"Functional Organization of the Transcriptome in Human Brain"

Michael C. Oldham, Steve Horvath, Genevieve Konopka, Kazuya Iwamoto, Peter Langfelder, Tadafumi Kato, and Daniel H. Geschwind

Nature Neuroscience

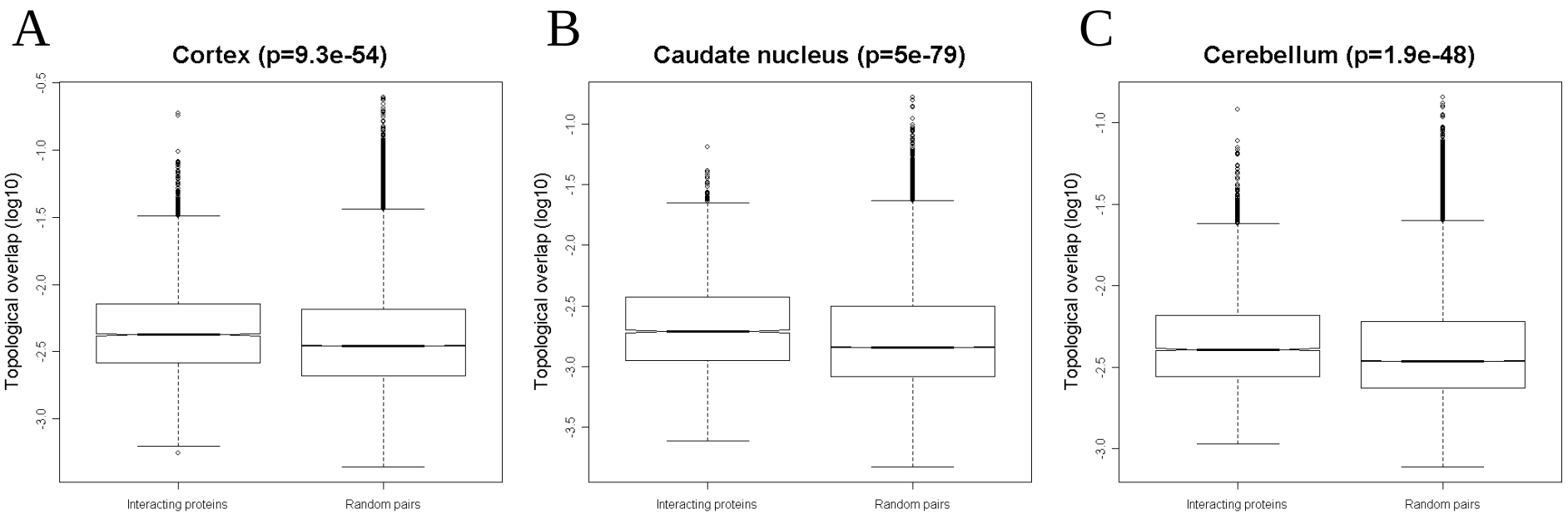

Supplementary Figure 1: Pairs of proteins that physically interact have higher topological overlap in gene coexpression networks than randomly selected pairs

Comparison of mean topological overlap (TO) for interacting protein pairs versus mean TO for randomly selected pairs in (**a**) CTX, (**b**) CN, and (**c**) CB. A set of experimentally validated interacting human protein pairs was obtained from ref. 26. Mean TO was calculated in each brain region for all expressed, interacting protein pairs (CTX = 5,980 pairs; CN = 4,901 pairs; CB = 5,347 pairs). For genes represented by multiple probe sets, the average was taken. The mean TO for interacting protein pairs was then compared to the mean TO for randomly selected pairs of probe sets in each network (n = 50,000). Data were highly skewed and log-transformed. Significance was assessed using the Kruskal-Wallis test.

“Functional Organization of the Transcriptome in Human Brain”

Michael C. Oldham, Steve Horvath, Genevieve Konopka, Kazuya Iwamoto, Peter Langfelder, Tadafumi Kato, and Daniel H. Geschwind

Nature Neuroscience

Supplementary Figure 2: Module summaries

Summaries for all modules from CTX (**a–s**), CTX_95 (**t–aj**), CN (**ak–bg**), and CB (**bh–cc**). Top left: heat map of gene expression levels for all genes assigned to the module in Fig. 1 (red = increased expression; black = neutral expression; green = decreased expression). Genes were ranked from top to bottom by the absolute value of module membership (MM). Bottom left: barplot of the module eigengene (ME; i.e. the first principal component following singular value decomposition). The ordering of samples in heat maps and ME barplots is identical for all modules in each network. Sample labels appear on the x-axis of the ME barplot (H1 = Human 1, etc.; BA = Brodmann area). Note that many samples from CTX, CN, and CB were taken from the same individuals (as denoted by sample labels). Right: $\log_2$-transformed expression levels for the top 10 genes selected by |MM| (note: kme = MM). Some genes are represented by multiple probe sets.

Figure S2

Cortex

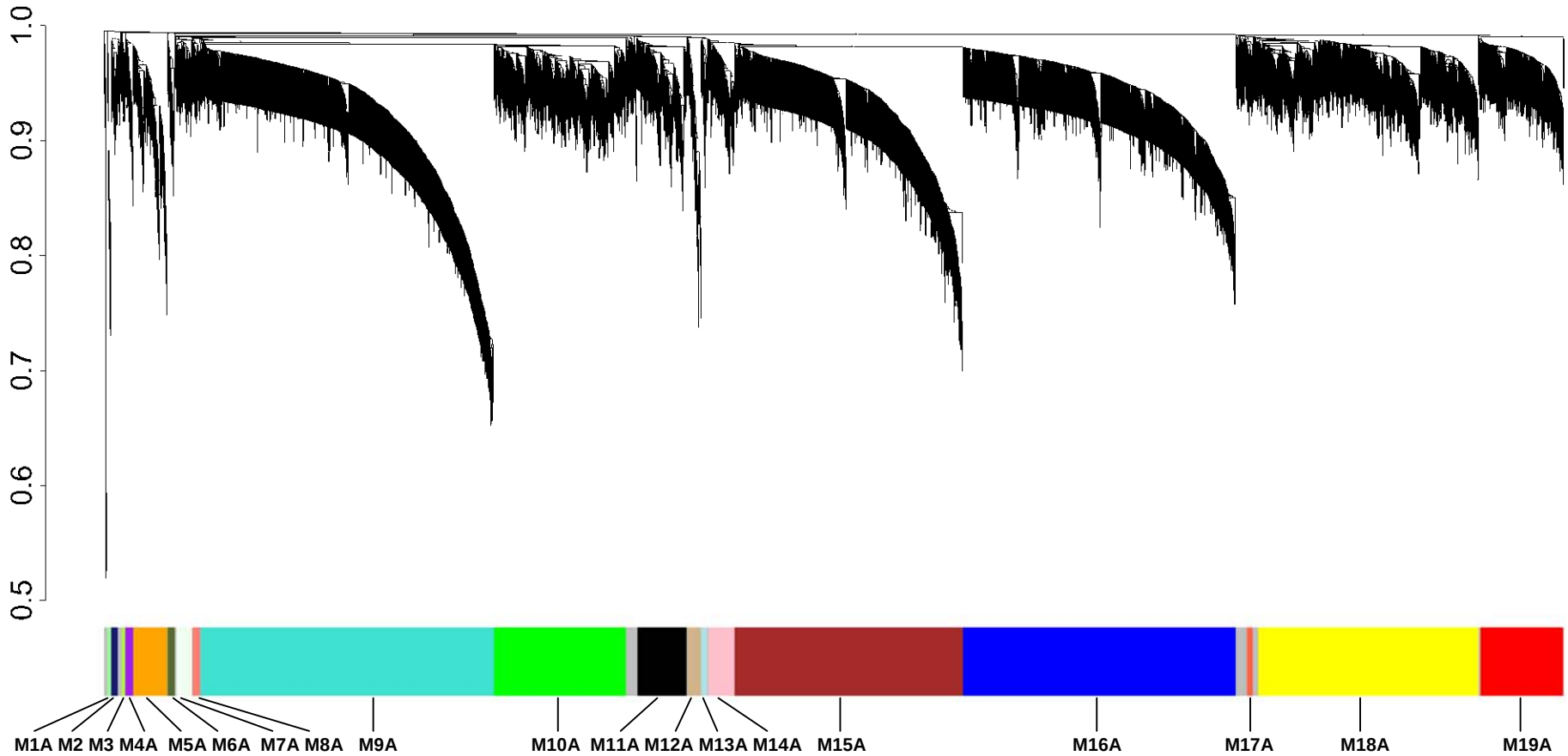

Figure S2A

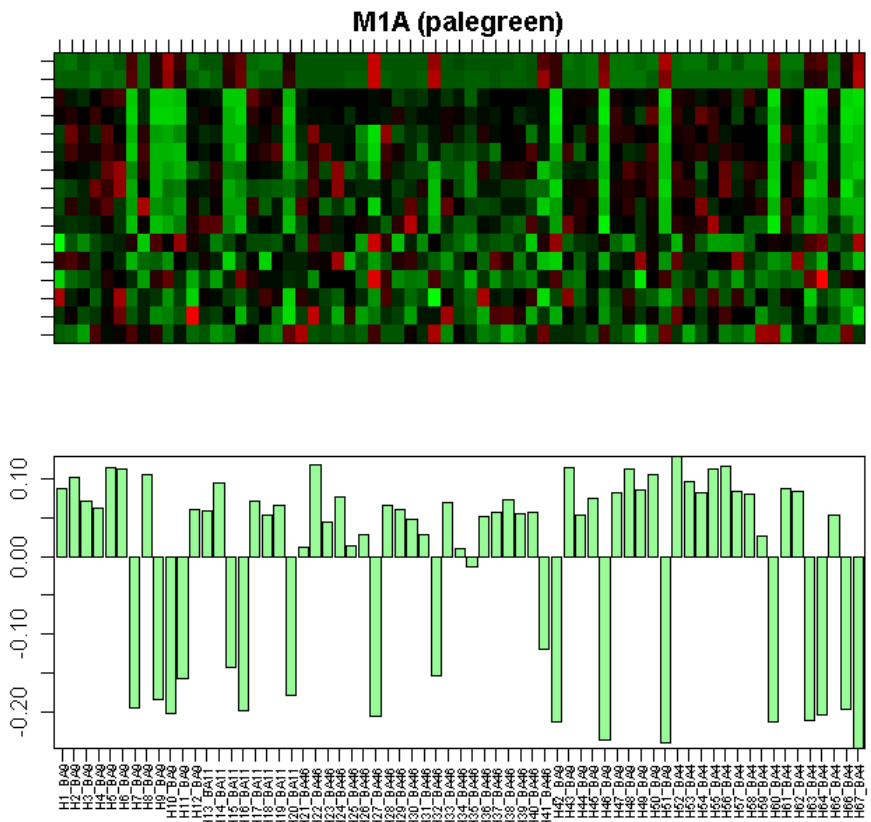
M1A (palegreen)
0.10
0.00
-0.10
-0.20

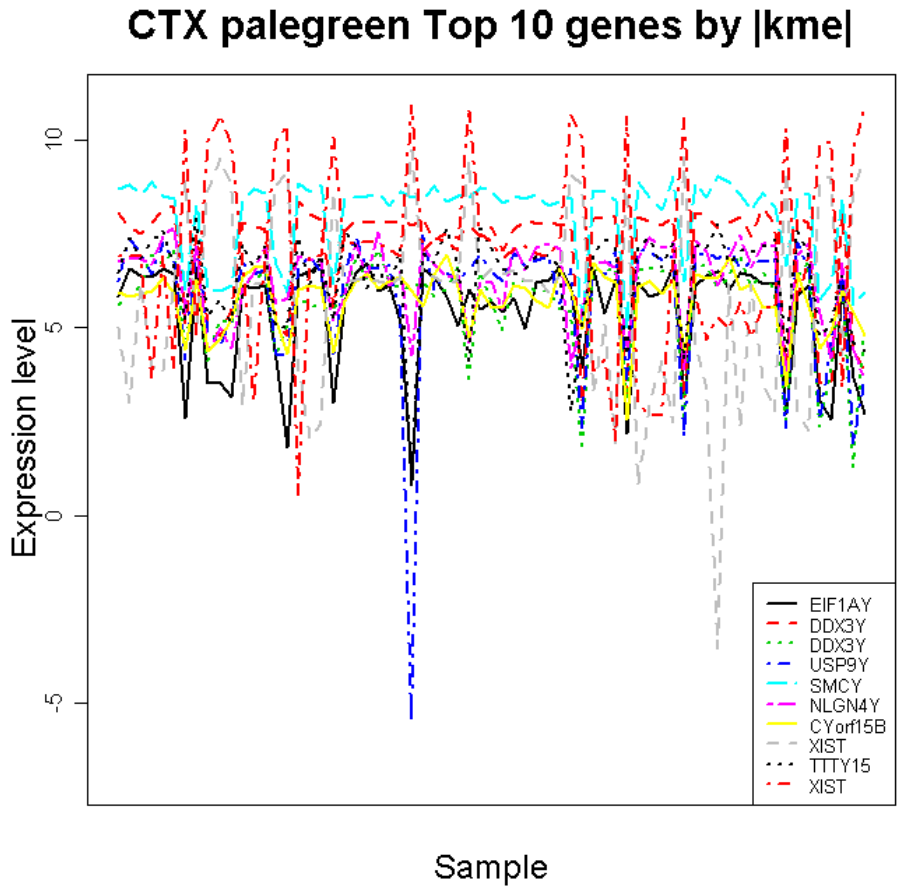
CTX palegreen Top 10 genes by |kme|
Expression level
10
5
0
-5
Sample
EIF1AY
DDX3Y
DDX3Y
USP9Y
SMCY
NLGN4Y
CYorf15B
XIST
TTTY15
XIST

Figure S2B

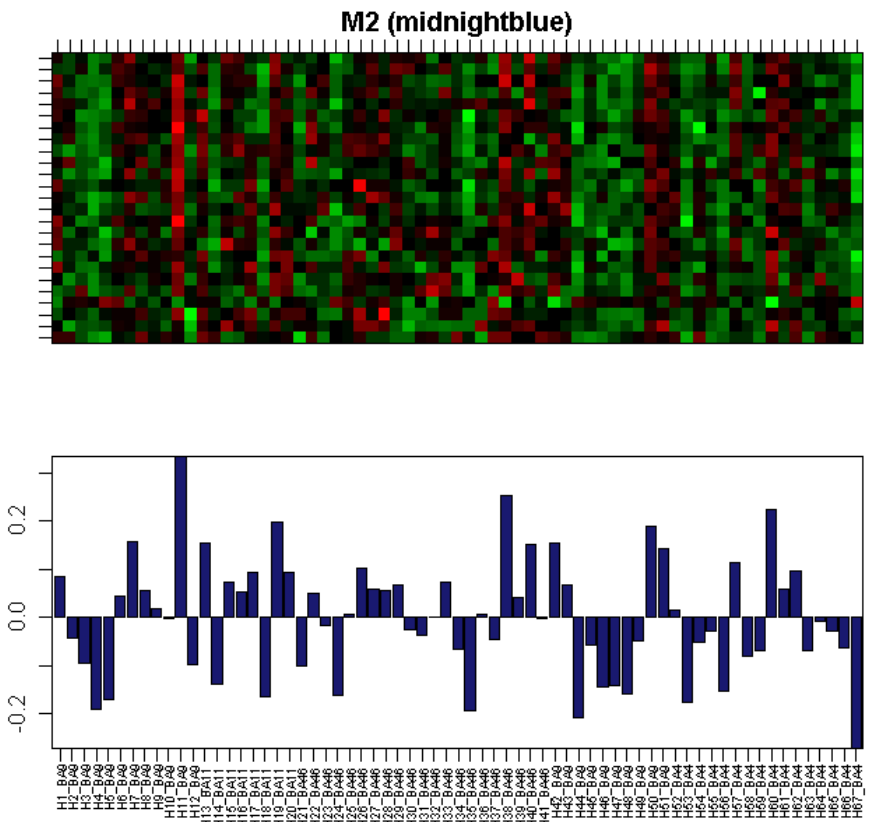
M2 (midnightblue)
0.2
0.0
-0.2

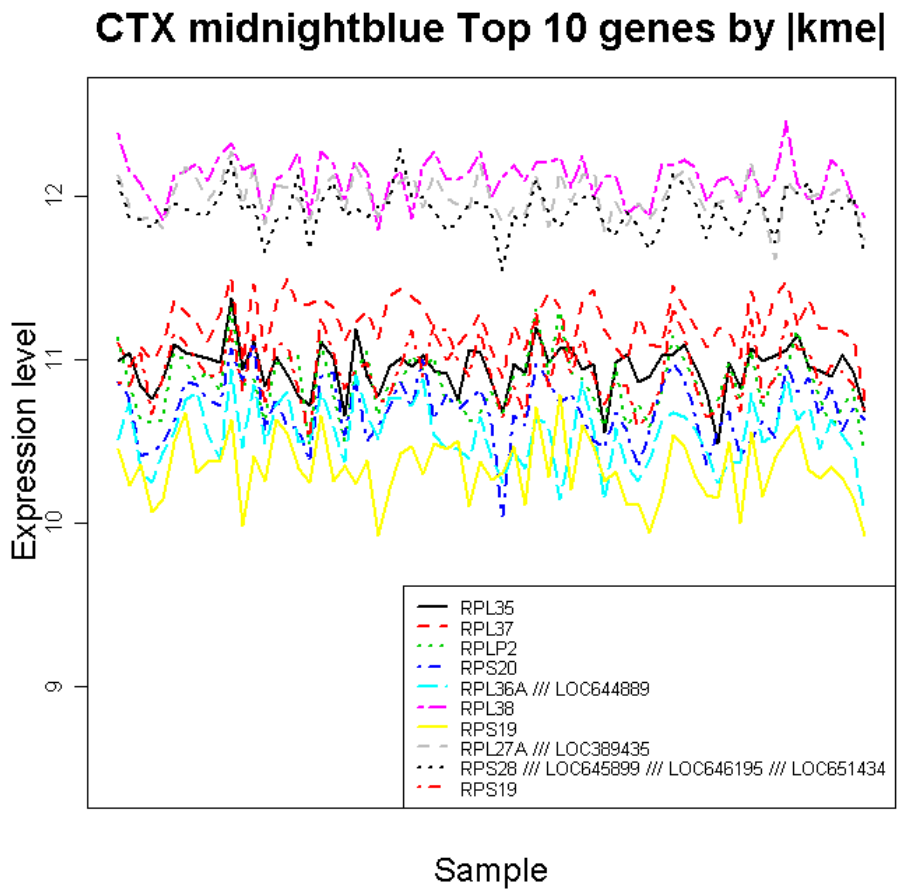
CTX midnightblue Top 10 genes by |kme|
Expression level
12
11
10
9
Sample
RPL35
RPL37
RPLP2
RPS20
RPL36A /// LOC644889
RPL38
RPS19
RPL27A /// LOC389435
RPS28 /// LOC645899 /// LOC646195 /// LOC651434
RPS19

Figure S2C

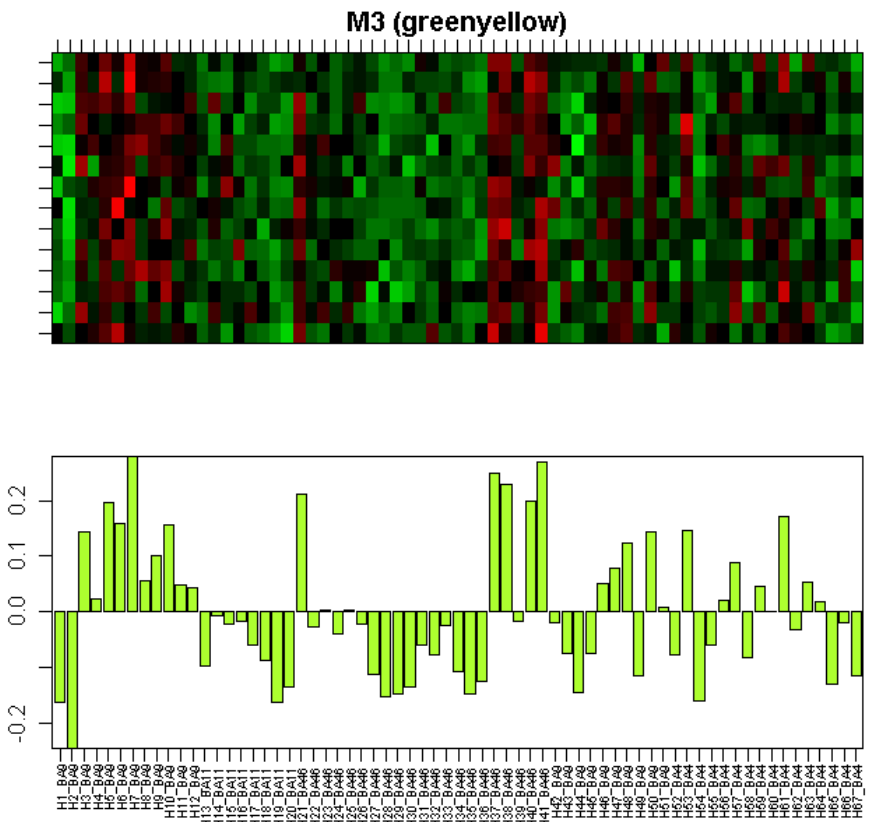
M3 (greenyellow)
0.2
0.1
0.0
-0.2

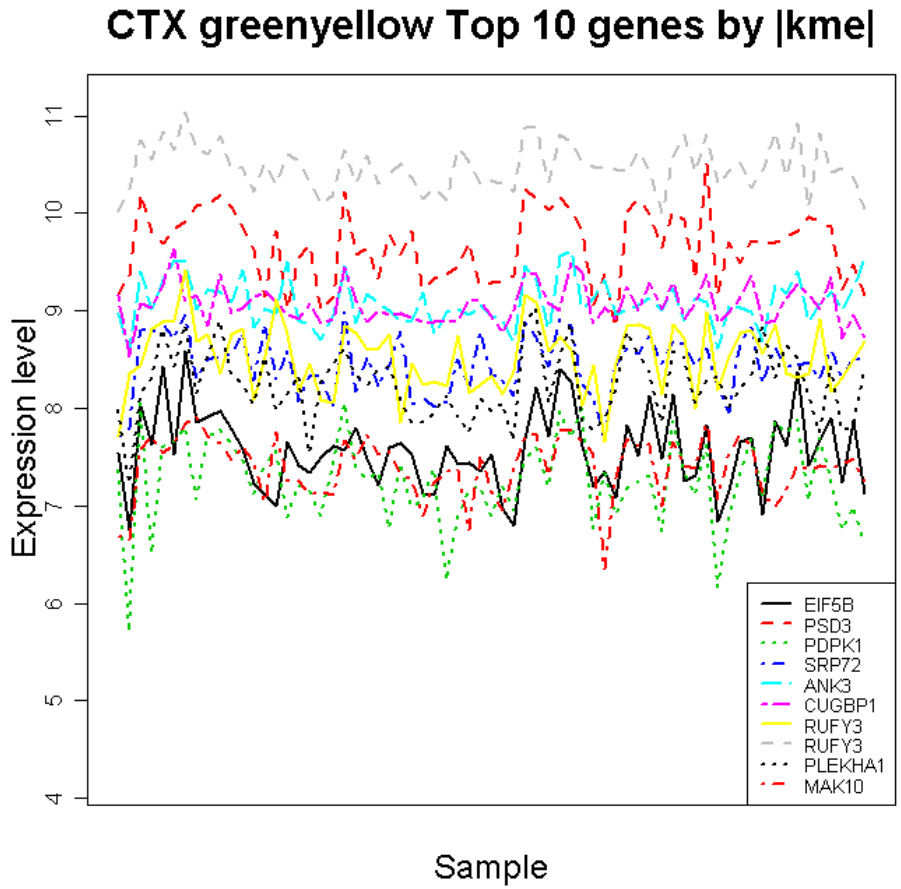
CTX greenyellow Top 10 genes by |kme|
Expression level
Sample
EIF5B
PSD3
PDPK1
SRP72
ANK3
CUGBP1
RUFY3
RUFY3
PLEKHA1
MAK10

Figure S2D

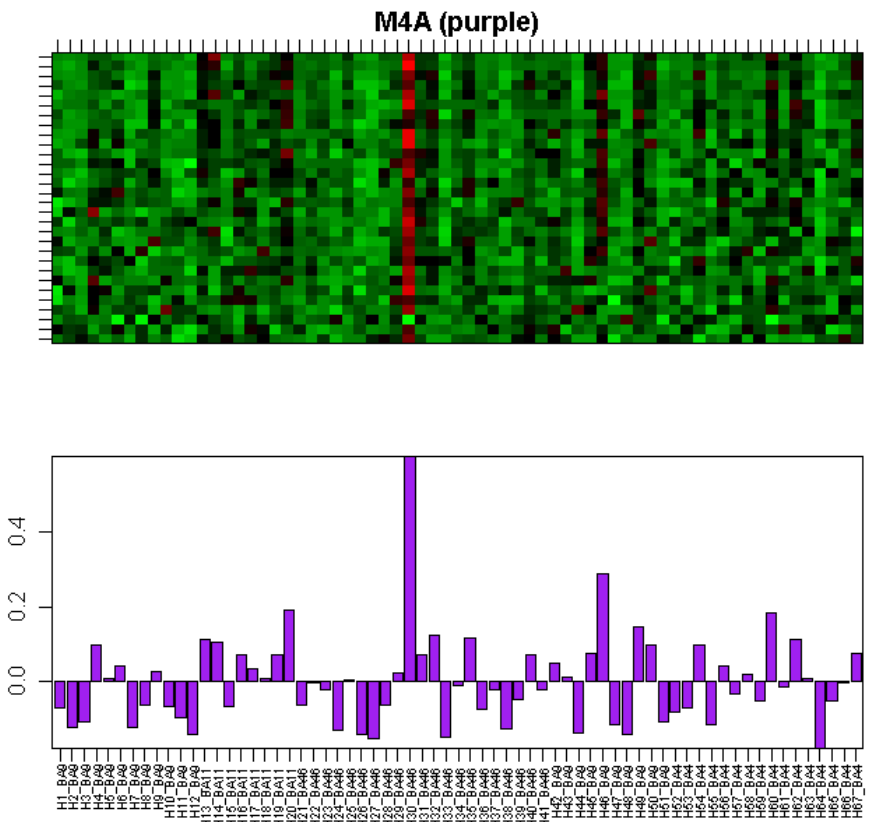
M4A (purple)
0.0
0.2
0.4

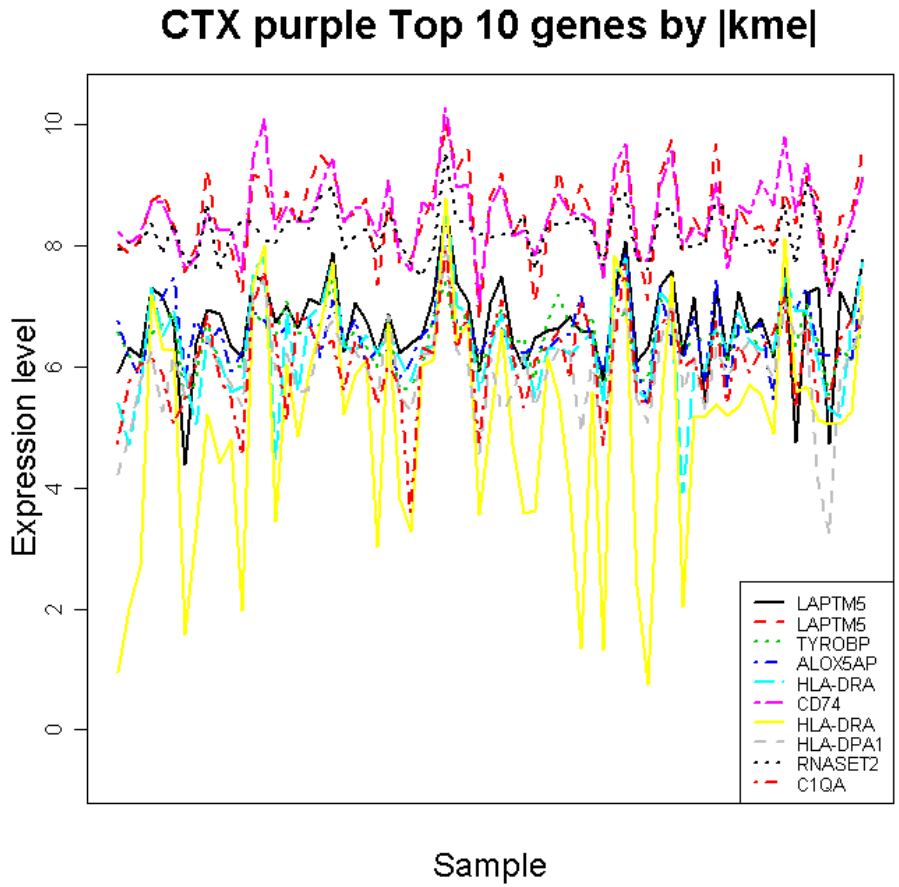
CTX purple Top 10 genes by |kme|
Expression level
0
2
4
6
8
10
Sample
LAPTM5
LAPTM5
TYROBP
ALOX5AP
HLA-DRA
CD74
HLA-DRA
HLA-DPA1
RNASET2
C1QA

Figure S2E

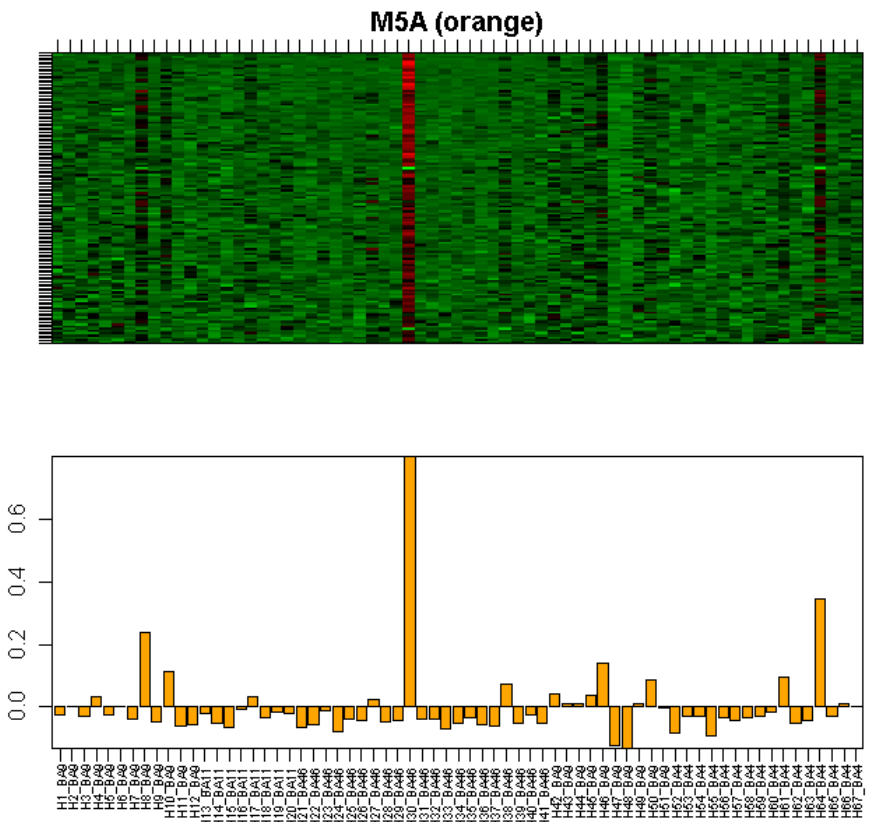
M5A (orange)
0.0
0.2
0.4
0.6

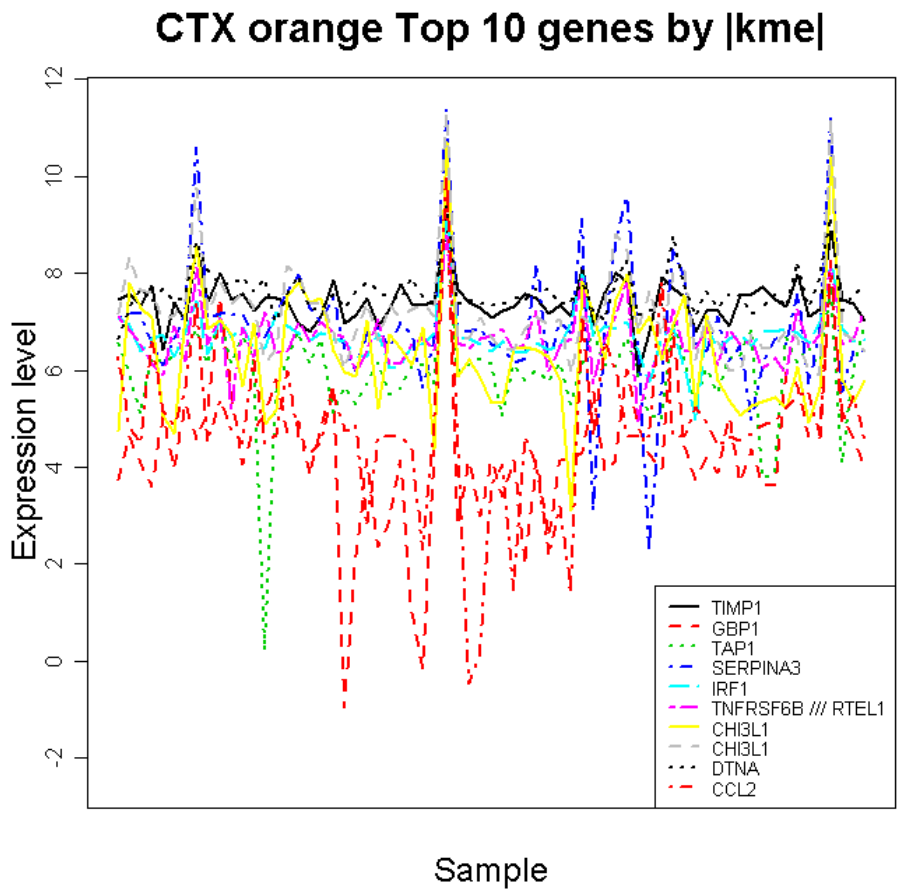
CTX orange Top 10 genes by |kme|
Expression level
-2
0
2
4
6
8
10
12
Sample
TIMP1
GBP1
TAP1
SERPINA3
IRF1
TNFRSF6B /// RTEL1
CHI3L1
CHI3L1
DTNA
CCL2

Figure S2F

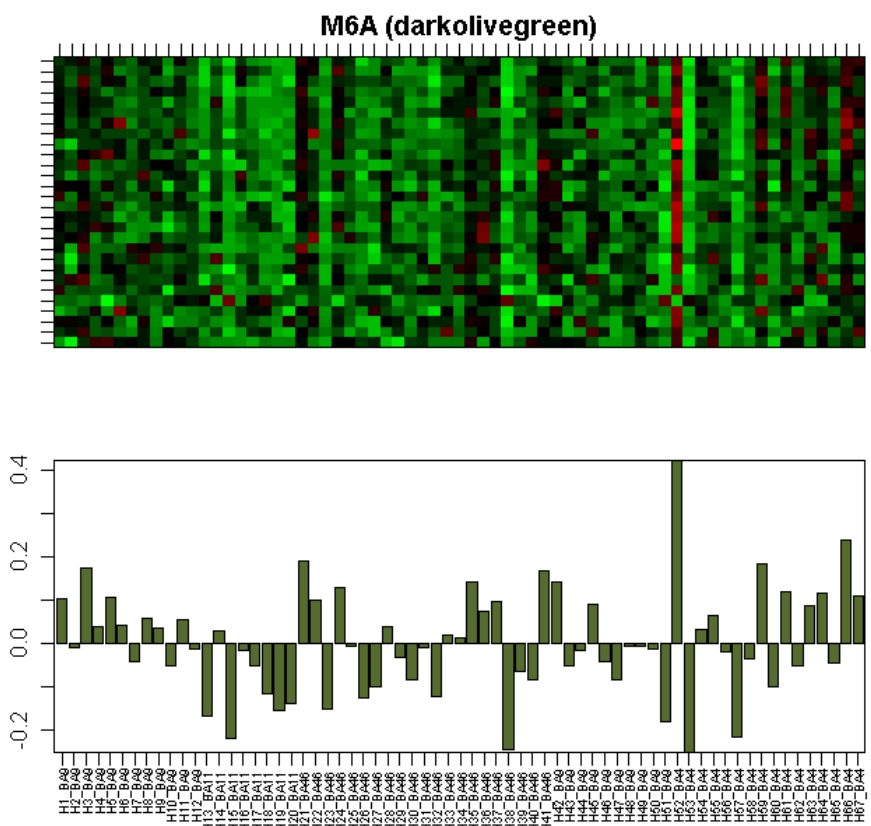
M6A (darkolivegreen)
0.4
0.2
0.0
-0.2

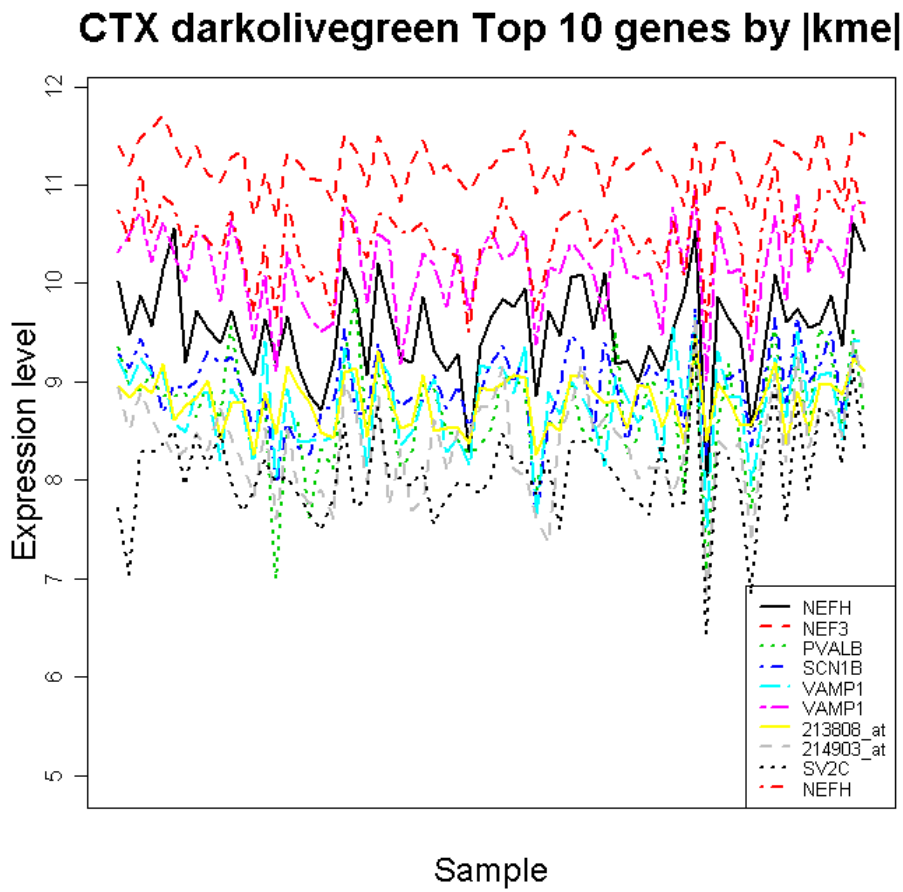
CTX darkolivegreen Top 10 genes by |kme|
Expression level
Sample
12
11
10
9
8
7
6
5
NEFH
NEF3
PVALB
SCN1B
VAMP1
VAMP1
213808_at
214903_at
SV2C
NEFH

Figure S2G

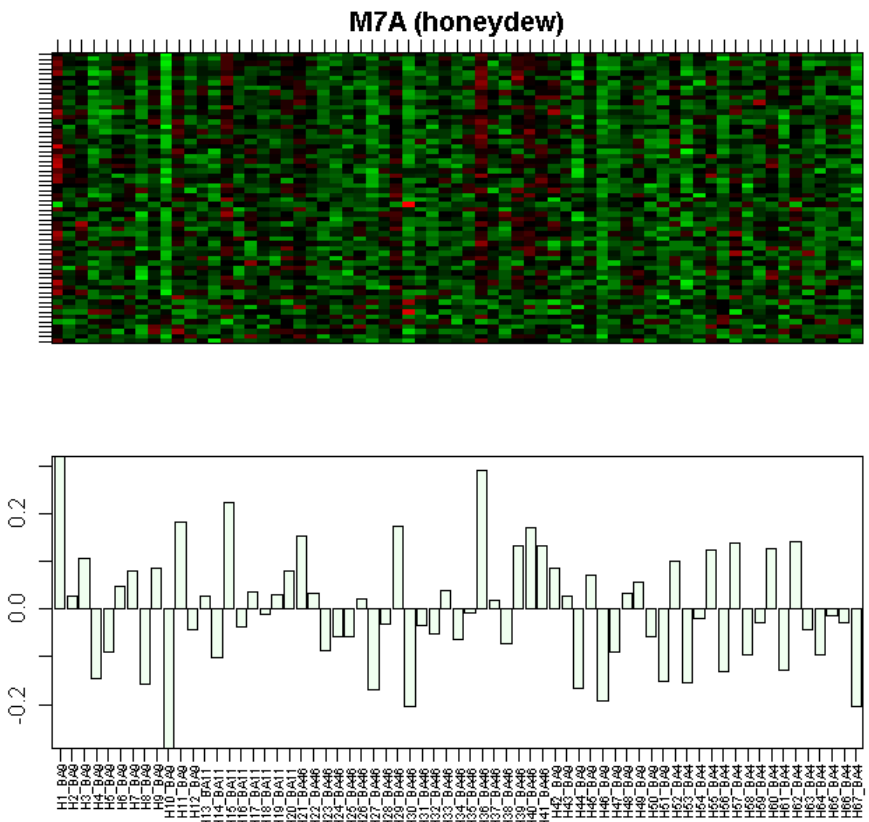
M7A (honeydew)
0.2
0.0
-0.2

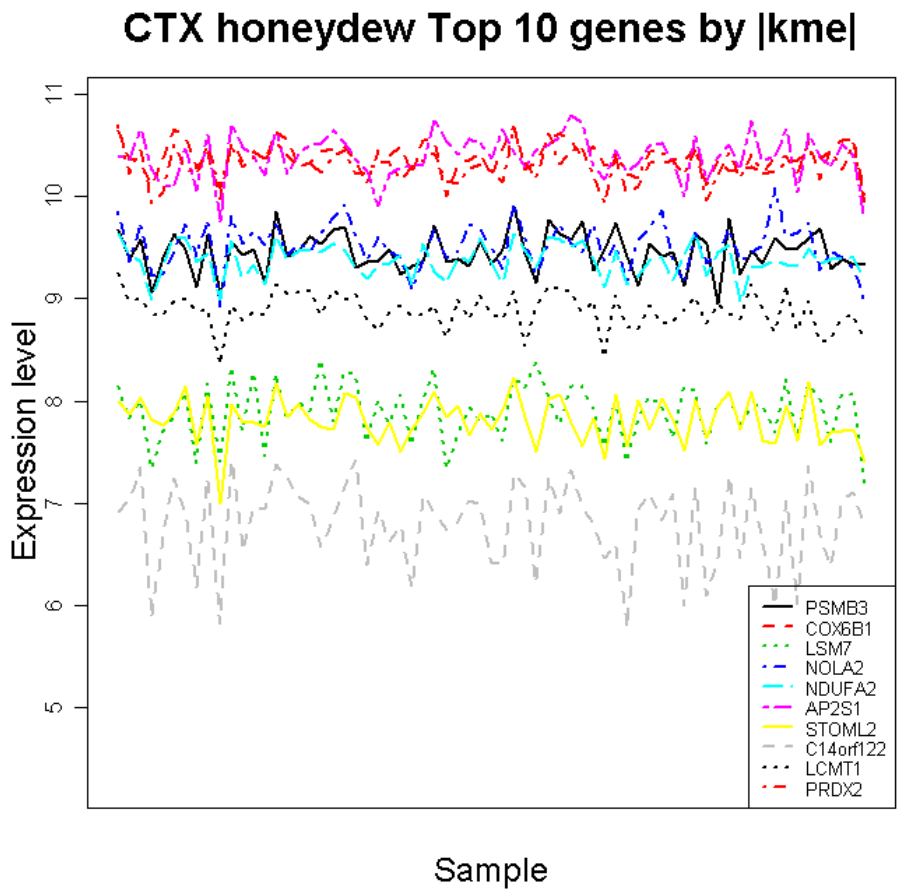
CTX honeydew Top 10 genes by |kme|
Expression level
Sample
PSMB3
COX6B1
LSM7
NOLA2
NDUFA2
AP2S1
STOML2
C14orf122
LCMT1
PRDX2

Figure S2H

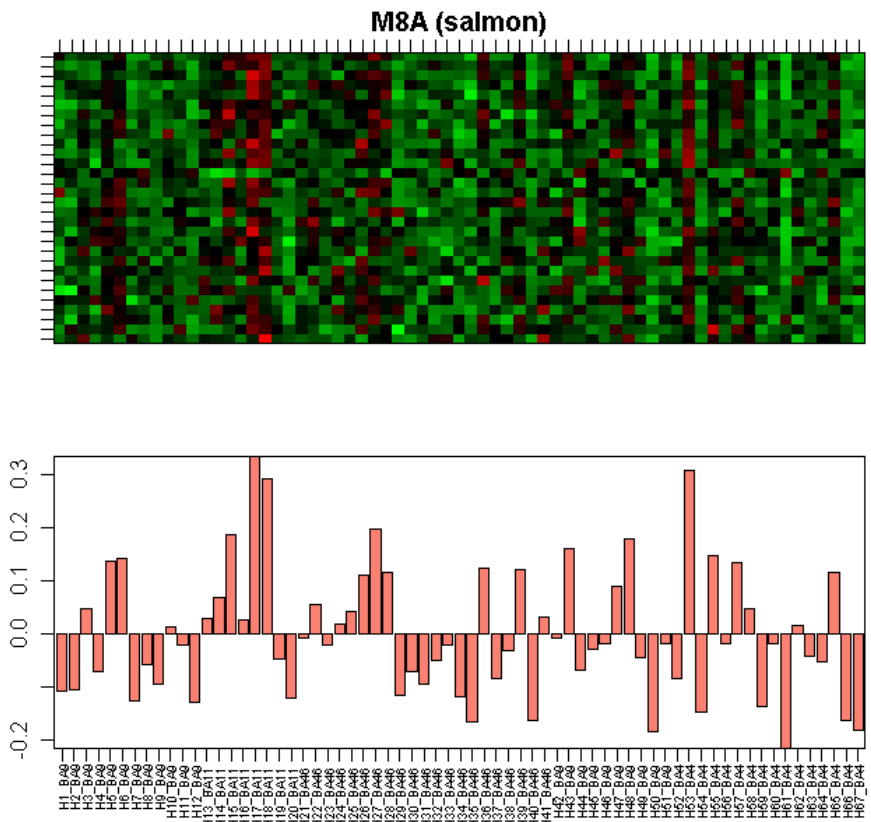
M8A (salmon)
0.3
0.2
0.1
0.0
-0.2

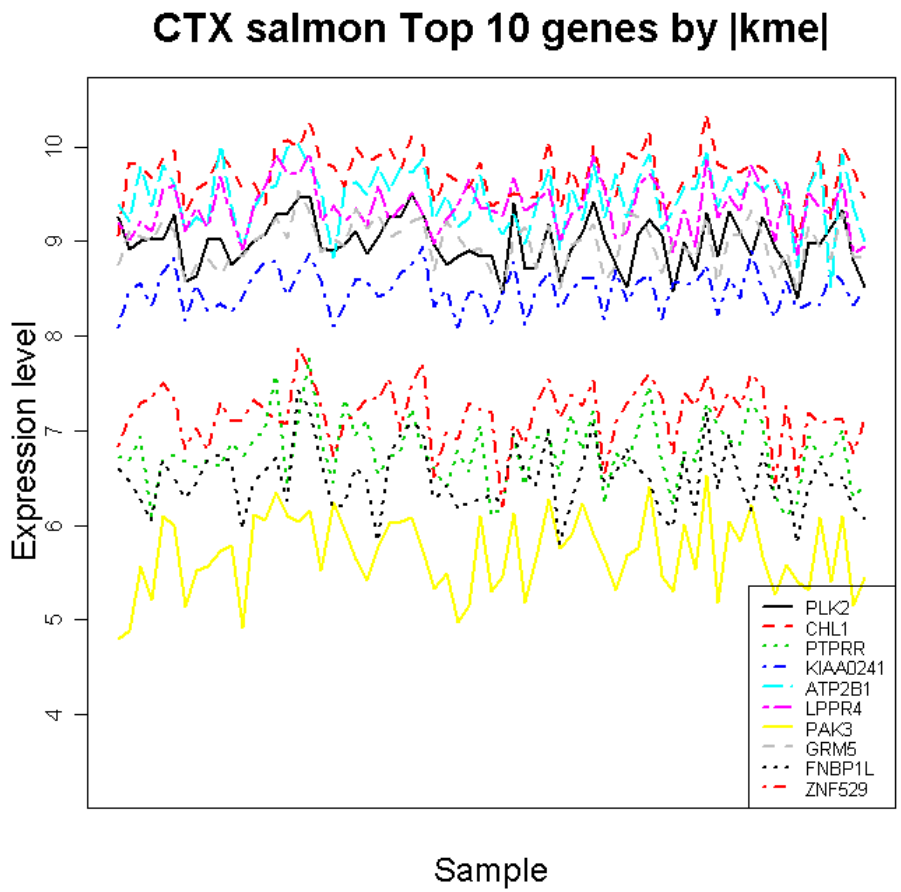
CTX salmon Top 10 genes by |kme|
Expression level
Sample
10
9
8
7
6
5
4
PLK2
CHL1
PTPRR
KIAA0241
ATP2B1
LPPR4
PAK3
GRM5
FNBP1L
ZNF529

Figure S2I

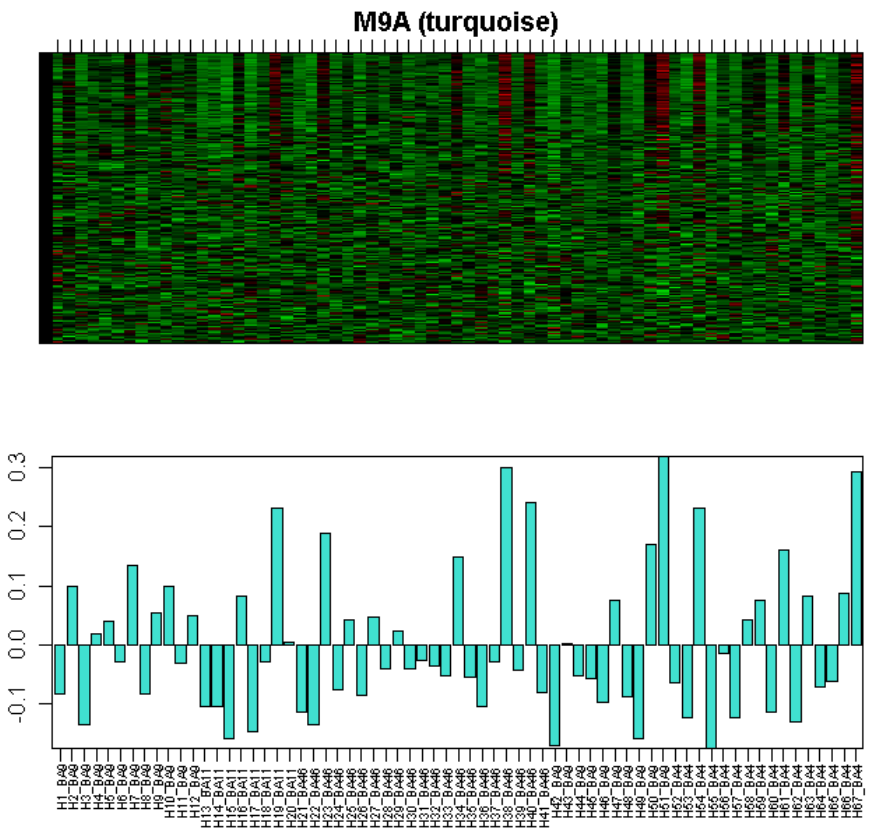
M9A (turquoise)
0.3
0.2
0.1
0.0
-0.1

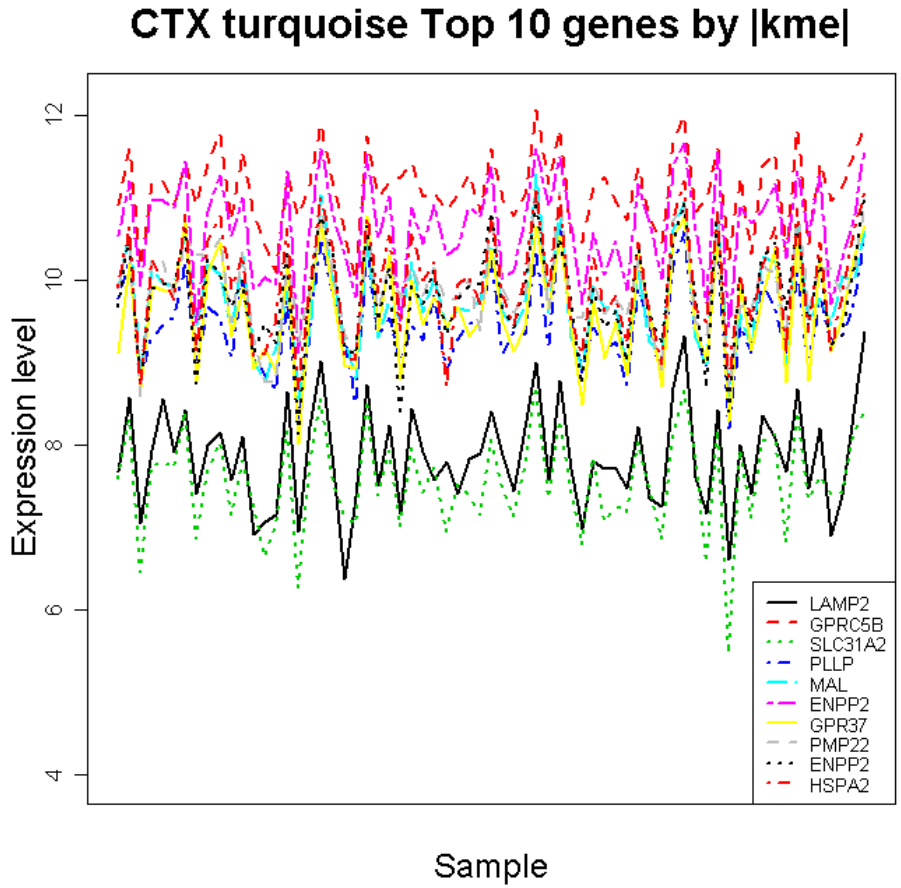
CTX turquoise Top 10 genes by |kme|
Expression level
12
10
8
6
4
Sample
LAMP2
GPRC5B
SLC31A2
PLLP
MAL
ENPP2
GPR37
PMP22
ENPP2
HSPA2

Figure S2J

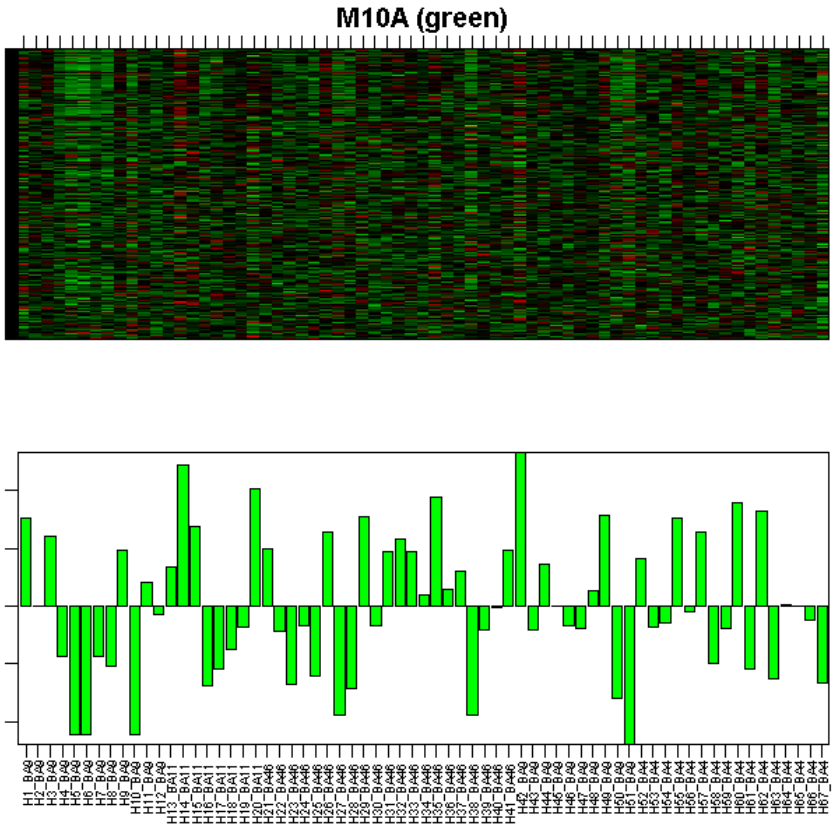

Figure S2K

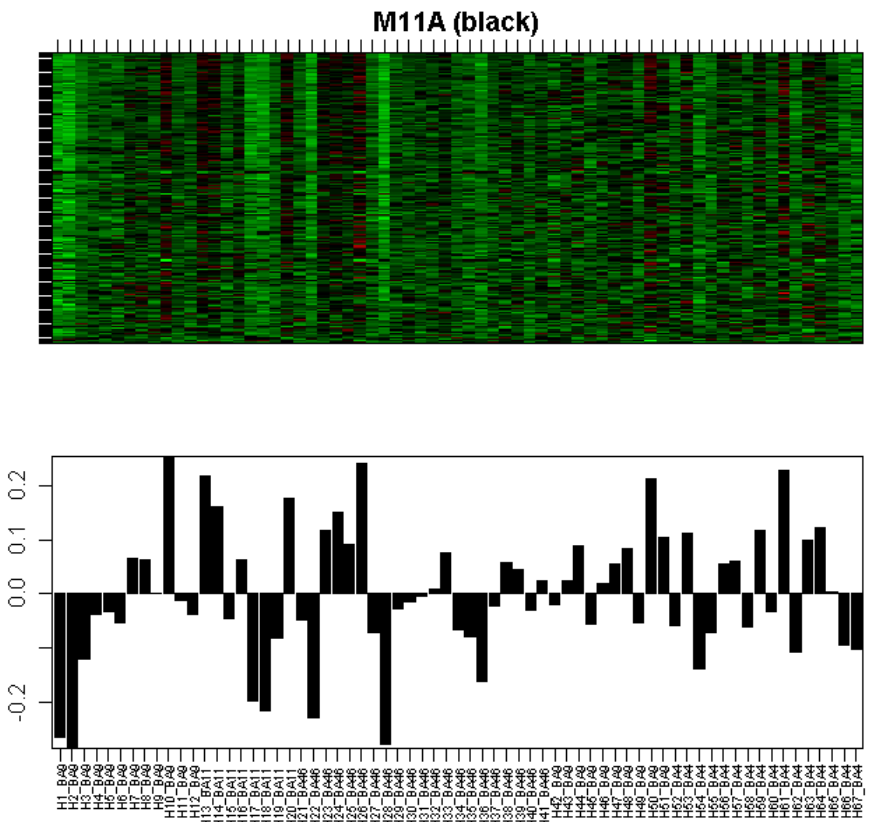
M11A (black)
0.2
0.1
0.0
-0.2

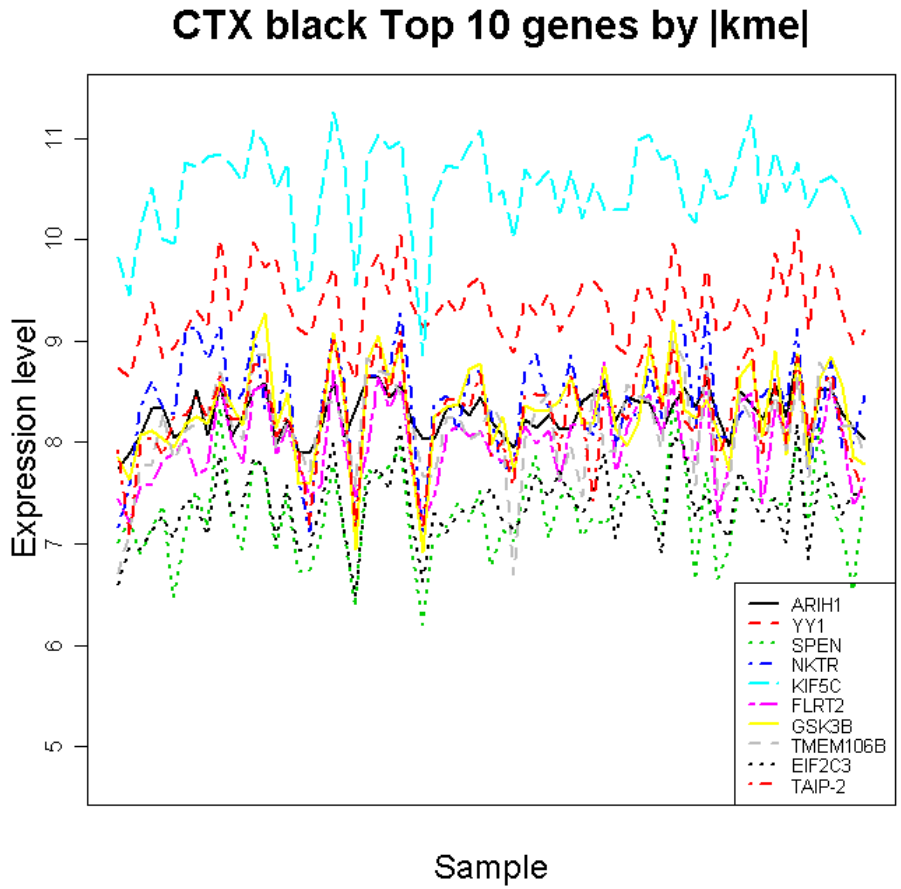
CTX black Top 10 genes by |kme|
Expression level
5
6
7
8
9
10
11
Sample
ARIH1
YY1
SPEN
NKTR
KIF5C
FLRT2
GSK3B
TMEM106B
EIF2C3
TAIP-2

Figure S2L

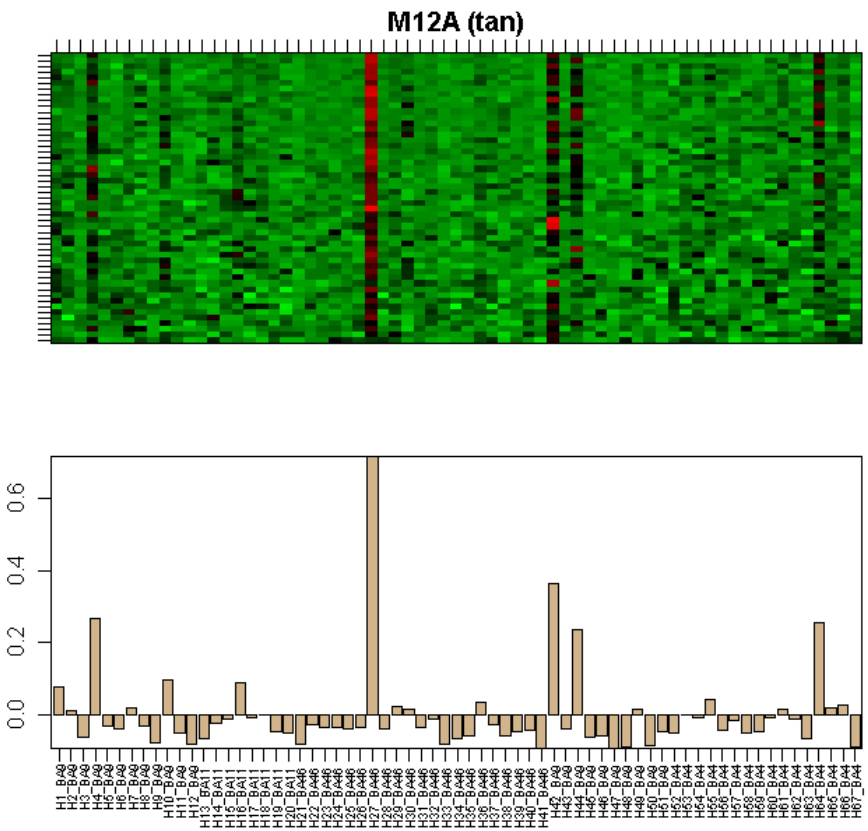
M12A (tan)
0.0
0.2
0.4
0.6

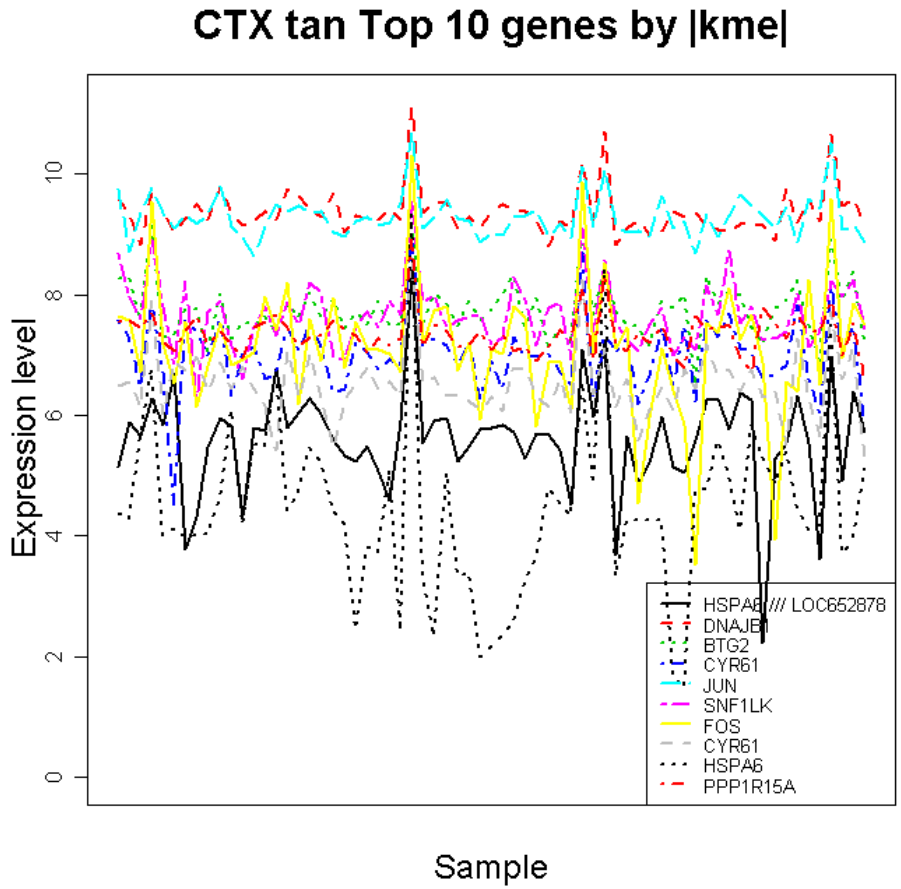
CTX tan Top 10 genes by |kme|
Expression level
0
2
4
6
8
10
Sample
HSPA8 /// LOC652878
DNAJB1
BTG2
CYR61
JUN
SNF1LK
FOS
CYR61
HSPA6
PPP1R15A

Figure S2M

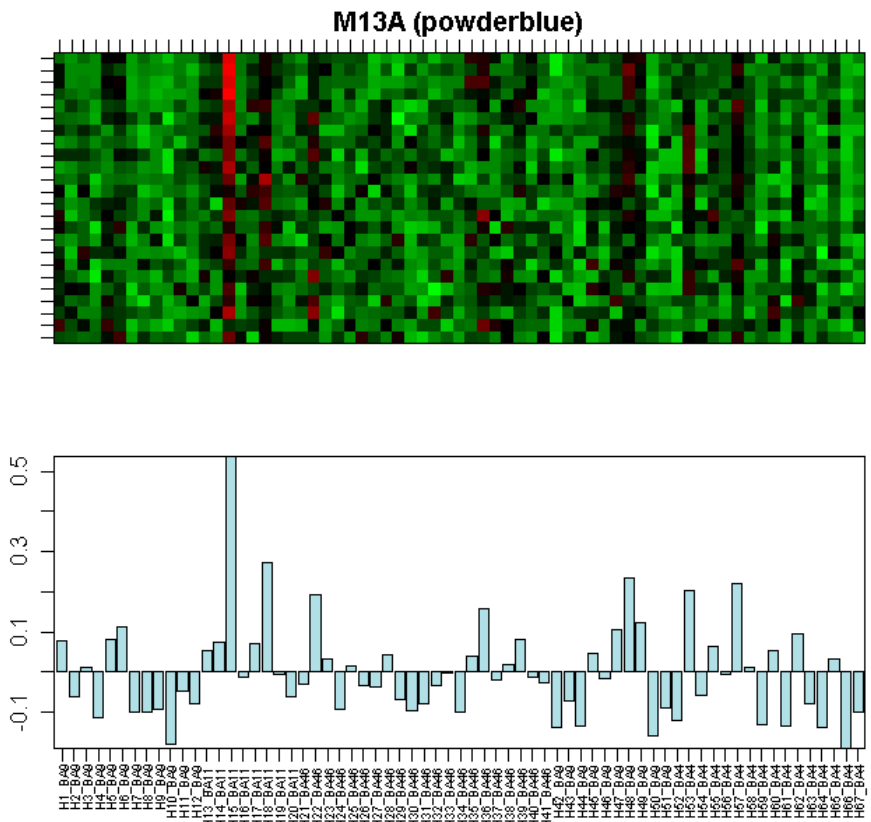
M13A (powderblue)
0.5
0.3
0.1
-0.1

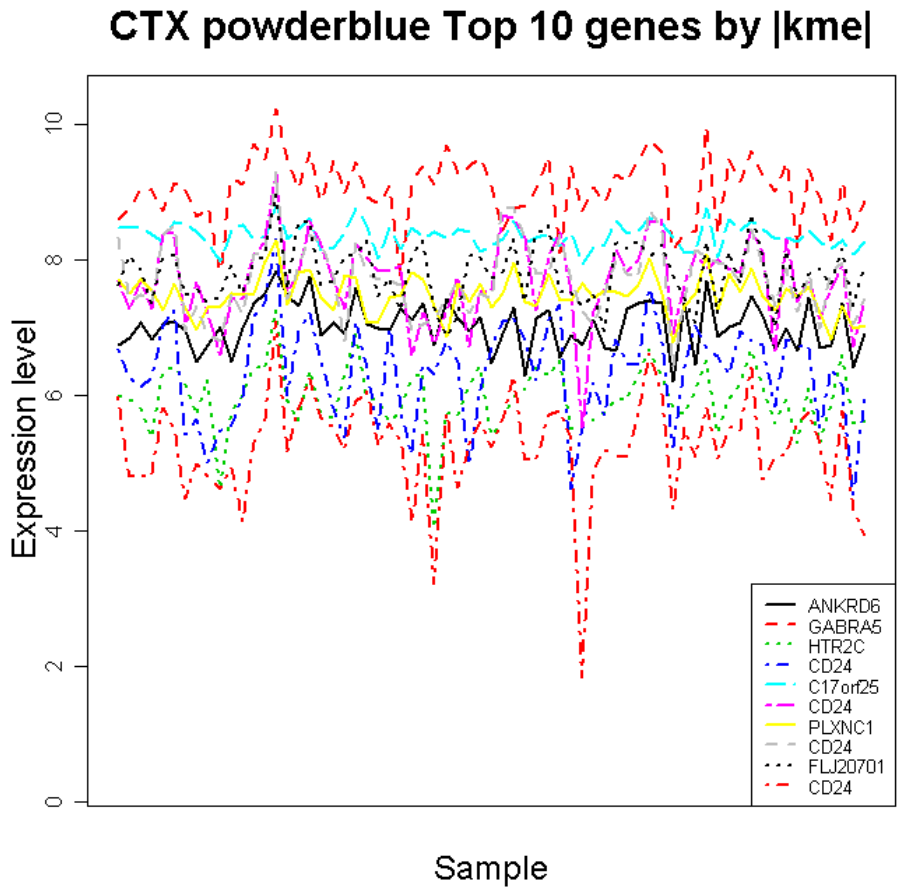
CTX powderblue Top 10 genes by |kme|
Expression level
0
2
4
6
8
10
Sample
ANKRD6
GABRA5
HTR2C
CD24
C17orf25
CD24
PLXNC1
CD24
FLJ20701
CD24

Figure S2N

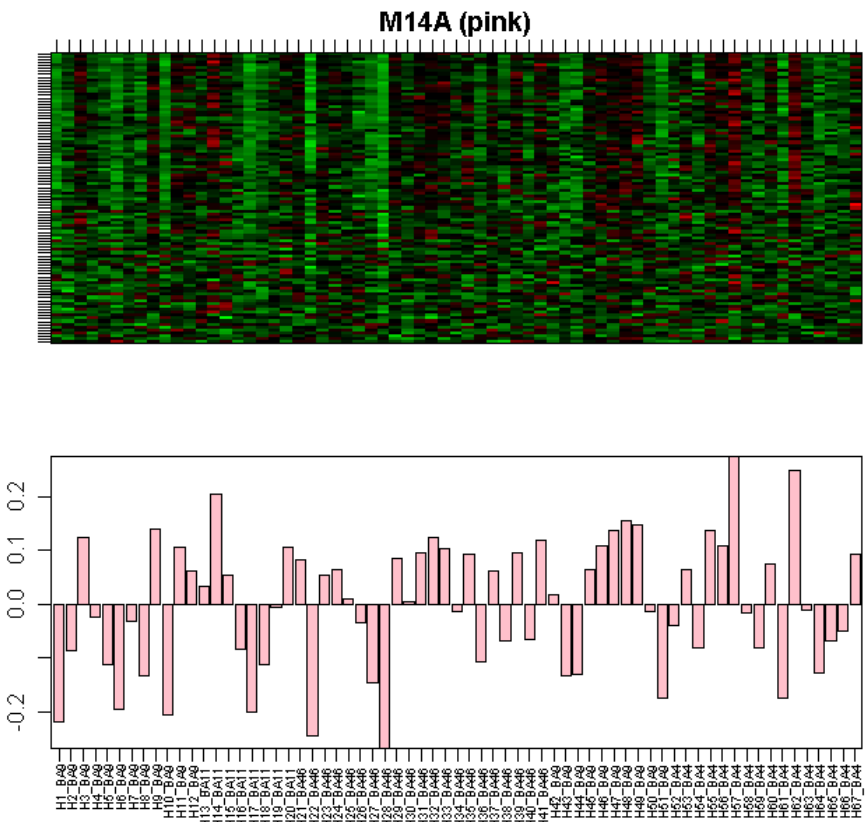
M14A (pink)
0.2
0.1
0.0
-0.2

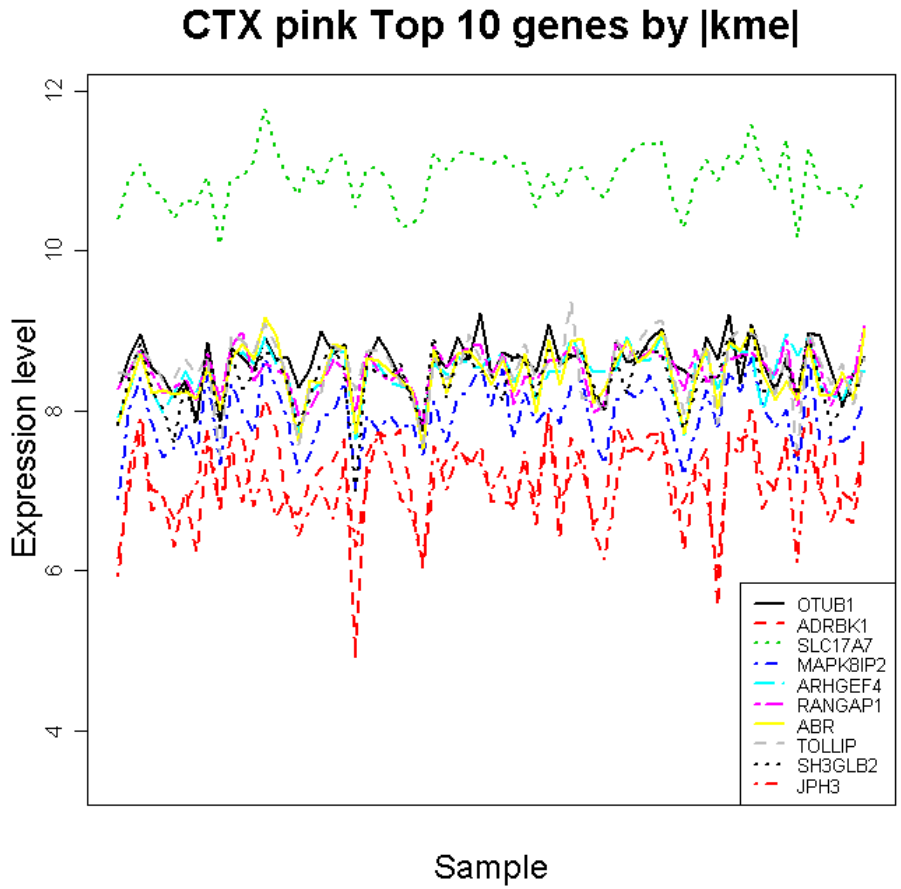
CTX pink Top 10 genes by |kme|
Expression level
12
10
8
6
4
Sample
OTUB1
ADRBK1
SLC17A7
MAPK8IP2
ARHGEF4
RANGAP1
ABR
TOLLIP
SH3GLB2
JPH3

Figure S2O

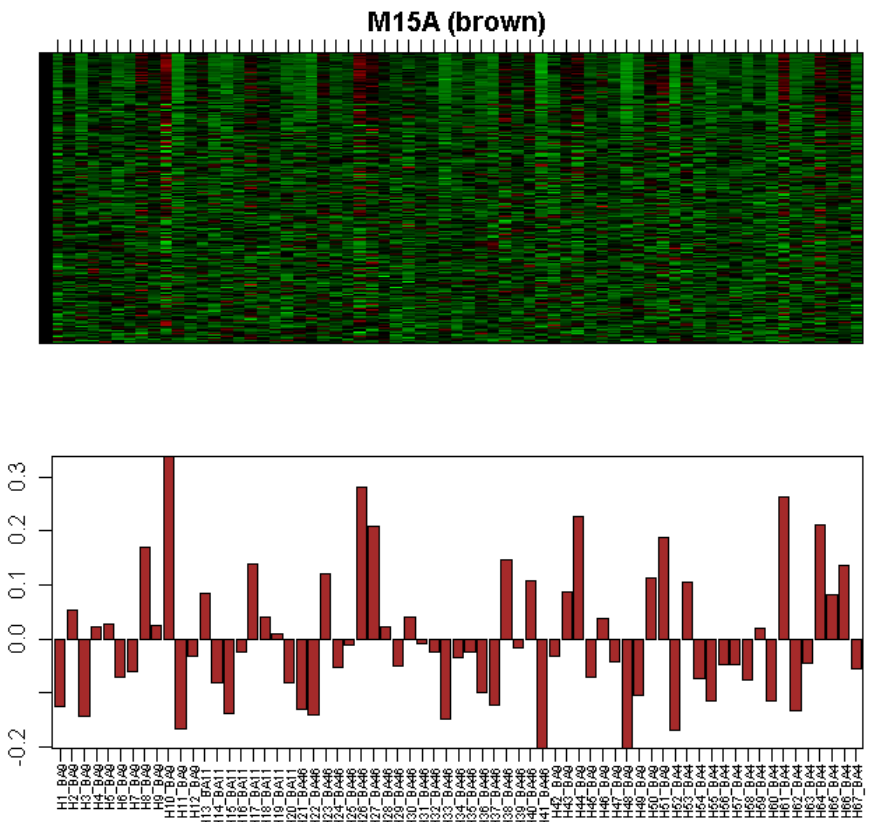
M15A (brown)
0.3
0.2
0.1
0.0
-0.2

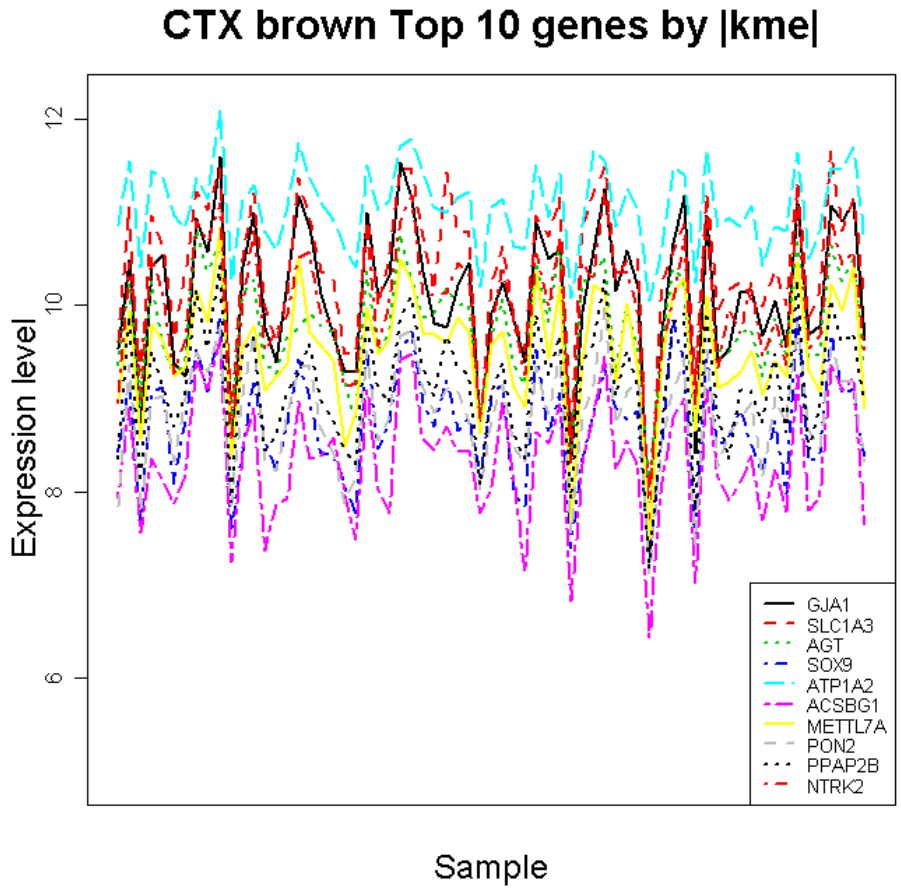
CTX brown Top 10 genes by |kme|
Expression level
12
10
8
6
Sample
GJA1
SLC1A3
AGT
SOX9
ATP1A2
ACSBG1
METTL7A
PON2
PPAP2B
NTRK2

Figure S2P

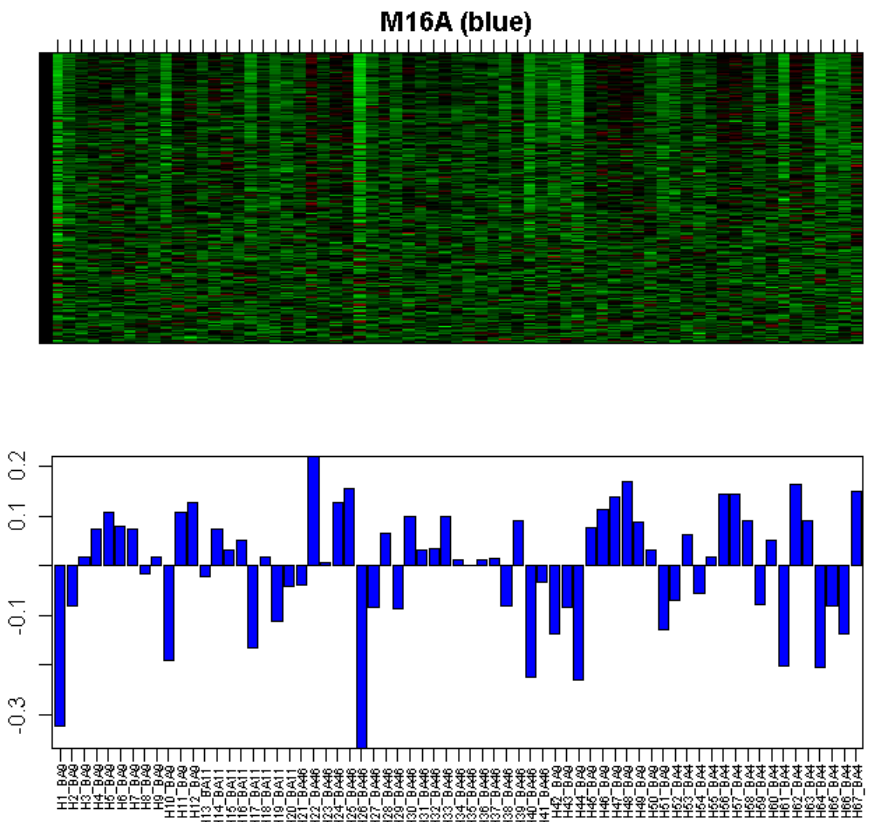
M16A (blue)
0.2
0.1
-0.1
-0.3

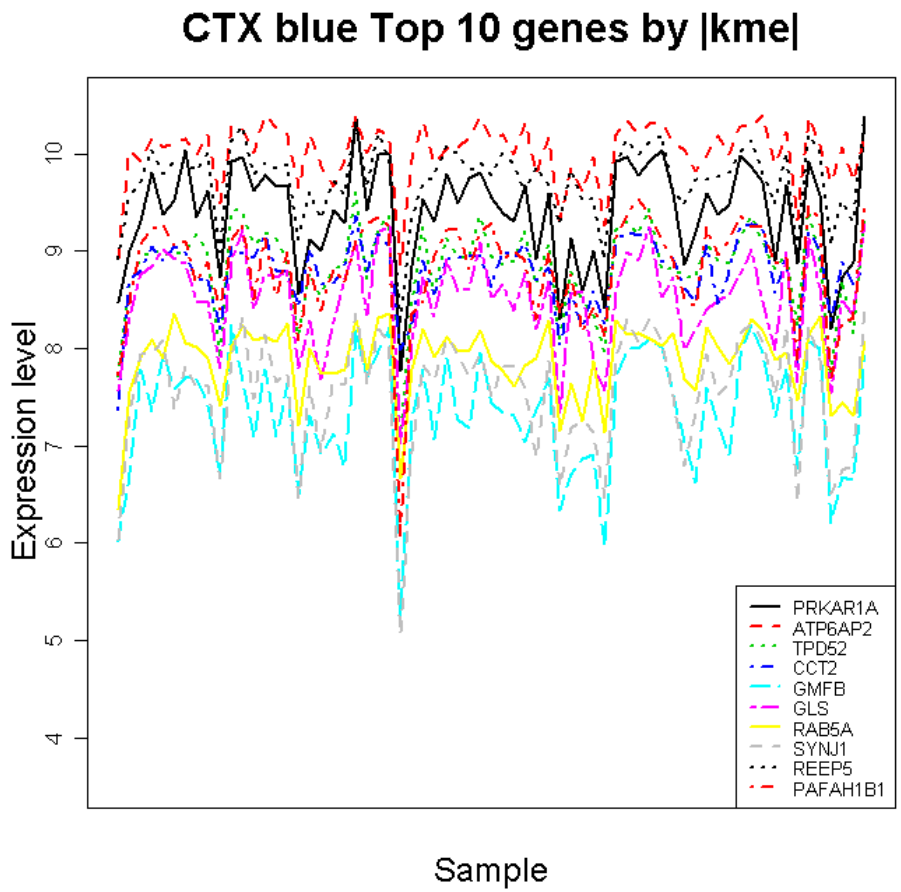
CTX blue Top 10 genes by |kme|
Expression level
4
5
6
7
8
9
10
Sample
PRKAR1A
ATP6AP2
TPD52
CCT2
GMFB
GLS
RAB5A
SYNJ1
REEP5
PAFAH1B1

Figure S2Q

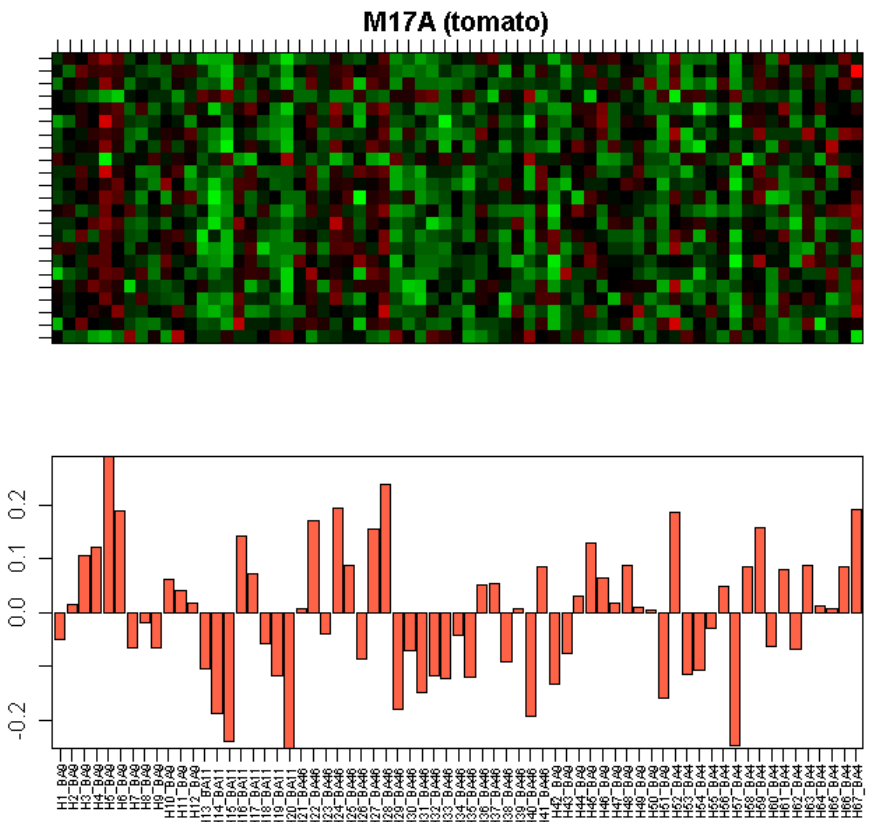
M17A (tomato)
0.2
0.1
0.0
-0.2

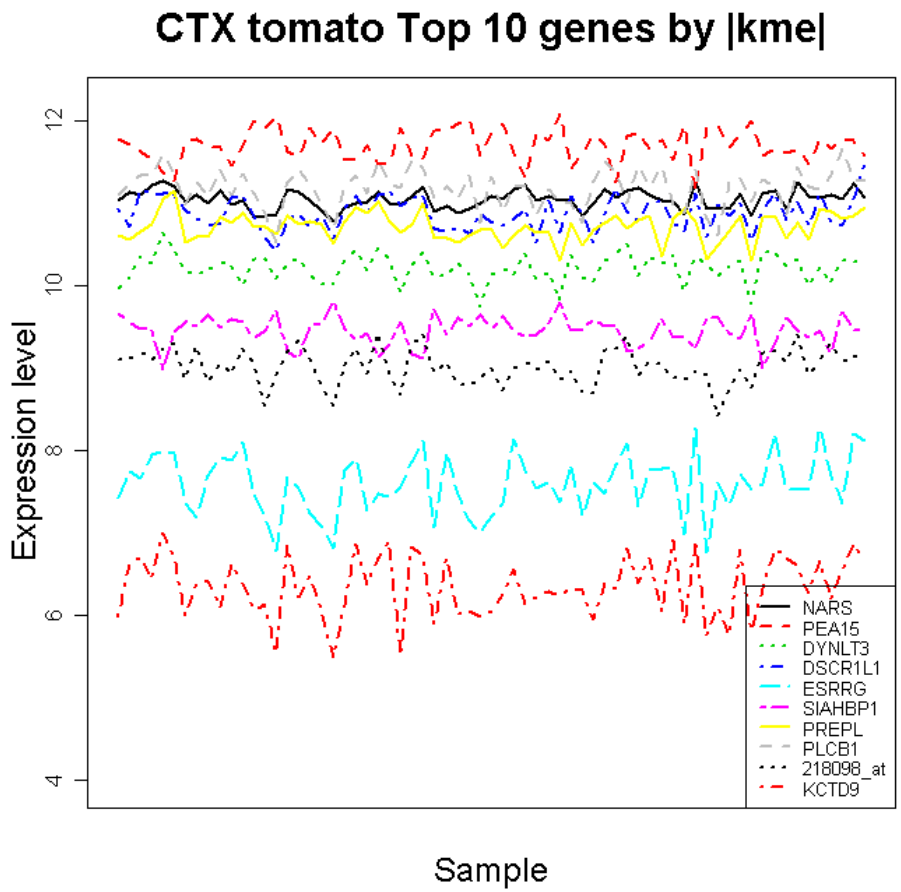
CTX tomato Top 10 genes by |kme|
Expression level
Sample
12
10
8
6
4
NARS
PEA15
DYNLT3
DSCR1L1
ESRRG
SIAHBP1
PREPL
PLCB1
218098_at
KCTD9

Figure S2R

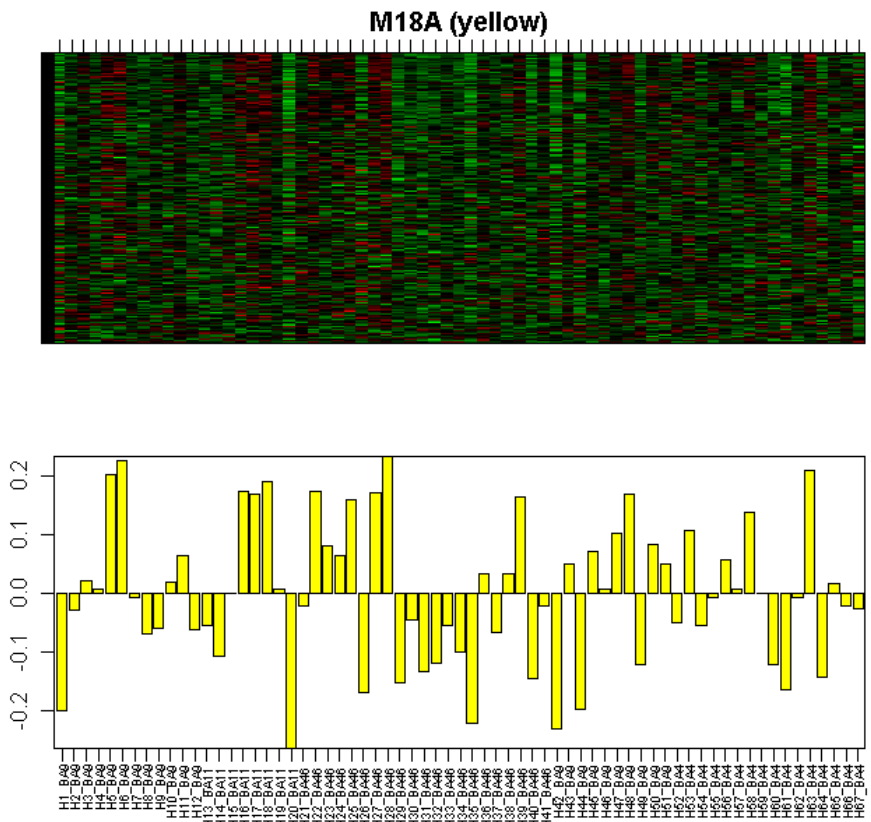
M18A (yellow)
0.2
0.1
0.0
-0.1
-0.2

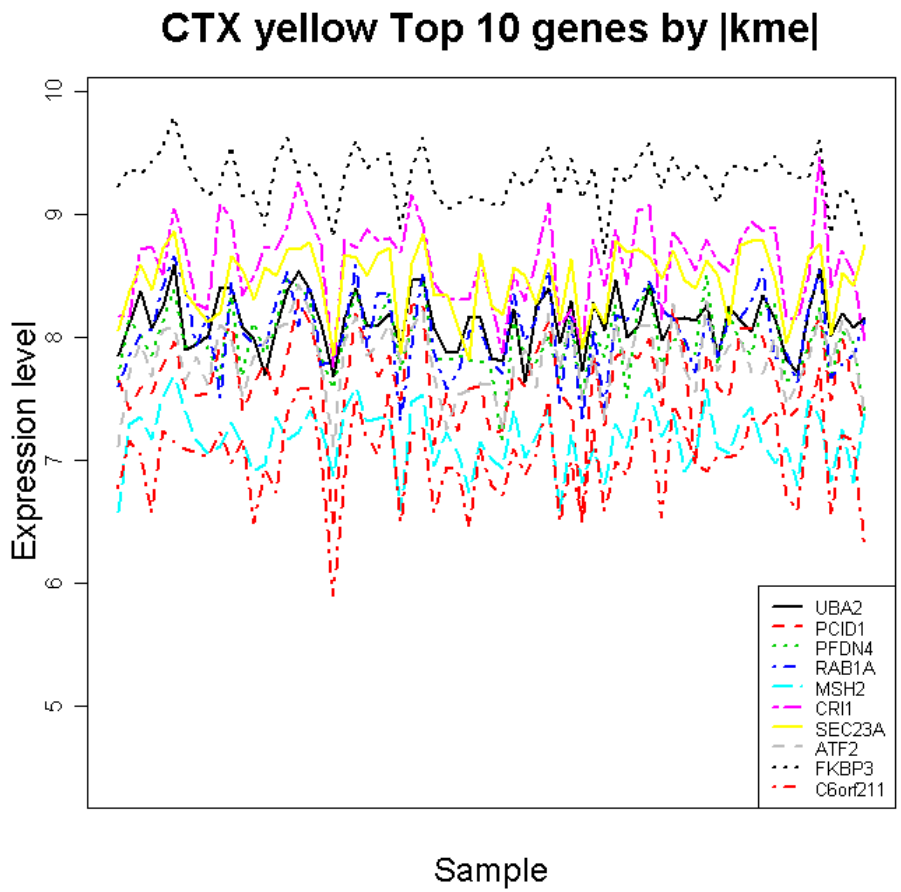
CTX yellow Top 10 genes by |kme|
Expression level
Sample
10
9
8
7
6
5
UBA2
PCID1
PFDN4
RAB1A
MSH2
CRI1
SEC23A
ATF2
FKBP3
C6orf211

Figure S2S

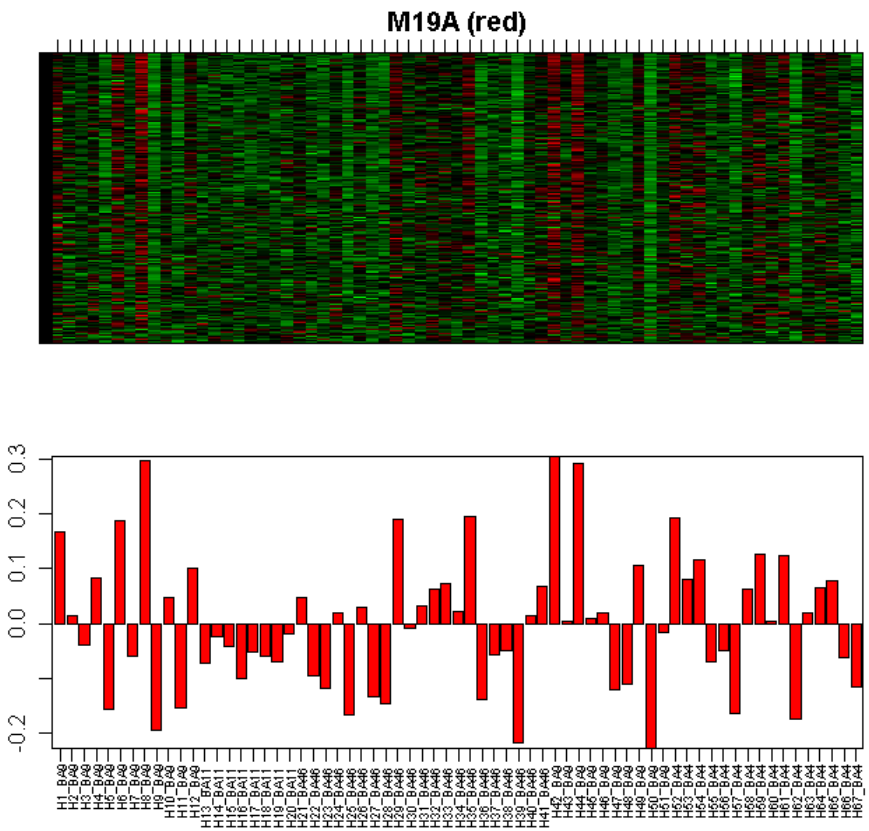
M19A (red)
0.3
0.2
0.1
0.0
-0.2

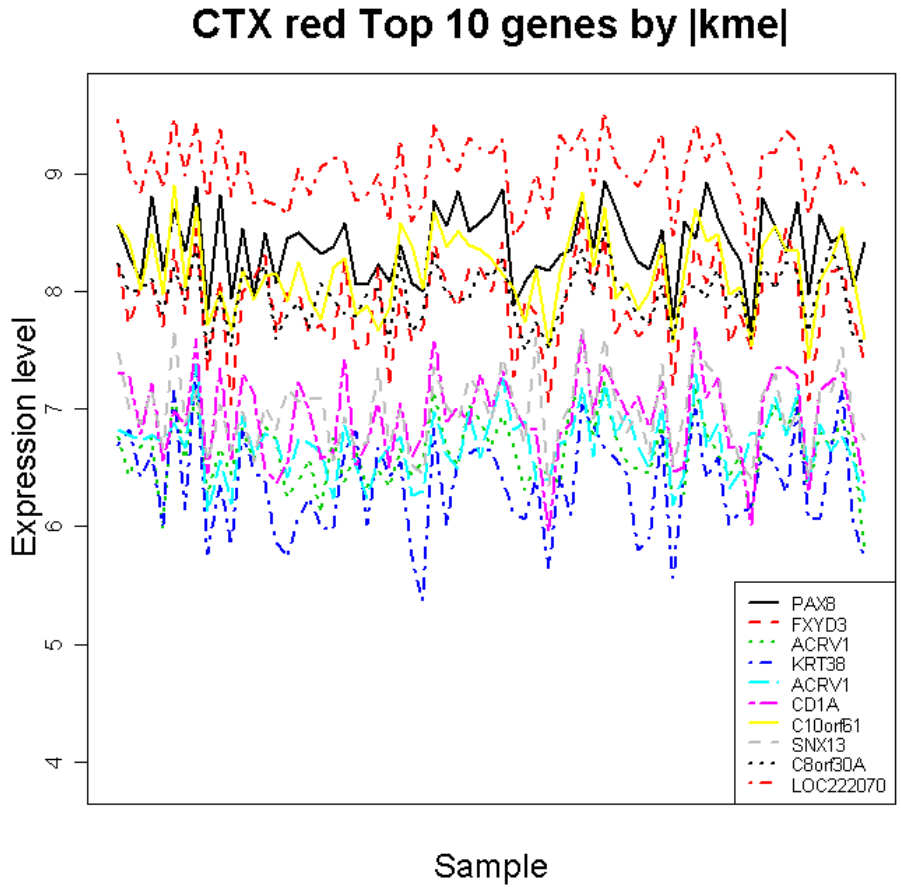
CTX red Top 10 genes by |kme|
Expression level
Sample
PAX8
FXYD3
ACRV1
KRT38
ACRV1
CD1A
C10orf61
SNX13
C8orf30A
LOC222070

Figure S2

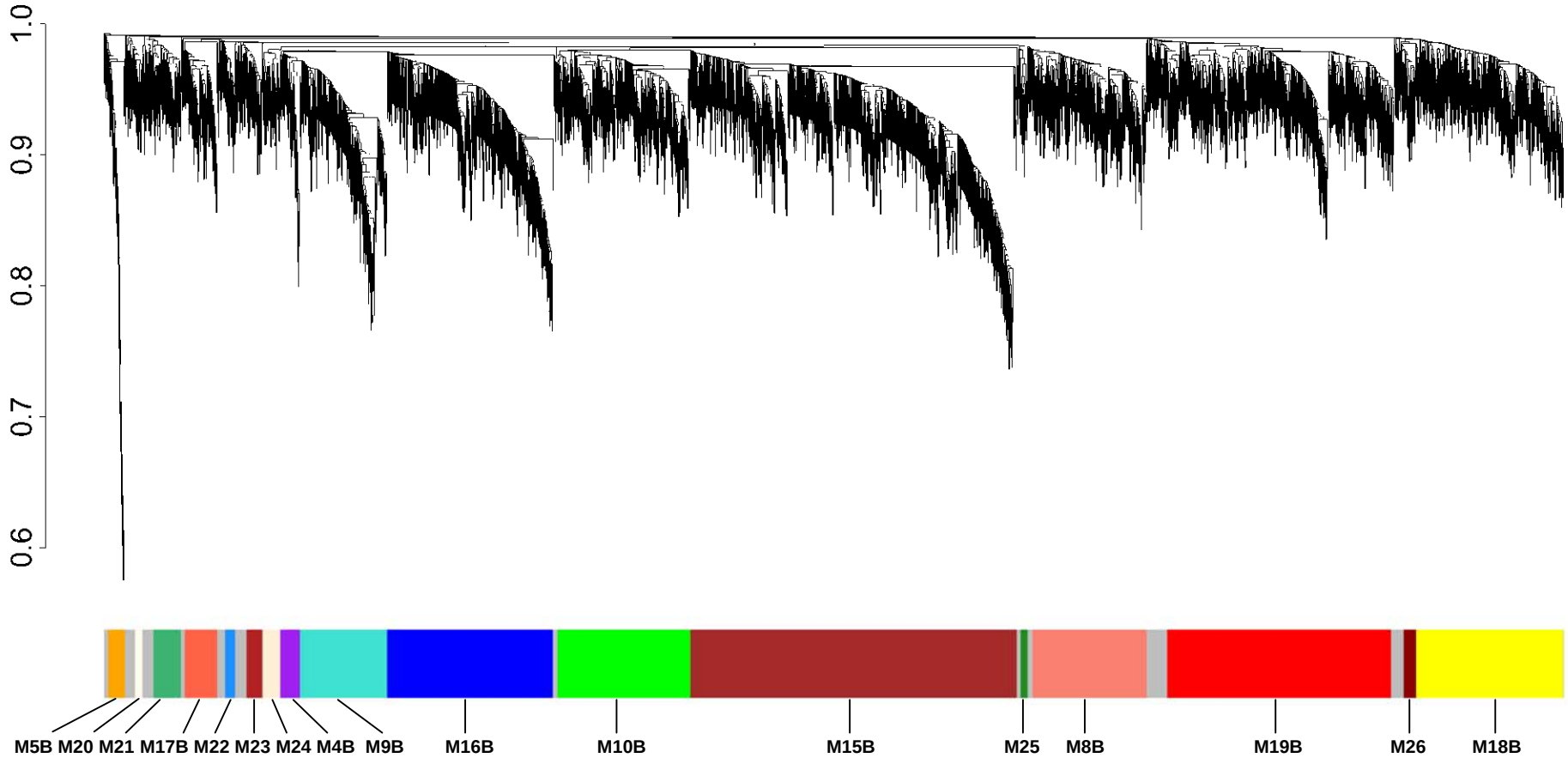
Cortex (U95)
1.0
0.9
0.8
0.7
0.6
M5B M20 M21 M17B M22 M23 M24 M4B M9B M16B M10B M15B M25 M8B M19B M26 M18B

Figure S2T

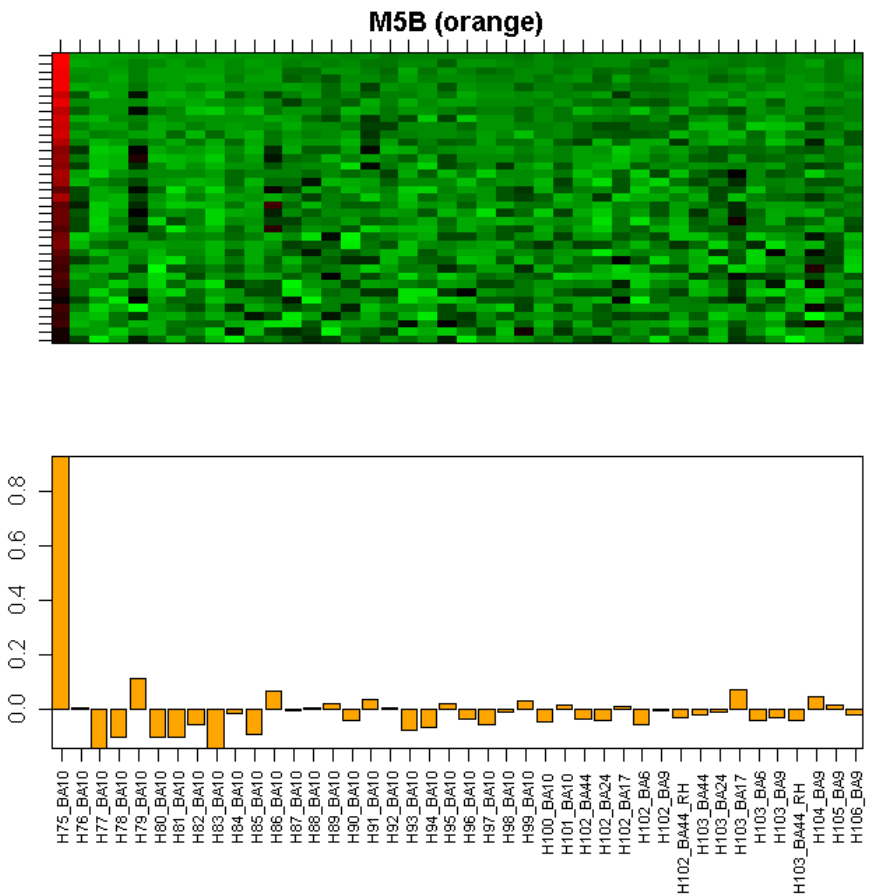
M5B (orange)
0.0
0.2
0.4
0.6
0.8
H75_BA10
H76_BA10
H77_BA10
H78_BA10
H79_BA10
H80_BA10
H81_BA10
H82_BA10
H83_BA10
H84_BA10
H85_BA10
H86_BA10
H87_BA10
H88_BA10
H89_BA10
H90_BA10
H91_BA10
H92_BA10
H93_BA10
H94_BA10
H95_BA10
H96_BA10
H97_BA10
H98_BA10
H99_BA10
H100_BA10
H101_BA10
H102_BA44
H102_BA24
H102_BA17
H102_BA6
H102_BA9
H102_BA44_RH
H103_BA44
H103_BA24
H103_BA17
H103_BA6
H103_BA9
H103_BA44_RH
H104_BA9
H105_BA9
H106_BA9

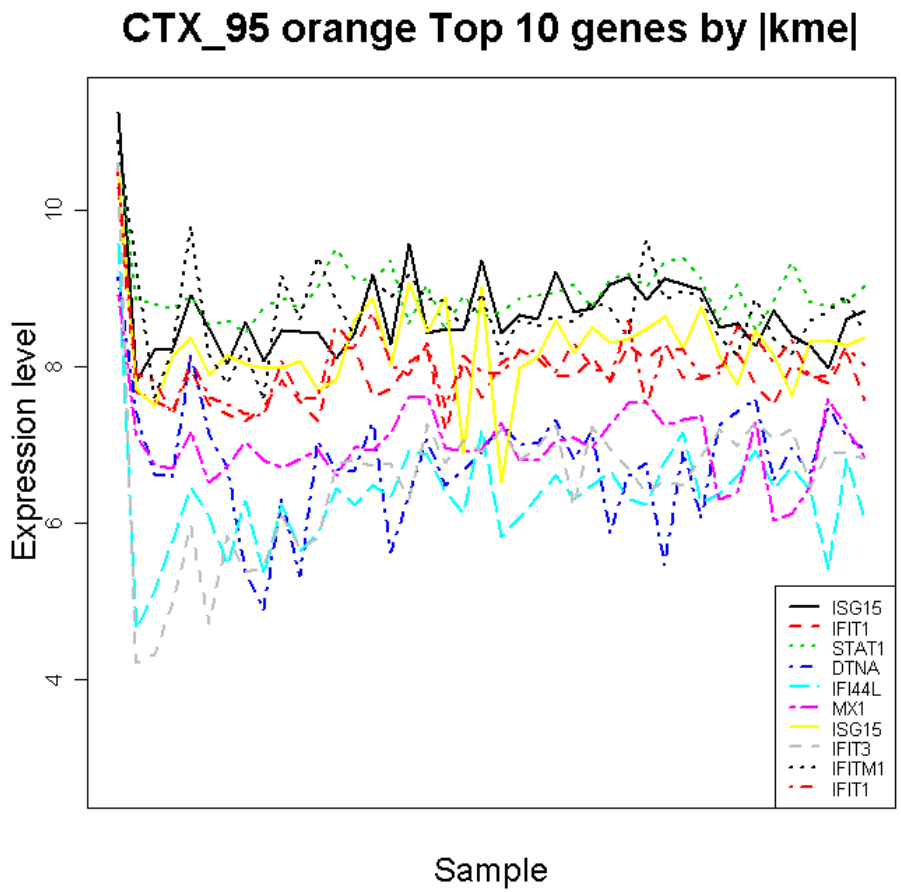
CTX_95 orange Top 10 genes by |kme|
Expression level
4
6
8
10
Sample
ISG15
IFIT1
STAT1
DTNA
IFI44L
MX1
ISG15
IFIT3
IFITM1
IFIT1

Figure S2U

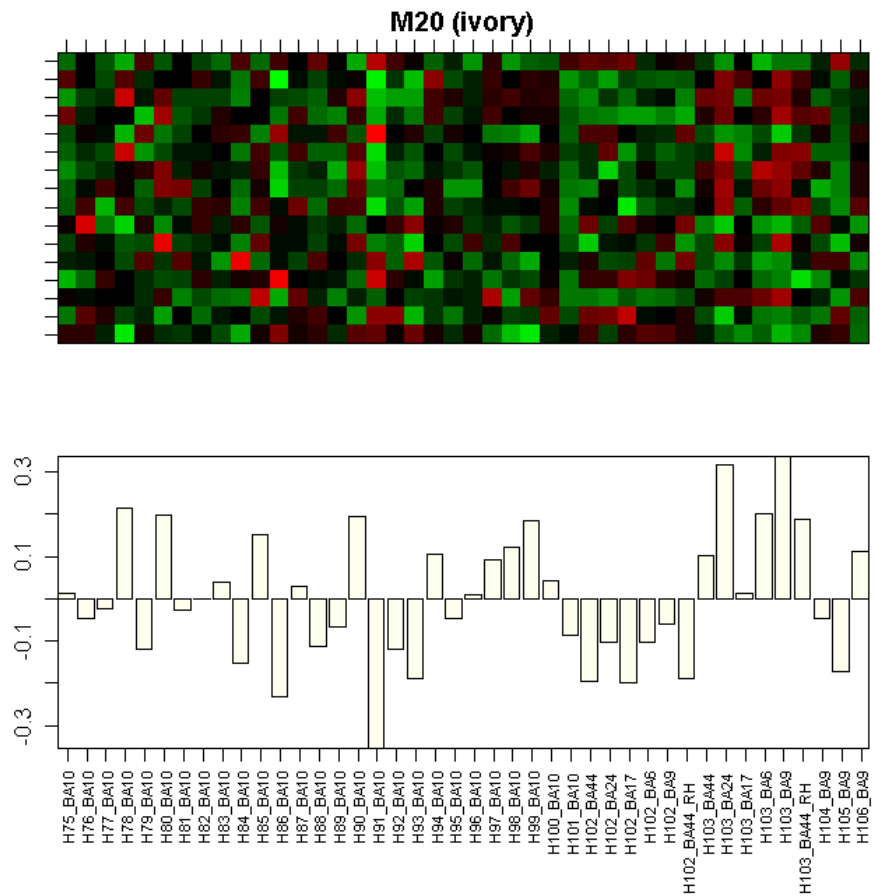
M20 (ivory)
0.3
0.1
-0.1
-0.3
H75_BA10
H76_BA10
H77_BA10
H78_BA10
H79_BA10
H80_BA10
H81_BA10
H82_BA10
H83_BA10
H84_BA10
H85_BA10
H86_BA10
H87_BA10
H88_BA10
H89_BA10
H90_BA10
H91_BA10
H92_BA10
H93_BA10
H94_BA10
H95_BA10
H96_BA10
H97_BA10
H98_BA10
H99_BA10
H100_BA10
H101_BA10
H102_BA44
H102_BA24
H102_BA17
H102_BA6
H102_BA9
H102_BA44_RH
H103_BA44
H103_BA24
H103_BA17
H103_BA6
H103_BA9
H103_BA44_RH
H104_BA9
H105_BA9
H106_BA9

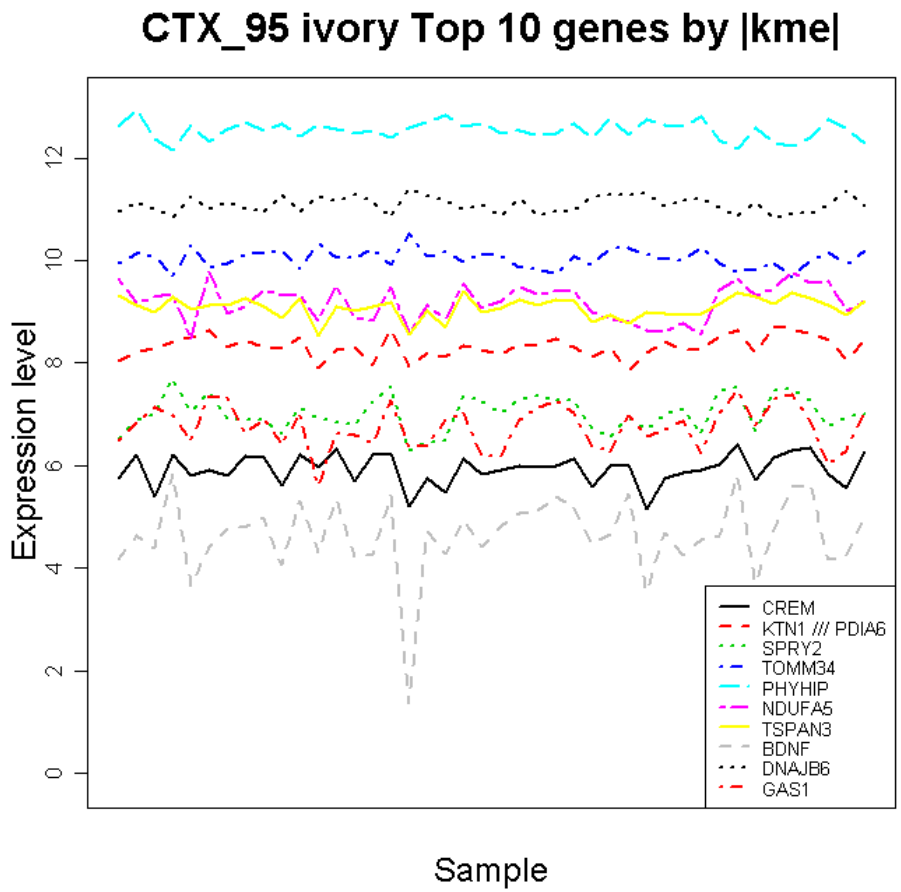
CTX_95 ivory Top 10 genes by |kme|
Expression level
0
2
4
6
8
10
12
Sample
CREM
KTN1 /// PDIA6
SPRY2
TOMM34
PHYHIP
NDUFA5
TSPAN3
BDNF
DNAJB6
GAS1

Figure S2V

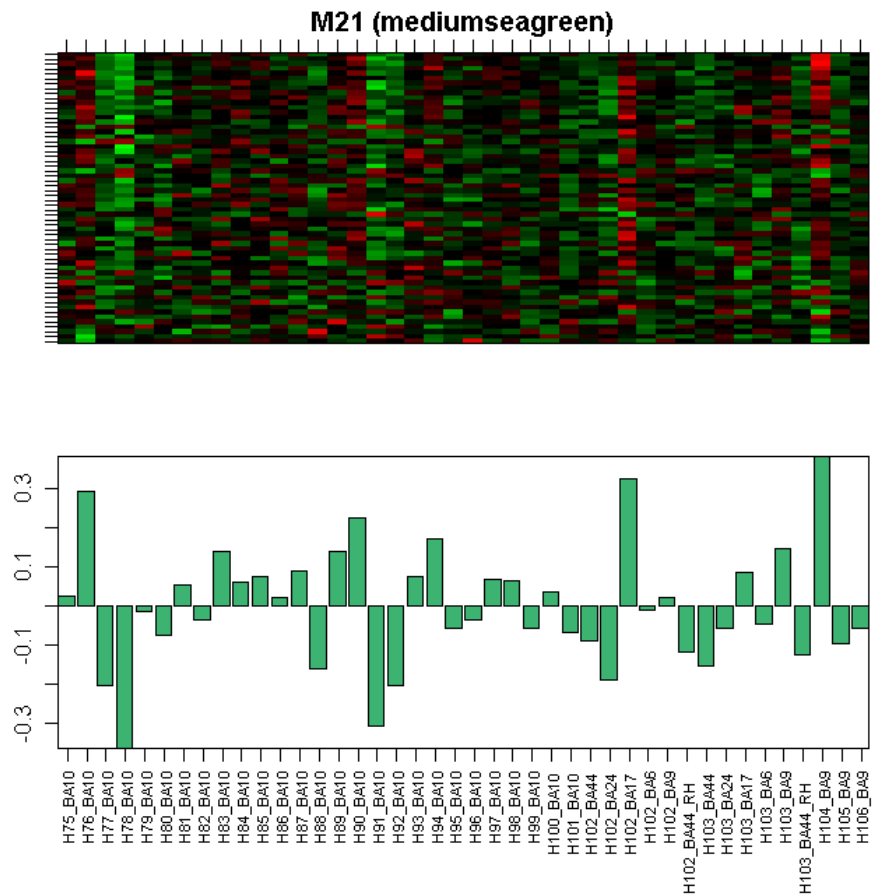
M21 (mediumseagreen)
0.3
0.1
-0.1
-0.3
H75_BA10
H76_BA10
H77_BA10
H78_BA10
H79_BA10
H80_BA10
H81_BA10
H82_BA10
H83_BA10
H84_BA10
H85_BA10
H86_BA10
H87_BA10
H88_BA10
H89_BA10
H90_BA10
H91_BA10
H92_BA10
H93_BA10
H94_BA10
H95_BA10
H96_BA10
H97_BA10
H98_BA10
H99_BA10
H100_BA10
H101_BA10
H102_BA44
H102_BA24
H102_BA17
H102_BA6
H102_BA9
H102_BA44_RH
H103_BA44
H103_BA24
H103_BA17
H103_BA6
H103_BA9
H103_BA44_RH
H104_BA9
H105_BA9
H106_BA9

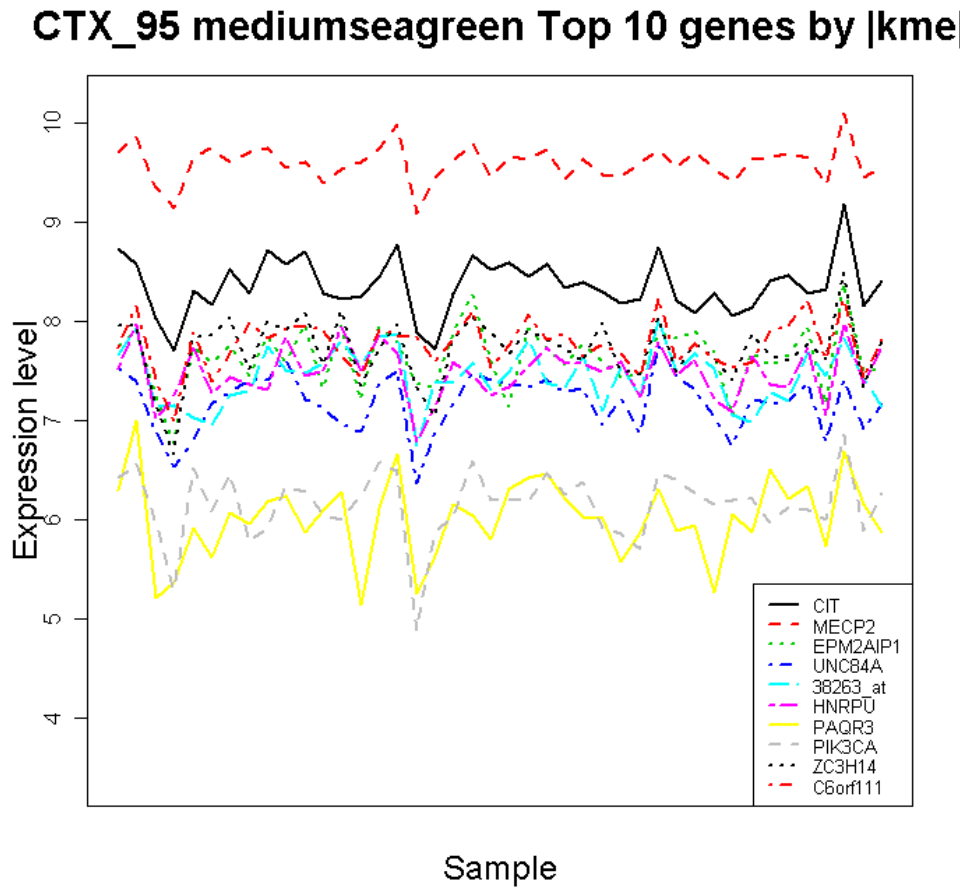
CTX_95 mediumseagreen Top 10 genes by |kme|
Expression level
4
5
6
7
8
9
10
Sample
CIT
MECP2
EPM2AIP1
UNC84A
38263_at
HNRPU
PAQR3
PIK3CA
ZC3H14
C6orf111

Figure S2W

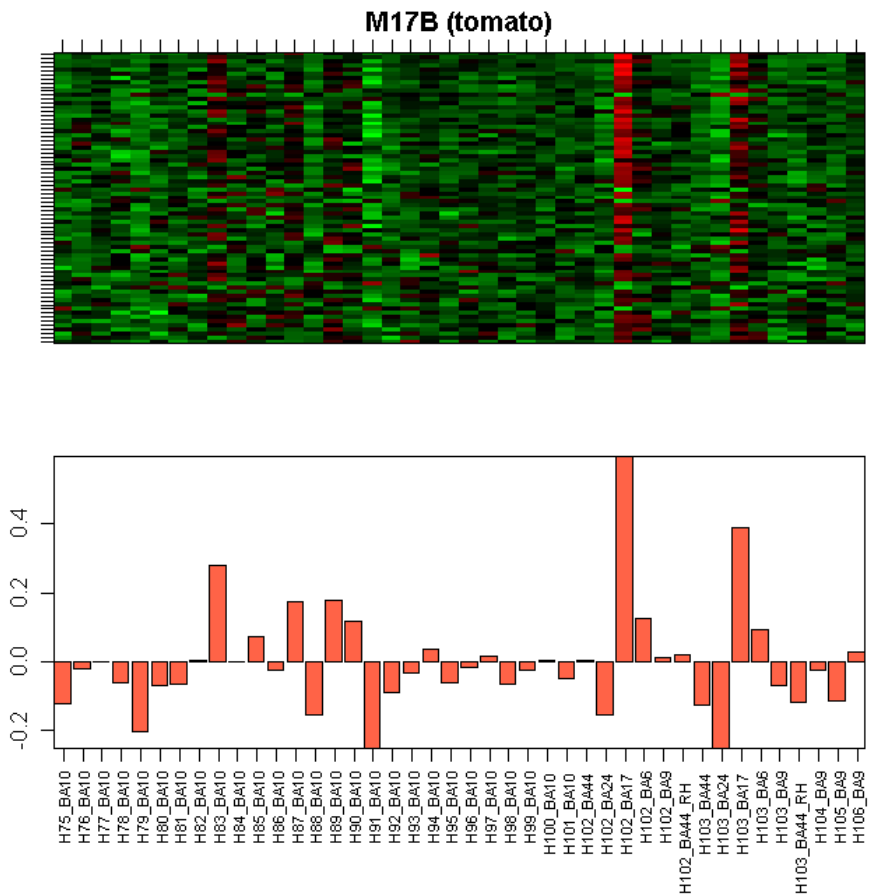
M17B (tomato)
0.4
0.2
0.0
-0.2
H75_BA10
H76_BA10
H77_BA10
H78_BA10
H79_BA10
H80_BA10
H81_BA10
H82_BA10
H83_BA10
H84_BA10
H85_BA10
H86_BA10
H87_BA10
H88_BA10
H89_BA10
H90_BA10
H91_BA10
H92_BA10
H93_BA10
H94_BA10
H95_BA10
H96_BA10
H97_BA10
H98_BA10
H99_BA10
H100_BA10
H101_BA10
H102_BA44
H102_BA24
H102_BA17
H102_BA6
H102_BA9
H102_BA44_RH
H103_BA44
H103_BA24
H103_BA17
H103_BA6
H103_BA9
H103_BA44_RH
H104_BA9
H105_BA9
H106_BA9

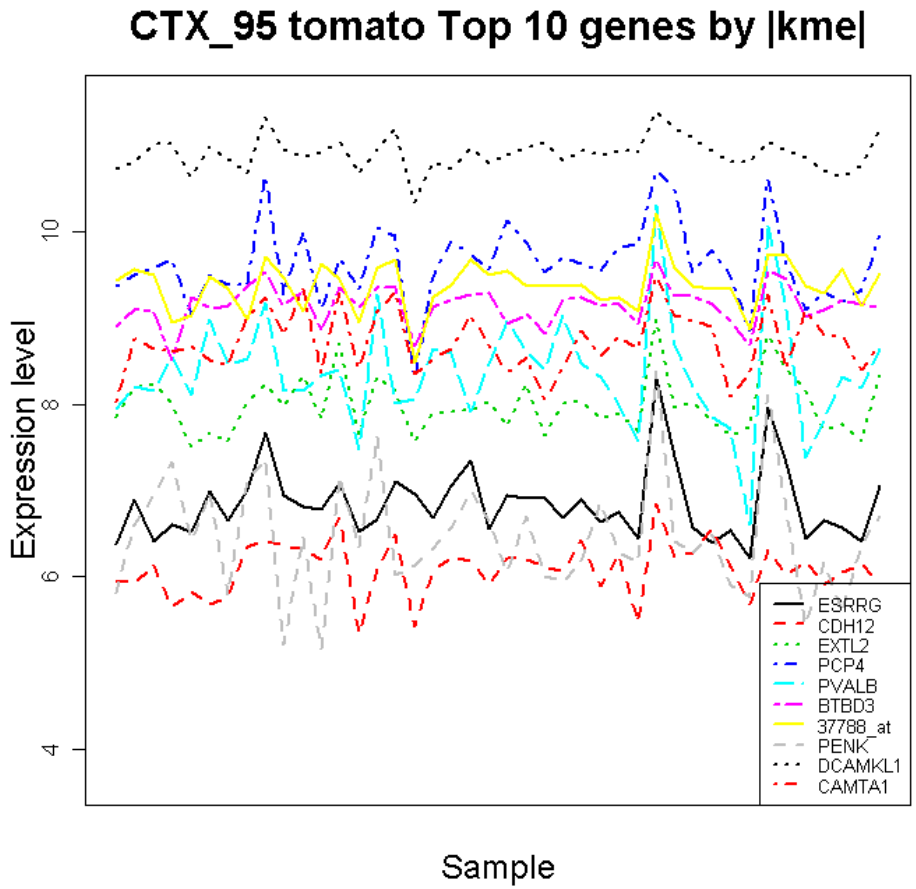
CTX_95 tomato Top 10 genes by |kme|
Expression level
4
6
8
10
Sample
ESRRG
CDH12
EXTL2
PCP4
PVALB
BTBD3
37788_at
PENK
DCAMKL1
CAMTA1

Figure S2X

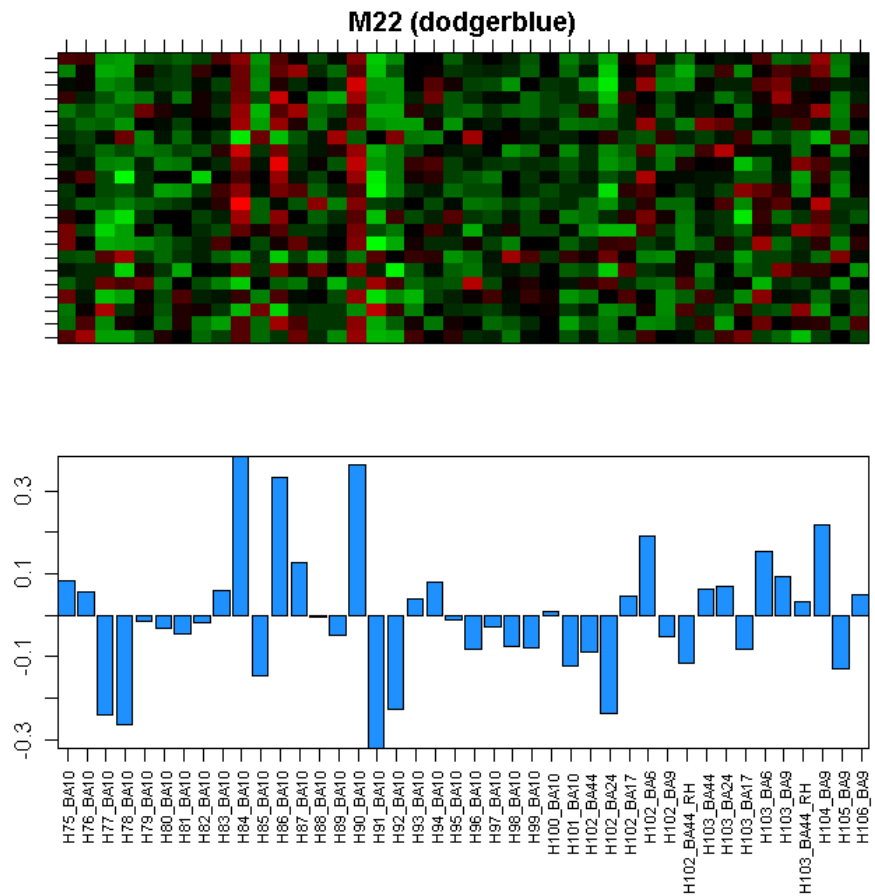
M22 (dodgerblue)
0.3
0.1
-0.1
-0.3
H75_BA10
H76_BA10
H77_BA10
H78_BA10
H79_BA10
H80_BA10
H81_BA10
H82_BA10
H83_BA10
H84_BA10
H85_BA10
H86_BA10
H87_BA10
H88_BA10
H89_BA10
H90_BA10
H91_BA10
H92_BA10
H93_BA10
H94_BA10
H95_BA10
H96_BA10
H97_BA10
H98_BA10
H99_BA10
H100_BA10
H101_BA10
H102_BA44
H102_BA24
H102_BA17
H102_BA6
H102_BA9
H102_BA44_RH
H103_BA44
H103_BA24
H103_BA17
H103_BA6
H103_BA9
H103_BA44_RH
H104_BA9
H105_BA9
H106_BA9

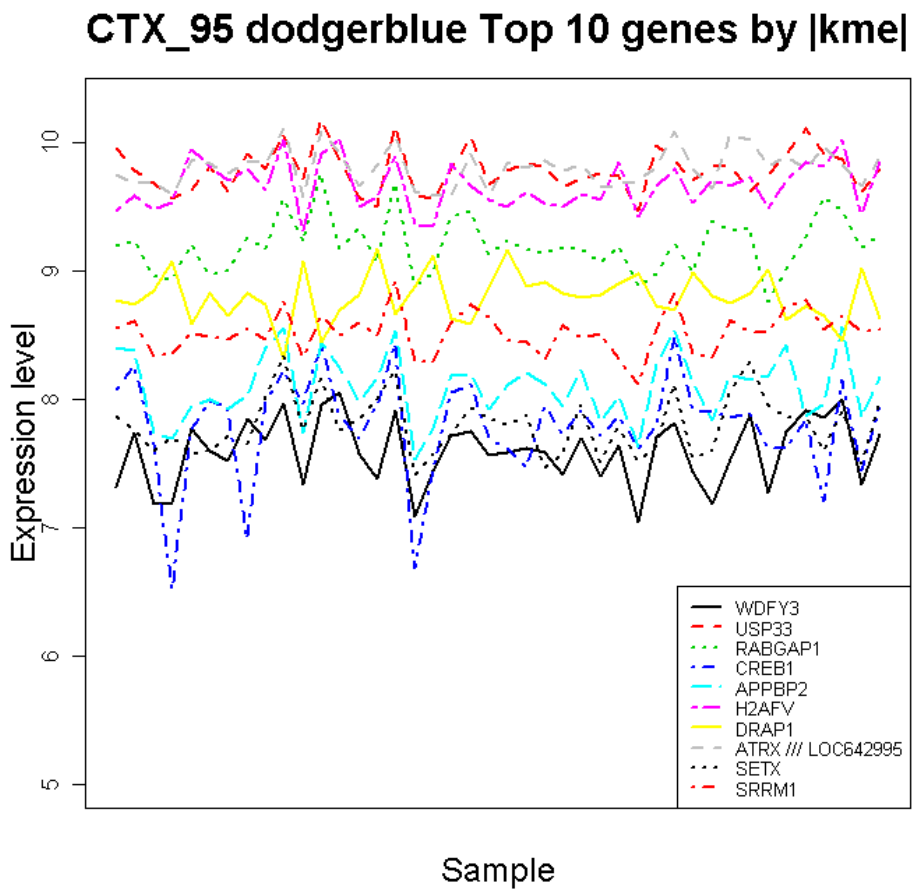
CTX_95 dodgerblue Top 10 genes by |kme|
Expression level
5
6
7
8
9
10
Sample
WDFY3
USP33
RABGAP1
CREB1
APPBP2
H2AFV
DRAP1
ATRX /// LOC642995
SETX
SRRM1

Figure S2Y

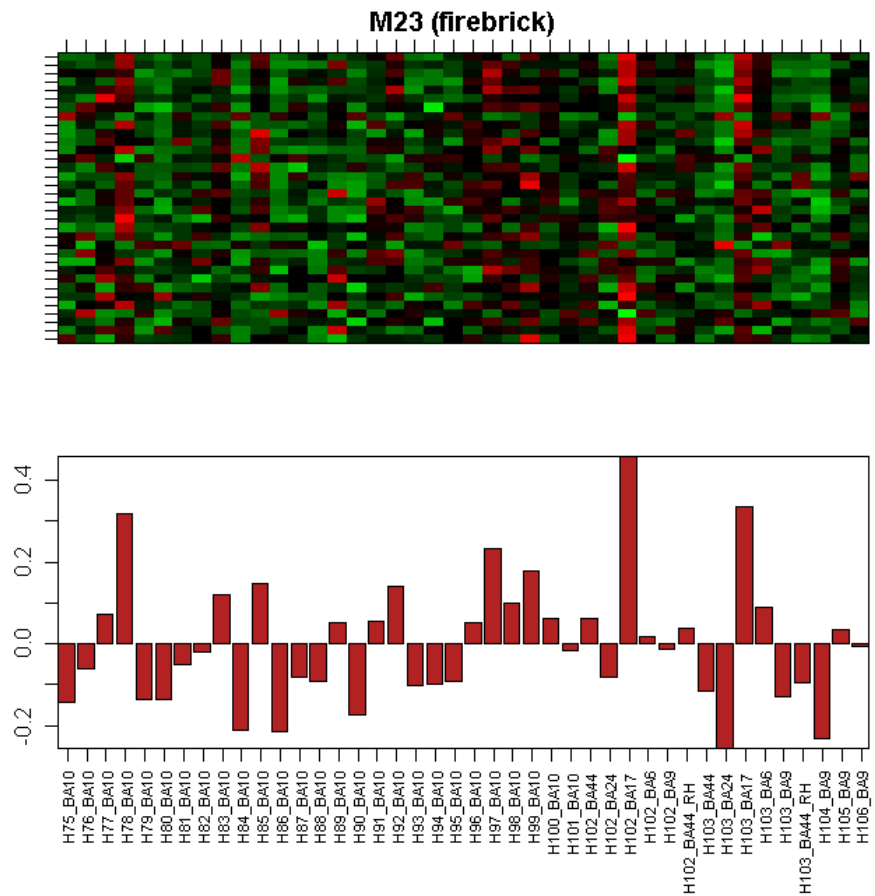
M23 (firebrick)
0.4
0.2
0.0
-0.2
H75_BA10
H76_BA10
H77_BA10
H78_BA10
H79_BA10
H80_BA10
H81_BA10
H82_BA10
H83_BA10
H84_BA10
H85_BA10
H86_BA10
H87_BA10
H88_BA10
H89_BA10
H90_BA10
H91_BA10
H92_BA10
H93_BA10
H94_BA10
H95_BA10
H96_BA10
H97_BA10
H98_BA10
H99_BA10
H100_BA10
H101_BA10
H102_BA44
H102_BA24
H102_BA17
H102_BA6
H102_BA9
H102_BA44_RH
H103_BA44
H103_BA24
H103_BA17
H103_BA6
H103_BA9
H103_BA44_RH
H104_BA9
H105_BA9
H106_BA9

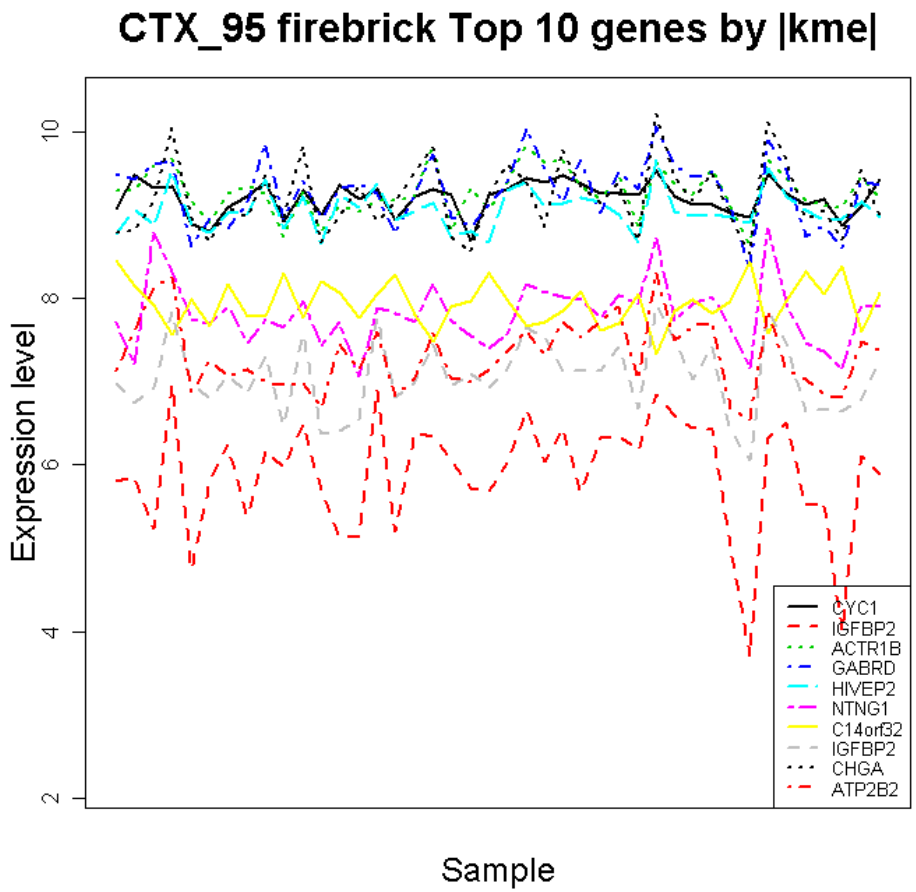
CTX_95 firebrick Top 10 genes by |kme|
Expression level
2
4
6
8
10
Sample
GYC1
IGFBP2
ACTR1B
GABRD
HIVEP2
NTNG1
C14orf32
IGFBP2
CHGA
ATP2B2

Figure S2Z

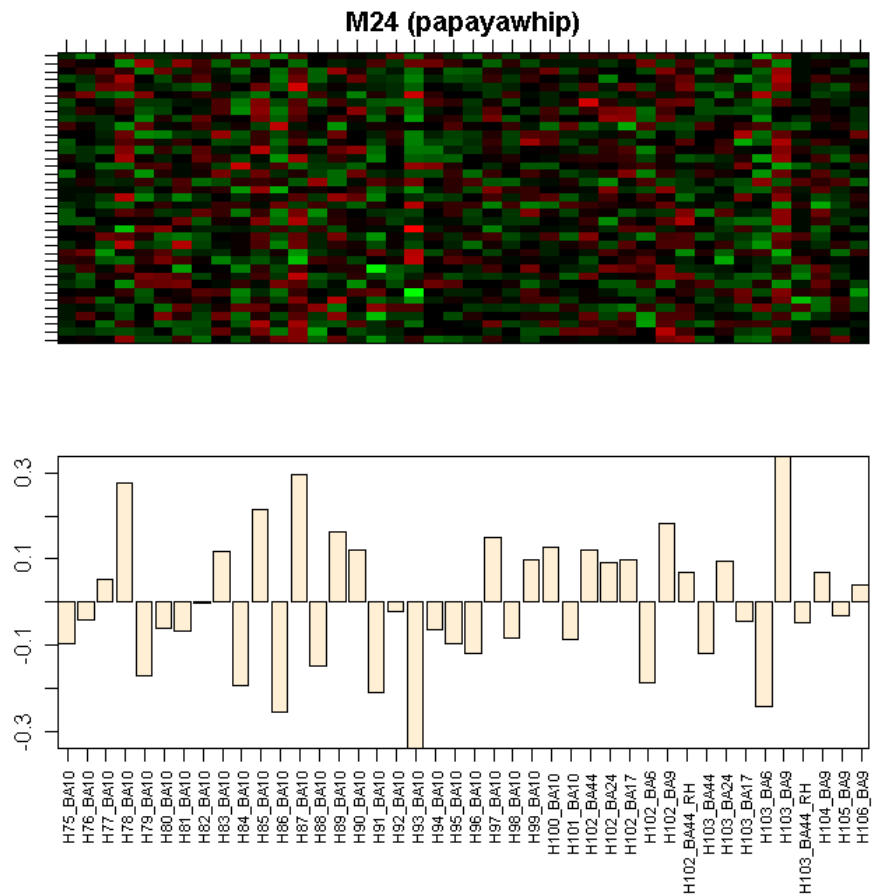
M24 (papayawhip)
0.3
0.1
-0.1
-0.3
H75_BA10
H76_BA10
H77_BA10
H78_BA10
H79_BA10
H80_BA10
H81_BA10
H82_BA10
H83_BA10
H84_BA10
H85_BA10
H86_BA10
H87_BA10
H88_BA10
H89_BA10
H90_BA10
H91_BA10
H92_BA10
H93_BA10
H94_BA10
H95_BA10
H96_BA10
H97_BA10
H98_BA10
H99_BA10
H100_BA10
H101_BA10
H102_BA44
H102_BA24
H102_BA17
H102_BA6
H102_BA9
H102_BA44_RH
H103_BA44
H103_BA24
H103_BA17
H103_BA6
H103_BA9
H103_BA44_RH
H104_BA9
H105_BA9
H106_BA9

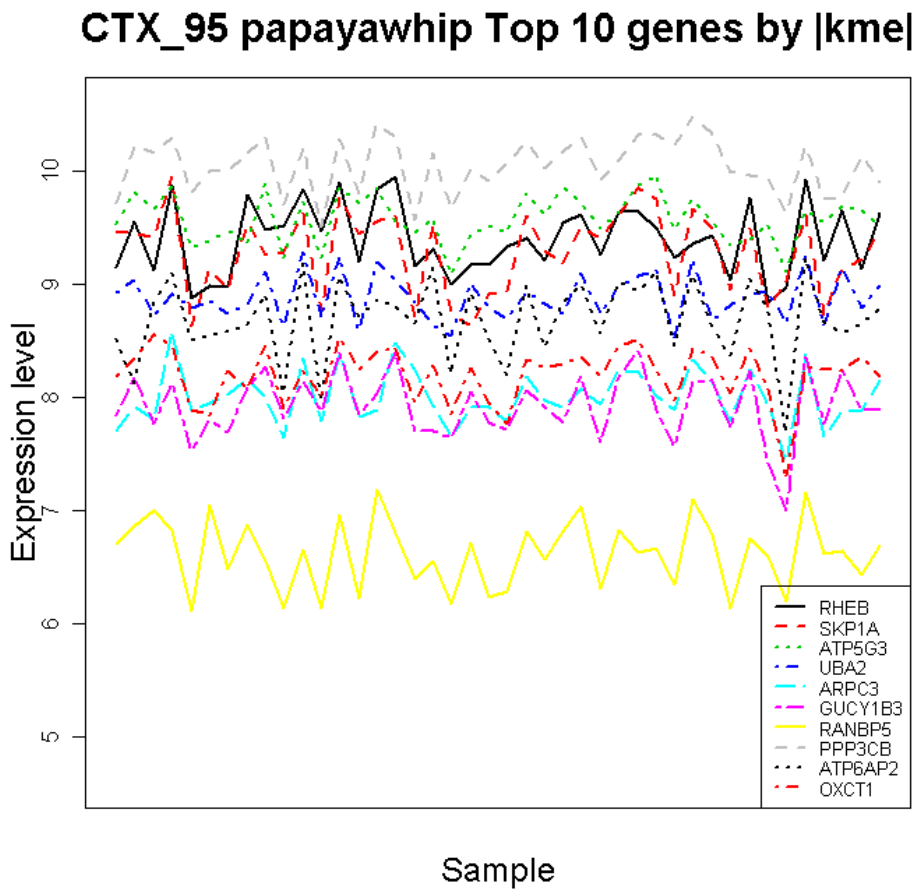
CTX_95 papayawhip Top 10 genes by |kme|
Expression level
5
6
7
8
9
10
Sample
RHEB
SKP1A
ATP5G3
UBA2
ARPC3
GUCY1B3
RANBP5
PPP3CB
ATP6AP2
OXCT1

Figure S2AA

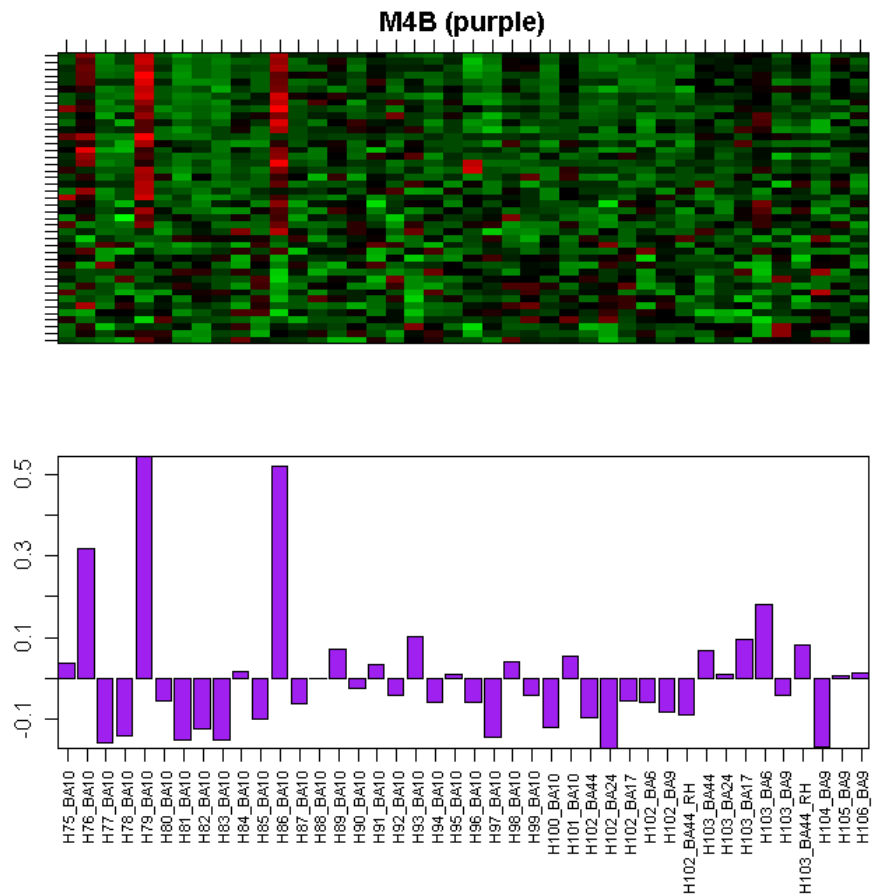
M4B (purple)
0.5
0.3
0.1
-0.1
H75_BA10
H76_BA10
H77_BA10
H78_BA10
H79_BA10
H80_BA10
H81_BA10
H82_BA10
H83_BA10
H84_BA10
H85_BA10
H86_BA10
H87_BA10
H88_BA10
H89_BA10
H90_BA10
H91_BA10
H92_BA10
H93_BA10
H94_BA10
H95_BA10
H96_BA10
H97_BA10
H98_BA10
H99_BA10
H100_BA10
H101_BA10
H102_BA44
H102_BA24
H102_BA17
H102_BA6
H102_BA9
H102_BA44_RH
H103_BA44
H103_BA24
H103_BA17
H103_BA6
H103_BA9
H103_BA44_RH
H104_BA9
H105_BA9
H106_BA9

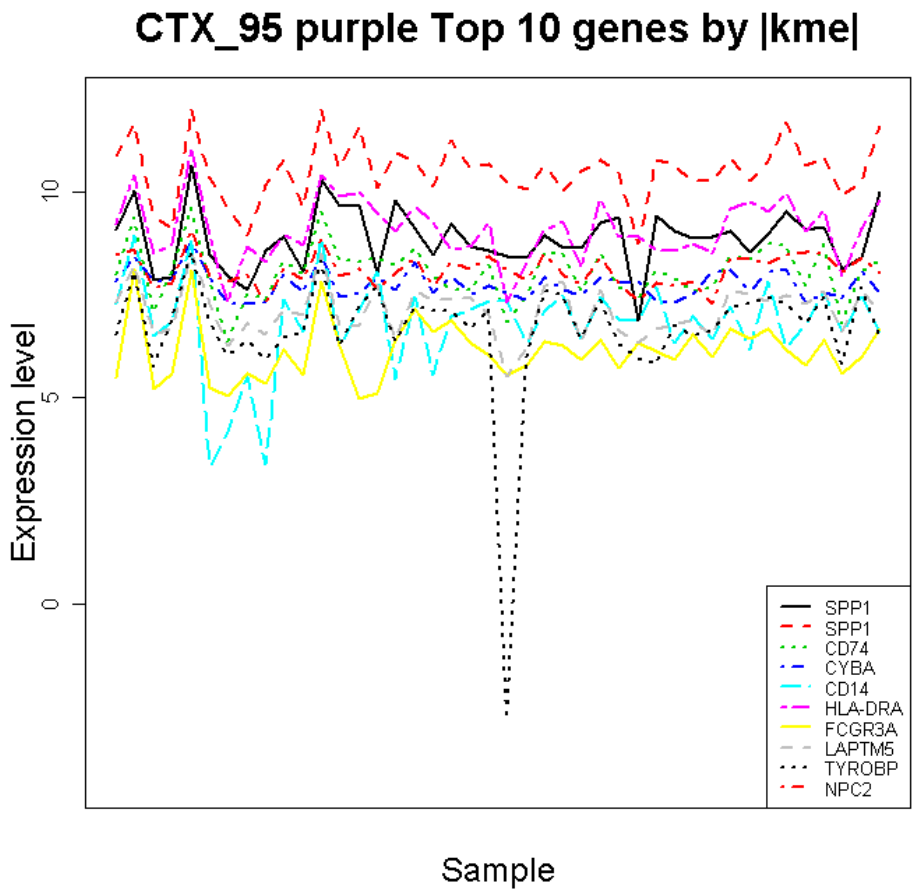
CTX_95 purple Top 10 genes by |kme|
Expression level
0
5
10
Sample
SPP1
SPP1
CD74
CYBA
CD14
HLA-DRA
FCGR3A
LAPTM5
TYROBP
NPC2

Figure S2AB

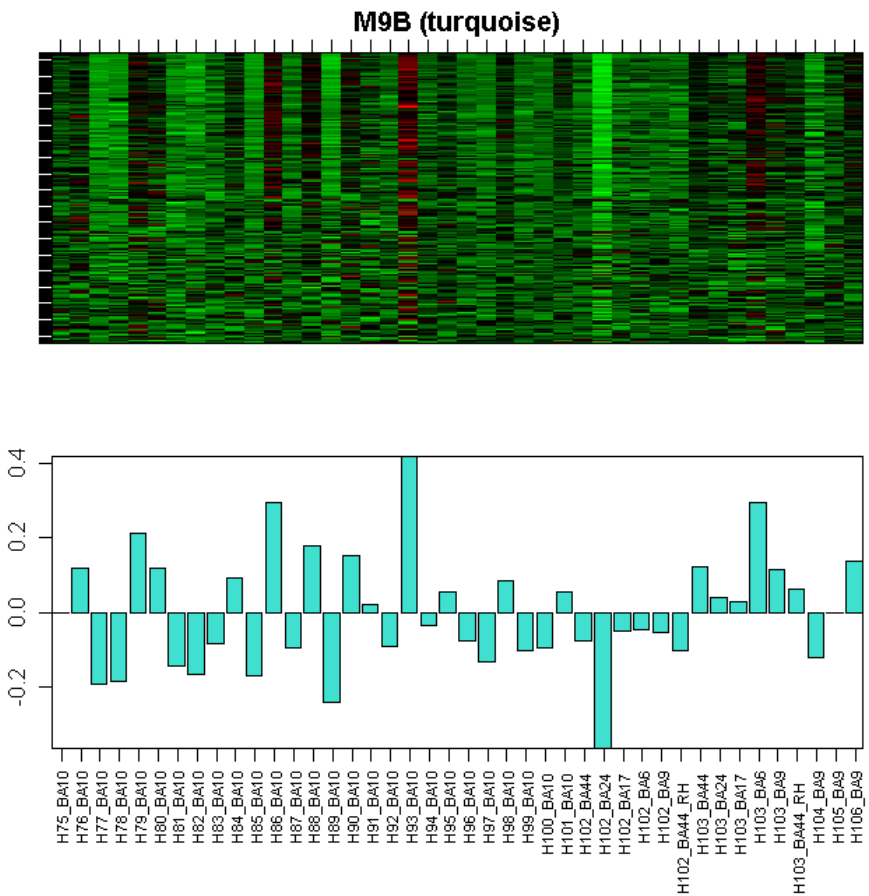
M9B (turquoise)
0.4
0.2
0.0
-0.2
H75_BA10
H76_BA10
H77_BA10
H78_BA10
H79_BA10
H80_BA10
H81_BA10
H82_BA10
H83_BA10
H84_BA10
H85_BA10
H86_BA10
H87_BA10
H88_BA10
H89_BA10
H90_BA10
H91_BA10
H92_BA10
H93_BA10
H94_BA10
H95_BA10
H96_BA10
H97_BA10
H98_BA10
H99_BA10
H100_BA10
H101_BA10
H102_BA44
H102_BA24
H102_BA17
H102_BA6
H102_BA9
H102_BA44_RH
H103_BA44
H103_BA24
H103_BA17
H103_BA6
H103_BA9
H103_BA44_RH
H104_BA9
H105_BA9
H106_BA9

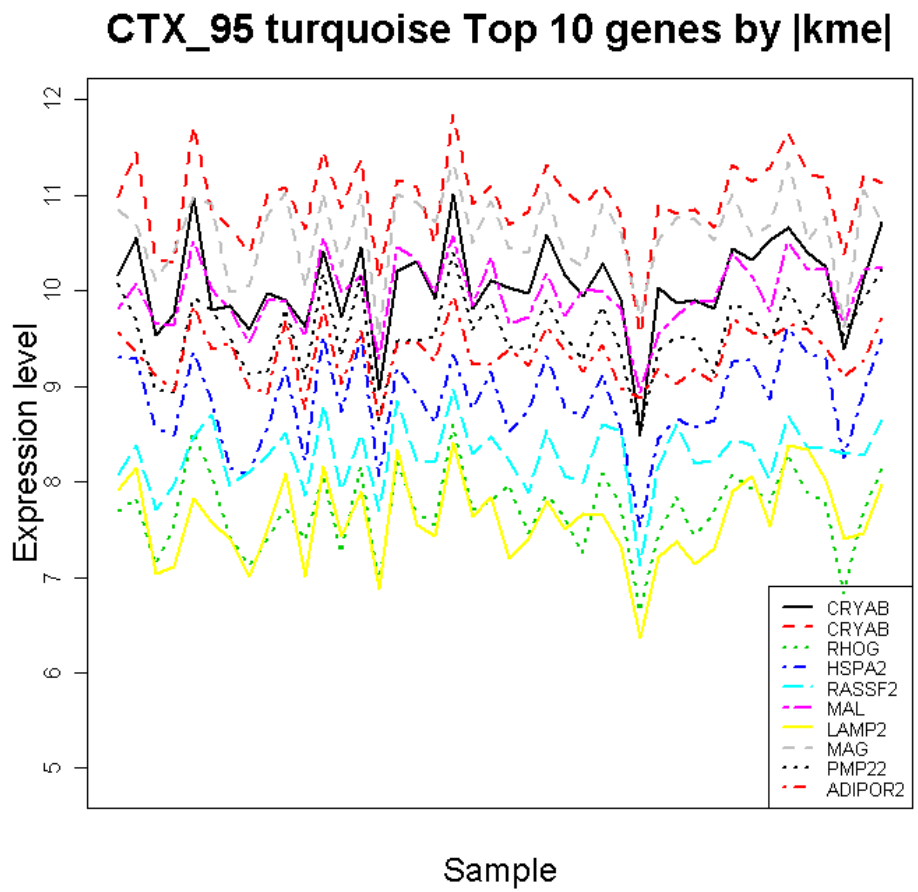
CTX_95 turquoise Top 10 genes by |kme|
Expression level
5
6
7
8
9
10
11
12
Sample
CRYAB
CRYAB
RHOG
HSPA2
RASSF2
MAL
LAMP2
MAG
PMP22
ADIPOR2

Figure S2AC

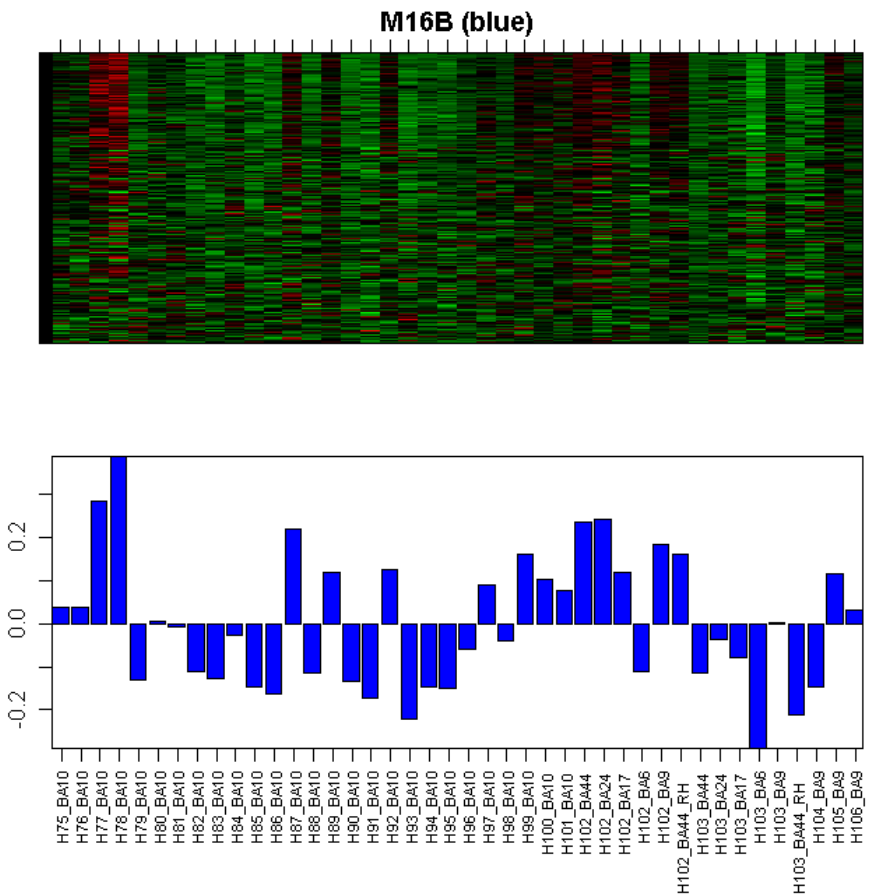
M16B (blue)
0.2
0.0
-0.2
H75_BA10
H76_BA10
H77_BA10
H78_BA10
H79_BA10
H80_BA10
H81_BA10
H82_BA10
H83_BA10
H84_BA10
H85_BA10
H86_BA10
H87_BA10
H88_BA10
H89_BA10
H90_BA10
H91_BA10
H92_BA10
H93_BA10
H94_BA10
H95_BA10
H96_BA10
H97_BA10
H98_BA10
H99_BA10
H100_BA10
H101_BA10
H102_BA44
H102_BA24
H102_BA17
H102_BA6
H102_BA9
H102_BA44_RH
H103_BA44
H103_BA24
H103_BA17
H103_BA6
H103_BA9
H103_BA44_RH
H104_BA9
H105_BA9
H106_BA9

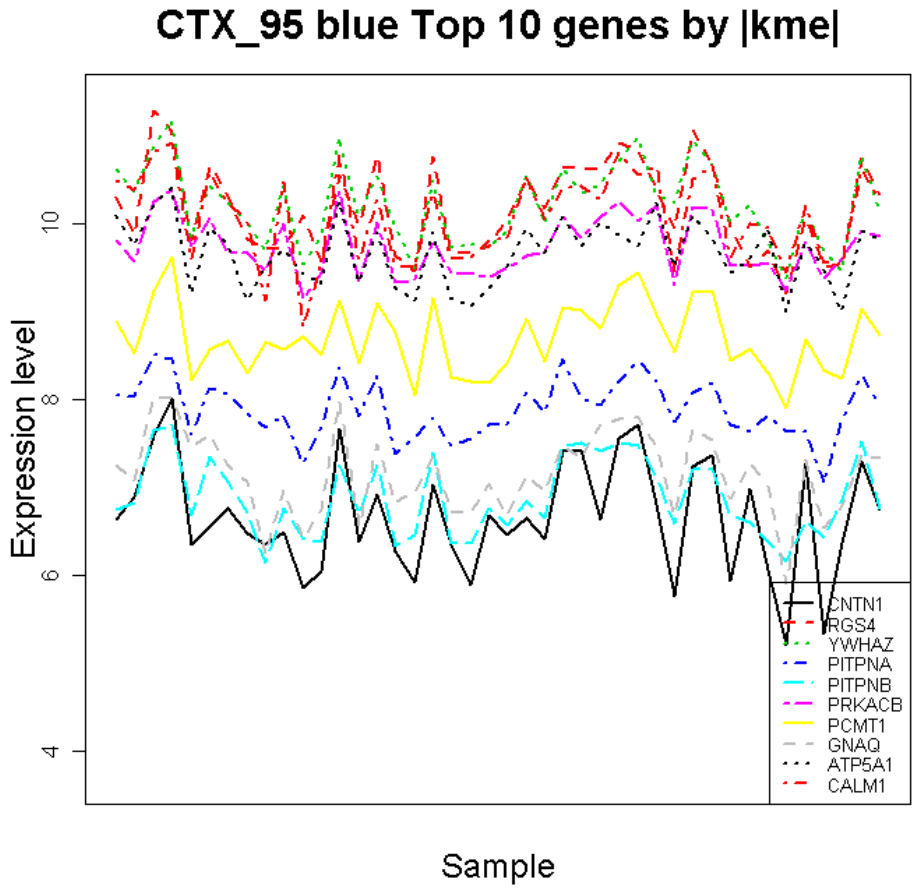
CTX_95 blue Top 10 genes by |kme|
Expression level
4
6
8
10
Sample
CNTN1
RGS4
YWHAZ
PITPNA
PITPNB
PRKACB
PCMT1
GNAQ
ATP5A1
CALM1

Figure S2AD

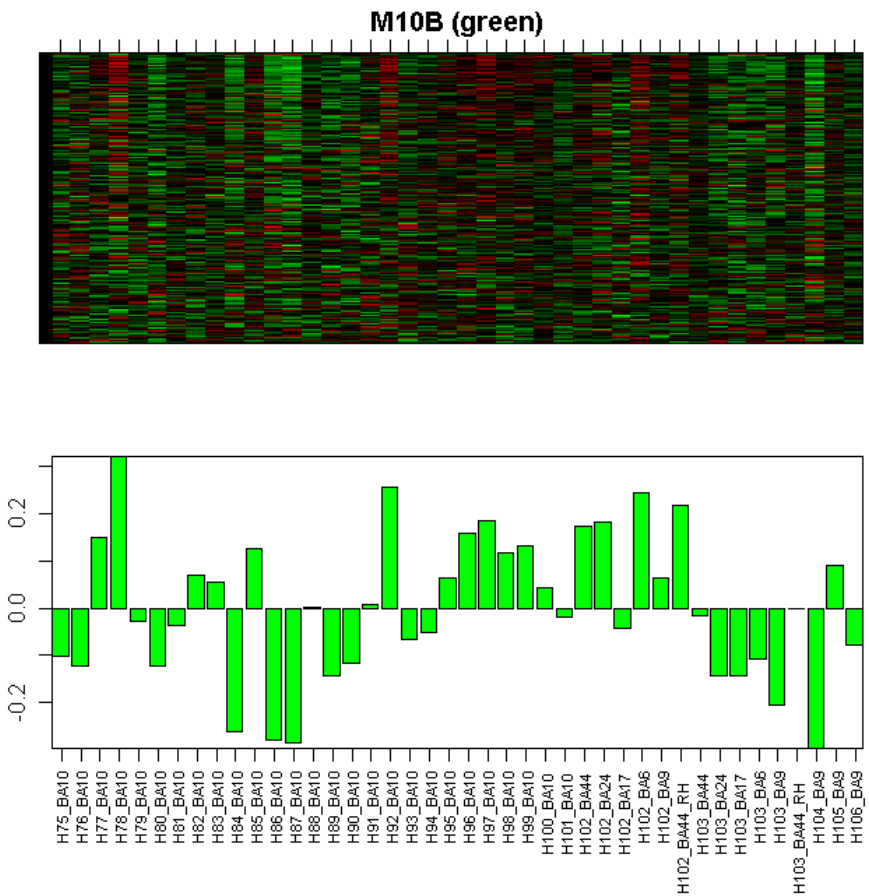
M10B (green)
0.2
0.0
-0.2
H75_BA10
H76_BA10
H77_BA10
H78_BA10
H79_BA10
H80_BA10
H81_BA10
H82_BA10
H83_BA10
H84_BA10
H85_BA10
H86_BA10
H87_BA10
H88_BA10
H89_BA10
H90_BA10
H91_BA10
H92_BA10
H93_BA10
H94_BA10
H95_BA10
H96_BA10
H97_BA10
H98_BA10
H99_BA10
H100_BA10
H101_BA10
H102_BA44
H102_BA24
H102_BA17
H102_BA6
H102_BA9
H102_BA44_RH
H103_BA44
H103_BA24
H103_BA17
H103_BA6
H103_BA9
H103_BA44_RH
H104_BA9
H105_BA9
H106_BA9

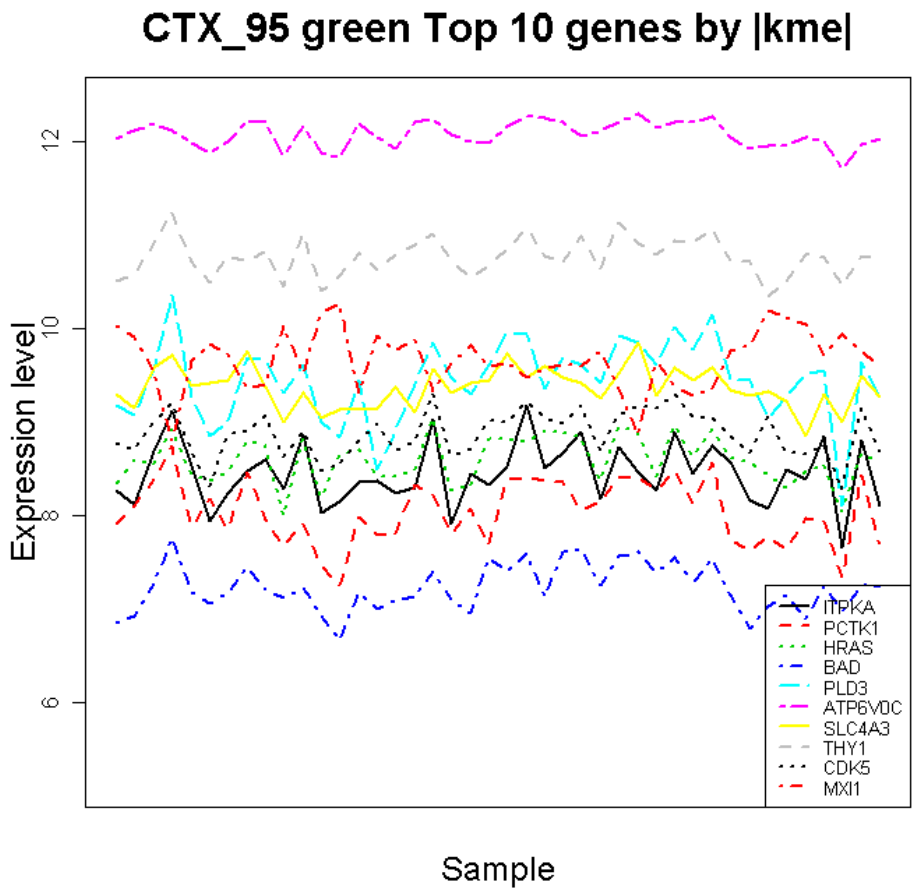
CTX_95 green Top 10 genes by |kme|
Expression level
6
8
10
12
Sample
ITPKA
PCTK1
HRAS
BAD
PLD3
ATP6V0C
SLC4A3
THY1
CDK5
MXI1

Figure S2AE

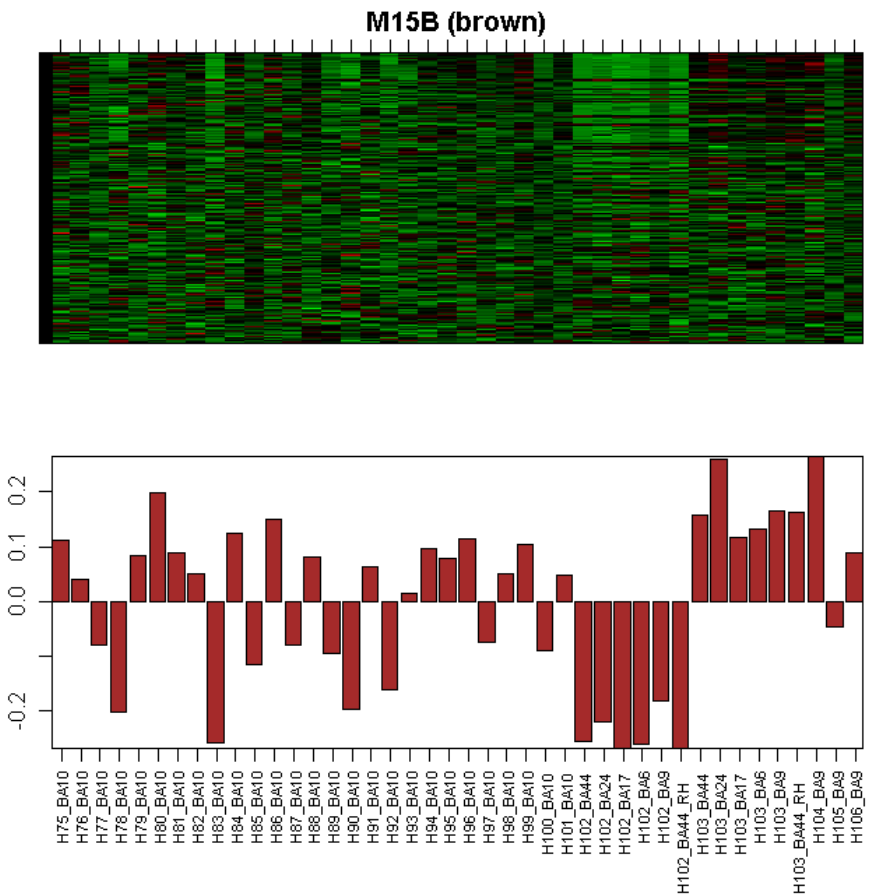
M15B (brown)
0.2
0.1
0.0
-0.2
H75_BA10
H76_BA10
H77_BA10
H78_BA10
H79_BA10
H80_BA10
H81_BA10
H82_BA10
H83_BA10
H84_BA10
H85_BA10
H86_BA10
H87_BA10
H88_BA10
H89_BA10
H90_BA10
H91_BA10
H92_BA10
H93_BA10
H94_BA10
H95_BA10
H96_BA10
H97_BA10
H98_BA10
H99_BA10
H100_BA10
H101_BA10
H102_BA44
H102_BA24
H102_BA17
H102_BA6
H102_BA9
H102_BA44_RH
H103_BA44
H103_BA24
H103_BA17
H103_BA6
H103_BA9
H103_BA44_RH
H104_BA9
H105_BA9
H106_BA9

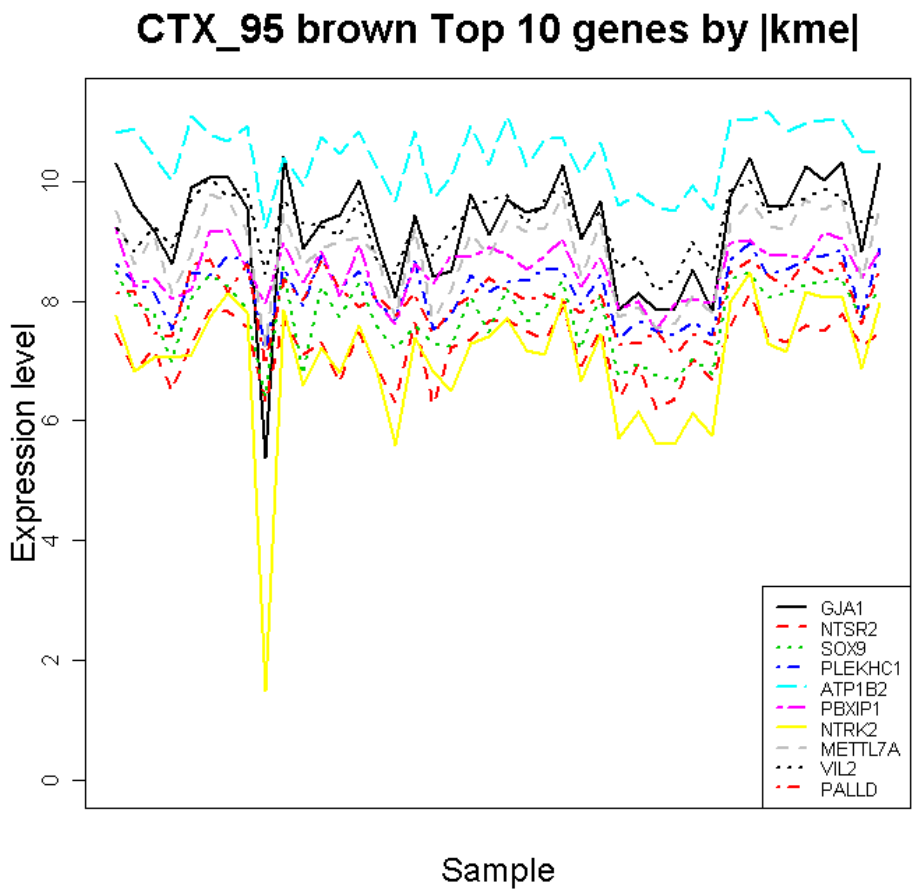
CTX_95 brown Top 10 genes by |kme|
Expression level
0
2
4
6
8
10
Sample
GJA1
NTSR2
SOX9
PLEKHC1
ATP1B2
PBXIP1
NTRK2
METTL7A
VIL2
PALLD

Figure S2AF

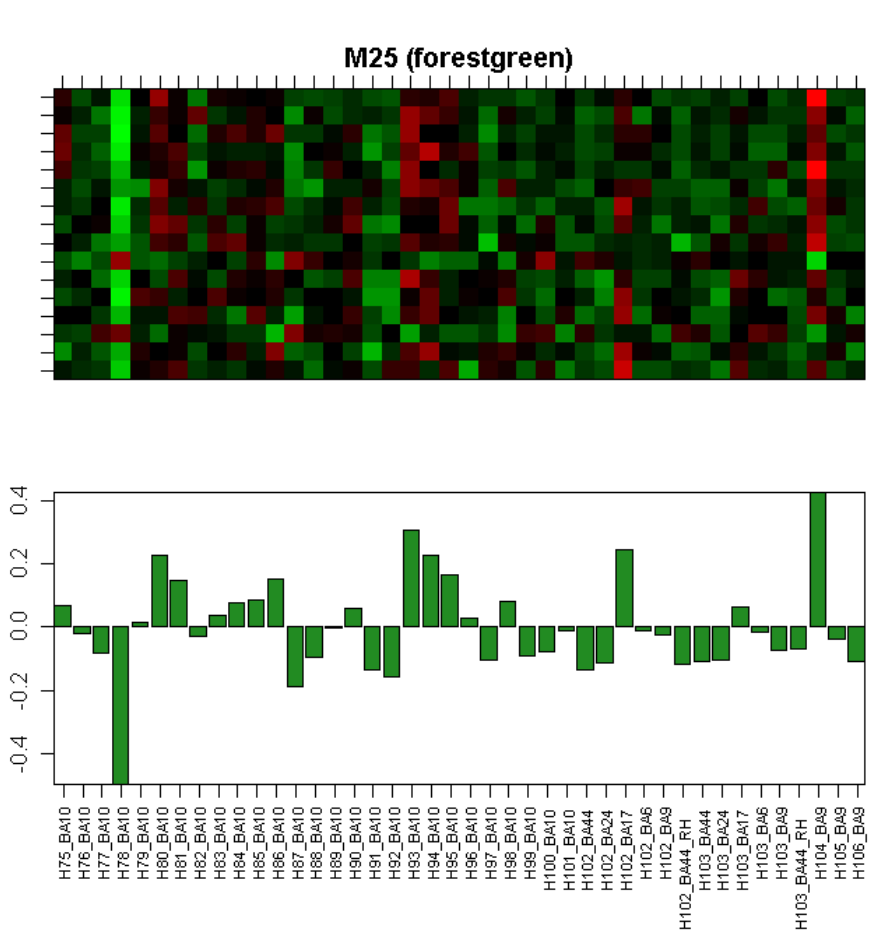
M25 (forestgreen)
0.4
0.2
0.0
-0.2
-0.4
H75_BA10
H76_BA10
H77_BA10
H78_BA10
H79_BA10
H80_BA10
H81_BA10
H82_BA10
H83_BA10
H84_BA10
H85_BA10
H86_BA10
H87_BA10
H88_BA10
H89_BA10
H90_BA10
H91_BA10
H92_BA10
H93_BA10
H94_BA10
H95_BA10
H96_BA10
H97_BA10
H98_BA10
H99_BA10
H100_BA10
H101_BA10
H102_BA44
H102_BA24
H102_BA17
H102_BA6
H102_BA9
H102_BA44_RH
H103_BA44
H103_BA24
H103_BA17
H103_BA6
H103_BA9
H103_BA44_RH
H104_BA9
H105_BA9
H106_BA9

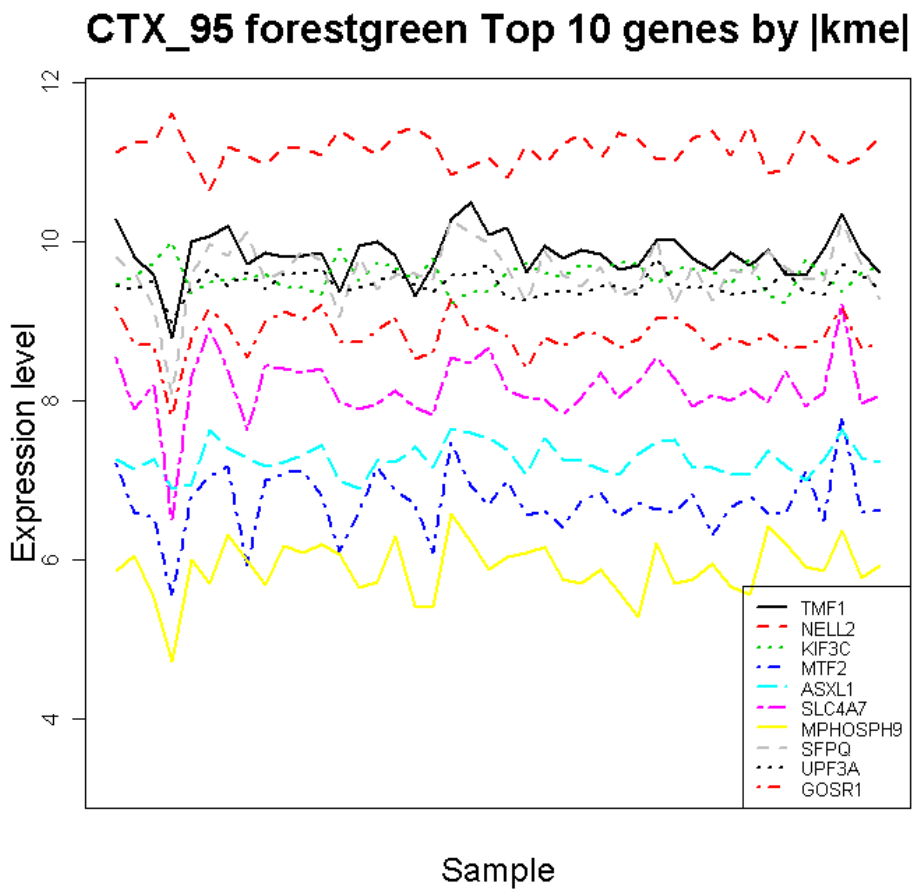
CTX_95 forestgreen Top 10 genes by |kme|
Expression level
12
10
8
6
4
Sample
TMF1
NELL2
KIF3C
MTF2
ASXL1
SLC4A7
MPHOSPH9
SFPQ
UPF3A
GOSR1

Figure S2AG

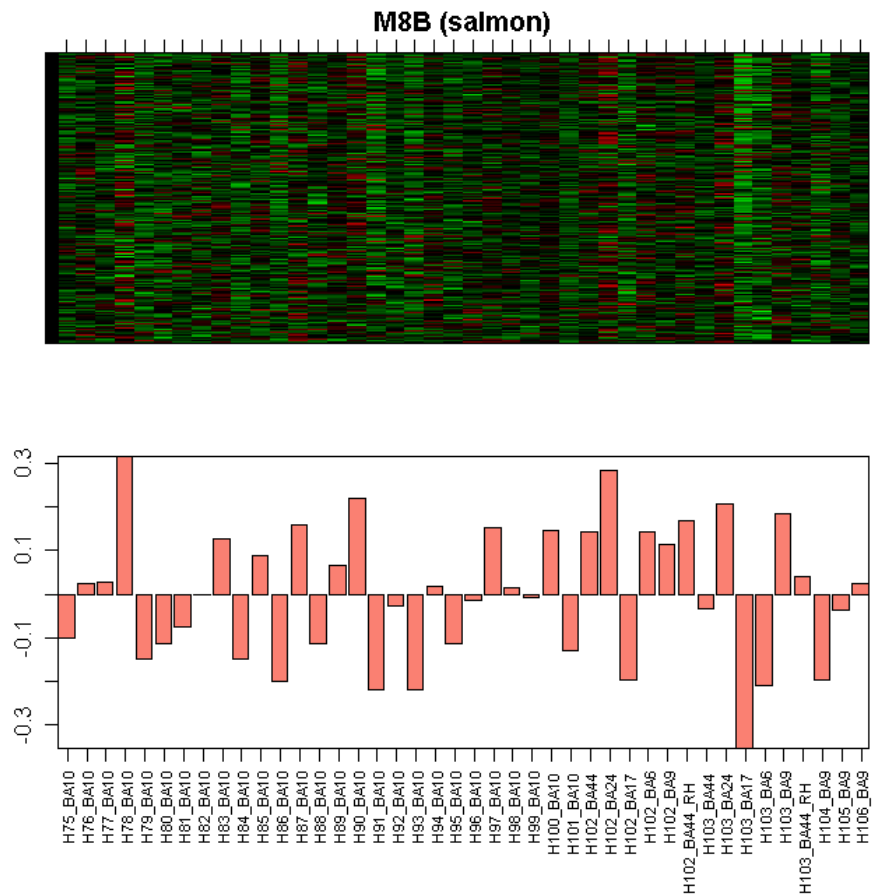
M8B (salmon)
0.3
0.1
-0.1
-0.3
H75_BA10
H76_BA10
H77_BA10
H78_BA10
H79_BA10
H80_BA10
H81_BA10
H82_BA10
H83_BA10
H84_BA10
H85_BA10
H86_BA10
H87_BA10
H88_BA10
H89_BA10
H90_BA10
H91_BA10
H92_BA10
H93_BA10
H94_BA10
H95_BA10
H96_BA10
H97_BA10
H98_BA10
H99_BA10
H100_BA10
H101_BA10
H102_BA44
H102_BA24
H102_BA17
H102_BA6
H102_BA9
H102_BA44_RH
H103_BA44
H103_BA24
H103_BA17
H103_BA6
H103_BA9
H103_BA44_RH
H104_BA9
H105_BA9
H106_BA9

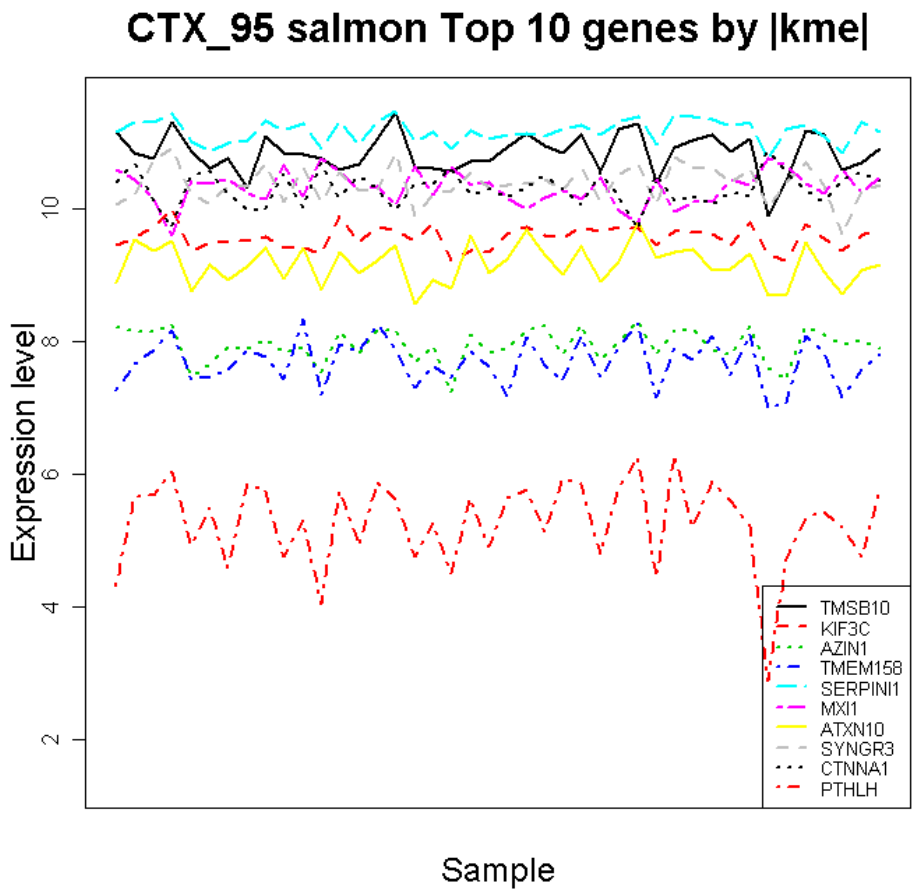
CTX_95 salmon Top 10 genes by |kme|
Expression level
2
4
6
8
10
Sample
TMSB10
KIF3C
AZIN1
TMEM158
SERPINI1
MXI1
ATXN10
SYNGR3
CTNNA1
PTHLH

Figure S2AH

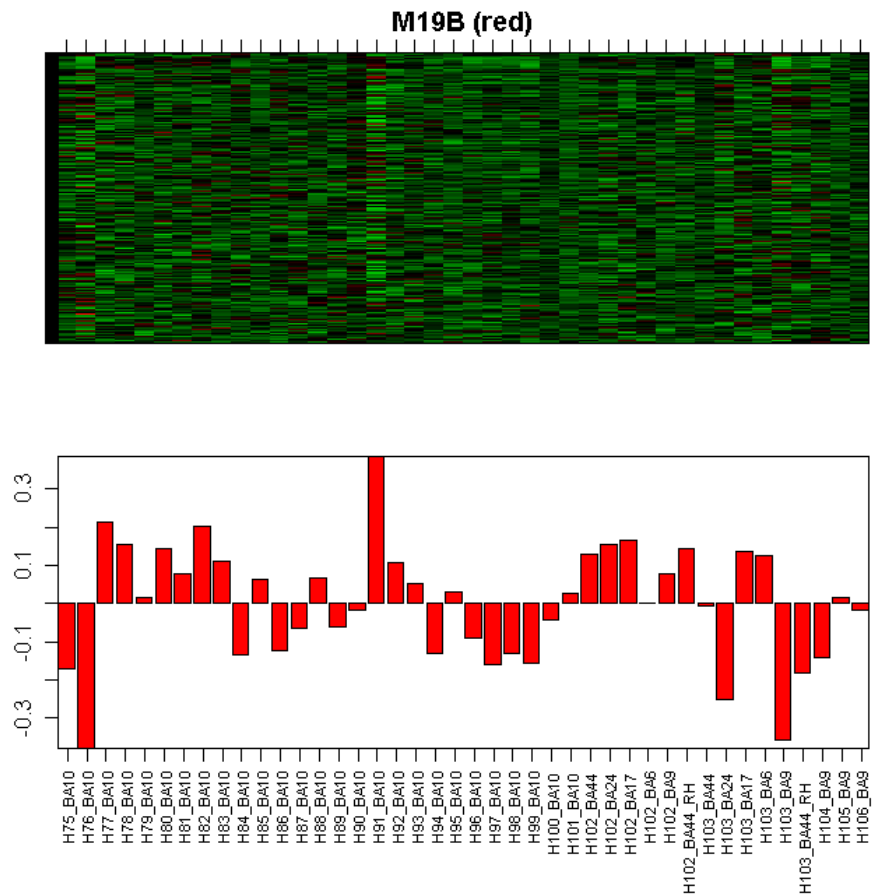
M19B (red)
0.3
0.1
-0.1
-0.3
H75_BA10
H76_BA10
H77_BA10
H78_BA10
H79_BA10
H80_BA10
H81_BA10
H82_BA10
H83_BA10
H84_BA10
H85_BA10
H86_BA10
H87_BA10
H88_BA10
H89_BA10
H90_BA10
H91_BA10
H92_BA10
H93_BA10
H94_BA10
H95_BA10
H96_BA10
H97_BA10
H98_BA10
H99_BA10
H100_BA10
H101_BA10
H102_BA44
H102_BA24
H102_BA17
H102_BA6
H102_BA9
H102_BA44_RH
H103_BA44
H103_BA24
H103_BA17
H103_BA6
H103_BA9
H103_BA44_RH
H104_BA9
H105_BA9
H106_BA9

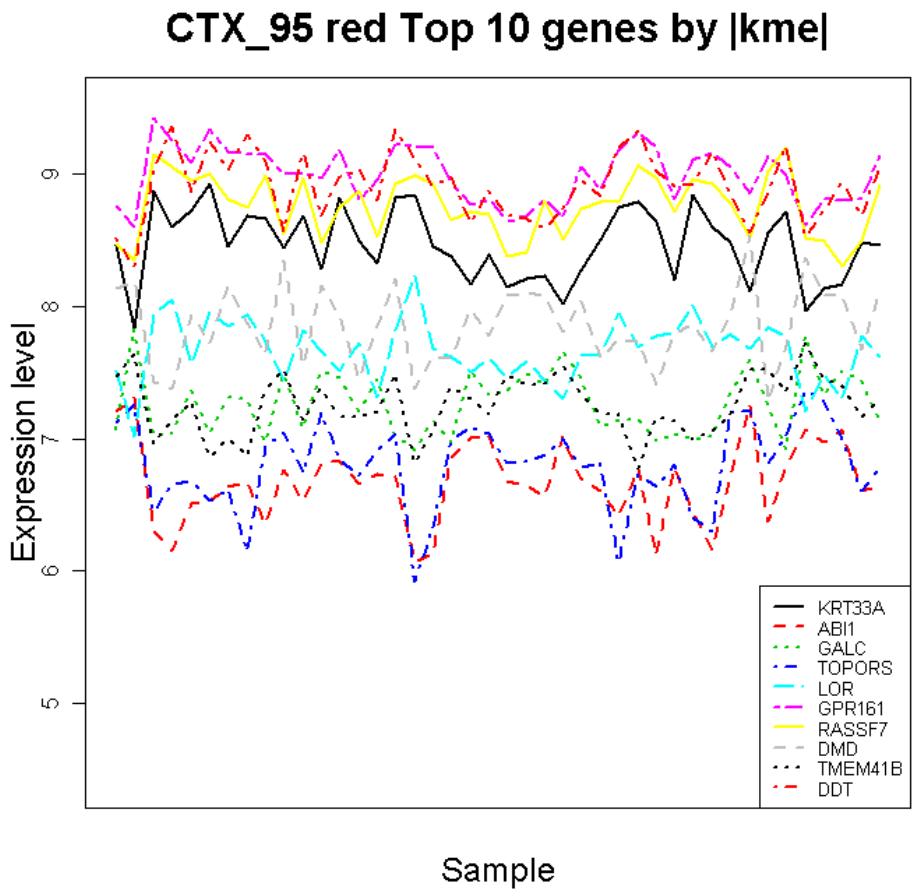
CTX_95 red Top 10 genes by |kme|
Expression level
5
6
7
8
9
Sample
KRT33A
ABI1
GALC
TOPORS
LOR
GPR161
RASSF7
DMD
TMEM41B
DDT

Figure S2AI

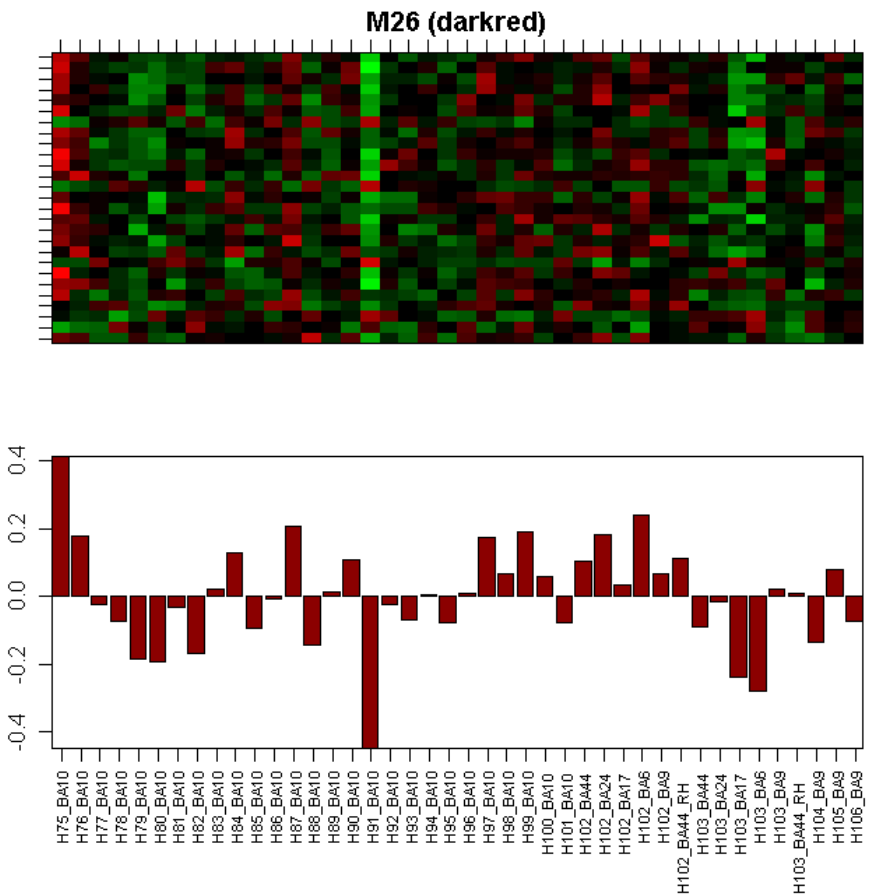
M26 (darkred)
0.4
0.2
0.0
-0.2
-0.4
H75_BA10
H76_BA10
H77_BA10
H78_BA10
H79_BA10
H80_BA10
H81_BA10
H82_BA10
H83_BA10
H84_BA10
H85_BA10
H86_BA10
H87_BA10
H88_BA10
H89_BA10
H90_BA10
H91_BA10
H92_BA10
H93_BA10
H94_BA10
H95_BA10
H96_BA10
H97_BA10
H98_BA10
H99_BA10
H100_BA10
H101_BA10
H102_BA44
H102_BA24
H102_BA17
H102_BA6
H102_BA9
H102_BA44_RH
H103_BA44
H103_BA24
H103_BA17
H103_BA6
H103_BA9
H103_BA44_RH
H104_BA9
H105_BA9
H106_BA9

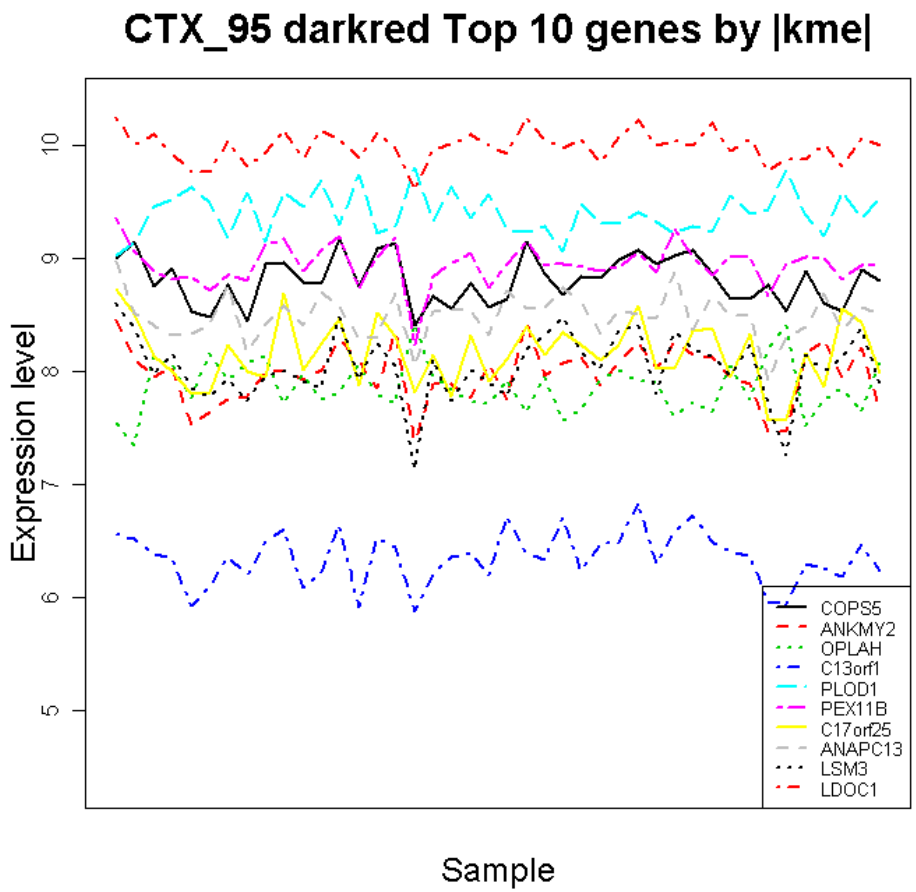
CTX_95 darkred Top 10 genes by |kme|
Expression level
5
6
7
8
9
10
Sample
COPS5
ANKMY2
OPLAH
C13orf1
PLOD1
PEX11B
C17orf25
ANAPC13
LSM3
LDOC1

Figure S2AJ

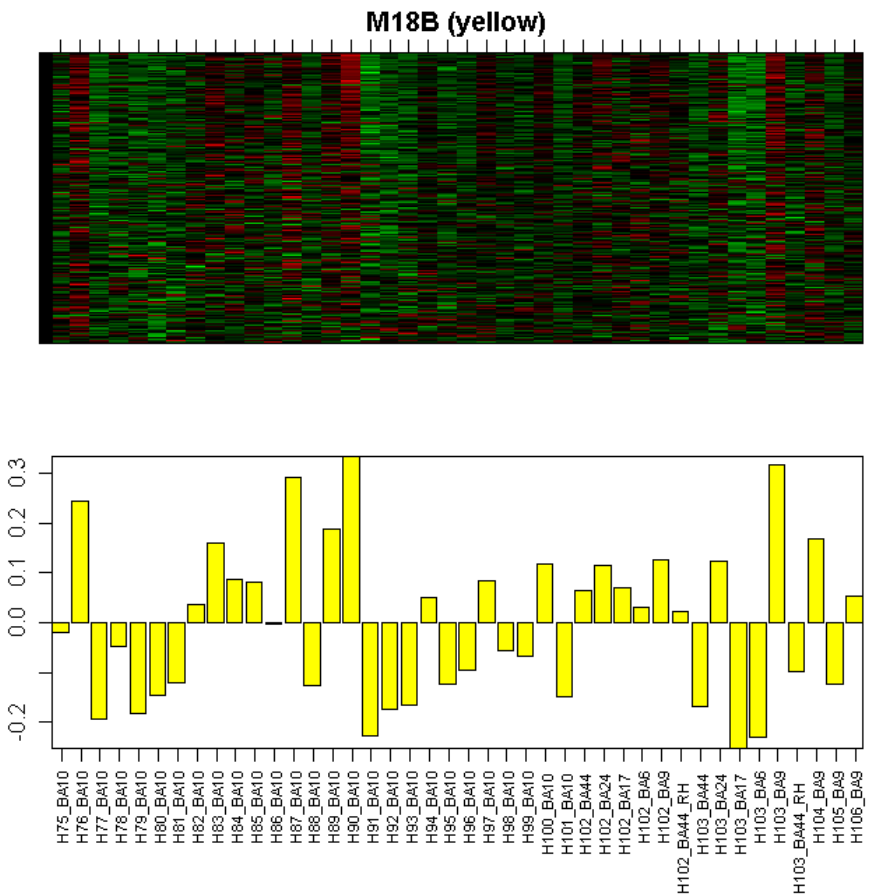
M18B (yellow)
0.3
0.2
0.1
0.0
-0.2
H75_BA10
H76_BA10
H77_BA10
H78_BA10
H79_BA10
H80_BA10
H81_BA10
H82_BA10
H83_BA10
H84_BA10
H85_BA10
H86_BA10
H87_BA10
H88_BA10
H89_BA10
H90_BA10
H91_BA10
H92_BA10
H93_BA10
H94_BA10
H95_BA10
H96_BA10
H97_BA10
H98_BA10
H99_BA10
H100_BA10
H101_BA10
H102_BA44
H102_BA24
H102_BA17
H102_BA6
H102_BA9
H102_BA44_RH
H103_BA44
H103_BA24
H103_BA17
H103_BA6
H103_BA9
H103_BA44_RH
H104_BA9
H105_BA9
H106_BA9

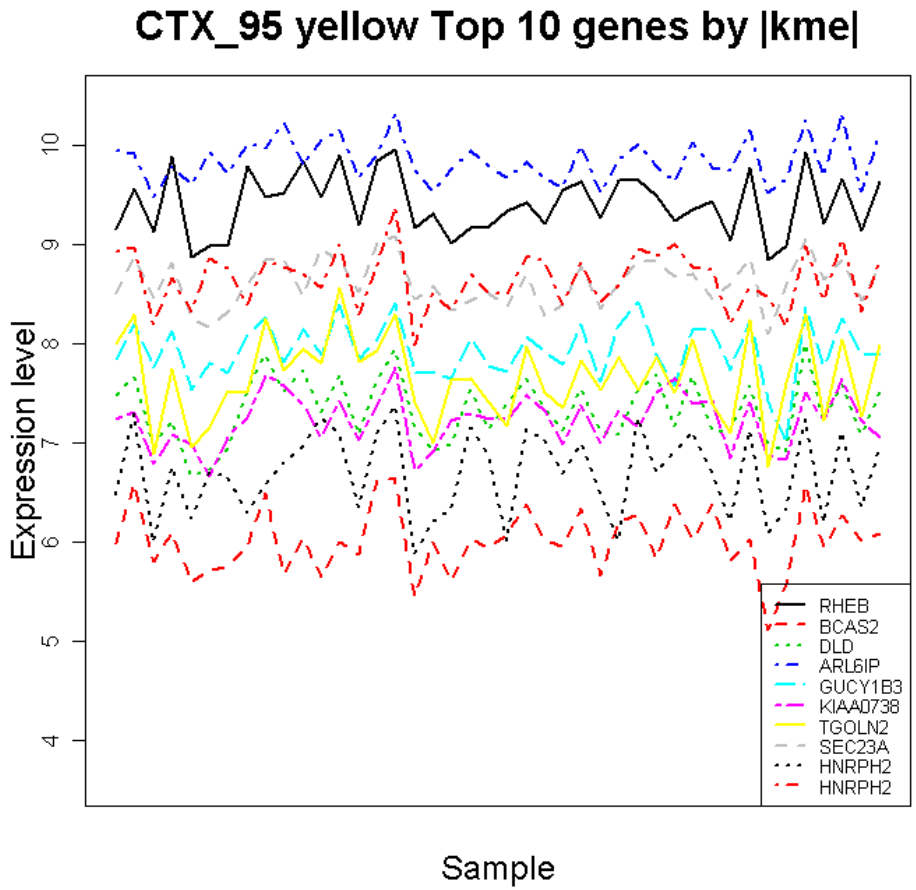
CTX_95 yellow Top 10 genes by |kme|
Expression level
10
9
8
7
6
5
4
Sample
RHEB
BCAS2
DLD
ARL6IP
GUCY1B3
KIAA0738
TGOLN2
SEC23A
HNRPH2
HNRPH2

Figure S2

Caudate nucleus

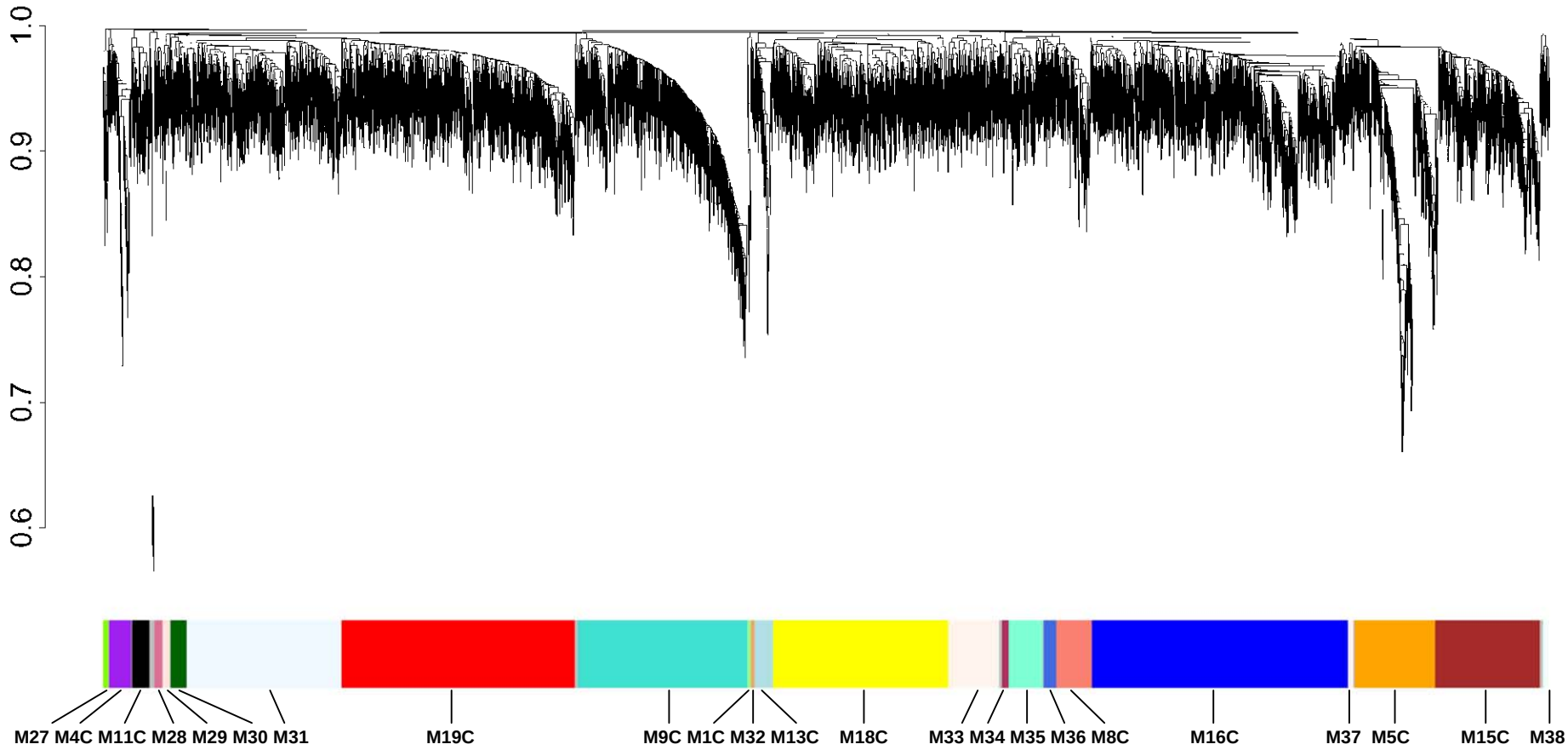

Figure S2AK

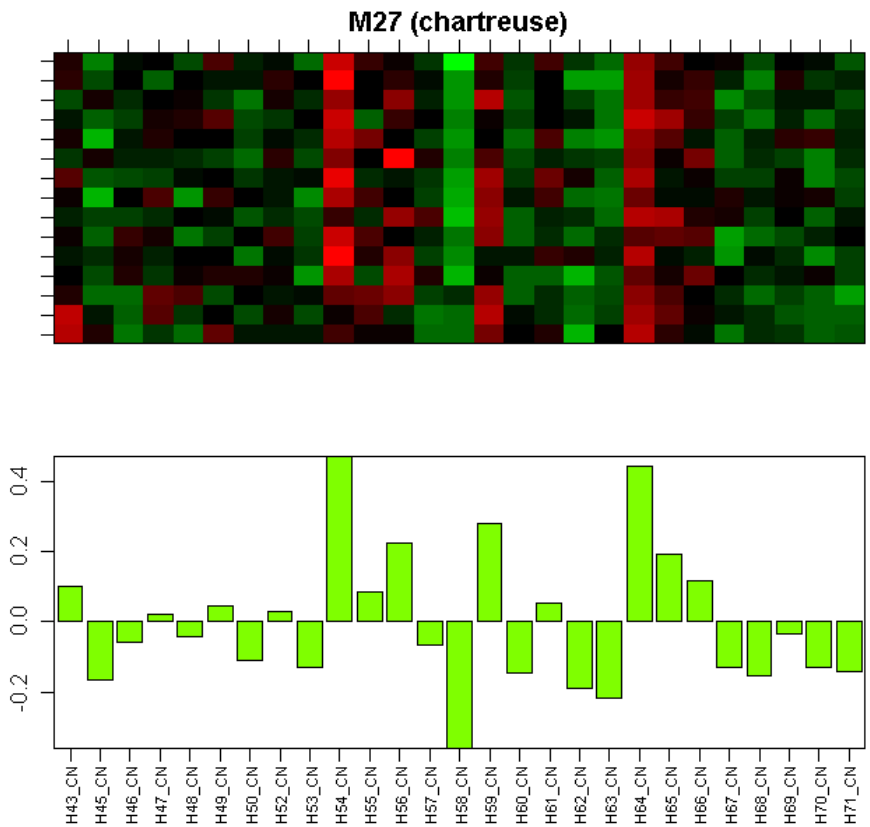
M27 (chartreuse)
-0.2
0.0
0.2
0.4
H43_CN
H45_CN
H46_CN
H47_CN
H48_CN
H49_CN
H50_CN
H52_CN
H53_CN
H54_CN
H55_CN
H56_CN
H57_CN
H58_CN
H59_CN
H60_CN
H61_CN
H62_CN
H63_CN
H64_CN
H65_CN
H66_CN
H67_CN
H68_CN
H69_CN
H70_CN
H71_CN

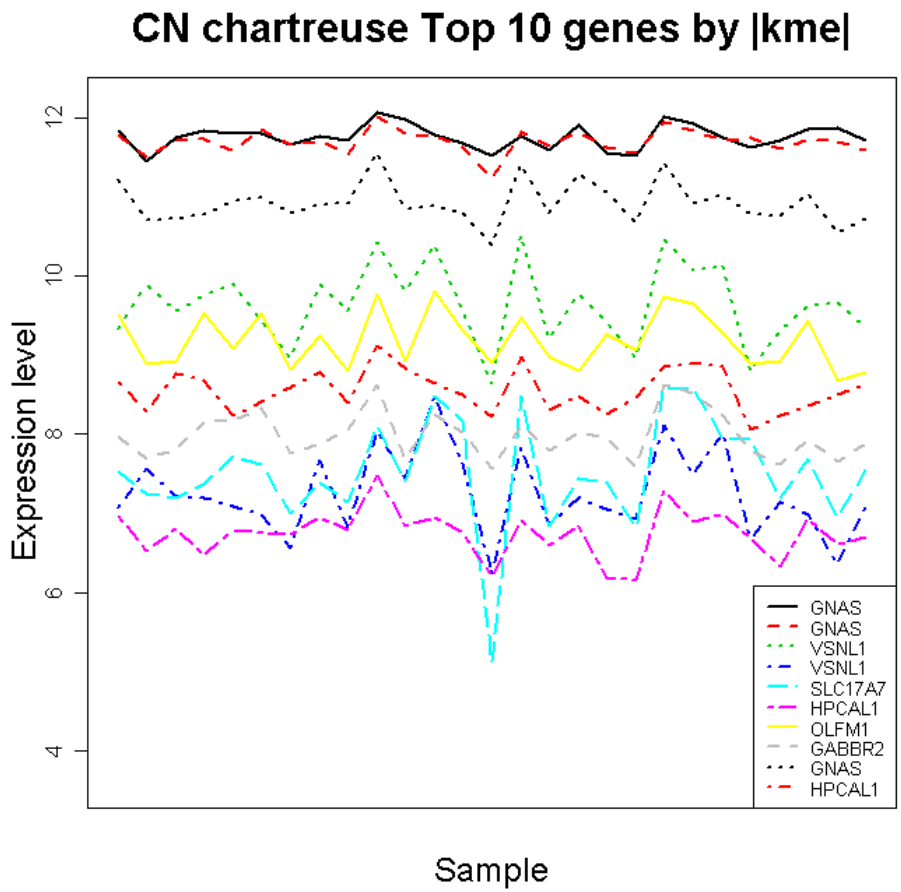
CN chartreuse Top 10 genes by |kme|
Expression level
4
6
8
10
12
Sample
GNAS
GNAS
VSNL1
VSNL1
SLC17A7
HPCAL1
OLFM1
GABBR2
GNAS
HPCAL1

Figure S2AL

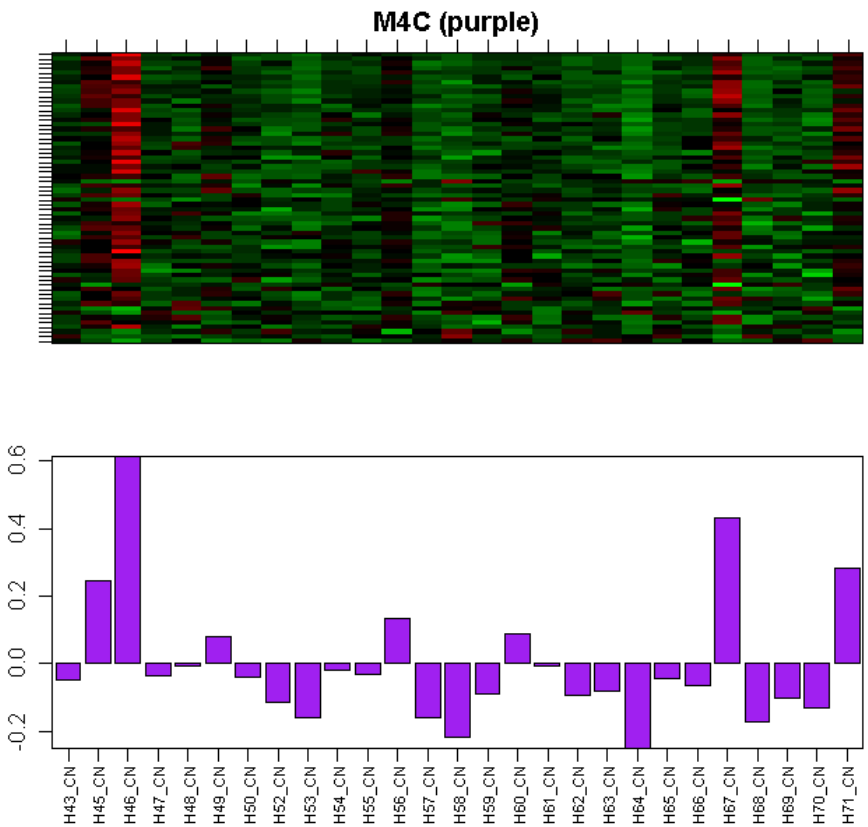
M4C (purple)
0.6
0.4
0.2
0.0
-0.2
H43_CN
H45_CN
H46_CN
H47_CN
H48_CN
H49_CN
H50_CN
H52_CN
H53_CN
H54_CN
H55_CN
H56_CN
H57_CN
H58_CN
H59_CN
H60_CN
H61_CN
H62_CN
H63_CN
H64_CN
H65_CN
H66_CN
H67_CN
H68_CN
H69_CN
H70_CN
H71_CN

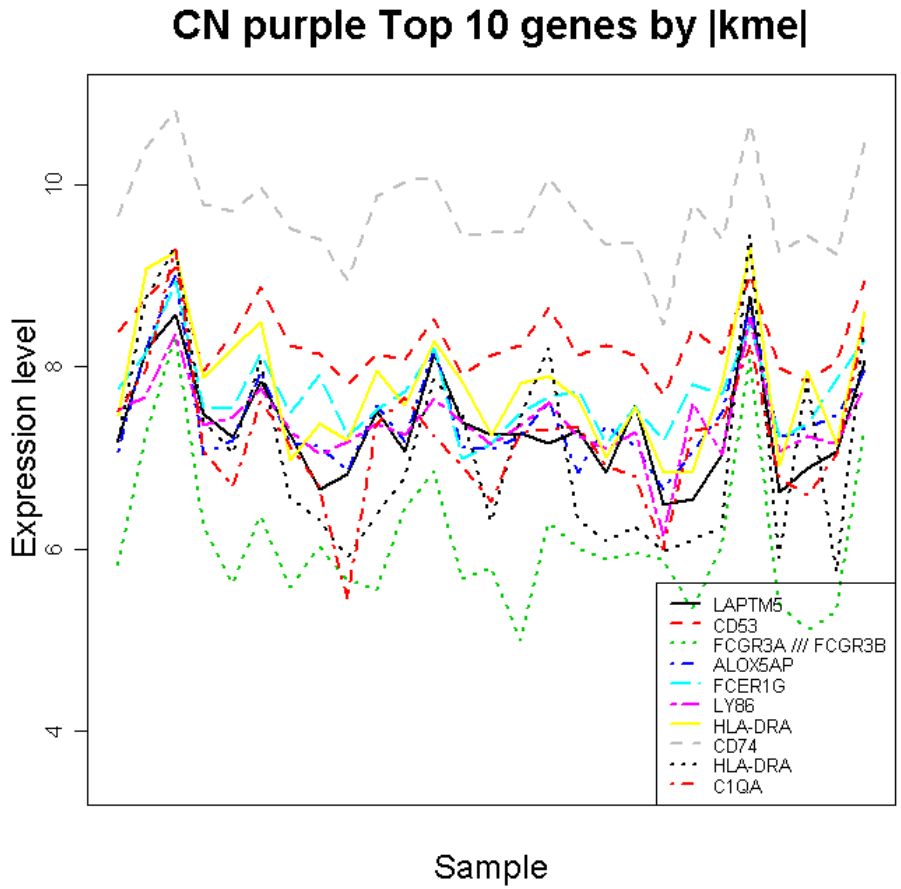
CN purple Top 10 genes by |kme|
Expression level
10
8
6
4
Sample
LAPTM5
CD53
FCGR3A /// FCGR3B
ALOX5AP
FCER1G
LY86
HLA-DRA
CD74
HLA-DRA
C1QA

Figure S2AM

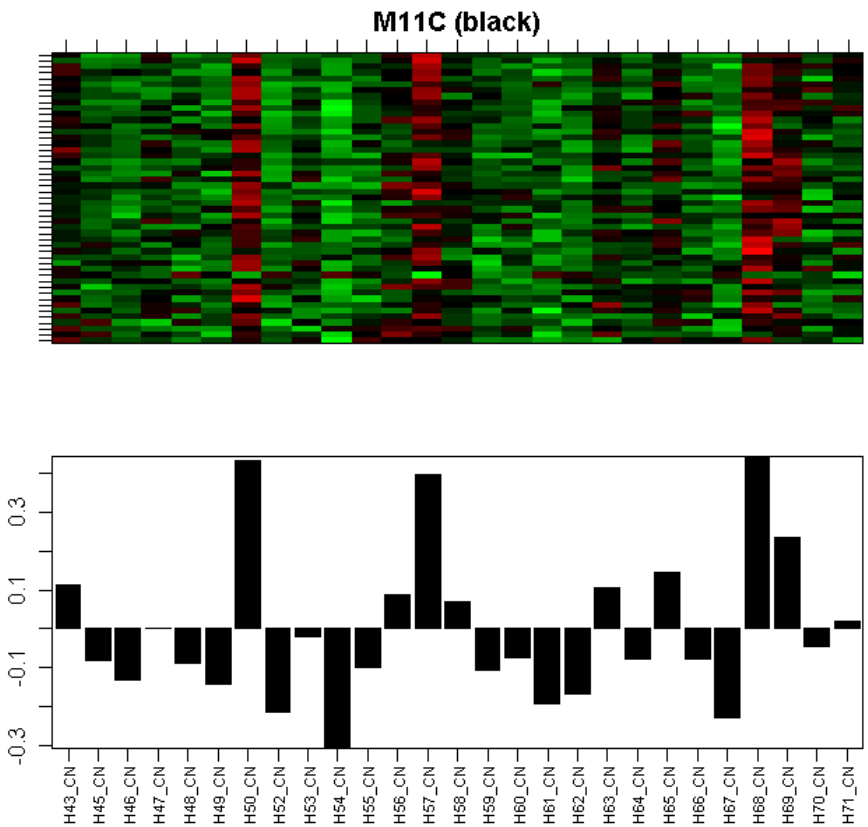
M11C (black)
0.3
0.1
-0.1
-0.3
H43_CN
H45_CN
H46_CN
H47_CN
H48_CN
H49_CN
H50_CN
H52_CN
H53_CN
H54_CN
H55_CN
H56_CN
H57_CN
H58_CN
H59_CN
H60_CN
H61_CN
H62_CN
H63_CN
H64_CN
H65_CN
H66_CN
H67_CN
H68_CN
H69_CN
H70_CN
H71_CN

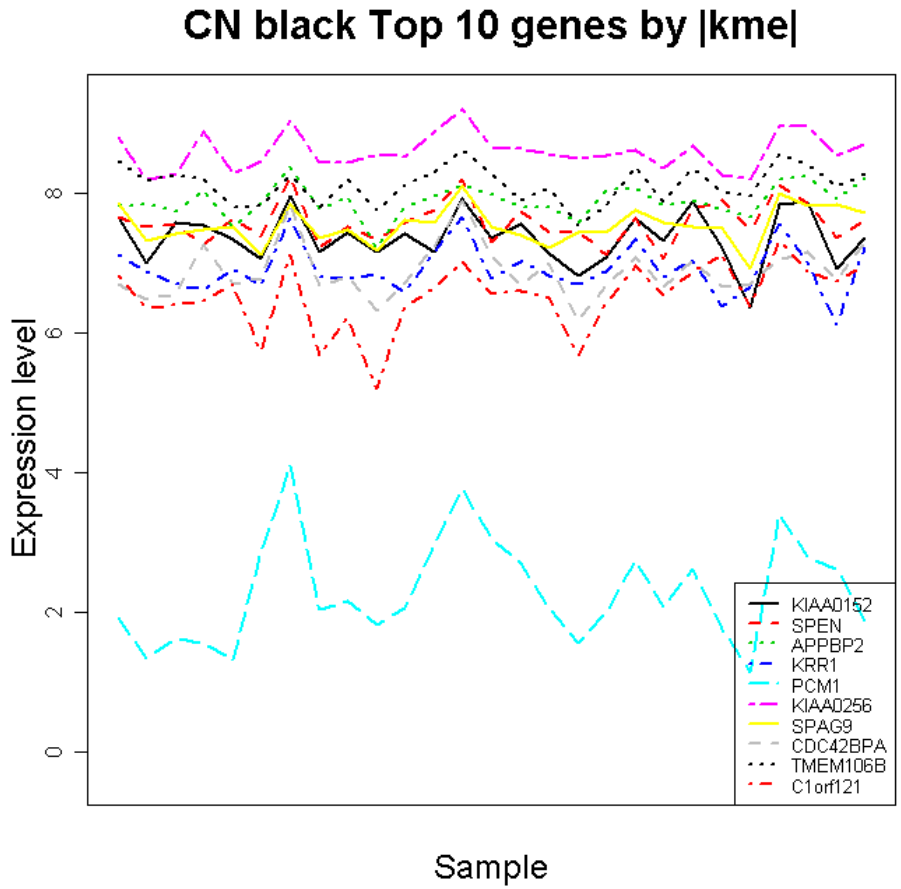
CN black Top 10 genes by |kme|
Expression level
0
2
4
6
8
Sample
KIAA0152
SPEN
APPBP2
KRR1
PCM1
KIAA0256
SPAG9
CDC42BPA
TMEM106B
C1orf121

Figure S2AN

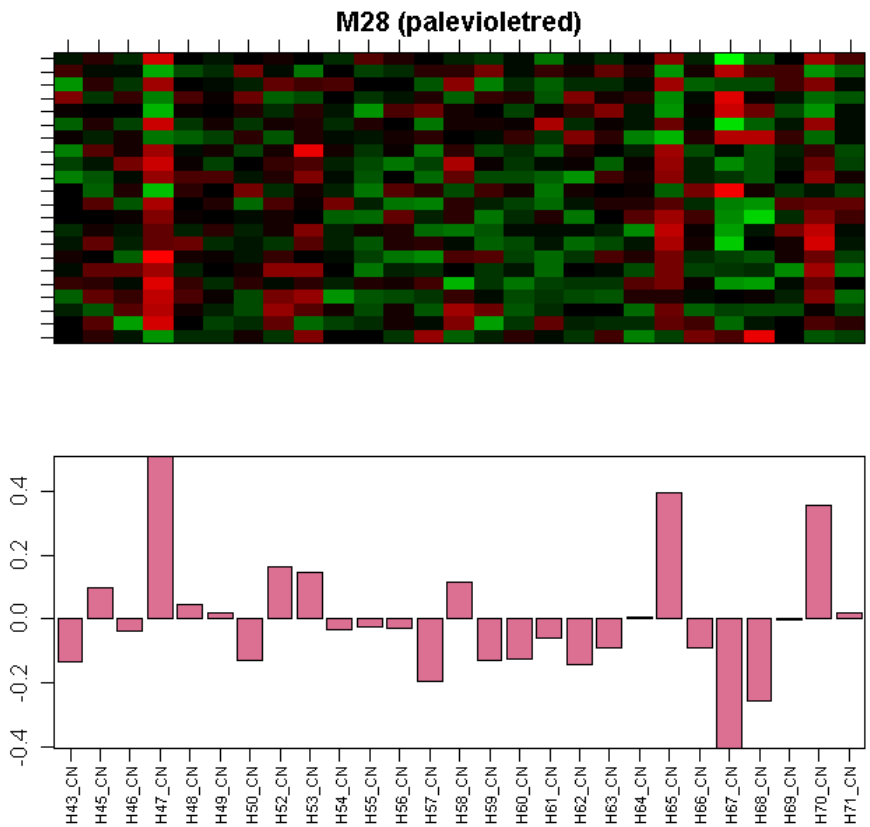
M28 (palevioletred)
0.4
0.2
0.0
-0.2
-0.4
H43_CN
H45_CN
H46_CN
H47_CN
H48_CN
H49_CN
H50_CN
H52_CN
H53_CN
H54_CN
H55_CN
H56_CN
H57_CN
H58_CN
H59_CN
H60_CN
H61_CN
H62_CN
H63_CN
H64_CN
H65_CN
H66_CN
H67_CN
H68_CN
H69_CN
H70_CN
H71_CN

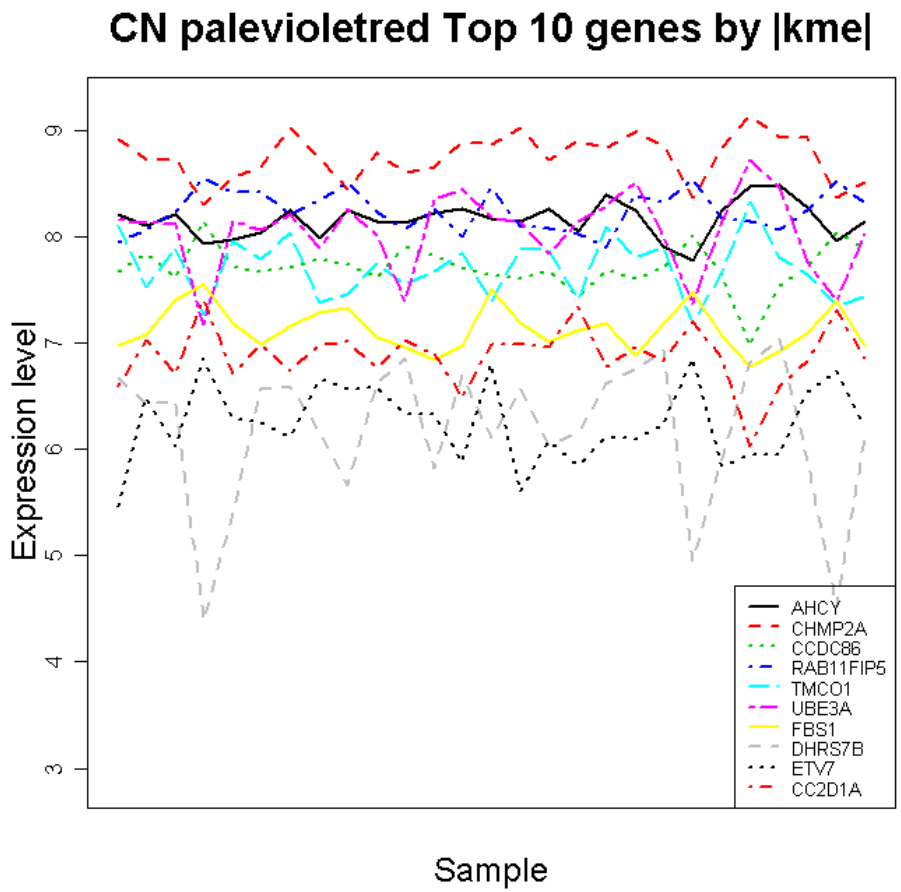
CN palevioletred Top 10 genes by |kme|
Expression level
3
4
5
6
7
8
9
Sample
AHCY
CHMP2A
CCDC86
RAB11FIP5
TMCO1
UBE3A
FBS1
DHRS7B
ETV7
CC2D1A

Figure S2AO

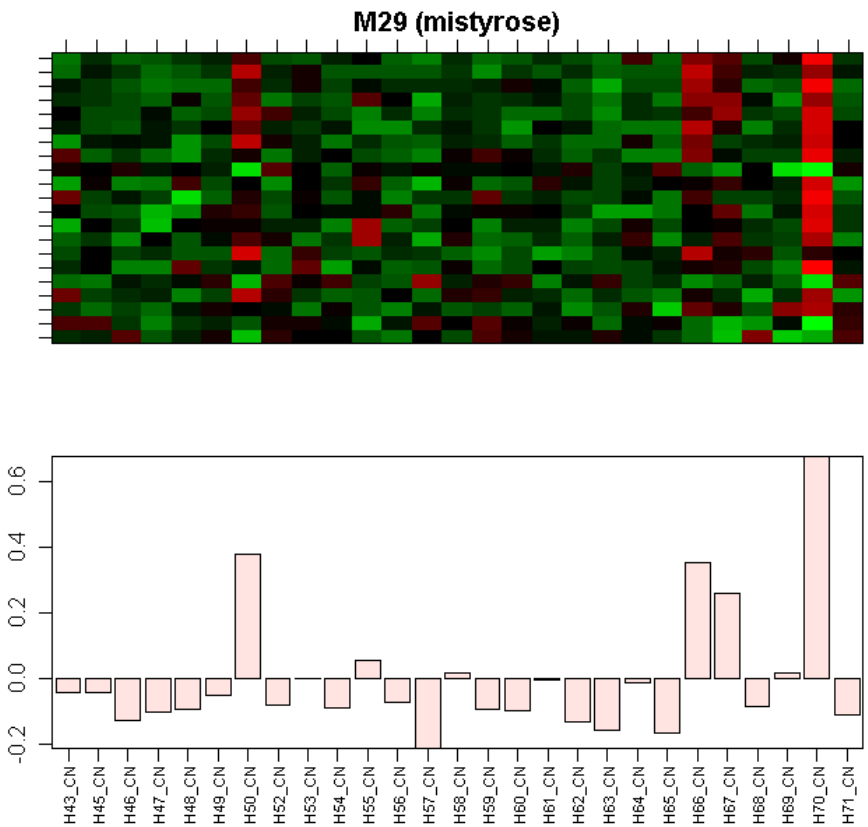
M29 (mistyrose)
0.6
0.4
0.2
0.0
-0.2
H43_CN
H45_CN
H46_CN
H47_CN
H48_CN
H49_CN
H50_CN
H52_CN
H53_CN
H54_CN
H55_CN
H56_CN
H57_CN
H58_CN
H59_CN
H60_CN
H61_CN
H62_CN
H63_CN
H64_CN
H65_CN
H66_CN
H67_CN
H68_CN
H69_CN
H70_CN
H71_CN

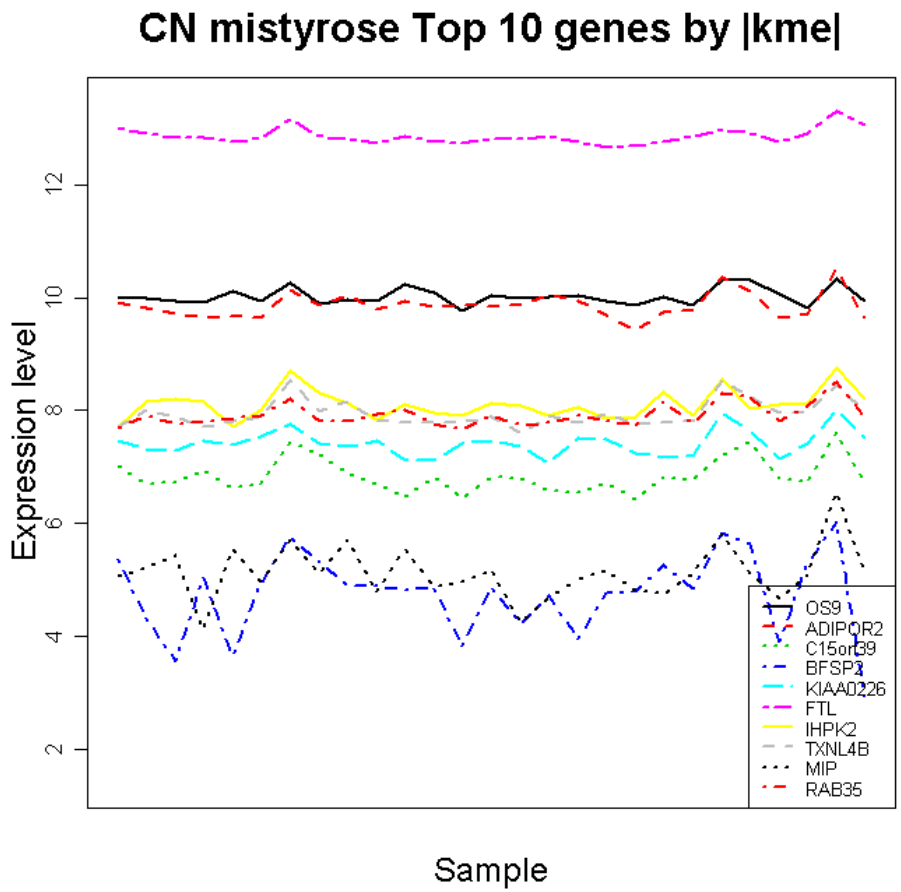
CN mistyrose Top 10 genes by |kme|
Expression level
2
4
6
8
10
12
Sample
OS9
ADIPOR2
C15orf39
BFSP1
KIAA0226
FTL
IHPK2
TXNL4B
MIP
RAB35

Figure S2AP

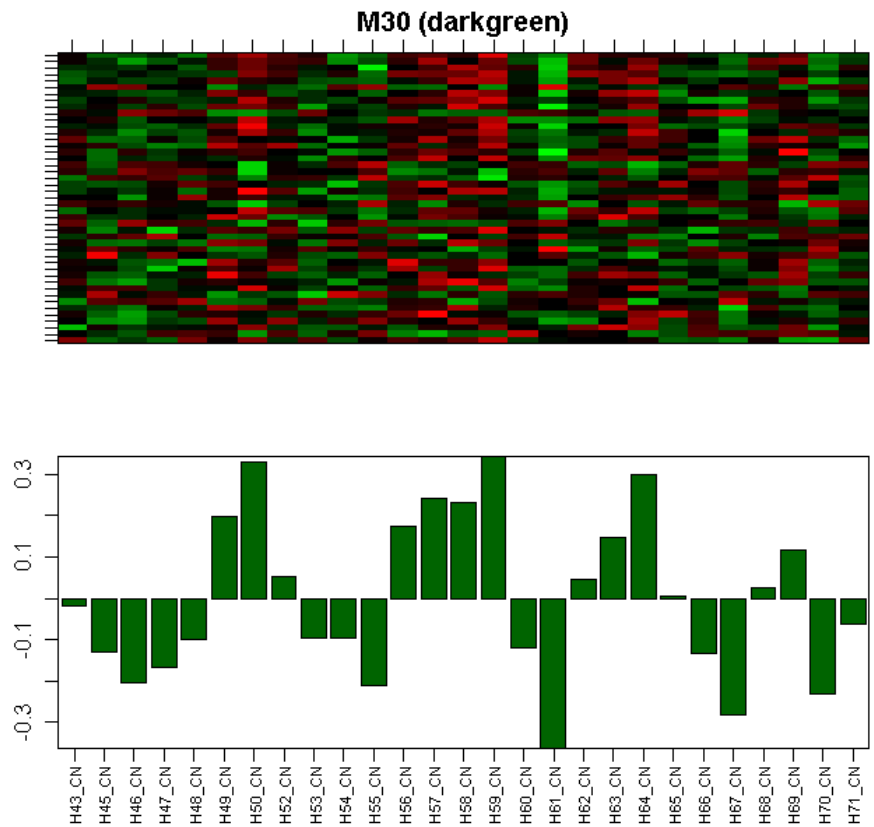
M30 (darkgreen)
0.3
0.1
-0.1
-0.3
H43_CN
H45_CN
H46_CN
H47_CN
H48_CN
H49_CN
H50_CN
H52_CN
H53_CN
H54_CN
H55_CN
H56_CN
H57_CN
H58_CN
H59_CN
H60_CN
H61_CN
H62_CN
H63_CN
H64_CN
H65_CN
H66_CN
H67_CN
H68_CN
H69_CN
H70_CN
H71_CN

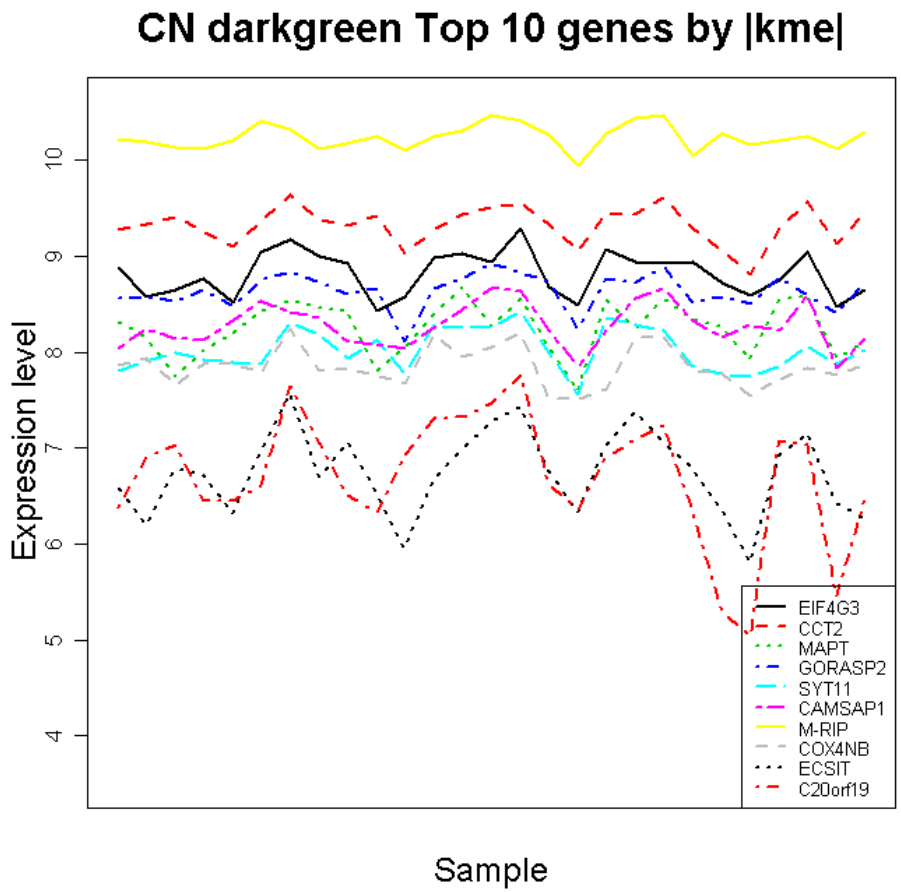
CN darkgreen Top 10 genes by |kme|
Expression level
4
5
6
7
8
9
10
Sample
EIF4G3
CCT2
MAPT
GORASP2
SYT11
CAMSAP1
M-RIP
COX4NB
ECSIT
C20orf19

Figure S2AQ

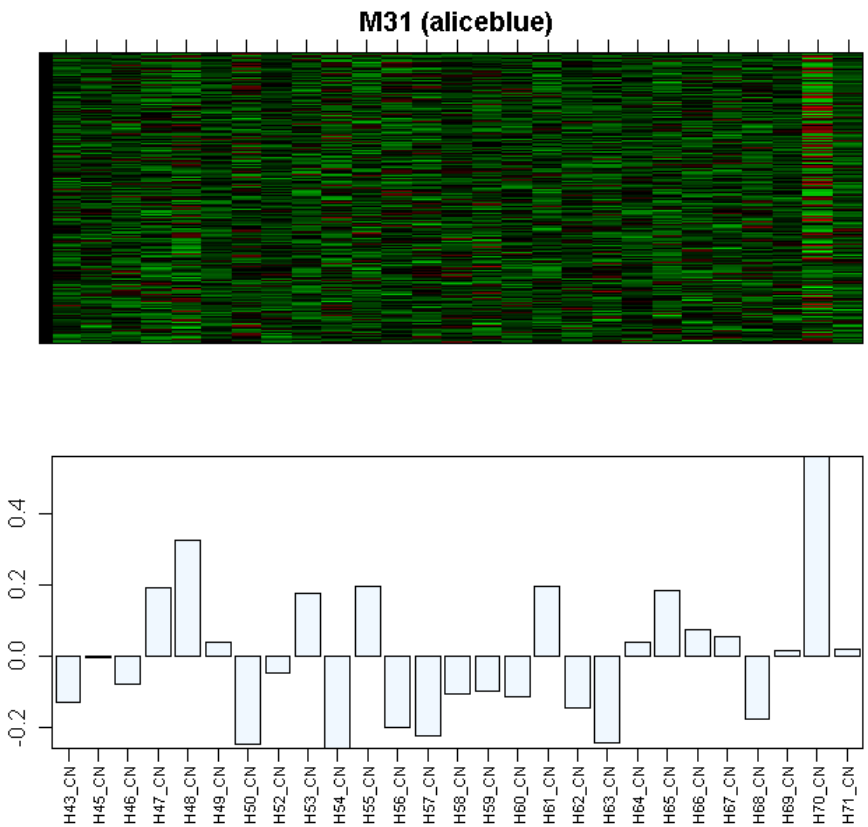
M31 (aliceblue)
0.4
0.2
0.0
-0.2
H43_CN
H45_CN
H46_CN
H47_CN
H48_CN
H49_CN
H50_CN
H52_CN
H53_CN
H54_CN
H55_CN
H56_CN
H57_CN
H58_CN
H59_CN
H60_CN
H61_CN
H62_CN
H63_CN
H64_CN
H65_CN
H66_CN
H67_CN
H68_CN
H69_CN
H70_CN
H71_CN

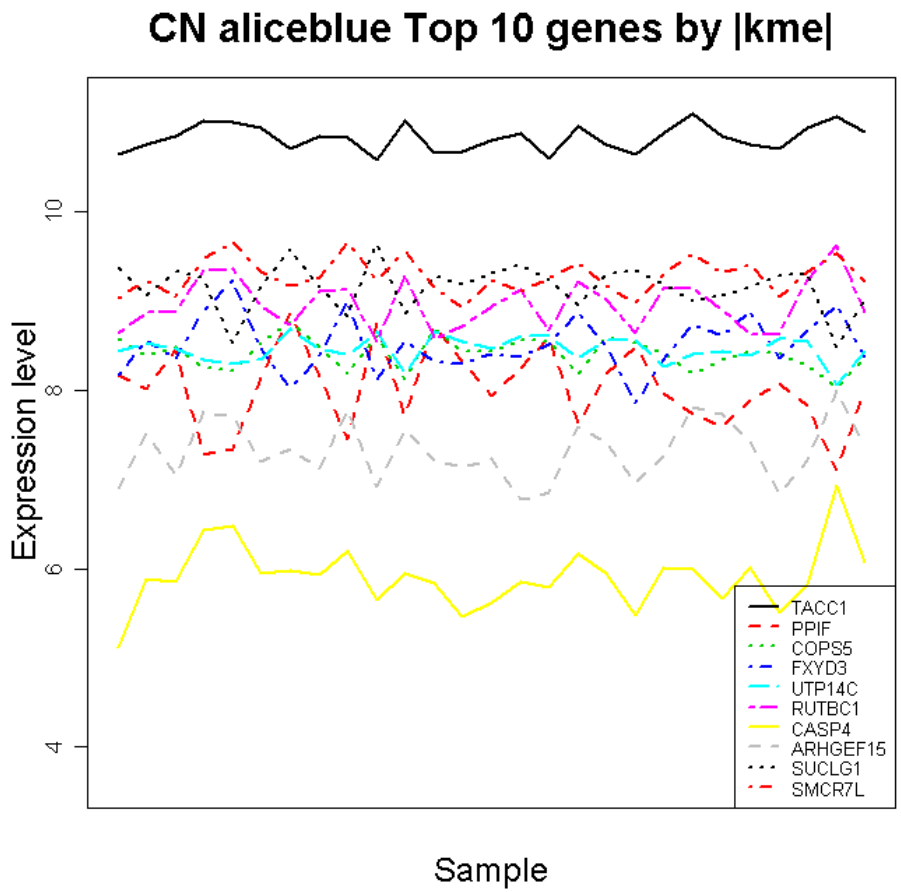
CN aliceblue Top 10 genes by |kme|
Expression level
10
8
6
4
Sample
TACC1
PPIF
COPS5
FXYD3
UTP14C
RUTBC1
CASP4
ARHGEF15
SUCLG1
SMCR7L

Figure S2AR

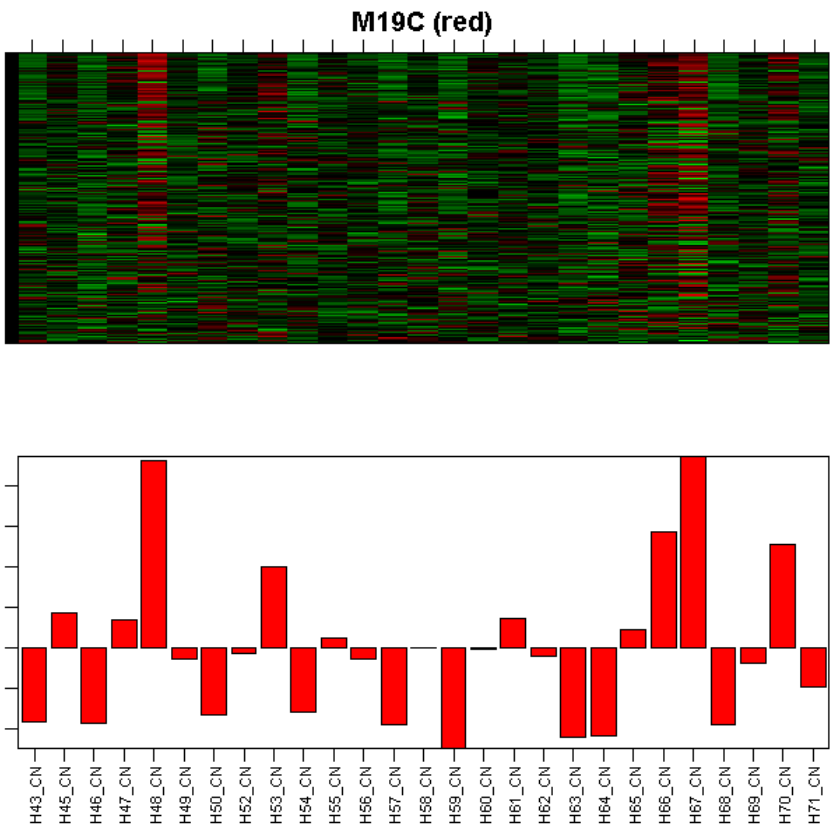
M19C (red)
0.4
0.2
0.0
-0.2
H43_CN
H45_CN
H46_CN
H47_CN
H48_CN
H49_CN
H50_CN
H52_CN
H53_CN
H54_CN
H55_CN
H56_CN
H57_CN
H58_CN
H59_CN
H60_CN
H61_CN
H62_CN
H63_CN
H64_CN
H65_CN
H66_CN
H67_CN
H68_CN
H69_CN
H70_CN
H71_CN

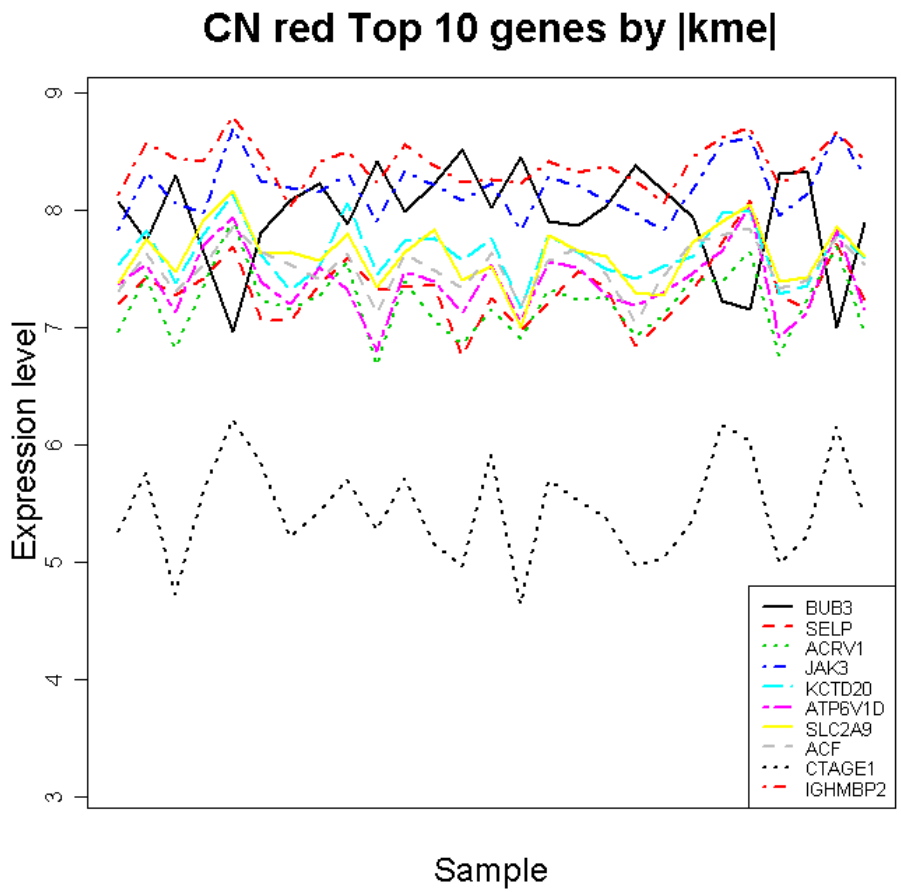
CN red Top 10 genes by |kme|
Expression level
3
4
5
6
7
8
9
Sample
BUB3
SELP
ACRV1
JAK3
KCTD20
ATP6V1D
SLC2A9
ACF
CTAGE1
IGHMBP2

Figure S2AS

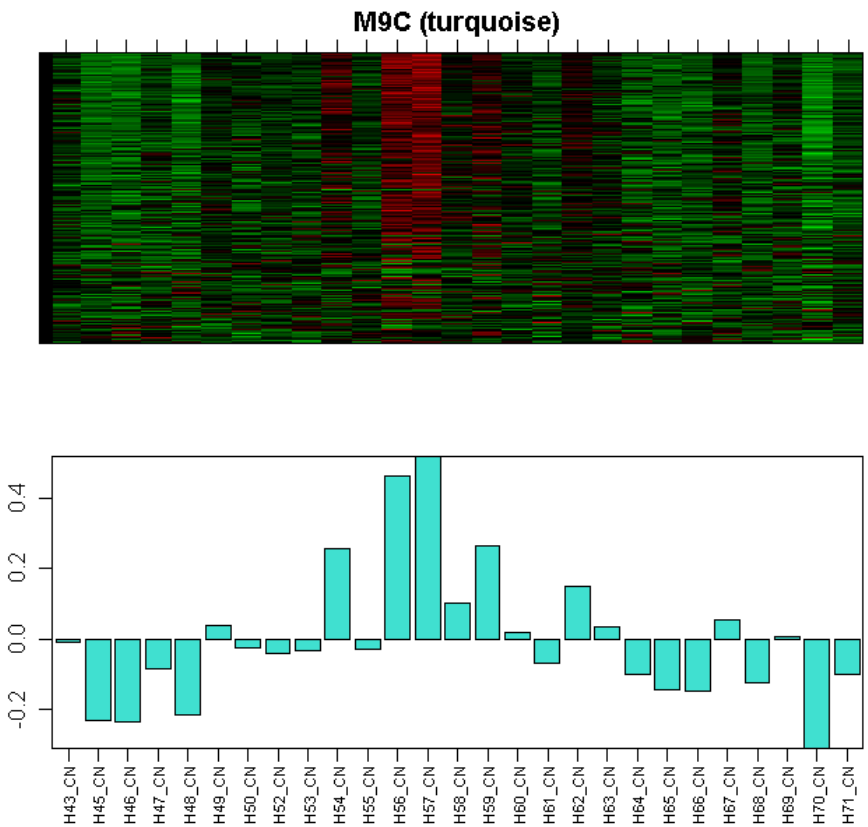
M9C (turquoise)
0.4
0.2
0.0
-0.2
H43_CN
H45_CN
H46_CN
H47_CN
H48_CN
H49_CN
H50_CN
H52_CN
H53_CN
H54_CN
H55_CN
H56_CN
H57_CN
H58_CN
H59_CN
H60_CN
H61_CN
H62_CN
H63_CN
H64_CN
H65_CN
H66_CN
H67_CN
H68_CN
H69_CN
H70_CN
H71_CN

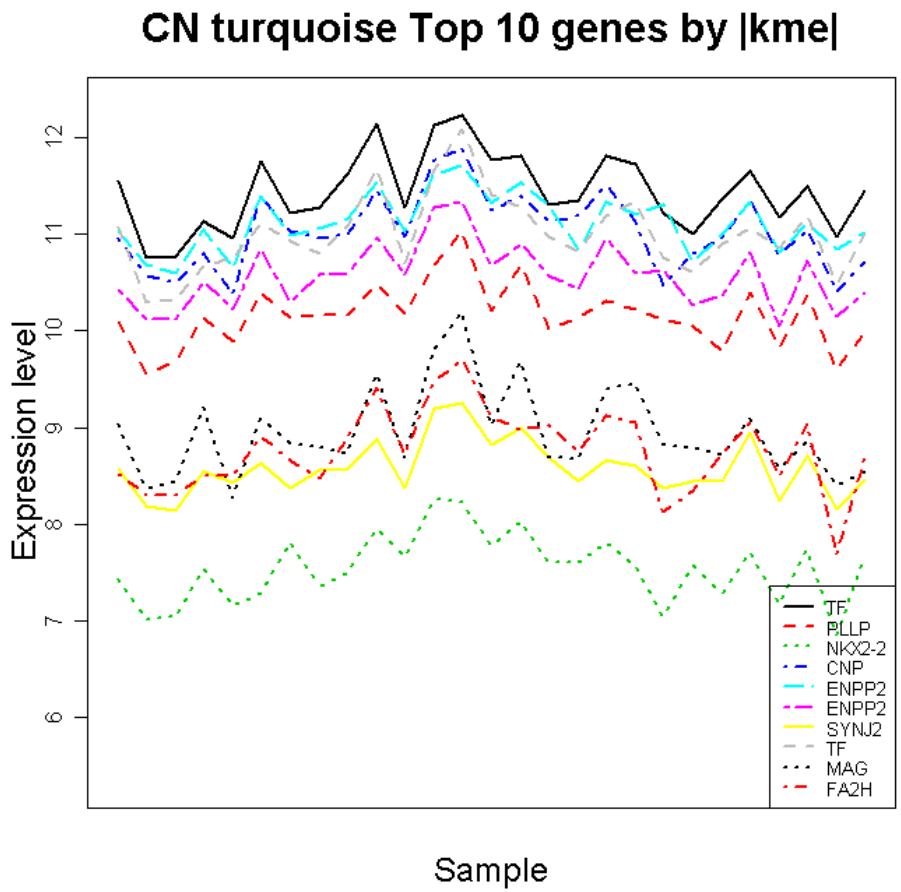
CN turquoise Top 10 genes by |kme|
Expression level
6
7
8
9
10
11
12
Sample
TF
PLLP
NKX2-2
CNP
ENPP2
ENPP2
SYNJ2
TF
MAG
FA2H

Figure S2AT

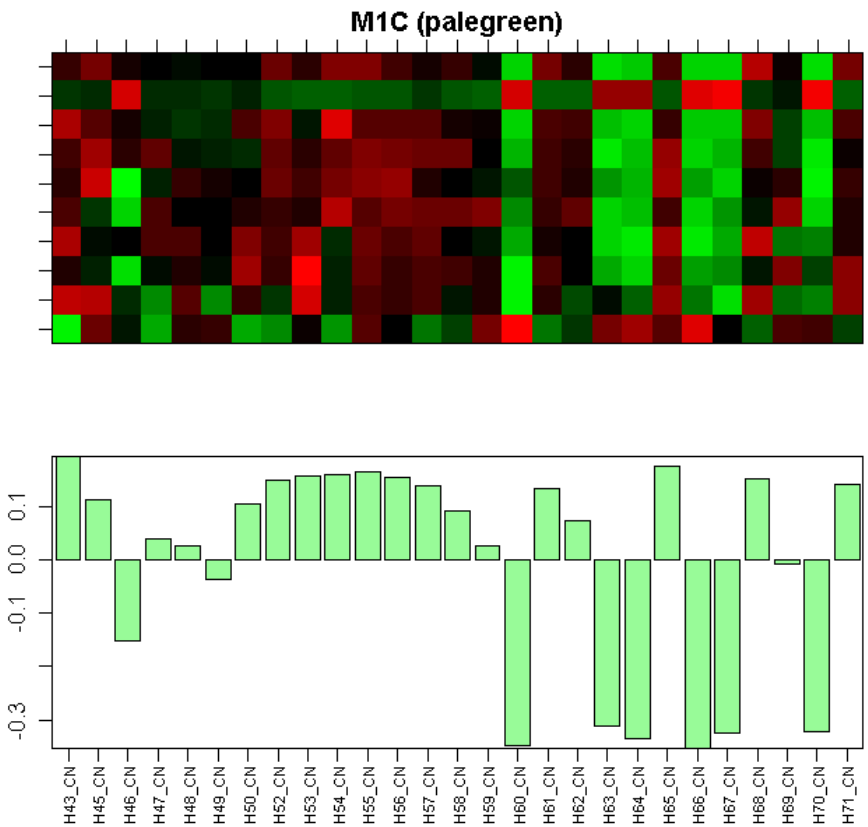
M1C (palegreen)
0.1
0.0
-0.1
-0.3
H43_CN
H45_CN
H46_CN
H47_CN
H48_CN
H49_CN
H50_CN
H52_CN
H53_CN
H54_CN
H55_CN
H56_CN
H57_CN
H58_CN
H59_CN
H60_CN
H61_CN
H62_CN
H63_CN
H64_CN
H65_CN
H66_CN
H67_CN
H68_CN
H69_CN
H70_CN
H71_CN

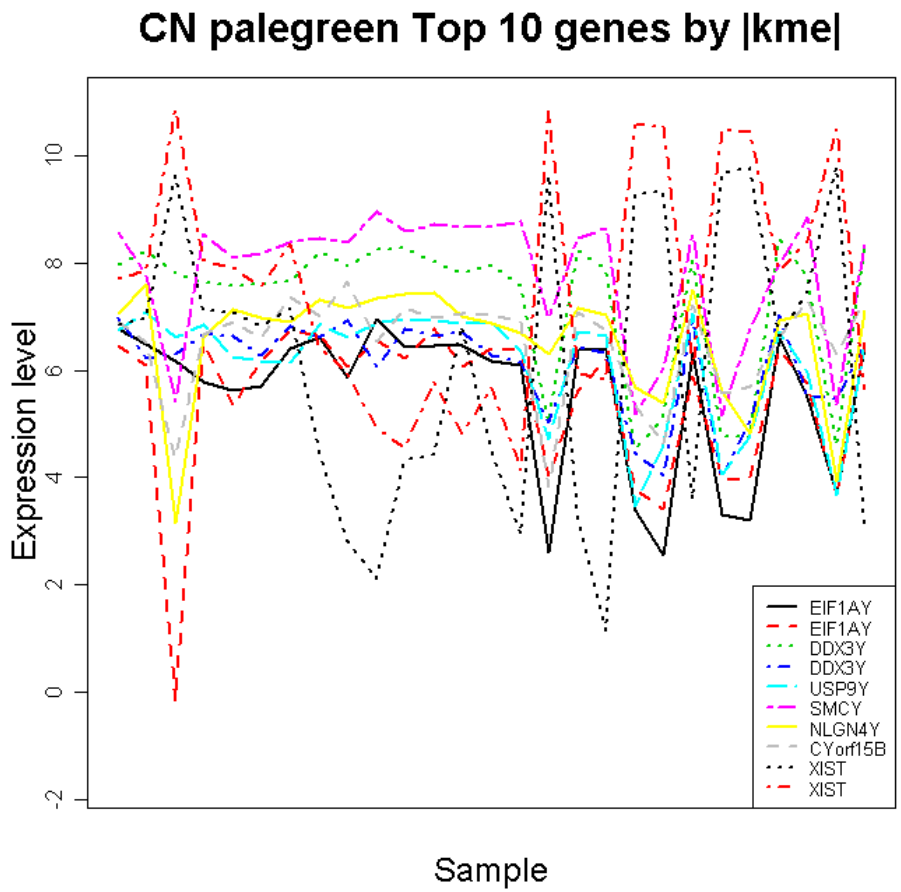
CN palegreen Top 10 genes by |kme|
Expression level
10
8
6
4
2
0
-2
Sample
EIF1AY
EIF1AY
DDX3Y
DDX3Y
USP9Y
SMCY
NLGN4Y
CYorf15B
XIST
XIST

Figure S2AU

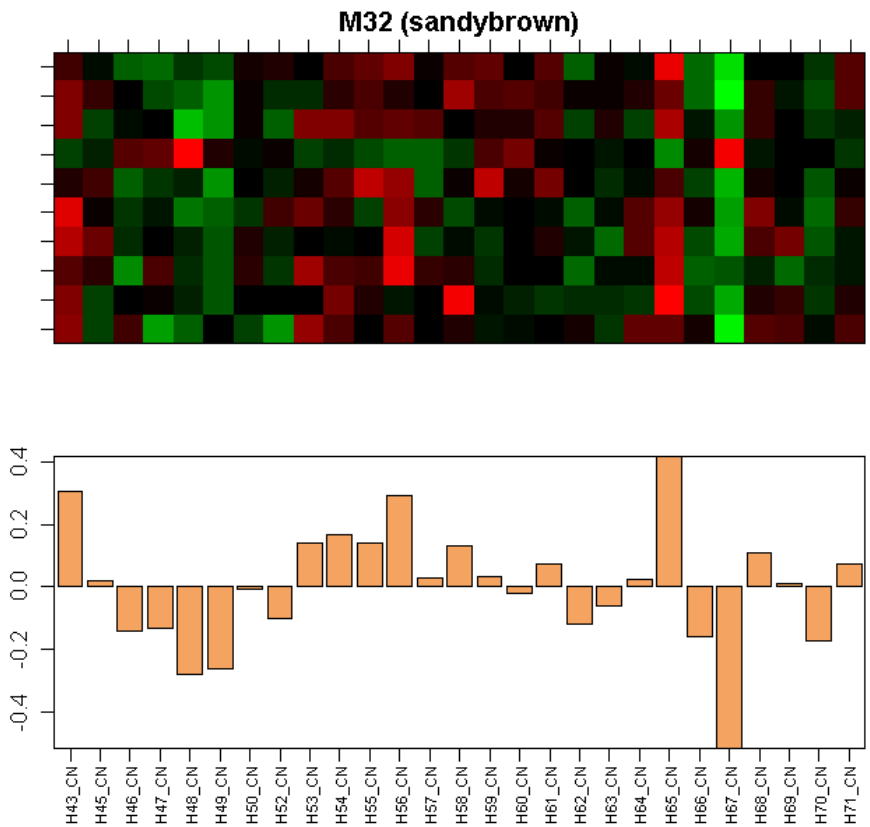
M32 (sandybrown)
0.4
0.2
0.0
-0.2
-0.4
H43_CN
H45_CN
H46_CN
H47_CN
H48_CN
H49_CN
H50_CN
H52_CN
H53_CN
H54_CN
H55_CN
H56_CN
H57_CN
H58_CN
H59_CN
H60_CN
H61_CN
H62_CN
H63_CN
H64_CN
H65_CN
H66_CN
H67_CN
H68_CN
H69_CN
H70_CN
H71_CN

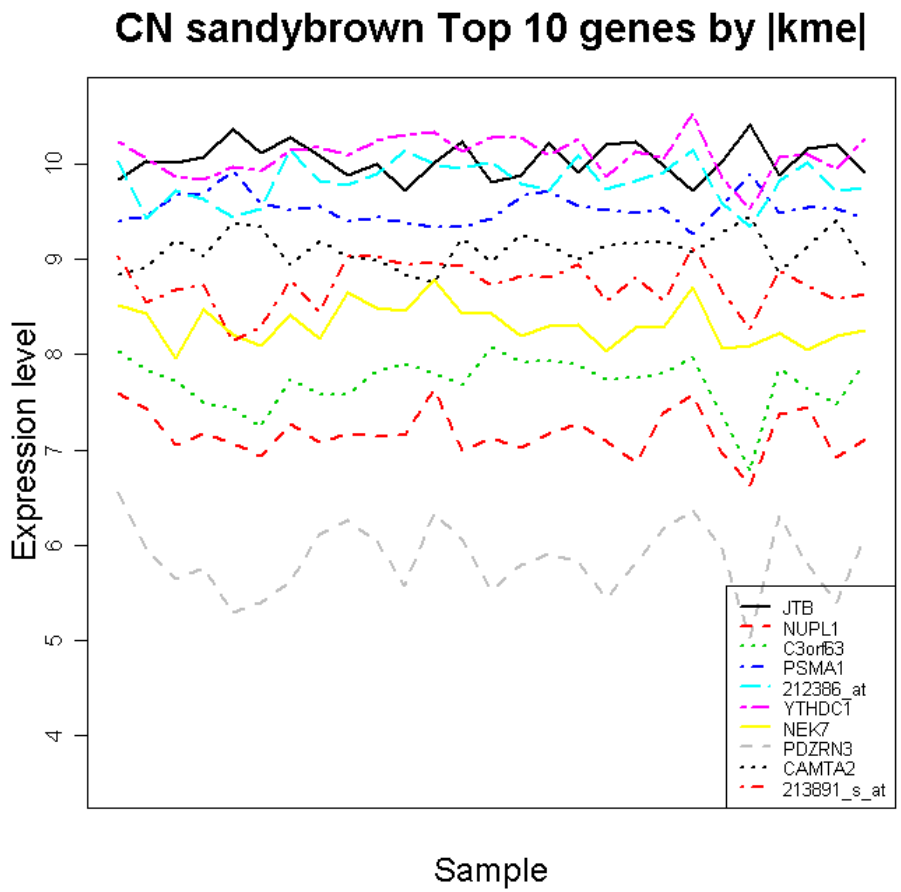
CN sandybrown Top 10 genes by |kme|
Expression level
4
5
6
7
8
9
10
Sample
JTB
NUPL1
C3orf63
PSMA1
212386_at
YTHDC1
NEK7
PDZRN3
CAMTA2
213891_s_at

Figure S2AV

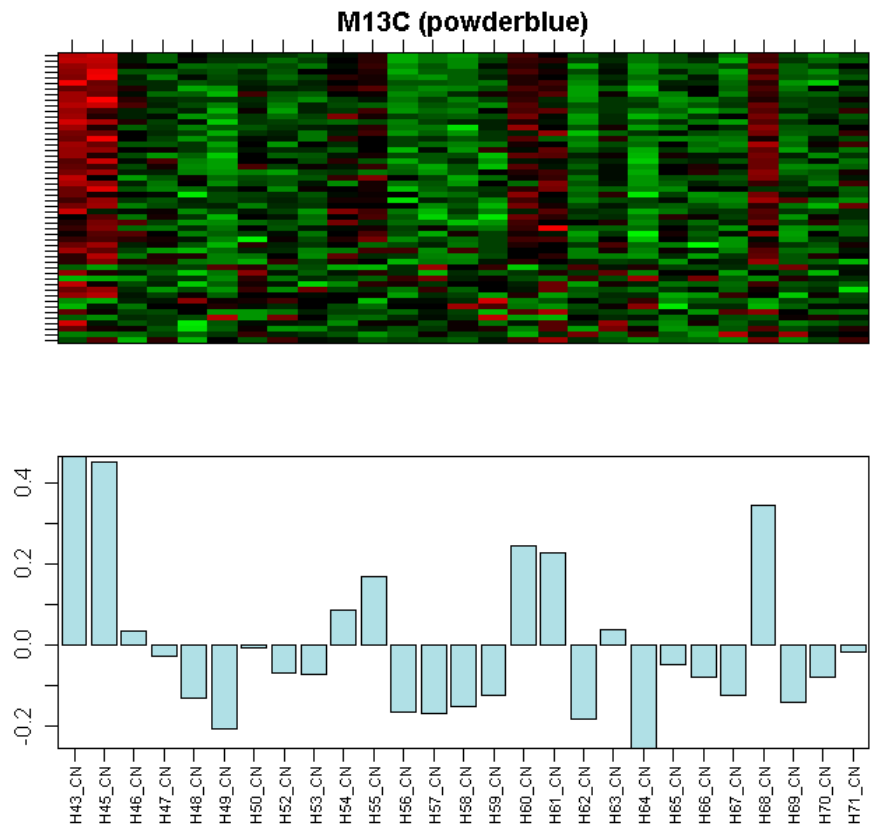
M13C (powderblue)
0.4
0.2
0.0
-0.2
H43_CN
H45_CN
H46_CN
H47_CN
H48_CN
H49_CN
H50_CN
H52_CN
H53_CN
H54_CN
H55_CN
H56_CN
H57_CN
H58_CN
H59_CN
H60_CN
H61_CN
H62_CN
H63_CN
H64_CN
H65_CN
H66_CN
H67_CN
H68_CN
H69_CN
H70_CN
H71_CN

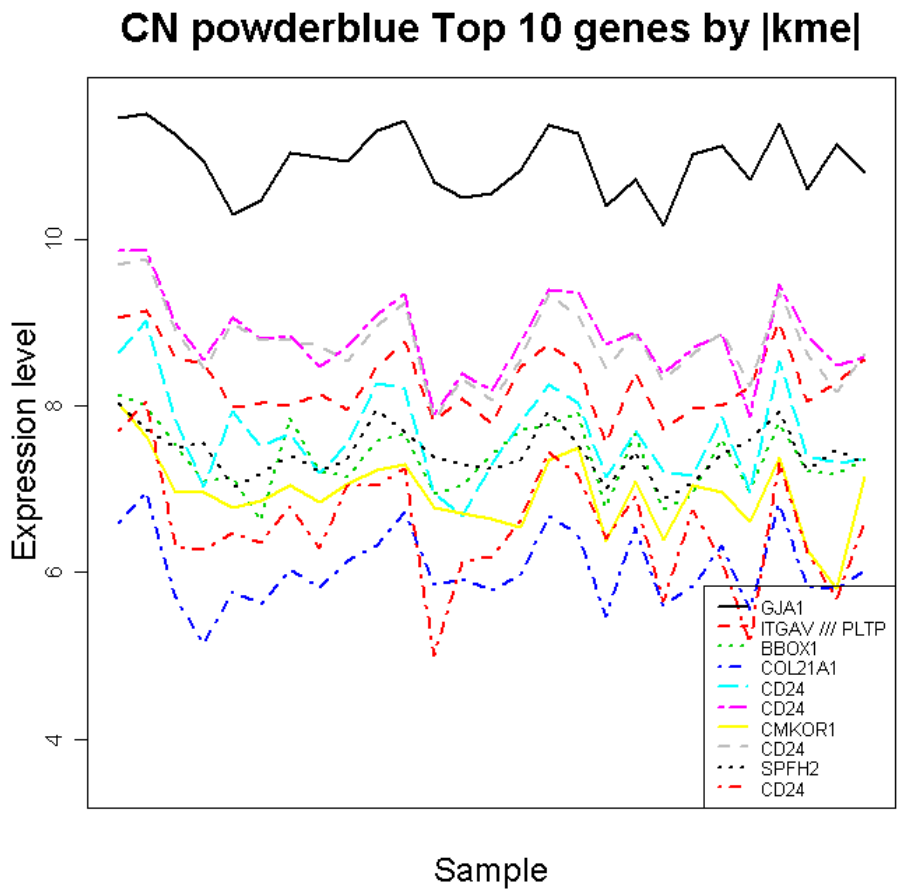
CN powderblue Top 10 genes by |kme|
Expression level
4
6
8
10
Sample
GJA1
ITGAV /// PLTP
BBOX1
COL21A1
CD24
CD24
CMKOR1
CD24
SPFH2
CD24

Figure S2AW

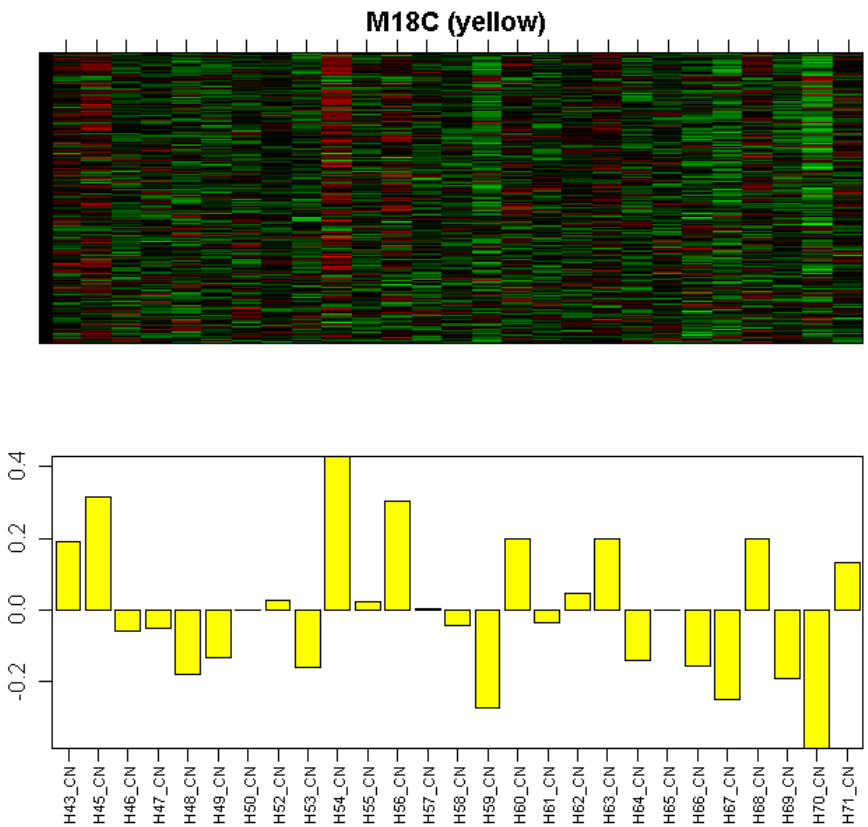
M18C (yellow)
0.4
0.2
0.0
-0.2
H43_CN
H45_CN
H46_CN
H47_CN
H48_CN
H49_CN
H50_CN
H52_CN
H53_CN
H54_CN
H55_CN
H56_CN
H57_CN
H58_CN
H59_CN
H60_CN
H61_CN
H62_CN
H63_CN
H64_CN
H65_CN
H66_CN
H67_CN
H68_CN
H69_CN
H70_CN
H71_CN

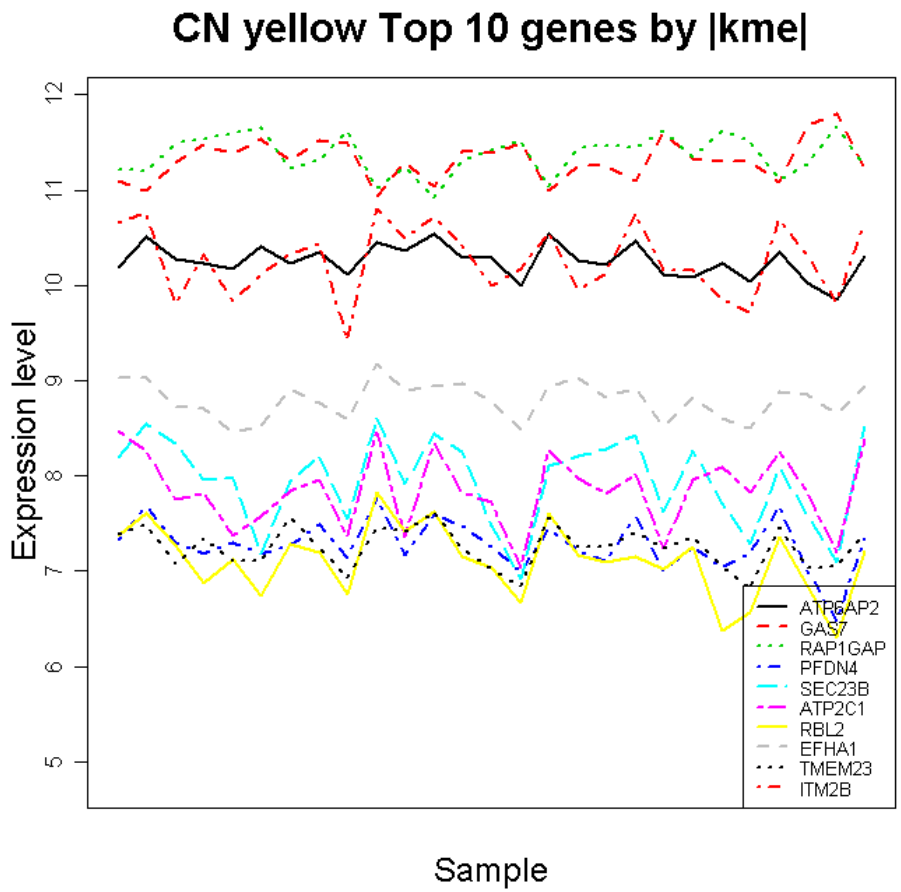
CN yellow Top 10 genes by |kme|
Expression level
5
6
7
8
9
10
11
12
Sample
ATP6AP2
GAS7
RAP1GAP
PFDN4
SEC23B
ATP2C1
RBL2
EFHA1
TMEM23
ITM2B

Figure S2AX

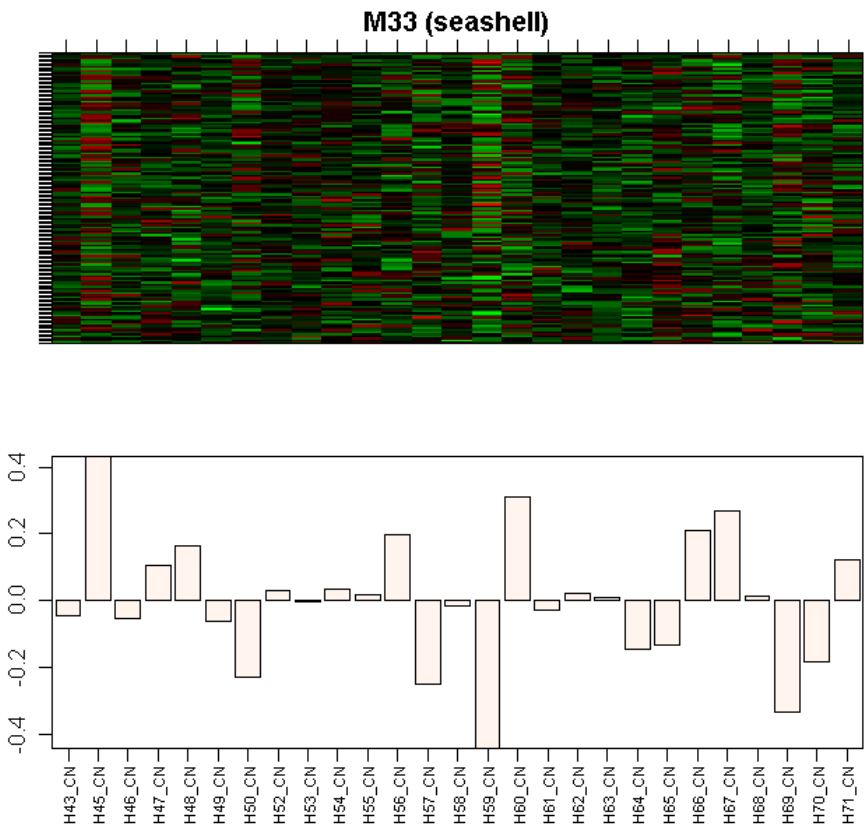
M33 (seashell)
0.4
0.2
0.0
-0.2
-0.4
H43_CN
H45_CN
H46_CN
H47_CN
H48_CN
H49_CN
H50_CN
H52_CN
H53_CN
H54_CN
H55_CN
H56_CN
H57_CN
H58_CN
H59_CN
H60_CN
H61_CN
H62_CN
H63_CN
H64_CN
H65_CN
H66_CN
H67_CN
H68_CN
H69_CN
H70_CN
H71_CN

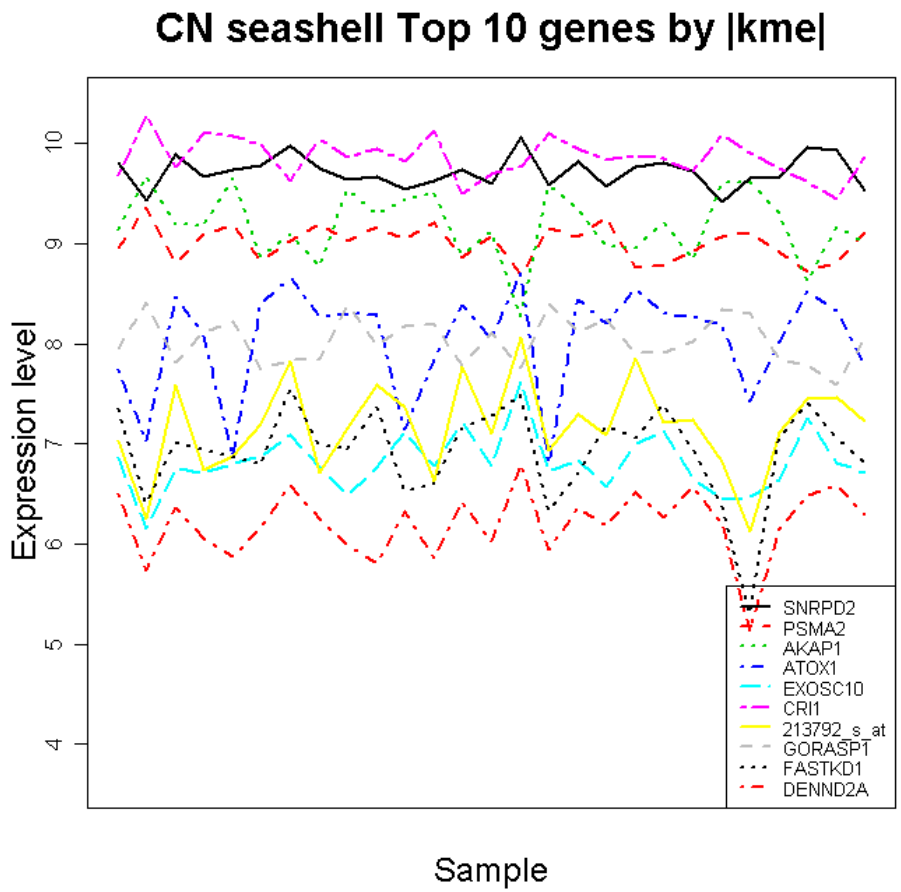
CN seashell Top 10 genes by |kme|
Expression level
4
5
6
7
8
9
10
Sample
SNRPD2
PSMA2
AKAP1
ATOX1
EXOSC10
CRI1
213792_s_at
GORASP1
FASTKD1
DENND2A

Figure S2AY

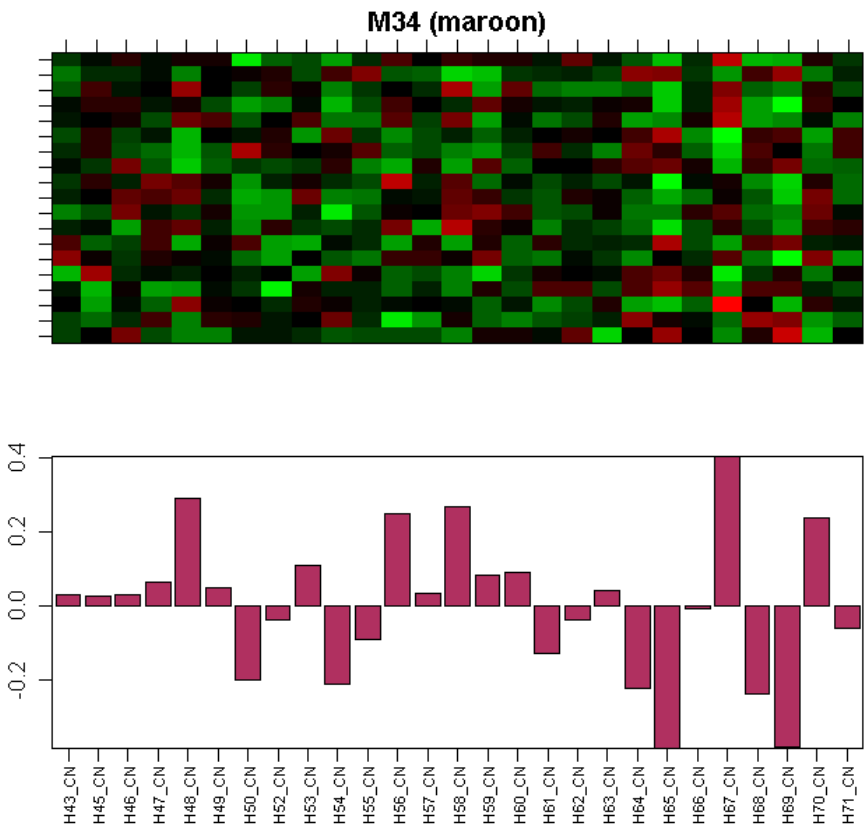
M34 (maroon)
0.4
0.2
0.0
-0.2
H43_CN
H45_CN
H46_CN
H47_CN
H48_CN
H49_CN
H50_CN
H52_CN
H53_CN
H54_CN
H55_CN
H56_CN
H57_CN
H58_CN
H59_CN
H60_CN
H61_CN
H62_CN
H63_CN
H64_CN
H65_CN
H66_CN
H67_CN
H68_CN
H69_CN
H70_CN
H71_CN

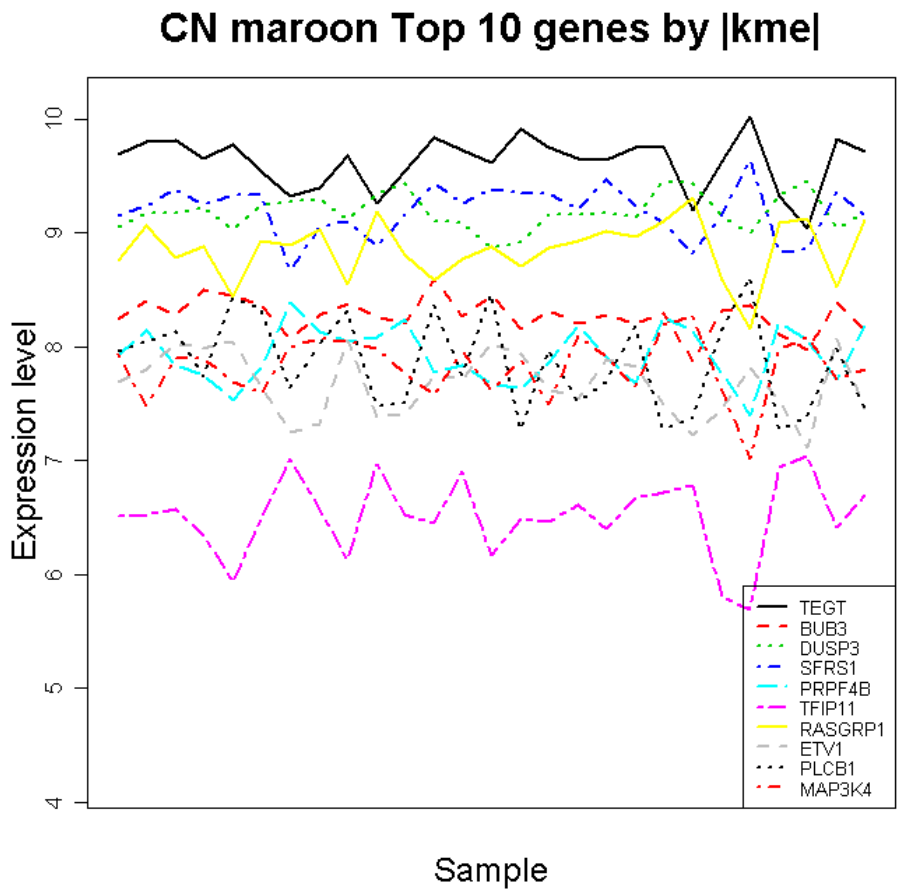
CN maroon Top 10 genes by |kme|
Expression level
Sample
4
5
6
7
8
9
10
TEGT
BUB3
DUSP3
SFRS1
PRPF4B
TFIP11
RASGRP1
ETV1
PLCB1
MAP3K4

Figure S2AZ

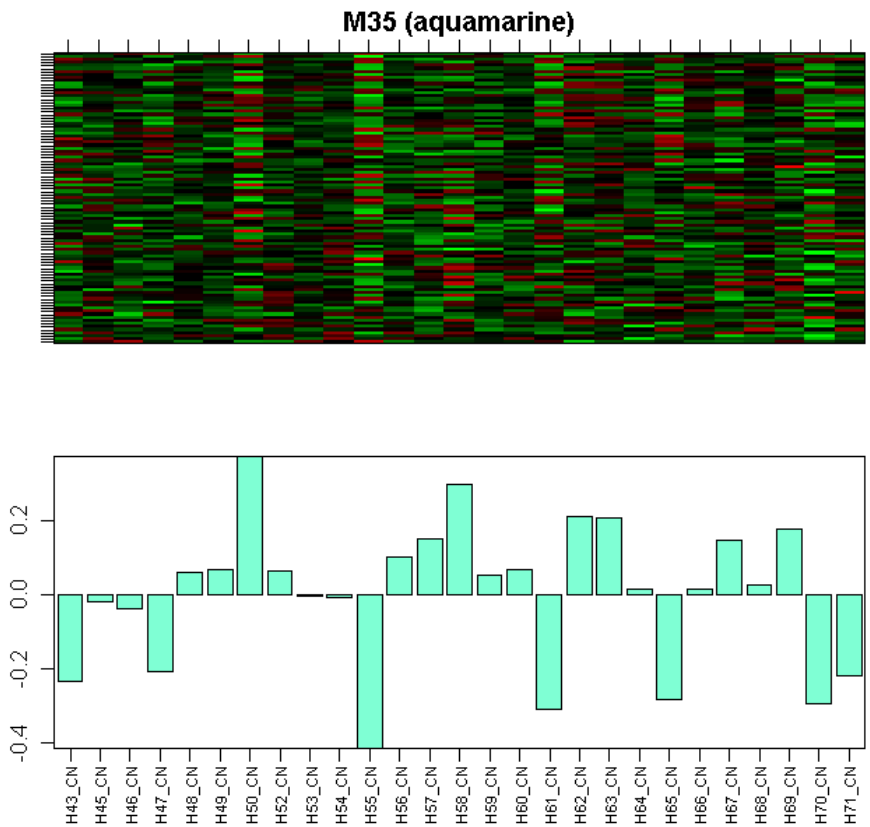
M35 (aquamarine)
0.2
0.0
-0.2
-0.4
H43_CN
H45_CN
H46_CN
H47_CN
H48_CN
H49_CN
H50_CN
H52_CN
H53_CN
H54_CN
H55_CN
H56_CN
H57_CN
H58_CN
H59_CN
H60_CN
H61_CN
H62_CN
H63_CN
H64_CN
H65_CN
H66_CN
H67_CN
H68_CN
H69_CN
H70_CN
H71_CN

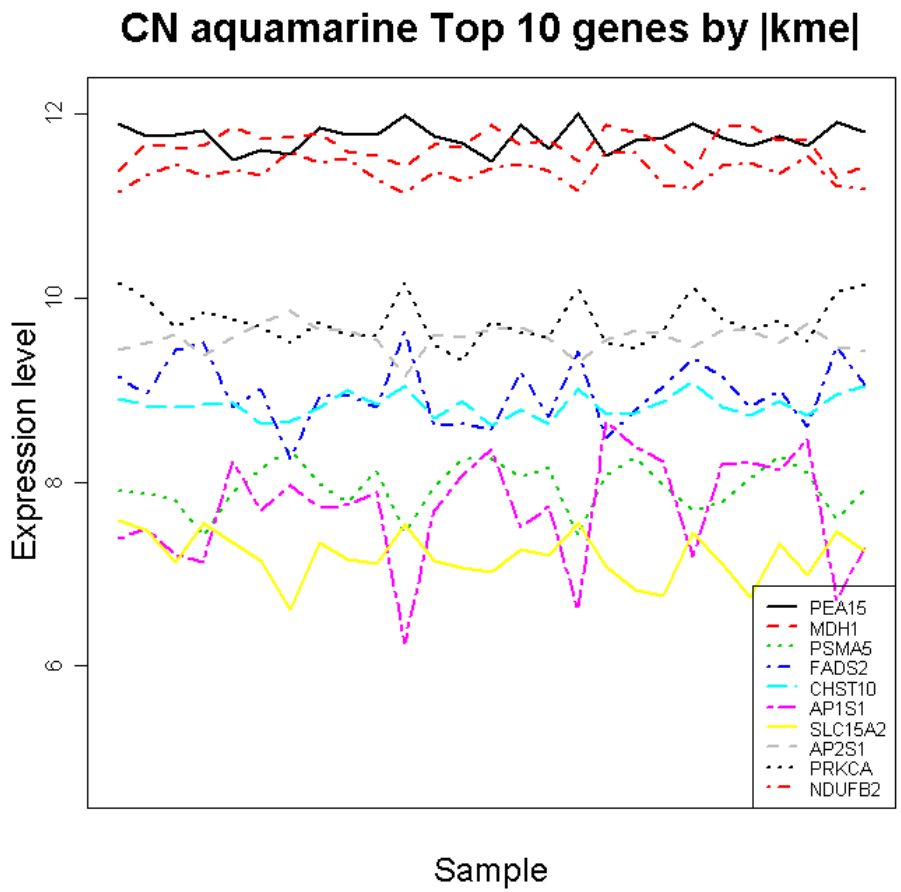
CN aquamarine Top 10 genes by |kme|
Expression level
12
10
8
6
Sample
PEA15
MDH1
PSMA5
FADS2
CHST10
AP1S1
SLC15A2
AP2S1
PRKCA
NDUFB2

Figure S2BA

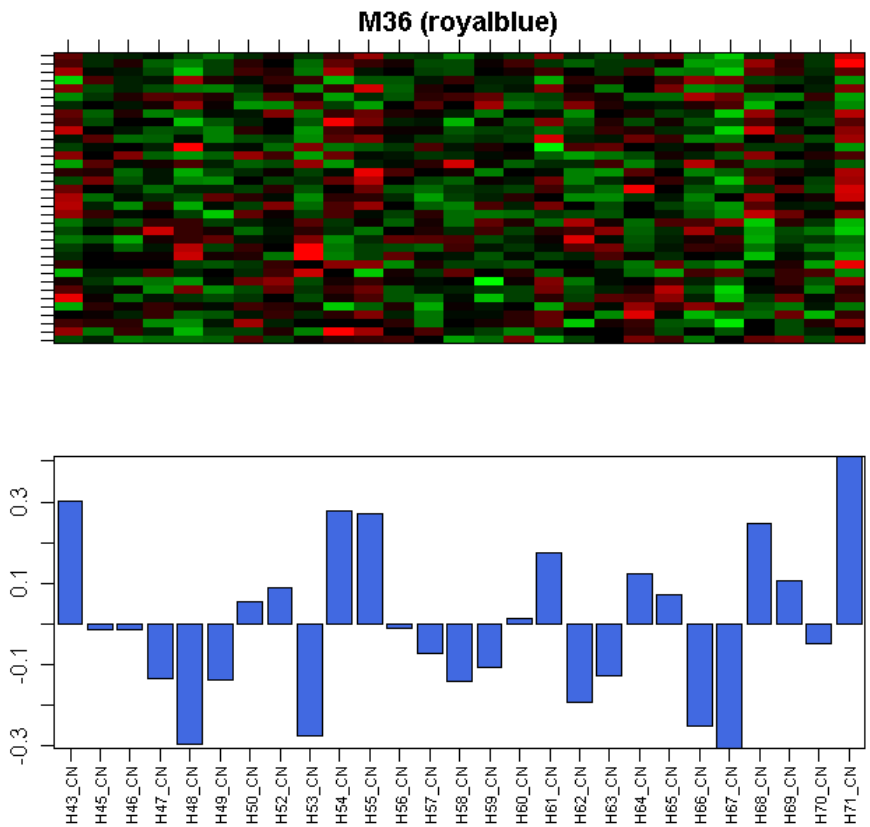
M36 (royalblue)
0.3
0.1
-0.1
-0.3
H43_CN
H45_CN
H46_CN
H47_CN
H48_CN
H49_CN
H50_CN
H52_CN
H53_CN
H54_CN
H55_CN
H56_CN
H57_CN
H58_CN
H59_CN
H60_CN
H61_CN
H62_CN
H63_CN
H64_CN
H65_CN
H66_CN
H67_CN
H68_CN
H69_CN
H70_CN
H71_CN

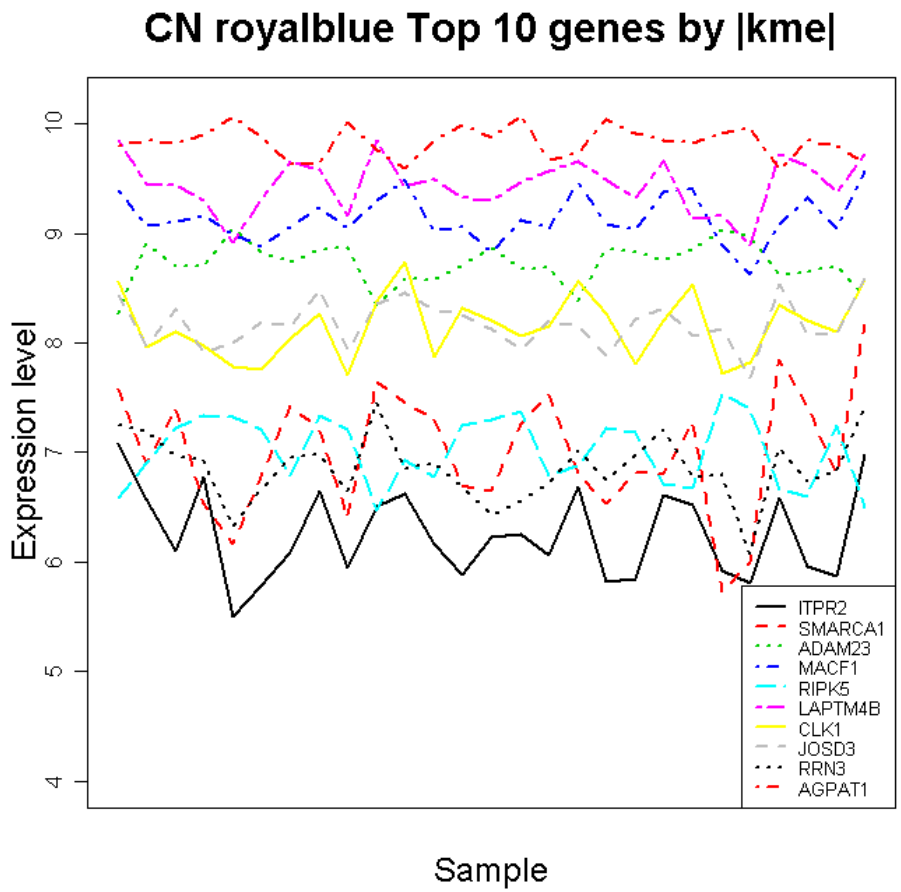
CN royalblue Top 10 genes by |kme|
Expression level
4
5
6
7
8
9
10
Sample
ITPR2
SMARCA1
ADAM23
MACF1
RIPK5
LAPTM4B
CLK1
JOSD3
RRN3
AGPAT1

Figure S2BB

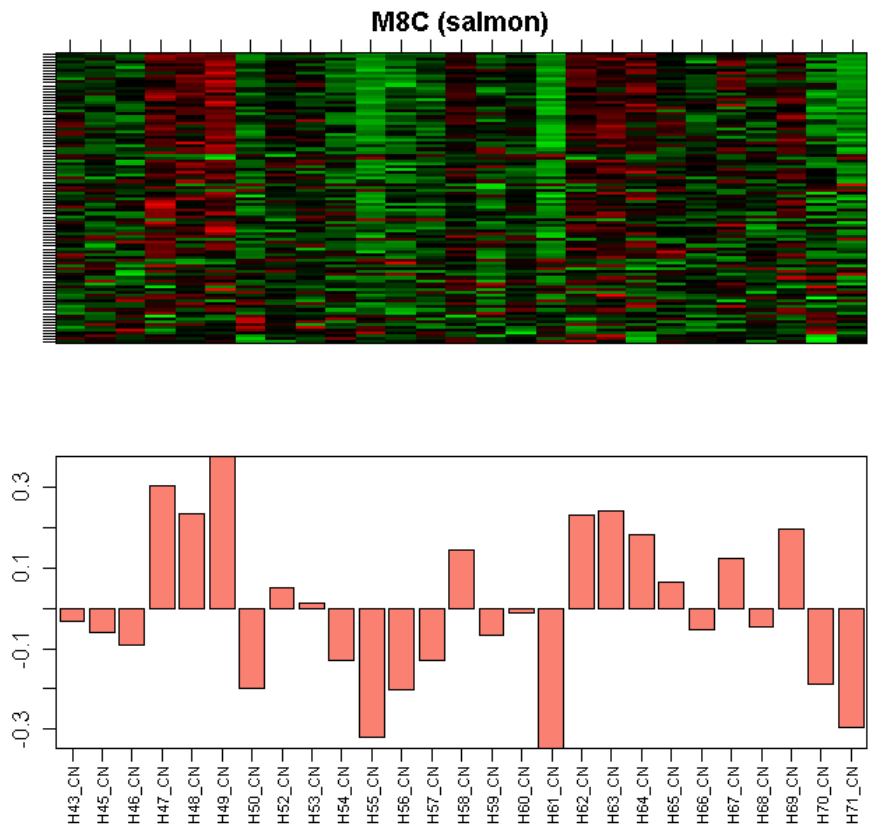
M8C (salmon)
0.3
0.1
-0.1
-0.3
H43_CN
H45_CN
H46_CN
H47_CN
H48_CN
H49_CN
H50_CN
H52_CN
H53_CN
H54_CN
H55_CN
H56_CN
H57_CN
H58_CN
H59_CN
H60_CN
H61_CN
H62_CN
H63_CN
H64_CN
H65_CN
H66_CN
H67_CN
H68_CN
H69_CN
H70_CN
H71_CN

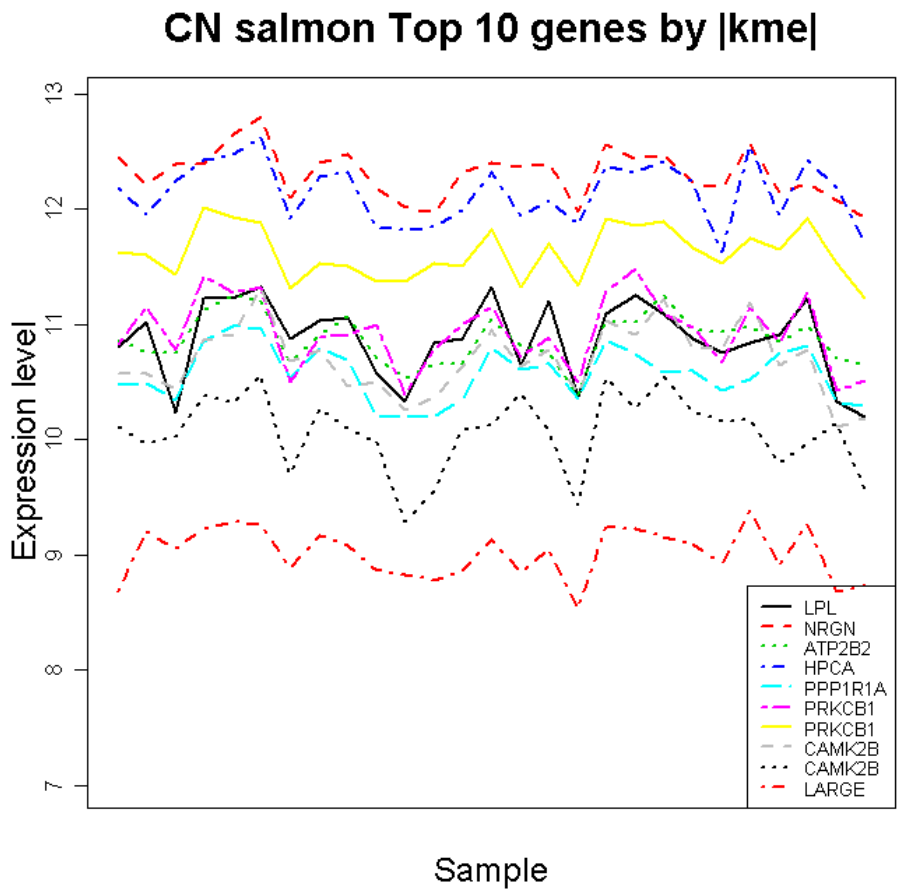
CN salmon Top 10 genes by |kme|
Expression level
13
12
11
10
9
8
7
Sample
LPL
NRGN
ATP2B2
HPCA
PPP1R1A
PRKCB1
PRKCB1
CAMK2B
CAMK2B
LARGE

Figure S2BC

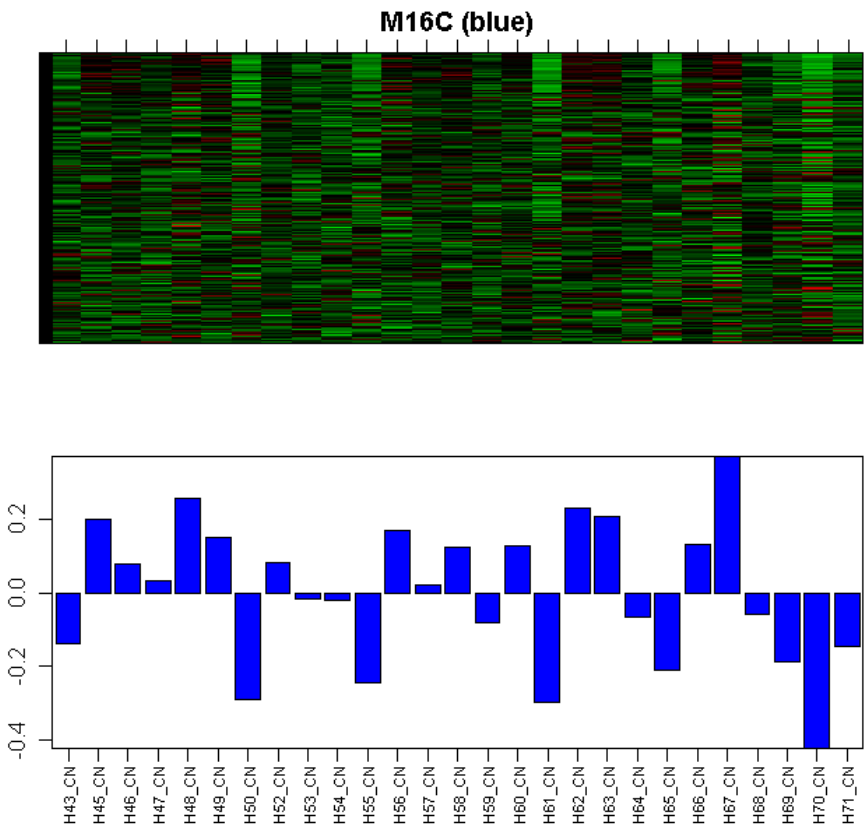
M16C (blue)
0.2
0.0
-0.2
-0.4
H43_CN
H45_CN
H46_CN
H47_CN
H48_CN
H49_CN
H50_CN
H52_CN
H53_CN
H54_CN
H55_CN
H56_CN
H57_CN
H58_CN
H59_CN
H60_CN
H61_CN
H62_CN
H63_CN
H64_CN
H65_CN
H66_CN
H67_CN
H68_CN
H69_CN
H70_CN
H71_CN

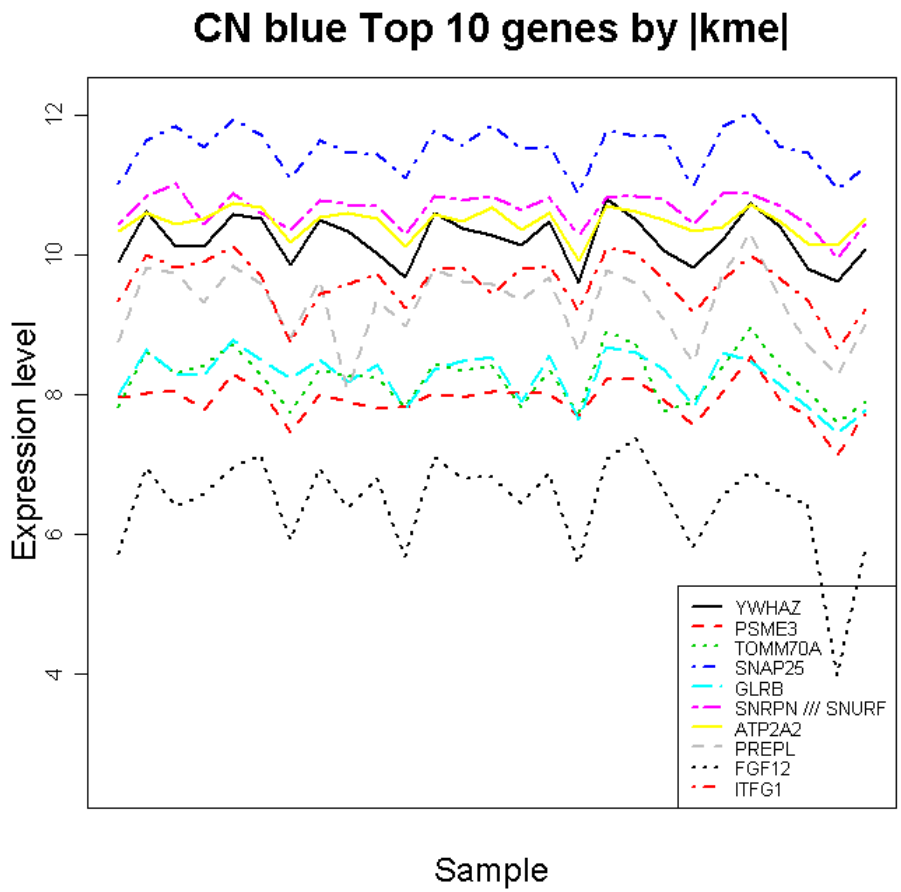
CN blue Top 10 genes by |kme|
Expression level
12
10
8
6
4
Sample
YWHAZ
PSME3
TOMM70A
SNAP25
GLRB
SNRPN /// SNURF
ATP2A2
PREPL
FGF12
ITFG1

Figure S2BD

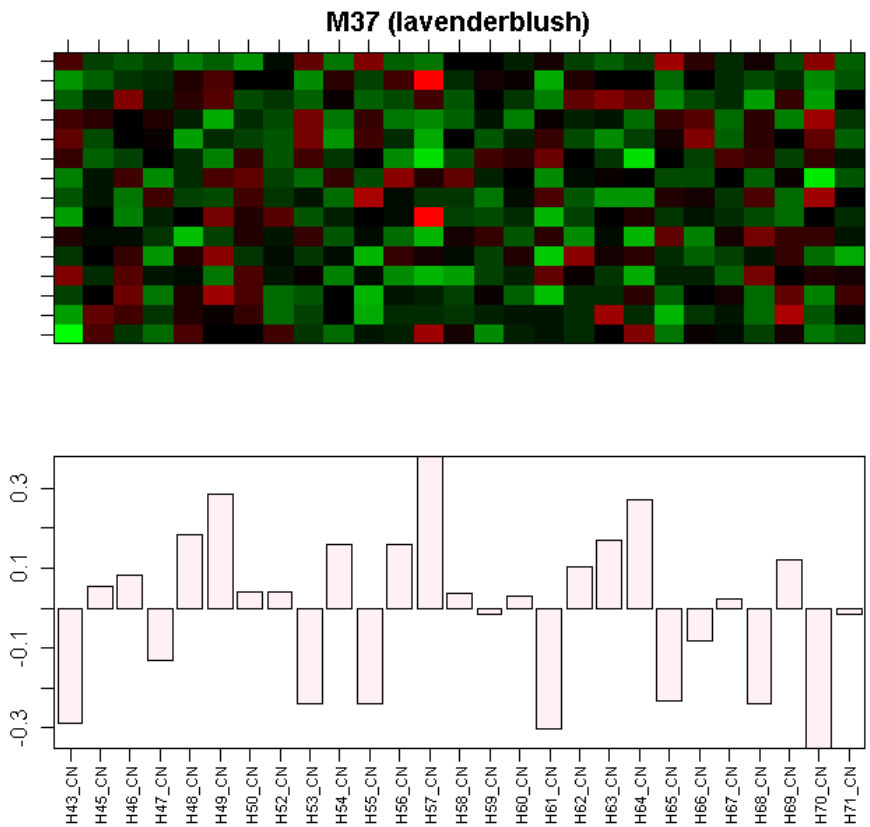
M37 (lavenderblush)
0.3
0.1
-0.1
-0.3
H43_CN
H45_CN
H46_CN
H47_CN
H48_CN
H49_CN
H50_CN
H52_CN
H53_CN
H54_CN
H55_CN
H56_CN
H57_CN
H58_CN
H59_CN
H60_CN
H61_CN
H62_CN
H63_CN
H64_CN
H65_CN
H66_CN
H67_CN
H68_CN
H69_CN
H70_CN
H71_CN

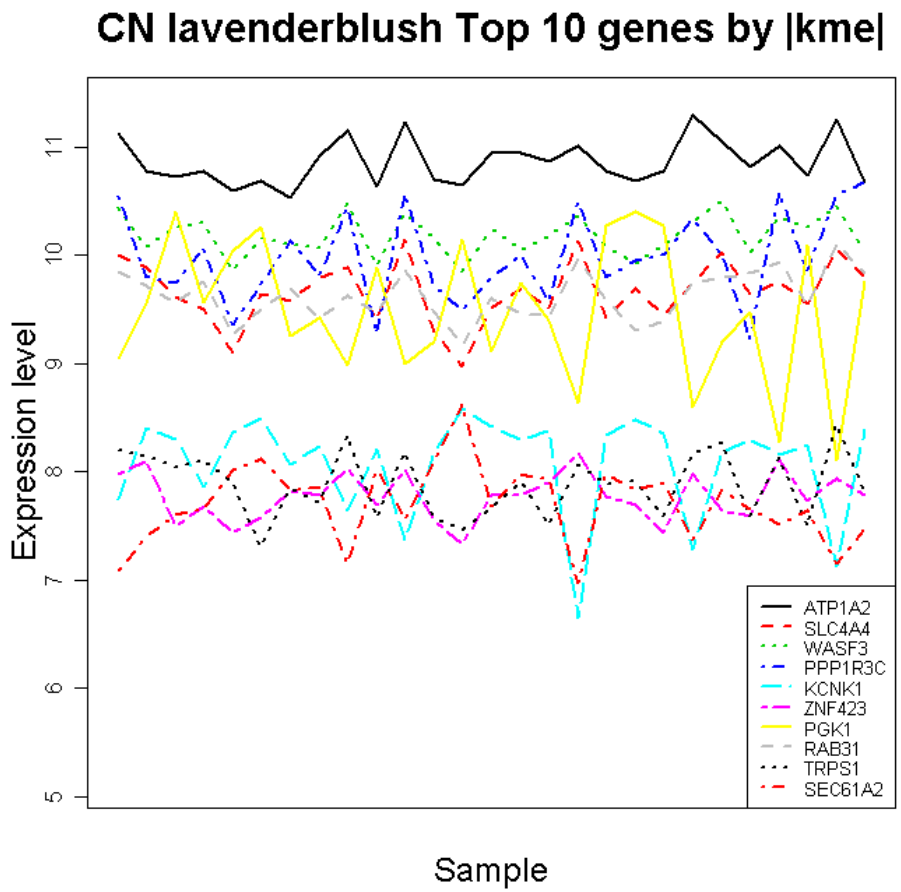
CN lavenderblush Top 10 genes by |kme|
Expression level
5
6
7
8
9
10
11
Sample
ATP1A2
SLC4A4
WASF3
PPP1R3C
KCNK1
ZNF423
PGK1
RAB31
TRPS1
SEC61A2

Figure S2BE

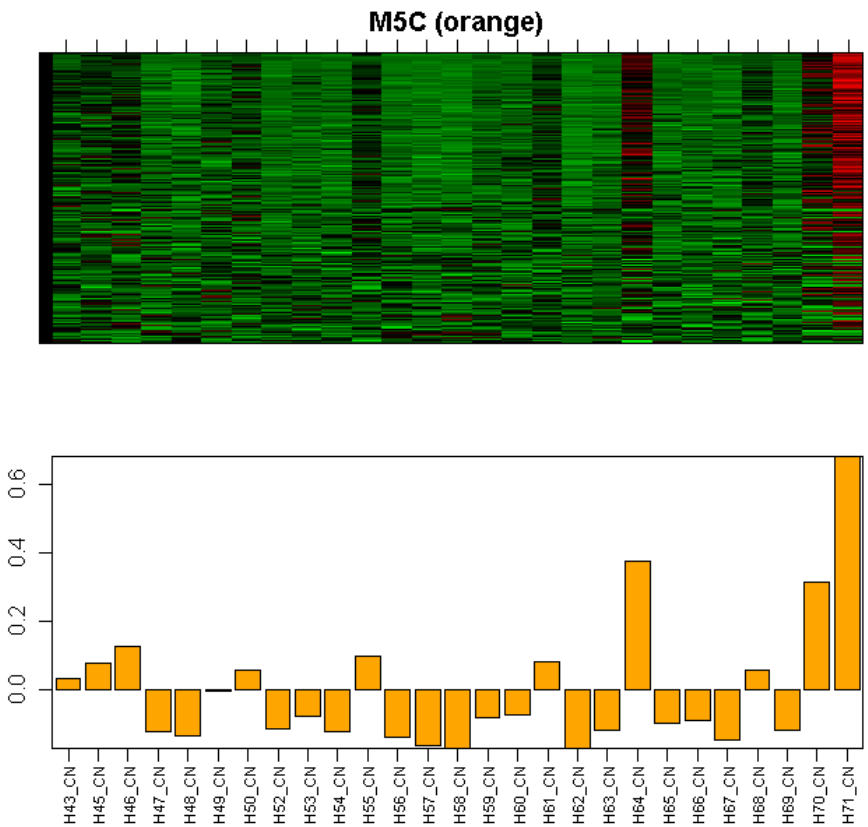
M5C (orange)
0.0
0.2
0.4
0.6
H43_CN
H45_CN
H46_CN
H47_CN
H48_CN
H49_CN
H50_CN
H52_CN
H53_CN
H54_CN
H55_CN
H56_CN
H57_CN
H58_CN
H59_CN
H60_CN
H61_CN
H62_CN
H63_CN
H64_CN
H65_CN
H66_CN
H67_CN
H68_CN
H69_CN
H70_CN
H71_CN

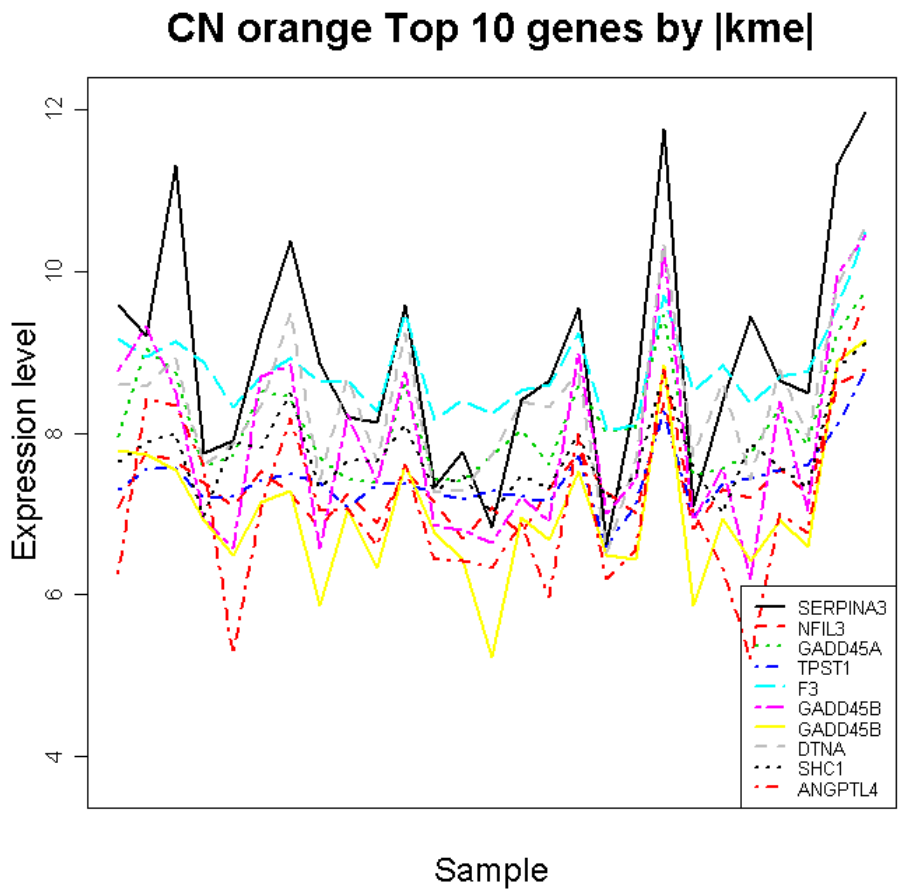
CN orange Top 10 genes by |kme|
Expression level
4
6
8
10
12
Sample
SERPINA3
NFIL3
GADD45A
TPST1
F3
GADD45B
GADD45B
DTNA
SHC1
ANGPTL4

Figure S2BF

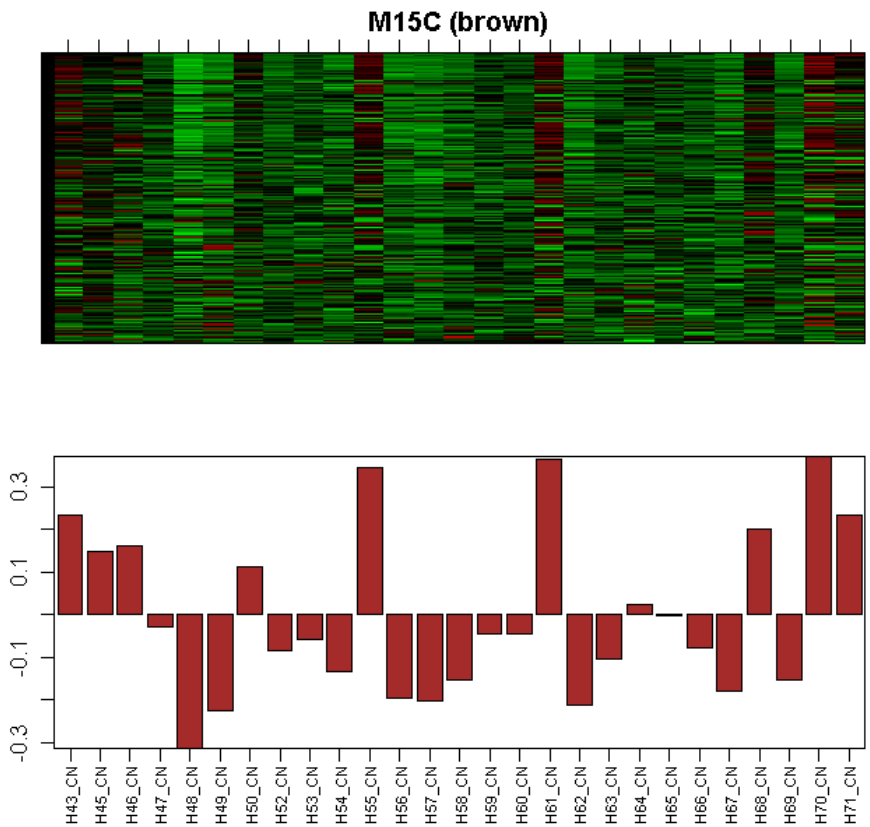
M15C (brown)
0.3
0.1
-0.1
-0.3
H43_CN
H45_CN
H46_CN
H47_CN
H48_CN
H49_CN
H50_CN
H52_CN
H53_CN
H54_CN
H55_CN
H56_CN
H57_CN
H58_CN
H59_CN
H60_CN
H61_CN
H62_CN
H63_CN
H64_CN
H65_CN
H66_CN
H67_CN
H68_CN
H69_CN
H70_CN
H71_CN

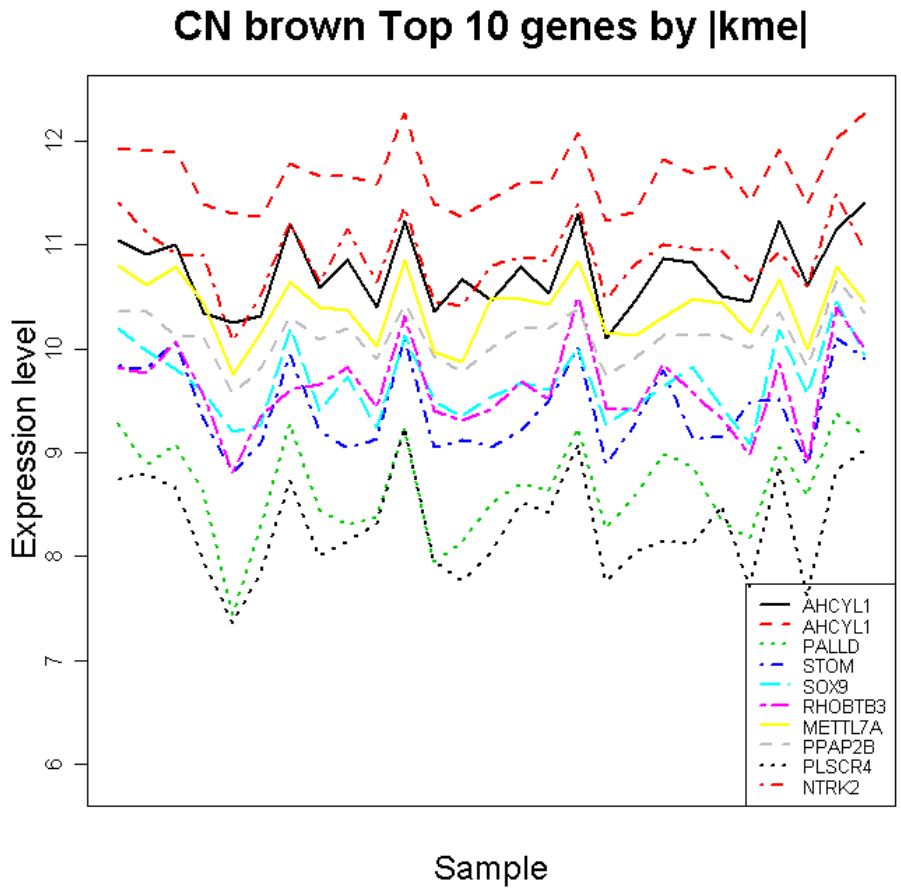
CN brown Top 10 genes by |kme|
Expression level
6
7
8
9
10
11
12
Sample
AHCYL1
AHCYL1
PALLD
STOM
SOX9
RHOBTB3
METTL7A
PPAP2B
PLSCR4
NTRK2

Figure S2BG

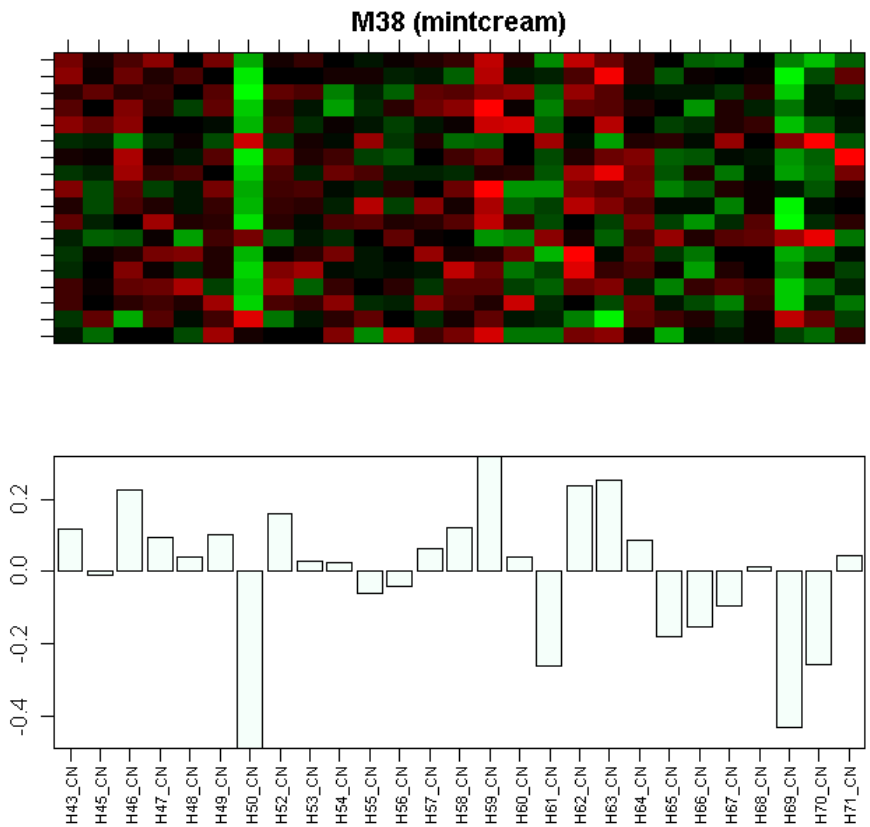
M38 (mintcream)
0.2
0.0
-0.2
-0.4
H43_CN
H45_CN
H46_CN
H47_CN
H48_CN
H49_CN
H50_CN
H52_CN
H53_CN
H54_CN
H55_CN
H56_CN
H57_CN
H58_CN
H59_CN
H60_CN
H61_CN
H62_CN
H63_CN
H64_CN
H65_CN
H66_CN
H67_CN
H68_CN
H69_CN
H70_CN
H71_CN

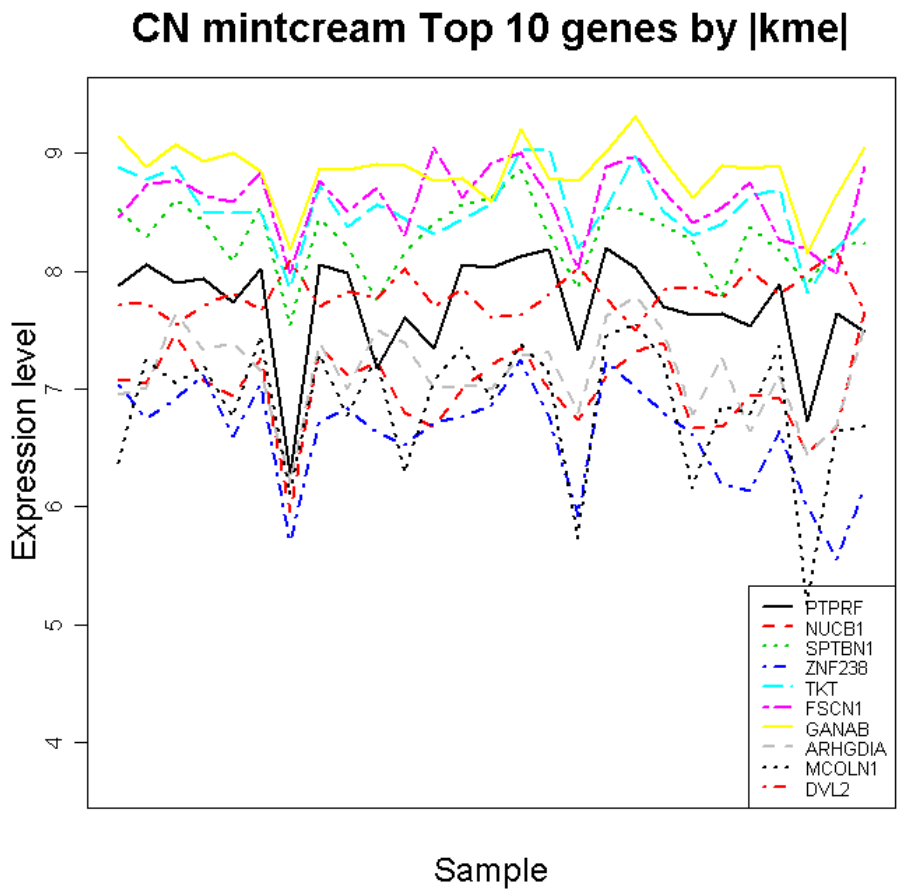
CN mintcream Top 10 genes by |kme|
Expression level
4
5
6
7
8
9
Sample
PTPRF
NUCB1
SPTBN1
ZNF238
TKT
FSCN1
GANAB
ARHGDIA
MCOLN1
DVL2

Figure S2

Cerebellum

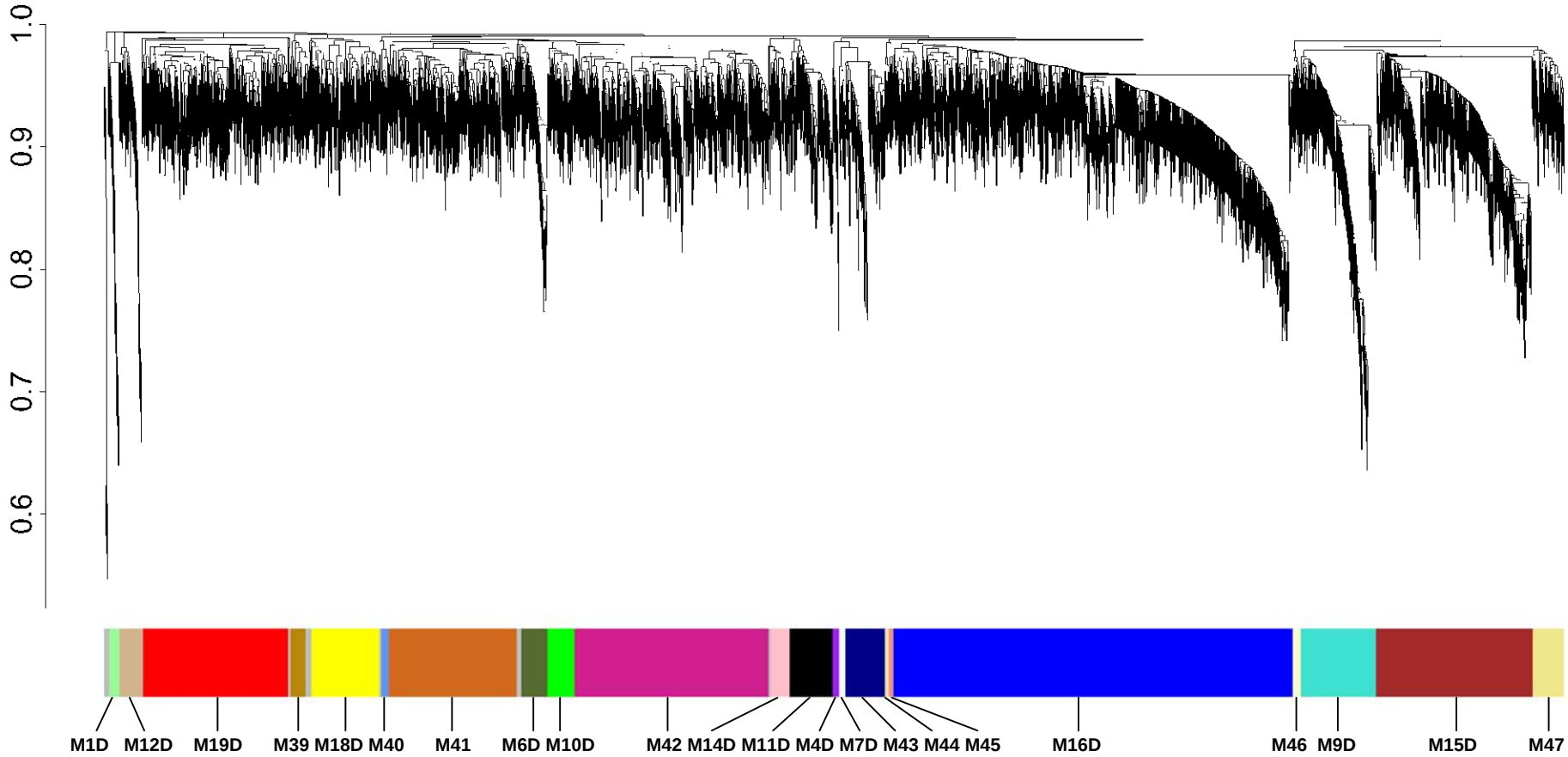

Figure S2BH

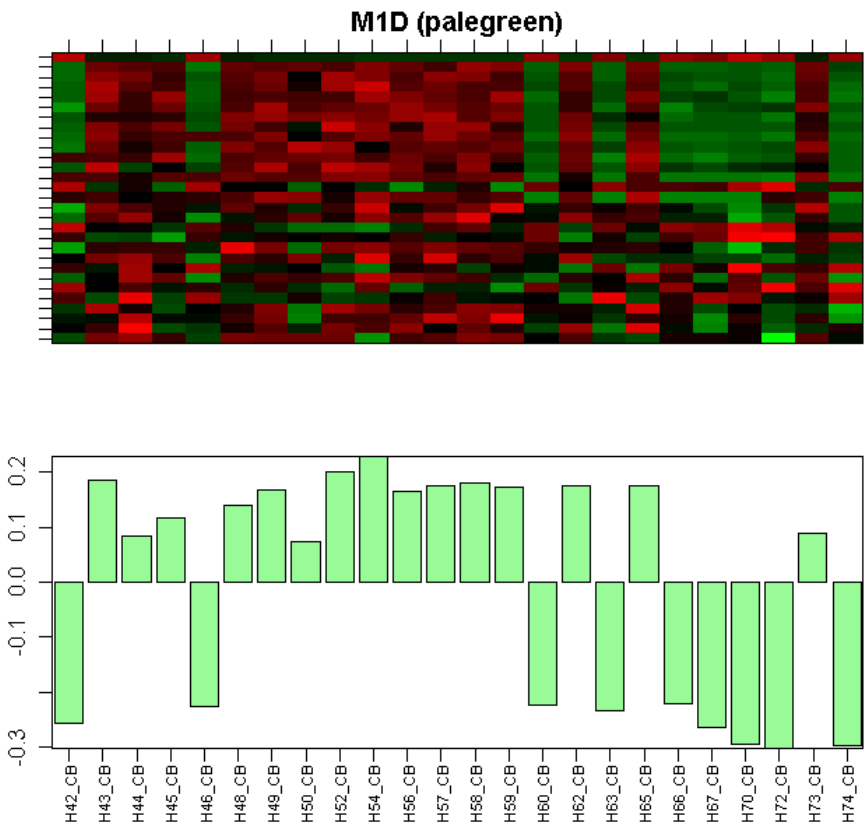
M1D (palegreen)
0.2
0.1
0.0
-0.1
-0.3
H42_CB
H43_CB
H44_CB
H45_CB
H46_CB
H48_CB
H49_CB
H50_CB
H52_CB
H54_CB
H56_CB
H57_CB
H58_CB
H59_CB
H60_CB
H62_CB
H63_CB
H65_CB
H66_CB
H67_CB
H70_CB
H72_CB
H73_CB
H74_CB

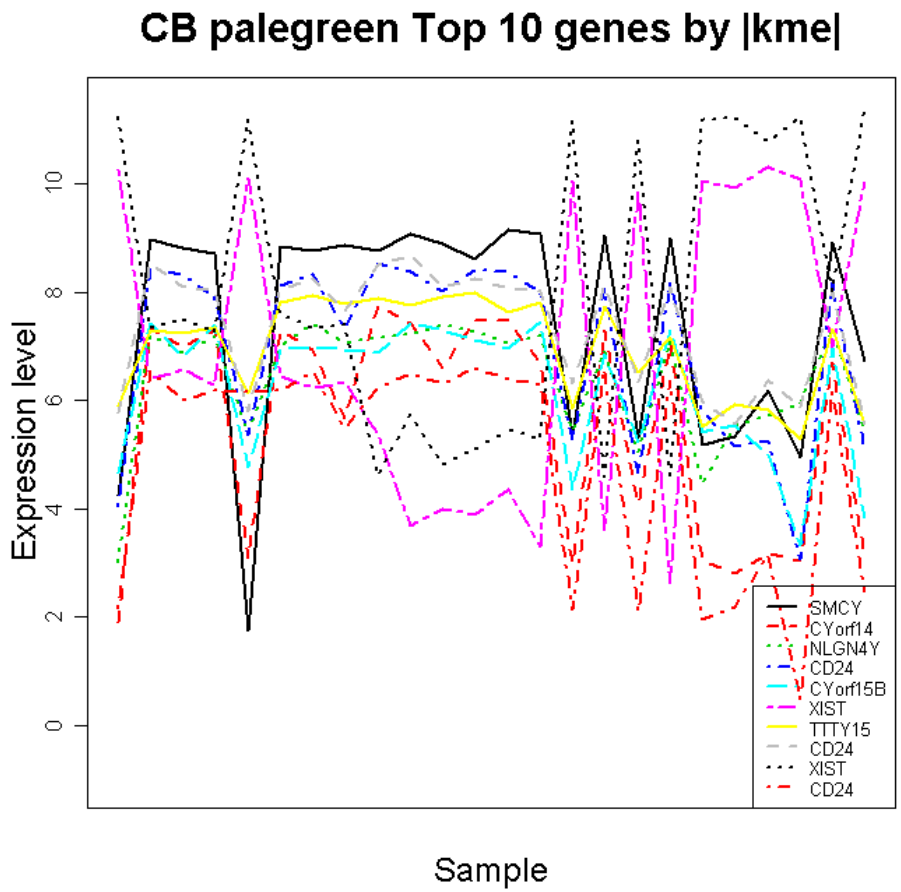
CB palegreen Top 10 genes by |kme|
Expression level
0
2
4
6
8
10
Sample
SMCY
CYorf14
NLGN4Y
CD24
CYorf15B
XIST
TTTY15
CD24
XIST
CD24

Figure S2BI

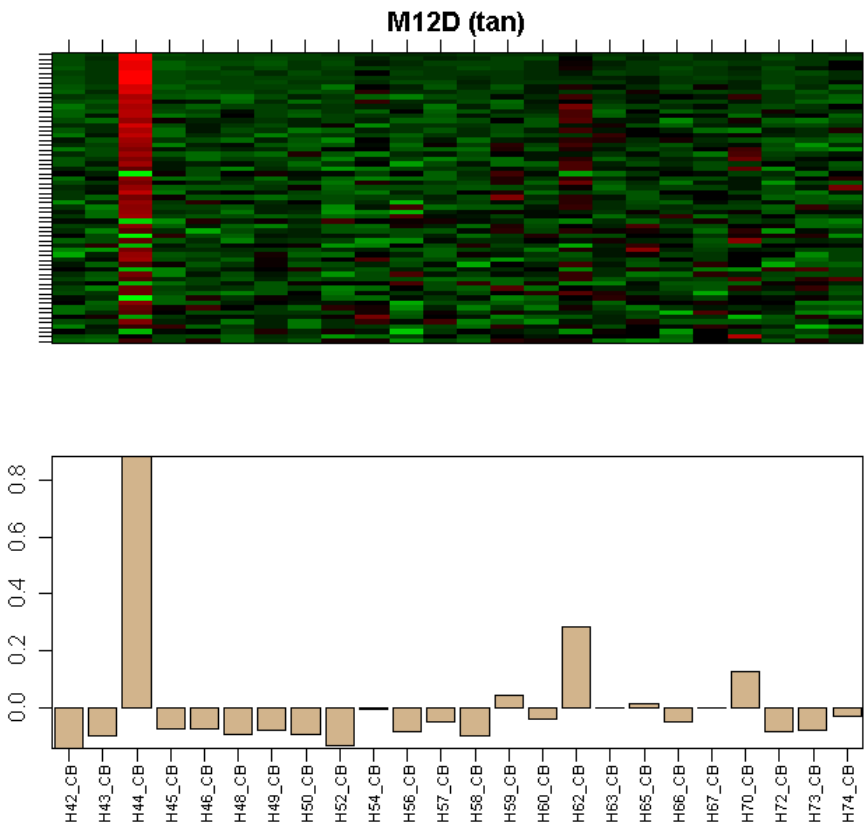
M12D (tan)
0.0
0.2
0.4
0.6
0.8
H42_CB
H43_CB
H44_CB
H45_CB
H46_CB
H48_CB
H49_CB
H50_CB
H52_CB
H54_CB
H56_CB
H57_CB
H58_CB
H59_CB
H60_CB
H62_CB
H63_CB
H65_CB
H66_CB
H67_CB
H70_CB
H72_CB
H73_CB
H74_CB

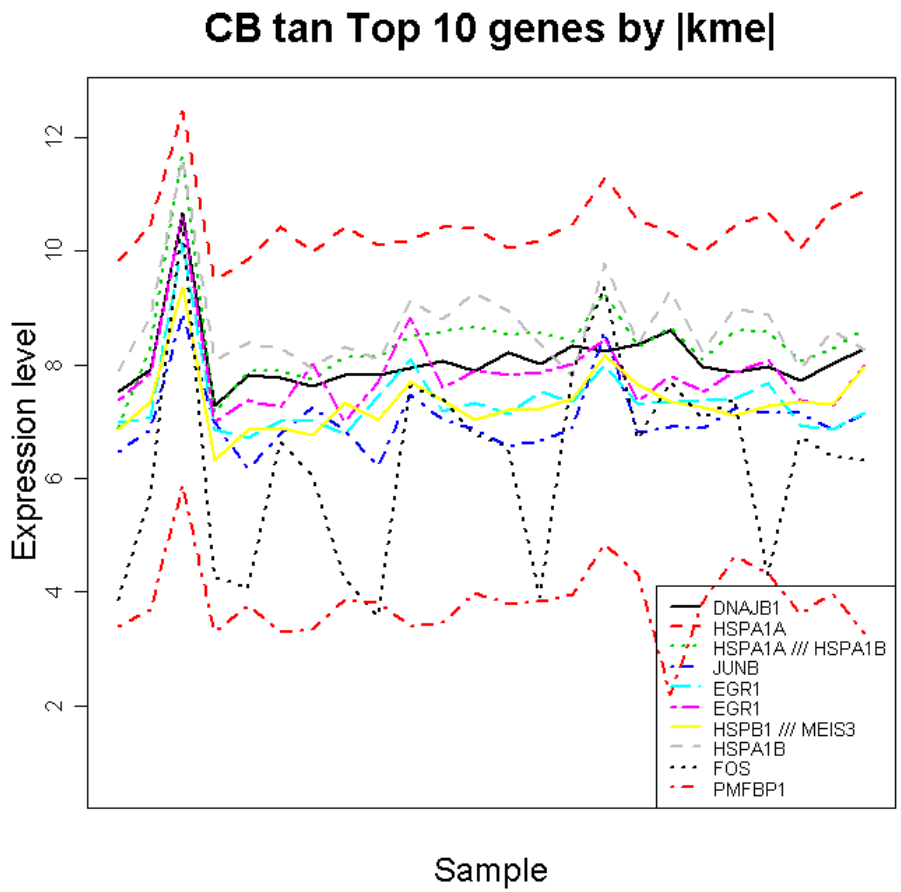
CB tan Top 10 genes by |kme|
Expression level
2
4
6
8
10
12
Sample
DNAJB1
HSPA1A
HSPA1A /// HSPA1B
JUNB
EGR1
EGR1
HSPB1 /// MEIS3
HSPA1B
FOS
PMFBP1

Figure S2BJ

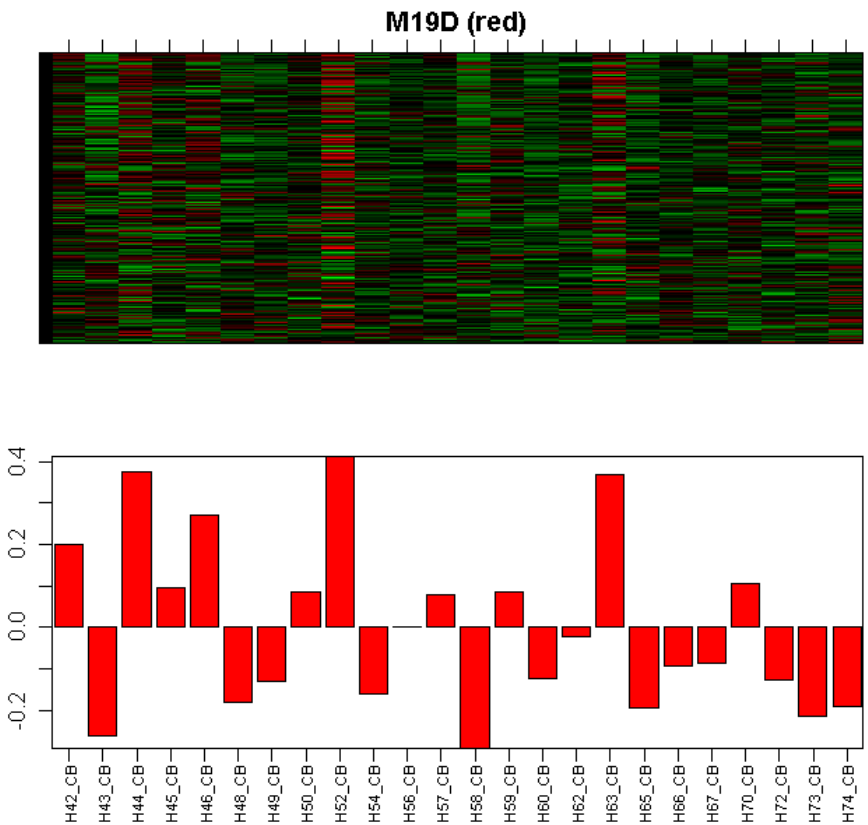
M19D (red)
0.4
0.2
0.0
-0.2
H42_CB
H43_CB
H44_CB
H45_CB
H46_CB
H48_CB
H49_CB
H50_CB
H52_CB
H54_CB
H56_CB
H57_CB
H58_CB
H59_CB
H60_CB
H62_CB
H63_CB
H65_CB
H66_CB
H67_CB
H70_CB
H72_CB
H73_CB
H74_CB

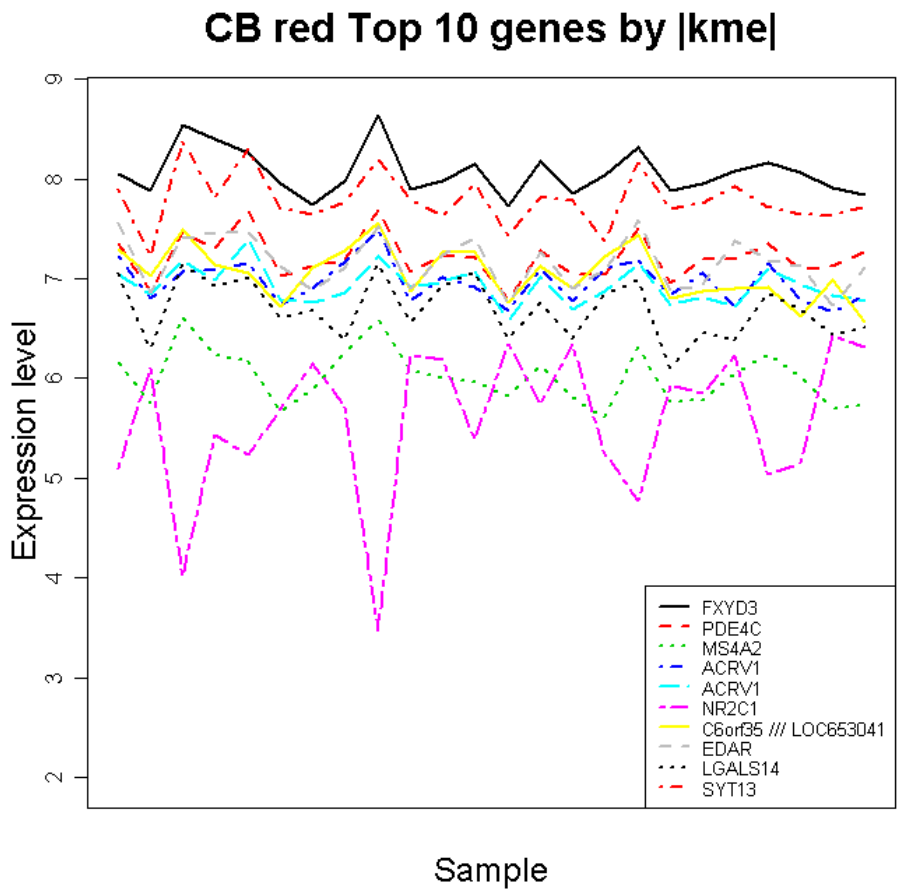
CB red Top 10 genes by |kme|
Expression level
Sample
2
3
4
5
6
7
8
9
FXYD3
PDE4C
MS4A2
ACRV1
ACRV1
NR2C1
C6orf35 /// LOC653041
EDAR
LGALS14
SYT13

Figure S2BK

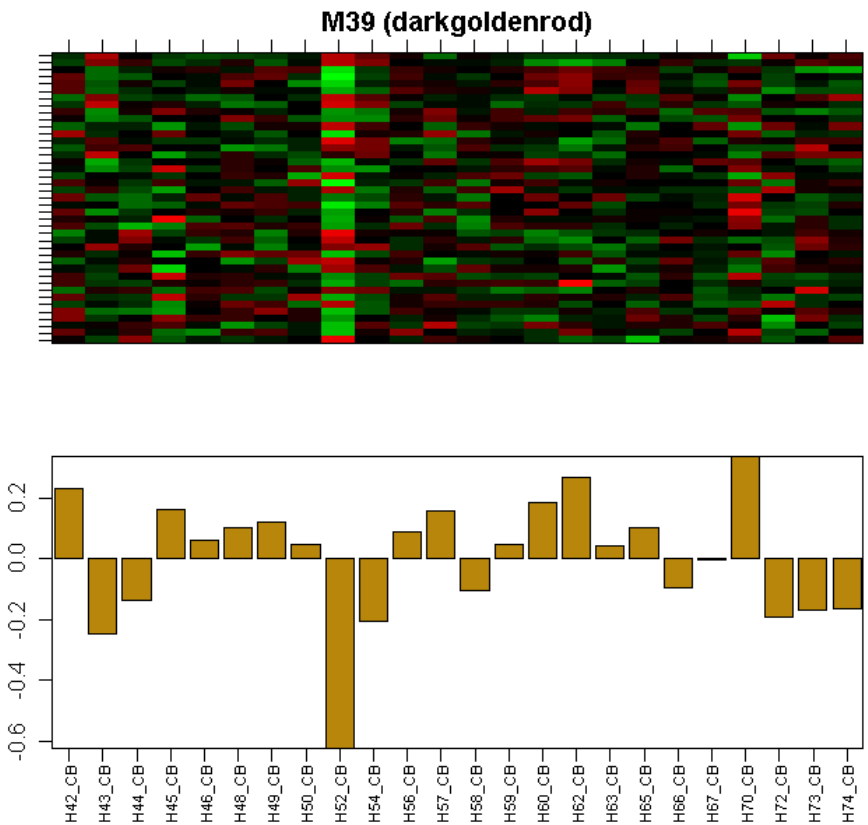
M39 (darkgoldenrod)
0.2
0.0
-0.2
-0.4
-0.6
H42_CB
H43_CB
H44_CB
H45_CB
H46_CB
H48_CB
H49_CB
H50_CB
H52_CB
H54_CB
H56_CB
H57_CB
H58_CB
H59_CB
H60_CB
H62_CB
H63_CB
H65_CB
H66_CB
H67_CB
H70_CB
H72_CB
H73_CB
H74_CB

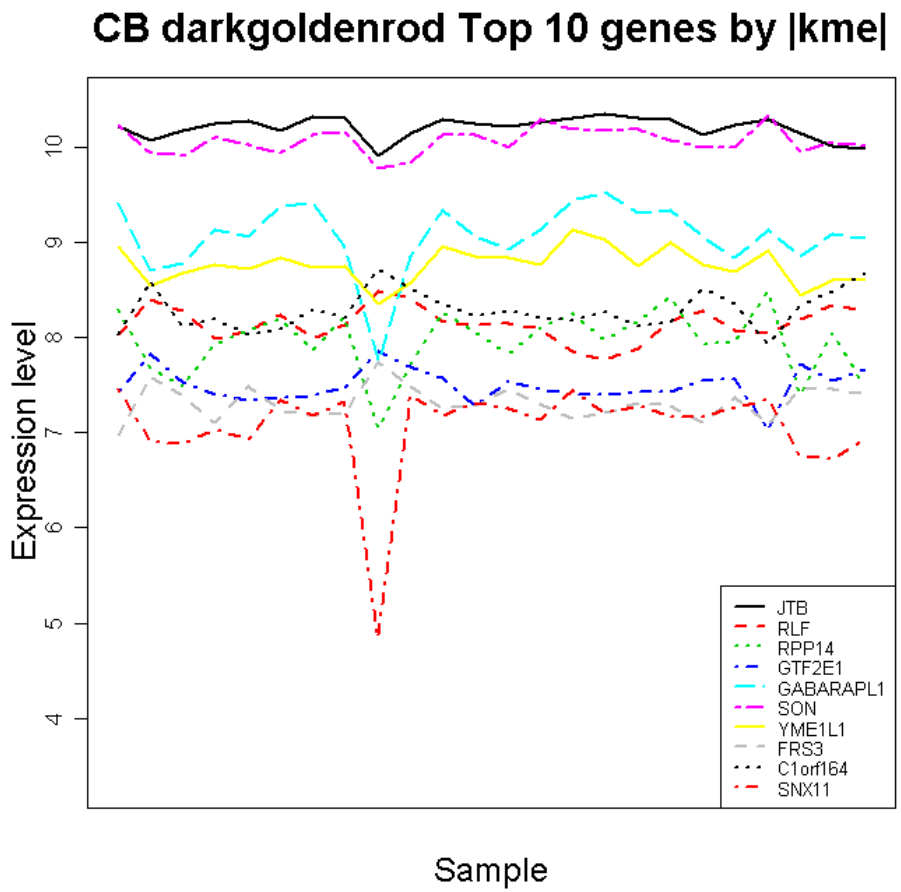
CB darkgoldenrod Top 10 genes by |kme|
Expression level
10
9
8
7
6
5
4
Sample
JTB
RLF
RPP14
GTF2E1
GABARAPL1
SON
YME1L1
FRS3
C1orf164
SNX11

Figure S2BL

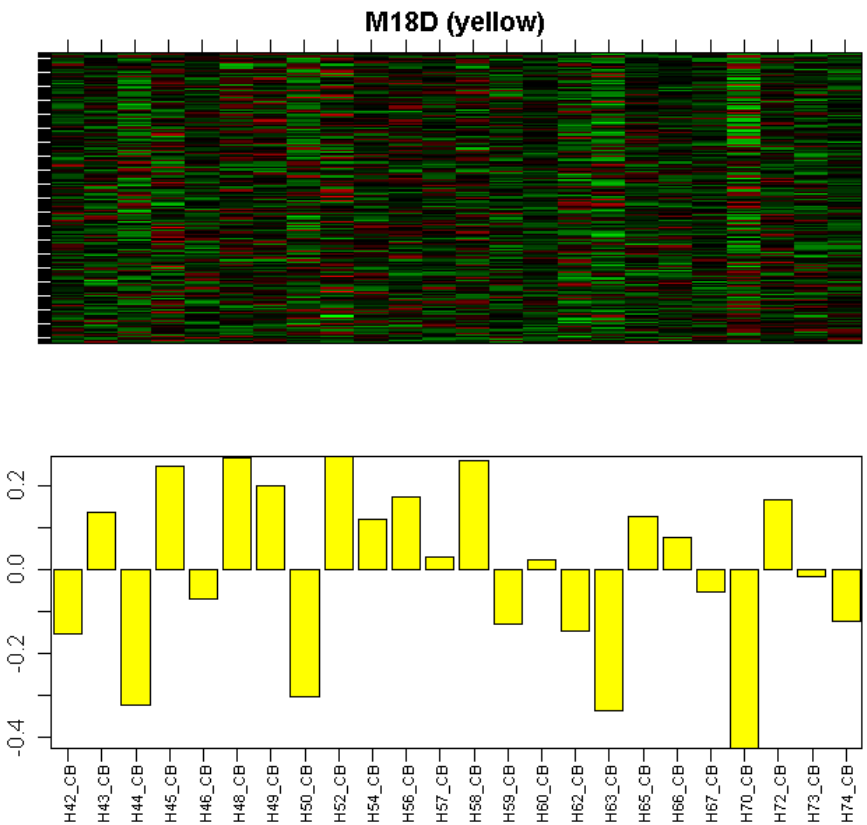
M18D (yellow)
0.2
0.0
-0.2
-0.4
H42_CB
H43_CB
H44_CB
H45_CB
H46_CB
H48_CB
H49_CB
H50_CB
H52_CB
H54_CB
H56_CB
H57_CB
H58_CB
H59_CB
H60_CB
H62_CB
H63_CB
H65_CB
H66_CB
H67_CB
H70_CB
H72_CB
H73_CB
H74_CB

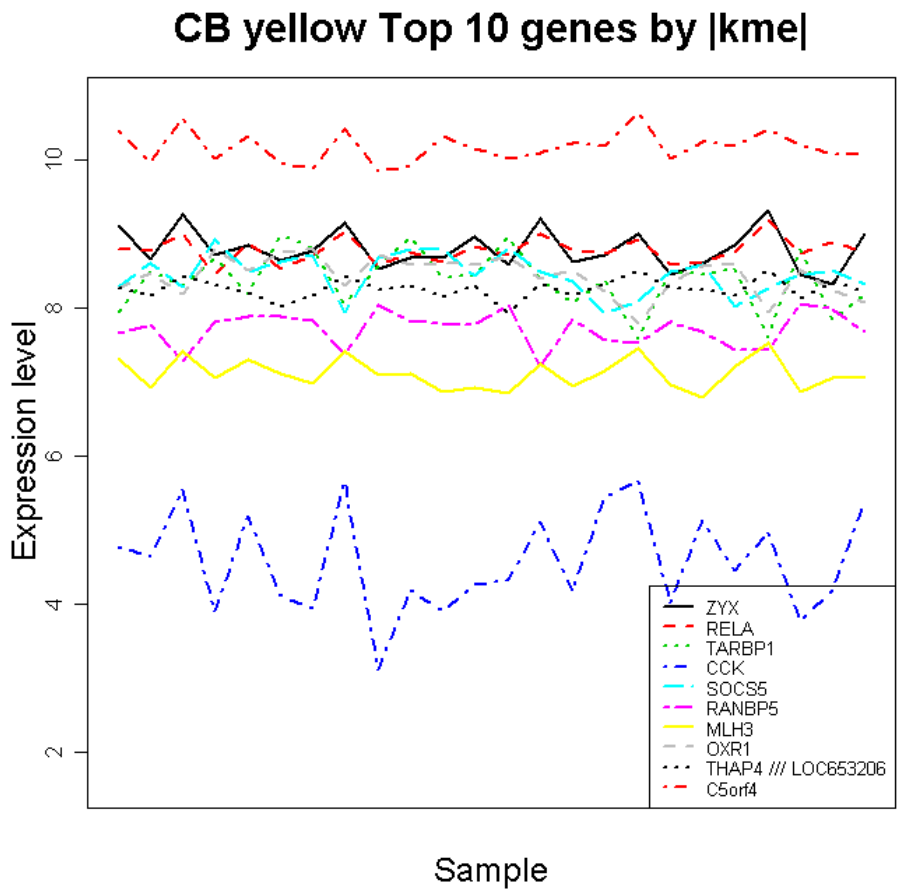
CB yellow Top 10 genes by |kme|
Expression level
2
4
6
8
10
Sample
ZYX
RELA
TARBP1
CCK
SOCS5
RANBP5
MLH3
OXR1
THAP4 /// LOC653206
C5orf4

Figure S2BM

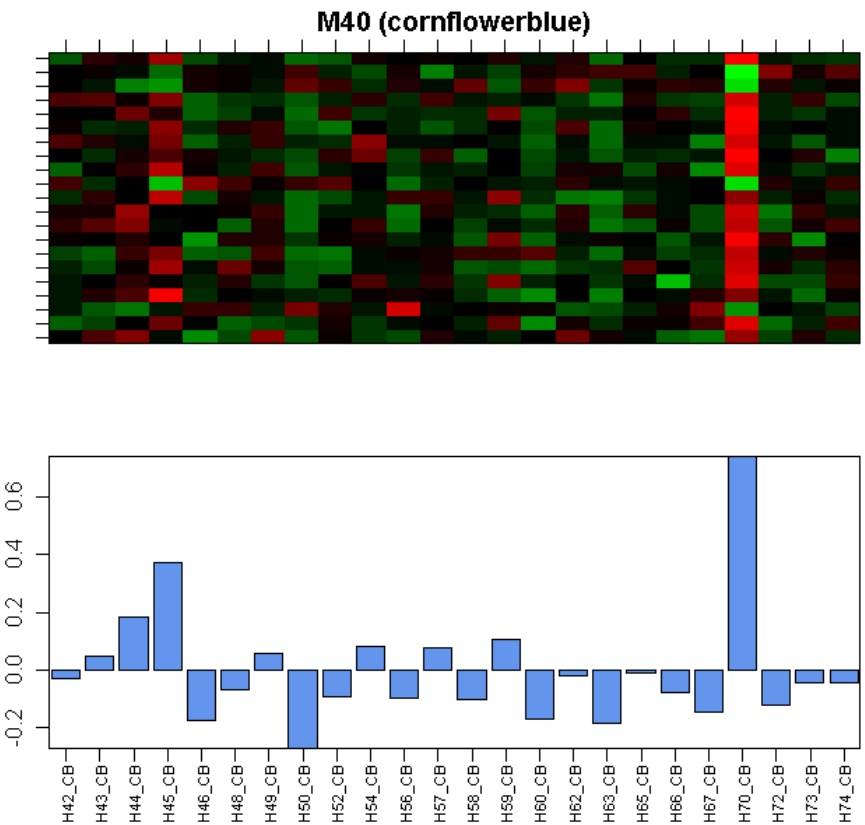
M40 (cornflowerblue)
-0.2
0.0
0.2
0.4
0.6
H42_CB
H43_CB
H44_CB
H45_CB
H46_CB
H48_CB
H49_CB
H50_CB
H52_CB
H54_CB
H56_CB
H57_CB
H58_CB
H59_CB
H60_CB
H62_CB
H63_CB
H65_CB
H66_CB
H67_CB
H70_CB
H72_CB
H73_CB
H74_CB

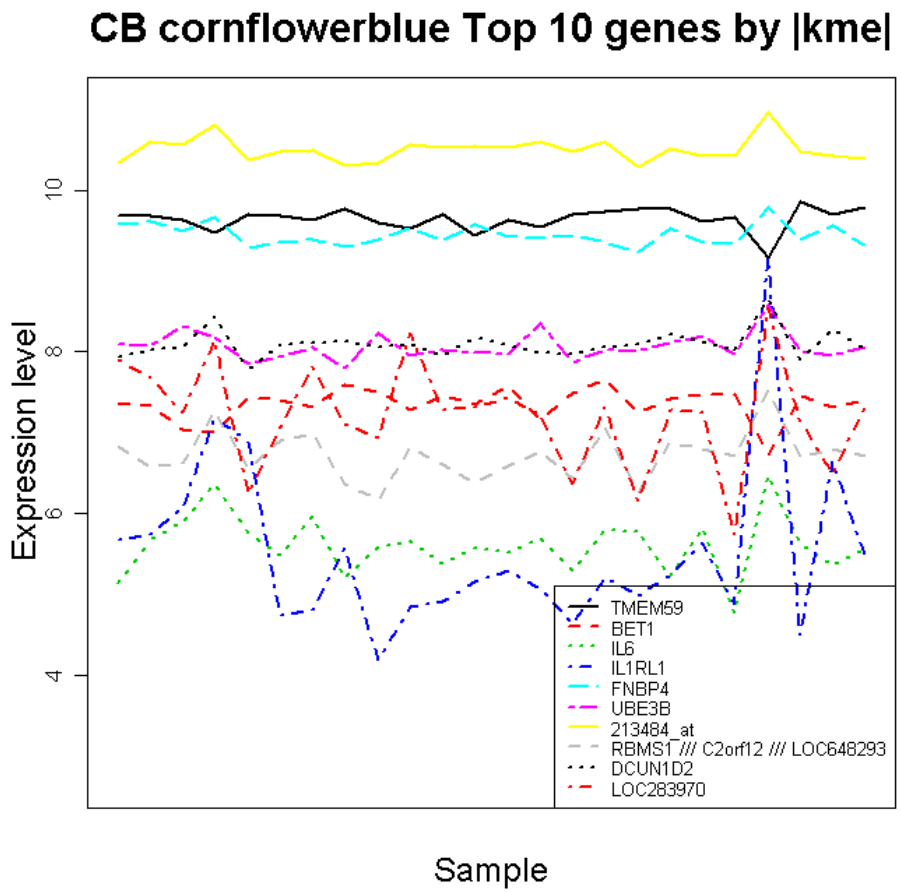
CB cornflowerblue Top 10 genes by |kme|
Expression level
4
6
8
10
Sample
TMEM59
BET1
IL6
IL1RL1
FNBP4
UBE3B
213484_at
RBMS1 /// C2orf12 /// LOC648293
DCUN1D2
LOC283970

Figure S2BN

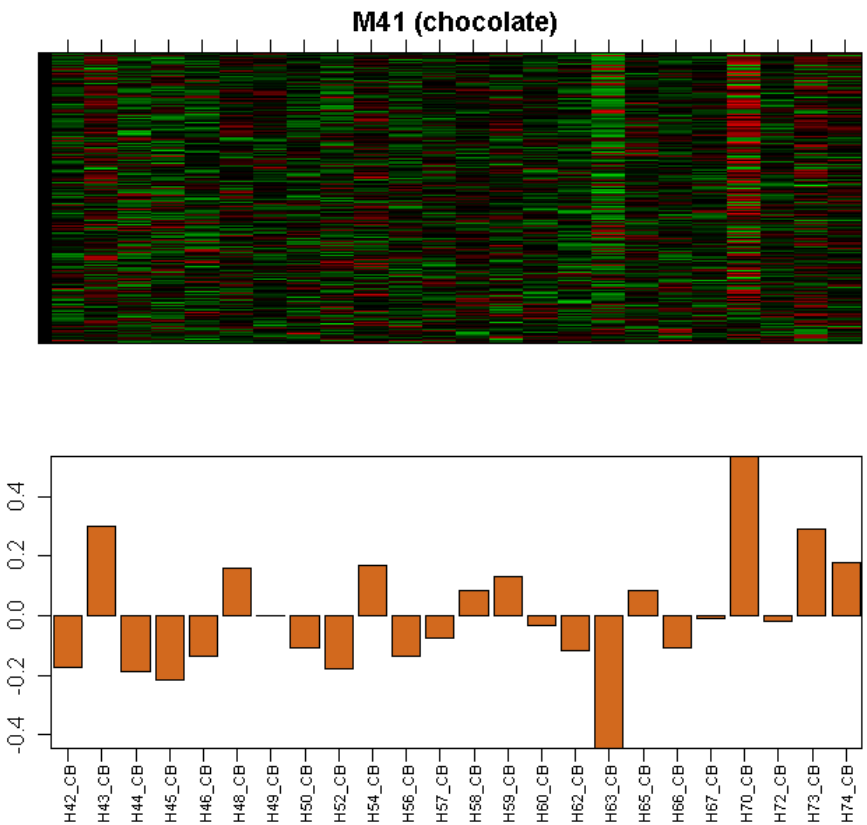
M41 (chocolate)
0.4
0.2
0.0
-0.2
-0.4
H42_CB
H43_CB
H44_CB
H45_CB
H46_CB
H48_CB
H49_CB
H50_CB
H52_CB
H54_CB
H56_CB
H57_CB
H58_CB
H59_CB
H60_CB
H62_CB
H63_CB
H65_CB
H66_CB
H67_CB
H70_CB
H72_CB
H73_CB
H74_CB

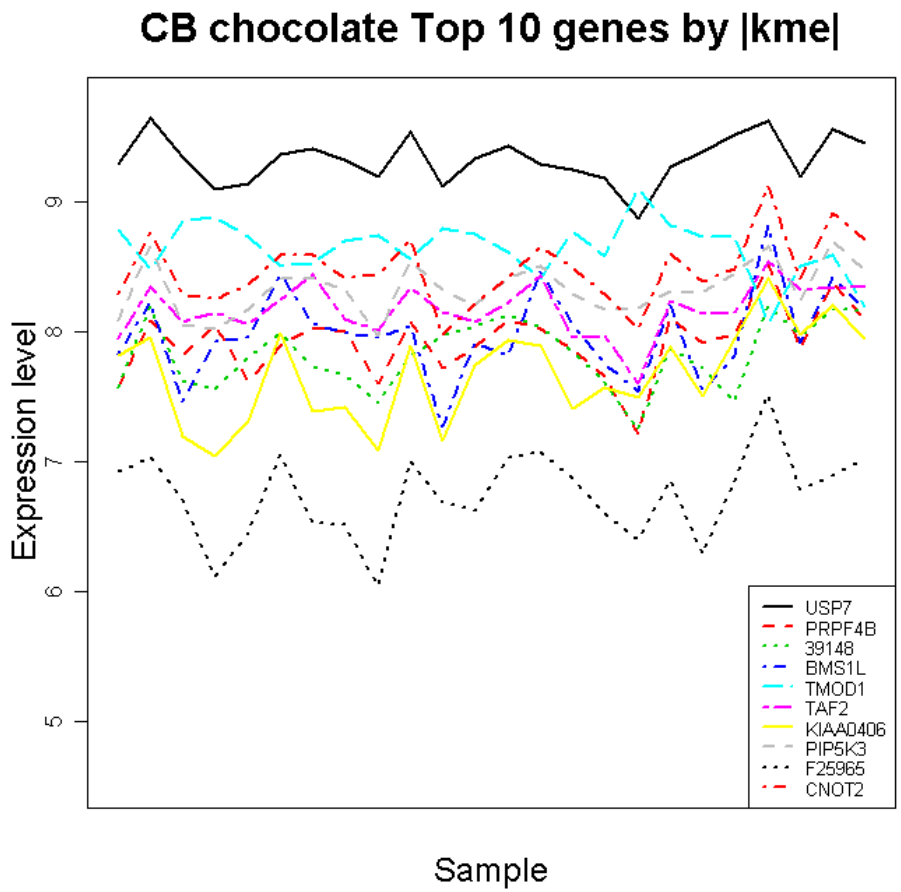
CB chocolate Top 10 genes by |kme|
Expression level
9
8
7
6
5
Sample
USP7
PRPF4B
39148
BMS1L
TMOD1
TAF2
KIAA0406
PIP5K3
F25965
CNOT2

Figure S2BO

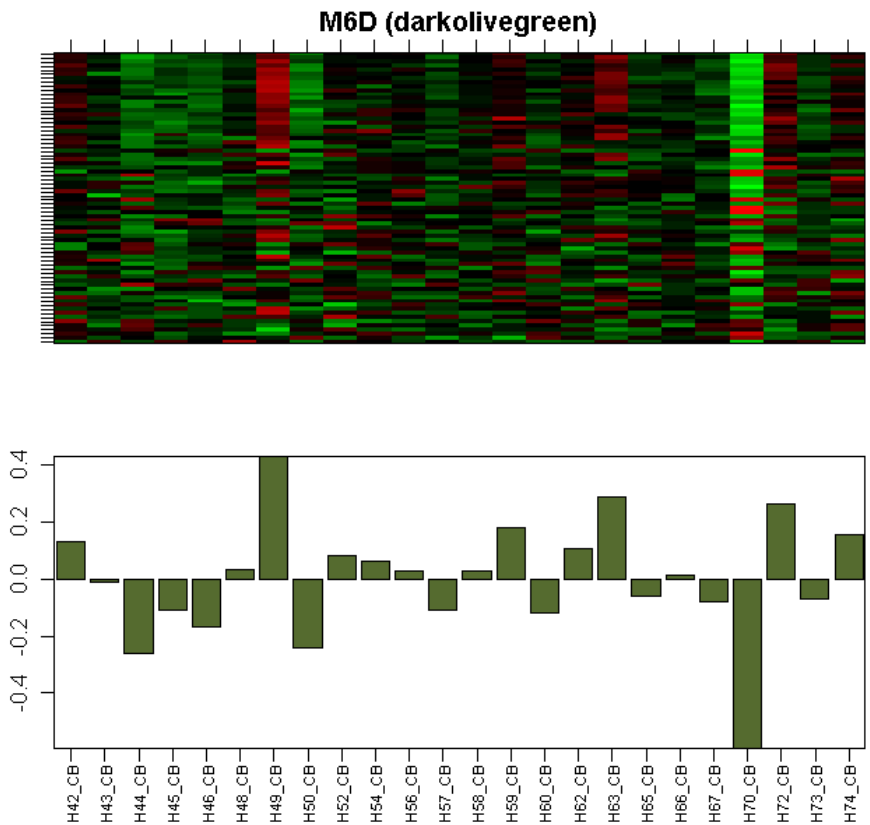
M6D (darkolivegreen)
0.4
0.2
0.0
-0.2
-0.4
H42_CB
H43_CB
H44_CB
H45_CB
H46_CB
H48_CB
H49_CB
H50_CB
H52_CB
H54_CB
H56_CB
H57_CB
H58_CB
H59_CB
H60_CB
H62_CB
H63_CB
H65_CB
H66_CB
H67_CB
H70_CB
H72_CB
H73_CB
H74_CB

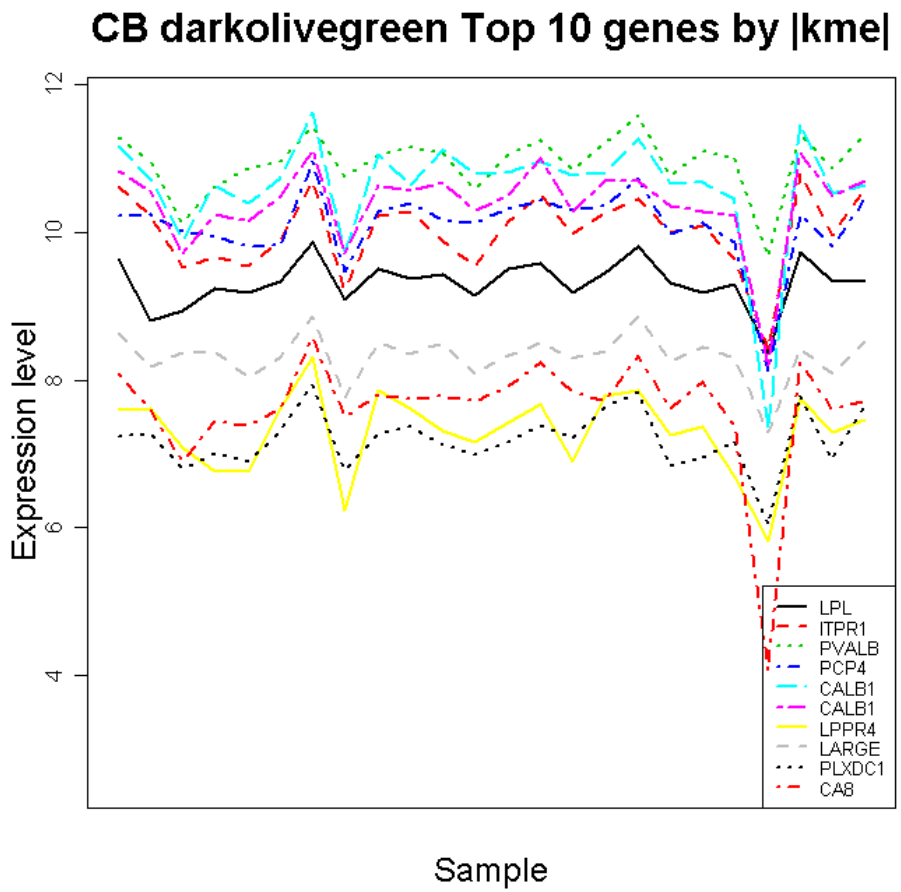
CB darkolivegreen Top 10 genes by |kme|
Expression level
12
10
8
6
4
Sample
LPL
ITPR1
PVALB
PCP4
CALB1
CALB1
LPPR4
LARGE
PLXDC1
CA8

Figure S2BP

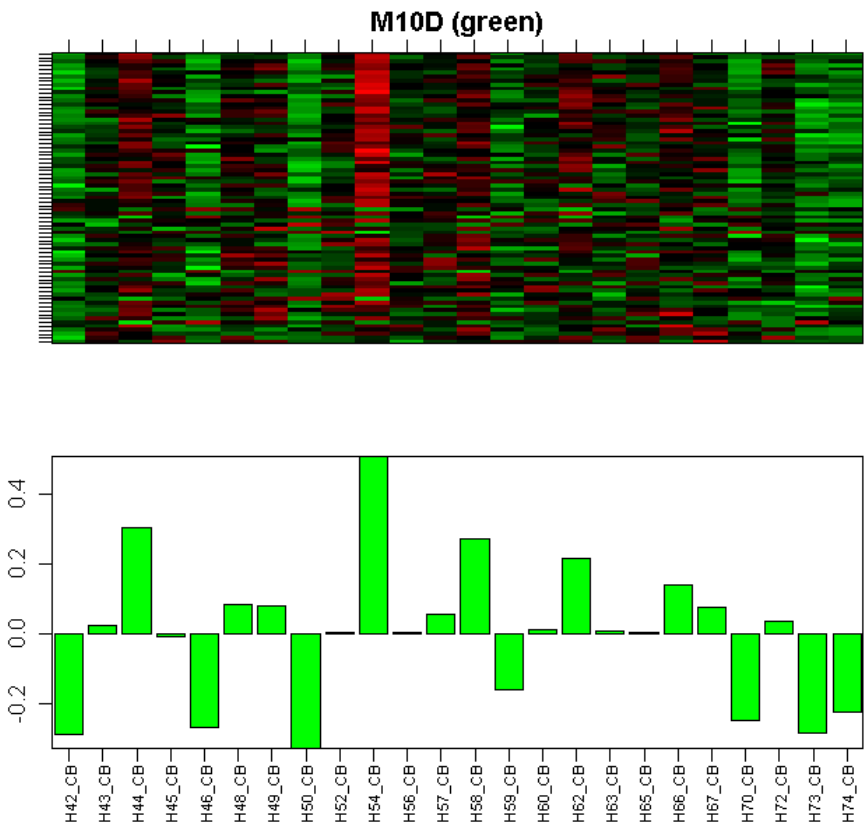
M10D (green)
0.4
0.2
0.0
-0.2
H42_CB
H43_CB
H44_CB
H45_CB
H46_CB
H48_CB
H49_CB
H50_CB
H52_CB
H54_CB
H56_CB
H57_CB
H58_CB
H59_CB
H60_CB
H62_CB
H63_CB
H65_CB
H66_CB
H67_CB
H70_CB
H72_CB
H73_CB
H74_CB

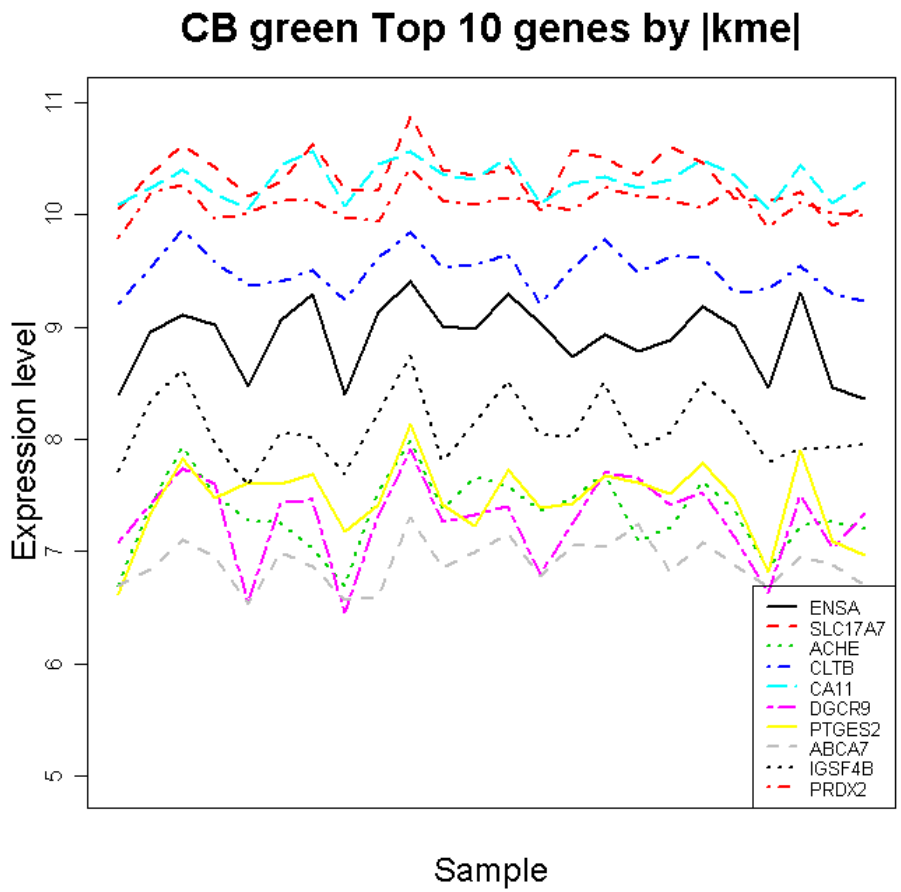
CB green Top 10 genes by |kme|
Expression level
Sample
5
6
7
8
9
10
11
ENSA
SLC17A7
ACHE
CLTB
CA11
DGCR9
PTGES2
ABCA7
IGSF4B
PRDX2

Figure S2BQ

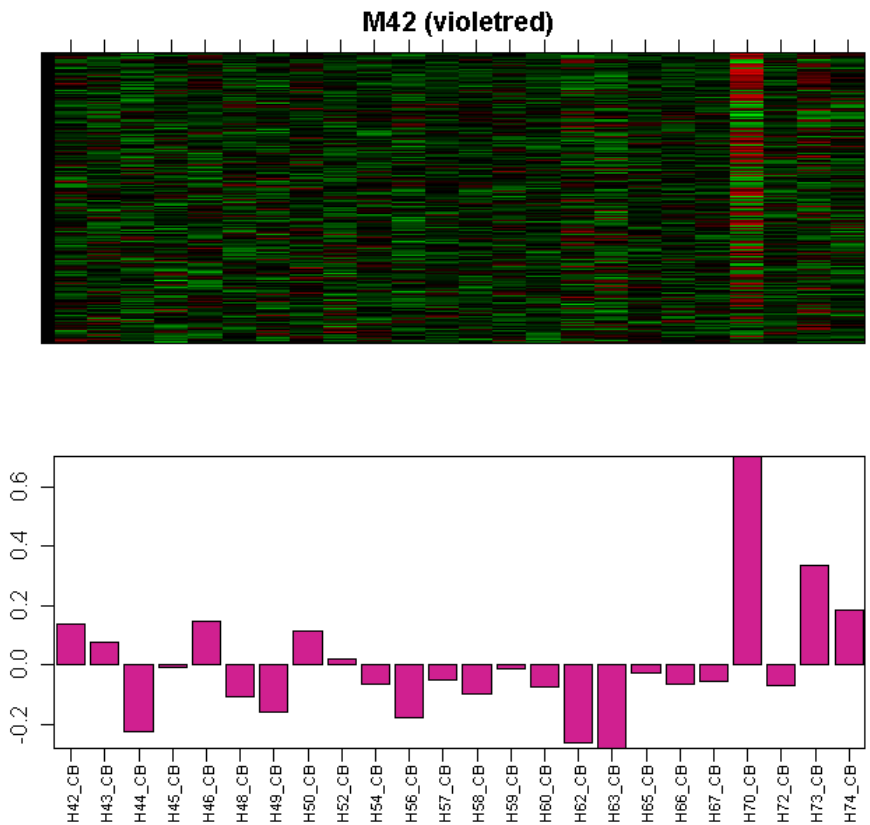
M42 (violetred)
-0.2
0.0
0.2
0.4
0.6
H42_CB
H43_CB
H44_CB
H45_CB
H46_CB
H48_CB
H49_CB
H50_CB
H52_CB
H54_CB
H56_CB
H57_CB
H58_CB
H59_CB
H60_CB
H62_CB
H63_CB
H65_CB
H66_CB
H67_CB
H70_CB
H72_CB
H73_CB
H74_CB

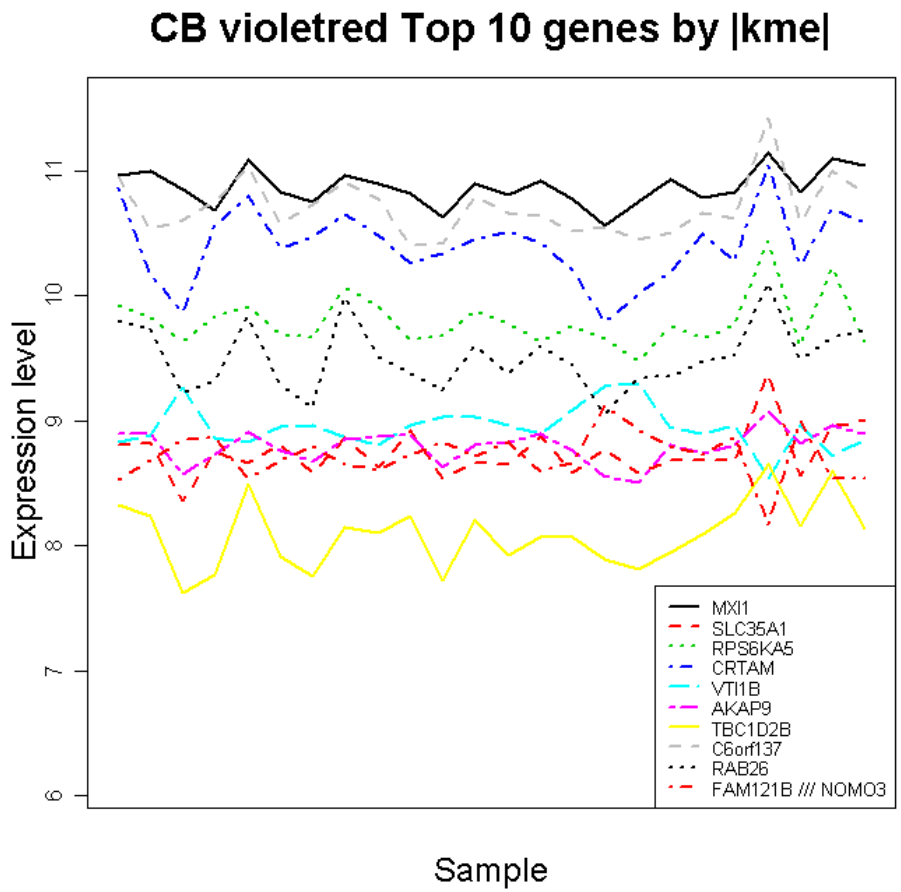
CB violetred Top 10 genes by |kme|
Expression level
6
7
8
9
10
11
Sample
MXI1
SLC35A1
RPS6KA5
CRTAM
VTI1B
AKAP9
TBC1D2B
C6orf137
RAB26
FAM121B /// NOMO3

Figure S2BR

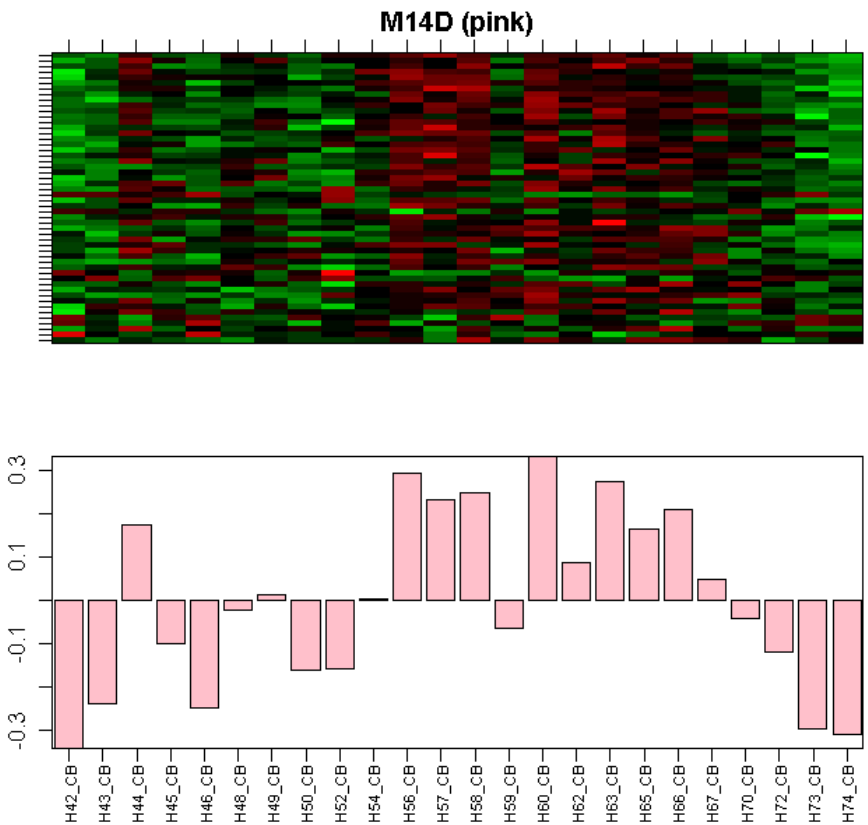
M14D (pink)
0.3
0.1
-0.1
-0.3
H42_CB
H43_CB
H44_CB
H45_CB
H46_CB
H48_CB
H49_CB
H50_CB
H52_CB
H54_CB
H56_CB
H57_CB
H58_CB
H59_CB
H60_CB
H62_CB
H63_CB
H65_CB
H66_CB
H67_CB
H70_CB
H72_CB
H73_CB
H74_CB

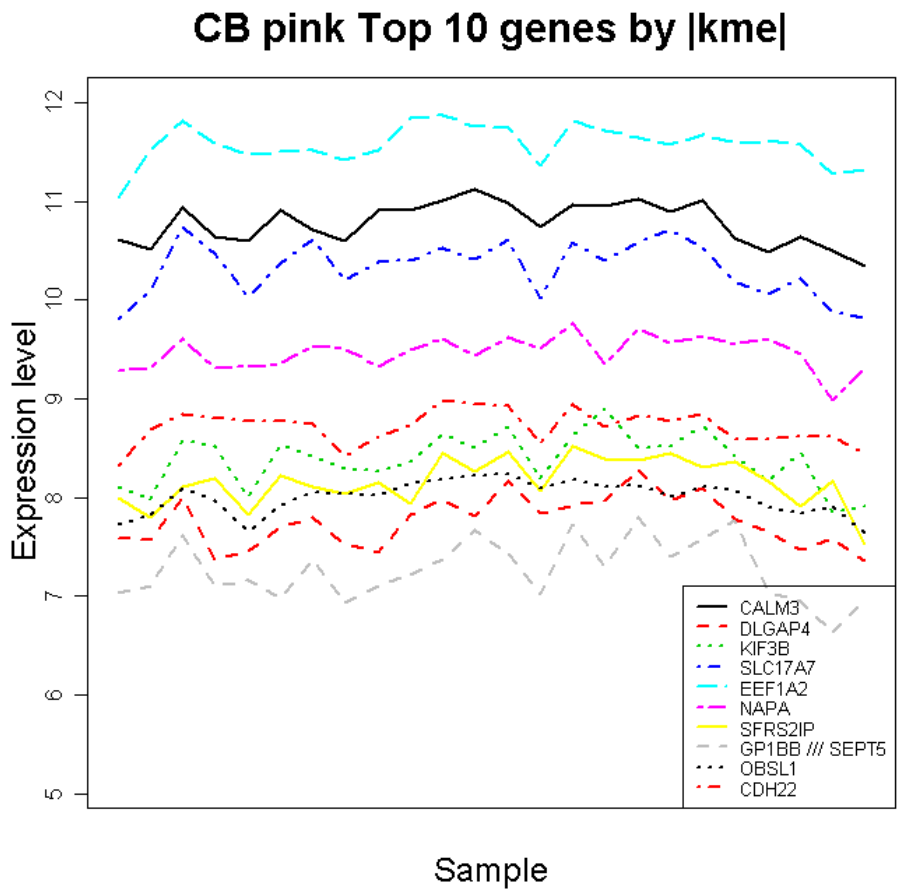
CB pink Top 10 genes by |kme|
Expression level
5
6
7
8
9
10
11
12
Sample
CALM3
DLGAP4
KIF3B
SLC17A7
EEF1A2
NAPA
SFRS2IP
GP1BB /// SEPT5
OBSL1
CDH22

Figure S2BS

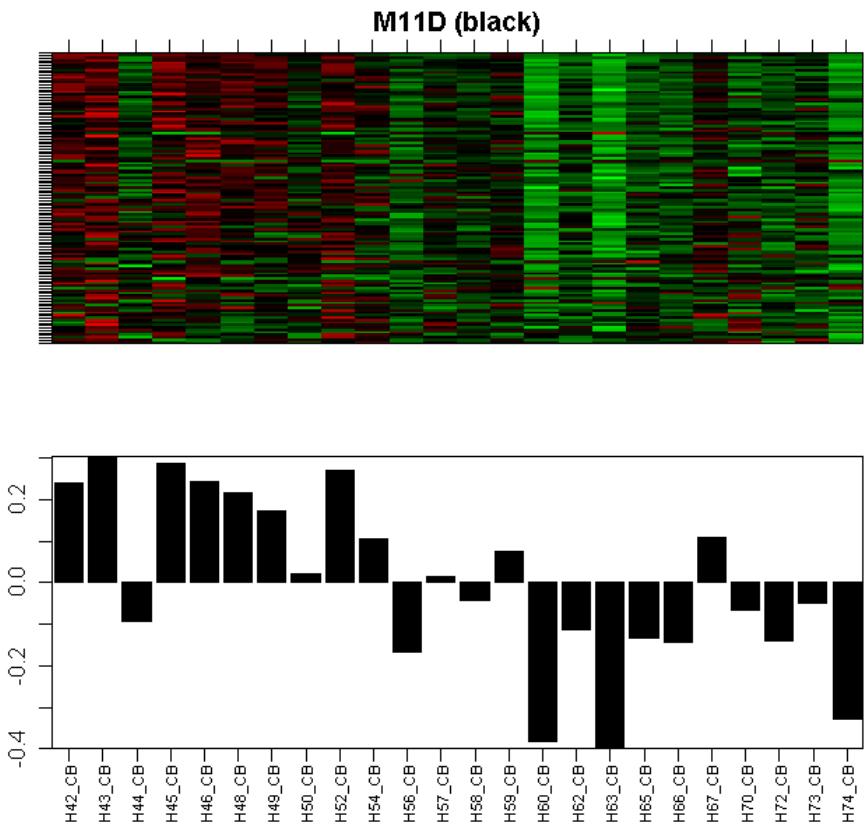
M11D (black)
0.2
0.0
-0.2
-0.4
H42_CB
H43_CB
H44_CB
H45_CB
H46_CB
H48_CB
H49_CB
H50_CB
H52_CB
H54_CB
H56_CB
H57_CB
H58_CB
H59_CB
H60_CB
H62_CB
H63_CB
H65_CB
H66_CB
H67_CB
H70_CB
H72_CB
H73_CB
H74_CB

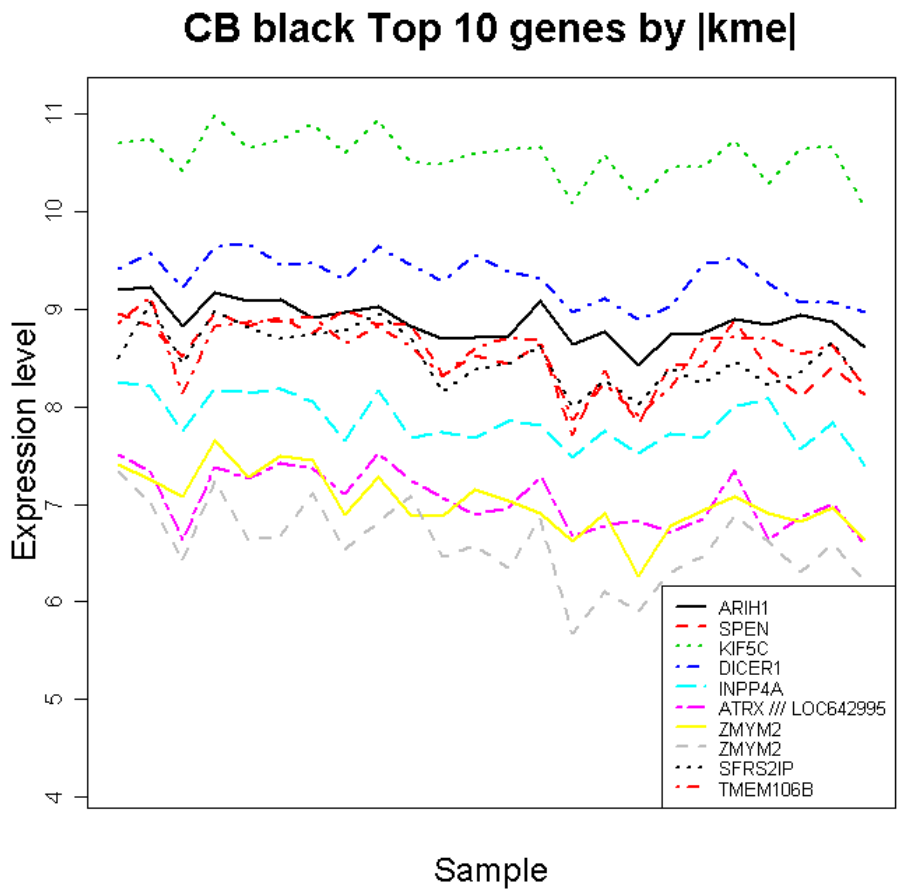
CB black Top 10 genes by |kme|
Expression level
4
5
6
7
8
9
10
11
Sample
ARIH1
SPEN
KIF5C
DICER1
INPP4A
ATRX /// LOC642995
ZMYM2
ZMYM2
SFRS2IP
TMEM106B

Figure S2BT

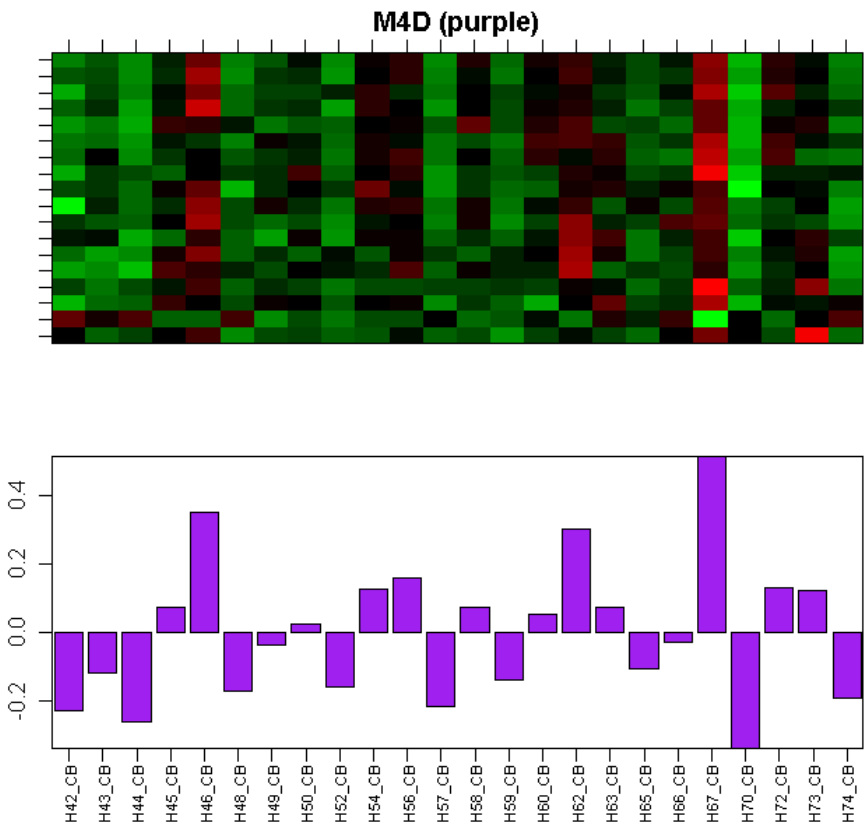
M4D (purple)
0.4
0.2
0.0
-0.2
H42_CB
H43_CB
H44_CB
H45_CB
H46_CB
H48_CB
H49_CB
H50_CB
H52_CB
H54_CB
H56_CB
H57_CB
H58_CB
H59_CB
H60_CB
H62_CB
H63_CB
H65_CB
H66_CB
H67_CB
H70_CB
H72_CB
H73_CB
H74_CB

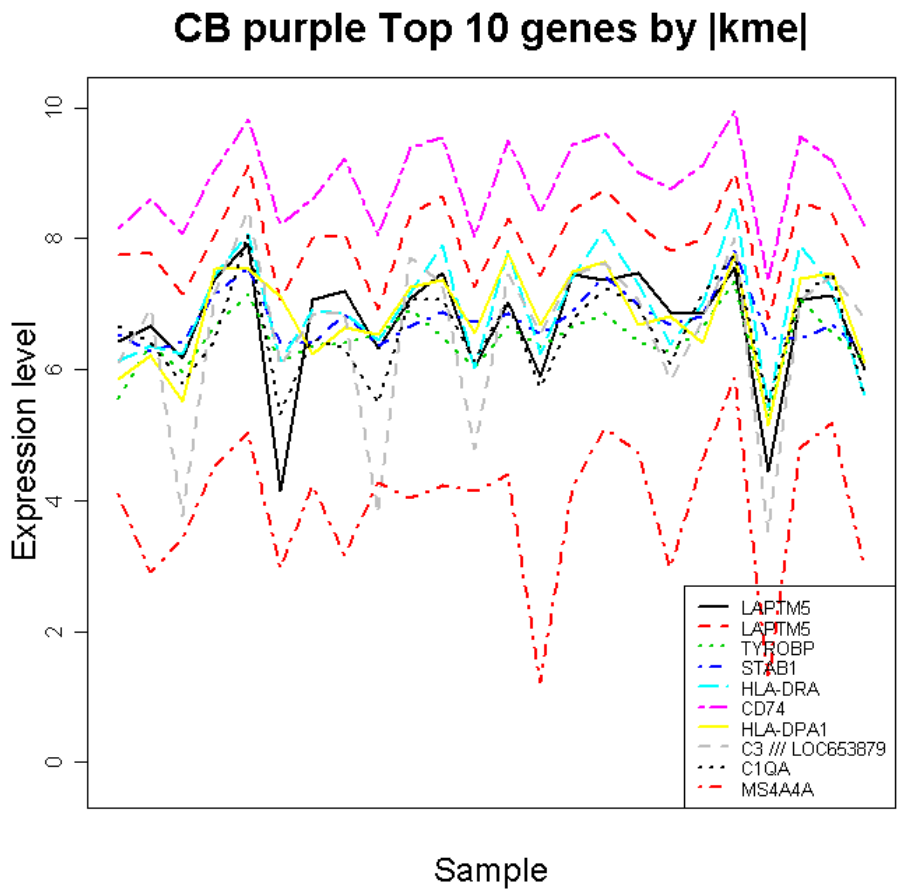
CB purple Top 10 genes by |kme|
Expression level
0
2
4
6
8
10
Sample
LAPTM5
LAPTM5
TYROBP
STAB1
HLA-DRA
CD74
HLA-DPA1
C3 /// LOC653879
C1QA
MS4A4A

Figure S2BU

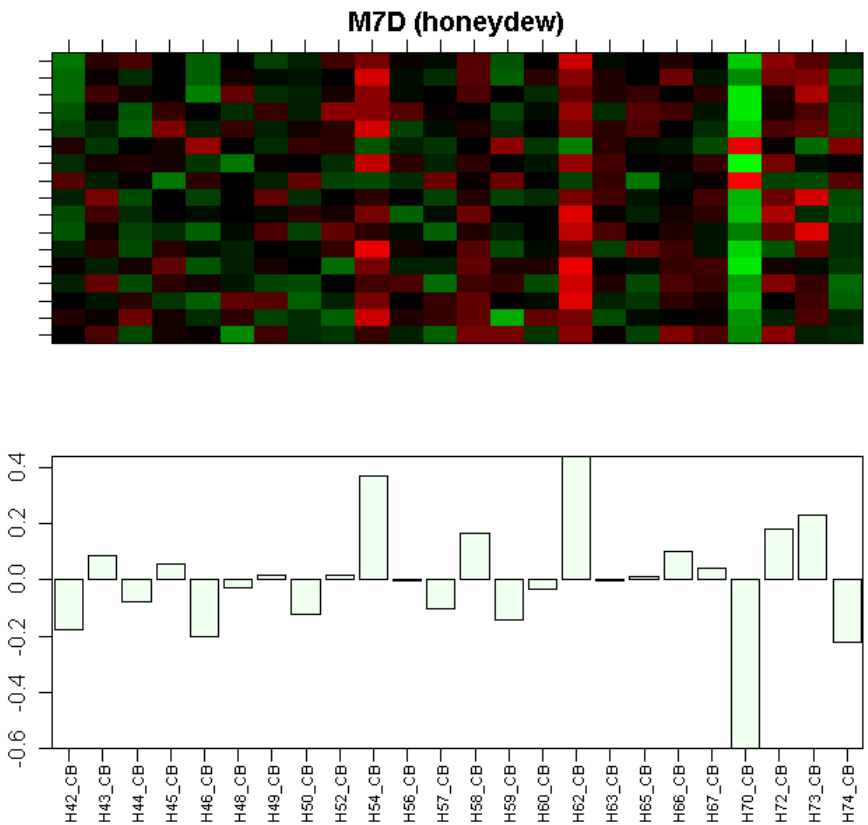
M7D (honeydew)
0.4
0.2
0.0
-0.2
-0.4
-0.6
H42_CB
H43_CB
H44_CB
H45_CB
H46_CB
H48_CB
H49_CB
H50_CB
H52_CB
H54_CB
H56_CB
H57_CB
H58_CB
H59_CB
H60_CB
H62_CB
H63_CB
H65_CB
H66_CB
H67_CB
H70_CB
H72_CB
H73_CB
H74_CB

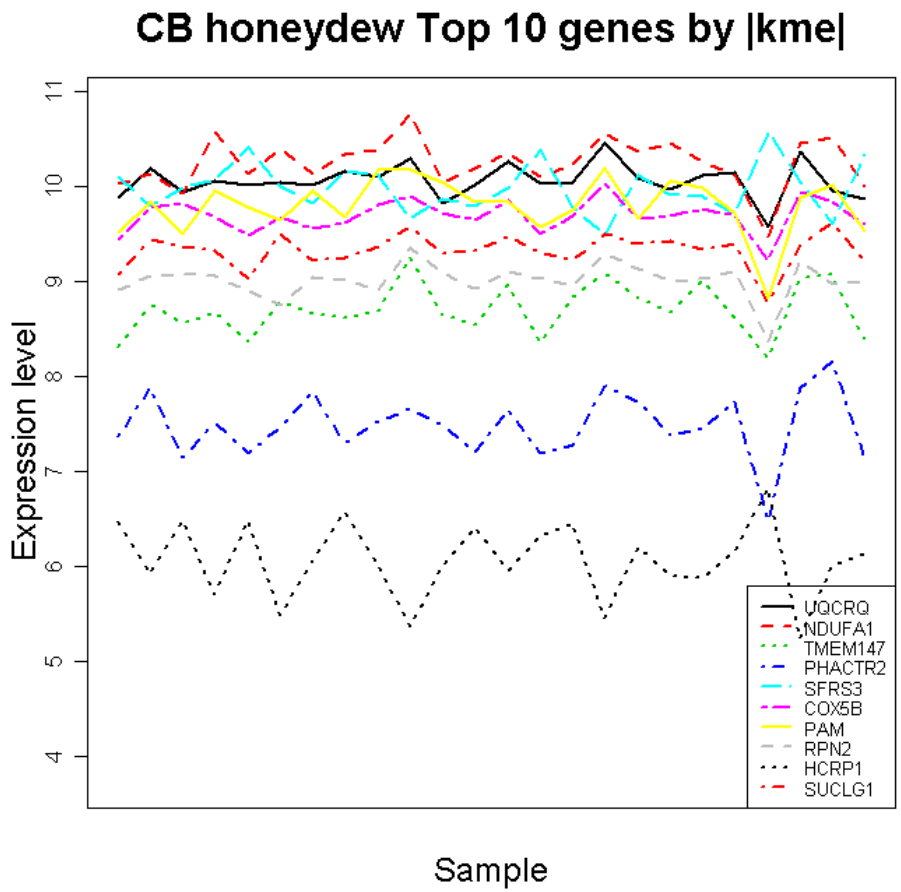
CB honeydew Top 10 genes by |kme|
Expression level
Sample
4
5
6
7
8
9
10
11
UQCRQ
NDUFA1
TMEM147
PHACTR2
SFRS3
COX5B
PAM
RPN2
HCRP1
SUCLG1

Figure S2BV

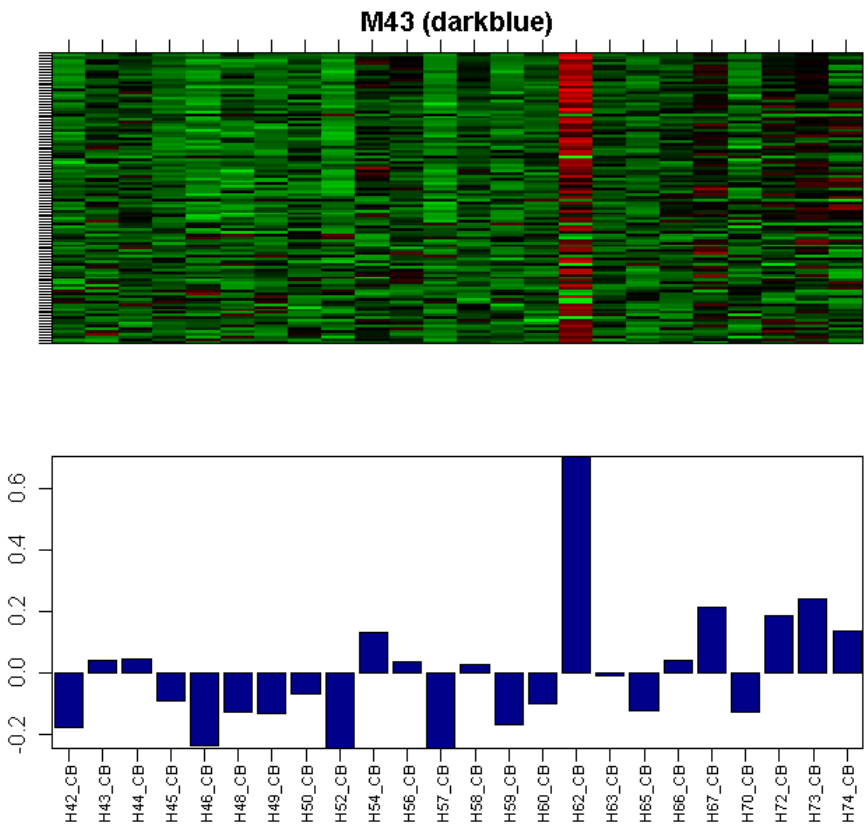
M43 (darkblue)
-0.2
0.0
0.2
0.4
0.6
H42_CB
H43_CB
H44_CB
H45_CB
H46_CB
H48_CB
H49_CB
H50_CB
H52_CB
H54_CB
H56_CB
H57_CB
H58_CB
H59_CB
H60_CB
H62_CB
H63_CB
H65_CB
H66_CB
H67_CB
H70_CB
H72_CB
H73_CB
H74_CB

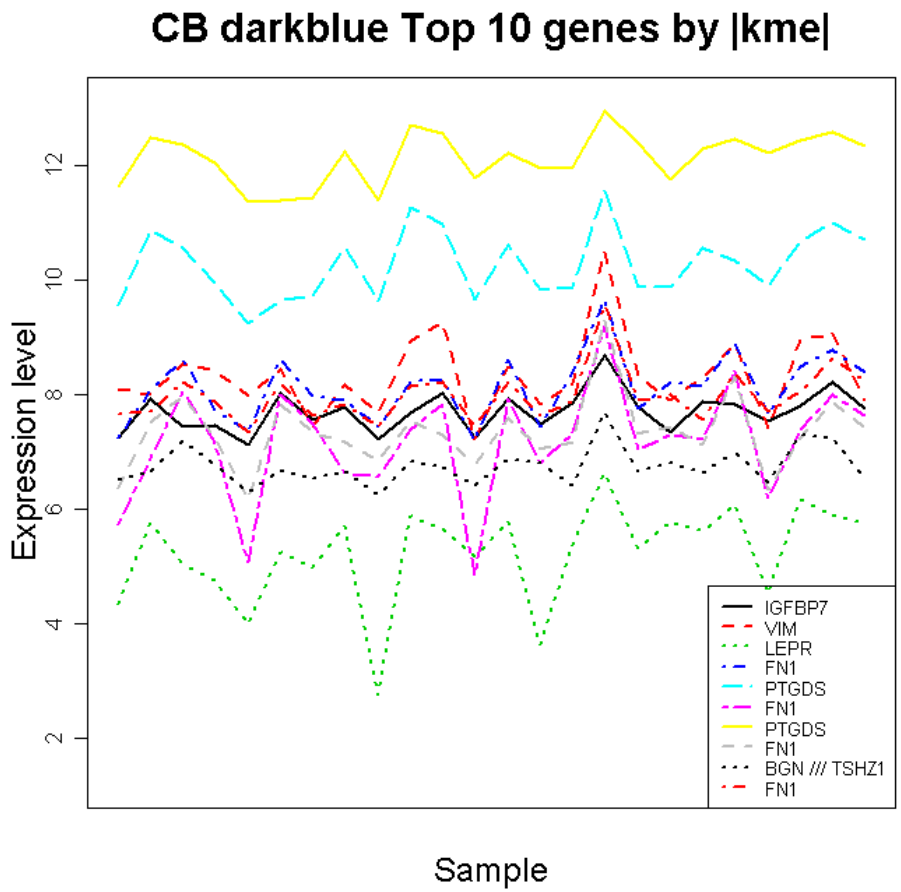
CB darkblue Top 10 genes by |kme|
Expression level
2
4
6
8
10
12
Sample
IGFBP7
VIM
LEPR
FN1
PTGDS
FN1
PTGDS
FN1
BGN /// TSHZ1
FN1

Figure S2BW

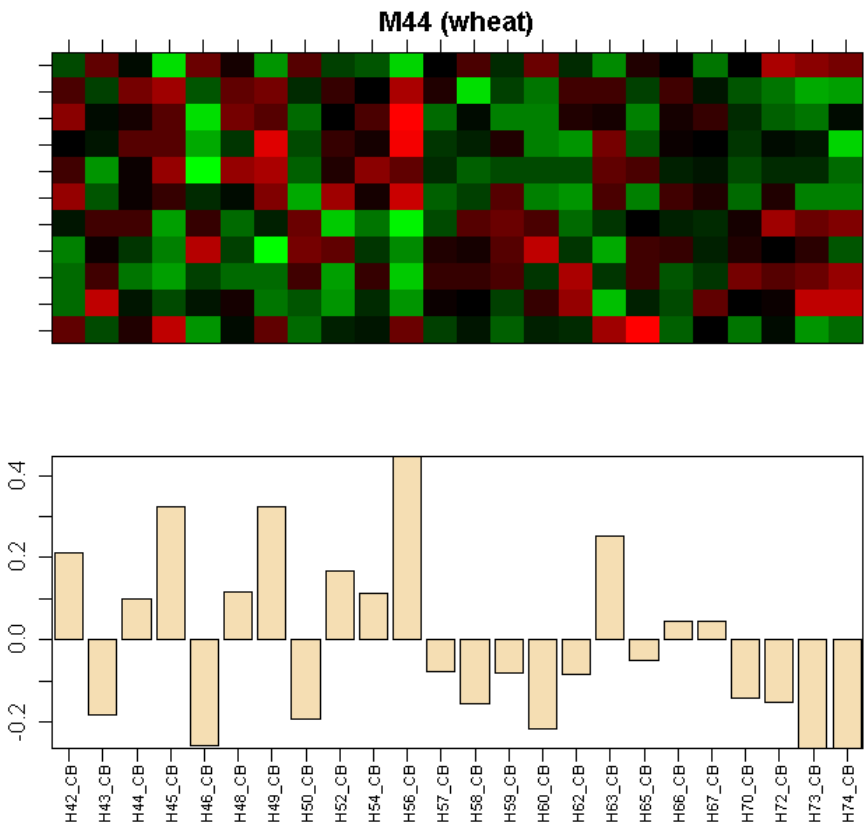
M44 (wheat)
0.4
0.2
0.0
-0.2
H42_CB
H43_CB
H44_CB
H45_CB
H46_CB
H48_CB
H49_CB
H50_CB
H52_CB
H54_CB
H56_CB
H57_CB
H58_CB
H59_CB
H60_CB
H62_CB
H63_CB
H65_CB
H66_CB
H67_CB
H70_CB
H72_CB
H73_CB
H74_CB

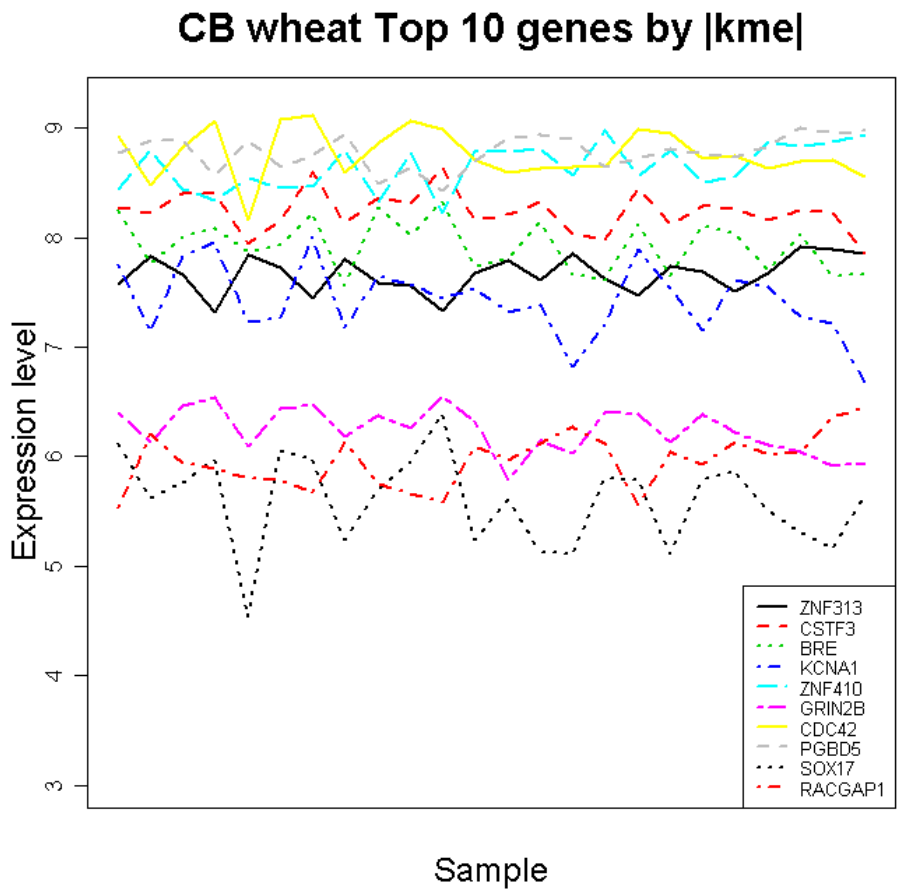
CB wheat Top 10 genes by |kme|
Expression level
3
4
5
6
7
8
9
Sample
ZNF313
CSTF3
BRE
KCNA1
ZNF410
GRIN2B
CDC42
PGBD5
SOX17
RACGAP1

Figure S2BX

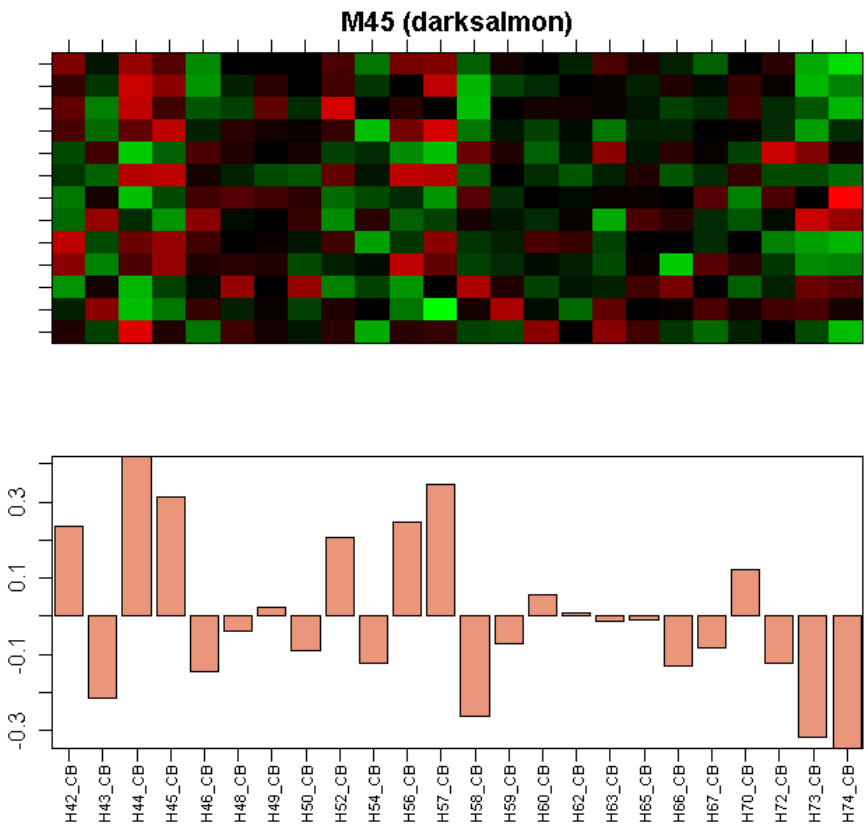
M45 (darksalmon)
0.3
0.1
-0.1
-0.3
H42_CB
H43_CB
H44_CB
H45_CB
H46_CB
H48_CB
H49_CB
H50_CB
H52_CB
H54_CB
H56_CB
H57_CB
H58_CB
H59_CB
H60_CB
H62_CB
H63_CB
H65_CB
H66_CB
H67_CB
H70_CB
H72_CB
H73_CB
H74_CB

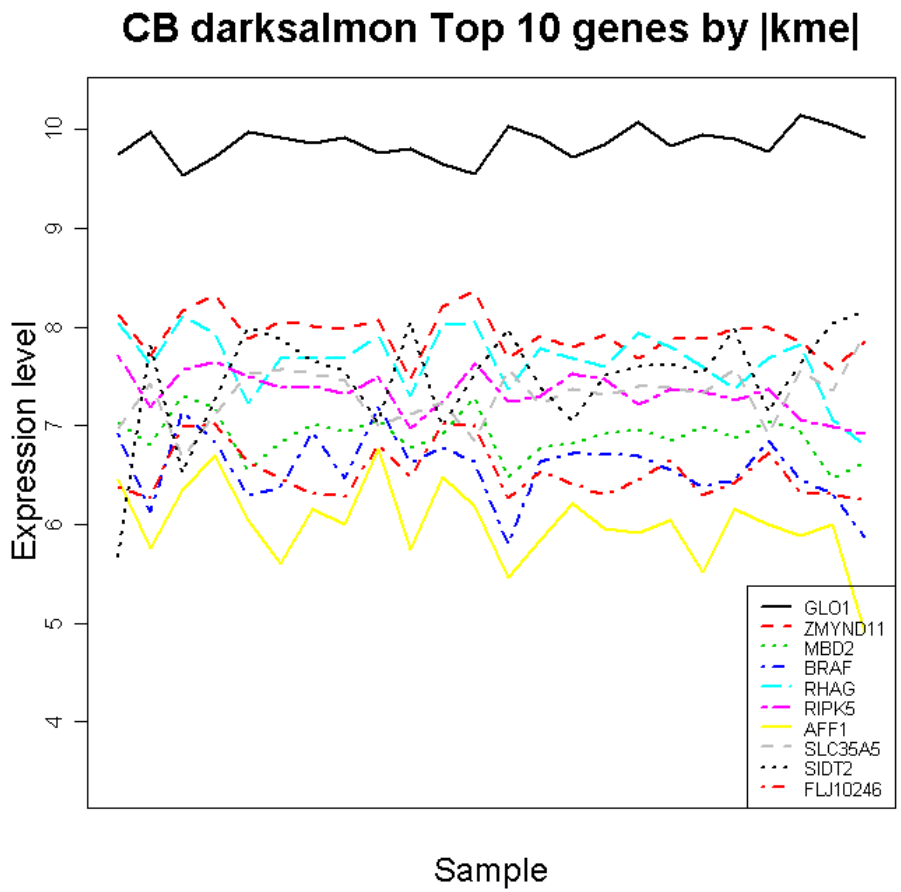
CB darksalmon Top 10 genes by |kme|
Expression level
4
5
6
7
8
9
10
Sample
GLO1
ZMYND11
MBD2
BRAF
RHAG
RIPK5
AFF1
SLC35A5
SIDT2
FLJ10246

Figure S2BY

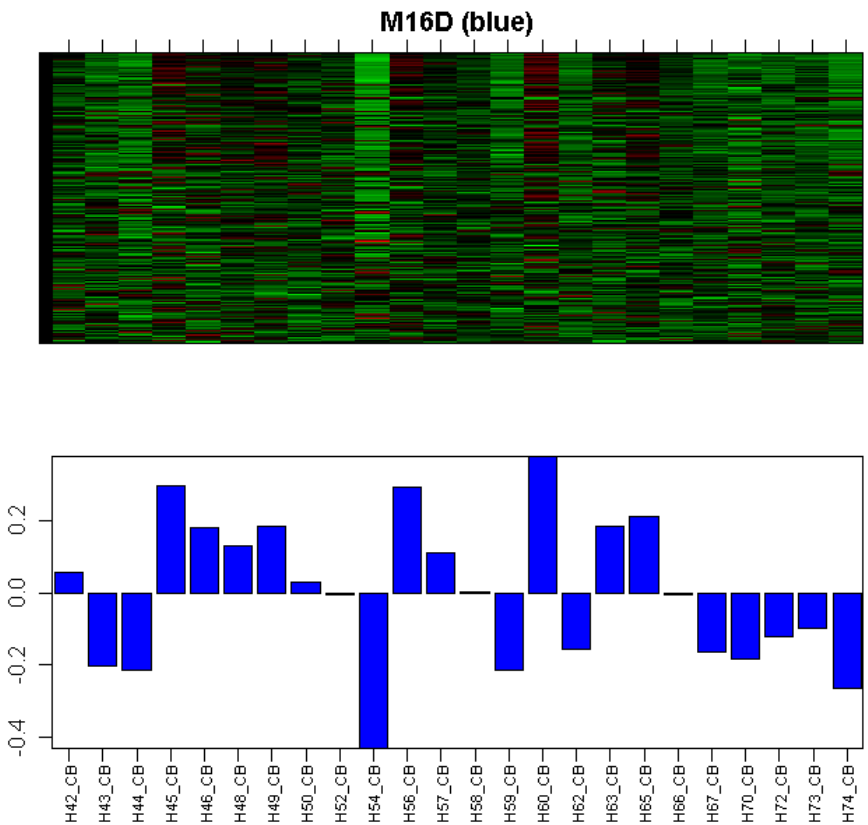
M16D (blue)
0.2
0.0
-0.2
-0.4
H42_CB
H43_CB
H44_CB
H45_CB
H46_CB
H48_CB
H49_CB
H50_CB
H52_CB
H54_CB
H56_CB
H57_CB
H58_CB
H59_CB
H60_CB
H62_CB
H63_CB
H65_CB
H66_CB
H67_CB
H70_CB
H72_CB
H73_CB
H74_CB

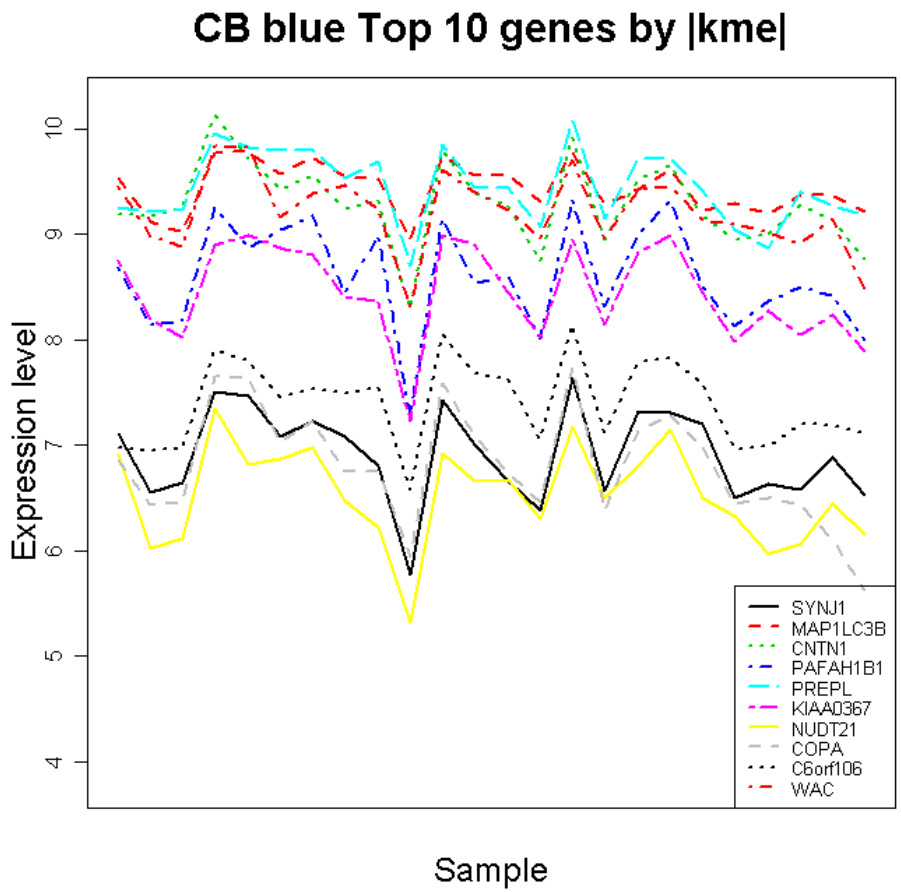
CB blue Top 10 genes by |kme|
Expression level
4
5
6
7
8
9
10
Sample
SYNJ1
MAP1LC3B
CNTN1
PAFAH1B1
PREPL
KIAA0367
NUDT21
COPA
C6orf106
WAC

Figure S2BZ

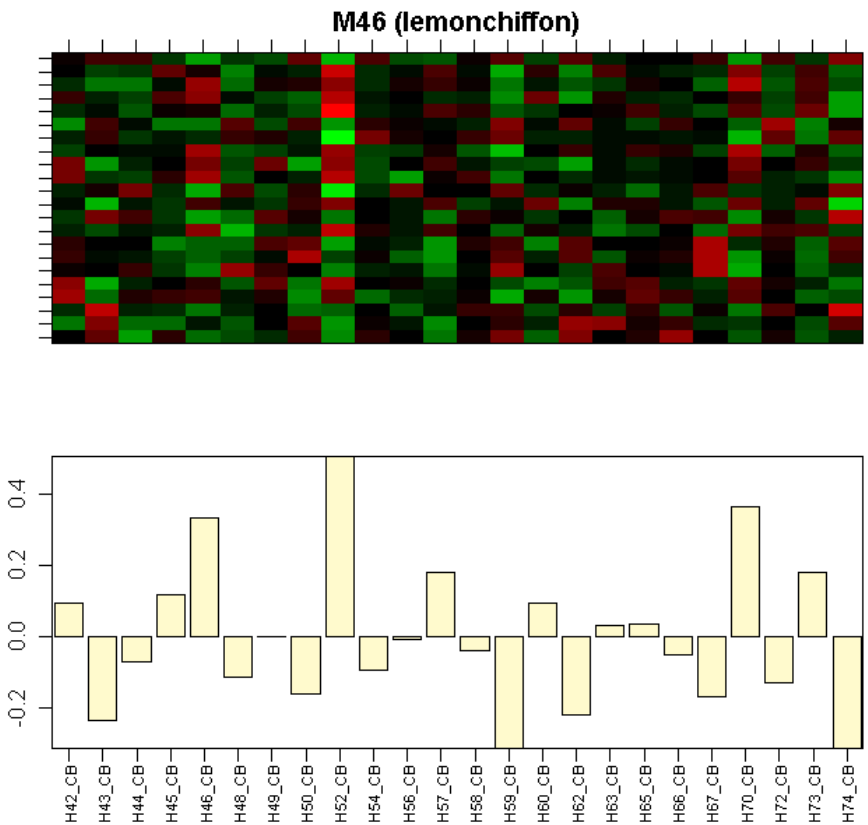
M46 (lemonchiffon)
-0.2
0.0
0.2
0.4
H42_CB
H43_CB
H44_CB
H45_CB
H46_CB
H48_CB
H49_CB
H50_CB
H52_CB
H54_CB
H56_CB
H57_CB
H58_CB
H59_CB
H60_CB
H62_CB
H63_CB
H65_CB
H66_CB
H67_CB
H70_CB
H72_CB
H73_CB
H74_CB

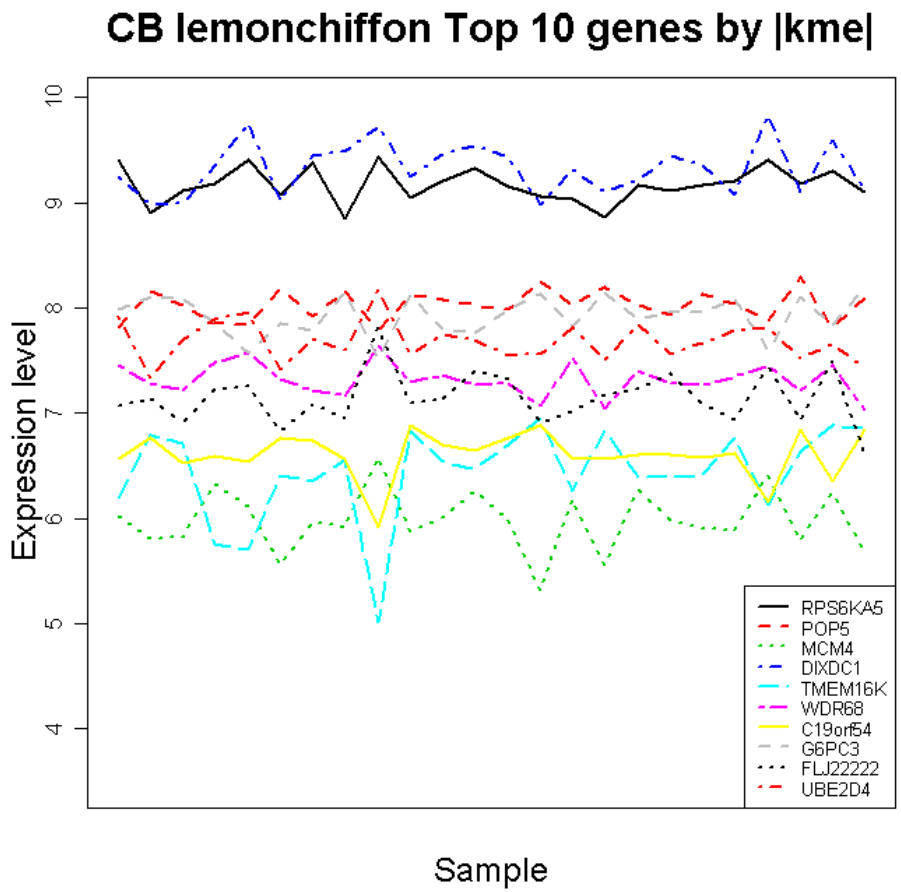
CB lemonchiffon Top 10 genes by |kme|
Expression level
4
5
6
7
8
9
10
Sample
RPS6KA5
POP5
MCM4
DIXDC1
TMEM16K
WDR68
C19orf54
G6PC3
FLJ22222
UBE2D4

Figure S2CA

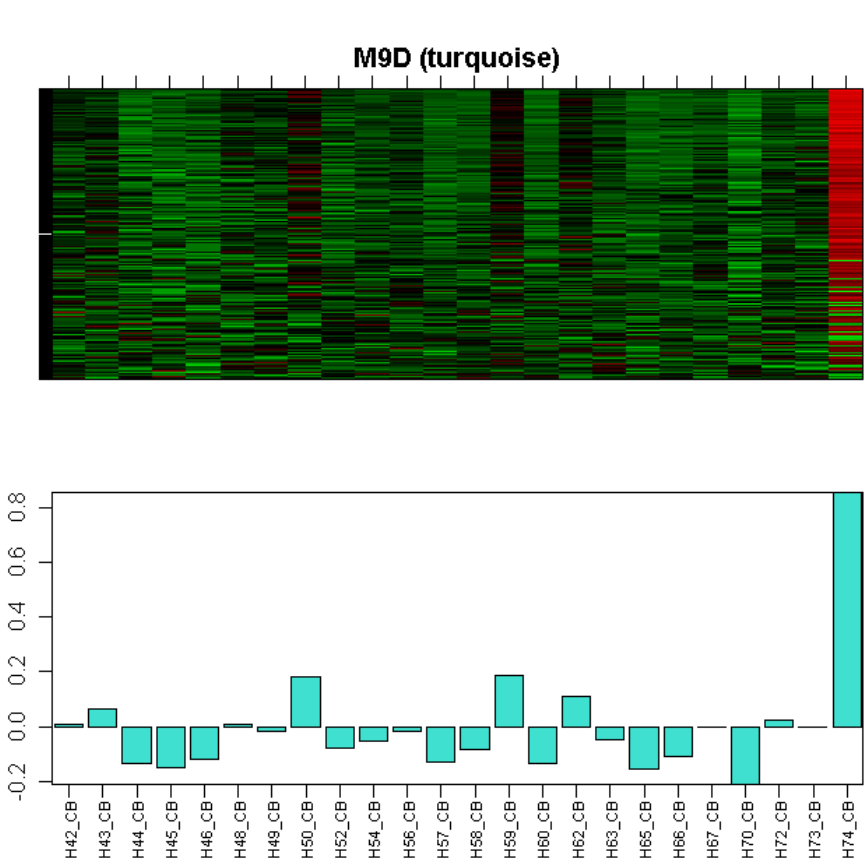
M9D (turquoise)
0.8
0.6
0.4
0.2
0.0
-0.2
H42_CB
H43_CB
H44_CB
H45_CB
H46_CB
H48_CB
H49_CB
H50_CB
H52_CB
H54_CB
H56_CB
H57_CB
H58_CB
H59_CB
H60_CB
H62_CB
H63_CB
H65_CB
H66_CB
H67_CB
H70_CB
H72_CB
H73_CB
H74_CB

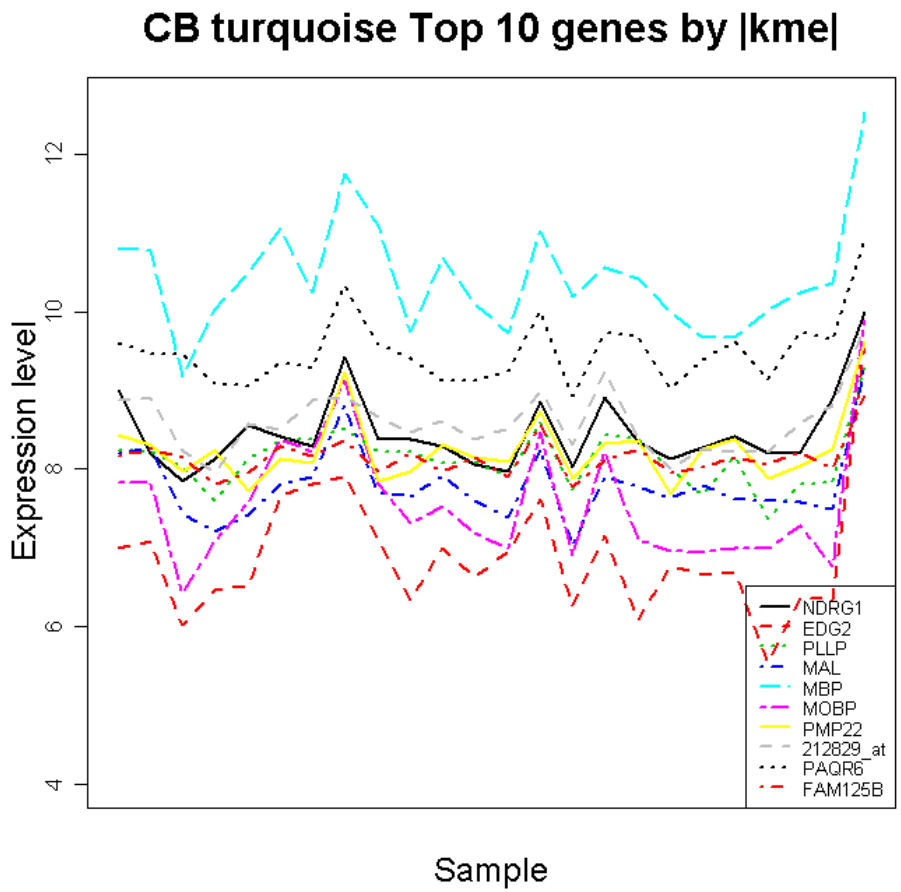
CB turquoise Top 10 genes by |kme|
Expression level
4
6
8
10
12
Sample
NDRG1
EDG2
PLLP
MAL
MBP
MOBP
PMP22
212829_at
PAQR6
FAM125B

Figure S2CB

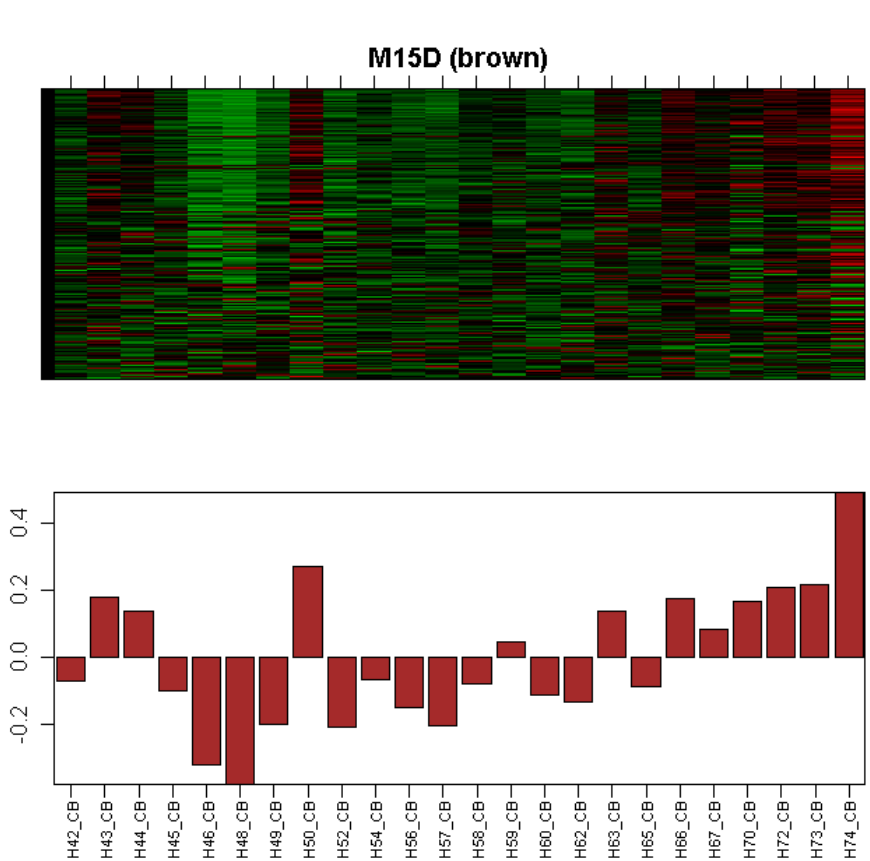
M15D (brown)
0.4
0.2
0.0
-0.2
H42_CB
H43_CB
H44_CB
H45_CB
H46_CB
H48_CB
H49_CB
H50_CB
H52_CB
H54_CB
H56_CB
H57_CB
H58_CB
H59_CB
H60_CB
H62_CB
H63_CB
H65_CB
H66_CB
H67_CB
H70_CB
H72_CB
H73_CB
H74_CB

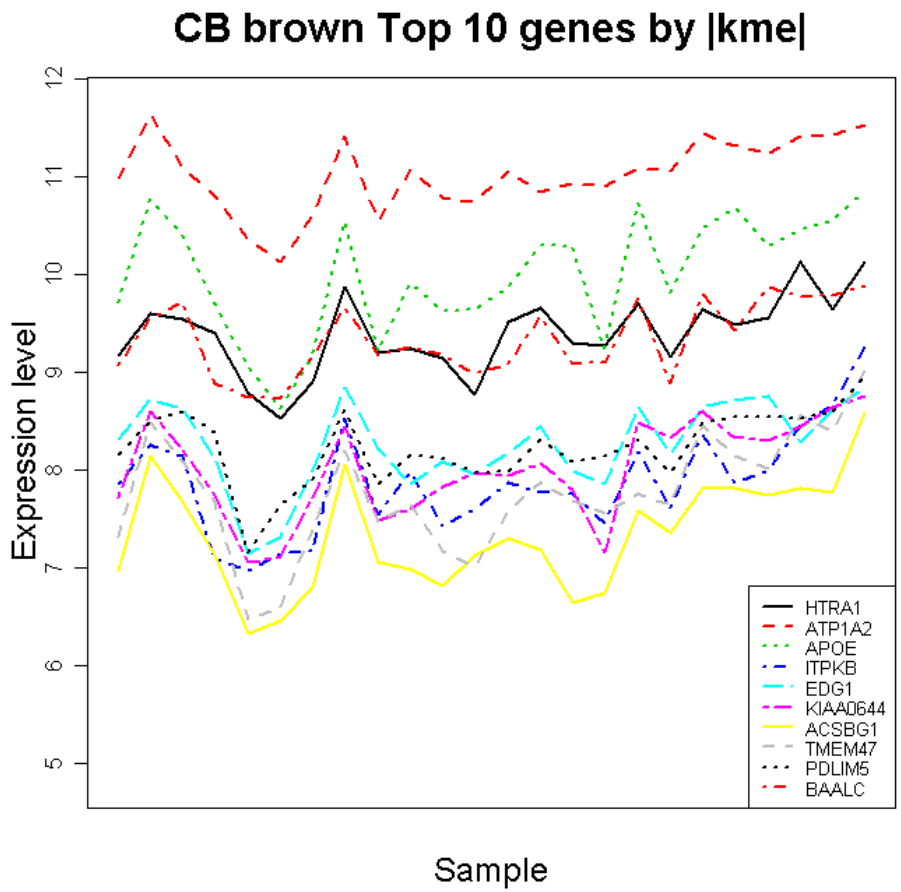
CB brown Top 10 genes by |kme|
Expression level
5
6
7
8
9
10
11
12
Sample
HTRA1
ATP1A2
APOE
ITPKB
EDG1
KIAA0644
ACSBG1
TMEM47
PDLIM5
BAALC

Figure S2CC

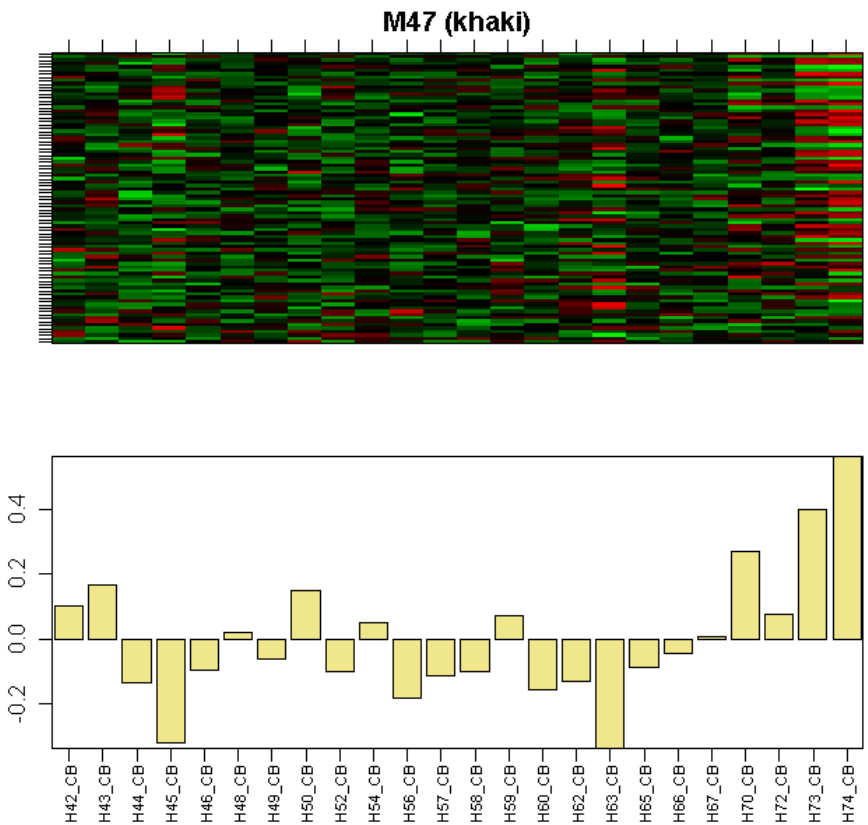
M47 (khaki)
0.4
0.2
0.0
-0.2
H42_CB
H43_CB
H44_CB
H45_CB
H46_CB
H48_CB
H49_CB
H50_CB
H52_CB
H54_CB
H56_CB
H57_CB
H58_CB
H59_CB
H60_CB
H62_CB
H63_CB
H65_CB
H66_CB
H67_CB
H70_CB
H72_CB
H73_CB
H74_CB

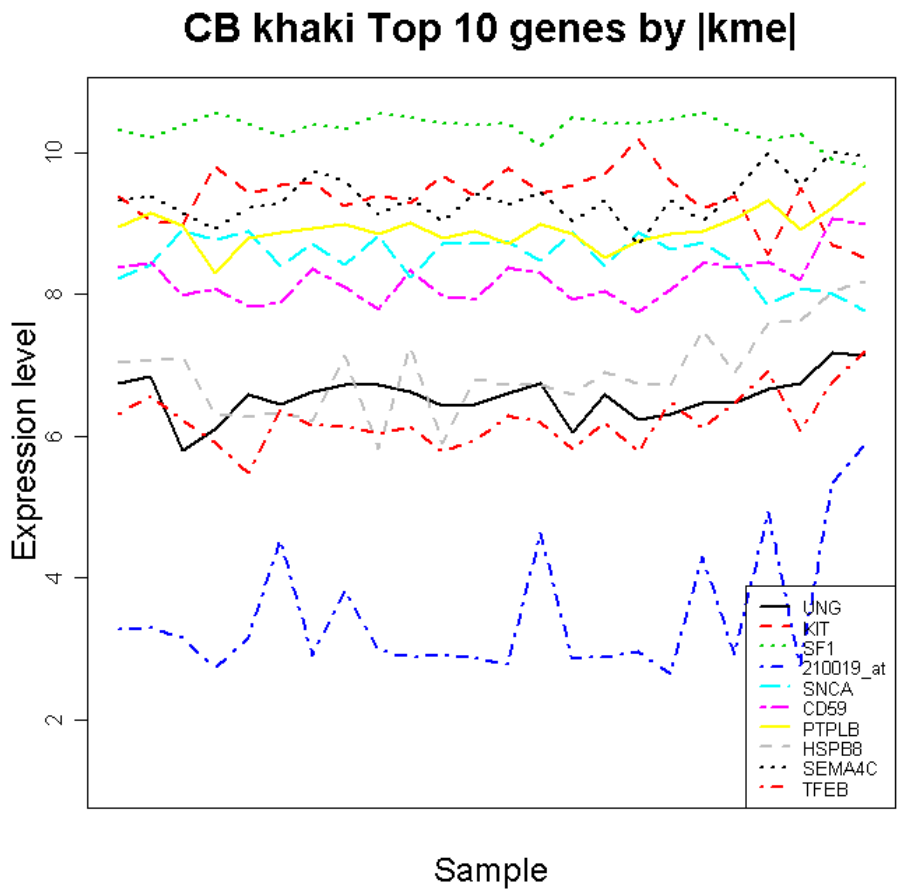
CB khaki Top 10 genes by |kme|
Expression level
2
4
6
8
10
Sample
UNG
KIT
SF1
210019_at
SNCA
CD59
PTPLB
HSPB8
SEMA4C
TFEB

"Functional Organization of the Transcriptome in Human Brain"

Michael C. Oldham, Steve Horvath, Genevieve Konopka, Kazuya Iwamoto, Peter Langfelder, Tadafumi Kato, and Daniel H. Geschwind

Nature Neuroscience

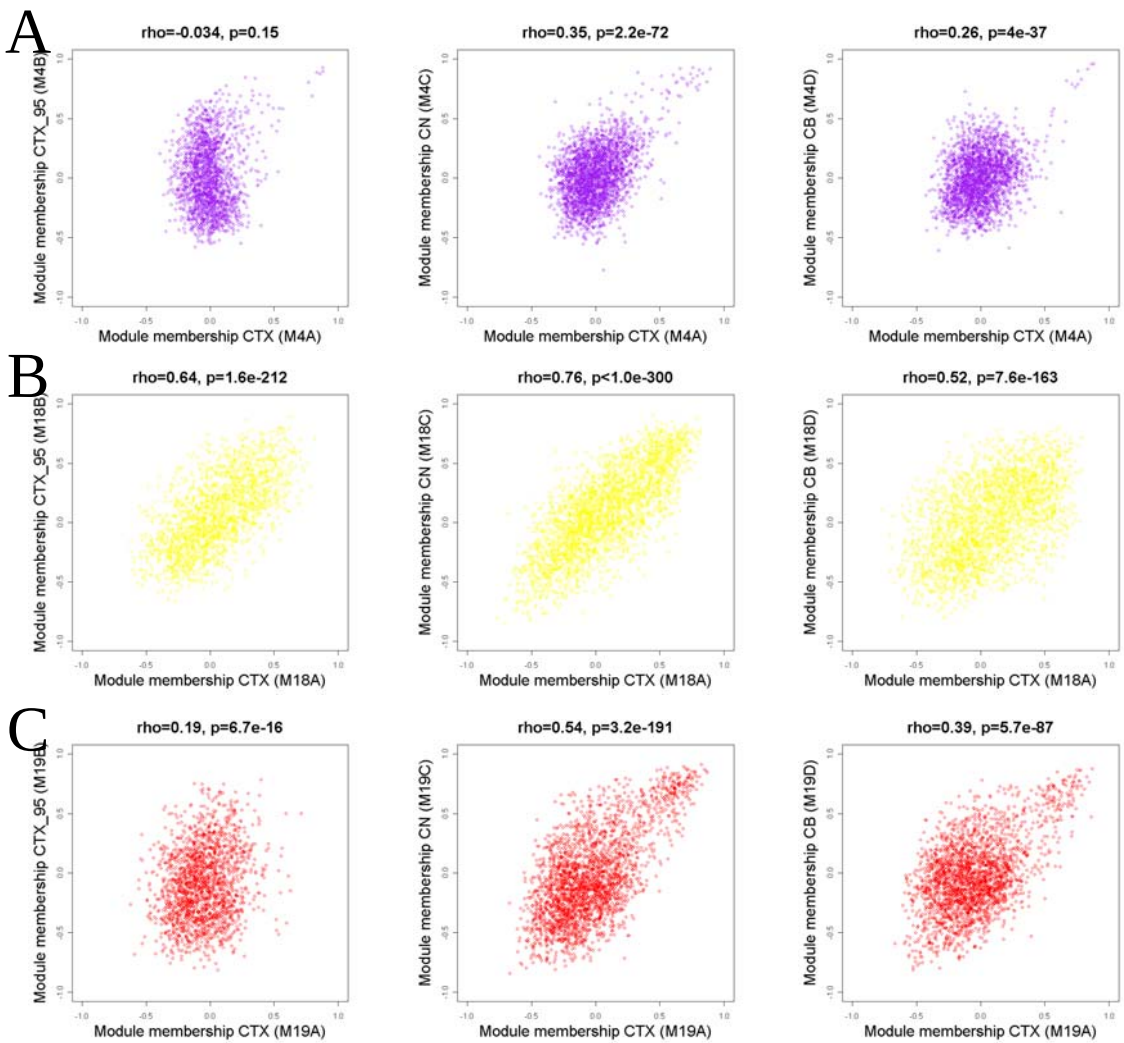

Supplementary Figure 3: Module membership is correlated in multiple human brain datasets (additional conserved modules)

Comparison of module membership between networks for M4 (**a**), M18 (**b**), and M19 (**c**). Data are presented as described in Fig. 3 of the journal article. Note that for smaller modules (e.g. M4), most genes were not significantly correlated with the module eigengene.

“Functional Organization of the Transcriptome in Human Brain”

Michael C. Oldham, Steve Horvath, Genevieve Konopka, Kazuya Iwamoto, Peter Langfelder, Tadafumi Kato, and Daniel H. Geschwind

Nature Neuroscience

Supplementary Figure 4: Module visualizations

150 pairs of genes with the highest topological overlap in each module are depicted for CTX (**a–s**), CN (**t–ap**), and CB (**aq–bl**) (Supplementary Methods). Genes with expression levels that were negatively correlated are connected by black lines. Where gene symbols are unknown, Affymetrix probe set IDs are shown (e.g. 214903_at). Numbers appended to gene symbols denote the rank |module membership| (RMM) for the corresponding probe set (some genes are represented by multiple probe sets). For example, *KIAA0103* exhibited the strongest membership of any gene for M10A (**j**). Genes with >= 20 depicted connections appear as large nodes, followed by genes with 10–19 connections that appear as medium nodes, followed by genes with < 10 connections that appear as small nodes.

Figure S4

Cortex

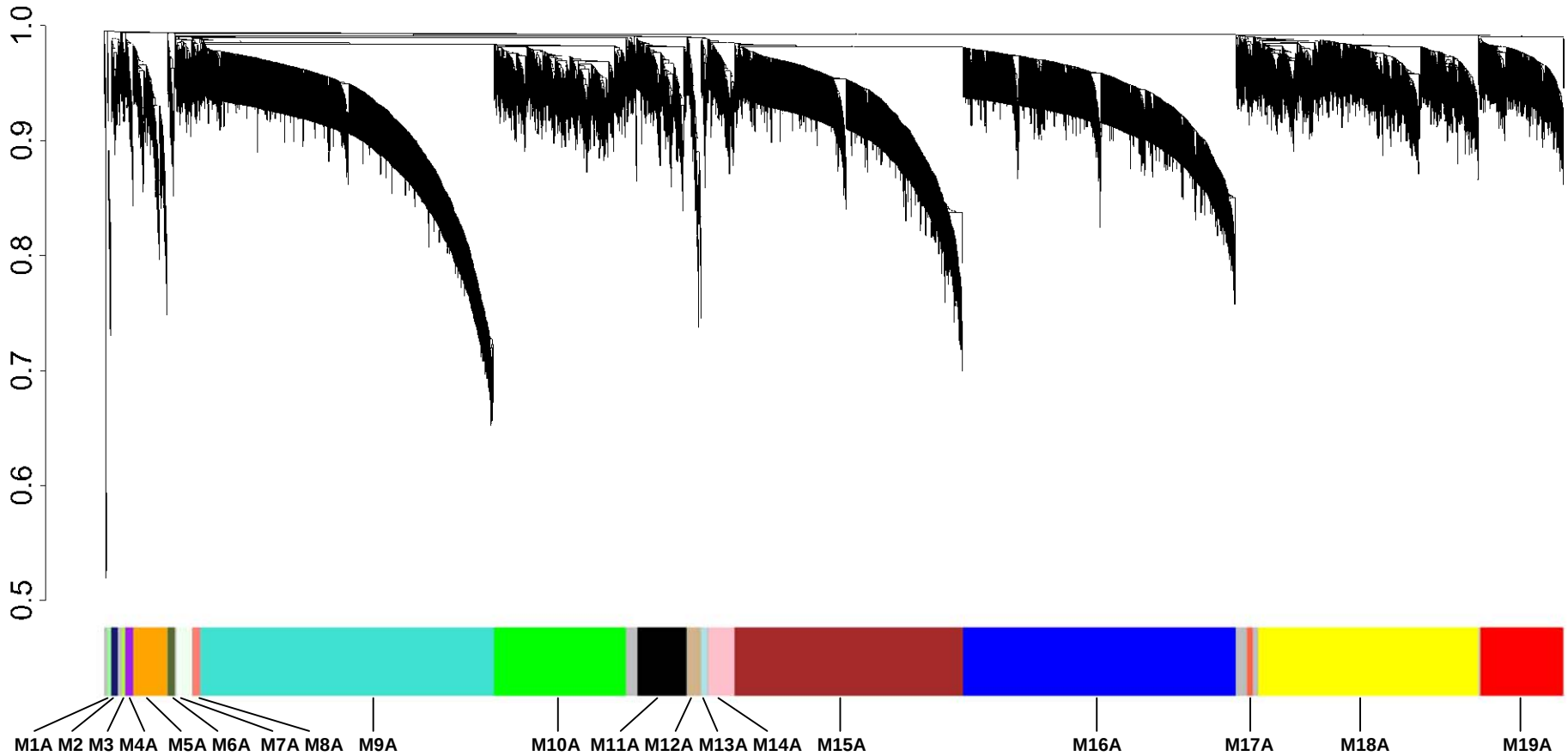

Figure S4A

M1A

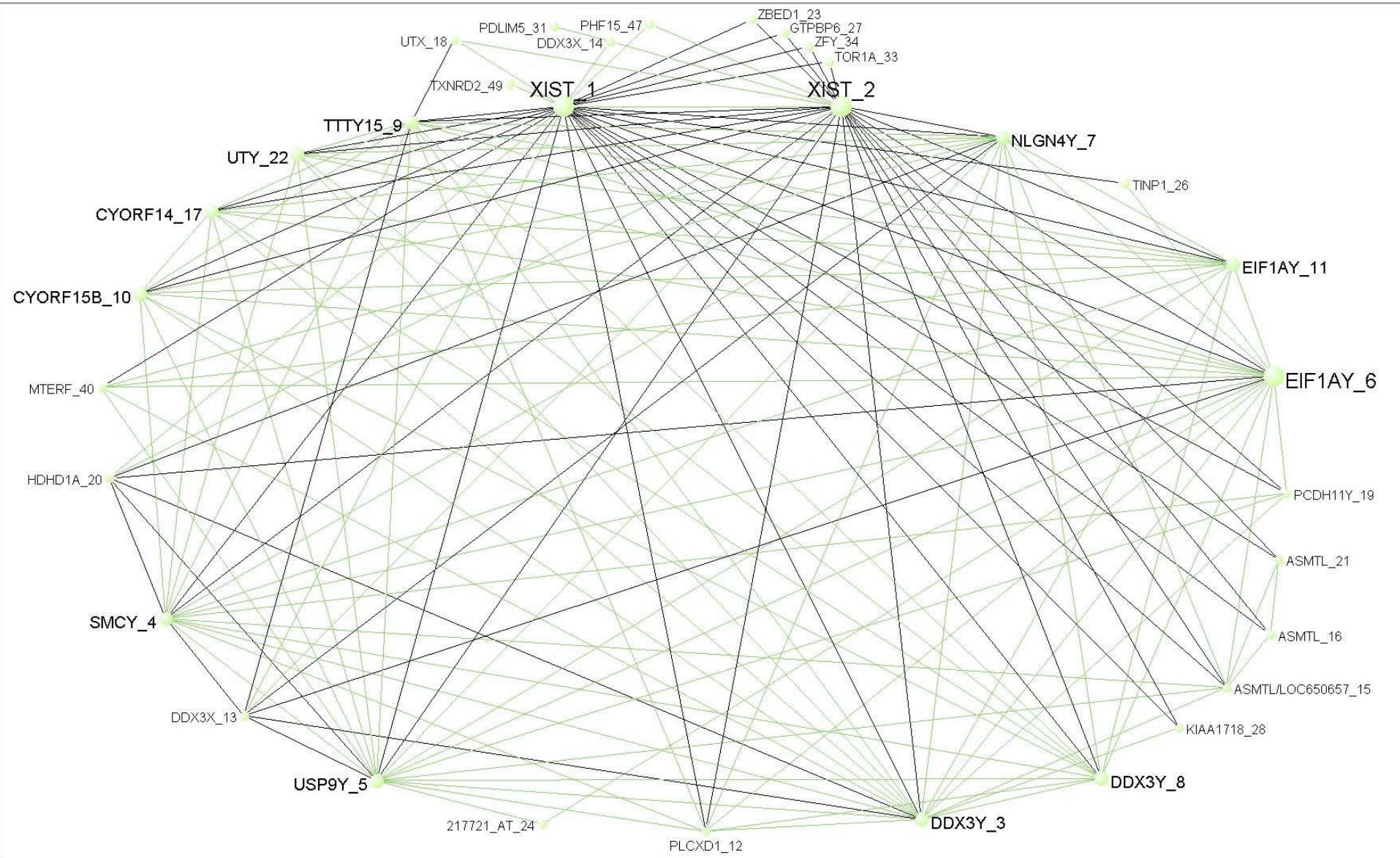

Figure S4B

M2

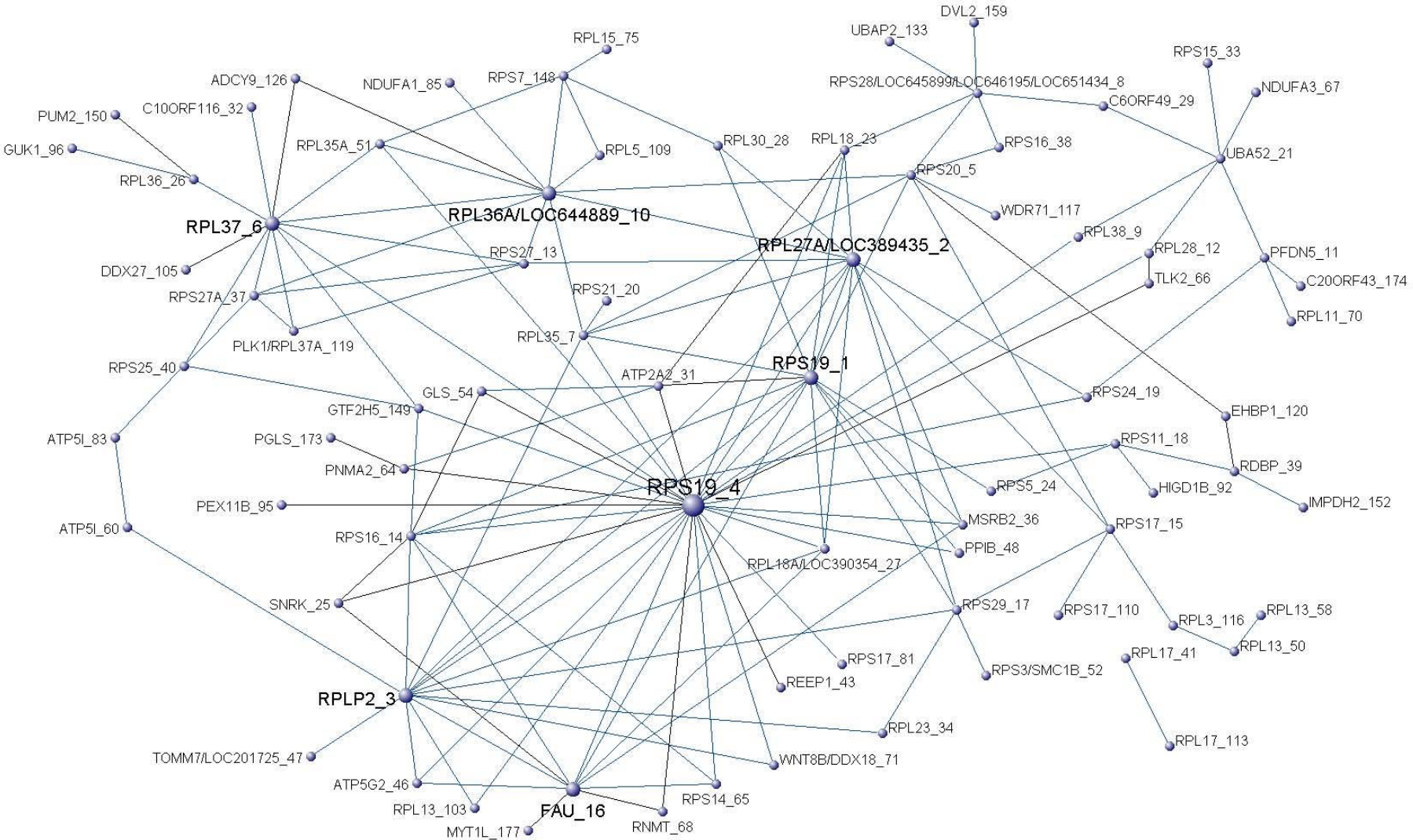

Figure S4C

M3

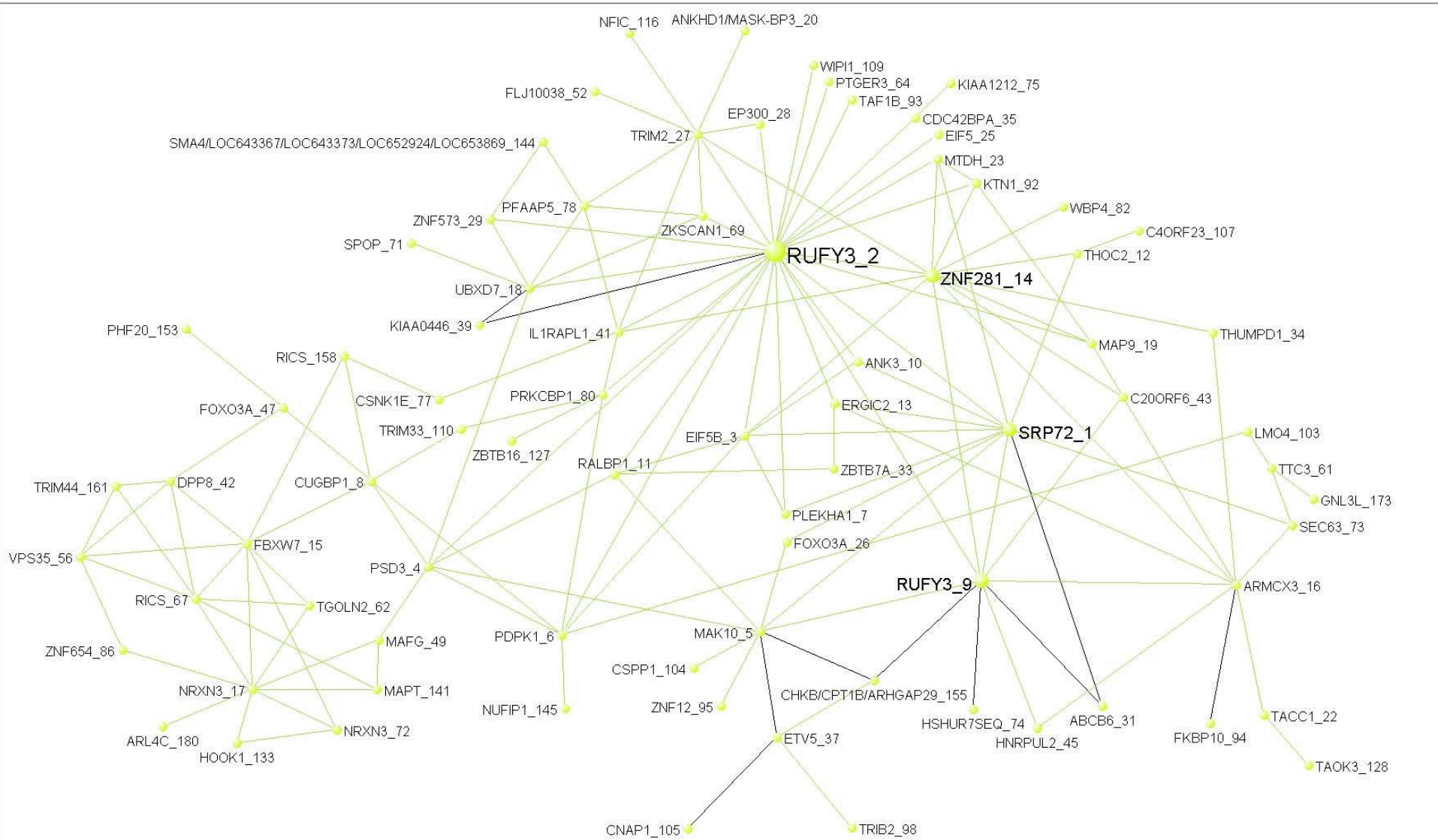

Figure S4D

M4A

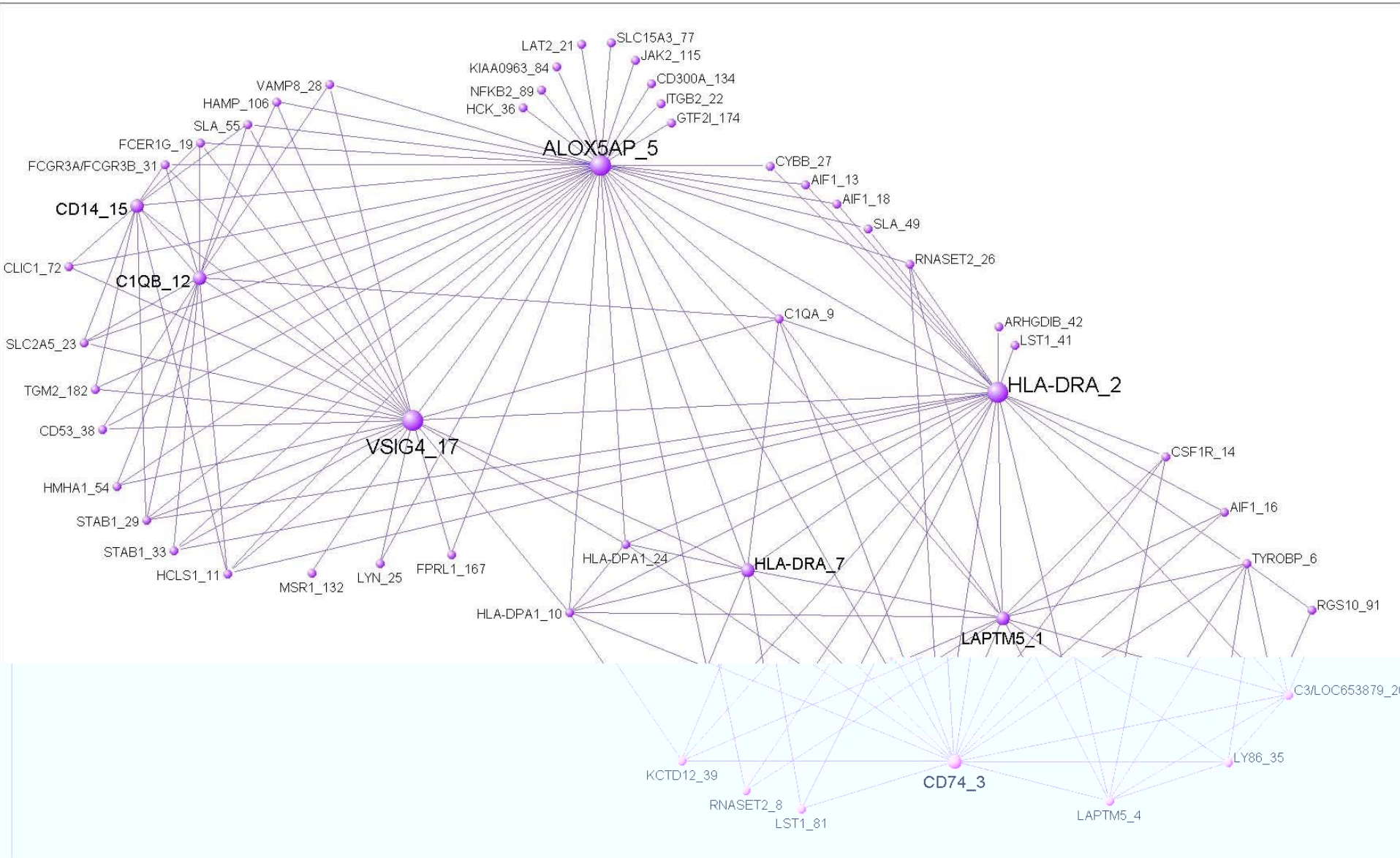

Figure S4E

M5A

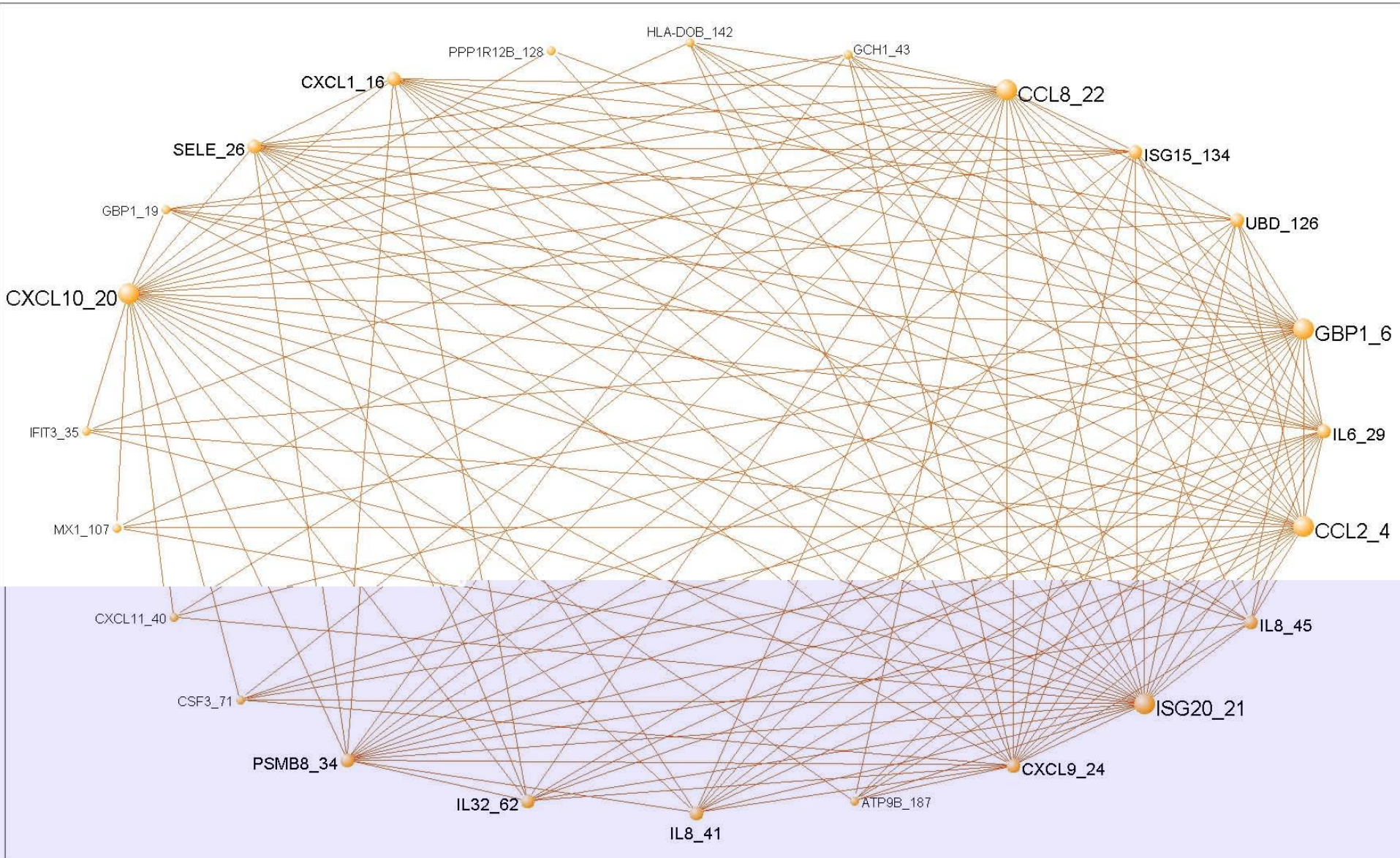

Figure S4F

M6A

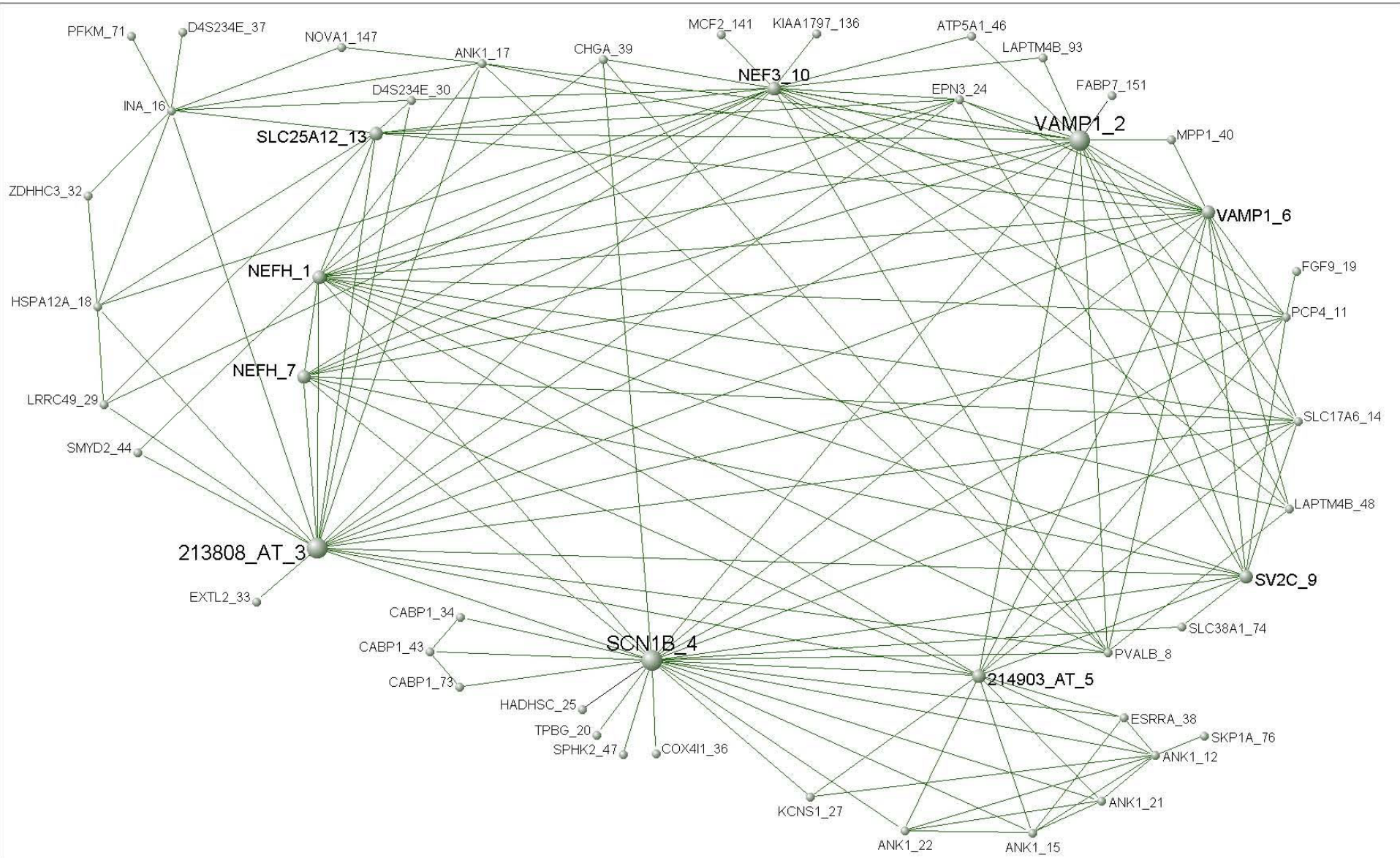

Figure S4G

M7A

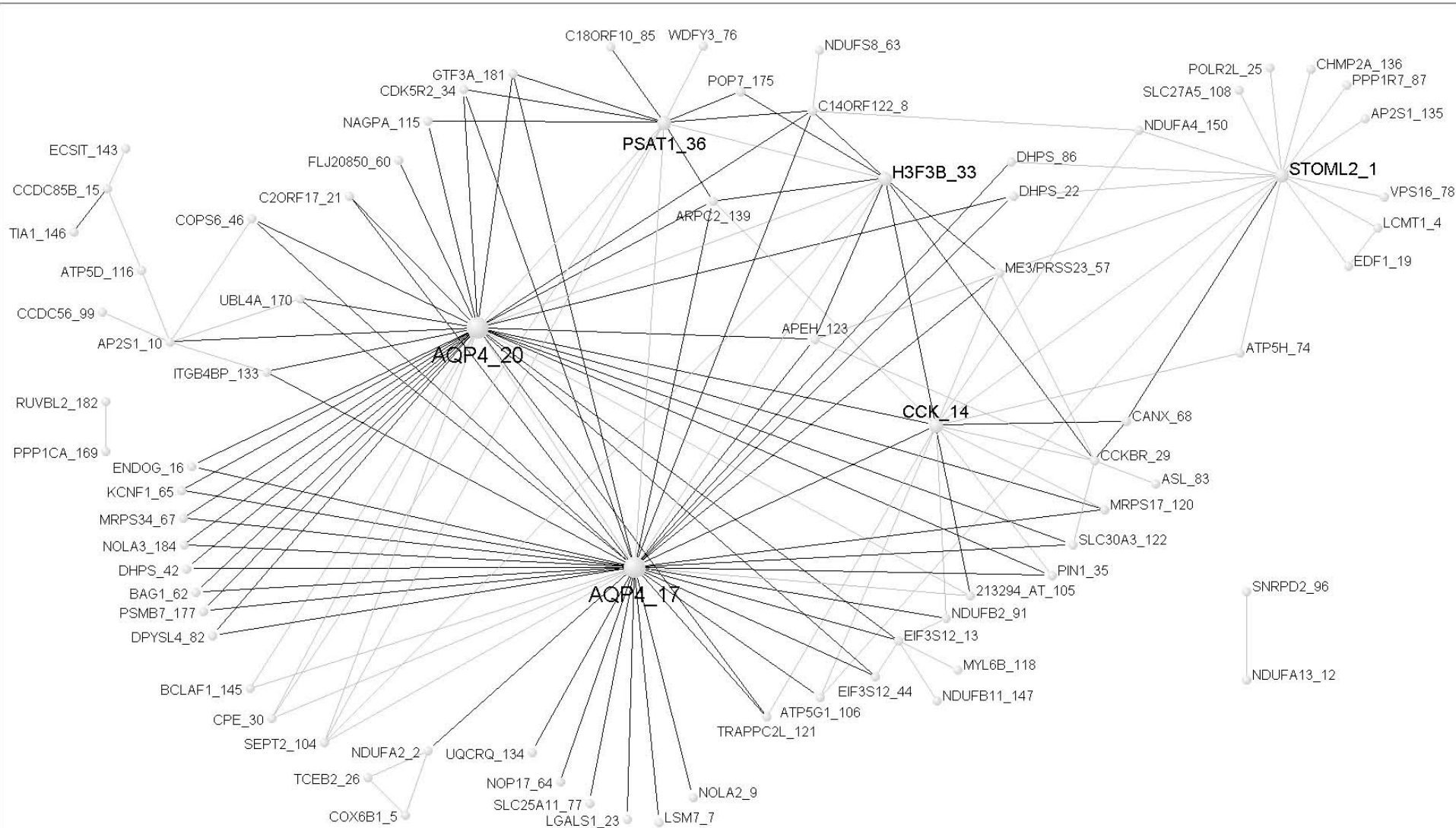

Figure S4H

M8A

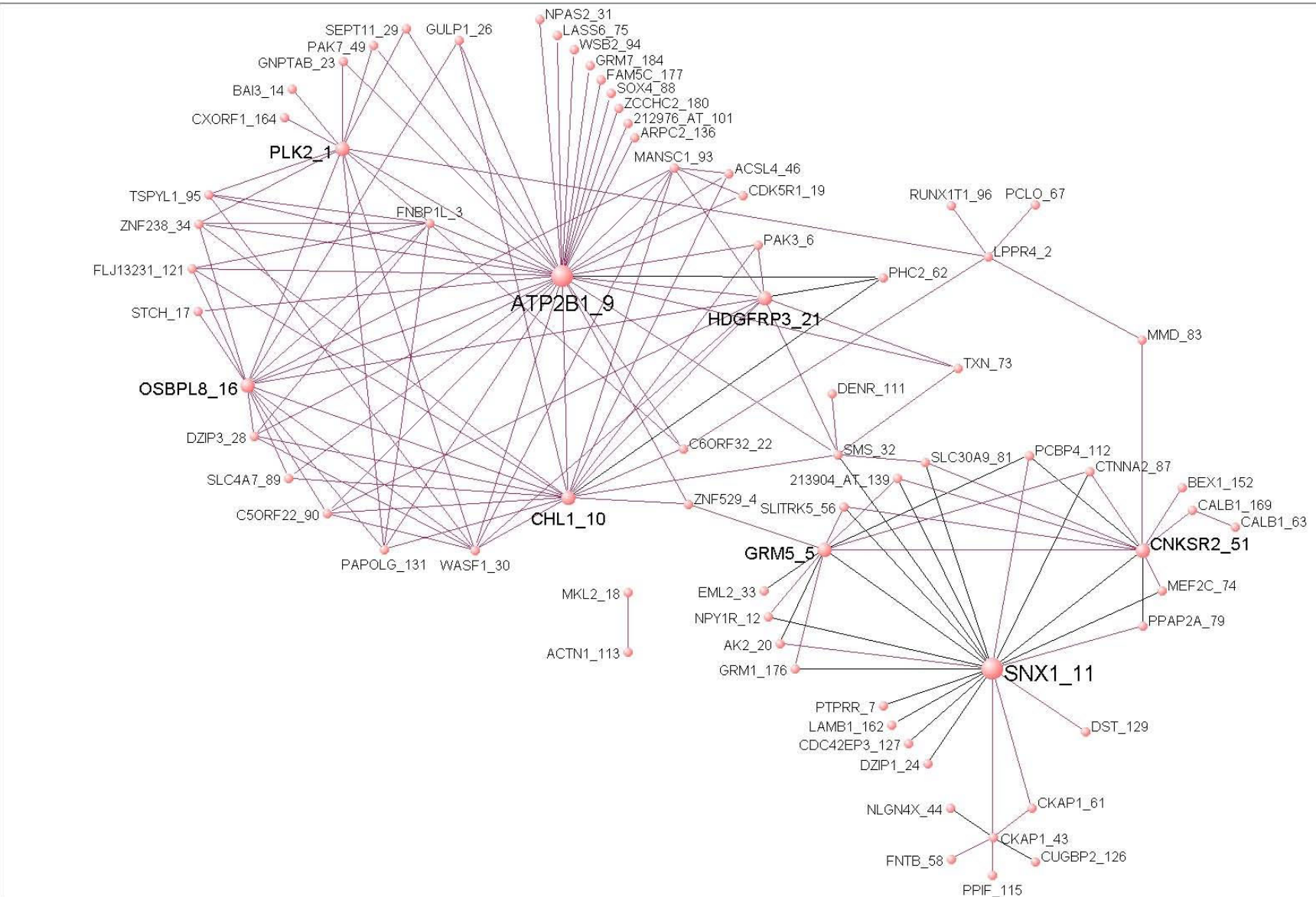

Figure S4I

M9A

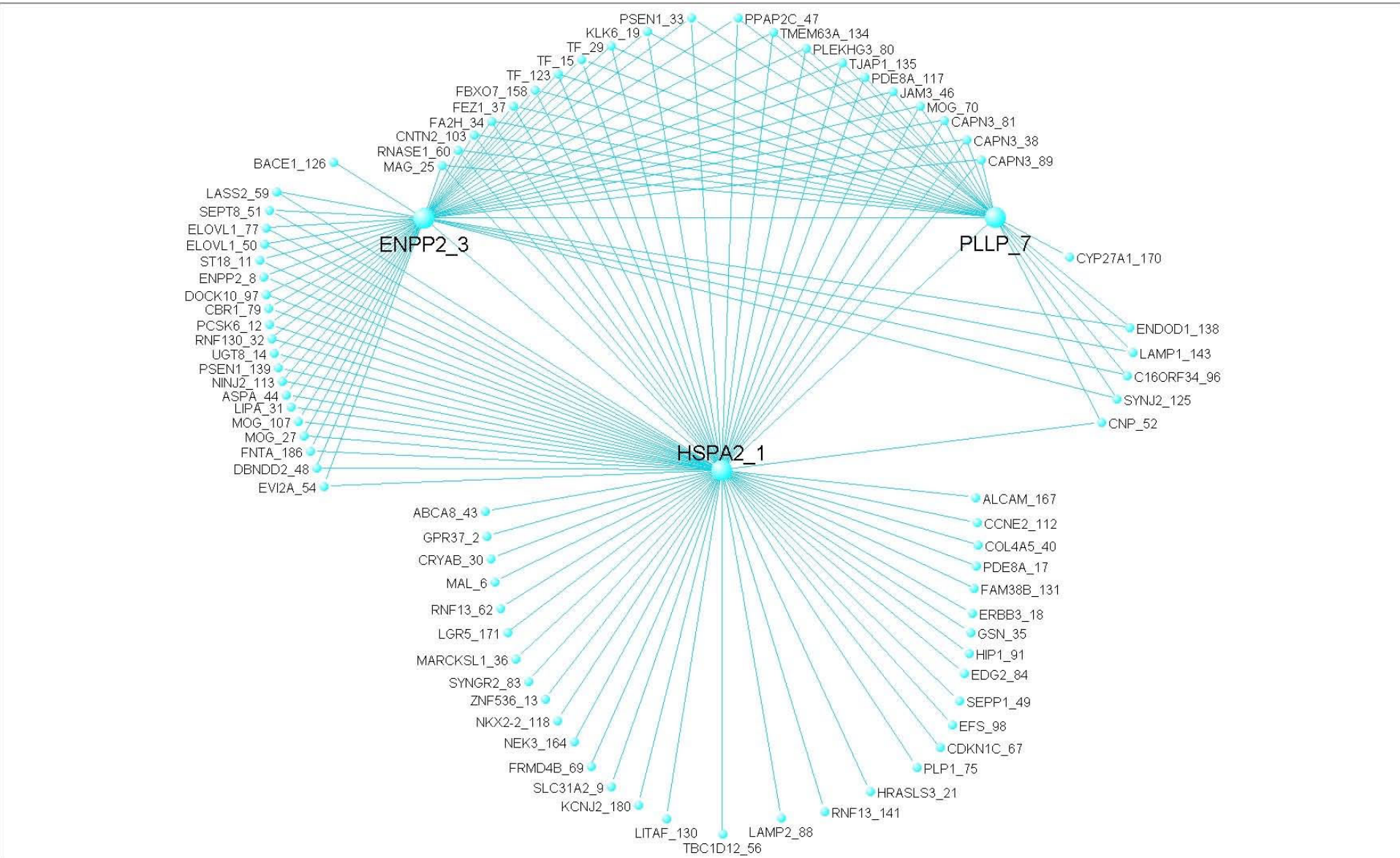

Figure S4J

M10A

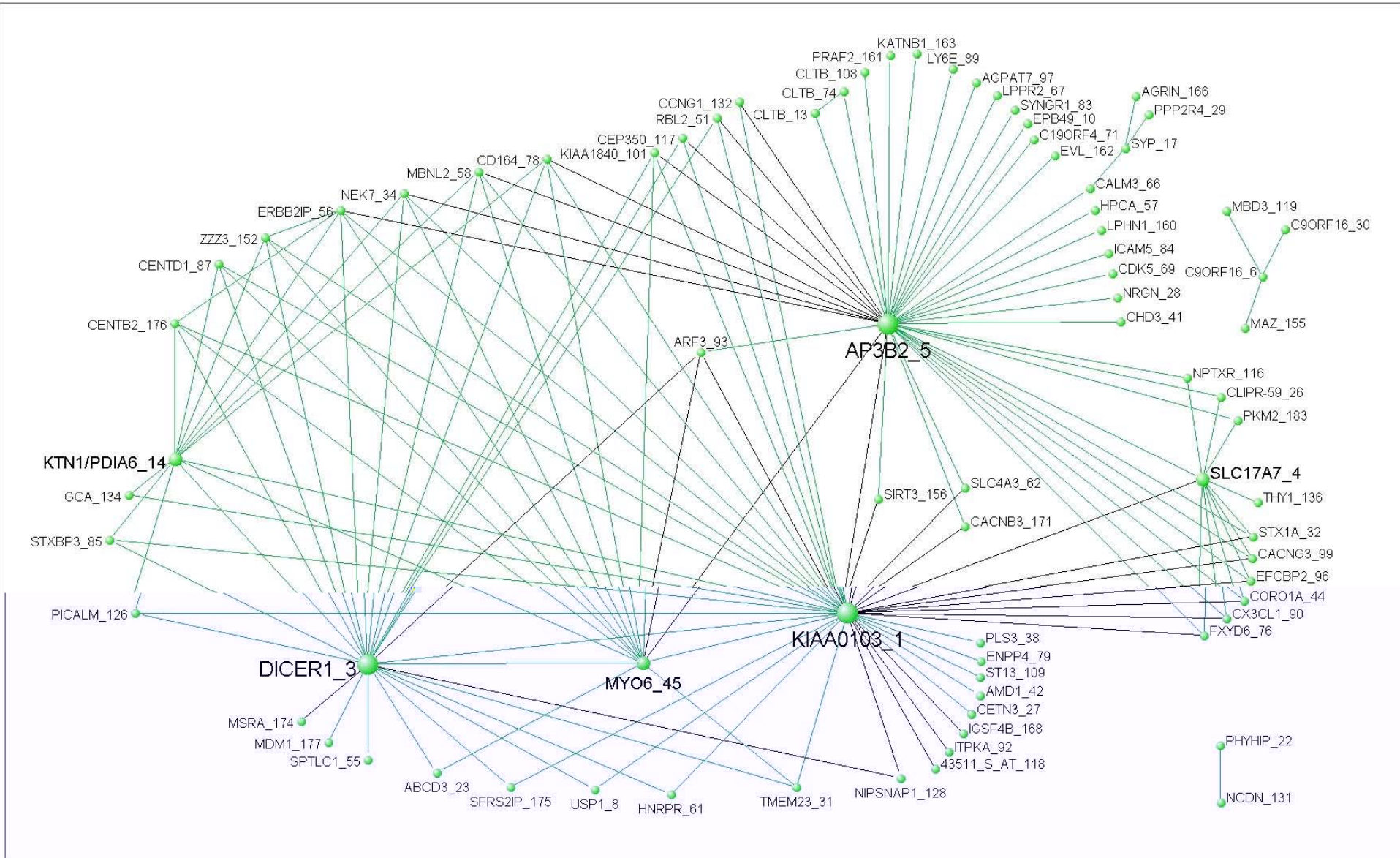

Figure S4K

M11A

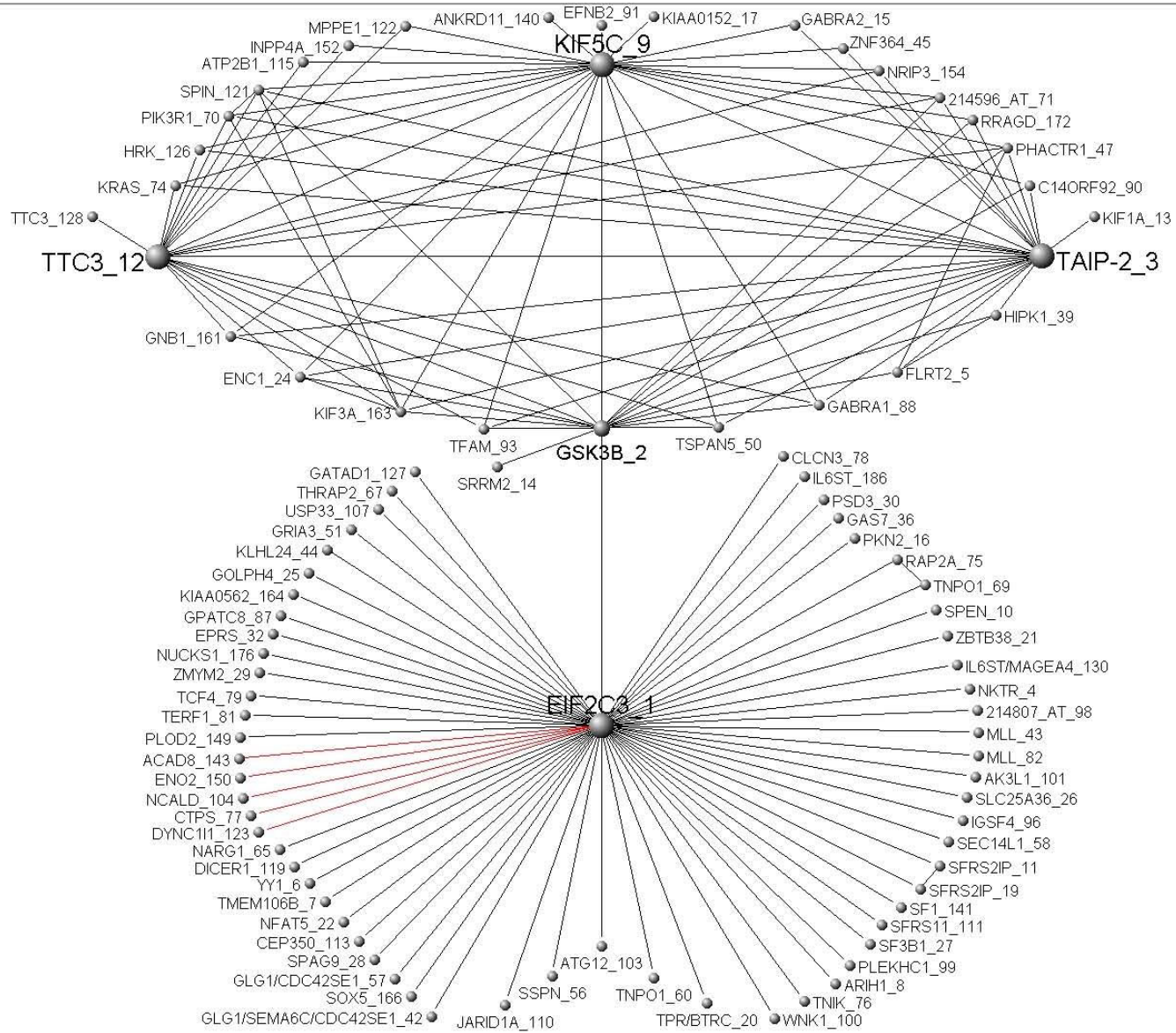

Figure S4L

M12A

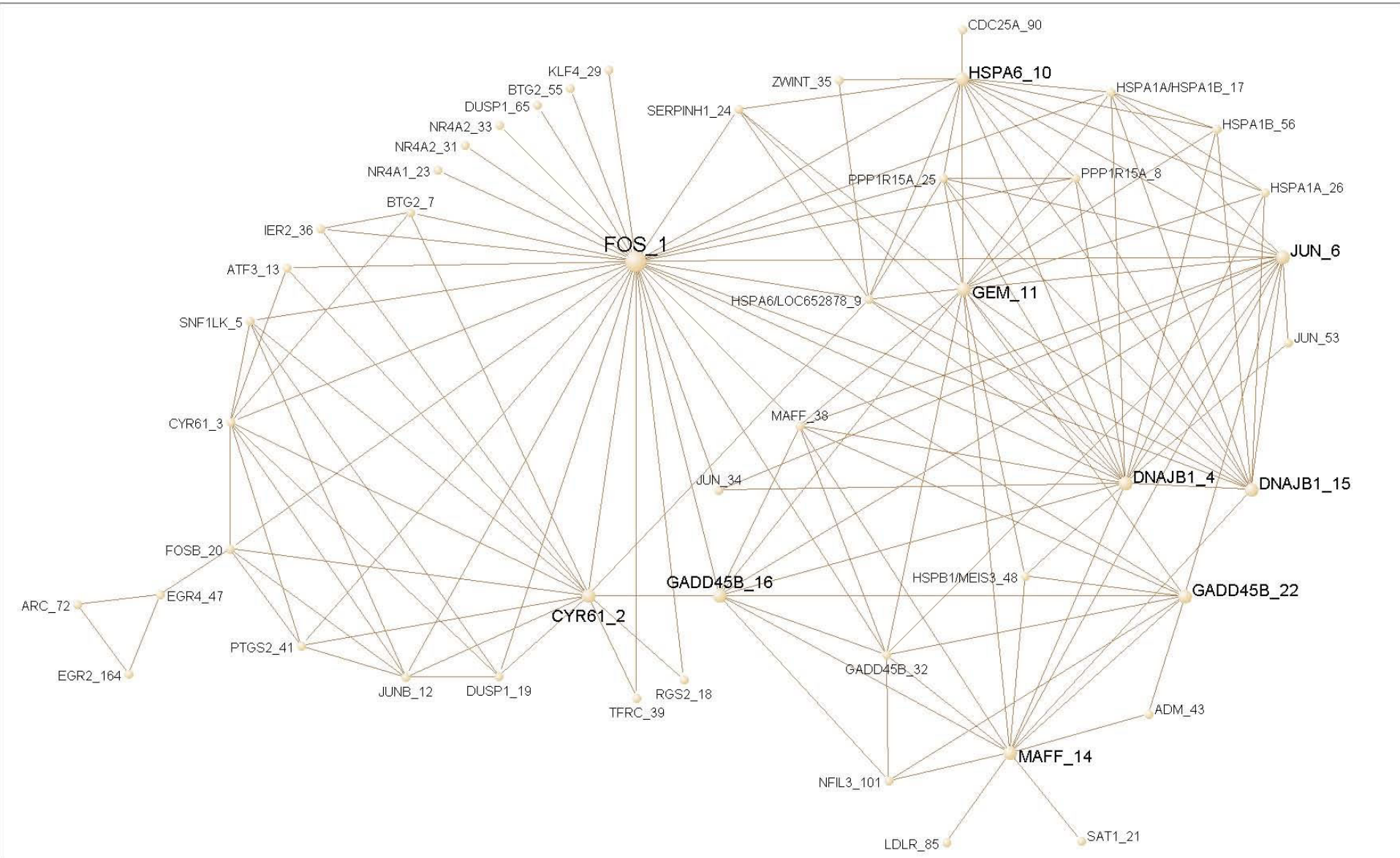

Figure S4M

M13A

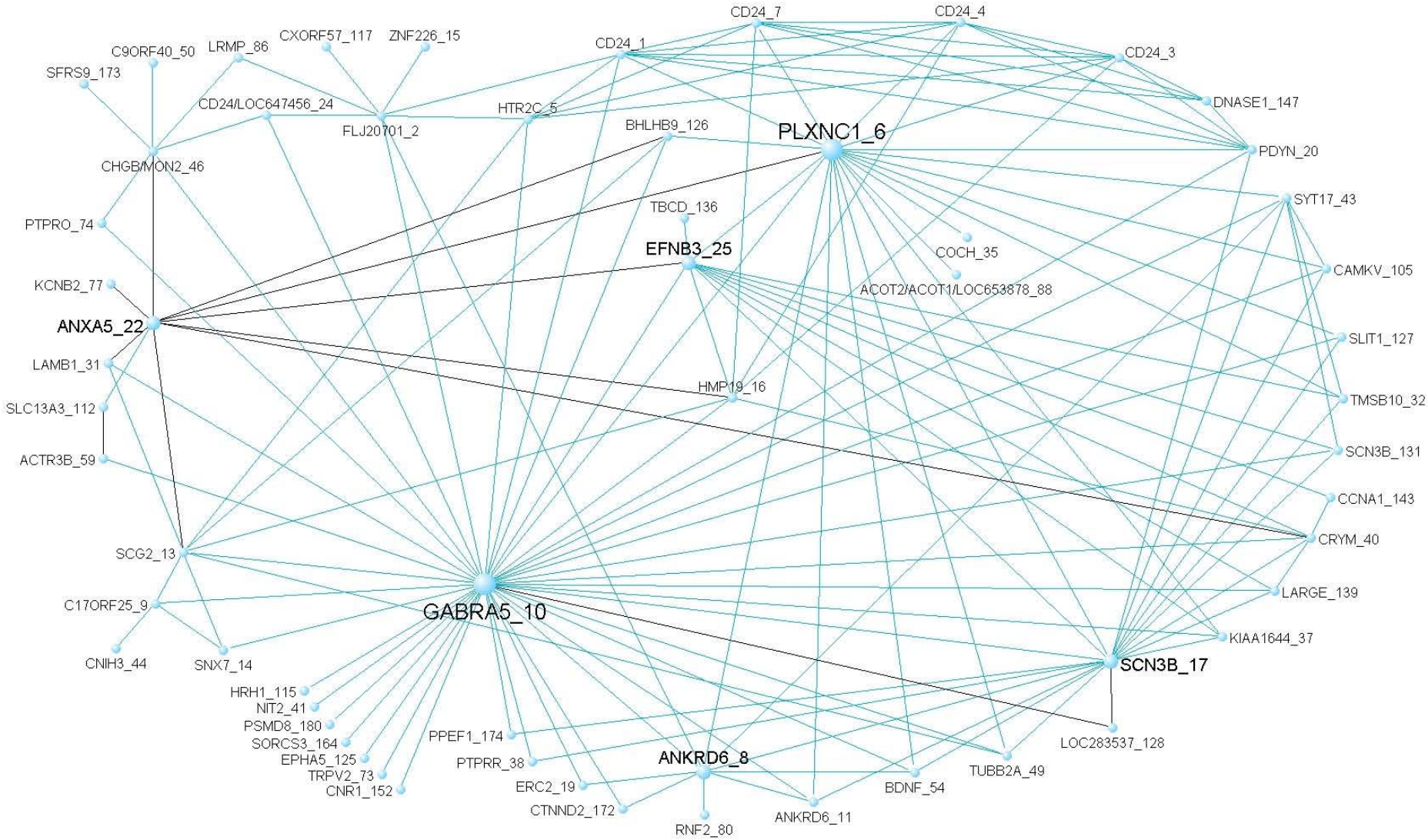

Figure S4N

M14A

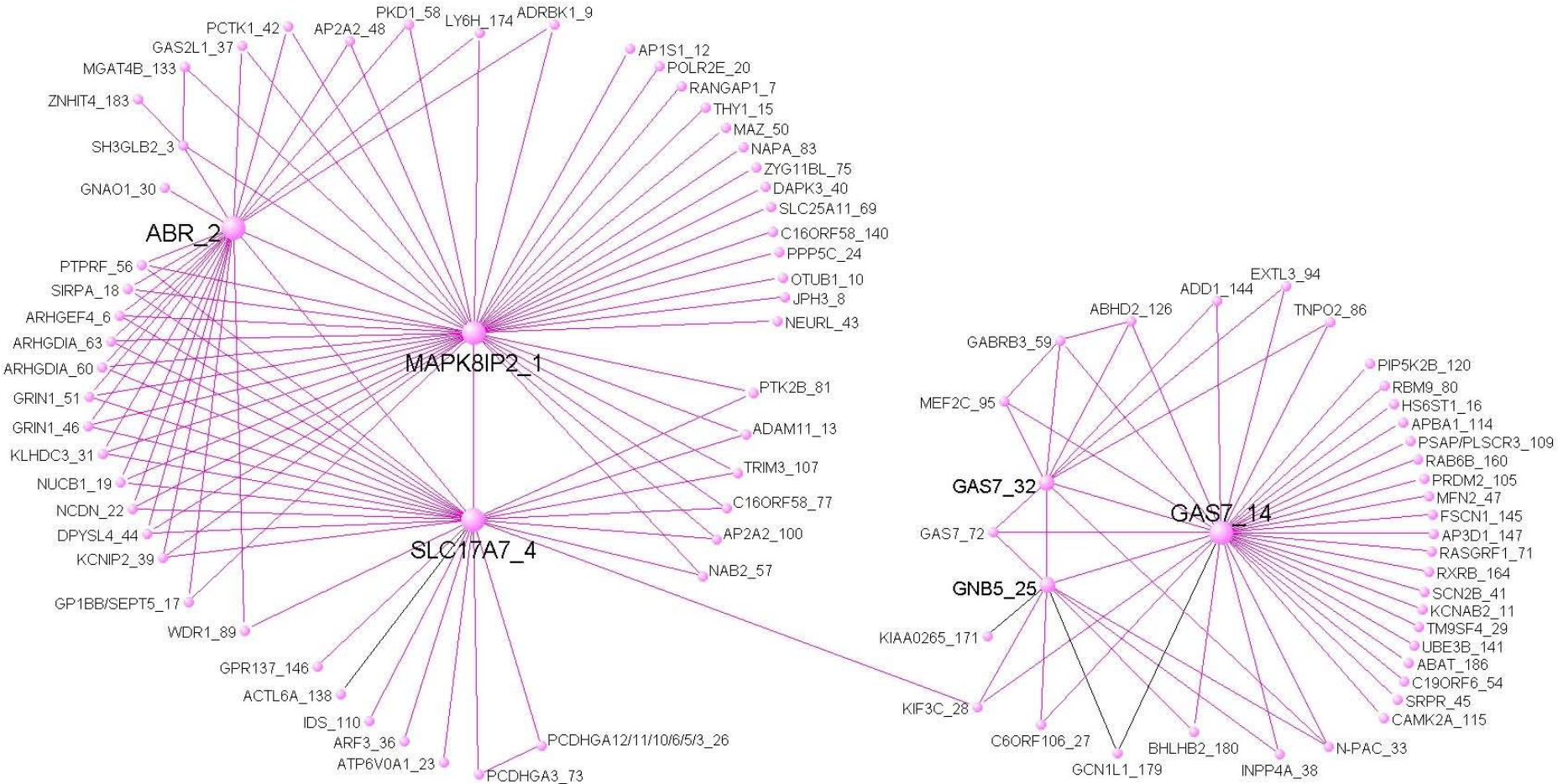

Figure S4O

M15A

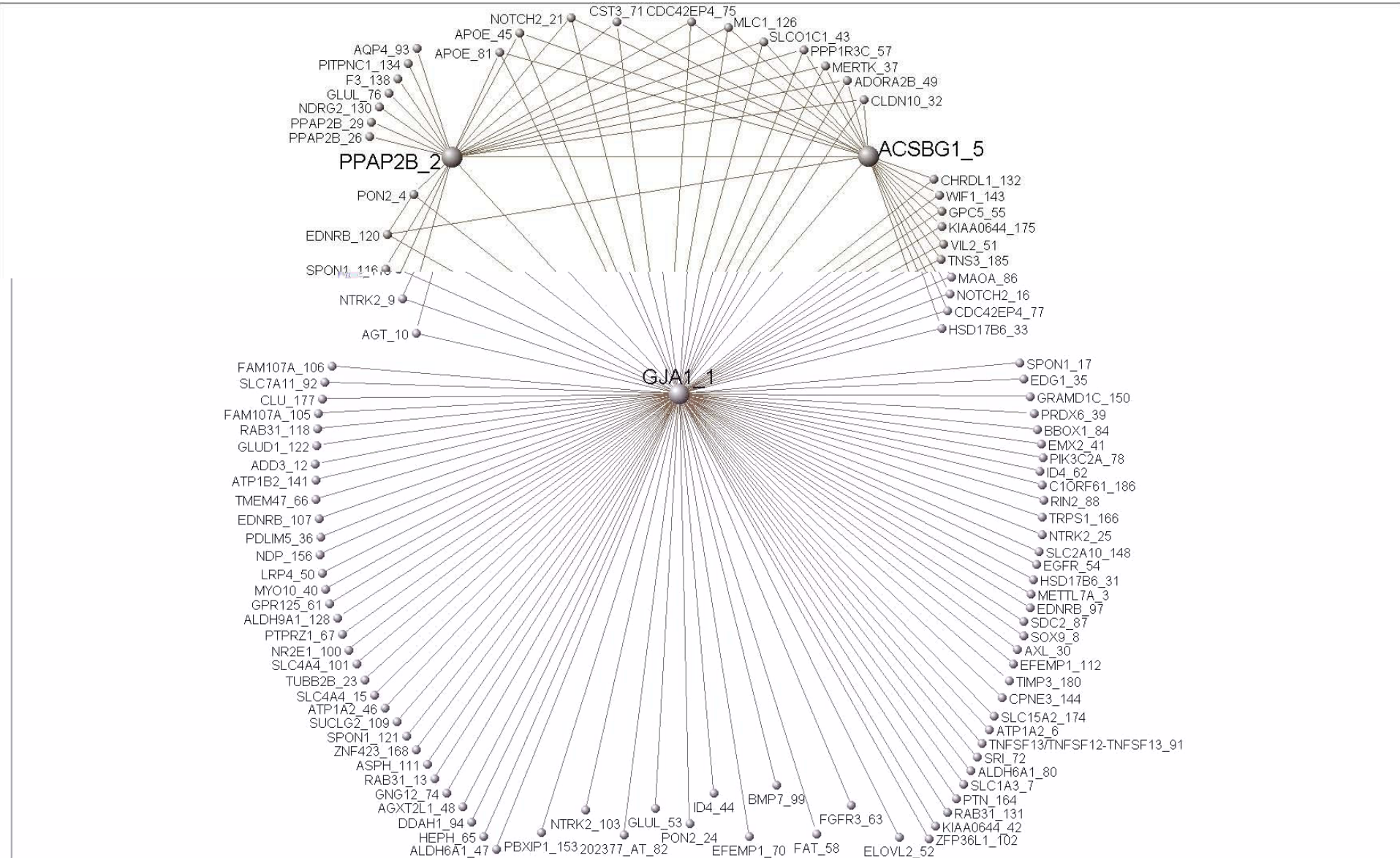

Figure S4P

M16A

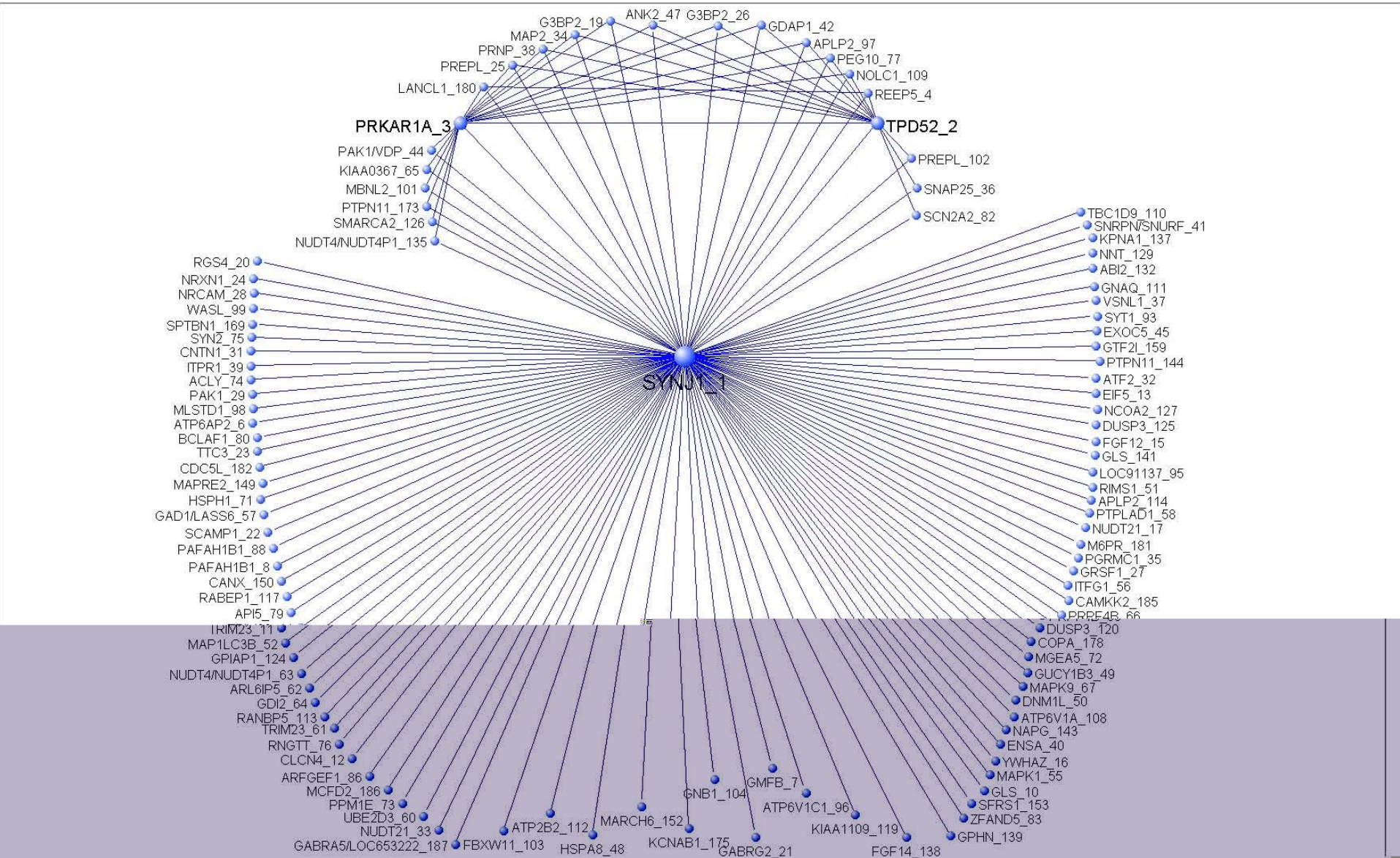

Figure S4Q

M17A

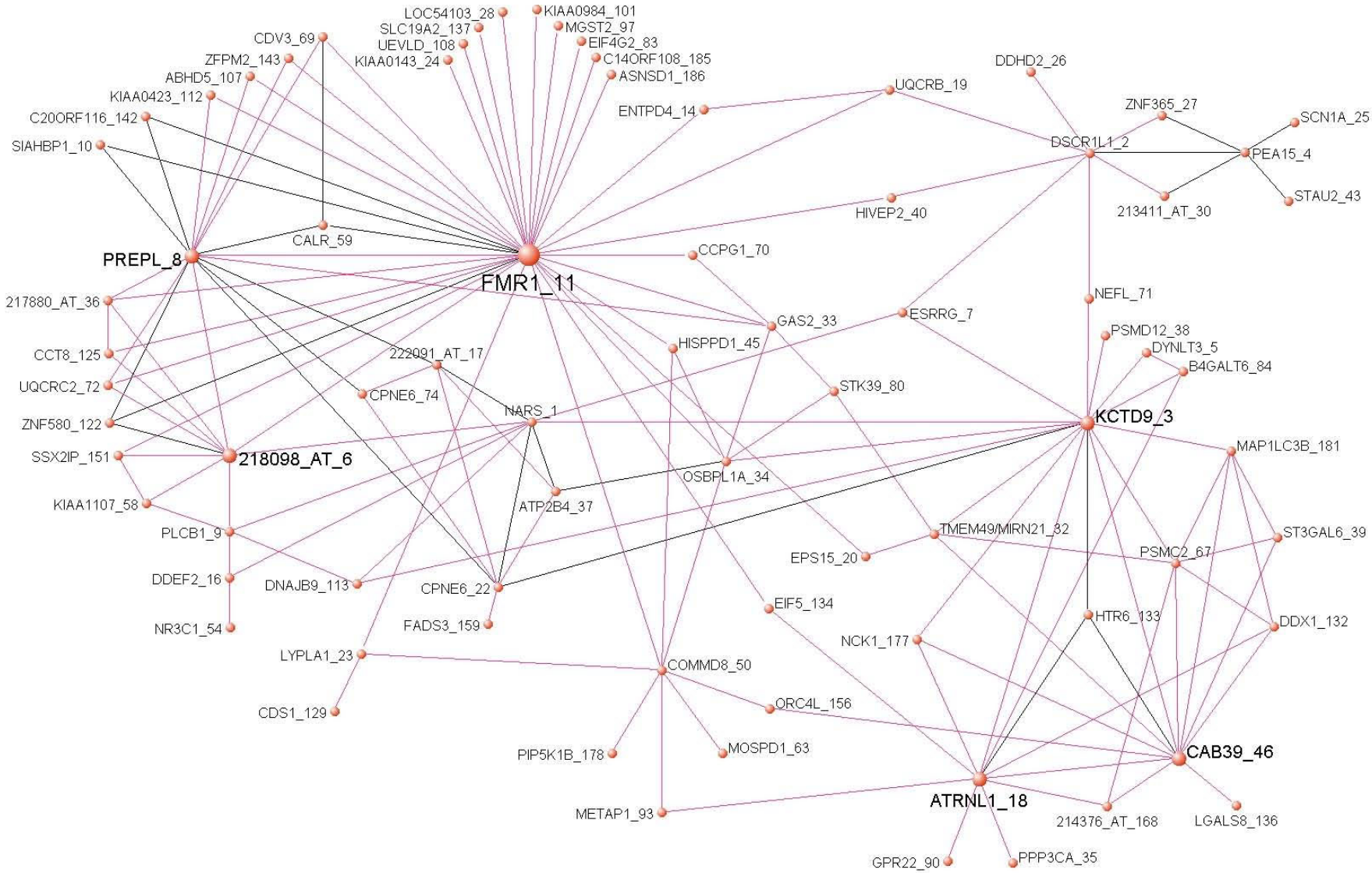

Figure S4R

M18A

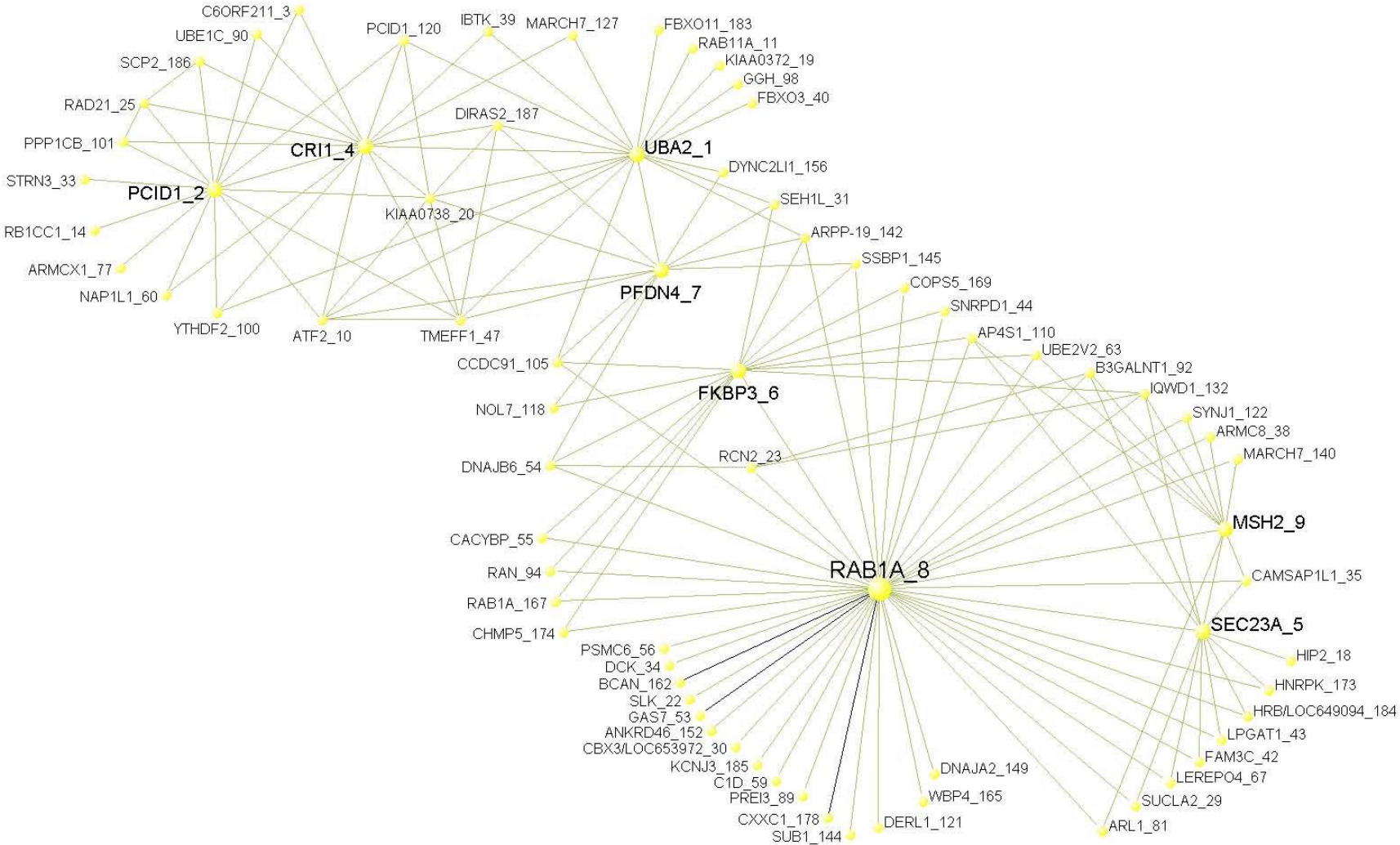

Figure S4S

M19A

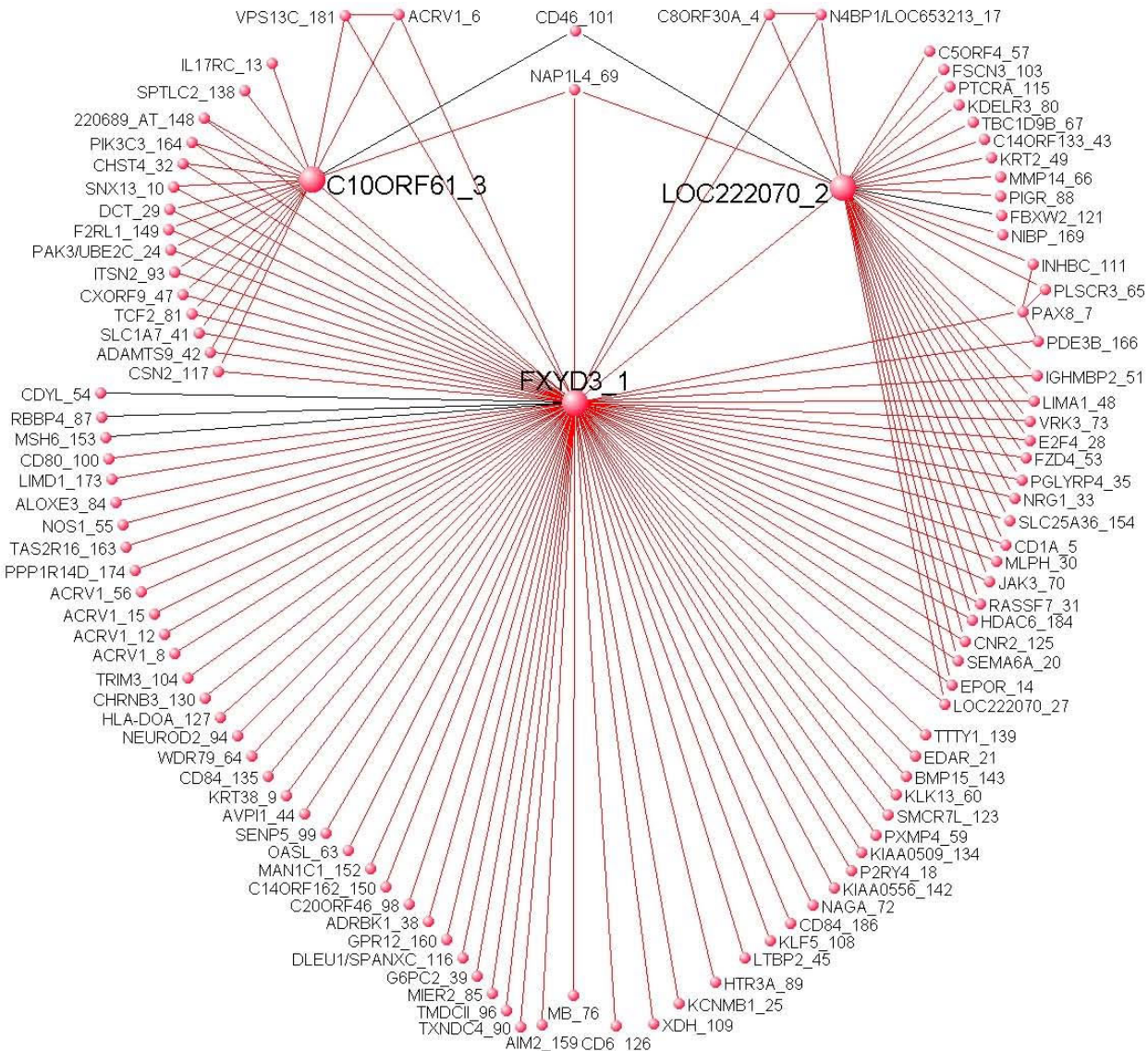

Figure S4

Caudate nucleus

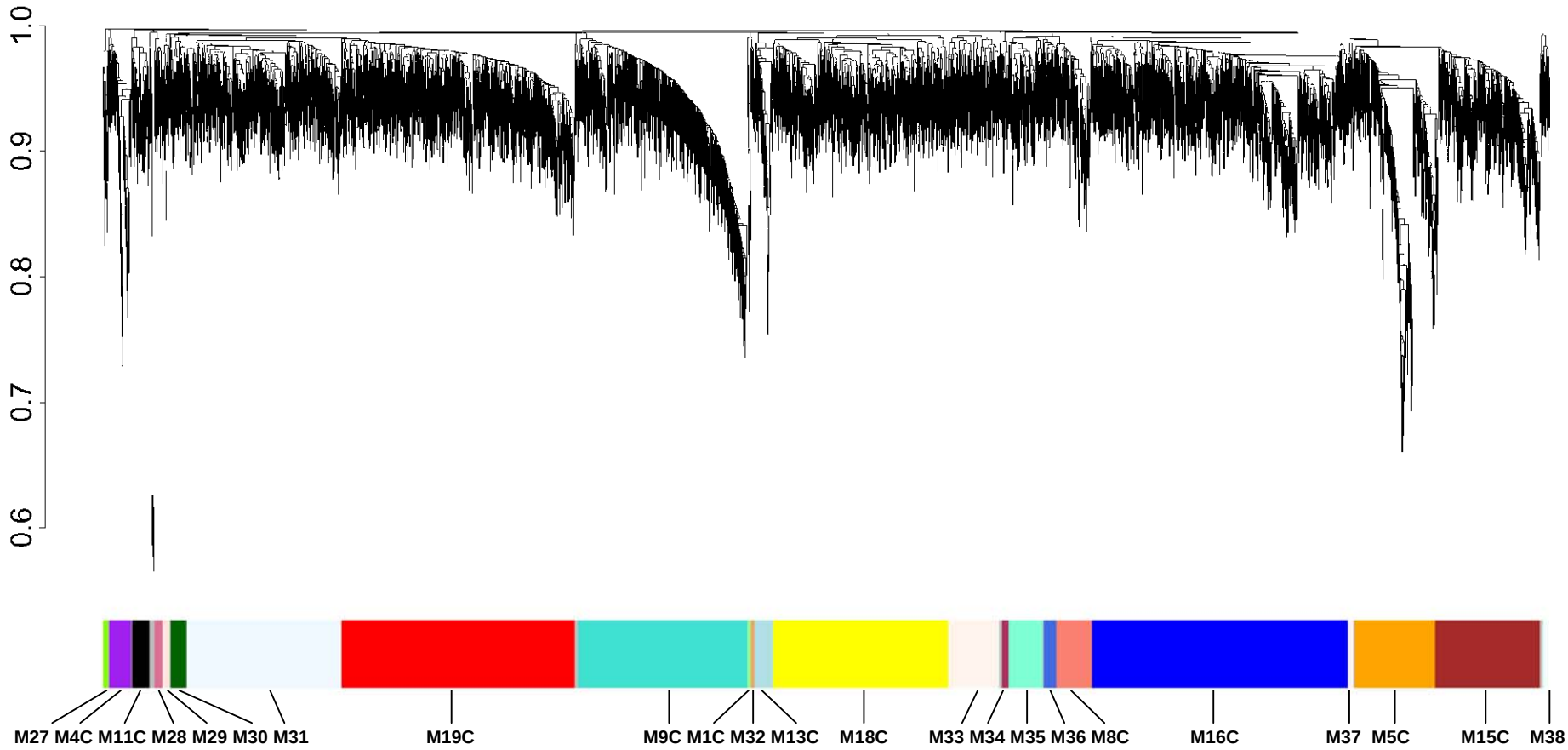

Figure S4T

M1C

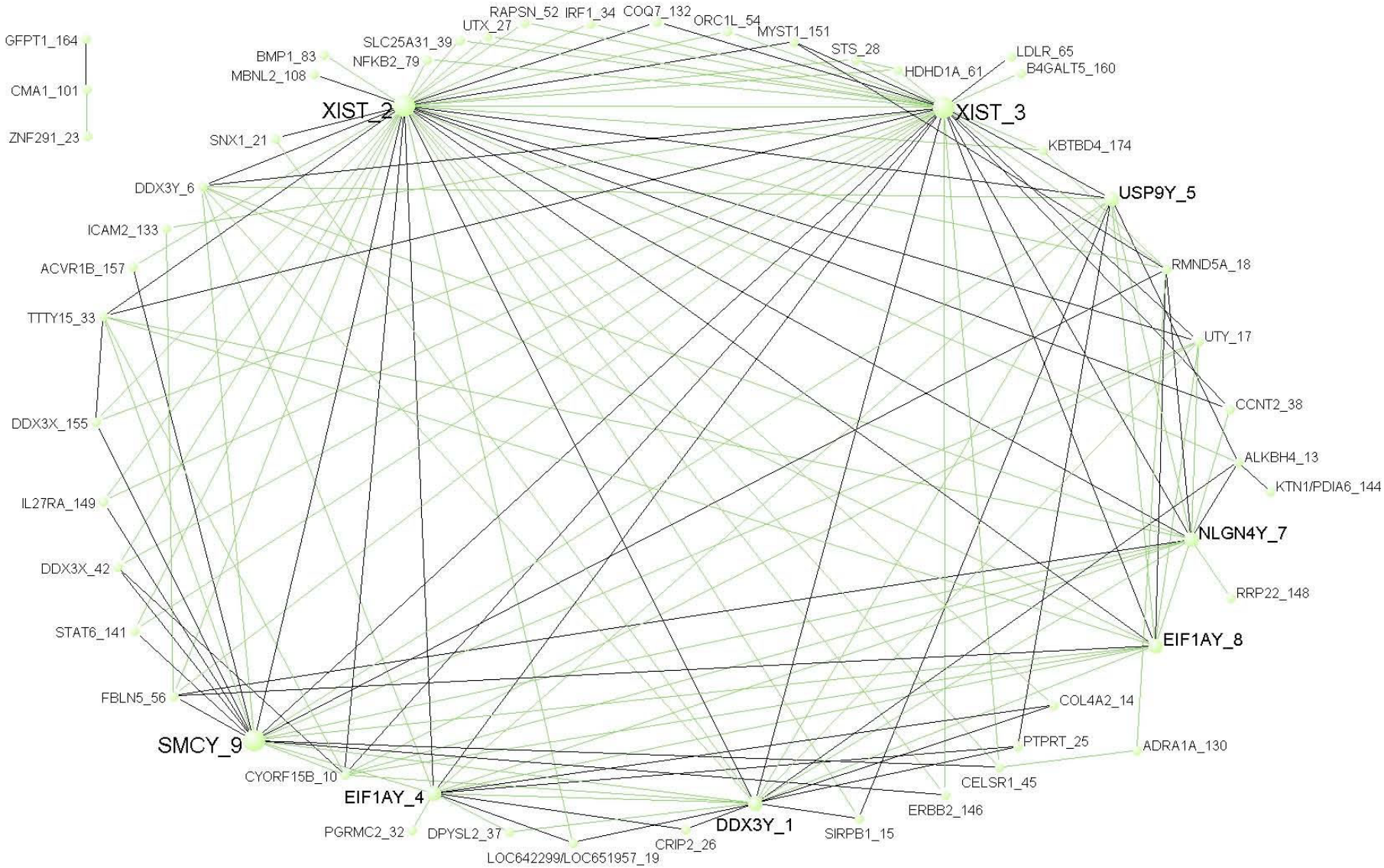

Figure S4U

M4C

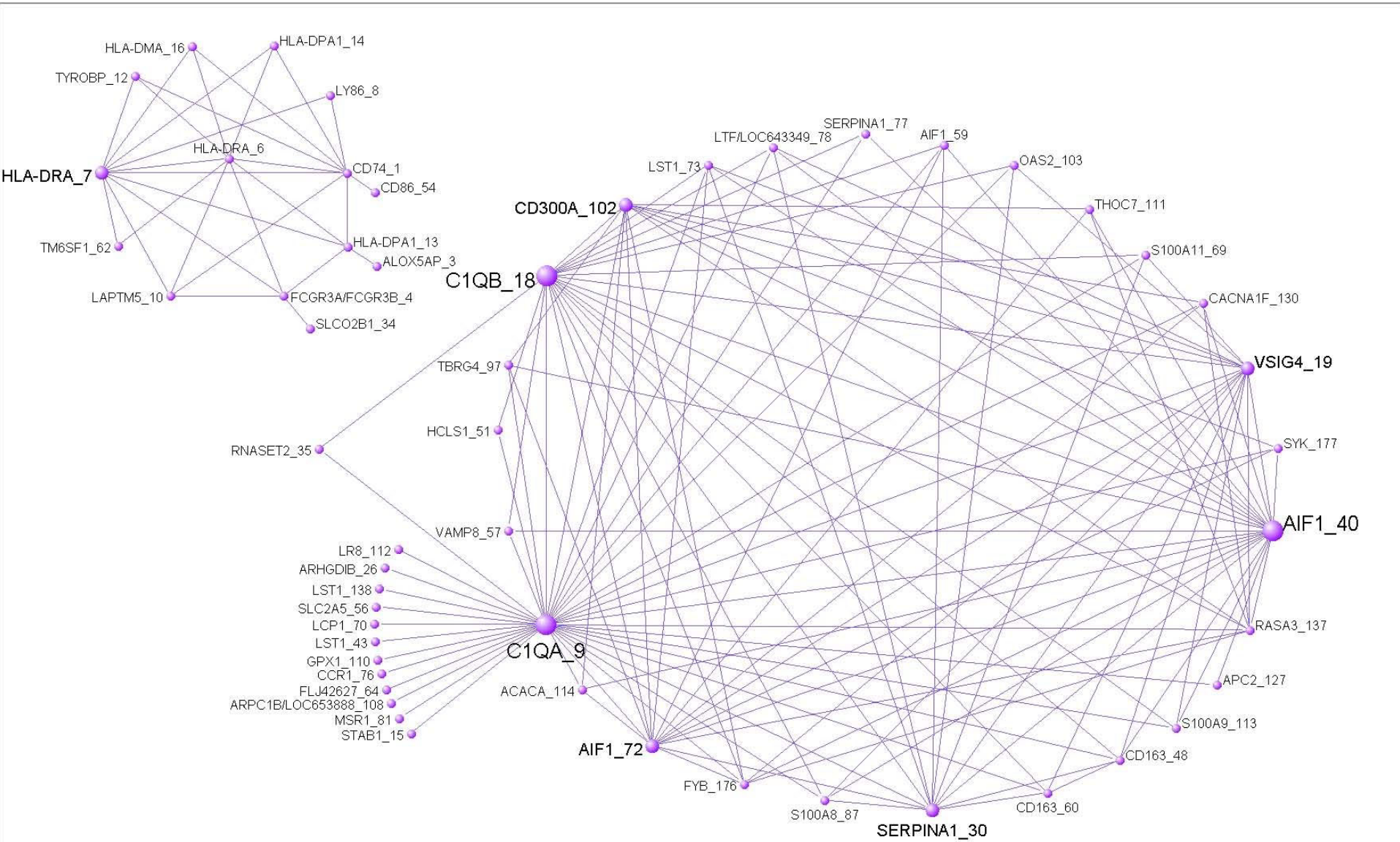

Figure S4V

M5C

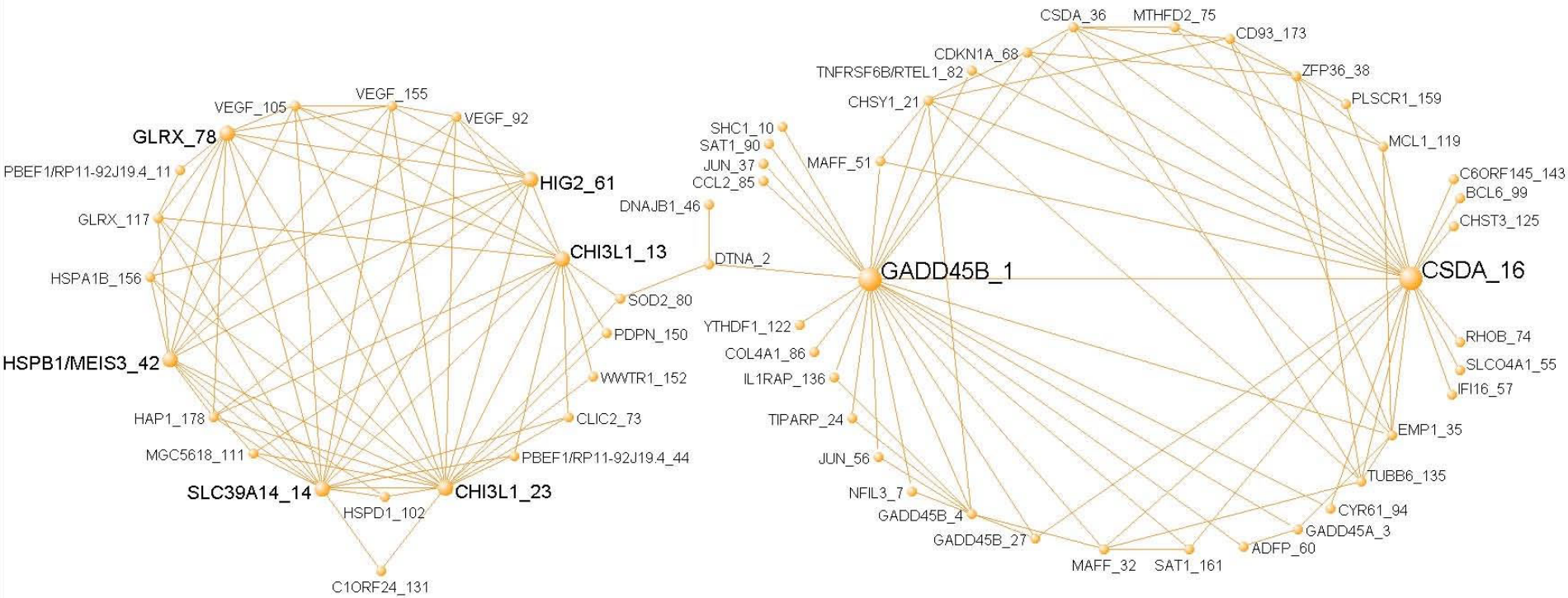

Figure S4W

M8C

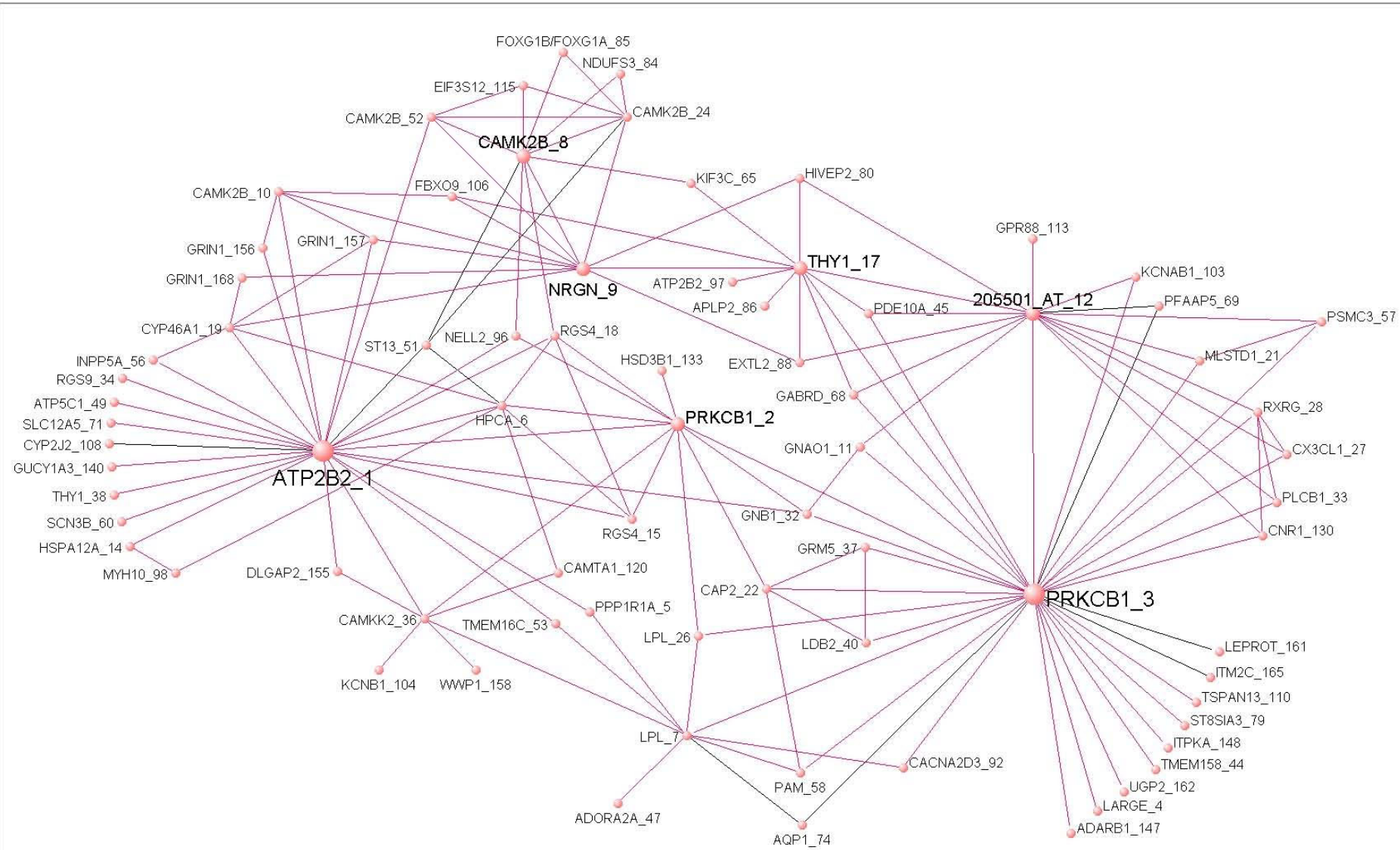

Figure S4X

M9C

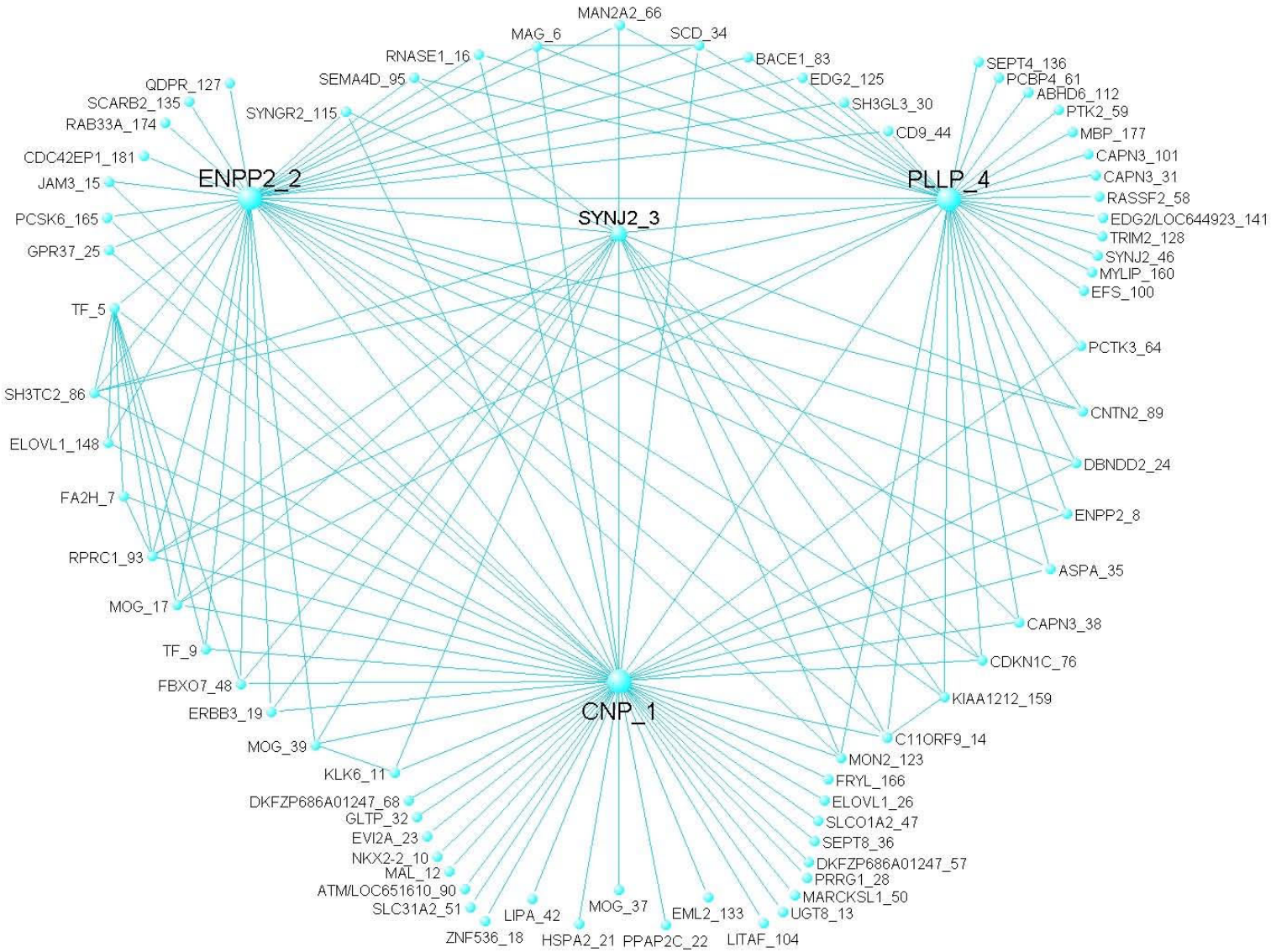

Figure S4Y

M11C

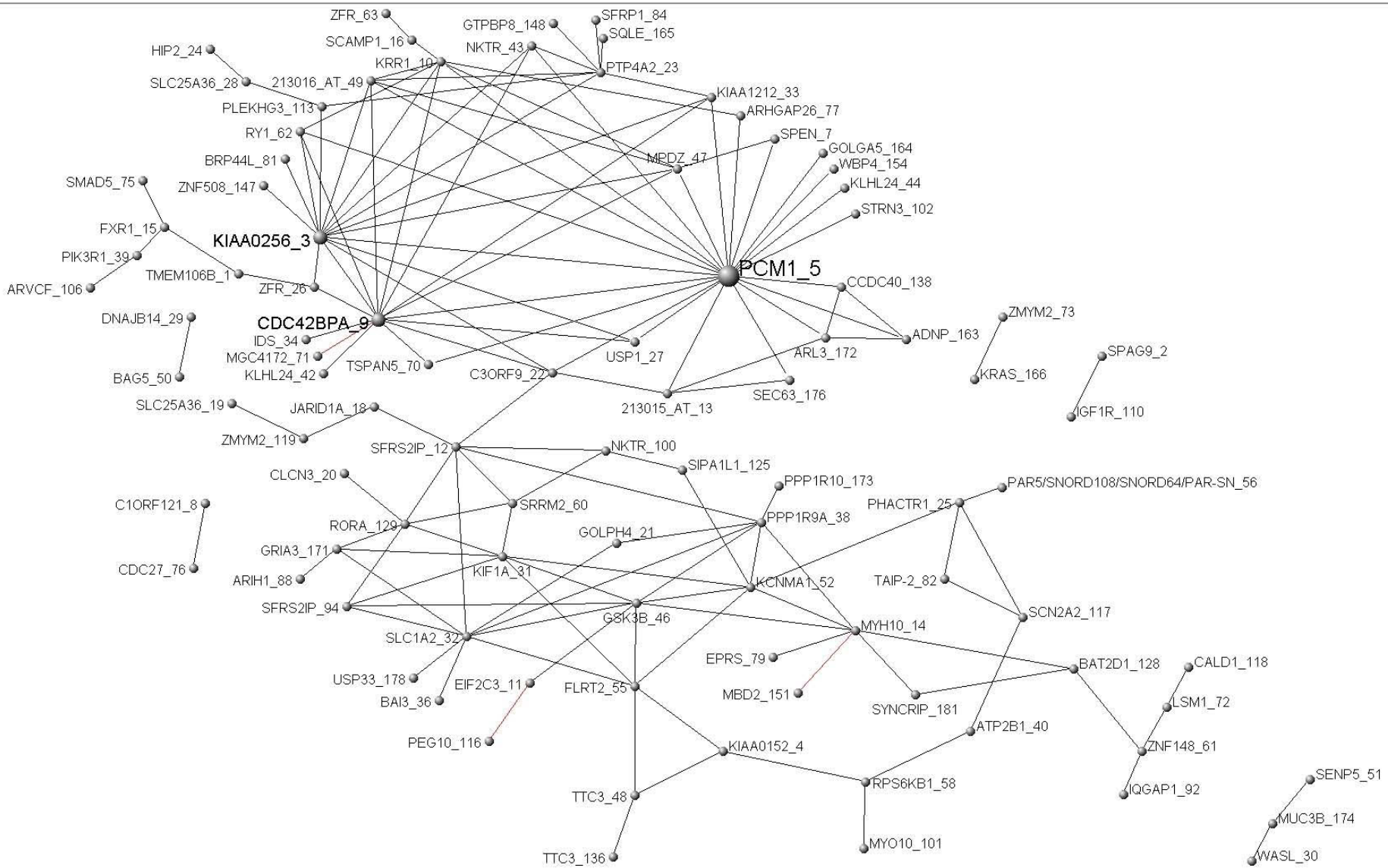

Figure S4Z

M13C

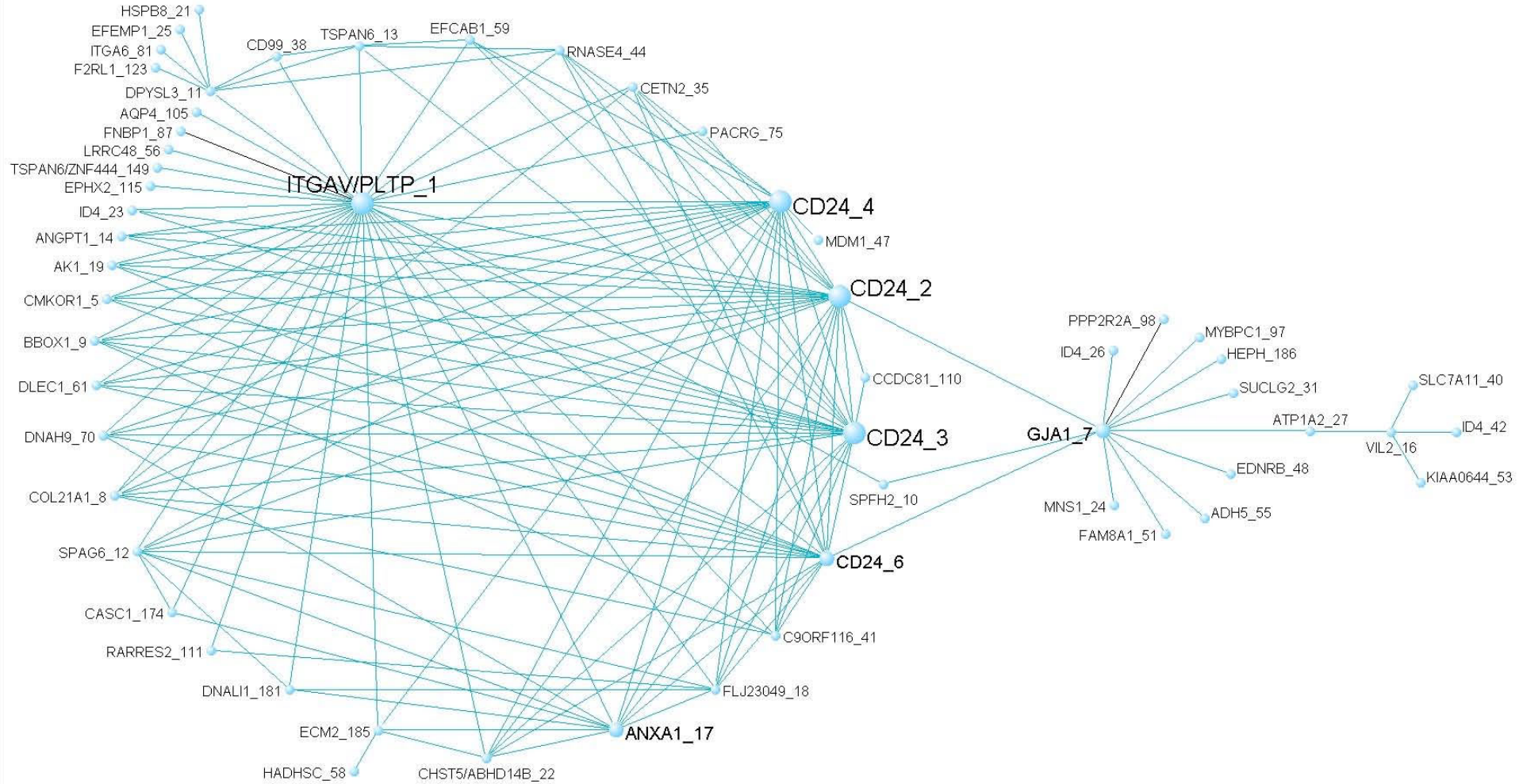

Figure S4AA

M15C

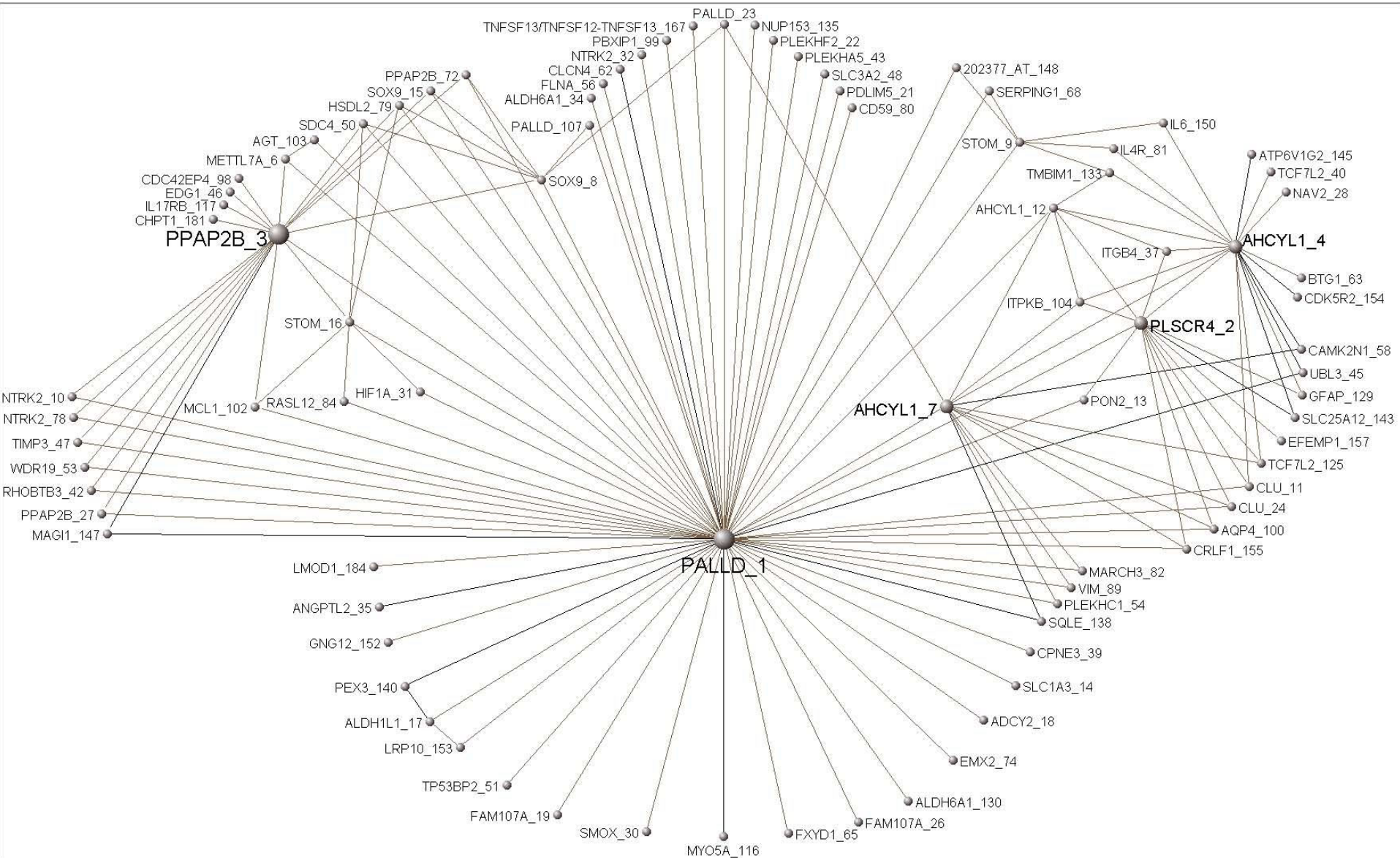

Figure S4AB

M16C

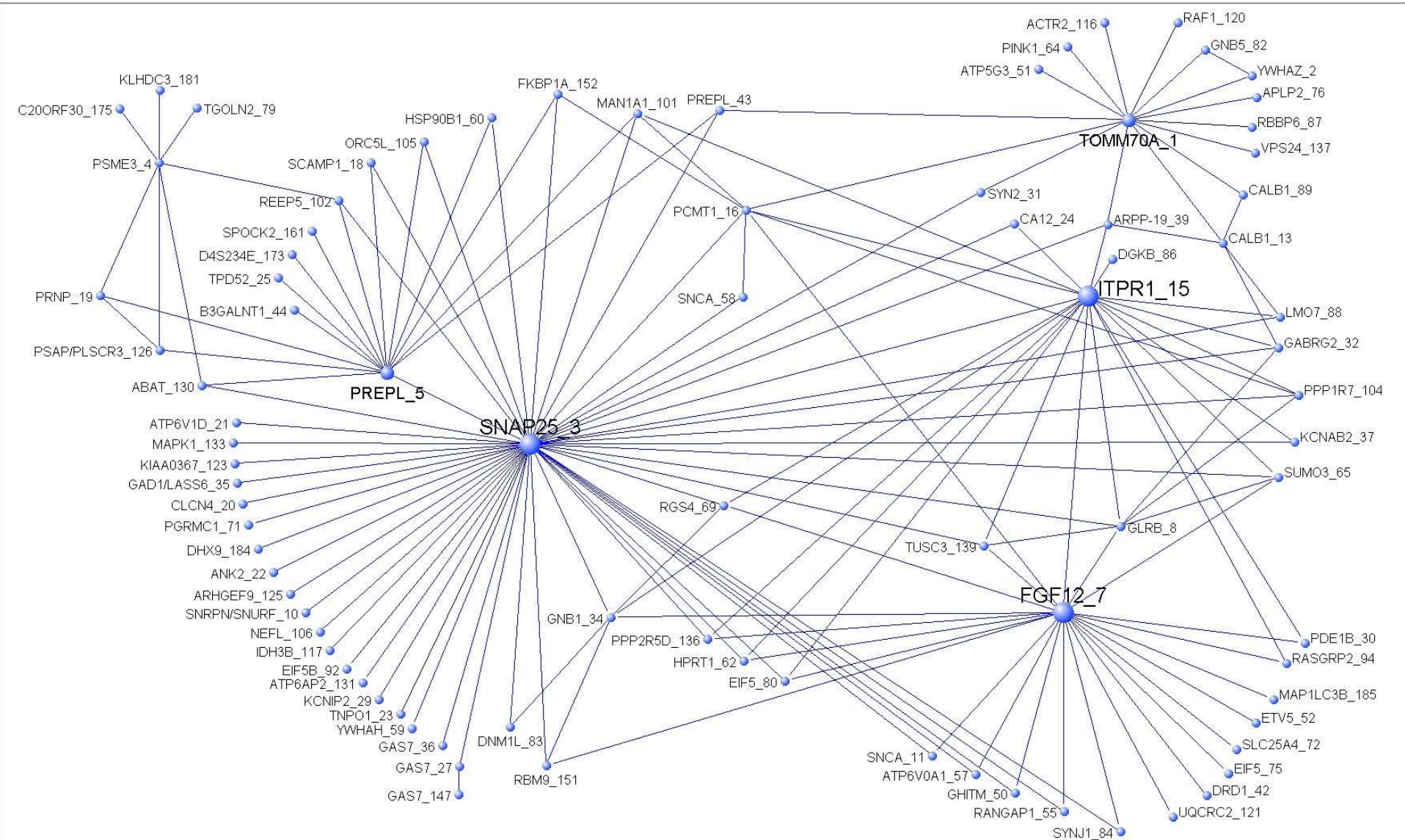

Figure S4AC

M18C

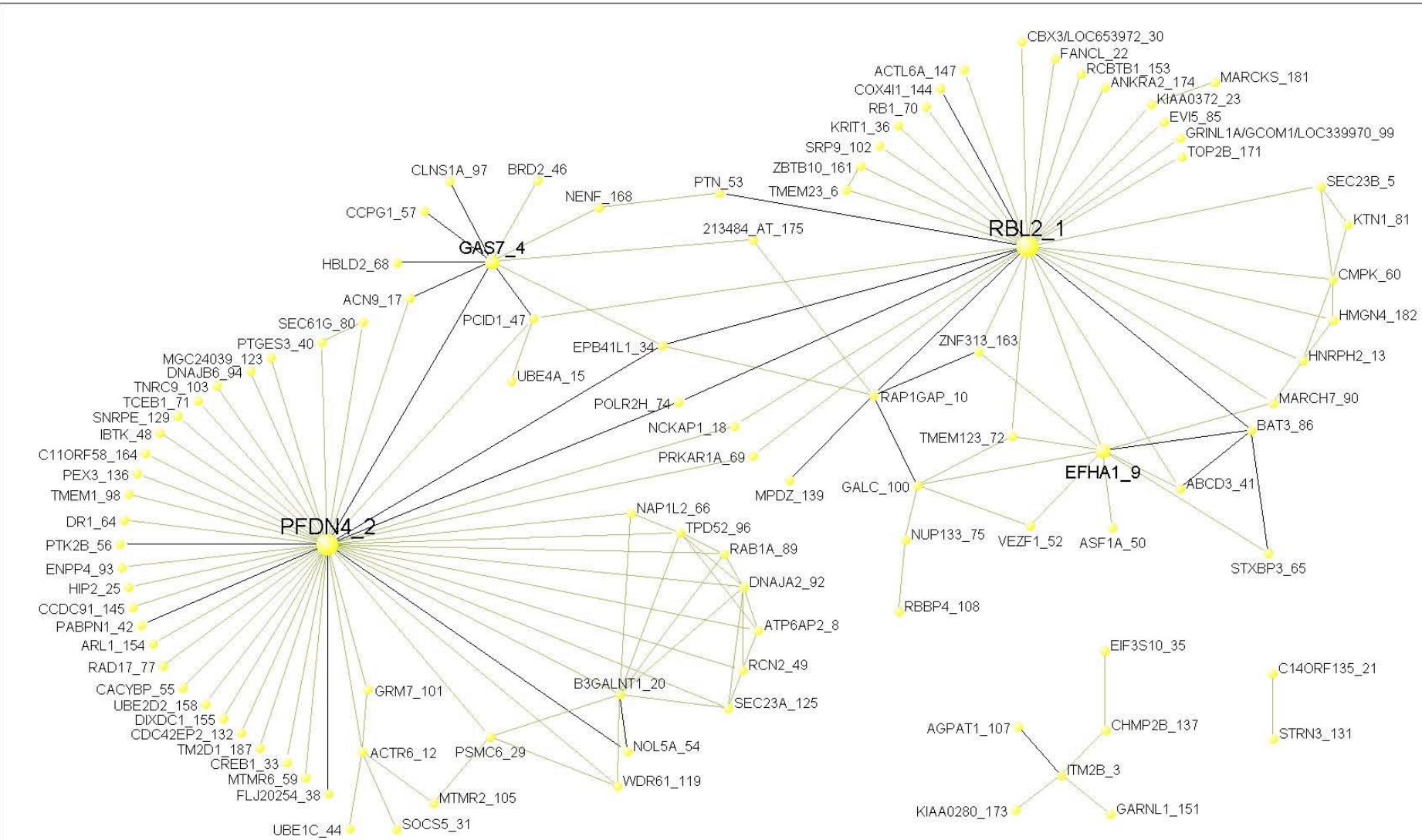

Figure S4AD

M19C

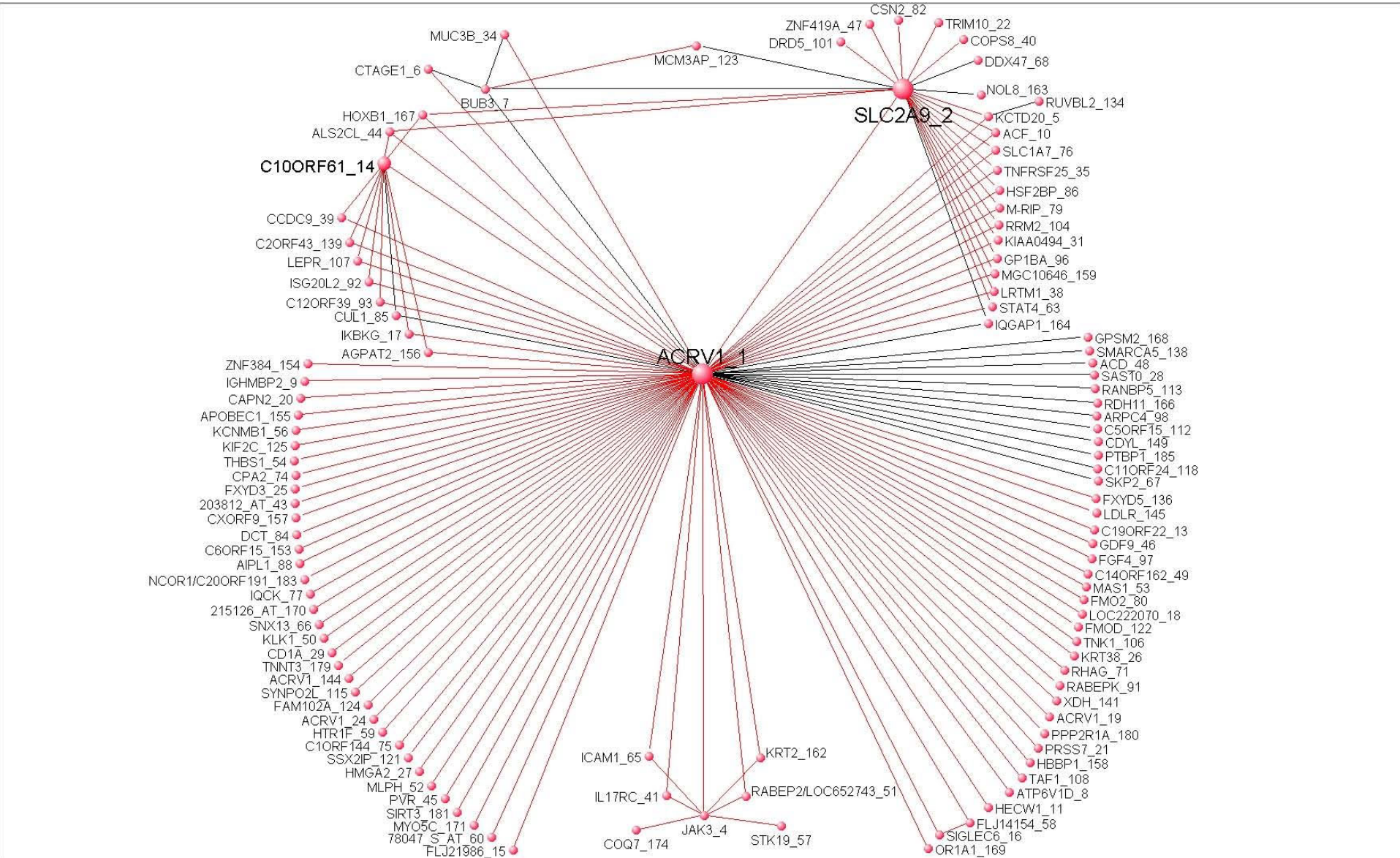

Figure S4AE

M27

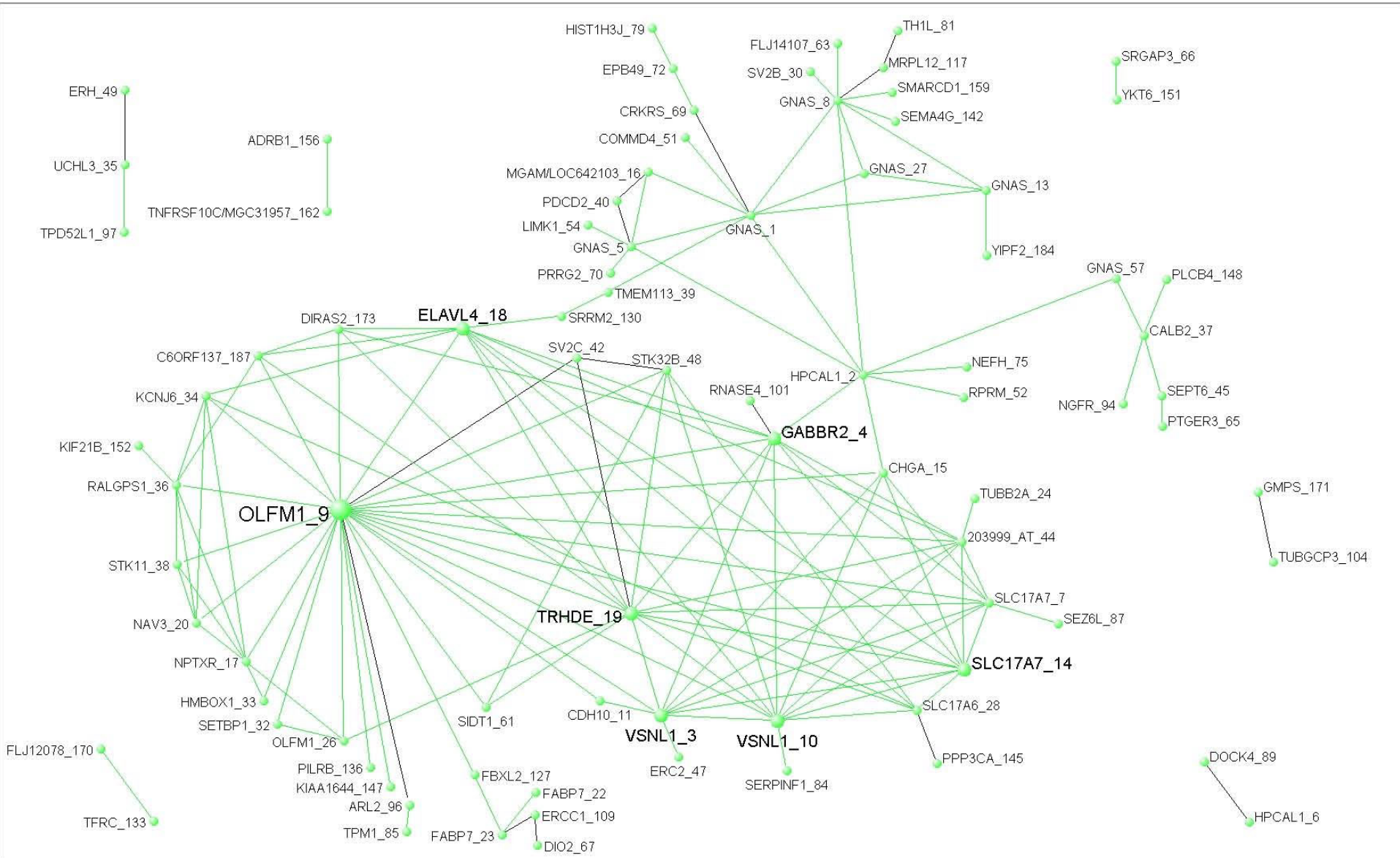

Figure S4AF

M28

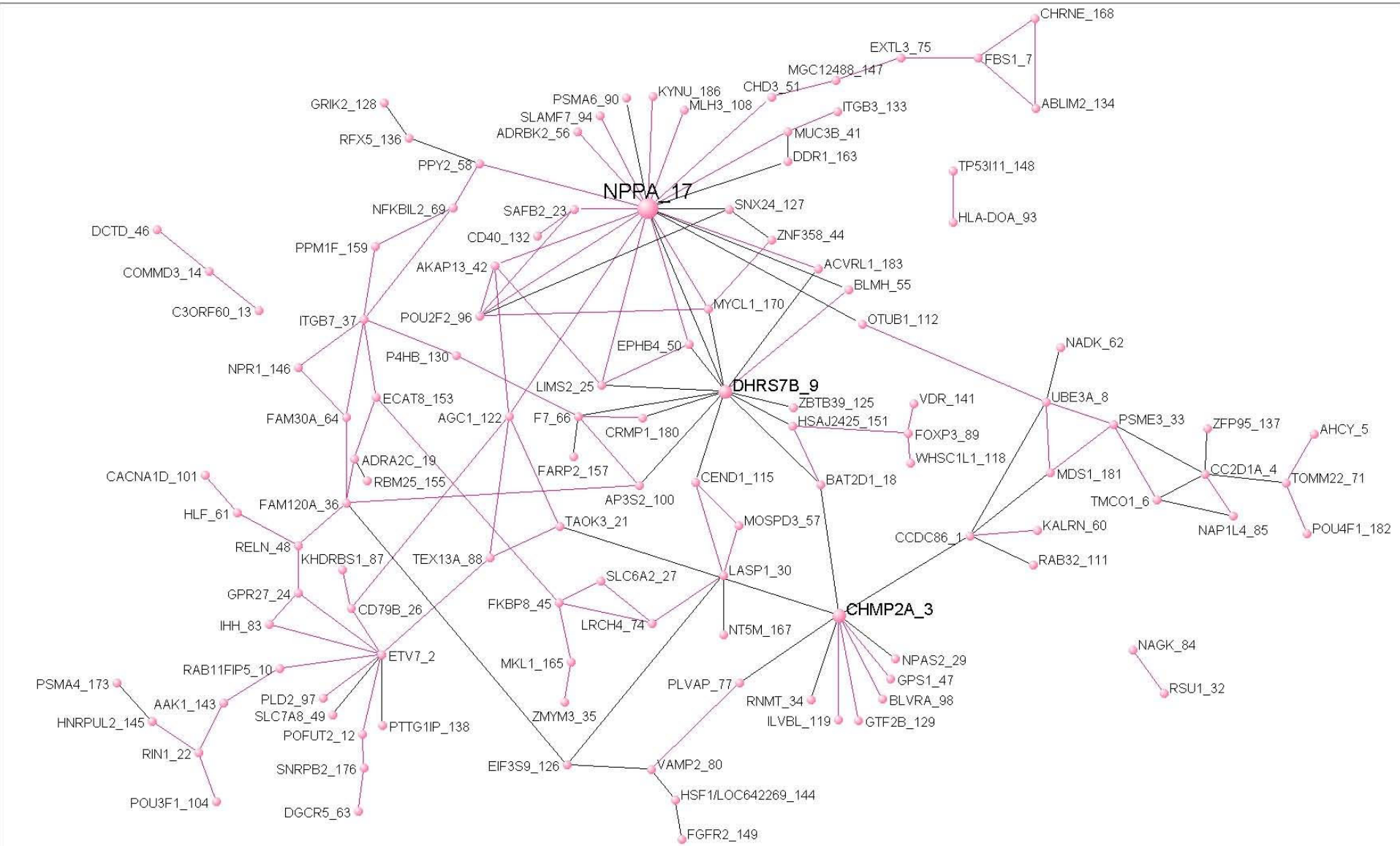

Figure S4AG

M29

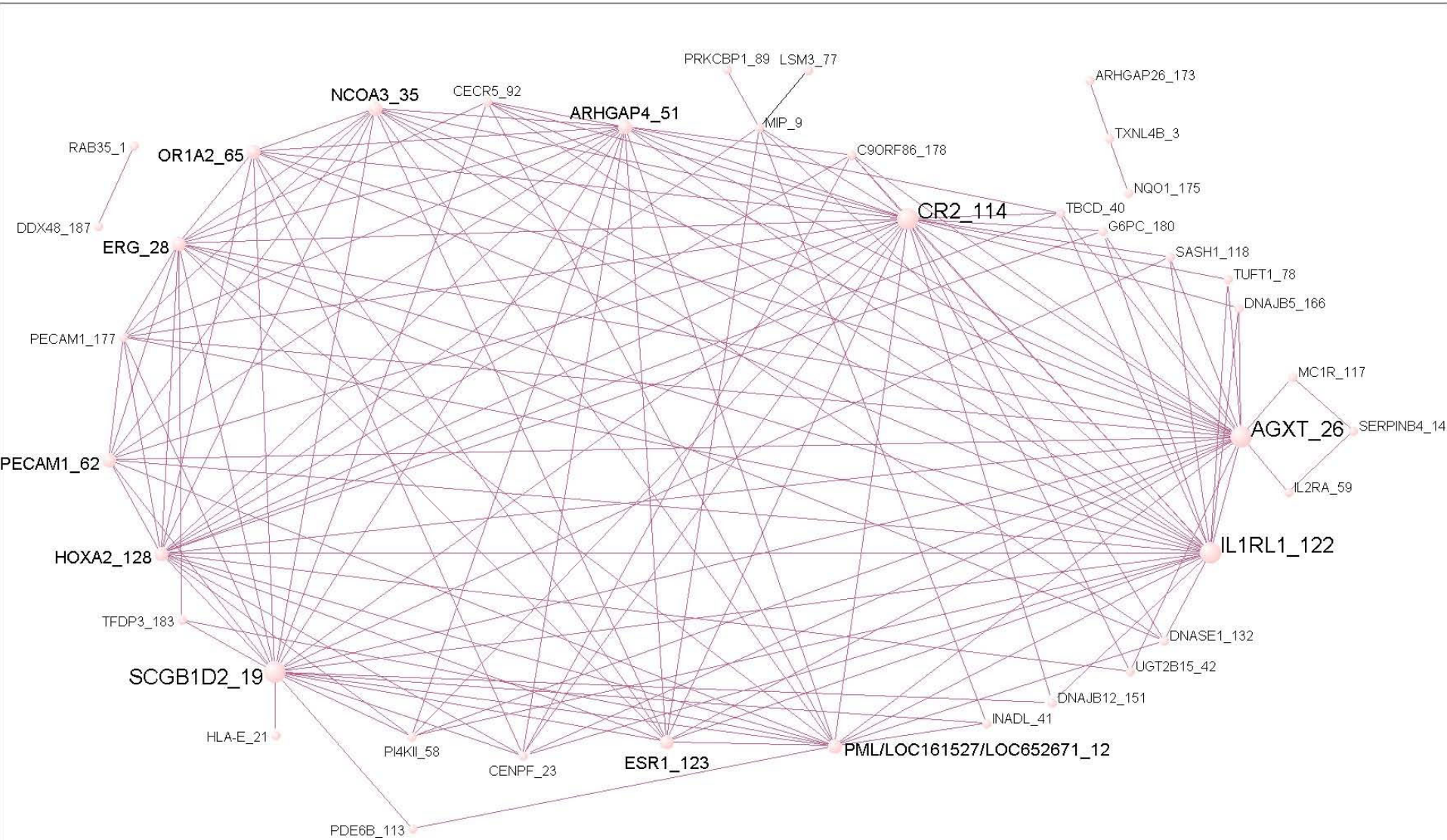

Figure S4AH

M30

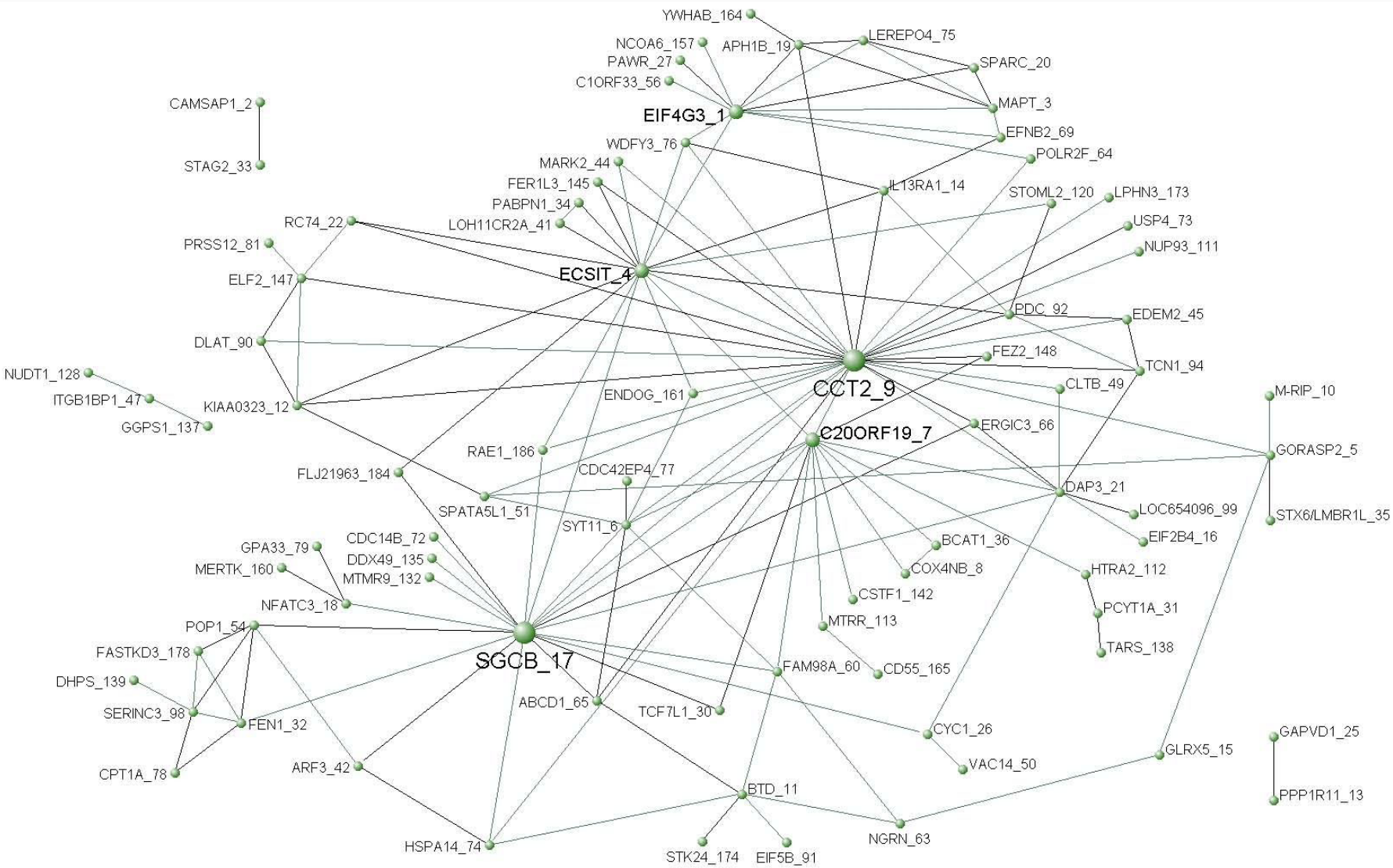

Figure S4AI

M31

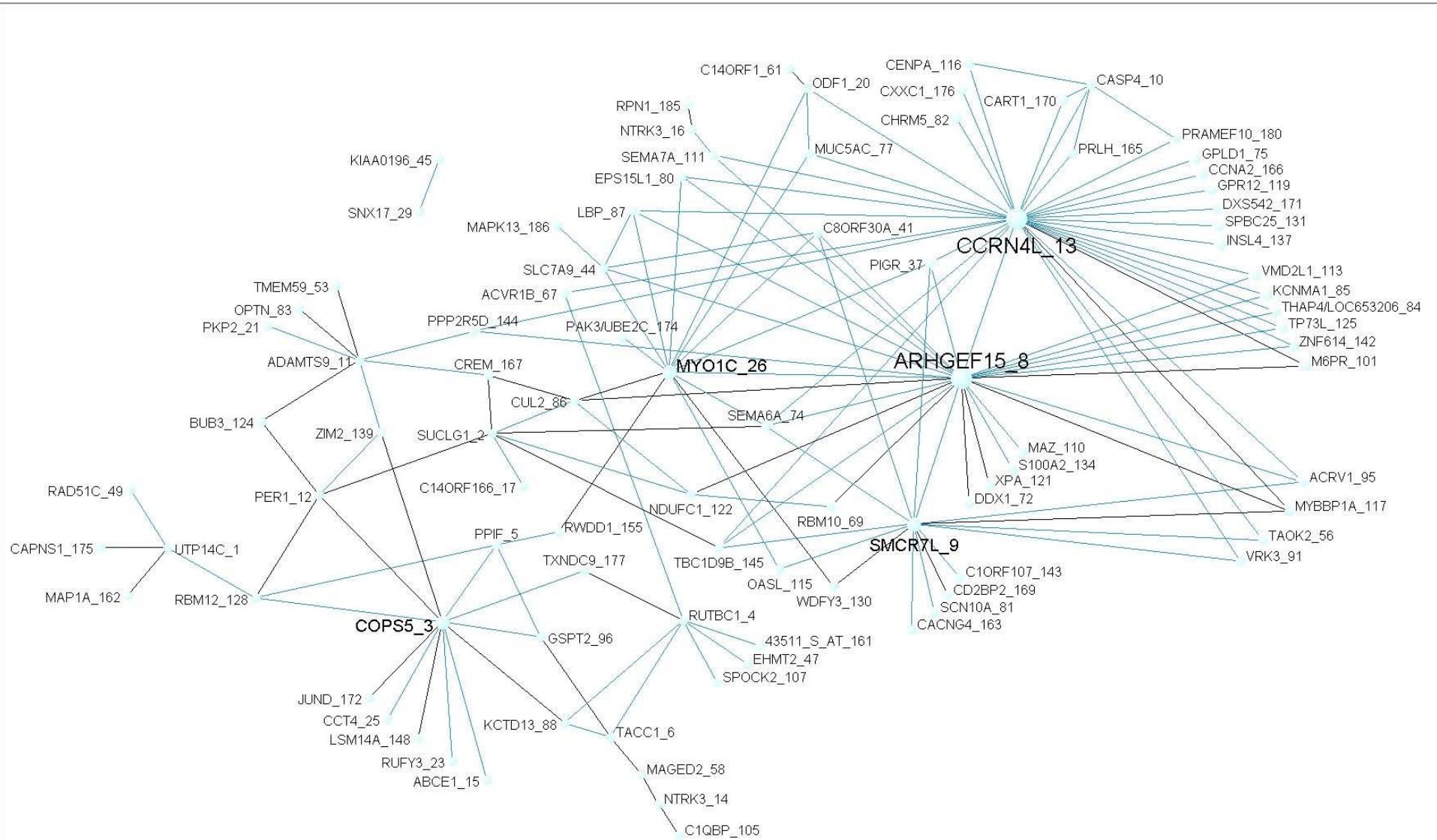

Figure S4AJ

M32

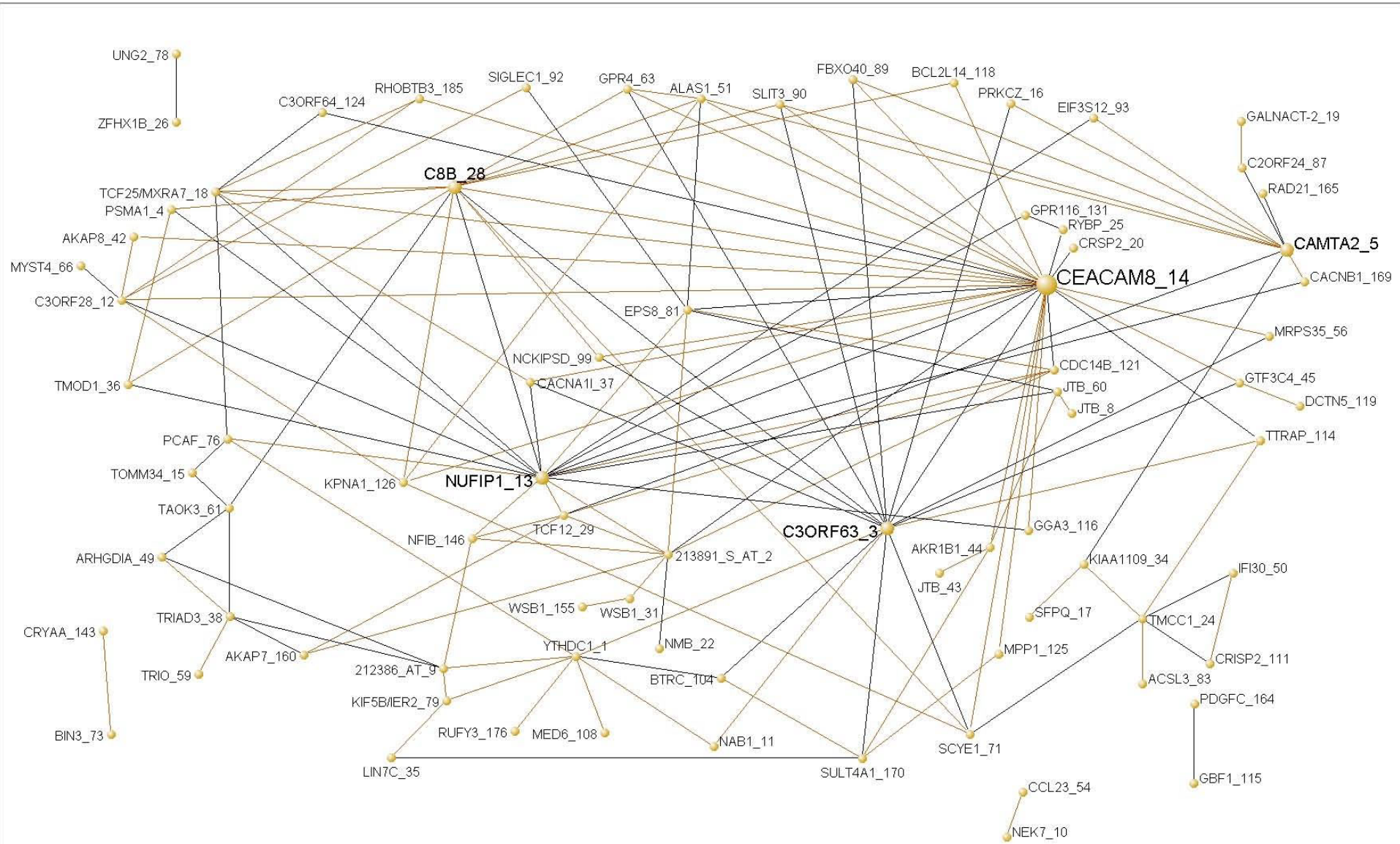

Figure S4AK

M33

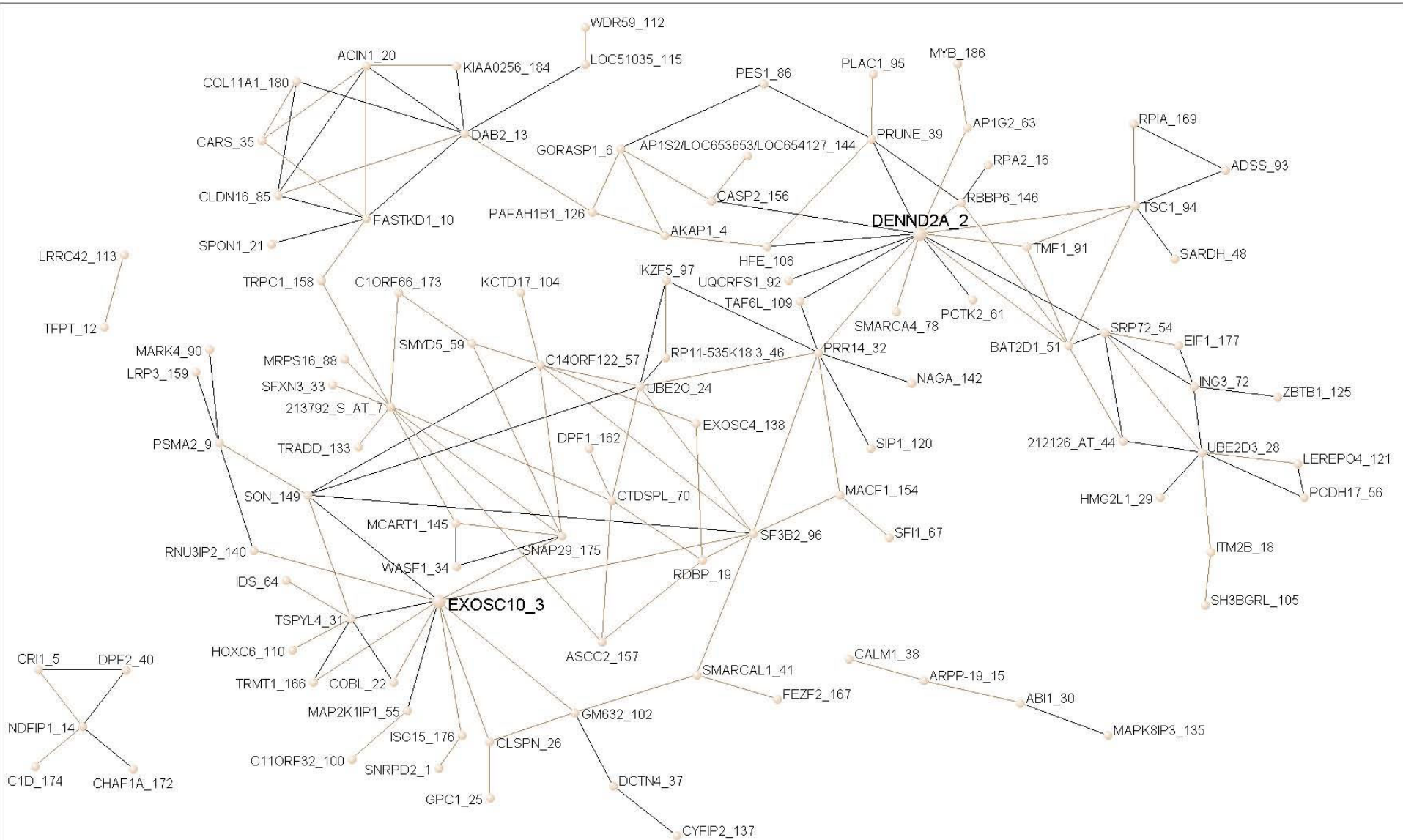

Figure S4AL

M34

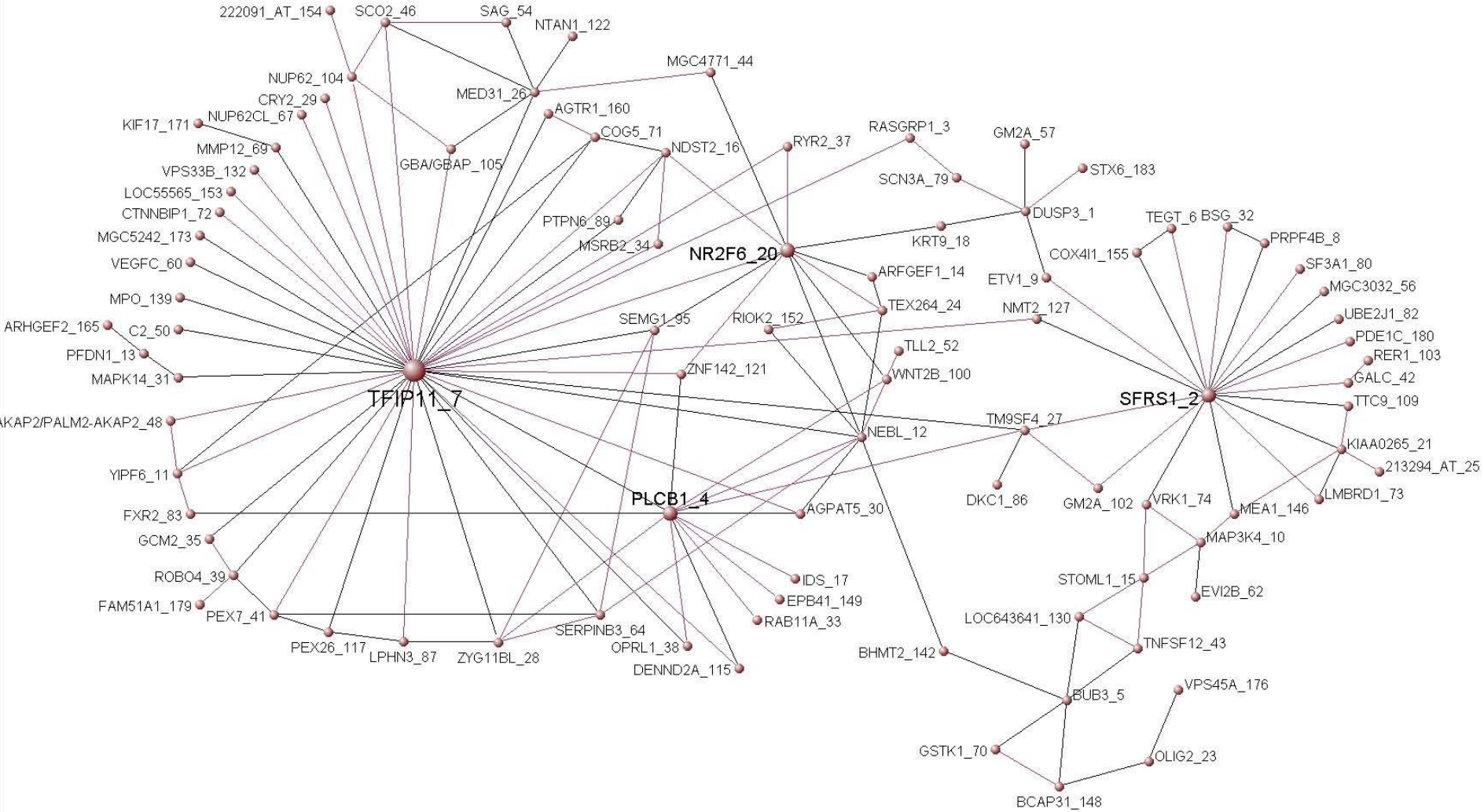

Figure S4AM

M35

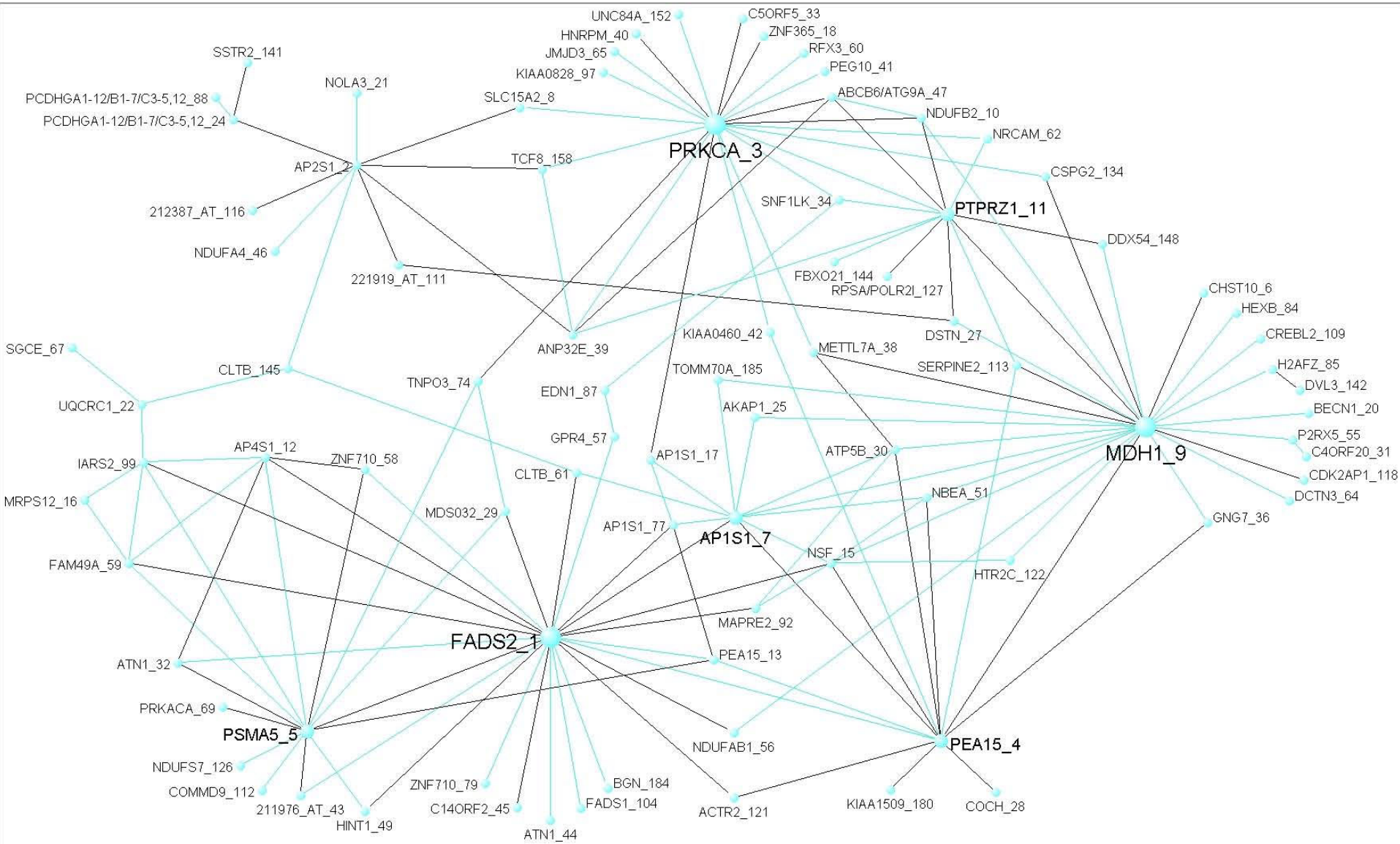

Figure S4AN

M36

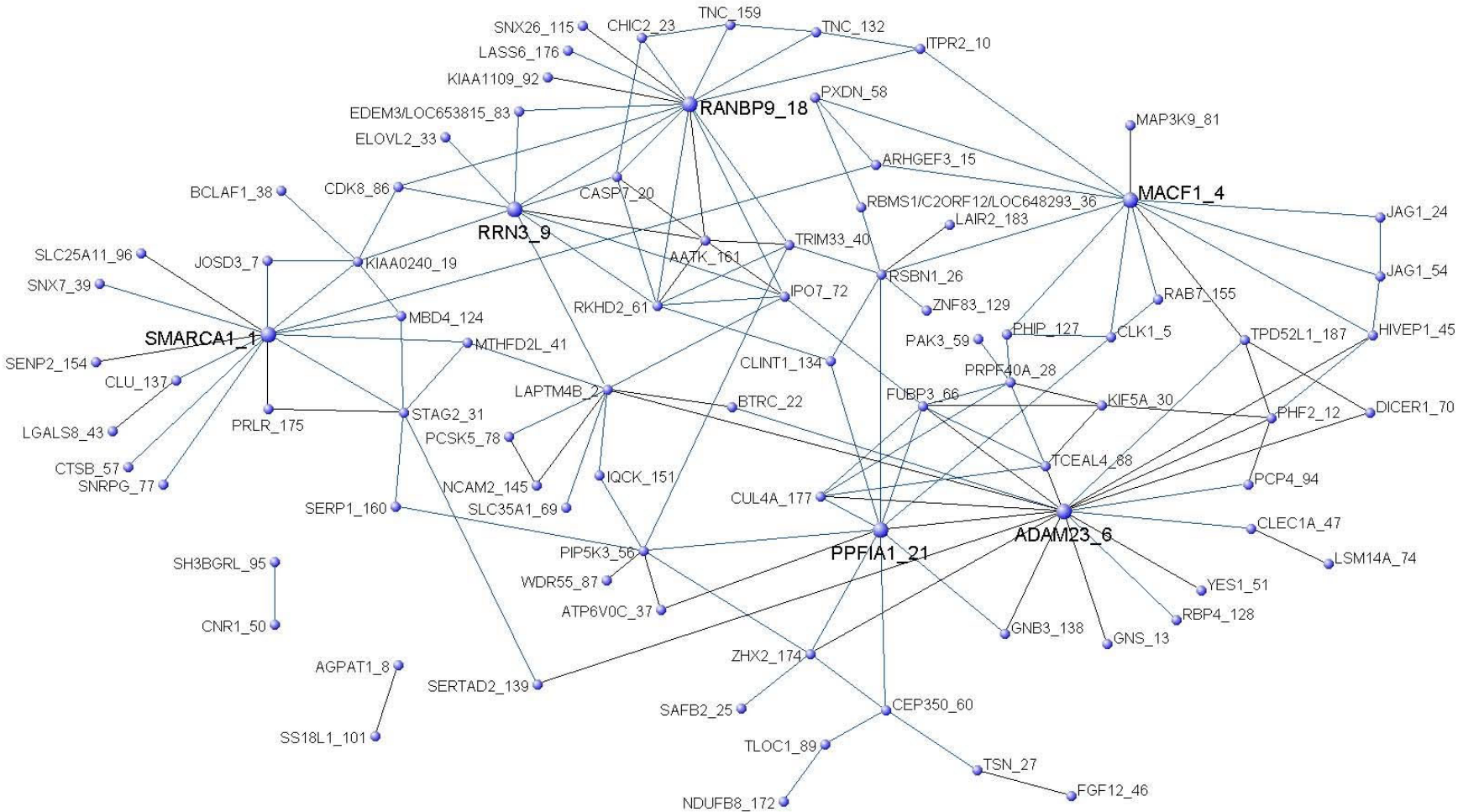

Figure S4AO

M37

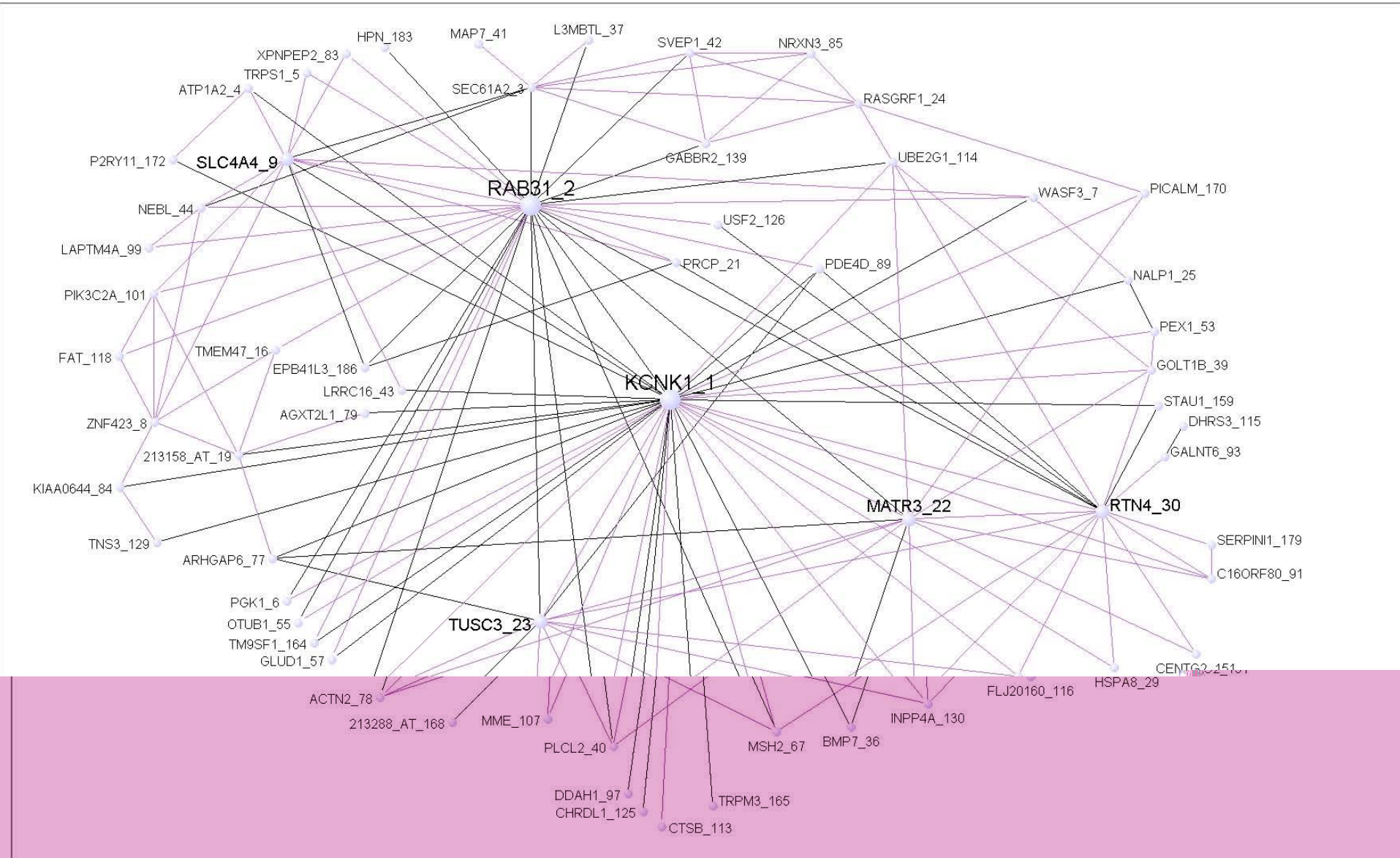

Figure S4AP

M38

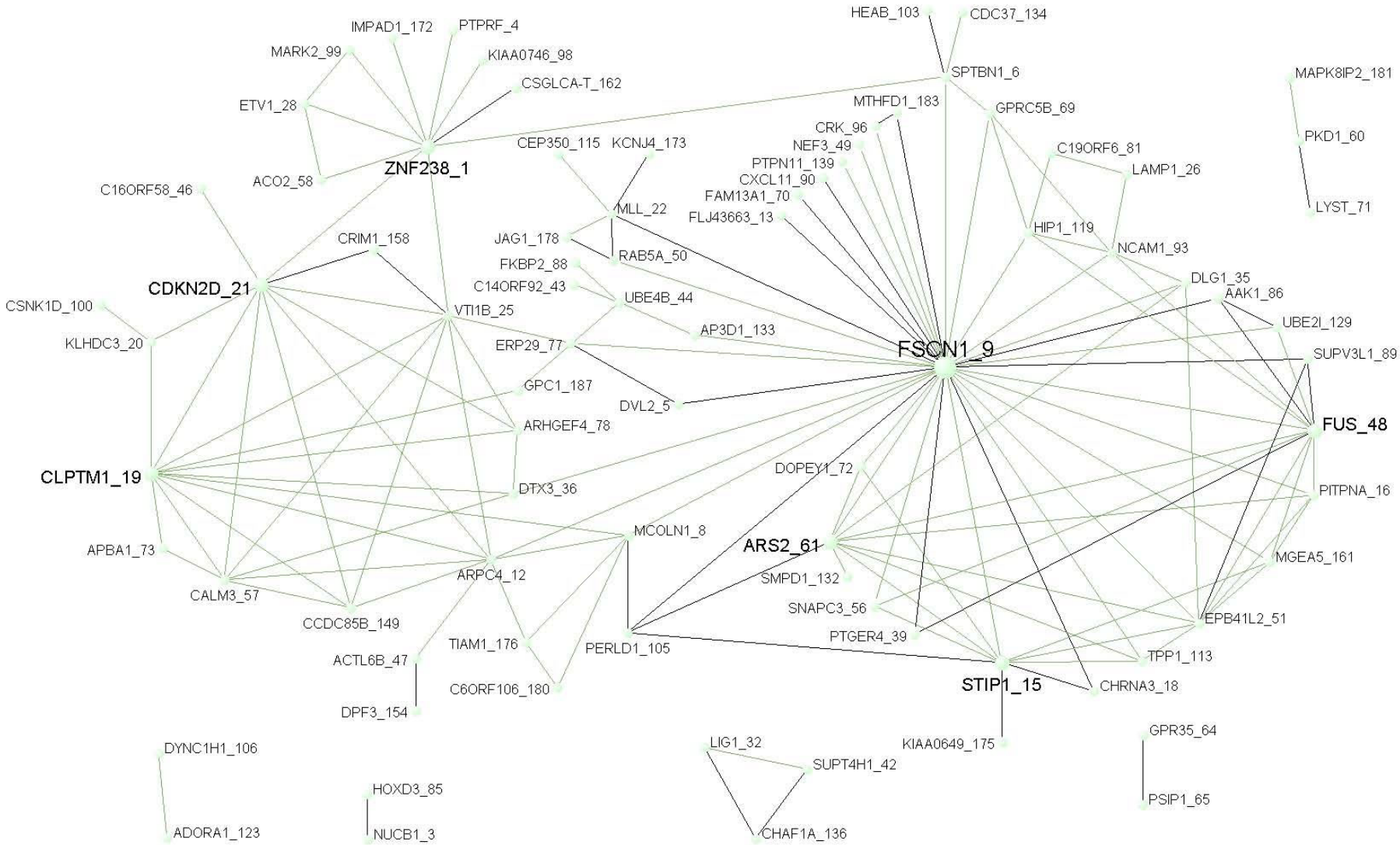

Figure S4

Cerebellum

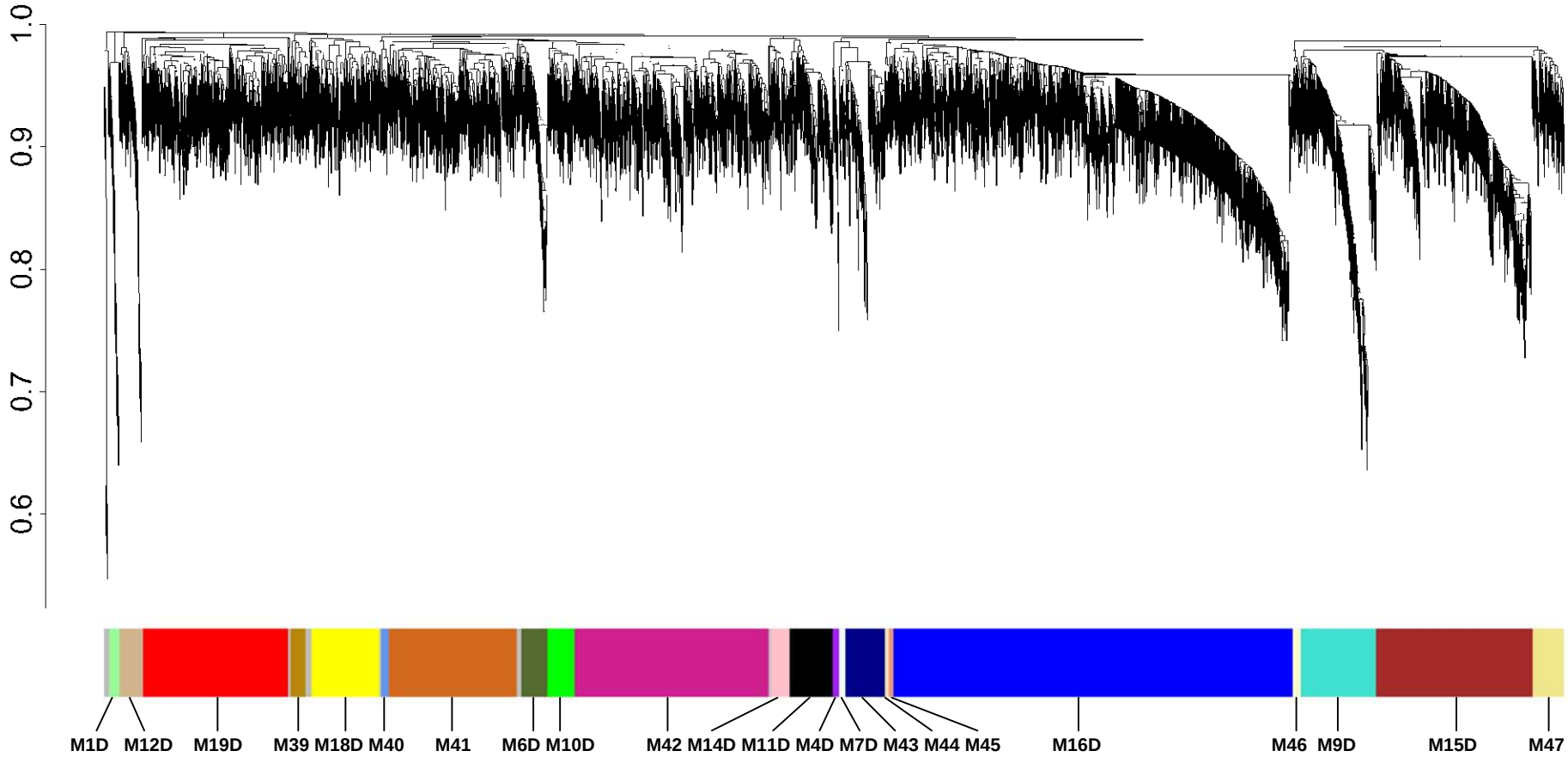

Figure S4AQ

M1D

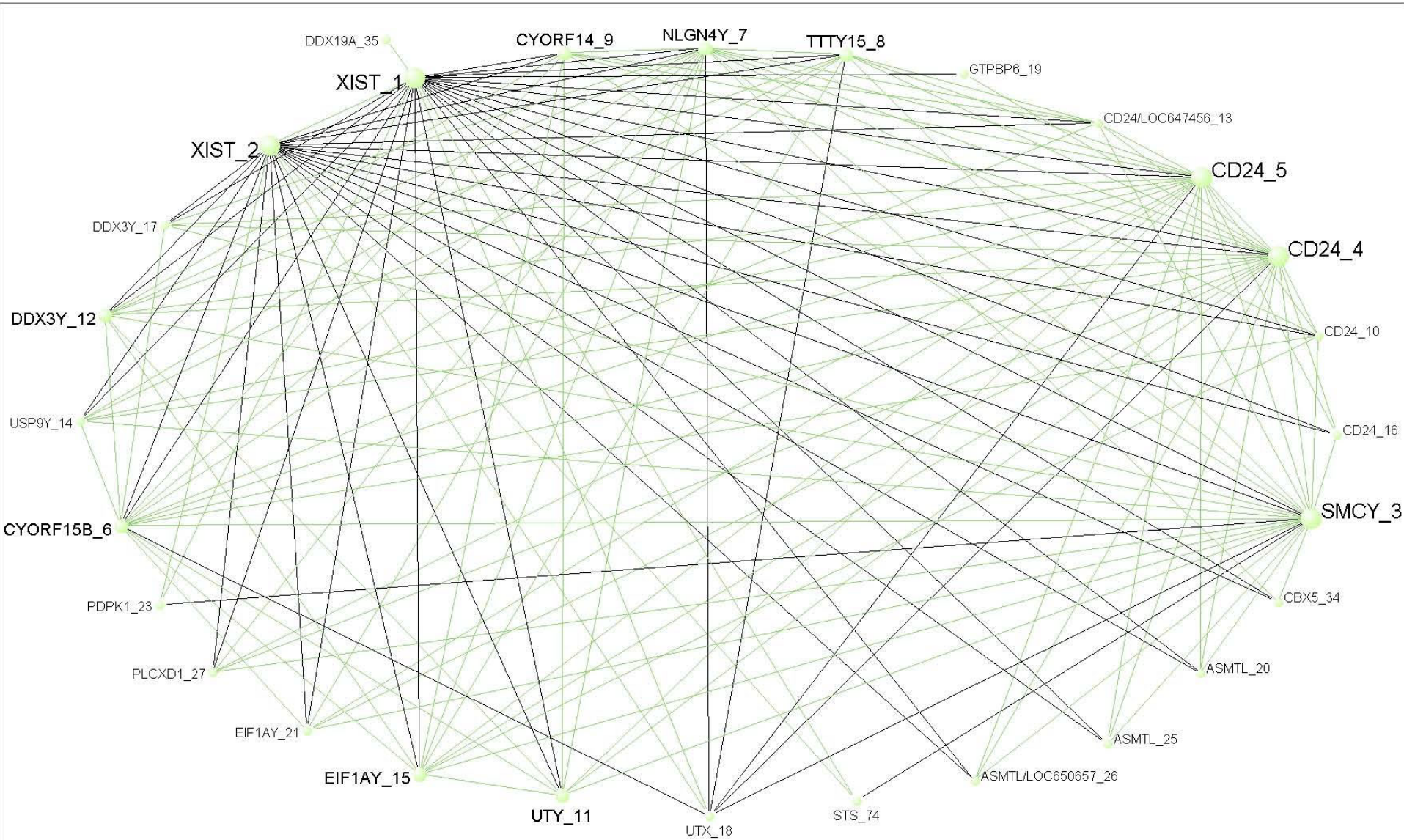

Figure S4AR

M4D

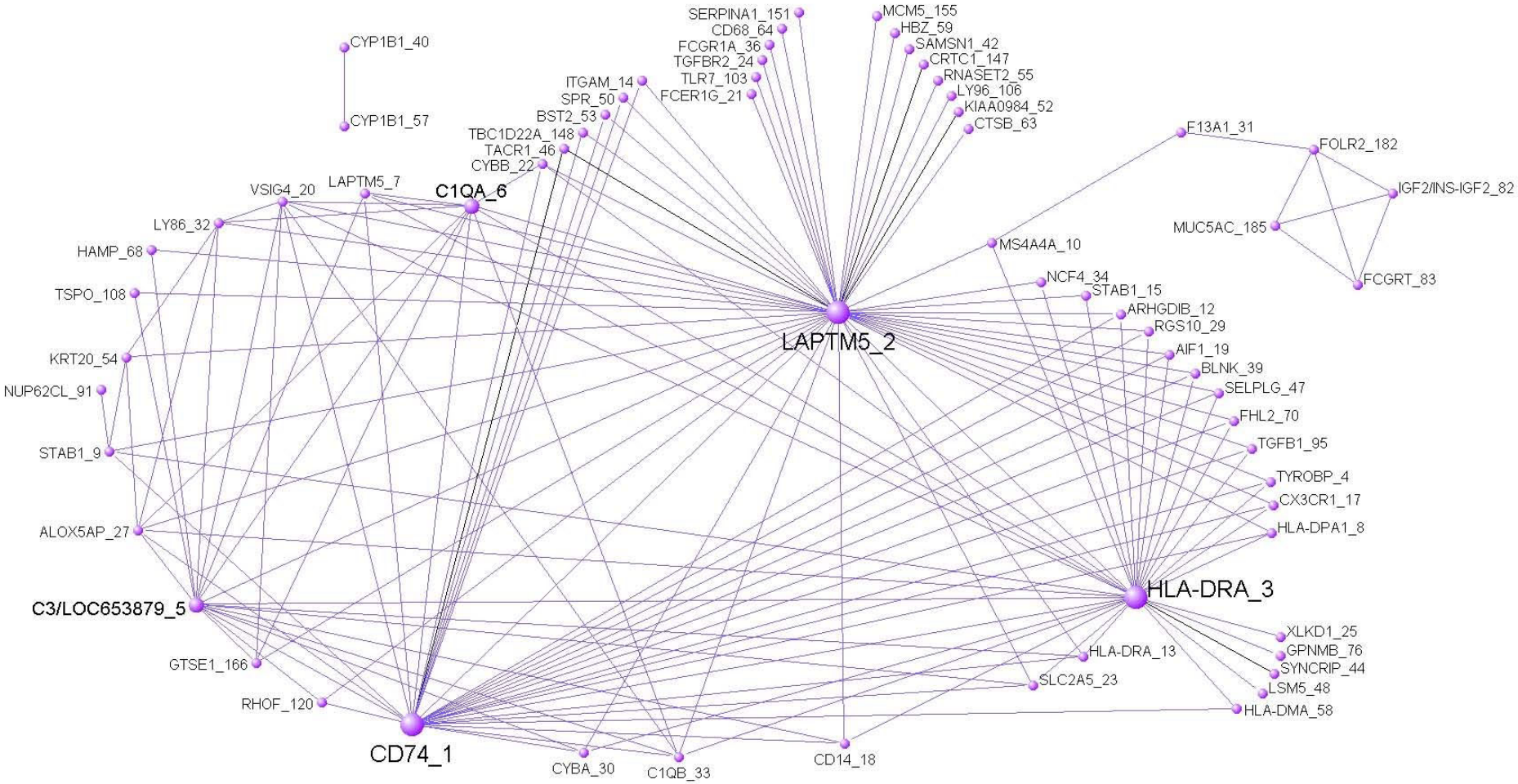

Figure S4AS

M6D

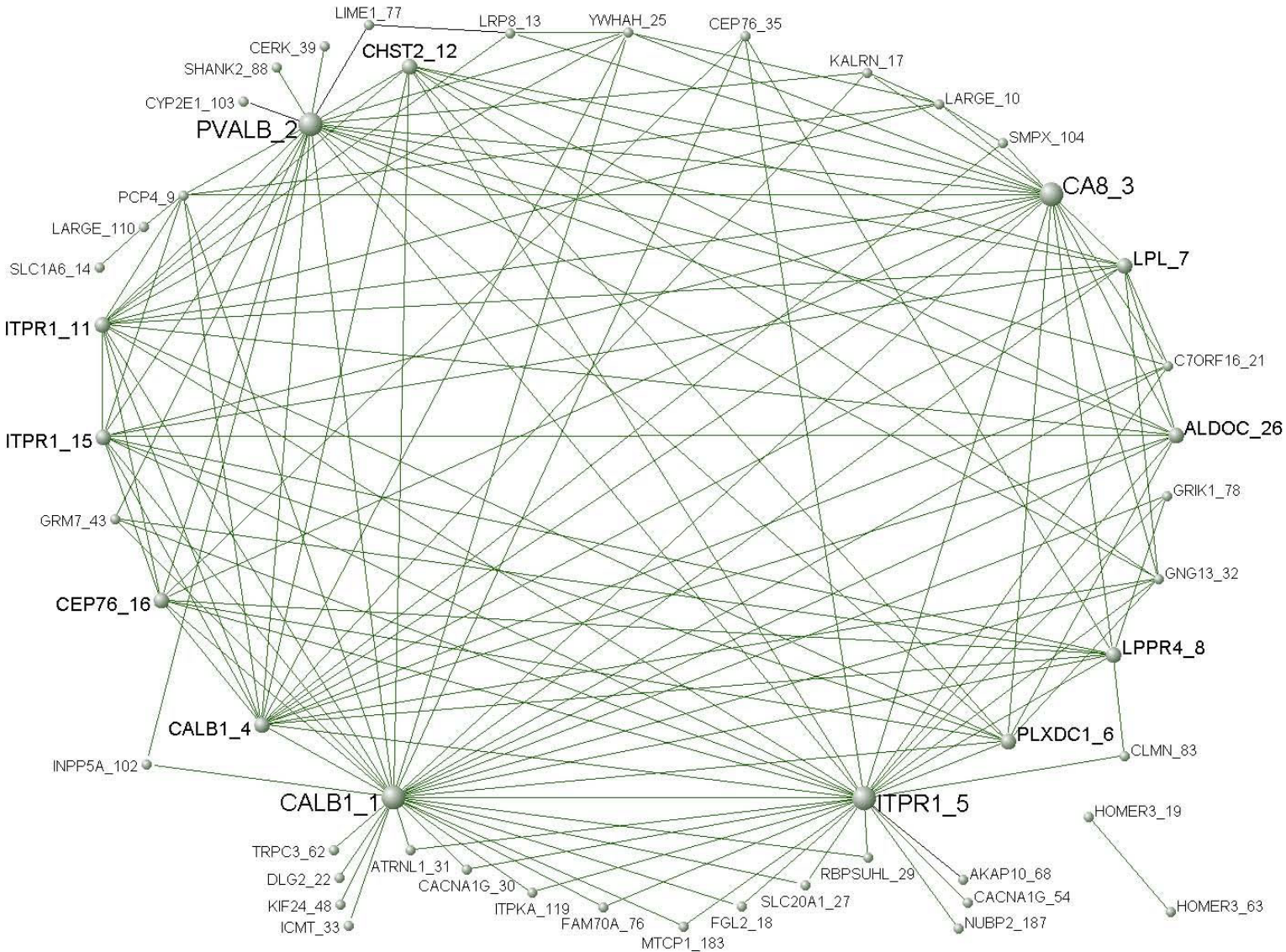

Figure S4AT

M7D

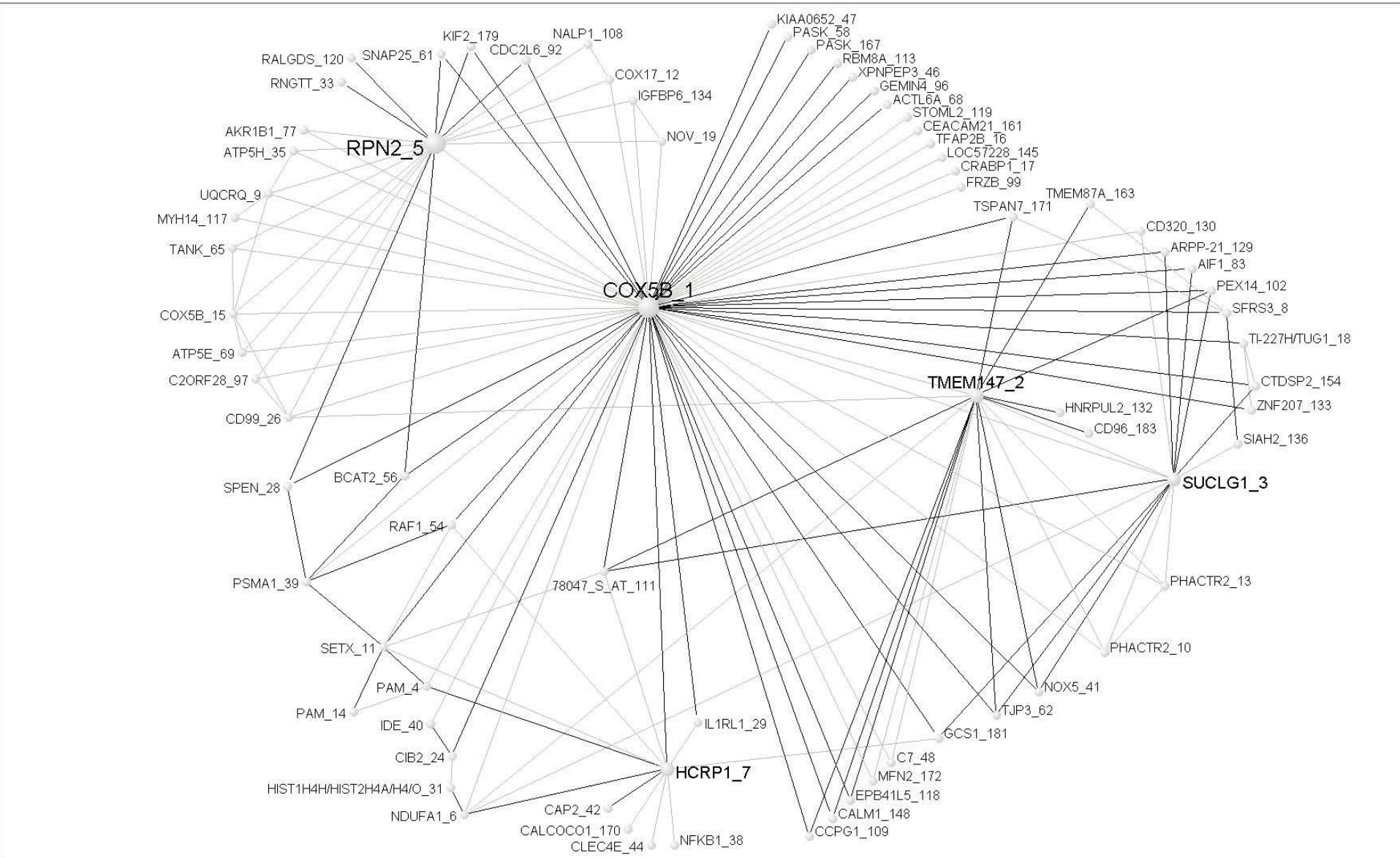

Figure S4AU

M9D

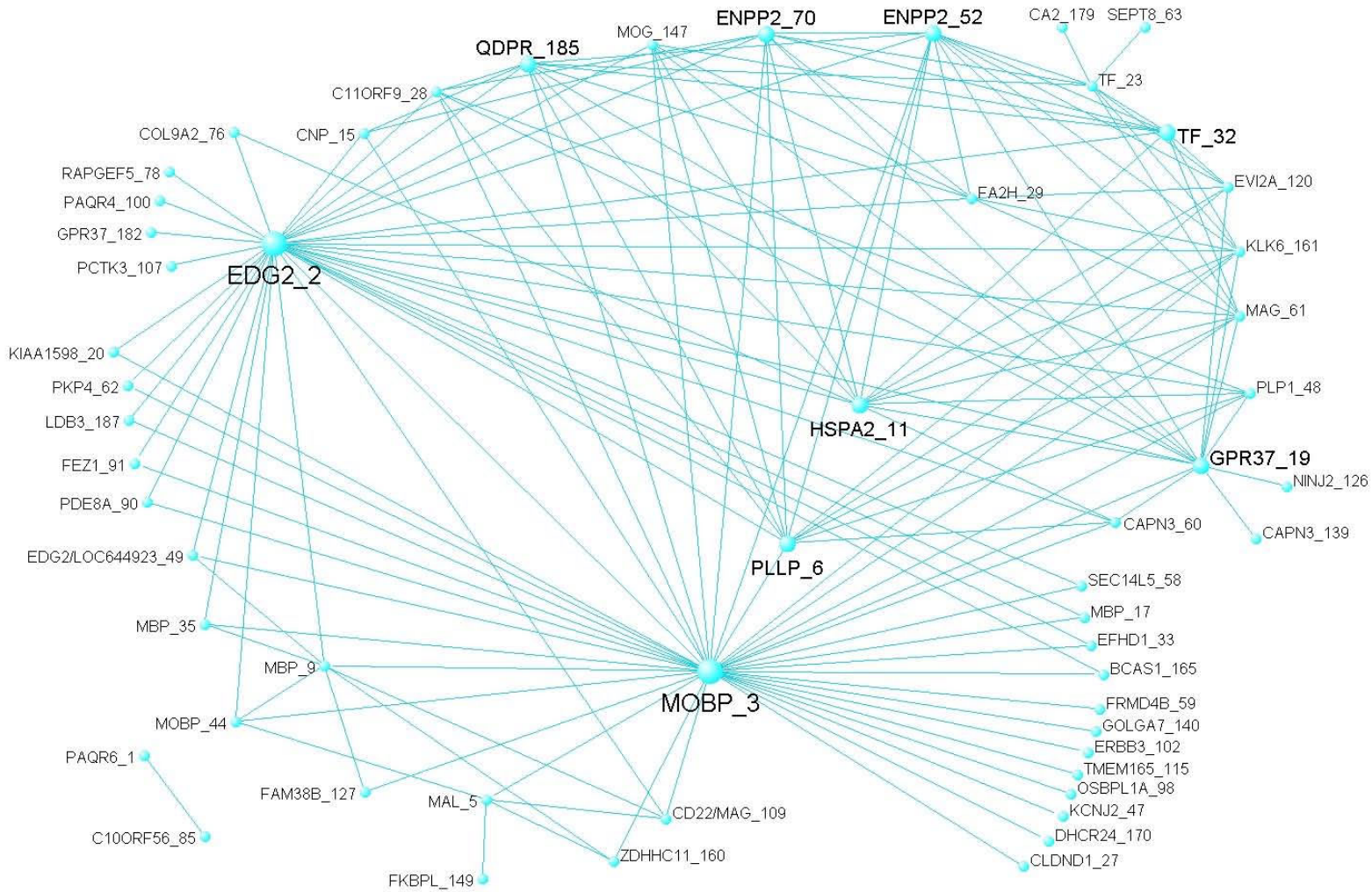

Figure S4AV

M10D

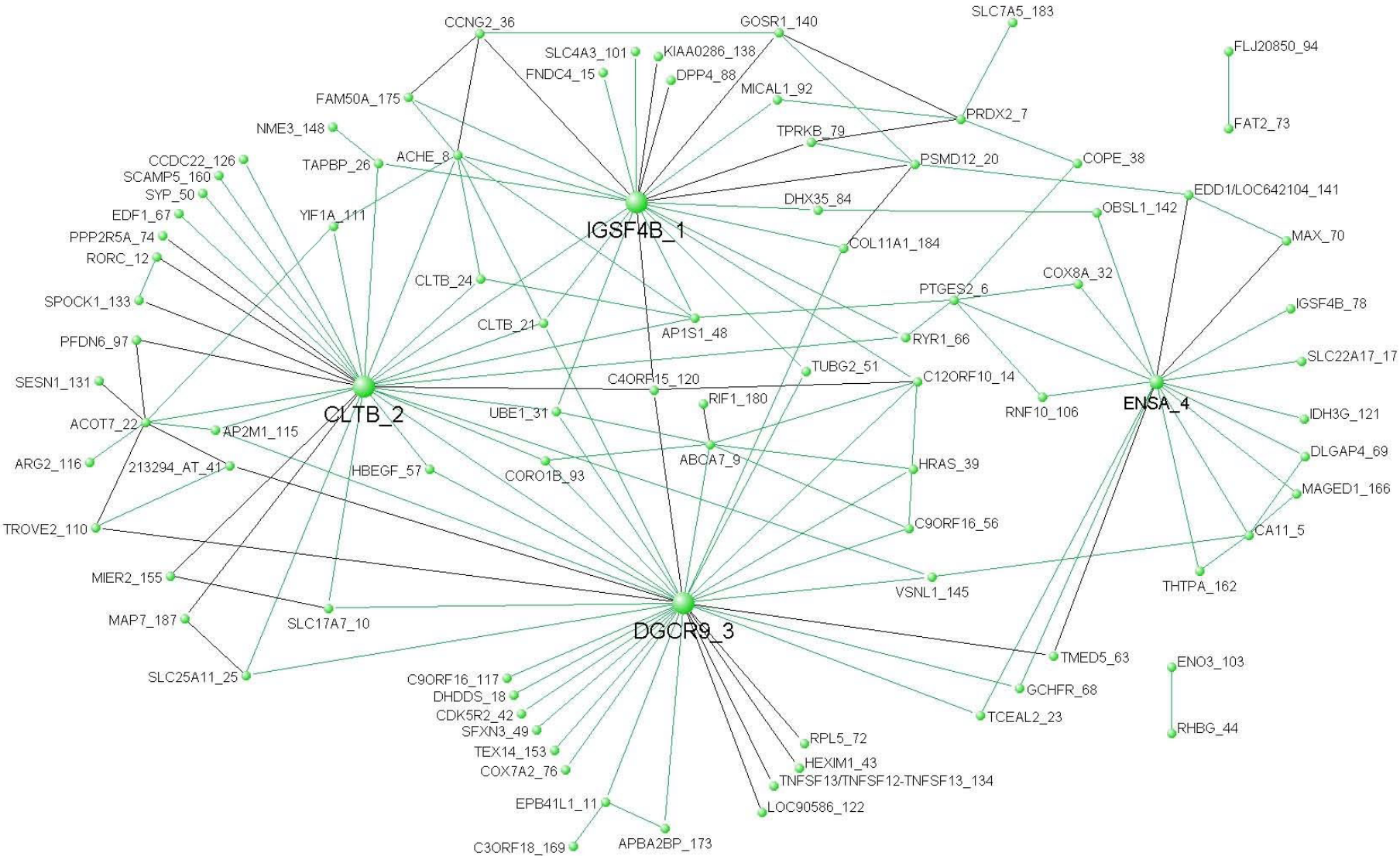

Figure S4AW

M11D

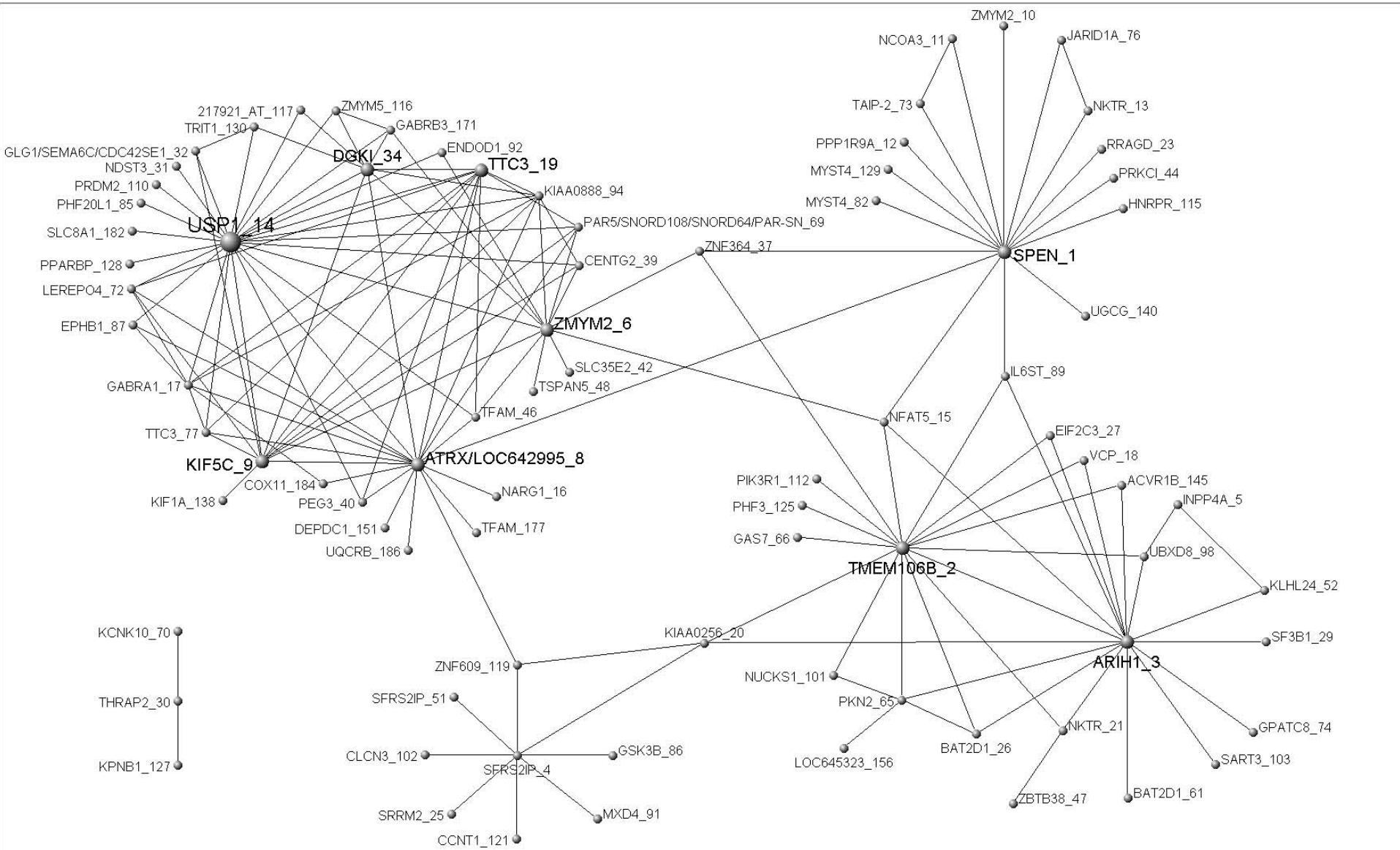

Figure S4AX

M12D

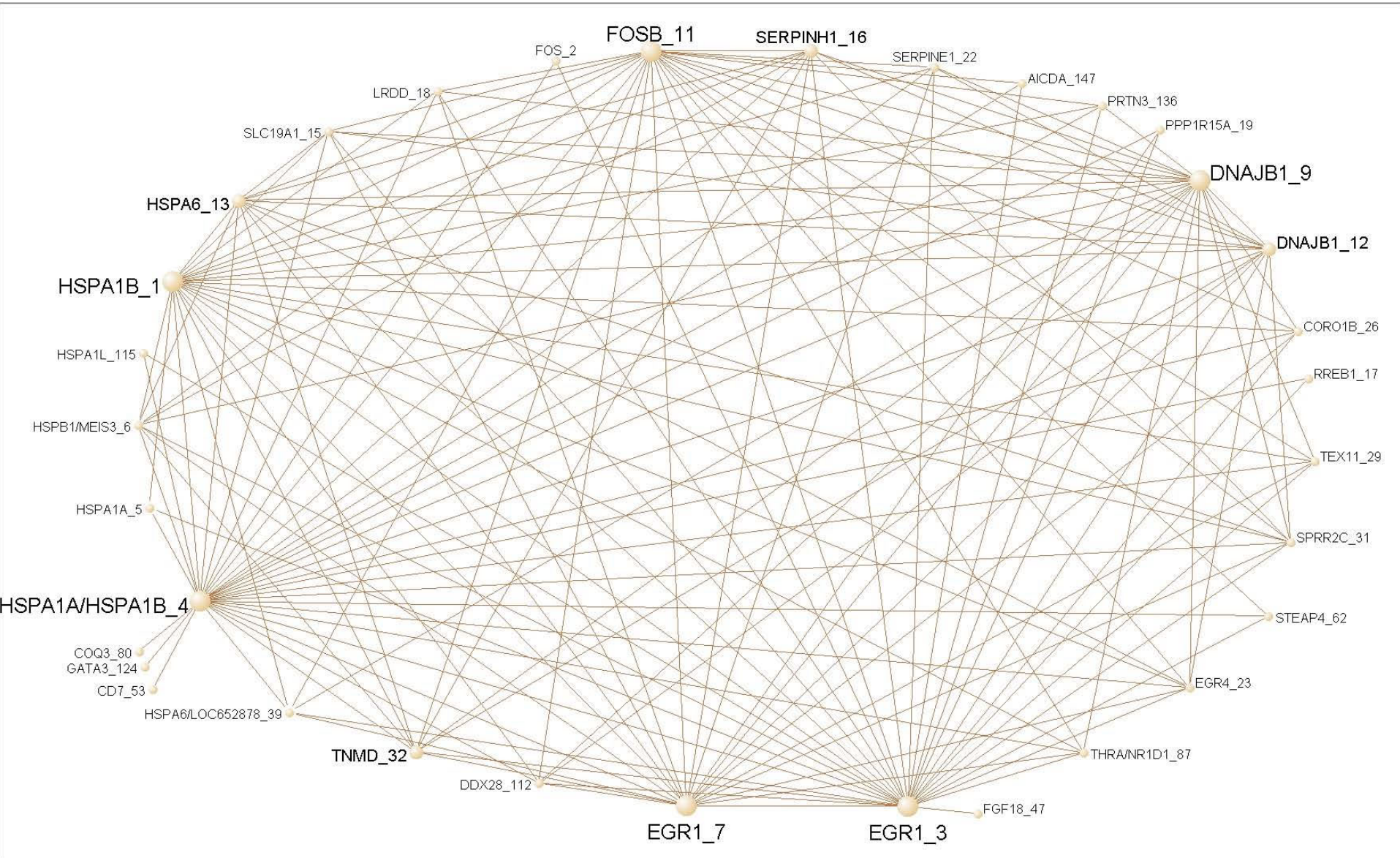

Figure S4AY

M14D

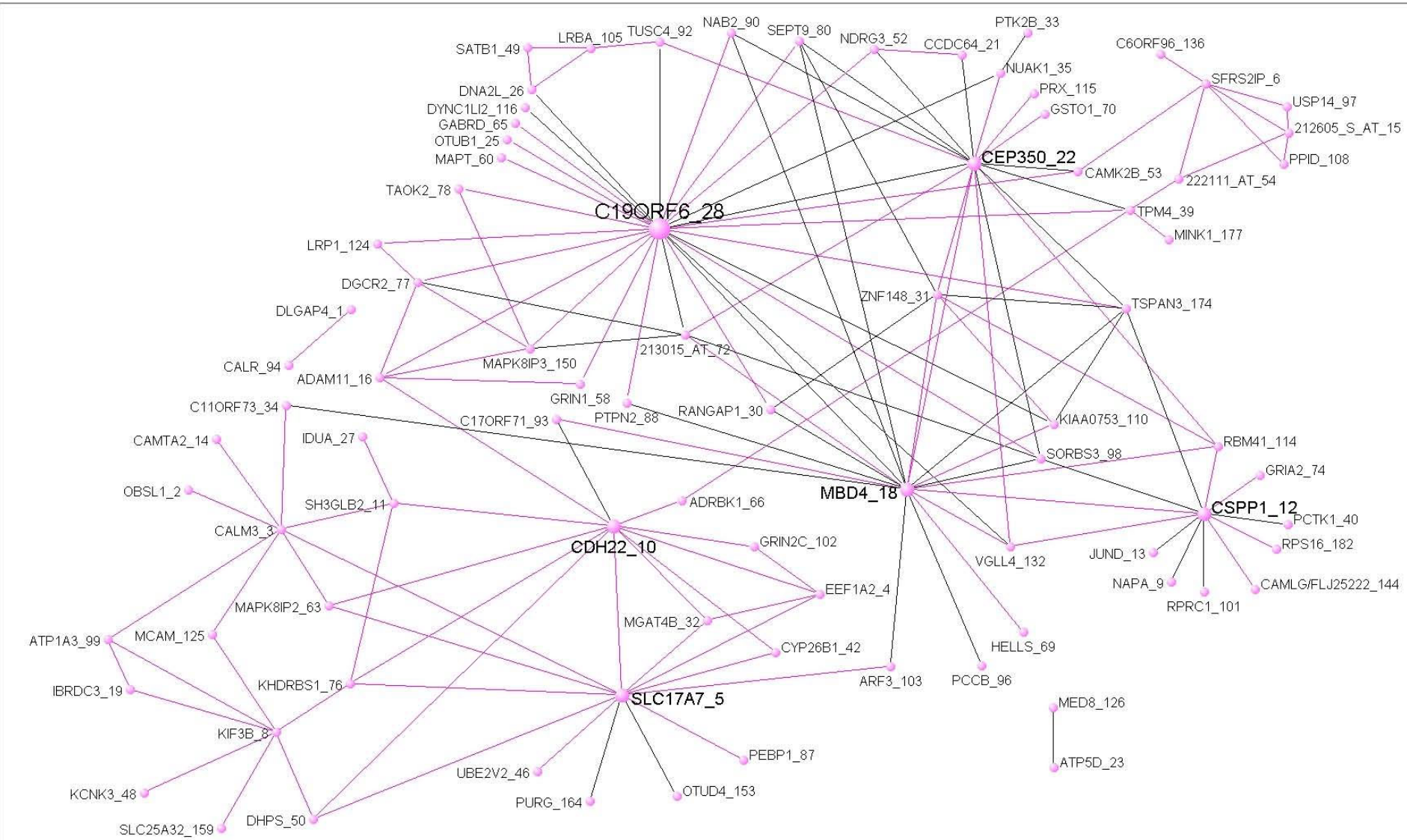

Figure S4AZ

M15D

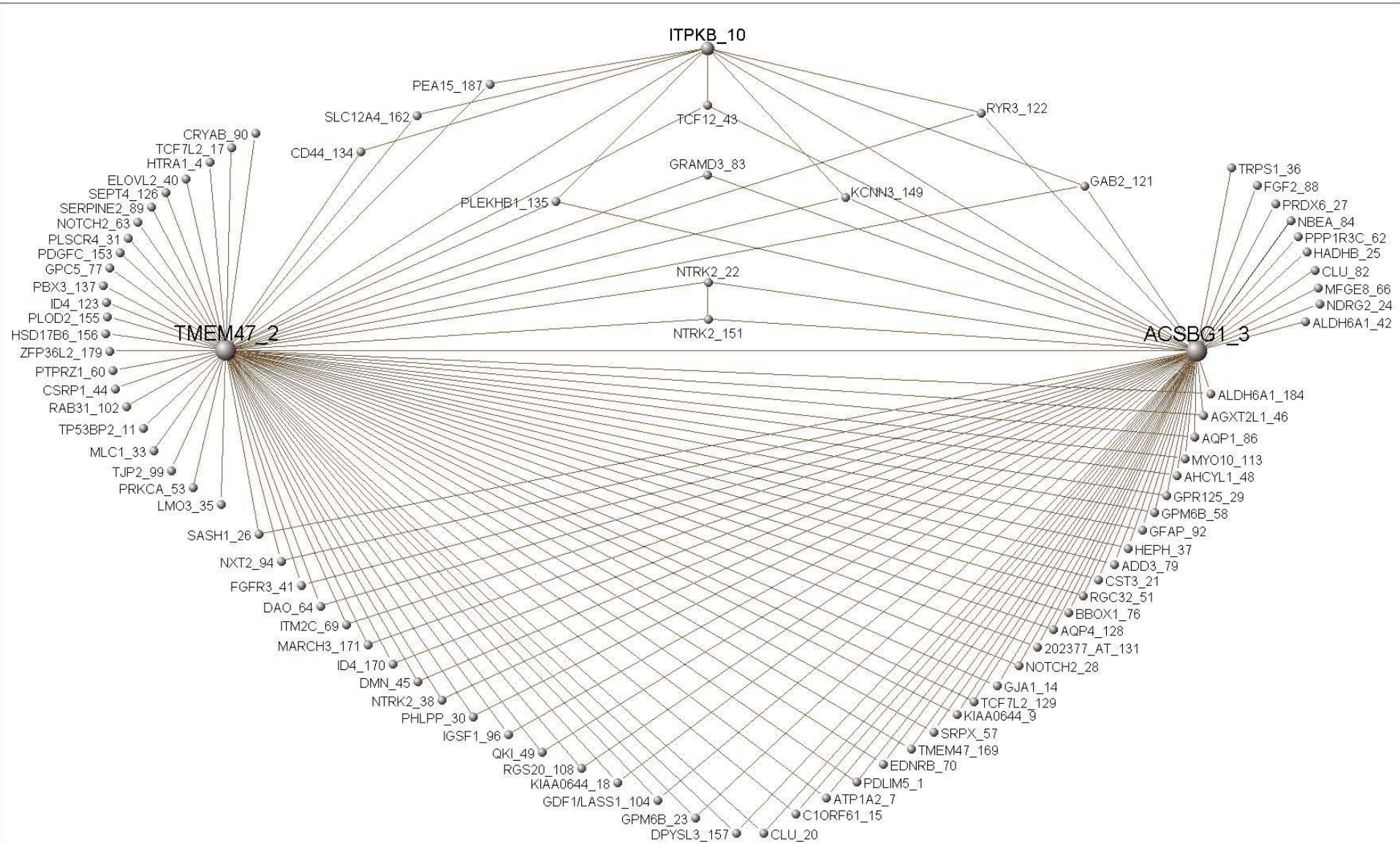

Figure S4BA

M16D

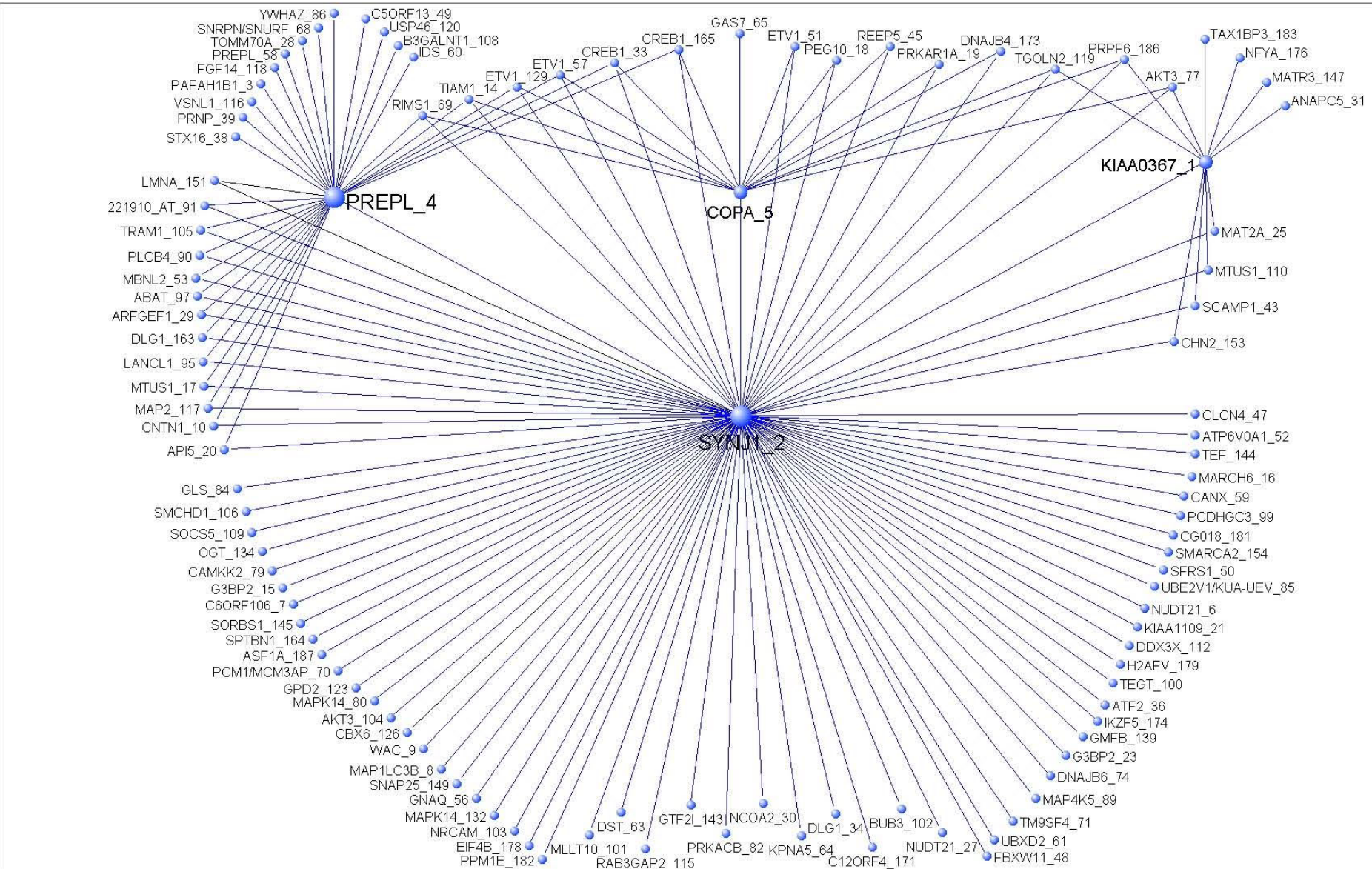

Figure S4BB

M18D

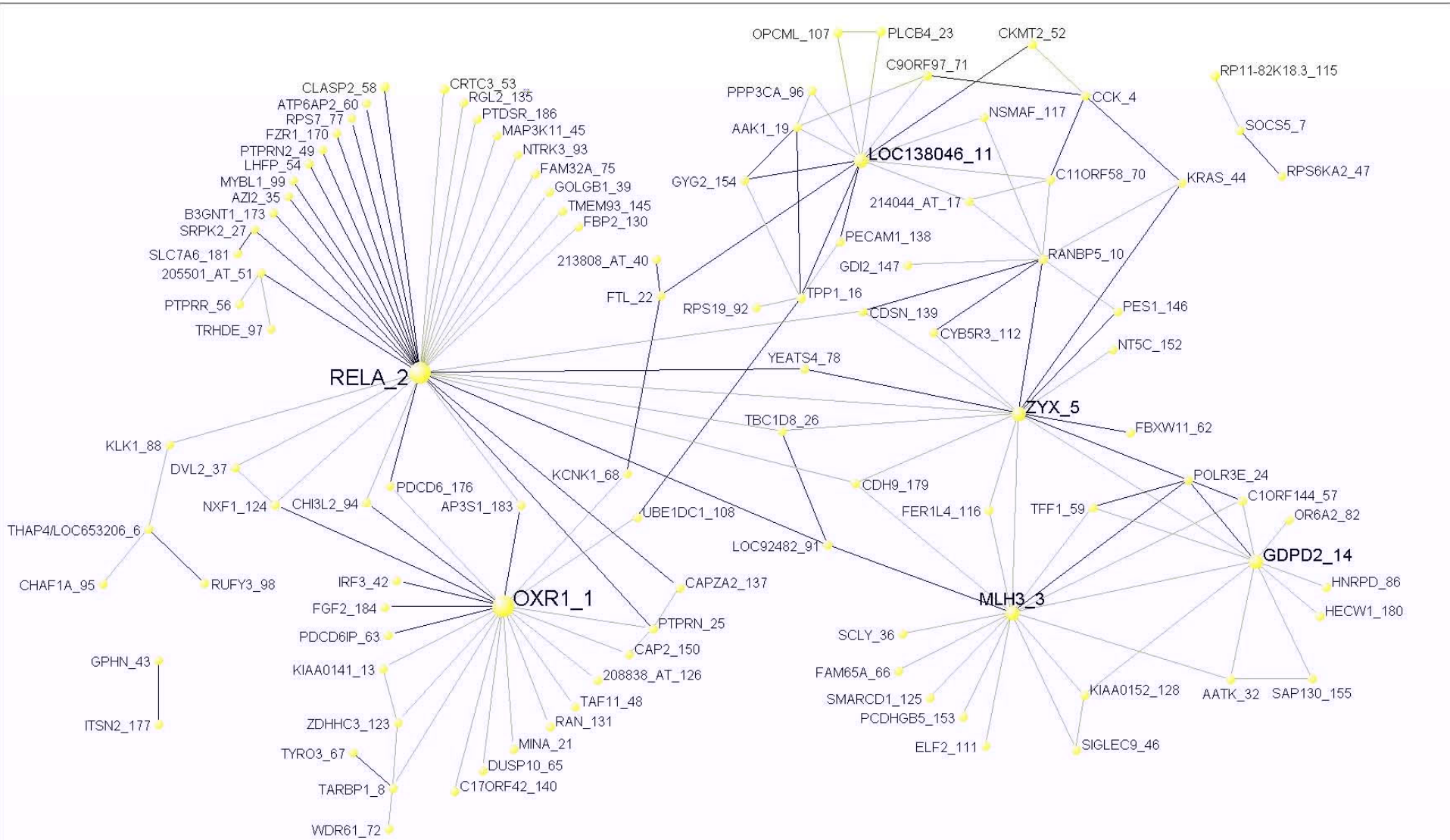

Figure S4BC

M19D

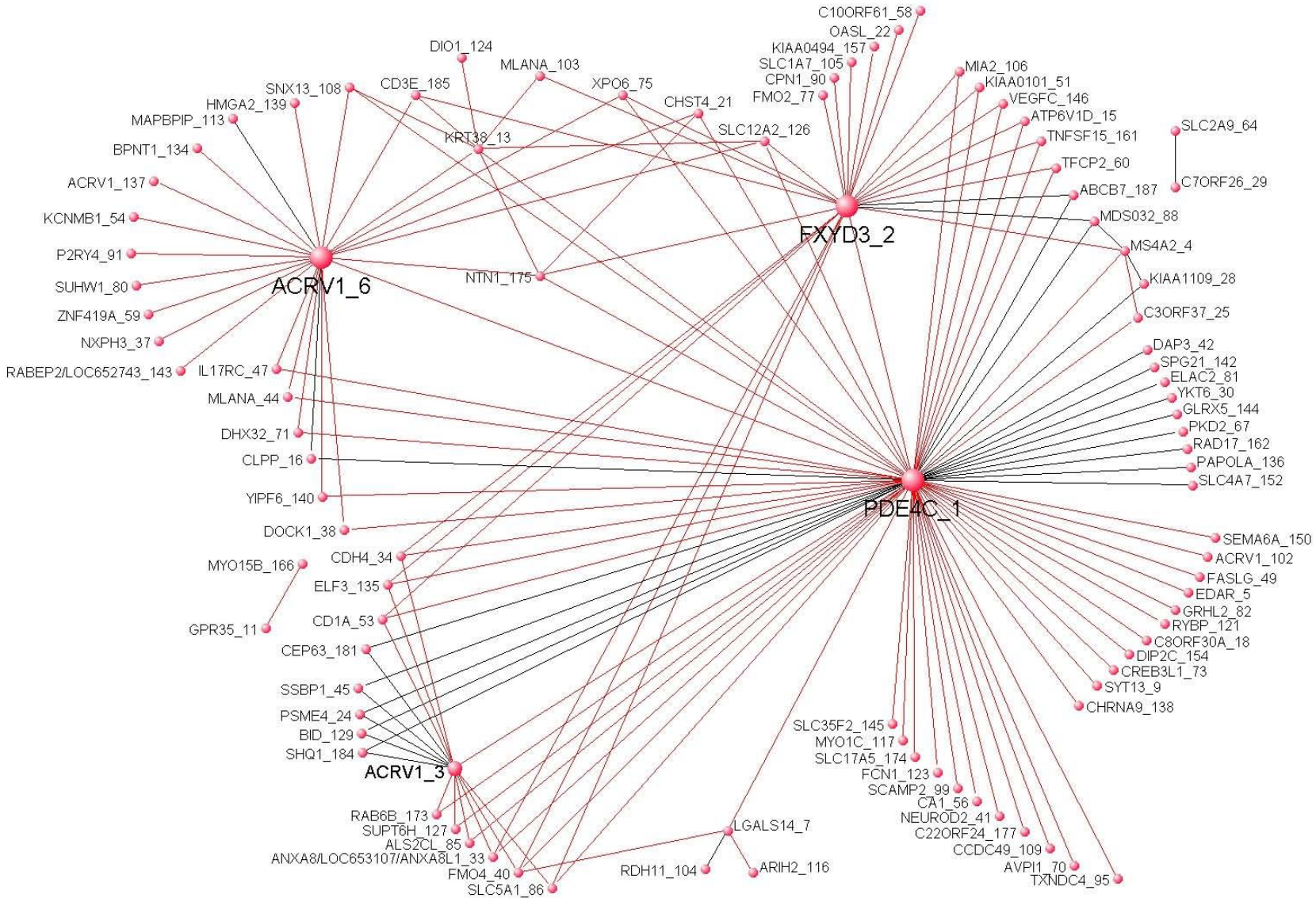

Figure S4BD

M39

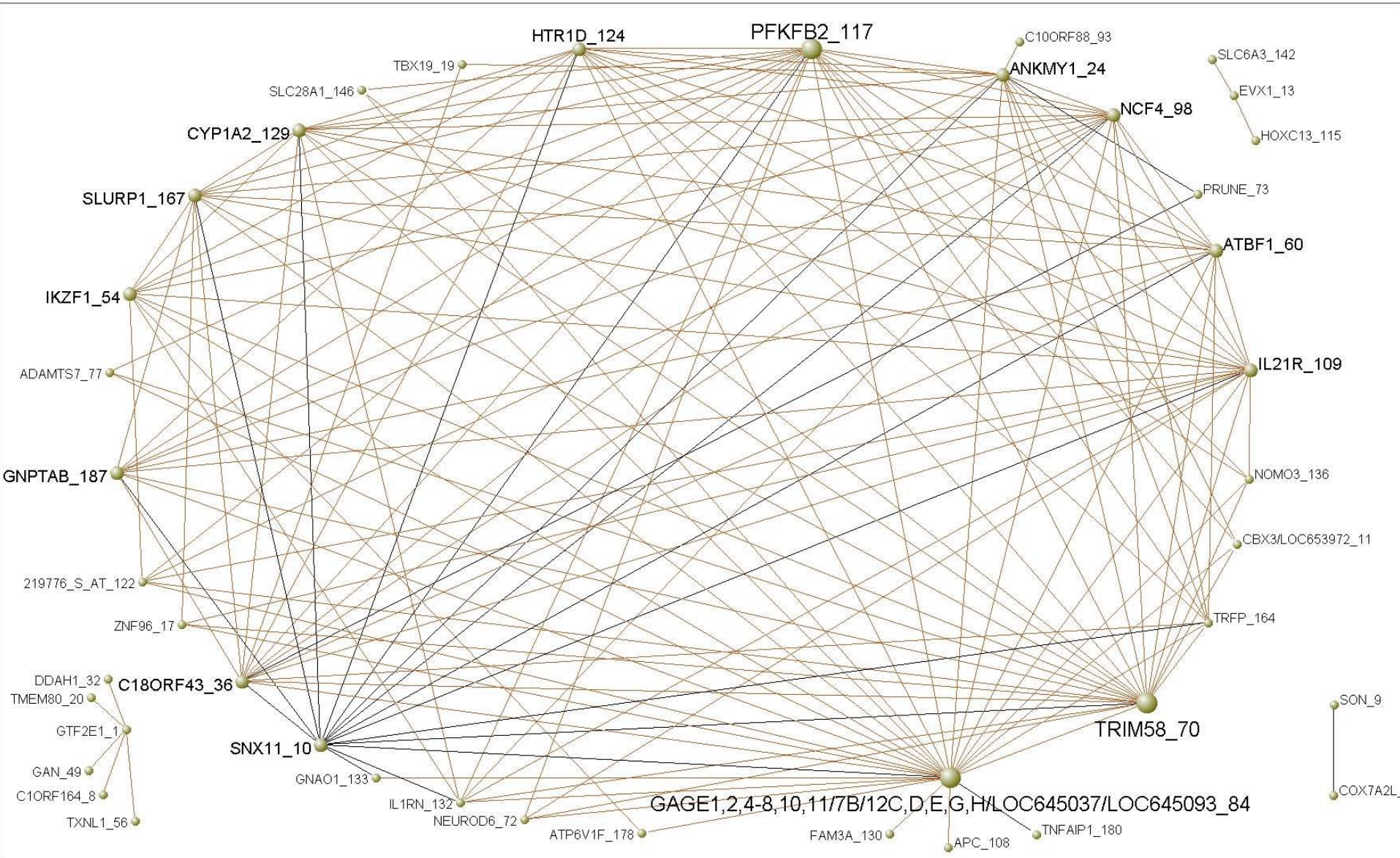

Figure S4BE

M40

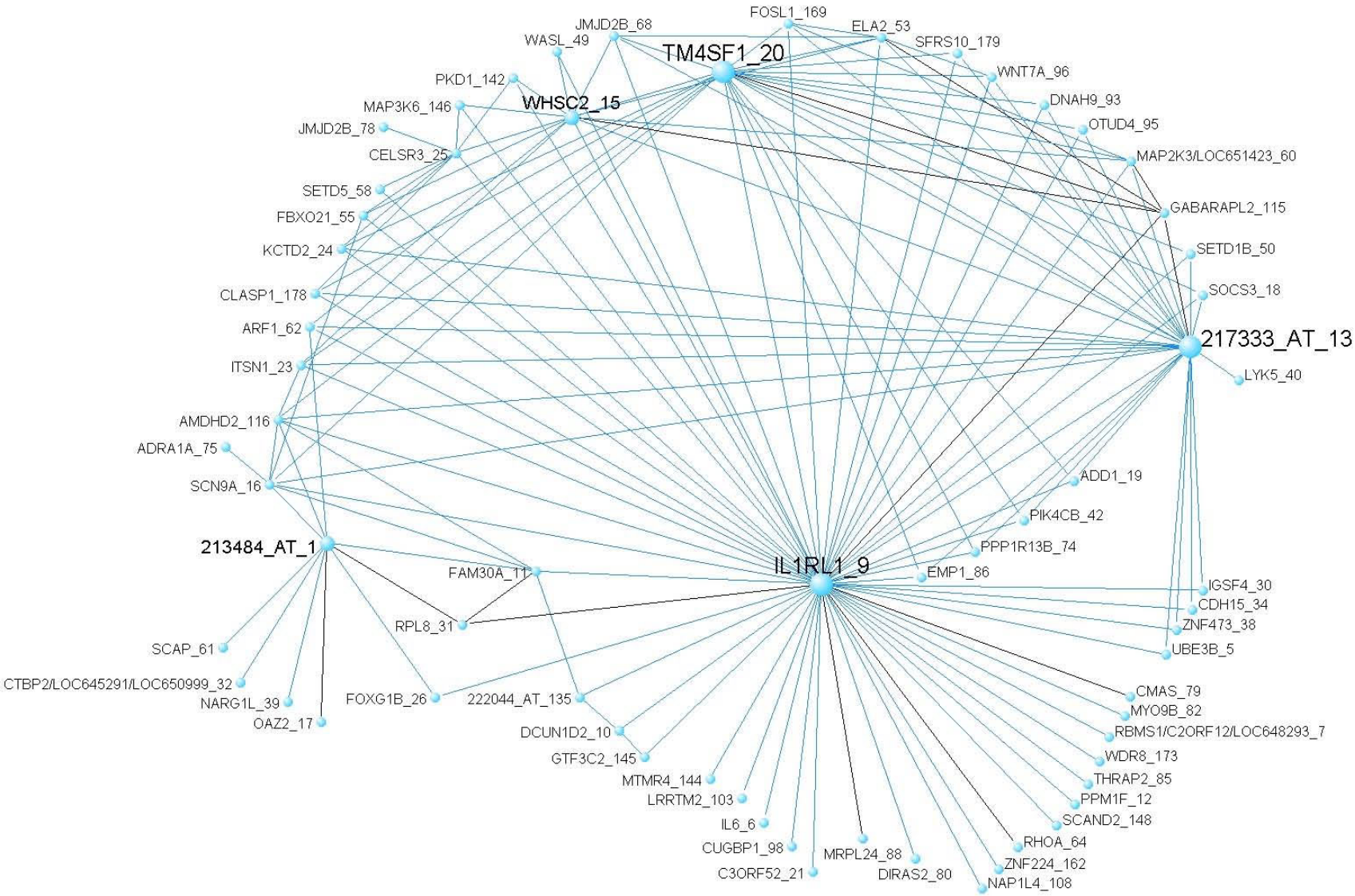

Figure S4BF

M41

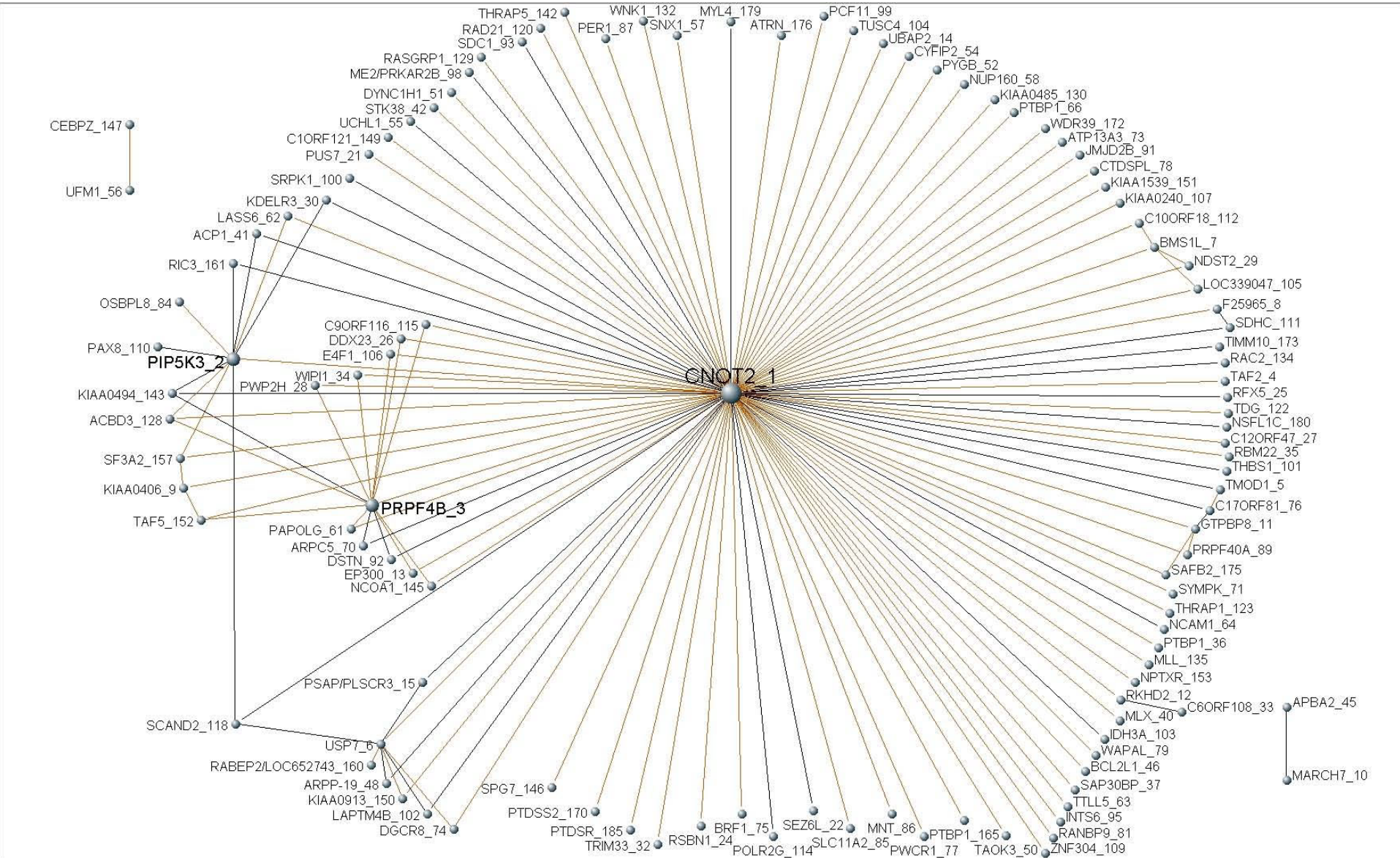

Figure S4BG

M42

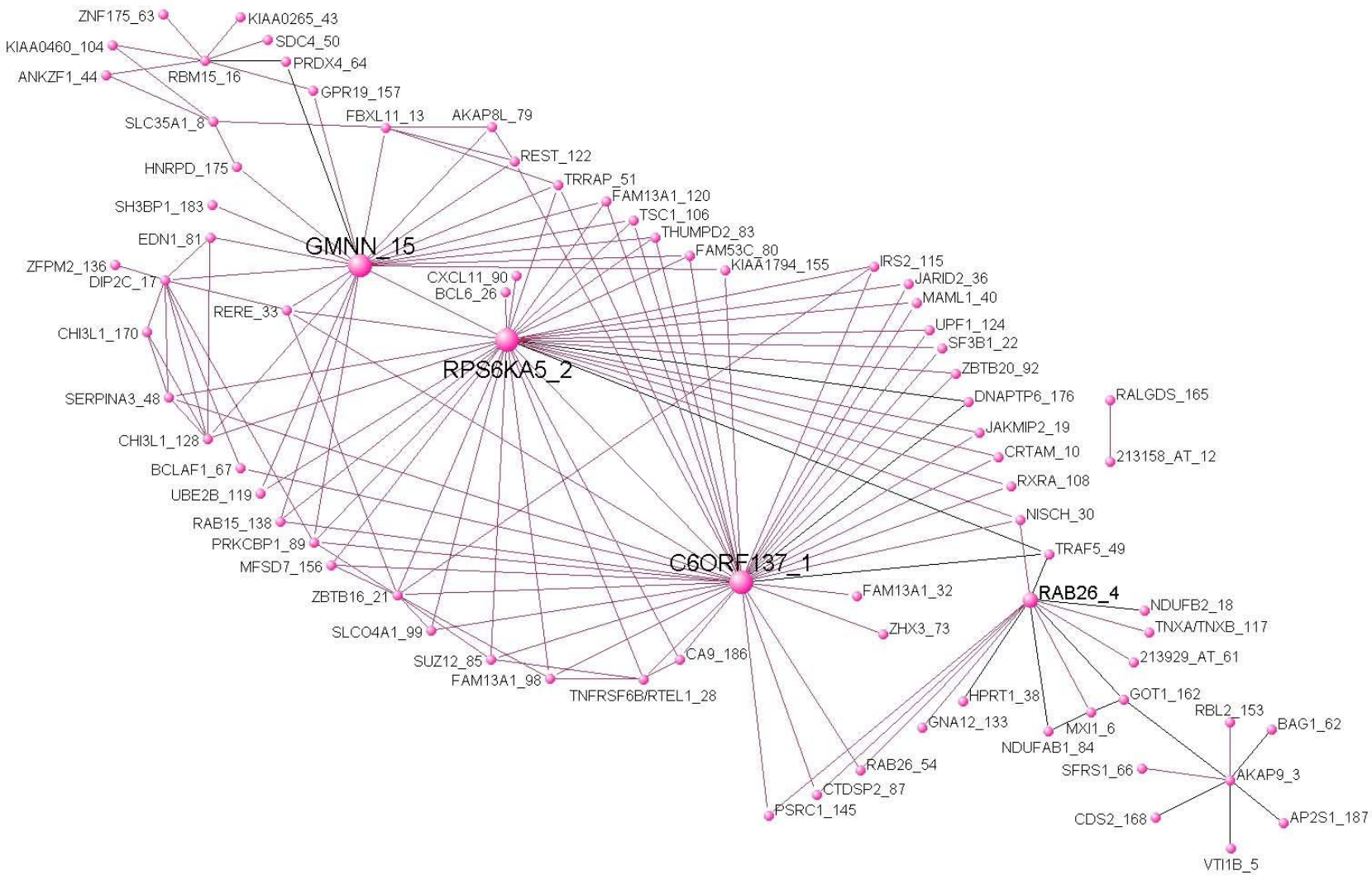

Figure S4BH

M43

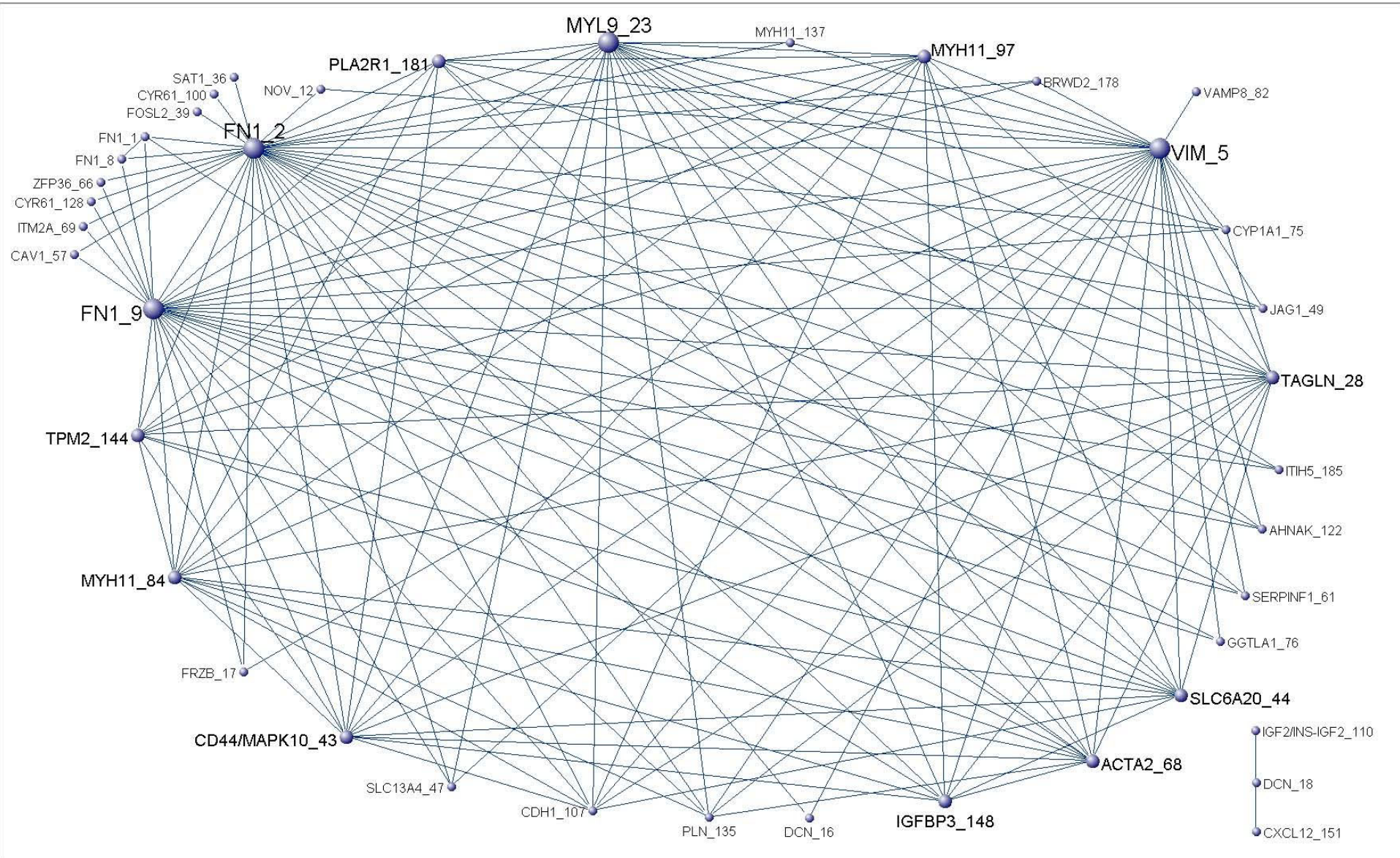

Figure S4BI

M44

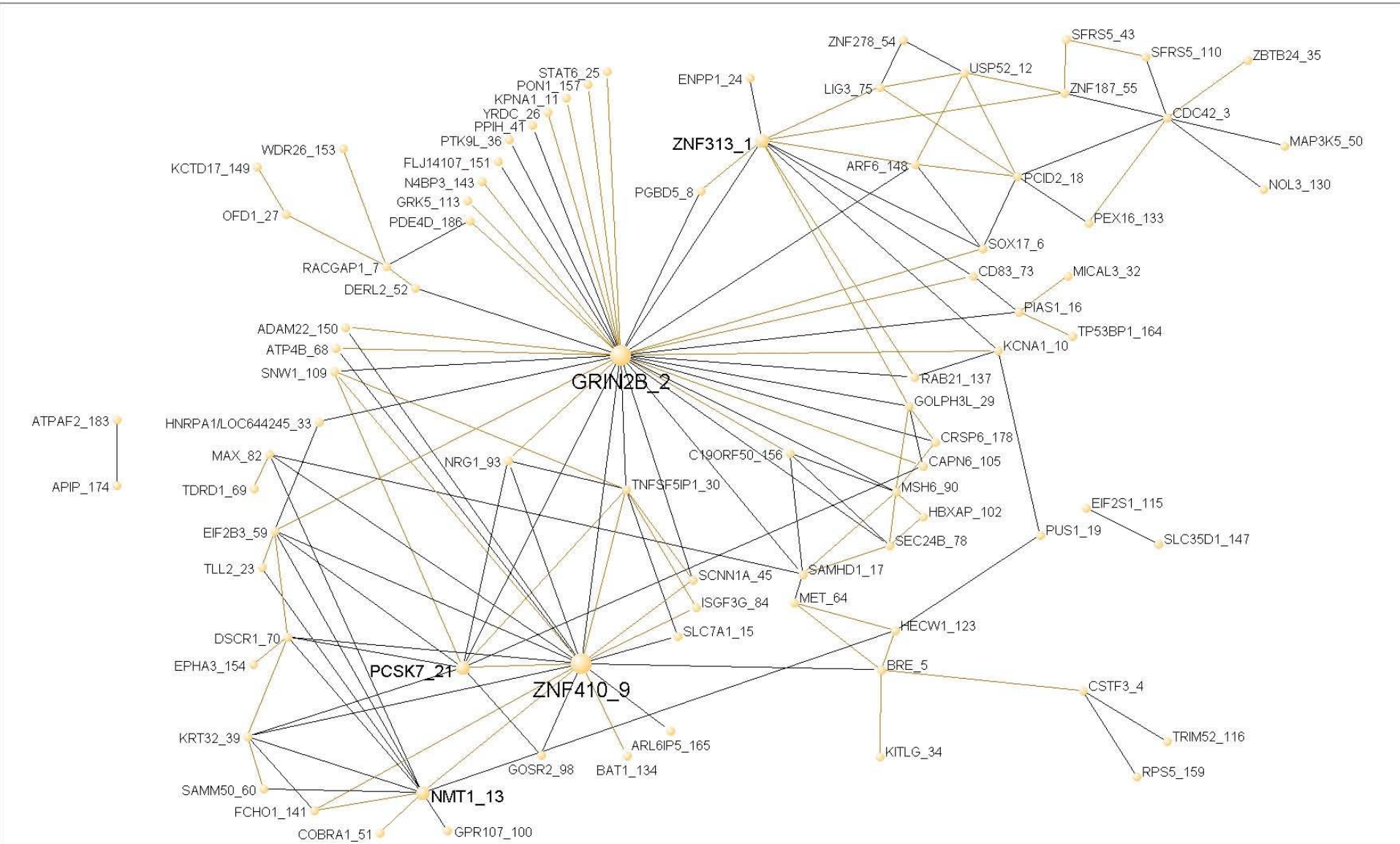

Figure S4BJ

M45

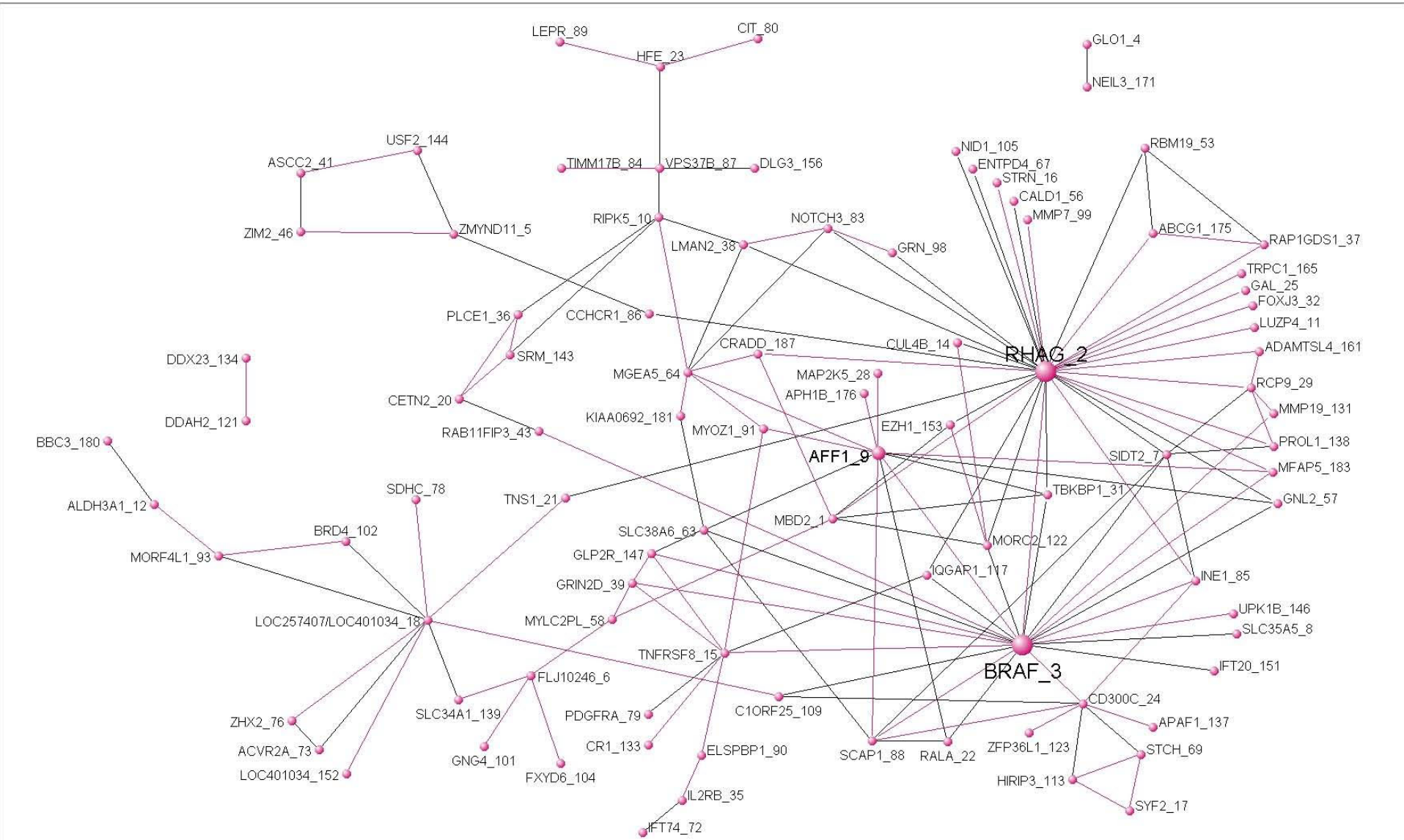

Figure S4BK

M46

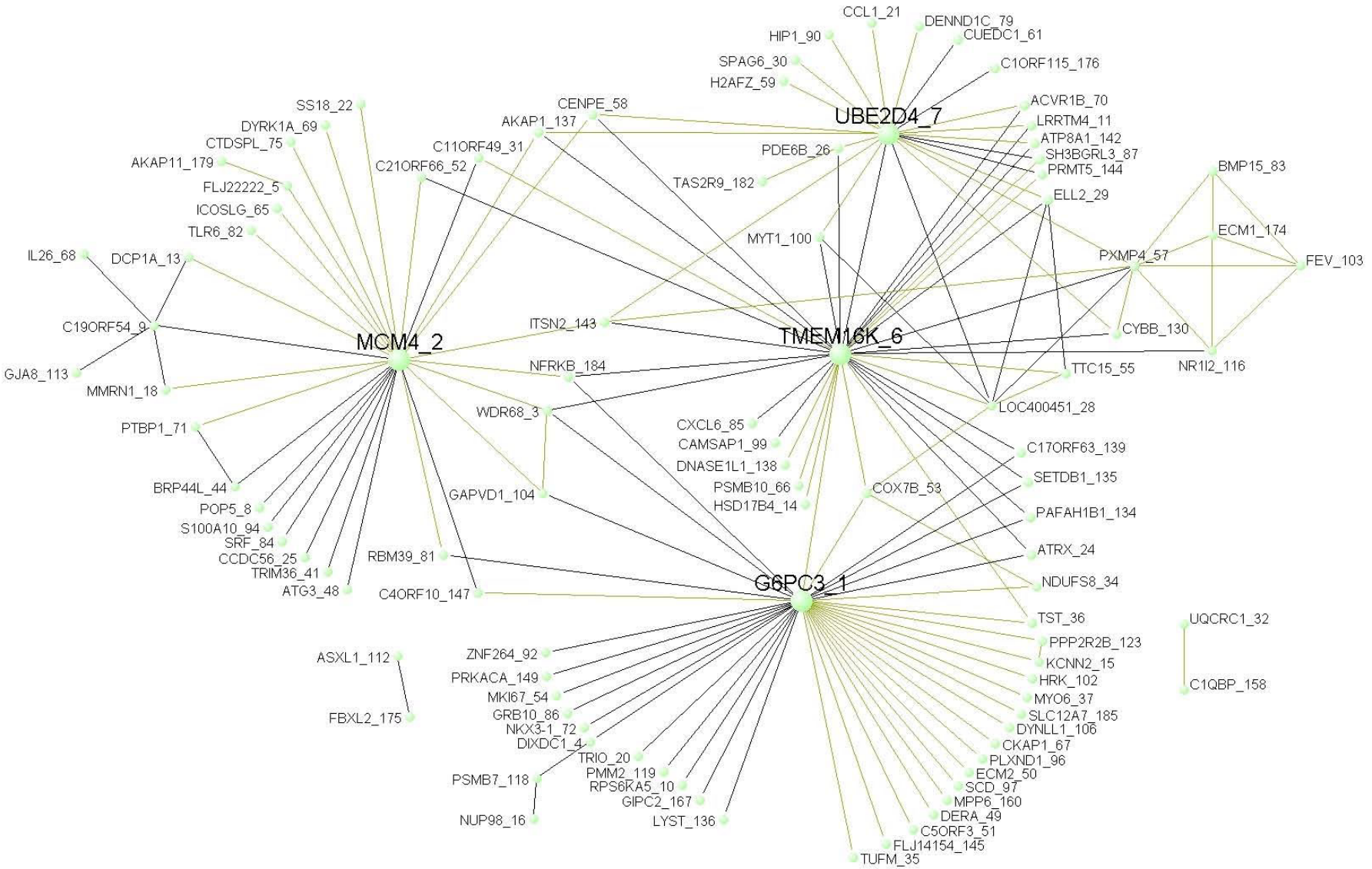

Figure S4BL

M47

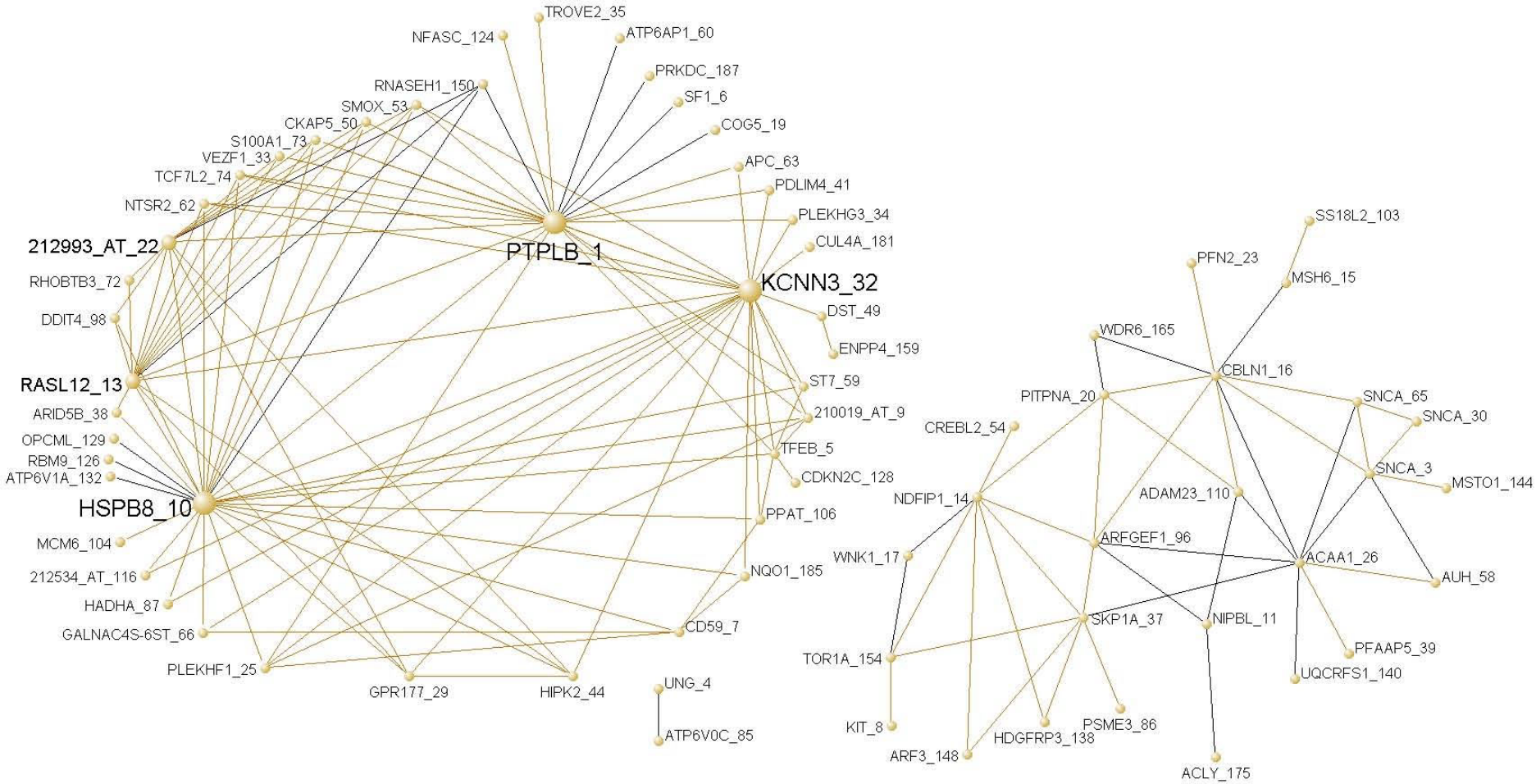

“Functional Organization of the Transcriptome in Human Brain”

Michael C. Oldham, Steve Horvath, Genevieve Konopka, Kazuya Iwamoto, Peter Langfelder, Tadafumi Kato, and Daniel H. Geschwind

Nature Neuroscience

Supplementary Figure 5: *In situ* hybridization confirms cellular/regional specificity of gene coexpression modules

Mouse *in situ* hybridization (ISH) data for genes from M6D (**a–j**) and M13C (**k–t**). ISH data were downloaded from the Allen Brain Atlas[31] (ABA) for available genes with the strongest membership for each module. Juxtaposed for each gene are the ISH image and corresponding expression level analysis (as calculated by the ABA). For genes in M6D, expression was strongest and most consistent in Purkinje neurons. For genes in M13C, the highest and most consistent expression levels in caudate nucleus were found in or near the subventricular zone.

Figure S5

Cerebellum

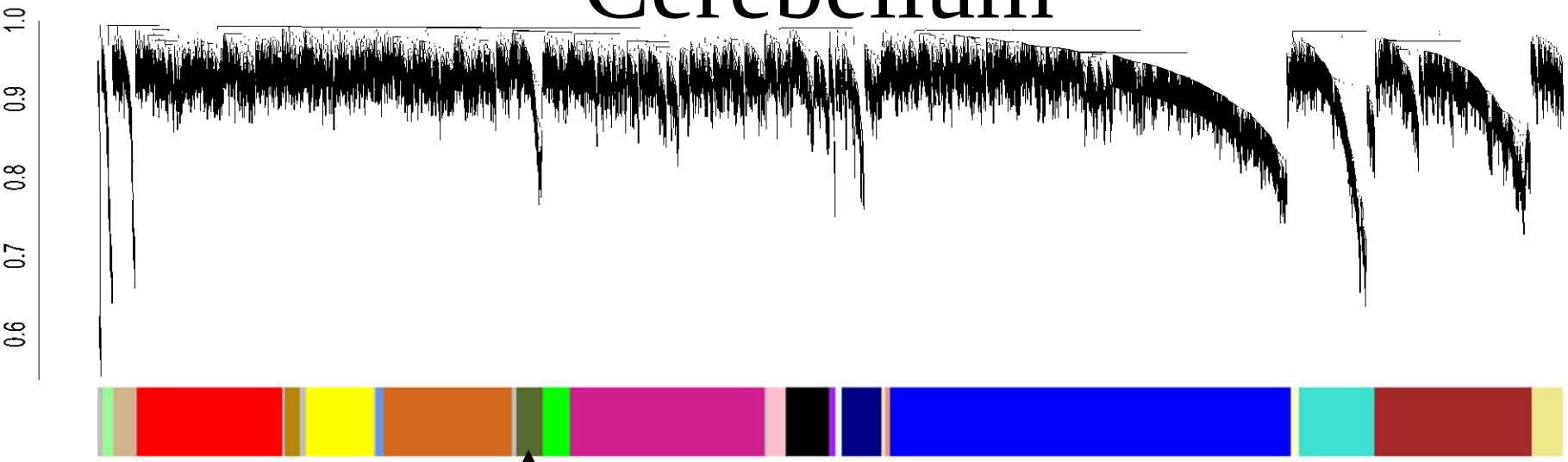

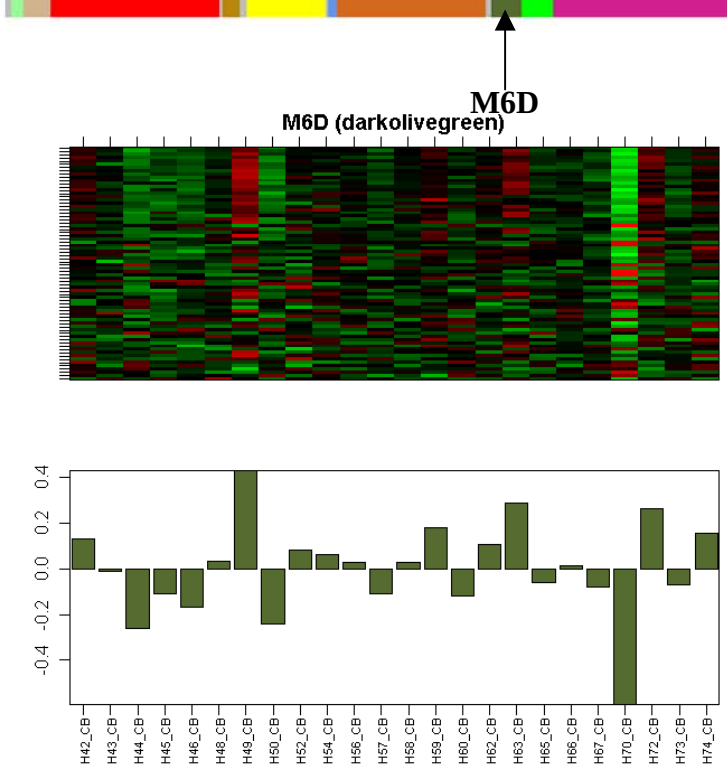

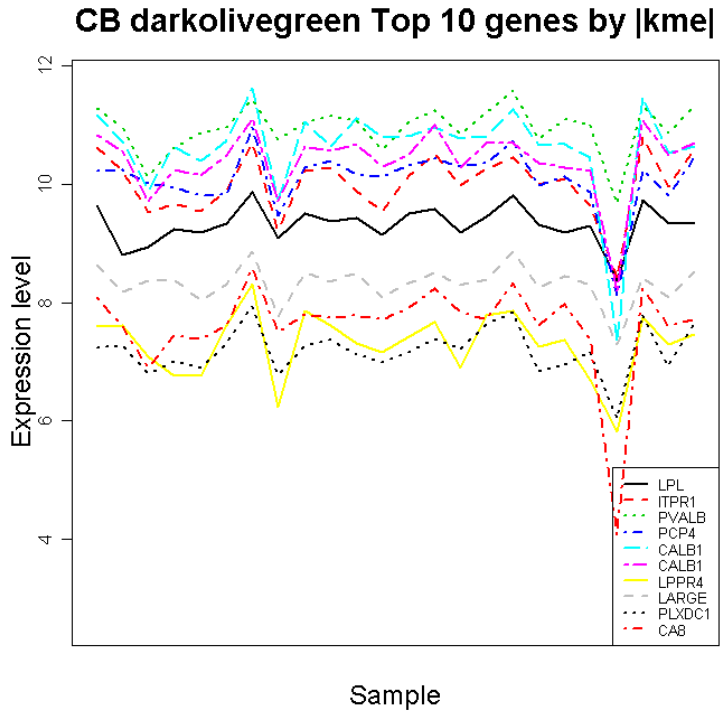

Figure S5A

M6D: *CALB1*

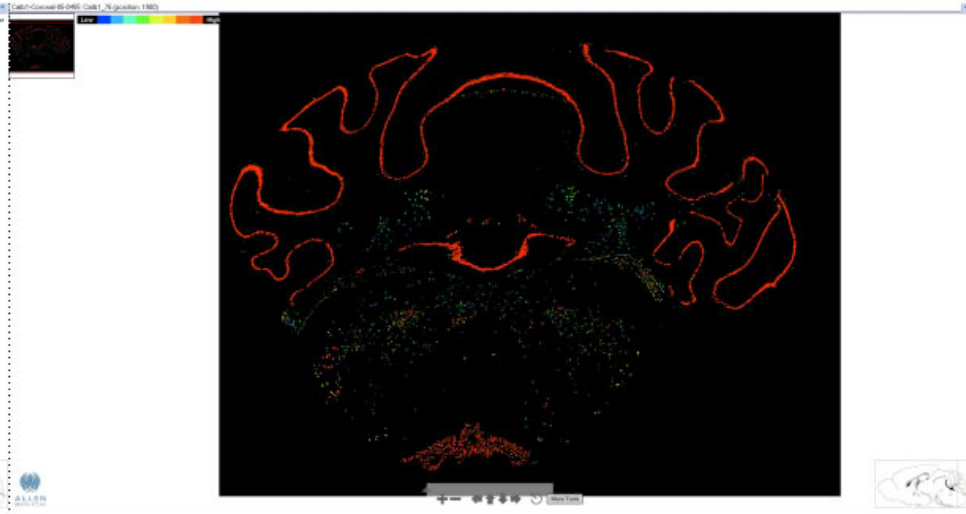

Figure S5B

M6D: *PVALB*

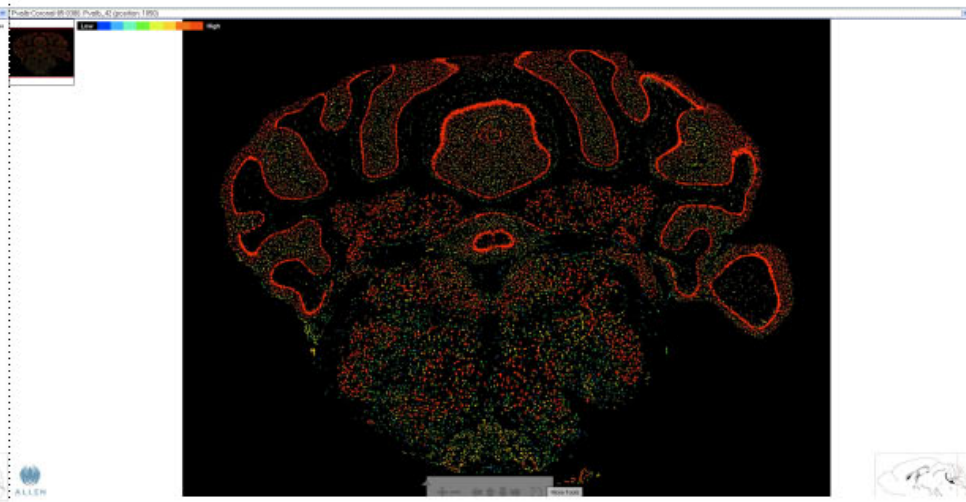

Figure S5C

M6D: *ITPR1*

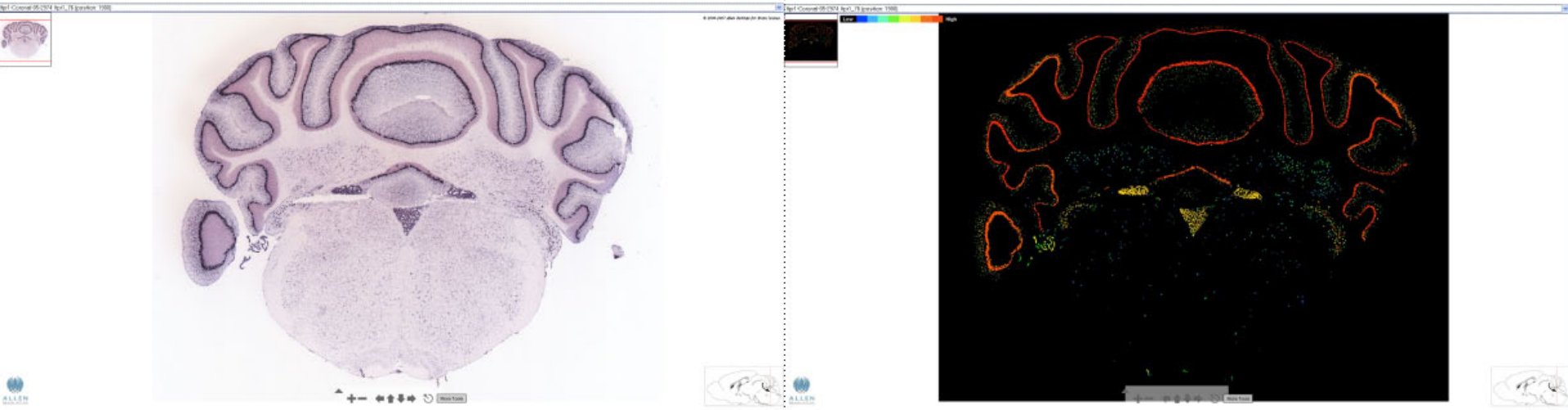

Figure S5D

M6D: *PLXDC1*

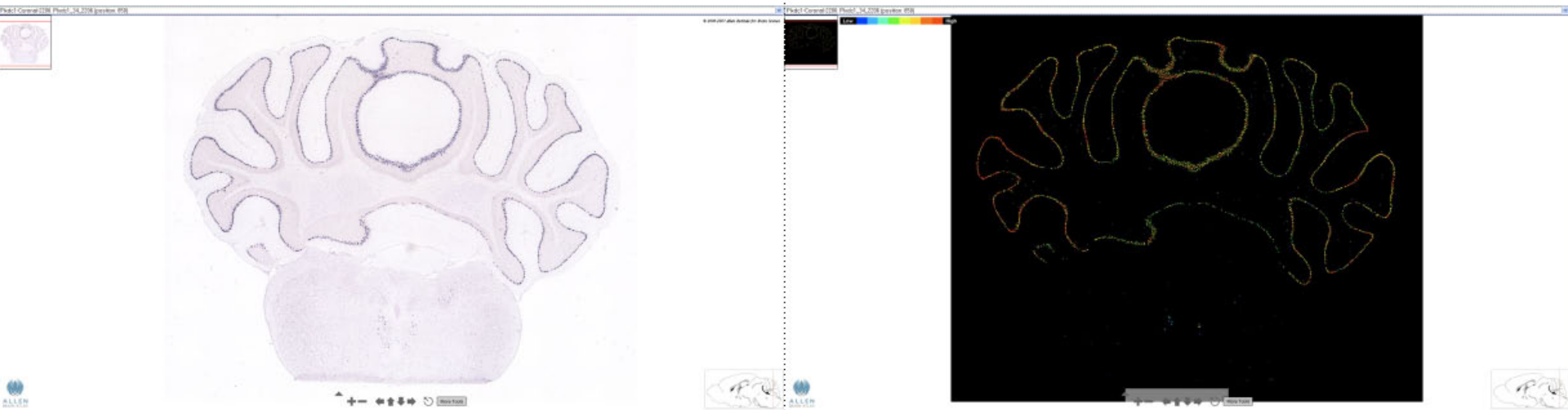

Figure S5E

M6D: *LPL*

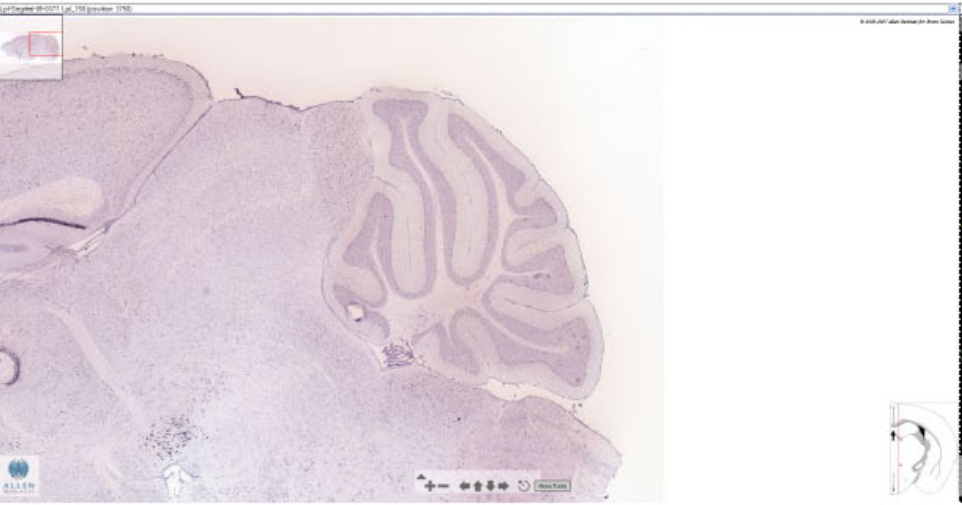

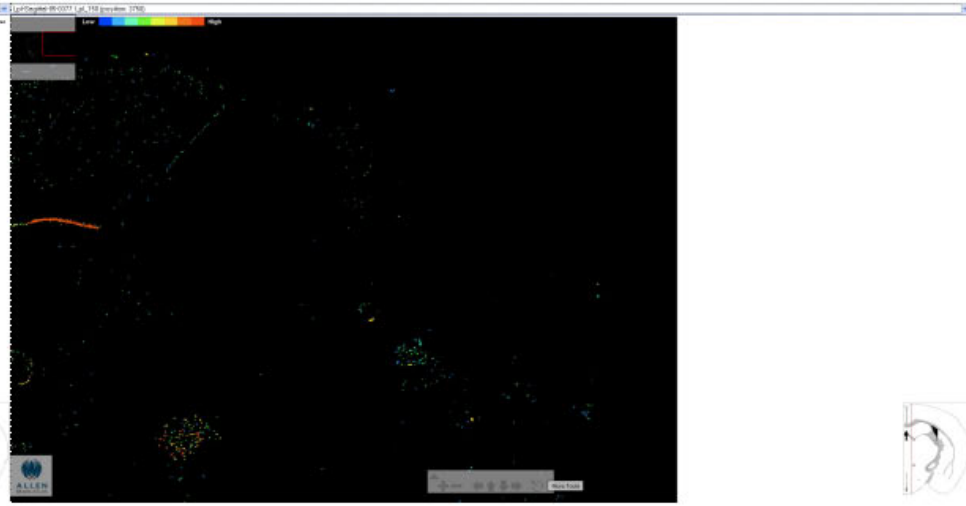

Figure S5F

M6D: *PCP4*

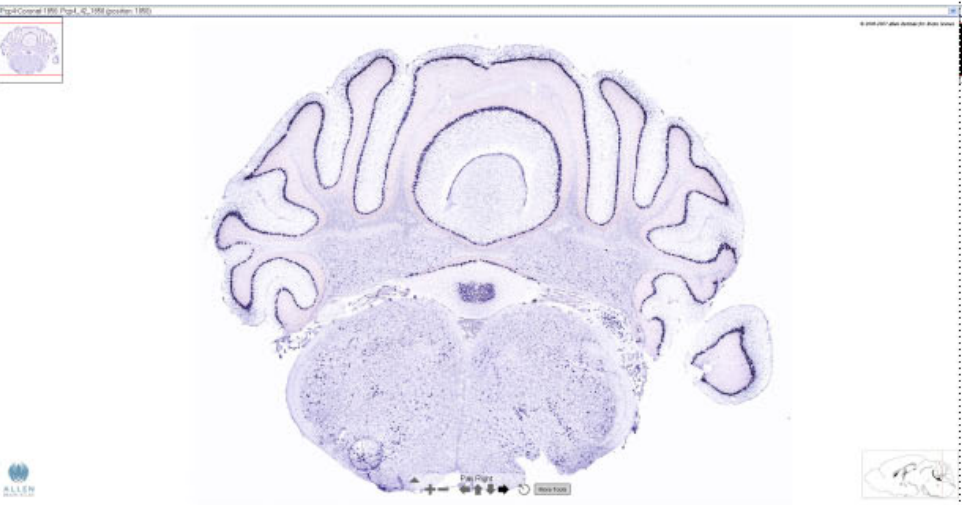

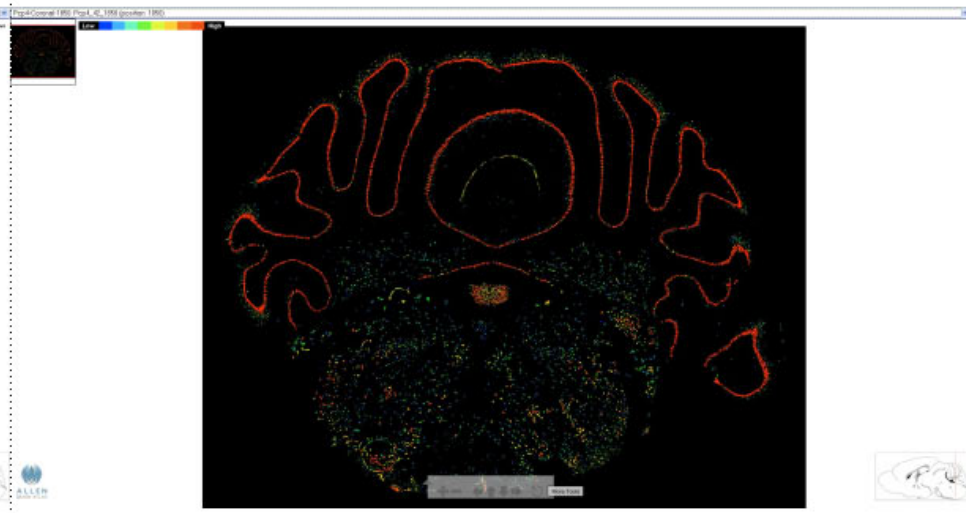

Figure S5G

M6D: *LARGE*

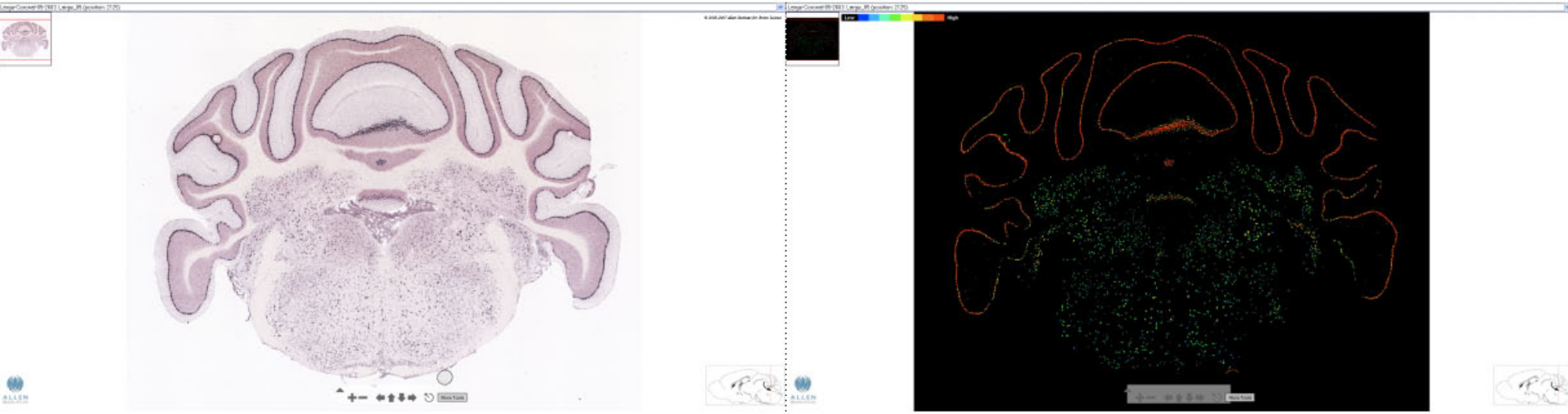

Figure S5H

M6D: *CHST2*

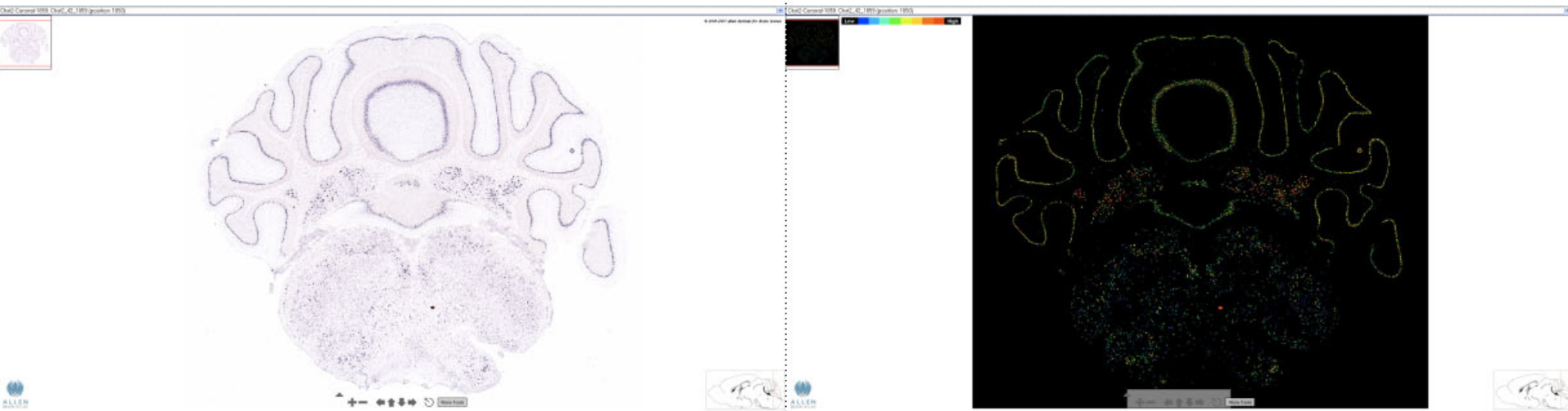

Figure S5I

M6D: *LRP8*

Figure S5J

M6D: *SLC1A6*

Figure S5

Caudate nucleus

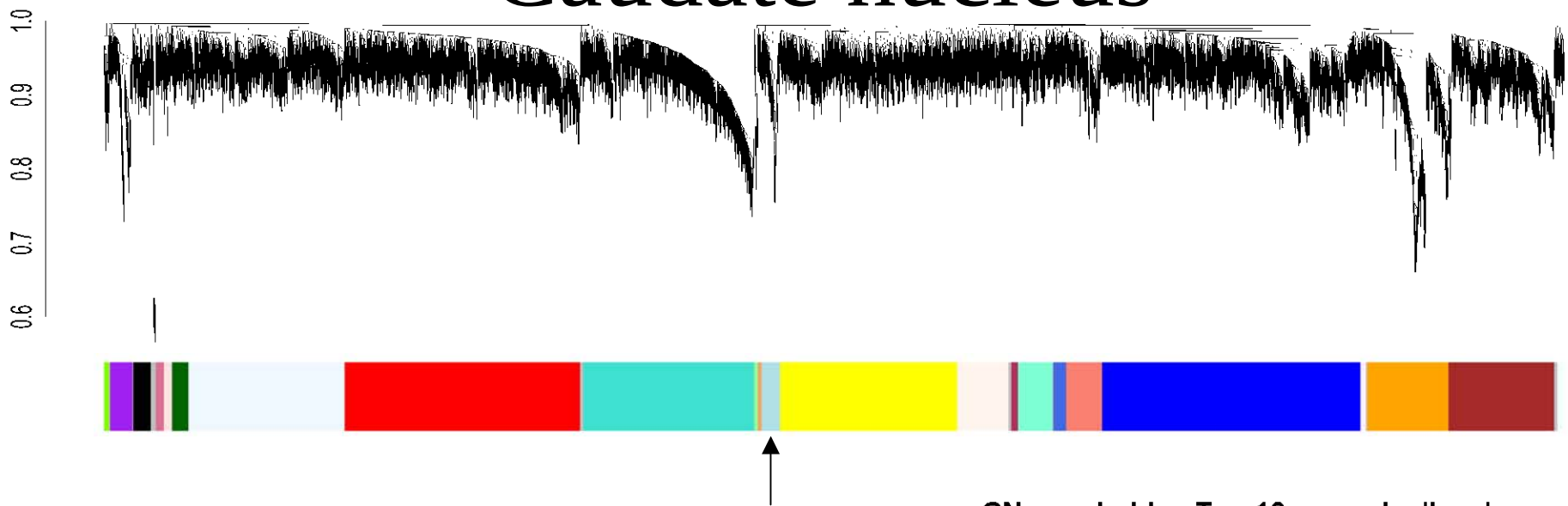

M13C

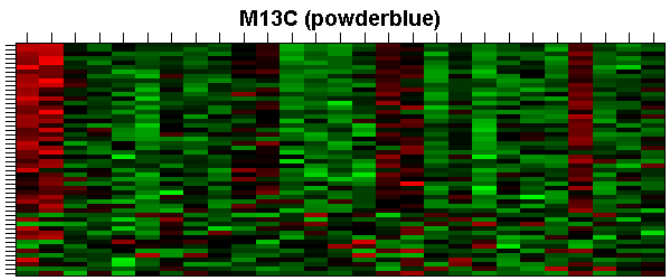

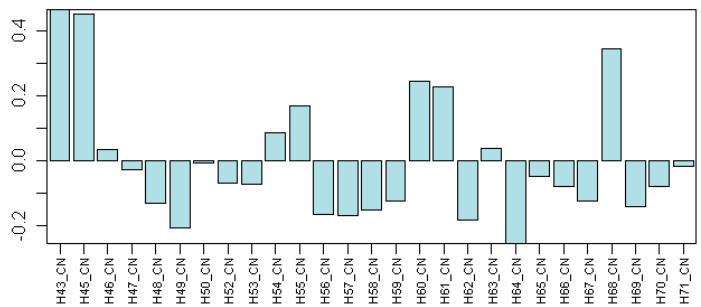

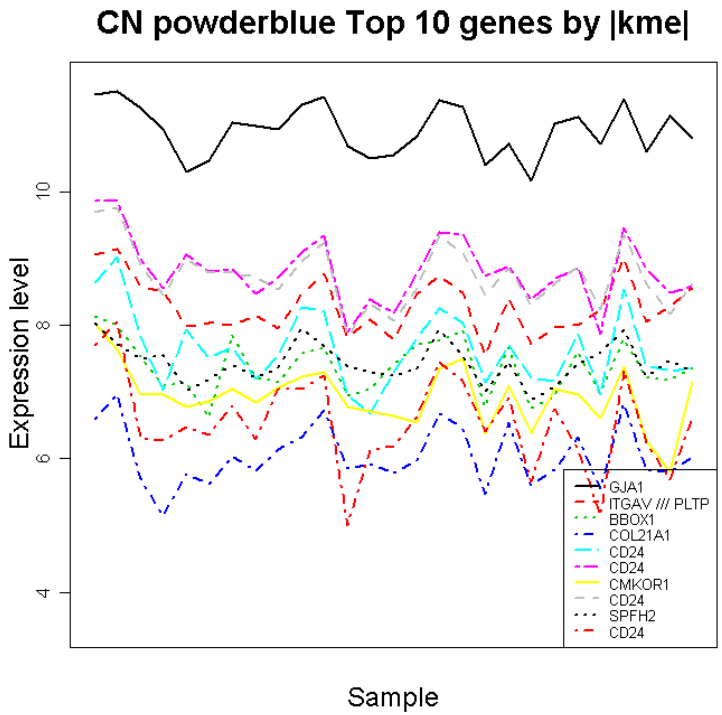

Figure S5K

M13C: *PLTP*

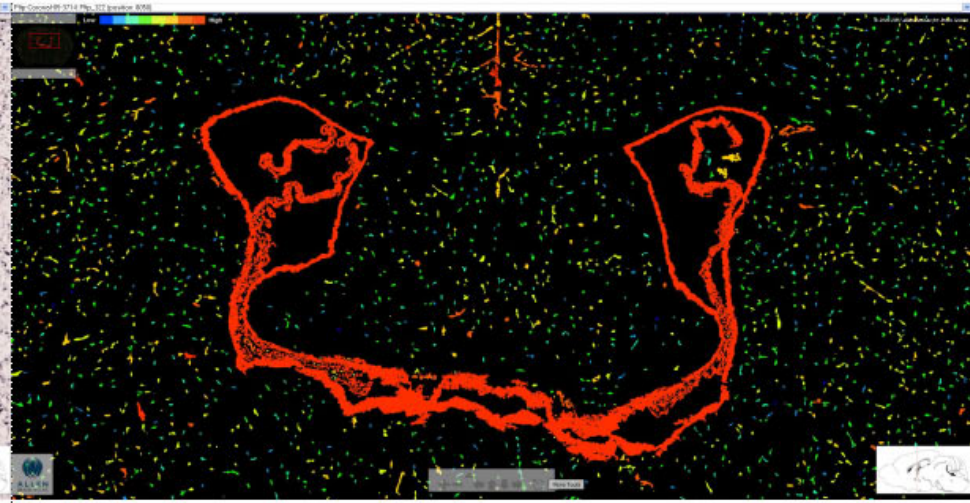

Figure S5L

M13C: *CD24*

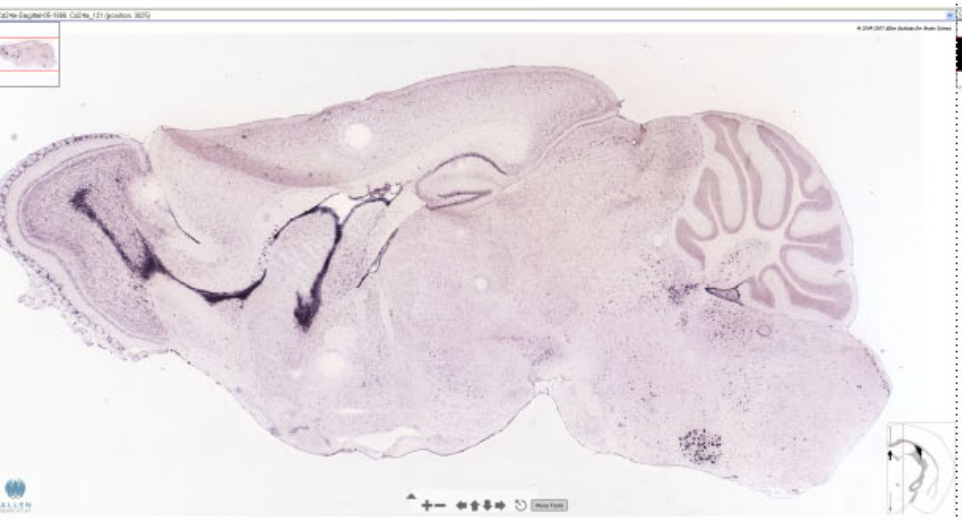

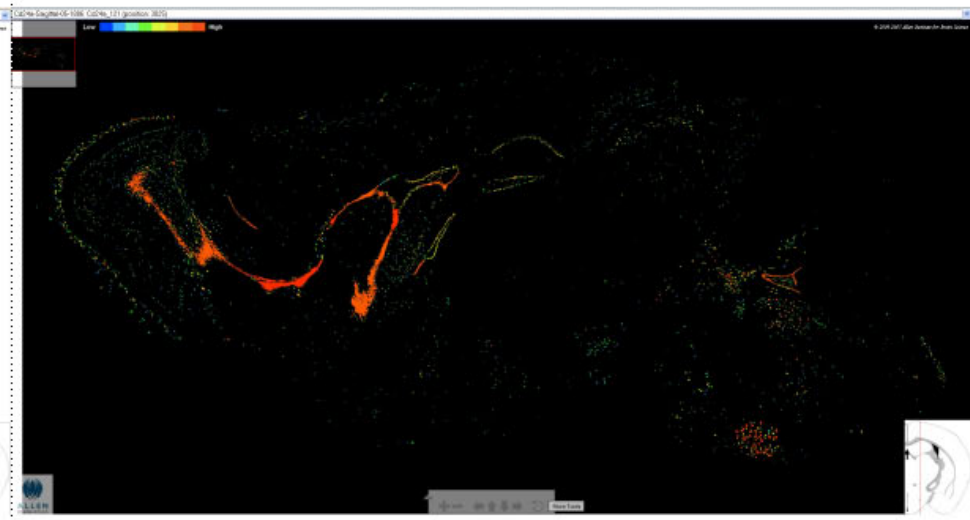

Figure S5M

M13C: *CD24*

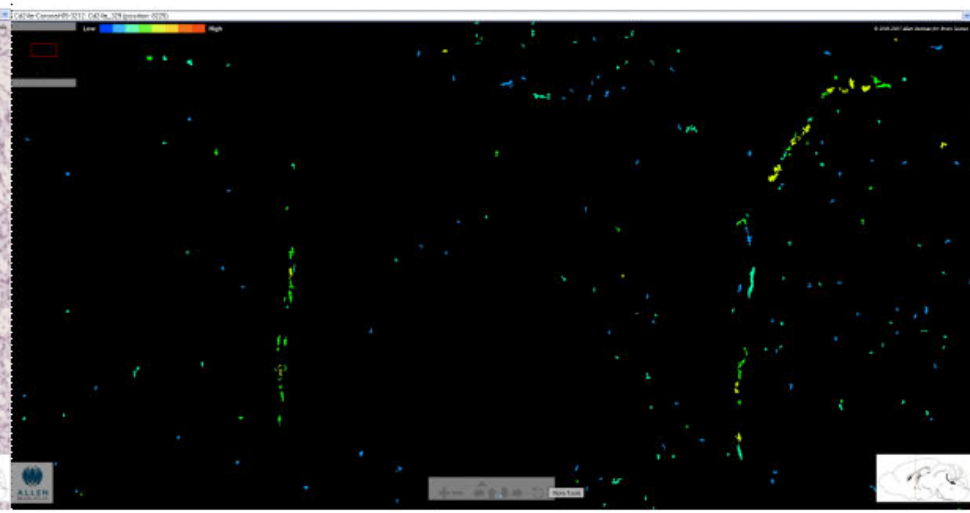

Figure S5N

M13C: *GJA1*

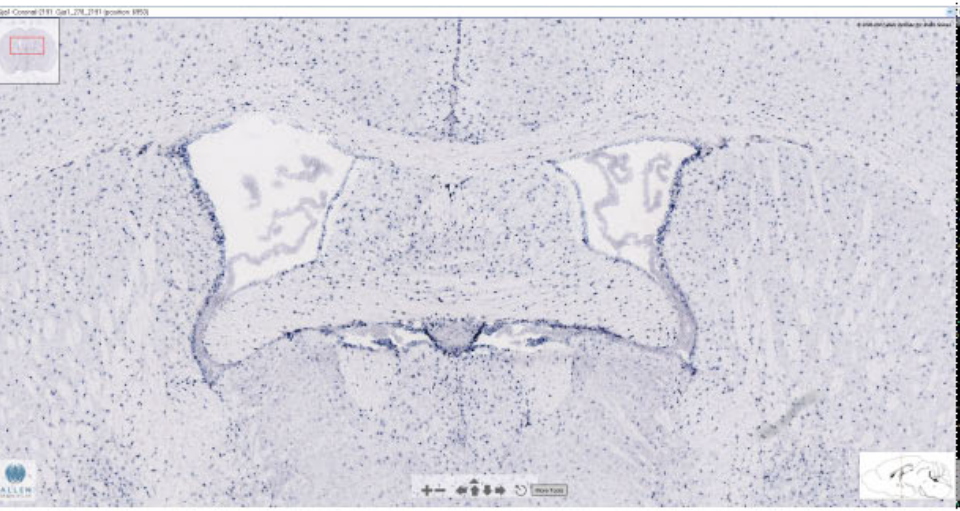

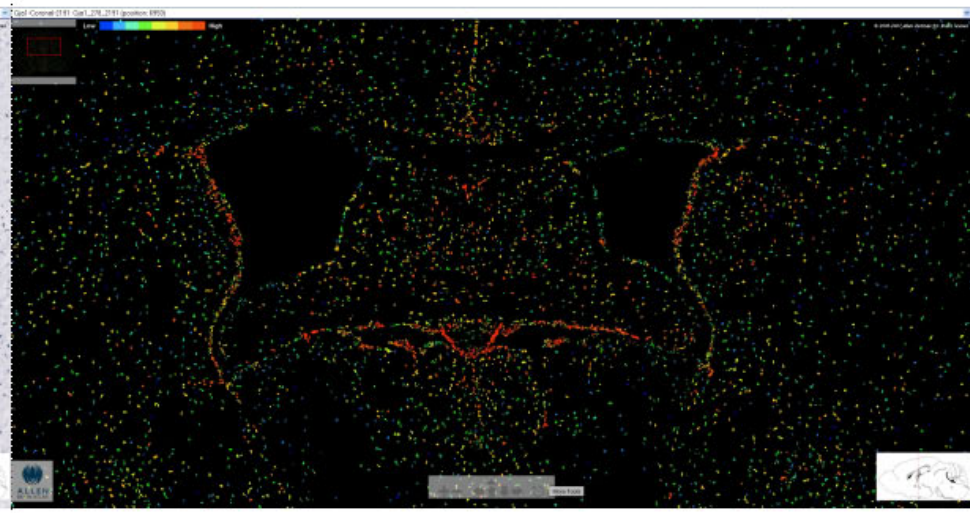

Figure S5O

M13C: *BBOX1*

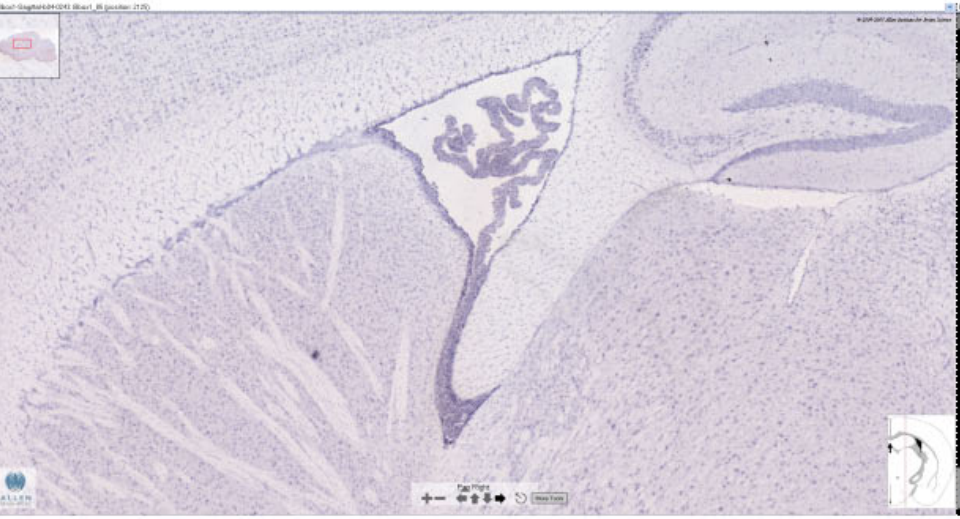

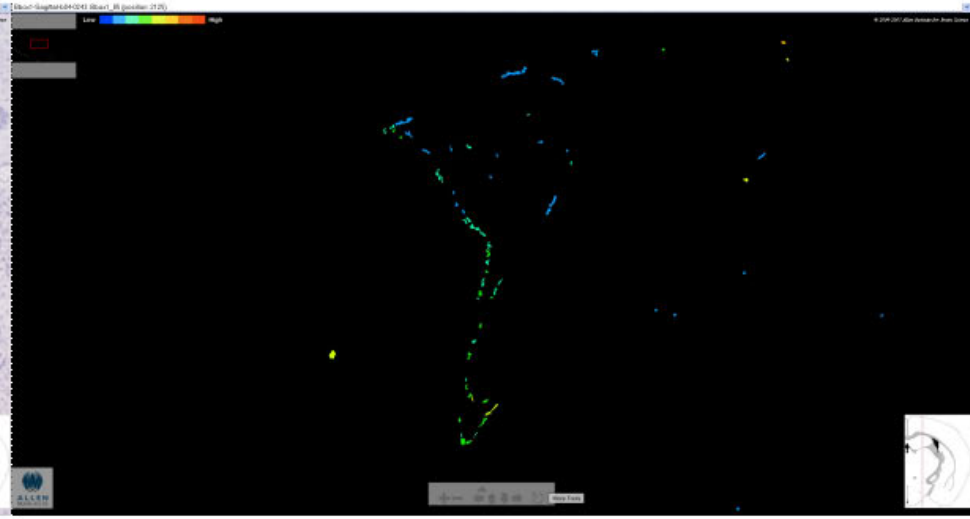

Figure S5P

M13C: *SPFH2*

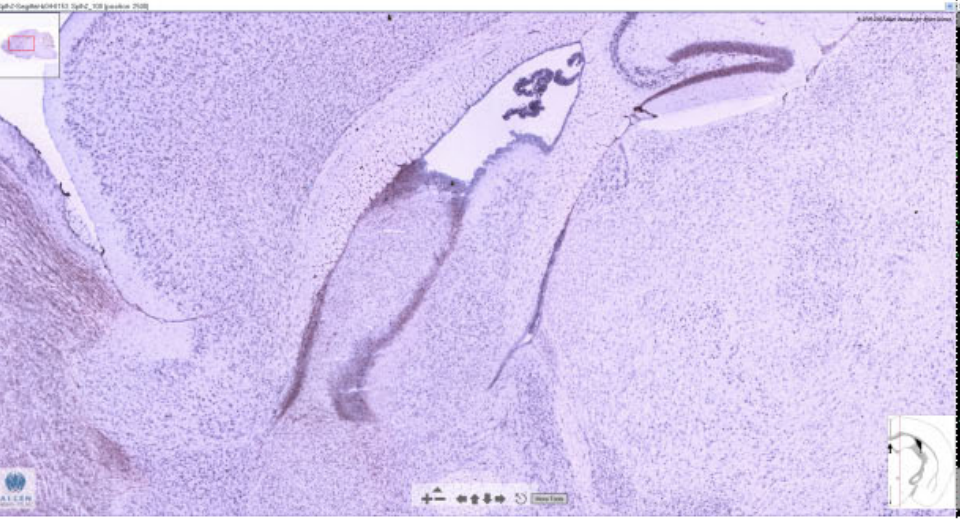

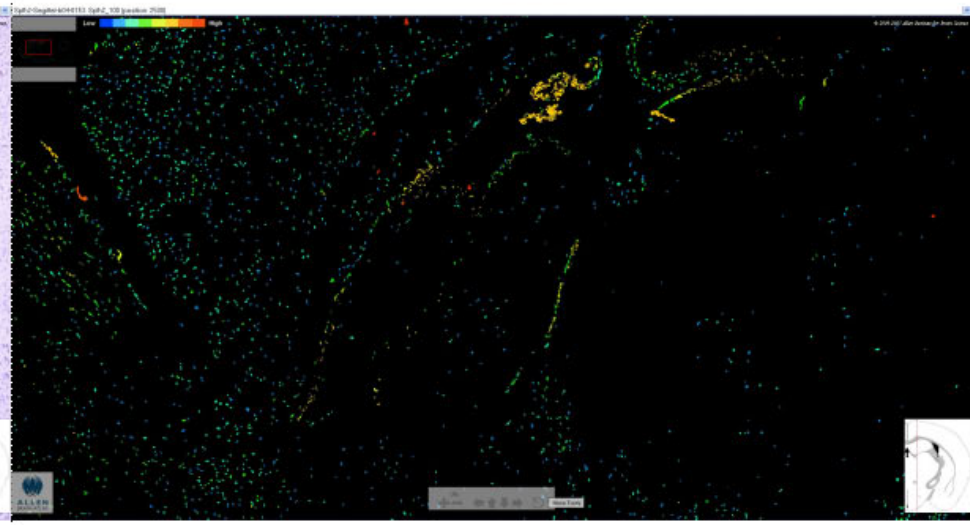

Figure S5Q

M13C: *DPYSL3*

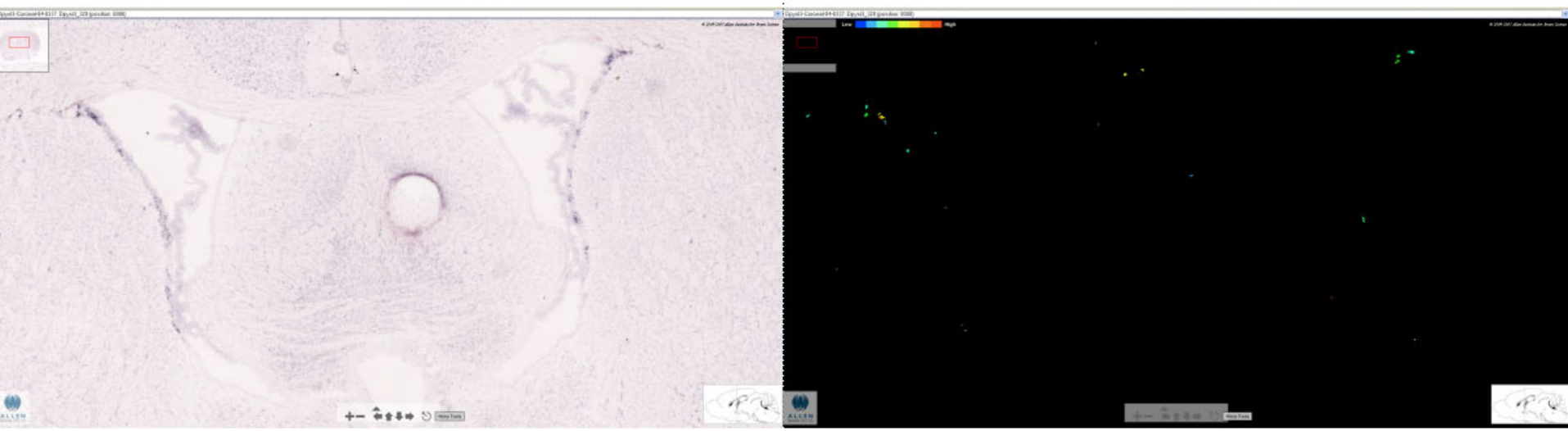

Figure S5R

M13C: *SPAG6*

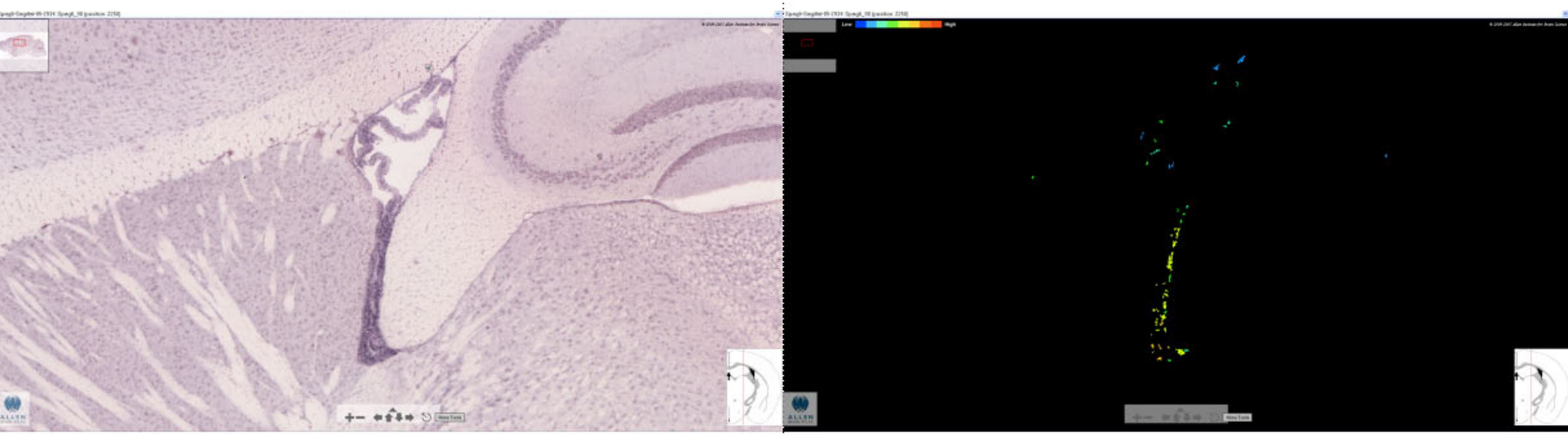

Figure S5S

M13C: *TSPAN6*

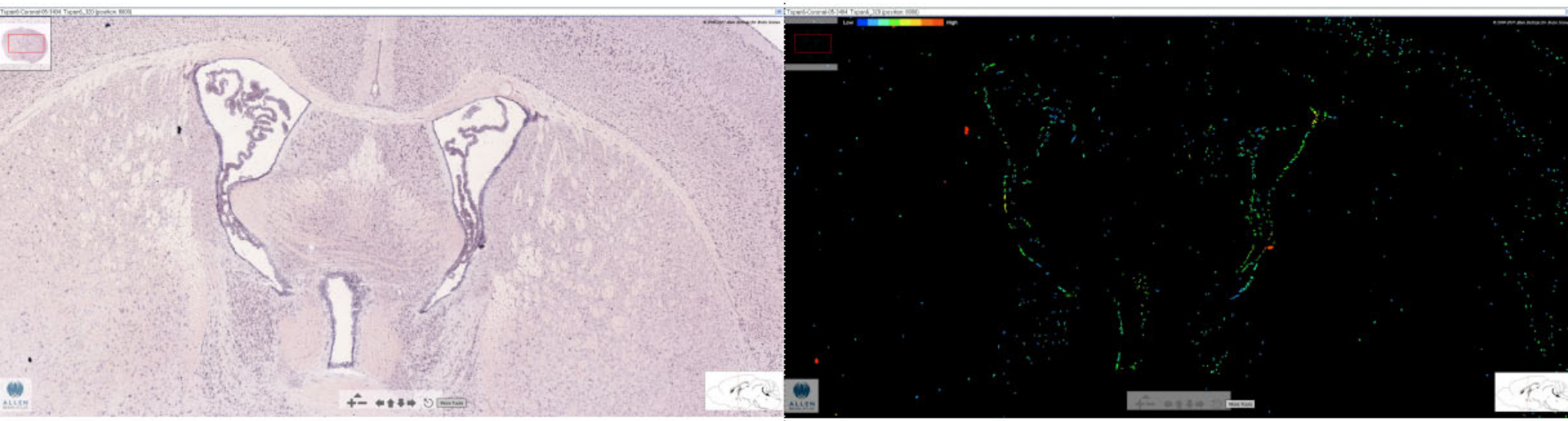

Figure S5T

M13C: *ANGPT1*

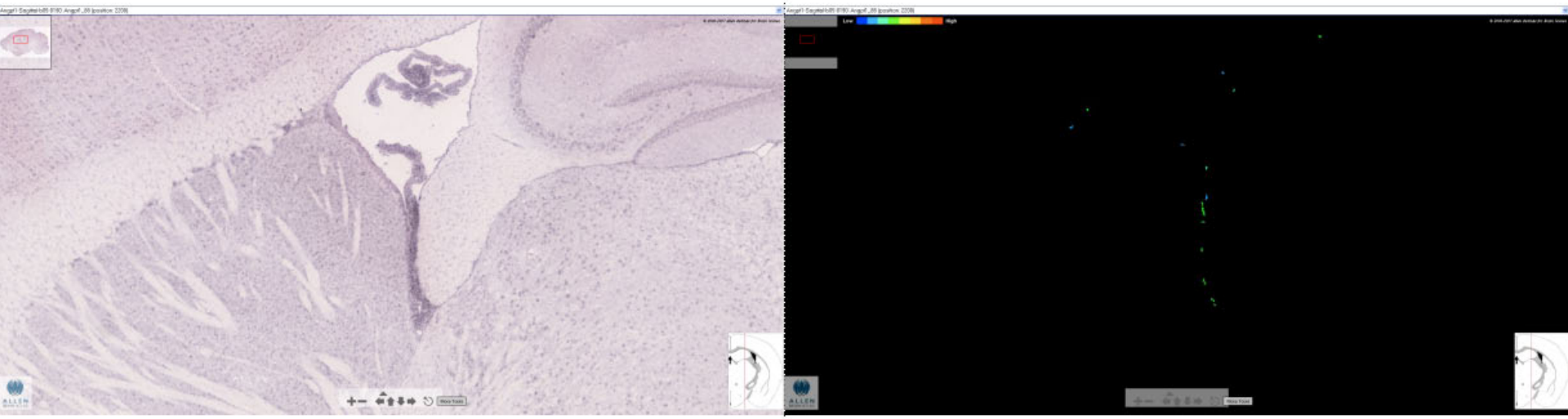

“Functional Organization of the Transcriptome in Human Brain”

Michael C. Oldham, Steve Horvath, Genevieve Konopka, Kazuya Iwamoto, Peter Langfelder, Tadafumi Kato, and Daniel H. Geschwind

Nature Neuroscience

Supplementary Figure 6: Module eigengene networks and comparisons between brain regions

Pearson correlation coefficients and corresponding p-values for all module eigengene (ME) comparisons in CTX (**a**), CTX_95 (**b**), CN (**c**), and CB (**d**). Red and green denote positive and negative correlations, respectively. MEs in each network were ordered to facilitate visual interpretation of the networks (Supplementary Methods). ME network comparisons between CTX and CN (**e**), CTX and CB (**f**), and CN and CB (**g**) were restricted to conserved modules and performed as described in Supplementary Methods.

Figure S6A

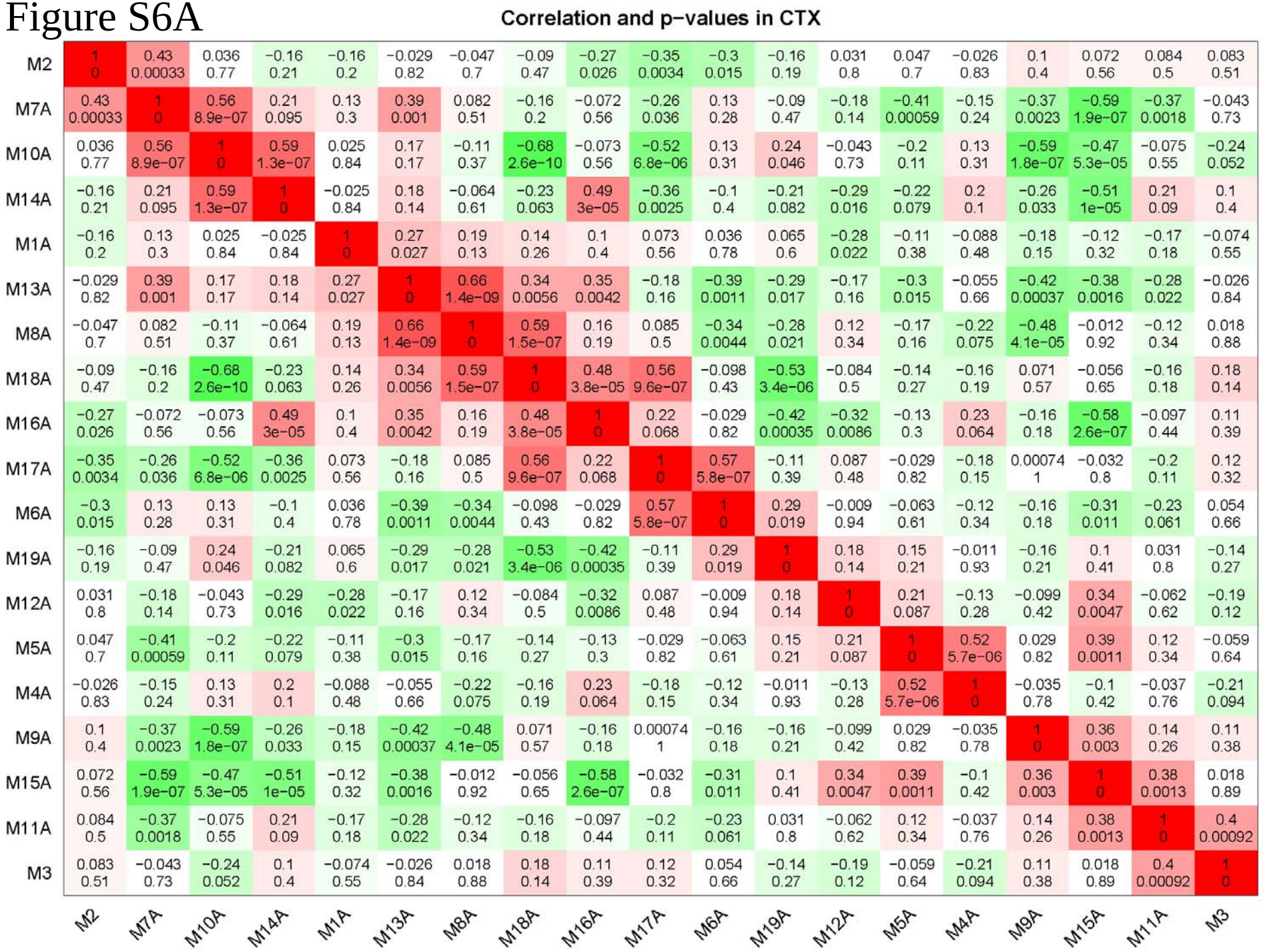
Correlation and p−values in CTX
M2 1 0 0.43 0.00033 0.036 0.77 −0.16 0.21 −0.16 0.2 −0.029 0.82 −0.047 0.7 −0.09 0.47 −0.27 0.026 −0.35 0.0034 −0.3 0.015 −0.16 0.19 0.031 0.8 0.047 0.7 −0.026 0.83 0.1 0.4 0.072 0.56 0.084 0.5 0.083 0.51
M7A 0.43 0.00033 1 0 0.56 8.9e−07 0.21 0.095 0.13 0.3 0.39 0.001 0.082 0.51 −0.16 0.2 −0.072 0.56 −0.26 0.036 0.13 0.28 −0.09 0.47 −0.18 0.14 −0.41 0.00059 −0.15 0.24 −0.37 0.0023 −0.59 1.9e−07 −0.37 0.0018 −0.043 0.73
M10A 0.036 0.77 0.56 8.9e−07 1 0 0.59 1.3e−07 0.025 0.84 0.17 0.17 −0.11 0.37 −0.68 2.6e−10 −0.073 0.56 −0.52 6.8e−06 0.13 0.31 0.24 0.046 −0.043 0.73 −0.2 0.11 0.13 0.31 −0.59 1.8e−07 −0.47 5.3e−05 −0.075 0.55 −0.24 0.052
M14A −0.16 0.21 0.21 0.095 0.59 1.3e−07 1 0 −0.025 0.84 0.18 0.14 −0.064 0.61 −0.23 0.063 0.49 3e−05 −0.36 0.0025 −0.1 0.4 −0.21 0.082 −0.29 0.016 −0.22 0.079 0.2 0.1 −0.26 0.033 −0.51 1e−05 0.21 0.09 0.1 0.4
M1A −0.16 0.2 0.13 0.3 0.025 0.84 −0.025 0.84 1 0 0.27 0.027 0.19 0.13 0.14 0.26 0.1 0.4 0.073 0.56 0.036 0.78 0.065 0.6 −0.28 0.022 −0.11 0.38 −0.088 0.48 −0.18 0.15 −0.12 0.32 −0.17 0.18 −0.074 0.55
M13A −0.029 0.82 0.39 0.001 0.17 0.17 0.18 0.14 0.27 0.027 1 0 0.66 1.4e−09 0.34 0.0056 0.35 0.0042 −0.18 0.16 −0.39 0.0011 −0.29 0.017 −0.17 0.16 −0.3 0.015 −0.055 0.66 −0.42 0.00037 −0.38 0.0016 −0.28 0.022 −0.026 0.84
M8A −0.047 0.7 0.082 0.51 −0.11 0.37 −0.064 0.61 0.19 0.13 0.66 1.4e−09 1 0 0.59 1.5e−07 0.16 0.19 0.085 0.5 −0.34 0.0044 −0.28 0.021 0.12 0.34 −0.17 0.16 −0.22 0.075 −0.48 4.1e−05 −0.012 0.92 −0.12 0.34 0.018 0.88
M18A −0.09 0.47 −0.16 0.2 −0.68 2.6e−10 −0.23 0.063 0.14 0.26 0.34 0.0056 0.59 1.5e−07 1 0 0.48 3.8e−05 0.56 9.6e−07 −0.098 0.43 −0.53 3.4e−06 −0.084 0.5 −0.14 0.27 −0.16 0.19 0.071 0.57 −0.056 0.65 −0.16 0.18 0.18 0.14
M16A −0.27 0.026 −0.072 0.56 −0.073 0.56 0.49 3e−05 0.1 0.4 0.35 0.0042 0.16 0.19 0.48 3.8e−05 1 0 0.22 0.068 −0.029 0.82 −0.42 0.00035 −0.32 0.0086 −0.13 0.3 0.23 0.064 −0.16 0.18 −0.58 2.6e−07 −0.097 0.44 0.11 0.39
M17A −0.35 0.0034 −0.26 0.036 −0.52 6.8e−06 −0.36 0.0025 0.073 0.56 −0.18 0.16 0.085 0.5 0.56 9.6e−07 0.22 0.068 1 0 0.57 5.8e−07 −0.11 0.39 0.087 0.48 −0.029 0.82 −0.18 0.15 0.00074 1 −0.032 0.8 −0.2 0.11 0.12 0.32
M6A −0.3 0.015 0.13 0.28 0.13 0.31 −0.1 0.4 0.036 0.78 −0.39 0.0011 −0.34 0.0044 −0.098 0.43 −0.029 0.82 0.57 5.8e−07 1 0 0.29 0.019 −0.009 0.94 −0.063 0.61 −0.12 0.34 −0.16 0.18 −0.31 0.011 −0.23 0.061 0.054 0.66
M19A −0.16 0.19 −0.09 0.47 0.24 0.046 −0.21 0.082 0.065 0.6 −0.29 0.017 −0.28 0.021 −0.53 3.4e−06 −0.42 0.00035 −0.11 0.39 0.29 0.019 1 0 0.18 0.14 0.15 0.21 −0.011 0.93 −0.16 0.21 0.1 0.41 0.031 0.8 −0.14 0.27
M12A 0.031 0.8 −0.18 0.14 −0.043 0.73 −0.29 0.016 −0.28 0.022 −0.17 0.16 0.12 0.34 −0.084 0.5 −0.32 0.0086 0.087 0.48 −0.009 0.94 0.18 0.14 1 0 0.21 0.087 −0.13 0.28 −0.099 0.42 0.34 0.0047 −0.062 0.62 −0.19 0.12
M5A 0.047 0.7 −0.41 0.00059 −0.2 0.11 −0.22 0.079 −0.11 0.38 −0.3 0.015 −0.17 0.16 −0.14 0.27 −0.13 0.3 −0.029 0.82 −0.063 0.61 0.15 0.21 0.21 0.087 1 0 0.52 5.7e−06 0.029 0.82 0.39 0.0011 0.12 0.34 −0.059 0.64
M4A −0.026 0.83 −0.15 0.24 0.13 0.31 0.2 0.1 −0.088 0.48 −0.055 0.66 −0.22 0.075 −0.16 0.19 0.23 0.064 −0.18 0.15 −0.12 0.34 −0.011 0.93 −0.13 0.28 0.52 5.7e−06 1 0 −0.035 0.78 −0.1 0.42 −0.037 0.76 −0.21 0.094
M9A 0.1 0.4 −0.37 0.0023 −0.59 1.8e−07 −0.26 0.033 −0.18 0.15 −0.42 0.00037 −0.48 4.1e−05 0.071 0.57 −0.16 0.18 0.00074 1 −0.16 0.18 −0.16 0.21 −0.099 0.42 0.029 0.82 −0.035 0.78 1 0 0.36 0.003 0.14 0.26 0.11 0.38
M15A 0.072 0.56 −0.59 1.9e−07 −0.47 5.3e−05 −0.51 1e−05 −0.12 0.32 −0.38 0.0016 −0.012 0.92 −0.056 0.65 −0.58 2.6e−07 −0.032 0.8 −0.31 0.011 0.1 0.41 0.34 0.0047 0.39 0.0011 −0.1 0.42 0.36 0.003 1 0 0.38 0.0013 0.018 0.89
M11A 0.084 0.5 −0.37 0.0018 −0.075 0.55 0.21 0.09 −0.17 0.18 −0.28 0.022 −0.12 0.34 −0.16 0.18 −0.097 0.44 −0.2 0.11 −0.23 0.061 0.031 0.8 −0.062 0.62 0.12 0.34 −0.037 0.76 0.14 0.26 0.38 0.0013 1 0 0.4 0.00092
M3 0.083 0.51 −0.043 0.73 −0.24 0.052 0.1 0.4 −0.074 0.55 −0.026 0.84 0.018 0.88 0.18 0.14 0.11 0.39 0.12 0.32 0.054 0.66 −0.14 0.27 −0.19 0.12 −0.059 0.64 −0.21 0.094 0.11 0.38 0.018 0.89 0.4 0.00092 1 0
M2 M7A M10A M14A M1A M13A M8A M18A M16A M17A M6A M19A M12A M5A M4A M9A M15A M11A M3

Figure S6B

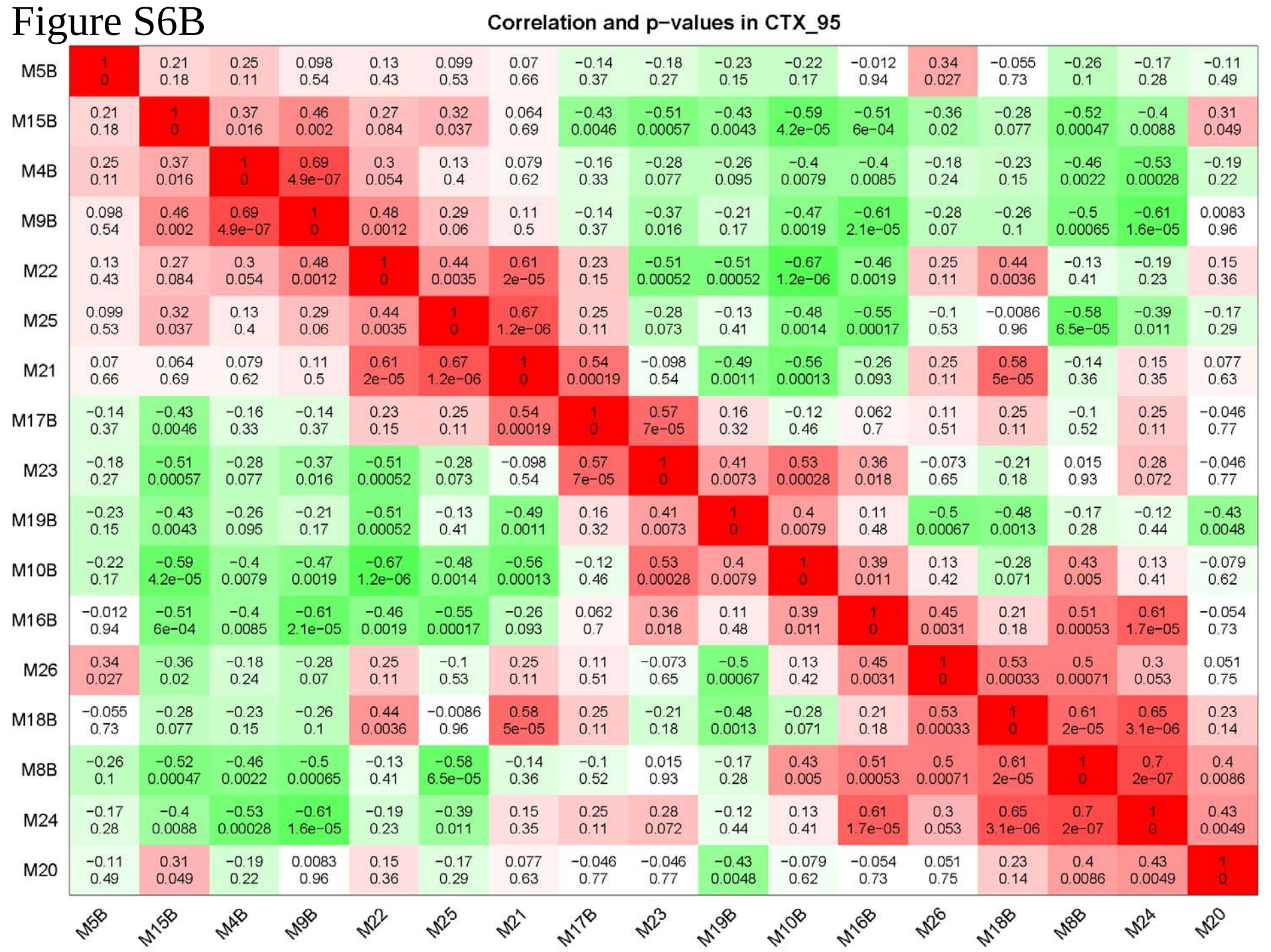
Correlation and p−values in CTX_95
M5B 1 0 0.21 0.18 0.25 0.11 0.098 0.54 0.13 0.43 0.099 0.53 0.07 0.66 −0.14 0.37 −0.18 0.27 −0.23 0.15 −0.22 0.17 −0.012 0.94 0.34 0.027 −0.055 0.73 −0.26 0.1 −0.17 0.28 −0.11 0.49
M15B 0.21 0.18 1 0 0.37 0.016 0.46 0.002 0.27 0.084 0.32 0.037 0.064 0.69 −0.43 0.0046 −0.51 0.00057 −0.43 0.0043 −0.59 4.2e−05 −0.51 6e−04 −0.36 0.02 −0.28 0.077 −0.52 0.00047 −0.4 0.0088 0.31 0.049
M4B 0.25 0.11 0.37 0.016 1 0 0.69 4.9e−07 0.3 0.054 0.13 0.4 0.079 0.62 −0.16 0.33 −0.28 0.077 −0.26 0.095 −0.4 0.0079 −0.4 0.0085 −0.18 0.24 −0.23 0.15 −0.46 0.0022 −0.53 0.00028 −0.19 0.22
M9B 0.098 0.54 0.46 0.002 0.69 4.9e−07 1 0 0.48 0.0012 0.29 0.06 0.11 0.5 −0.14 0.37 −0.37 0.016 −0.21 0.17 −0.47 0.0019 −0.61 2.1e−05 −0.28 0.07 −0.26 0.1 −0.5 0.00065 −0.61 1.6e−05 0.0083 0.96
M22 0.13 0.43 0.27 0.084 0.3 0.054 0.48 0.0012 1 0 0.44 0.0035 0.61 2e−05 0.23 0.15 −0.51 0.00052 −0.51 0.00052 −0.67 1.2e−06 −0.46 0.0019 0.25 0.11 0.44 0.0036 −0.13 0.41 −0.19 0.23 0.15 0.36
M25 0.099 0.53 0.32 0.037 0.13 0.4 0.29 0.06 0.44 0.0035 1 0 0.67 1.2e−06 0.25 0.11 −0.28 0.073 −0.13 0.41 −0.48 0.0014 −0.55 0.00017 −0.1 0.53 −0.0086 0.96 −0.58 6.5e−05 −0.39 0.011 −0.17 0.29
M21 0.07 0.66 0.064 0.69 0.079 0.62 0.11 0.5 0.61 2e−05 0.67 1.2e−06 1 0 0.54 0.00019 −0.098 0.54 −0.49 0.0011 −0.56 0.00013 −0.26 0.093 0.25 0.11 0.58 5e−05 −0.14 0.36 0.15 0.35 0.077 0.63
M17B −0.14 0.37 −0.43 0.0046 −0.16 0.33 −0.14 0.37 0.23 0.15 0.25 0.11 0.54 0.00019 1 0 0.57 7e−05 0.16 0.32 −0.12 0.46 0.062 0.7 0.11 0.51 0.25 0.11 −0.1 0.52 0.25 0.11 −0.046 0.77
M23 −0.18 0.27 −0.51 0.00057 −0.28 0.077 −0.37 0.016 −0.51 0.00052 −0.28 0.073 −0.098 0.54 0.57 7e−05 1 0 0.41 0.0073 0.53 0.00028 0.36 0.018 −0.073 0.65 −0.21 0.18 0.015 0.93 0.28 0.072 −0.046 0.77
M19B −0.23 0.15 −0.43 0.0043 −0.26 0.095 −0.21 0.17 −0.51 0.00052 −0.13 0.41 −0.49 0.0011 0.16 0.32 0.41 0.0073 1 0 0.4 0.0079 0.11 0.48 −0.5 0.00067 −0.48 0.0013 −0.17 0.28 −0.12 0.44 −0.43 0.0048
M10B −0.22 0.17 −0.59 4.2e−05 −0.4 0.0079 −0.47 0.0019 −0.67 1.2e−06 −0.48 0.0014 −0.56 0.00013 −0.12 0.46 0.53 0.00028 0.4 0.0079 1 0 0.39 0.011 0.13 0.42 −0.28 0.071 0.43 0.005 0.13 0.41 −0.079 0.62
M16B −0.012 0.94 −0.51 6e−04 −0.4 0.0085 −0.61 2.1e−05 −0.46 0.0019 −0.55 0.00017 −0.26 0.093 0.062 0.7 0.36 0.018 0.11 0.48 0.39 0.011 1 0 0.45 0.0031 0.21 0.18 0.51 0.00053 0.61 1.7e−05 −0.054 0.73
M26 0.34 0.027 −0.36 0.02 −0.18 0.24 −0.28 0.07 0.25 0.11 −0.1 0.53 0.25 0.11 0.11 0.51 −0.073 0.65 −0.5 0.00067 0.13 0.42 0.45 0.0031 1 0 0.53 0.00033 0.5 0.00071 0.3 0.053 0.051 0.75
M18B −0.055 0.73 −0.28 0.077 −0.23 0.15 −0.26 0.1 0.44 0.0036 −0.0086 0.96 0.58 5e−05 0.25 0.11 −0.21 0.18 −0.48 0.0013 −0.28 0.071 0.21 0.18 0.53 0.00033 1 0 0.61 2e−05 0.65 3.1e−06 0.23 0.14
M8B −0.26 0.1 −0.52 0.00047 −0.46 0.0022 −0.5 0.00065 −0.13 0.41 −0.58 6.5e−05 −0.14 0.36 −0.1 0.52 0.015 0.93 −0.17 0.28 0.43 0.005 0.51 0.00053 0.5 0.00071 0.61 2e−05 1 0 0.7 2e−07 0.4 0.0086
M24 −0.17 0.28 −0.4 0.0088 −0.53 0.00028 −0.61 1.6e−05 −0.19 0.23 −0.39 0.011 0.15 0.35 0.25 0.11 0.28 0.072 −0.12 0.44 0.13 0.41 0.61 1.7e−05 0.3 0.053 0.65 3.1e−06 0.7 2e−07 1 0 0.43 0.0049
M20 −0.11 0.49 0.31 0.049 −0.19 0.22 0.0083 0.96 0.15 0.36 −0.17 0.29 0.077 0.63 −0.046 0.77 −0.046 0.77 −0.43 0.0048 −0.079 0.62 −0.054 0.73 0.051 0.75 0.23 0.14 0.4 0.0086 0.43 0.0049 1 0
M5B M15B M4B M9B M22 M25 M21 M17B M23 M19B M10B M16B M26 M18B M8B M24 M20

Figure S6C

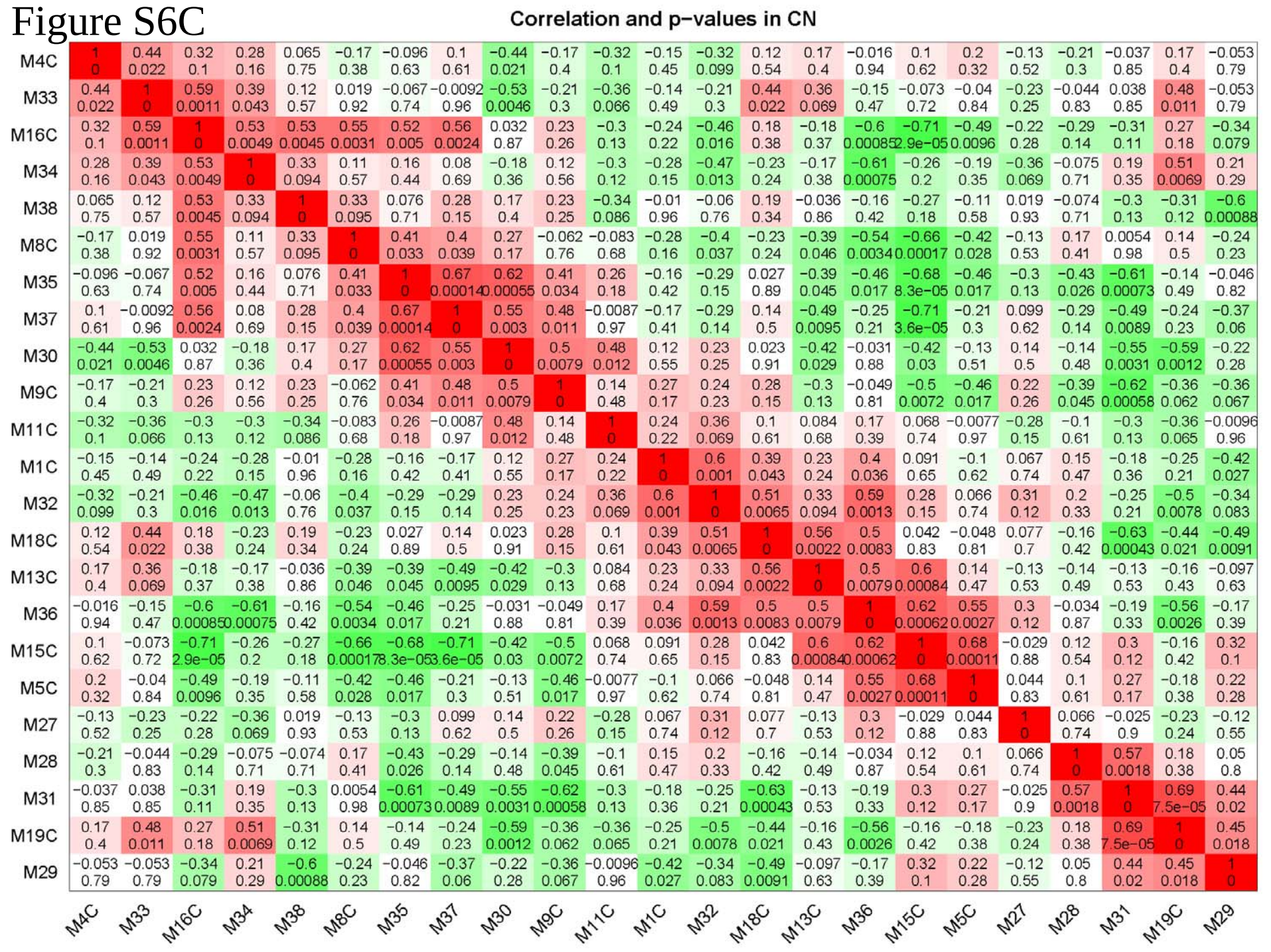
Correlation and p−values in CN
M4C 1 0 0.44 0.022 0.32 0.1 0.28 0.16 0.065 0.75 −0.17 0.38 −0.096 0.63 0.1 0.61 −0.44 0.021 −0.17 0.4 −0.32 0.1 −0.15 0.45 −0.32 0.099 0.12 0.54 0.17 0.4 −0.016 0.94 0.1 0.62 0.2 0.32 −0.13 0.52 −0.21 0.3 −0.037 0.85 0.17 0.4 −0.053 0.79
M33 0.44 0.022 1 0 0.59 0.0011 0.39 0.043 0.12 0.57 0.019 0.92 −0.067 0.74 −0.0092 0.96 −0.53 0.0046 −0.21 0.3 −0.36 0.066 −0.14 0.49 −0.21 0.3 0.44 0.022 0.36 0.069 −0.15 0.47 −0.073 0.72 −0.04 0.84 −0.23 0.25 −0.044 0.83 0.038 0.85 0.48 0.011 −0.053 0.79
M16C 0.32 0.1 0.59 0.0011 1 0 0.53 0.0049 0.53 0.0045 0.55 0.0031 0.52 0.005 0.56 0.0024 0.032 0.87 0.23 0.26 −0.3 0.13 −0.24 0.22 −0.46 0.016 0.18 0.38 −0.18 0.37 −0.6 0.00085 −0.71 2.9e−05 −0.49 0.0096 −0.22 0.28 −0.29 0.14 −0.31 0.11 0.27 0.18 −0.34 0.079
M34 0.28 0.16 0.39 0.043 0.53 0.0049 1 0 0.33 0.094 0.11 0.57 0.16 0.44 0.08 0.69 −0.18 0.36 0.12 0.56 −0.3 0.12 −0.28 0.15 −0.47 0.013 −0.23 0.24 −0.17 0.38 −0.61 0.00075 −0.26 0.2 −0.19 0.35 −0.36 0.069 −0.075 0.71 0.19 0.35 0.51 0.0069 0.21 0.29
M38 0.065 0.75 0.12 0.57 0.53 0.0045 0.33 0.094 1 0 0.33 0.095 0.076 0.71 0.28 0.15 0.17 0.4 0.23 0.25 −0.34 0.086 −0.01 0.96 −0.06 0.76 0.19 0.34 −0.036 0.86 −0.16 0.42 −0.27 0.18 −0.11 0.58 0.019 0.93 −0.074 0.71 −0.3 0.13 −0.31 0.12 −0.6 0.00088
M8C −0.17 0.38 0.019 0.92 0.55 0.0031 0.11 0.57 0.33 0.095 1 0 0.41 0.033 0.4 0.039 0.27 0.17 −0.062 0.76 −0.083 0.68 −0.28 0.16 −0.4 0.037 −0.23 0.24 −0.39 0.046 −0.54 0.0034 −0.66 0.00017 −0.42 0.028 −0.13 0.53 0.17 0.41 0.0054 0.98 0.14 0.5 −0.24 0.23
M35 −0.096 0.63 −0.067 0.74 0.52 0.005 0.16 0.44 0.076 0.71 0.41 0.033 1 0 0.67 0.00014 0.62 0.00055 0.41 0.034 0.26 0.18 −0.16 0.42 −0.29 0.15 0.027 0.89 −0.39 0.045 −0.46 0.017 −0.68 8.3e−05 −0.46 0.017 −0.3 0.13 −0.43 0.026 −0.61 0.00073 −0.14 0.49 −0.046 0.82
M37 0.1 0.61 −0.0092 0.96 0.56 0.0024 0.08 0.69 0.28 0.15 0.4 0.039 0.67 0.00014 1 0 0.55 0.003 0.48 0.011 −0.0087 0.97 −0.17 0.41 −0.29 0.14 0.14 0.5 −0.49 0.0095 −0.25 0.21 −0.71 3.6e−05 −0.21 0.3 0.099 0.62 −0.29 0.14 −0.49 0.0089 −0.24 0.23 −0.37 0.06
M30 −0.44 0.021 −0.53 0.0046 0.032 0.87 −0.18 0.36 0.17 0.4 0.27 0.17 0.62 0.00055 0.55 0.003 1 0 0.5 0.0079 0.48 0.012 0.12 0.55 0.23 0.25 0.023 0.91 −0.42 0.029 −0.031 0.88 −0.42 0.03 −0.13 0.51 0.14 0.5 −0.14 0.48 −0.55 0.0031 −0.59 0.0012 −0.22 0.28
M9C −0.17 0.4 −0.21 0.3 0.23 0.26 0.12 0.56 0.23 0.25 −0.062 0.76 0.41 0.034 0.48 0.011 0.5 0.0079 1 0 0.14 0.48 0.27 0.17 0.24 0.23 0.28 0.15 −0.3 0.13 −0.049 0.81 −0.5 0.0072 −0.46 0.017 0.22 0.26 −0.39 0.045 −0.62 0.00058 −0.36 0.062 −0.36 0.067
M11C −0.32 0.1 −0.36 0.066 −0.3 0.13 −0.3 0.12 −0.34 0.086 −0.083 0.68 0.26 0.18 −0.0087 0.97 0.48 0.012 0.14 0.48 1 0 0.24 0.22 0.36 0.069 0.1 0.61 0.084 0.68 0.17 0.39 0.068 0.74 −0.0077 0.97 −0.28 0.15 −0.1 0.61 −0.3 0.13 −0.36 0.065 −0.0096 0.96
M1C −0.15 0.45 −0.14 0.49 −0.24 0.22 −0.28 0.15 −0.01 0.96 −0.28 0.16 −0.16 0.42 −0.17 0.41 0.12 0.55 0.27 0.17 0.24 0.22 1 0 0.6 0.001 0.39 0.043 0.23 0.24 0.4 0.036 0.091 0.65 −0.1 0.62 0.067 0.74 0.15 0.47 −0.18 0.36 −0.25 0.21 −0.42 0.027
M32 −0.32 0.099 −0.21 0.3 −0.46 0.016 −0.47 0.013 −0.06 0.76 −0.4 0.037 −0.29 0.15 −0.29 0.14 0.23 0.25 0.24 0.23 0.36 0.069 0.6 0.001 1 0 0.51 0.0065 0.33 0.094 0.59 0.0013 0.28 0.15 0.066 0.74 0.31 0.12 0.2 0.33 −0.25 0.21 −0.5 0.0078 −0.34 0.083
M18C 0.12 0.54 0.44 0.022 0.18 0.38 −0.23 0.24 0.19 0.34 −0.23 0.24 0.027 0.89 0.14 0.5 0.023 0.91 0.28 0.15 0.1 0.61 0.39 0.043 0.51 0.0065 1 0 0.56 0.0022 0.5 0.0083 0.042 0.83 −0.048 0.81 0.077 0.7 −0.16 0.42 −0.63 0.00043 −0.44 0.021 −0.49 0.0091
M13C 0.17 0.4 0.36 0.069 −0.18 0.37 −0.17 0.38 −0.036 0.86 −0.39 0.046 −0.39 0.045 −0.49 0.0095 −0.42 0.029 −0.3 0.13 0.084 0.68 0.23 0.24 0.33 0.094 0.56 0.0022 1 0 0.5 0.0079 0.6 0.00084 0.14 0.47 −0.13 0.53 −0.14 0.49 −0.13 0.53 −0.16 0.43 −0.097 0.63
M36 −0.016 0.94 −0.15 0.47 −0.6 0.00085 −0.61 0.00075 −0.16 0.42 −0.54 0.0034 −0.46 0.017 −0.25 0.21 −0.031 0.88 −0.049 0.81 0.17 0.39 0.4 0.036 0.59 0.0013 0.5 0.0083 0.5 0.0079 1 0 0.62 0.00062 0.55 0.0027 0.3 0.12 −0.034 0.87 −0.19 0.33 −0.56 0.0026 −0.17 0.39
M15C 0.1 0.62 −0.073 0.72 −0.71 2.9e−05 −0.26 0.2 −0.27 0.18 −0.66 0.00017 −0.68 8.3e−05 −0.71 3.6e−05 −0.42 0.03 −0.5 0.0072 0.068 0.74 0.091 0.65 0.28 0.15 0.042 0.83 0.6 0.00084 0.62 0.00062 1 0 0.68 0.00011 −0.029 0.88 0.12 0.54 0.3 0.12 −0.16 0.42 0.32 0.1
M5C 0.2 0.32 −0.04 0.84 −0.49 0.0096 −0.19 0.35 −0.11 0.58 −0.42 0.028 −0.46 0.017 −0.21 0.3 −0.13 0.51 −0.46 0.017 −0.0077 0.97 −0.1 0.62 0.066 0.74 −0.048 0.81 0.14 0.47 0.55 0.0027 0.68 0.00011 1 0 0.044 0.83 0.1 0.61 0.27 0.17 −0.18 0.38 0.22 0.28
M27 −0.13 0.52 −0.23 0.25 −0.22 0.28 −0.36 0.069 0.019 0.93 −0.13 0.53 −0.3 0.13 0.099 0.62 0.14 0.5 0.22 0.26 −0.28 0.15 0.067 0.74 0.31 0.12 0.077 0.7 −0.13 0.53 0.3 0.12 −0.029 0.88 0.044 0.83 1 0 0.066 0.74 −0.025 0.9 −0.23 0.24 −0.12 0.55
M28 −0.21 0.3 −0.044 0.83 −0.29 0.14 −0.075 0.71 −0.074 0.71 0.17 0.41 −0.43 0.026 −0.29 0.14 −0.14 0.48 −0.39 0.045 −0.1 0.61 0.15 0.47 0.2 0.33 −0.16 0.42 −0.14 0.49 −0.034 0.87 0.12 0.54 0.1 0.61 0.066 0.74 1 0 0.57 0.0018 0.18 0.38 0.05 0.8
M31 −0.037 0.85 0.038 0.85 −0.31 0.11 0.19 0.35 −0.3 0.13 0.0054 0.98 −0.61 0.00073 −0.49 0.0089 −0.55 0.0031 −0.62 0.00058 −0.3 0.13 −0.18 0.36 −0.25 0.21 −0.63 0.00043 −0.13 0.53 −0.19 0.33 0.3 0.12 0.27 0.17 −0.025 0.9 0.57 0.0018 1 0 0.69 7.5e−05 0.44 0.02
M19C 0.17 0.4 0.48 0.011 0.27 0.18 0.51 0.0069 −0.31 0.12 0.14 0.5 −0.14 0.49 −0.24 0.23 −0.59 0.0012 −0.36 0.062 −0.36 0.065 −0.25 0.21 −0.5 0.0078 −0.44 0.021 −0.16 0.43 −0.56 0.0026 −0.16 0.42 −0.18 0.38 −0.23 0.24 0.18 0.38 0.69 7.5e−05 1 0 0.45 0.018
M29 −0.053 0.79 −0.053 0.79 −0.34 0.079 0.21 0.29 −0.6 0.00088 −0.24 0.23 −0.046 0.82 −0.37 0.06 −0.22 0.28 −0.36 0.067 −0.0096 0.96 −0.42 0.027 −0.34 0.083 −0.49 0.0091 −0.097 0.63 −0.17 0.39 0.32 0.1 0.22 0.28 −0.12 0.55 0.05 0.8 0.44 0.02 0.45 0.018 1 0
M4C M33 M16C M34 M38 M8C M35 M37 M30 M9C M11C M1C M32 M18C M13C M36 M15C M5C M27 M28 M31 M19C M29

Figure S6D

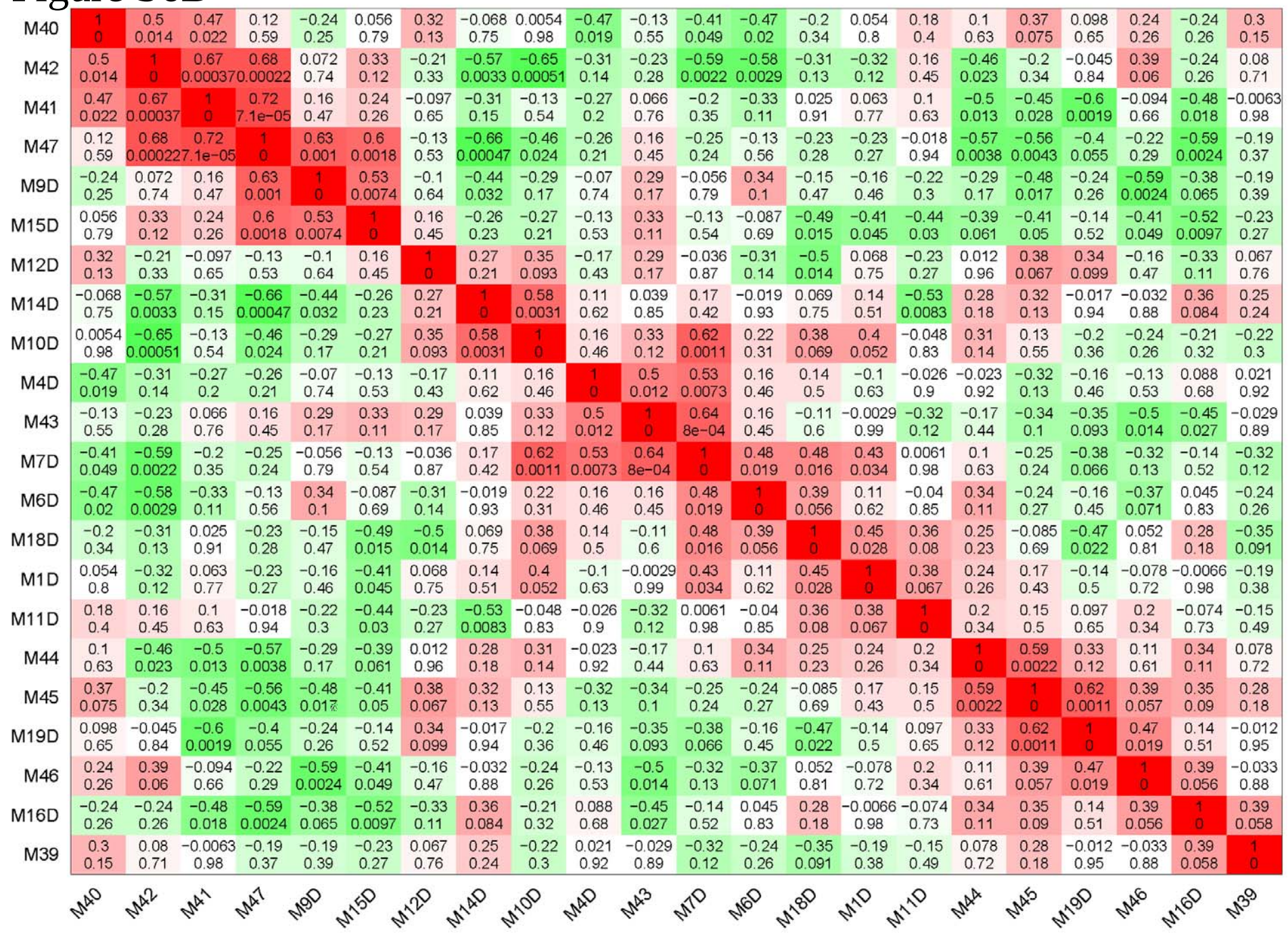
Correlation and p−values in CB
M40 1 0 0.5 0.014 0.47 0.022 0.12 0.59 −0.24 0.25 0.056 0.79 0.32 0.13 −0.068 0.75 0.0054 0.98 −0.47 0.019 −0.13 0.55 −0.41 0.049 −0.47 0.02 −0.2 0.34 0.054 0.8 0.18 0.4 0.1 0.63 0.37 0.075 0.098 0.65 0.24 0.26 −0.24 0.26 0.3 0.15
M42 0.5 0.014 1 0 0.67 0.00037 0.68 0.00022 0.072 0.74 0.33 0.12 −0.21 0.33 −0.57 0.0033 −0.65 0.00051 −0.31 0.14 −0.23 0.28 −0.59 0.0022 −0.58 0.0029 −0.31 0.13 −0.32 0.12 0.16 0.45 −0.46 0.023 −0.2 0.34 −0.045 0.84 0.39 0.06 −0.24 0.26 0.08 0.71
M41 0.47 0.022 0.67 0.00037 1 0 0.72 7.1e−05 0.16 0.47 0.24 0.26 −0.097 0.65 −0.31 0.15 −0.13 0.54 −0.27 0.2 0.066 0.76 −0.2 0.35 −0.33 0.11 0.025 0.91 0.063 0.77 0.1 0.63 −0.5 0.013 −0.45 0.028 −0.6 0.0019 −0.094 0.66 −0.48 0.018 −0.0063 0.98
M47 0.12 0.59 0.68 0.00022 0.72 7.1e−05 1 0 0.63 0.001 0.6 0.0018 −0.13 0.53 −0.66 0.00047 −0.46 0.024 −0.26 0.21 0.16 0.45 −0.25 0.24 −0.13 0.56 −0.23 0.28 −0.23 0.27 −0.018 0.94 −0.57 0.0038 −0.56 0.0043 −0.4 0.055 −0.22 0.29 −0.59 0.0024 −0.19 0.37
M9D −0.24 0.25 0.072 0.74 0.16 0.47 0.63 0.001 1 0 0.53 0.0074 −0.1 0.64 −0.44 0.032 −0.29 0.17 −0.07 0.74 0.29 0.17 −0.056 0.79 0.34 0.1 −0.15 0.47 −0.16 0.46 −0.22 0.3 −0.29 0.17 −0.48 0.017 −0.24 0.26 −0.59 0.0024 −0.38 0.065 −0.19 0.39
M15D 0.056 0.79 0.33 0.12 0.24 0.26 0.6 0.0018 0.53 0.0074 1 0 0.16 0.45 −0.26 0.23 −0.27 0.21 −0.13 0.53 0.33 0.11 −0.13 0.54 −0.087 0.69 −0.49 0.015 −0.41 0.045 −0.44 0.03 −0.39 0.061 −0.41 0.05 −0.14 0.52 −0.41 0.049 −0.52 0.0097 −0.23 0.27
M12D 0.32 0.13 −0.21 0.33 −0.097 0.65 −0.13 0.53 −0.1 0.64 0.16 0.45 1 0 0.27 0.21 0.35 0.093 −0.17 0.43 0.29 0.17 −0.036 0.87 −0.31 0.14 −0.5 0.014 0.068 0.75 −0.23 0.27 0.012 0.96 0.38 0.067 0.34 0.099 −0.16 0.47 −0.33 0.11 0.067 0.76
M14D −0.068 0.75 −0.57 0.0033 −0.31 0.15 −0.66 0.00047 −0.44 0.032 −0.26 0.23 0.27 0.21 1 0 0.58 0.0031 0.11 0.62 0.039 0.85 0.17 0.42 −0.019 0.93 0.069 0.75 0.14 0.51 −0.53 0.0083 0.28 0.18 0.32 0.13 −0.017 0.94 −0.032 0.88 0.36 0.084 0.25 0.24
M10D 0.0054 0.98 −0.65 0.00051 −0.13 0.54 −0.46 0.024 −0.29 0.17 −0.27 0.21 0.35 0.093 0.58 0.0031 1 0 0.16 0.46 0.33 0.12 0.62 0.0011 0.22 0.31 0.38 0.069 0.4 0.052 −0.048 0.83 0.31 0.14 0.13 0.55 −0.2 0.36 −0.24 0.26 −0.21 0.32 −0.22 0.3
M4D −0.47 0.019 −0.31 0.14 −0.27 0.2 −0.26 0.21 −0.07 0.74 −0.13 0.53 −0.17 0.43 0.11 0.62 0.16 0.46 1 0 0.5 0.012 0.53 0.0073 0.16 0.46 0.14 0.5 −0.1 0.63 −0.026 0.9 −0.023 0.92 −0.32 0.13 −0.16 0.46 −0.13 0.53 0.088 0.68 0.021 0.92
M43 −0.13 0.55 −0.23 0.28 0.066 0.76 0.16 0.45 0.29 0.17 0.33 0.11 0.29 0.17 0.039 0.85 0.33 0.12 0.5 0.012 1 0 0.64 8e−04 0.16 0.45 −0.11 0.6 −0.0029 0.99 −0.32 0.12 −0.17 0.44 −0.34 0.1 −0.35 0.093 −0.5 0.014 −0.45 0.027 −0.029 0.89
M7D −0.41 0.049 −0.59 0.0022 −0.2 0.35 −0.25 0.24 −0.056 0.79 −0.13 0.54 −0.036 0.87 0.17 0.42 0.62 0.0011 0.53 0.0073 0.64 8e−04 1 0 0.48 0.019 0.48 0.016 0.43 0.034 0.0061 0.98 0.1 0.63 −0.25 0.24 −0.38 0.066 −0.32 0.13 −0.14 0.52 −0.32 0.12
M6D −0.47 0.02 −0.58 0.0029 −0.33 0.11 −0.13 0.56 0.34 0.1 −0.087 0.69 −0.31 0.14 −0.019 0.93 0.22 0.31 0.16 0.46 0.16 0.45 0.48 0.019 1 0 0.39 0.056 0.11 0.62 −0.04 0.85 0.34 0.11 −0.24 0.27 −0.16 0.45 −0.37 0.071 0.045 0.83 −0.24 0.26
M18D −0.2 0.34 −0.31 0.13 0.025 0.91 −0.23 0.28 −0.15 0.47 −0.49 0.015 −0.5 0.014 0.069 0.75 0.38 0.069 0.14 0.5 −0.11 0.6 0.48 0.016 0.39 0.056 1 0 0.45 0.028 0.36 0.08 0.25 0.23 −0.085 0.69 −0.47 0.022 0.052 0.81 0.28 0.18 −0.35 0.091
M1D 0.054 0.8 −0.32 0.12 0.063 0.77 −0.23 0.27 −0.16 0.46 −0.41 0.045 0.068 0.75 0.14 0.51 0.4 0.052 −0.1 0.63 −0.0029 0.99 0.43 0.034 0.11 0.62 0.45 0.028 1 0 0.38 0.067 0.24 0.26 0.17 0.43 −0.14 0.5 −0.078 0.72 −0.0066 0.98 −0.19 0.38
M11D 0.18 0.4 0.16 0.45 0.1 0.63 −0.018 0.94 −0.22 0.3 −0.44 0.03 −0.23 0.27 −0.53 0.0083 −0.048 0.83 −0.026 0.9 −0.32 0.12 0.0061 0.98 −0.04 0.85 0.36 0.08 0.38 0.067 1 0 0.2 0.34 0.15 0.5 0.097 0.65 0.2 0.34 −0.074 0.73 −0.15 0.49
M44 0.1 0.63 −0.46 0.023 −0.5 0.013 −0.57 0.0038 −0.29 0.17 −0.39 0.061 0.012 0.96 0.28 0.18 0.31 0.14 −0.023 0.92 −0.17 0.44 0.1 0.63 0.34 0.11 0.25 0.23 0.24 0.26 0.2 0.34 1 0 0.59 0.0022 0.33 0.12 0.11 0.61 0.34 0.11 0.078 0.72
M45 0.37 0.075 −0.2 0.34 −0.45 0.028 −0.56 0.0043 −0.48 0.017 −0.41 0.05 0.38 0.067 0.32 0.13 0.13 0.55 −0.32 0.13 −0.34 0.1 −0.25 0.24 −0.24 0.27 −0.085 0.69 0.17 0.43 0.15 0.5 0.59 0.0022 1 0 0.62 0.0011 0.39 0.057 0.35 0.09 0.28 0.18
M19D 0.098 0.65 −0.045 0.84 −0.6 0.0019 −0.4 0.055 −0.24 0.26 −0.14 0.52 0.34 0.099 −0.017 0.94 −0.2 0.36 −0.16 0.46 −0.35 0.093 −0.38 0.066 −0.16 0.45 −0.47 0.022 −0.14 0.5 0.097 0.65 0.33 0.12 0.62 0.0011 1 0 0.47 0.019 0.14 0.51 −0.012 0.95
M46 0.24 0.26 0.39 0.06 −0.094 0.66 −0.22 0.29 −0.59 0.0024 −0.41 0.049 −0.16 0.47 −0.032 0.88 −0.24 0.26 −0.13 0.53 −0.5 0.014 −0.32 0.13 −0.37 0.071 0.052 0.81 −0.078 0.72 0.2 0.34 0.11 0.61 0.39 0.057 0.47 0.019 1 0 0.39 0.056 −0.033 0.88
M16D −0.24 0.26 −0.24 0.26 −0.48 0.018 −0.59 0.0024 −0.38 0.065 −0.52 0.0097 −0.33 0.11 0.36 0.084 −0.21 0.32 0.088 0.68 −0.45 0.027 −0.14 0.52 0.045 0.83 0.28 0.18 −0.0066 0.98 −0.074 0.73 0.34 0.11 0.35 0.09 0.14 0.51 0.39 0.056 1 0 0.39 0.058
M39 0.3 0.15 0.08 0.71 −0.0063 0.98 −0.19 0.37 −0.19 0.39 −0.23 0.27 0.067 0.76 0.25 0.24 −0.22 0.3 0.021 0.92 −0.029 0.89 −0.32 0.12 −0.24 0.26 −0.35 0.091 −0.19 0.38 −0.15 0.49 0.078 0.72 0.28 0.18 −0.012 0.95 −0.033 0.88 0.39 0.058 1 0
M40 M42 M41 M47 M9D M15D M12D M14D M10D M4D M43 M7D M6D M18D M1D M11D M44 M45 M19D M46 M16D M39

Figure S6E

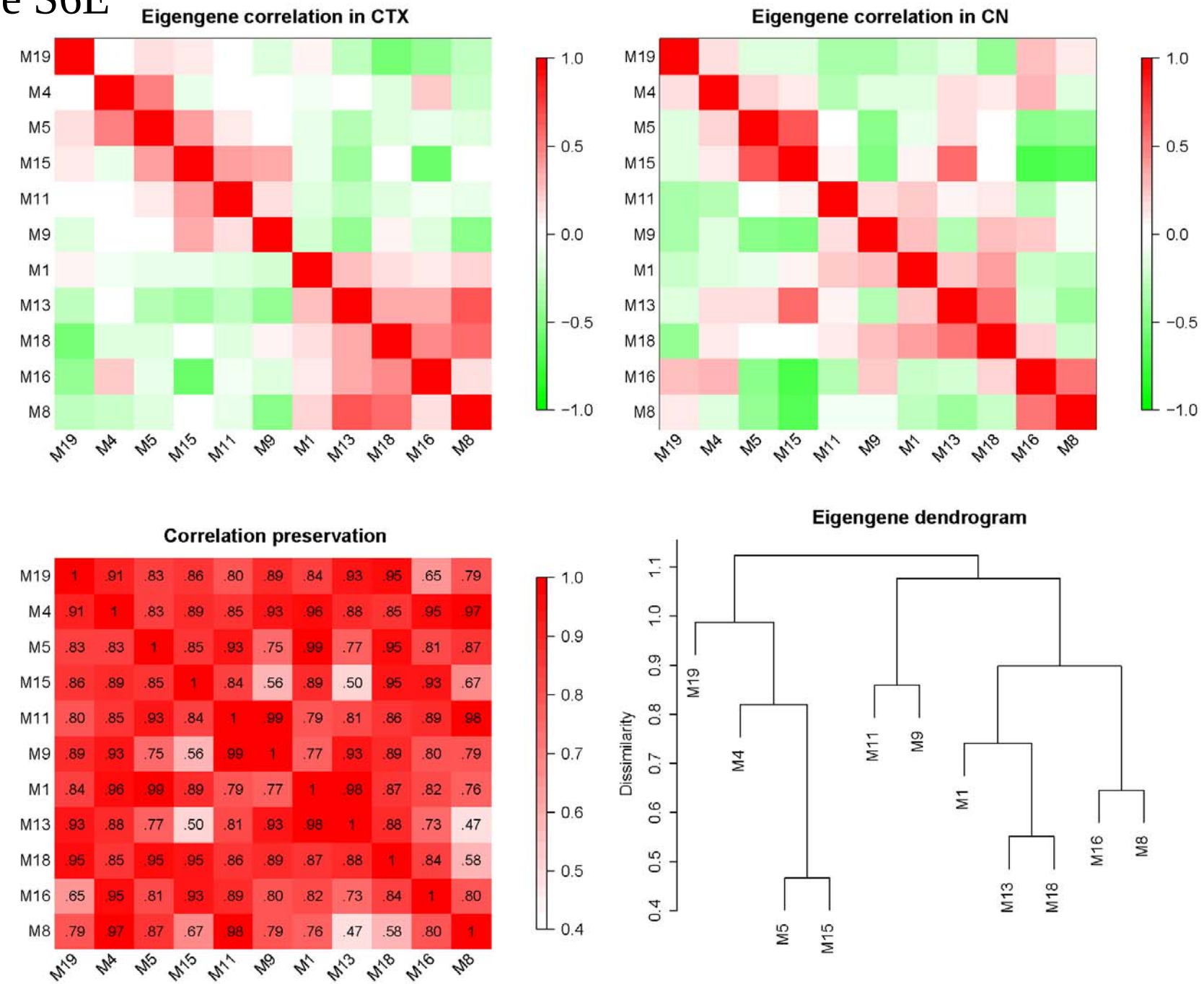
Eigengene correlation in CTX
Eigengene correlation in CN
Correlation preservation
Eigengene dendrogram
M19
M4
M5
M15
M11
M9
M1
M13
M18
M16
M8
1.0
0.5
0.0
−0.5
−1.0
Dissimilarity
0.4
0.5
0.6
0.7
0.8
0.9
1.0
1.1

Figure S6F

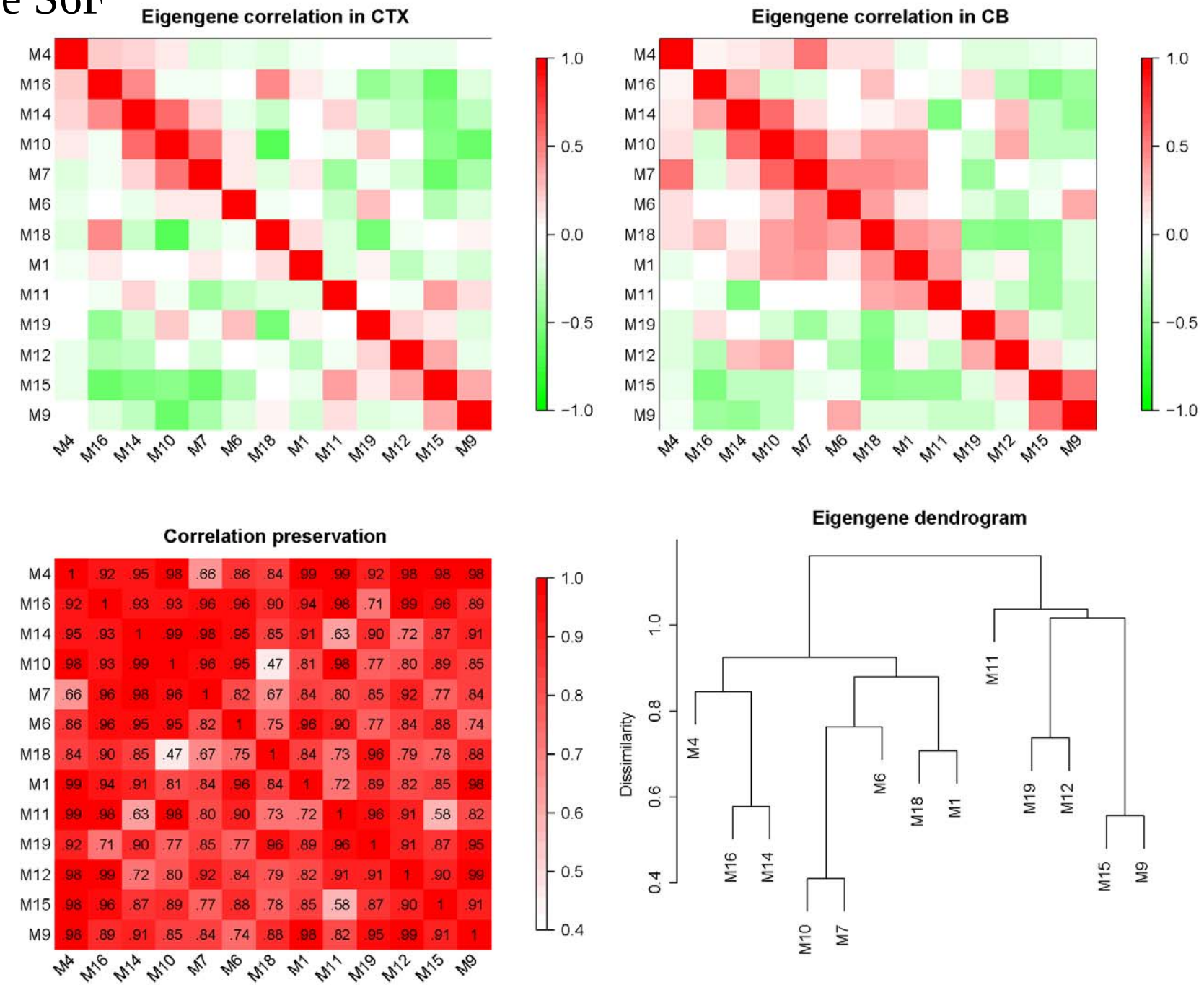
Eigengene correlation in CTX
Eigengene correlation in CB
Correlation preservation
Eigengene dendrogram
M4 M16 M14 M10 M7 M6 M18 M1 M11 M19 M12 M15 M9
1.0 0.5 0.0 −0.5 −1.0
1.0 0.9 0.8 0.7 0.6 0.5 0.4
Dissimilarity
0.4 0.6 0.8 1.0

Figure S6G

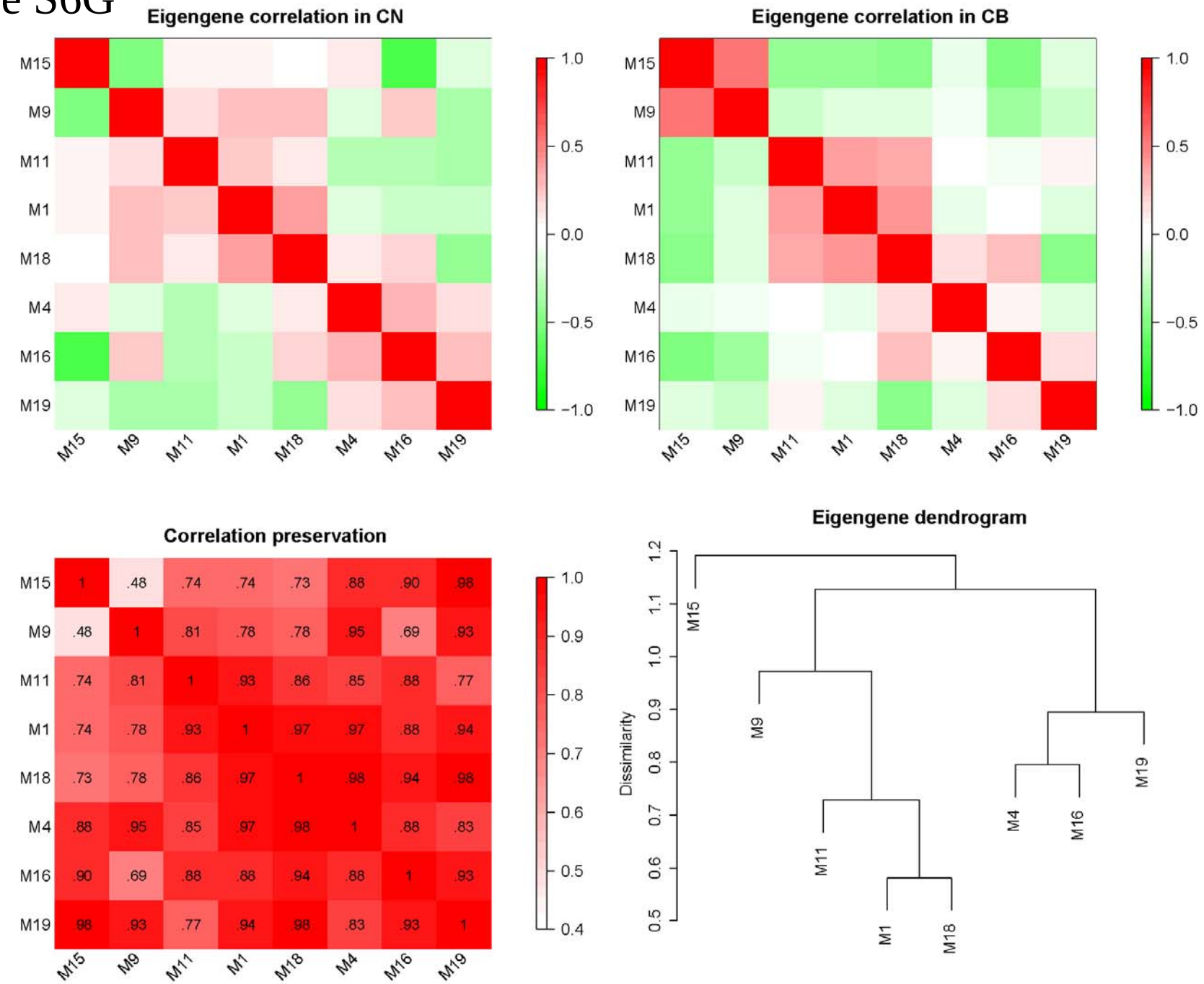
Eigengene correlation in CN
Eigengene correlation in CB
Correlation preservation
Eigengene dendrogram
M15
M9
M11
M1
M18
M4
M16
M19
1.0
0.5
0.0
−0.5
−1.0
Dissimilarity
1.2
1.1
1.0
0.9
0.8
0.7
0.6
0.5
0.4
1 .48 .74 .74 .73 .88 .90 .98
.48 1 .81 .78 .78 .95 .69 .93
.74 .81 1 .93 .86 .85 .88 .77
.74 .78 .93 1 .97 .97 .88 .94
.73 .78 .86 .97 1 .98 .94 .98
.88 .95 .85 .97 .98 1 .88 .83
.90 .69 .88 .88 .94 .88 1 .93
.98 .93 .77 .94 .98 .83 .93 1

"Functional Organization of the Transcriptome in Human Brain"

Michael C. Oldham, Steve Horvath, Genevieve Konopka, Kazuya Iwamoto, Peter Langfelder, Tadafumi Kato, and Daniel H. Geschwind

Nature Neuroscience

Supplementary Figure 7: Relationships between modules in cortical networks are highly reproducible

Heat maps depicting Pearson correlation matrices (PCMs) of module eigengenes (MEs) for modules found in both CTX (**a**) and CTX_95 (**b**). Red and green denote positive and negative correlations, respectively. MEs in each network were ordered to facilitate visual interpretation of the networks (Supplementary Methods). (**c**) Correlation preservation for each pair of MEs (1 = perfect preservation; Supplementary Methods). (**d**) Average linkage hierarchical clustering of MEs based on the average of the PCMs depicted in (**a**) and (**b**). Three main clusters were evident in the consensus dendrogram, corresponding to modules that were primarily glial, synaptic/membranal, or neuronal in nature.

Figure S7

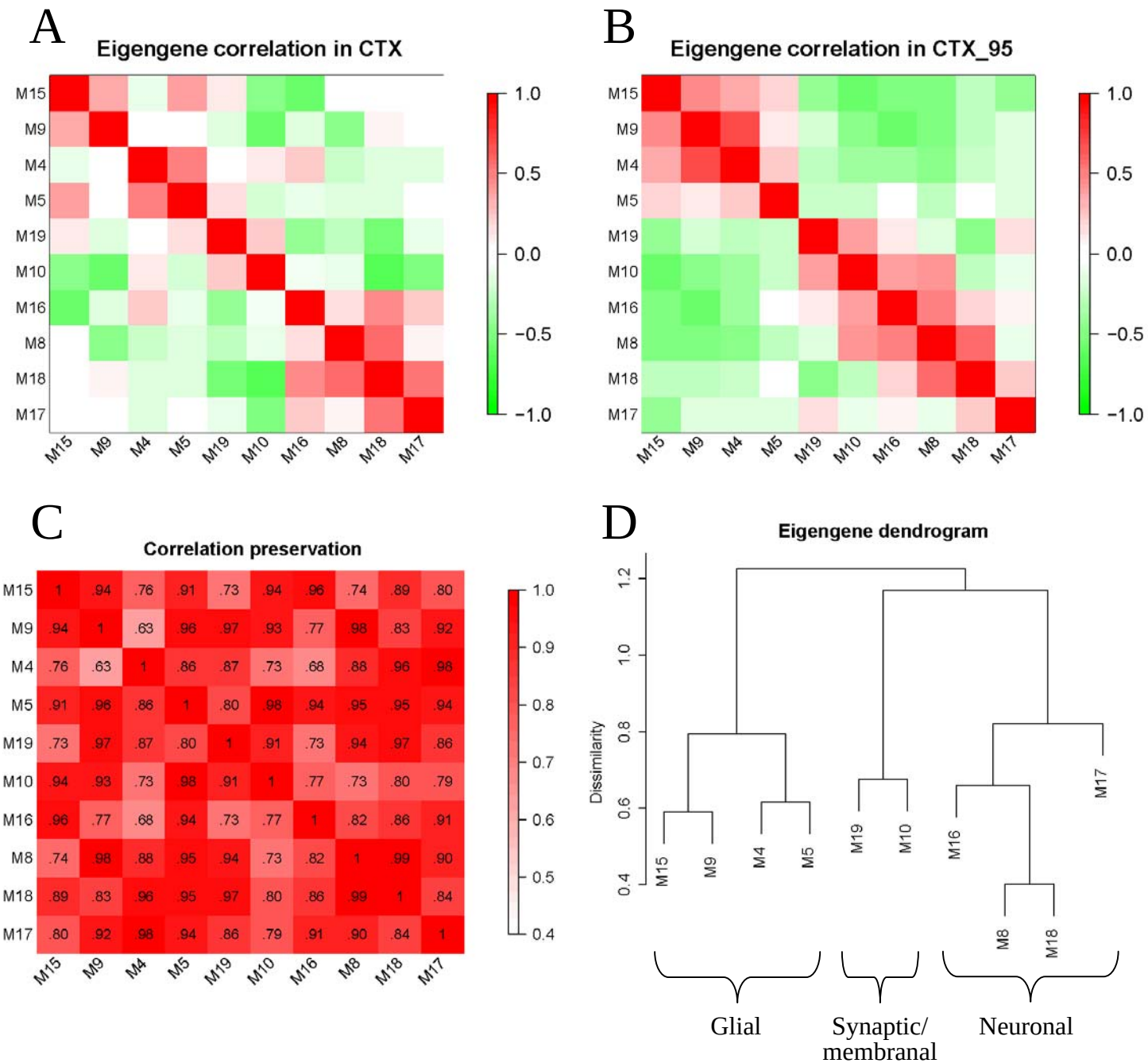
A
Eigengene correlation in CTX
M15
M9
M4
M5
M19
M10
M16
M8
M18
M17
1.0
0.5
0.0
−0.5
−1.0
B
Eigengene correlation in CTX_95
C
Correlation preservation
D
Eigengene dendrogram
Dissimilarity
0.4
0.6
0.8
1.0
1.2
Glial
Synaptic/
membranal
Neuronal

Supplementary Methods

Michael C. Oldham, Steve Horvath, Genevieve Konopka, Kazuya Iwamoto, Peter Langfelder, Tadafumi Kato, and Daniel H. Geschwind

"Functional Organization of the Transcriptome in Human Brain"

Term	Definition
Coexpression network	A coexpression network is defined as an undirected, weighted network in which nodes correspond to genes and edges are based upon the pairwise Pearson correlations between measured expression levels. Pearson correlations are weighted by raising their absolute value to a power (a process known as "soft thresholding"), thereby emphasizing strong correlations at the expense of weak correlations.
Topological overlap	Topological overlap (TO) is a quantity that describes the similarity of a pair of genes by comparing their weighted correlations with all other genes in the coexpression network. TO is converted to a measure of dissimilarity (1-TO) in order to identify modules of coexpressed genes via unsupervised hierarchical clustering.
Module	A module is a group of genes with high TO. Genes within a module have expression levels that are much more highly correlated (or anti-correlated) with each other than they are with genes outside the module.
Module eigengene	A module eigengene (ME) is defined as the first principal component of a given module. The ME summarizes the characteristic expression pattern of a module.
Module eigengene network	A module eigengene network (ME network) is defined as the Pearson correlation matrix for all of the MEs in a coexpression network. The ME network describes the higher-order structure of gene coexpression networks by quantifying relationships between modules.
Module membership	Module membership (MM) is defined as the Pearson correlation between the expression level of a given gene and a given ME. This quantity describes the extent to which a gene "belongs" to a module. When referencing individual genes in the text, a gene's rank |MM| (RMM) is reported.
Differential network analysis	Differential network analysis refers to the comparison of two or more gene coexpression networks. With this approach, genes are compared between groups not on the basis of mean expression levels, but rather on the strength of membership for identified modules.

Table 1: Glossary of WGCNA terminology.

Microarray data processing

Microarray data generated from control samples of human cerebral cortex, caudate nucleus, and cerebellum were gathered from nine published studies[1-9]. Four datasets were assembled. Gene coexpression analyses are particularly sensitive to the presence of outlier samples and systematic biases in microarray data. Therefore, rigorous quality control procedures were implemented to ensure the highest possible level of quality for each dataset. First, non-specific and mis-targeted microarray probes were masked prior to generating expression values[10]. Second, outlier samples were identified and removed from each dataset. Third, data were normalized to eliminate systematic biases introduced by combining data from different studies ("batch effects")[11].

Prior to removal of outlier and duplicate samples, dataset 1 ("CTX") consisted of 104 samples from various cortical areas[3,4,8], dataset 2 ("CTX_95") consisted of 82 samples from various cortical areas[1,2,5-7,9], dataset 3 ("CN") consisted of 32 samples from the head of the caudate nucleus[3], and dataset 4 ("CB") consisted of 27 samples from cerebellar hemisphere[3]. To eliminate non-specific and mis-targeted probes prior to generating expression values, mask files were obtained for both microarrays (http://masker.nci.nih.gov/ev/)[10] and applied to the raw data using GCOSv1.2 or the R package "ProbeFilter" (http://arrayanalysis.mbni.med.umich.edu/MBNIUM.html#ProbeFilter)[12]. After applying the mask files, only probe sets with at least seven (HG-U133A) or ten (HG-U95A/v2) remaining probes were retained for further analysis (n = 18,631 and n = 10,553, respectively).

Expression values for CTX, CN, and CB were generated using GCOSv1.2. All arrays were scaled to the same average intensity (200). For CTX_95, expression values were generated in R using the "expresso" function of the "affy" package (http://www.bioconductor.org/)[13] with "mas" settings and no normalization, followed by scaling of arrays to the same average intensity

(200). Scaled expression values were imported into R for outlier detection and removal prior to normalization. A detailed supplement containing all of the relevant R code and corresponding figure images that were used to guide our decisions to remove outlier samples in each of the four datasets analyzed in this study is available on our web page (http://www.genetics.ucla.edu/labs/horvath/CoexpressionNetwork/HumanBrainTranscriptome/). For each dataset, samples were correlated with one another using expression levels for all probe sets. These inter-array correlations (IACs) were averaged for each array and compared to the resulting distribution of IACs for the dataset. In general, samples with an average IAC < 2.0 standard deviations below the mean IAC for the dataset were removed. Samples were also hierarchically clustered using average linkage and 1-IAC as a distance metric to identify outliers. This process was repeated for each dataset until no outliers were evident. This approach constitutes an unbiased method for the identification and removal of samples with aberrant gene expression levels. In practice, such samples often possess long postmortem intervals or low pH values, which have been shown to alter the expression levels of certain classes of genes[14]. However, these variables are not perfect predictors of sample quality[15], and in many cases the underlying causes of aberrant gene expression levels are unknown. The number of samples identified as outliers in each dataset was as follows: 14 (CTX), 36 (CTX_95), 5 (CN), and 3 (CB). Following outlier removal, technical replicates were averaged (CTX_95). For CTX, additional samples were removed to account for the fact that many samples from refs. 4,8 were taken from the same individuals. 23 pairs of such samples were identified; for each pair, the sample with the lower average IAC was removed from the dataset. These samples were removed from CTX to ensure a 1:1 ratio of samples to unique individuals for this dataset, which was also the case for CN and CB. However, an interesting biological question concerns the extent to

which gene coexpression patterns are preserved across cortical areas within the same individual. It would have been difficult to interpret the extent of such preservation in CTX had these samples been retained, since a) each unique individual would have been represented by no more than two cortical areas, and b) the effect of regional variability would have been confounded by potential batch effects. However, the composition of the dataset from ref. 6 presented a tractable opportunity to explore this question in CTX_95, as each individual from this study was represented by six cortical areas.

Following outlier removal, quantile normalization[16] was performed for each dataset in R. Average linkage hierarchical clustering using 1-IAC as a distance metric revealed that most samples clustered by study (data not shown), indicating the presence of significant batch effects in the data. To eliminate batch effects, additional normalization was performed using the R package "ComBat" (http://statistics.byu.edu/johnson/ComBat/)[11] with default parameters. Within each dataset, each study was assigned a single batch number with the exception of ref. 3, which was assigned two batch numbers (samples from this study exhibited a batch effect that reflected country of origin [U.S. vs. New Zealand; data not shown]). ComBat successfully eliminated batch effects in each dataset as evidenced by hierarchical clustering and significant improvement of mean IAC (data not shown). Negative expression values introduced by ComBat (~0.01% of all expression values) were replaced with the median for the corresponding probe set.

Following microarray data processing, CTX consisted of 67 samples from 67 individuals representing four cortical areas (mean inter-array correlation [IAC] = 0.970), CTX_95 consisted of 42 samples from 32 individuals representing six cortical areas (mean IAC = 0.975), CN consisted of 27 samples from 27 individuals (mean IAC = 0.972), and CB consisted of 24 samples from 24 individuals (mean IAC = 0.975). Combined, these datasets comprised 160

samples from 106 individuals (CTX, CN, and CB samples from ref. 3 often represented the same individual). Additional sample information can be found in Supplementary Table 1.

Choice of genes for network analysis

For each dataset, WGCNA was performed on all expressed genes. (Note: although some genes are represented by multiple probe sets and other probe sets are not fully annotated, for consistency we refer to probe sets as "genes" throughout the journal article, unless otherwise noted.) A gene was considered expressed if it was called "present" or "marginal" in at least half of all samples in a given dataset. In CTX, a gene was also considered expressed if it was called present or marginal in at least three quarters of all samples from one cortical area. Finally, genes that were consistently called present or marginal in either males or females were also included in the analysis. Present/marginal/absent calls were determined using GCOSv1.2 (CTX, CN, and CB) or the "mas5calls" function (Bioconductor "affy" package) in R (CTX_95). The total number of expressed probe sets in each dataset was as follows: 10,865 (CTX), 5,392 (CTX_95), 9,363 (CN), and 9,714 (CB). These "brain-expressed" probe sets are indicated in the "BE" column of Supplementary Tables 3-6 (1 = expressed, 0 = not expressed).

Weighted gene coexpression network construction and module detection

Several alternative network approaches have been proposed for analyzing microarray data[17-23]. For example, graphical Gaussian models have been proposed for inferring gene association networks[24-27]. A comparison of these alternative methods is beyond the scope of this article, but will be important for future development of network approaches.

The use of weighted networks constitutes an improvement over unweighted networks produced by dichotomizing the Pearson correlation matrix, since a) the continuous nature of gene coexpression information is preserved, and b) the results of weighted network analyses are highly robust with respect to the choice of the parameter β (where connection strength = $|\text{correlation}|^{\beta}$), whereas unweighted networks display sensitivity to the choice of cutoff[28]. Gene coexpression networks, like many other types of biological networks, have been found to exhibit an approximate scale-free topology[28-30]. Zhang and Horvath[28] proposed a scale-free topology criterion for choosing β. Here, a power of β = 4 was chosen for both CTX and CTX_95, while slightly higher powers were chosen for CN (β = 6) and CB (β = 5) due to the smaller sizes of these datasets.

Unlike correlation, which considers each pair of genes in isolation, topological overlap (TO) considers each pair of genes in relation to all other genes in the network. TO thus serves as a filter to exclude spurious or isolated connections during network construction (see Figures S1 and S2 from ref. 31). Due to the large number of genes analyzed, we performed an additional step to enrich each network with genes with high TO. A dynamic tree-cutting algorithm[32] was used to "cut" each dendrogram and define an initial set of modules for each network (the minimum module size was arbitrarily set to ten probe sets). This algorithm uses the structure of a dendrogram to iteratively decompose and combine branches until the number of clusters stabilizes[32]. The density of the resulting modules (defined as the average intramodular TO) was compared to the density of modules of equivalent size selected randomly from the network (n = 5,000 permutations). Density p-values were determined for each initial module by calculating the percentage of trials in which the density of the "random" modules exceeded the density of the initial module. Modules for which this p-value exceeded 0.01, along with genes that were not

assigned to any initial modules, were removed from the network. This filter reduced the number of probe sets in each network to 5,549 (CTX), 3,203 (CTX_95), 4,050 (CN), and 4,029 (CB). Using only these probe sets, a new TO matrix was calculated for each network and average linkage hierarchical clustering was performed to group genes based upon the TO dissimilarity measure. The dynamic tree-cutting algorithm[32] was again used to identify modules in each network. To ensure the consistency of coexpression patterns within modules, the algorithm was tuned to first identify small modules, which were then progressively merged based on similarities in gene expression profiles. To assess similarities in gene expression profiles, singular value decomposition ($X = UDV^T$) was performed for all modules and the values of the module eigengenes, V_1 (i.e. the first principal components), were correlated with one another. In general, modules with highly correlated eigengenes (Pearson correlation >= 0.8) were merged. This process was performed iteratively until merging was no longer necessary. Small modules that consisted primarily of probe sets for a single gene (e.g. protocadherin, hemoglobin) were removed. Lastly, modules with a final density $P > 0.1$ (calculated as described above, but using random samples from the second [filtered] TO matrix instead of the first) were also removed. Genes belonging to each of the remaining modules were labeled by color (one color per module), while genes from modules that were removed and genes that were not assigned to modules were denoted with the color grey. Following these steps, the number of modules identified in each network was as follows: 19 (CTX), 17 (CTX_95), 23 (CN), and 22 (CB). Summaries of all modules are presented in Supplementary Figure 2.

Topological overlap of interacting protein pairs

To assess whether proteins that physically interact have higher TO in gene coexpression networks than proteins that do not, we downloaded a database of experimentally validated interacting protein pairs from EBI (European Bioinformatics Institute)/IntAct (http://www.ebi.ac.uk/intact/site/index.jsf)[33]. Analysis was restricted to interacting human protein pairs for which both gene symbols were known. After excluding self-self and duplicate interacting pairs, a total of 17,540 interacting human protein pairs were obtained. Using the TO matrices for all expressed genes in CTX, CN, and CB, we calculated the mean TO of all interacting protein pairs for which both members were present in the matrix (CTX = 5,980 pairs, CN = 4,901 pairs, and CB = 5,347 pairs). For genes represented by multiple probe sets, the average was taken. The mean TO for interacting protein pairs was then compared to the mean TO for randomly selected pairs of probe sets in each network (n = 50,000).

Module comparisons between networks

The overlap and corresponding significance for all pairwise comparisons of networks and modules can be found in Supplementary Table 2, and all of the information necessary for the calculation of the hypergeometric p-values can be found in Supplementary Tables 2-6. The "Module" column of Supplementary Tables 3-6 denotes the module assignments of all probe sets used to construct the networks depicted in Figure 1; probe sets that were not used for network construction are denoted by NA ("not available"). For example, 5,549 probe sets were used to construct the CTX network (Supplementary Table 3) and 4,050 probe sets were used to construct the CN network (Supplementary Table 5). Intersecting these lists identifies 2,542 probe sets common to CTX and CN network construction. Comparing M4 (purple), we find 30 probe sets

assigned to this module in CTX (Supplementary Table 3), 22 of which were represented among the probe sets used for CN network construction (Supplementary Table 5); in CN, we find 62 probe sets assigned to this module (Supplementary Table 5), 38 of which were represented among the probe sets used for CTX network construction (Supplementary Table 3). In total, 19 probe sets were shared in M4 between CTX and CN (Supplementary Table 2). The statistical significance of the reported overlap for this example corresponds to a one-sided p-value of 1.39e–34. After correcting for multiple comparisons, the adjusted p-value is 3.19e–33 (Supplementary Table 2).

Defining a measure of module membership (k_{ME})

In our study, we defined the module membership for each gene with respect to each module as the Pearson correlation between the expression level of the gene and the ME[34]. This quantity, which we refer to here as k_{ME}, is a natural summary of the extent to which a gene conforms to the characteristic expression pattern of a module. However, we note that other summary measures are possible. One advantage of using the ME is that it satisfies an optimality criterion: by definition, it provides the best summary of variation in gene expression within a module. The ME also has an intuitive interpretation when it is juxtaposed with the more familiar "heat map" depicting the expression levels of genes within a module (Supplementary Figure 2). On the other hand, the ME is not a real gene; it is a centroid of a module. Because modules have varying extents of heterogeneity in gene expression, not all modules are represented equally well by the ME. Summaries of such modules may benefit from the use of additional components.

Module characterization

Modules were characterized using several complementary approaches. One primary approach involved cross-referencing gene sets describing pertinent cellular or functional phenotypes with module composition. Lists of genes known to be preferentially expressed in mouse oligodendrocytes, astrocytes, and neurons were obtained from Tables S4-S6 of ref. 35 and Table S1 of ref. 36. For data from ref. 35, analysis was restricted to genes with at least threefold enrichment in a given cell type. A third list of astrocyte markers was obtained from Table S7 of ref. 37, and a list of markers for Purkinje cells was obtained from Table 3 of ref. 38. We also generated a list of genes with increased expression in differentiated rat oligodendrocytes relative to oligodendrocyte precursors by analyzing data from ref. 39. Raw data (.CEL files) were obtained from Gene Expression Omnibus (http://www.ncbi.nlm.nih.gov/geo/query/acc.cgi?acc=GSE5940) for nine samples (five precursor, four differentiated) analyzed on Affymetrix, Inc. RAE230A microarrays. Data were imported into R and processed as described above but without probe masking or batch normalization. To identify differentially expressed (DE) genes, a Bayesian t-test was applied using the R package "bayesreg"[40] with the following parameters: betaFit = 1, bayes = TRUE, winSize = 101, conf = 10. Genes with higher expression in differentiated oligodendrocytes relative to oligodendrocyte precursors and a posterior probability of differential expression (PPDE) > 0.999 were used for cross-referencing. Similarly, lists of genes up-regulated in mouse glutamatergic cortical neurons, GABAergic cortical neurons, or layer 4-6 interneurons were obtained by analyzing data from ref. 41. Raw data (.CEL files) were obtained from Gene Expression Omnibus (http://www.ncbi.nlm.nih.gov/geo/query/acc.cgi?acc=GSE2882) for 42

samples analyzed on Affymetrix, Inc. MG-430A microarrays. Non-specific and mis-targeted probes were masked using the R package "ProbeFilter"[12] prior to generation of expression values and normalization in R as described above (no batch normalization was necessary). DE genes were identified as described above. All comparisons were restricted to cortical neurons. For genes up-regulated in glutamatergic or GABAergic cortical neurons, PPDE > 0.999 was chosen as the threshold for differential expression. For genes up-regulated in layer 4–6 interneurons, a threshold of PPDE > 0.99 was chosen. For cross-referencing with the synaptic proteome, a list of proteins enriched in the post-synaptic density was obtained from the Genes2Cognition Consortium[42] (http://www.genes2cognition.org/cgi-bin/browser?action=bydataset;proteomics_id=psp_member;proteomics_value=Y), while a list of proteins enriched in synaptic vesicles and the pre-synaptic membrane compartment was obtained from ref. 43 (Tables 1 and 2). Finally, a list of genes with altered expression following ischemia and reperfusion in mouse hippocampus was obtained from Table 1 of ref. 44.

Gene symbols were used as unique identifiers to cross-reference each set of genes with all modules in each network in an unbiased manner. For each module, these comparisons were restricted to genes with positive k_{ME} values ($P < 0.001$). The significance of module enrichment was assessed using Fisher's exact test (one-sided). To account for multiple comparisons, a Bonferroni correction was applied based upon the number of modules in the network. Complete cross-referencing results can be found in Supplementary Table 7.

Another approach to module characterization involved searching for over-represented categorical systems using EASE[45] (p-values cited in the journal article refer to EASE scores from Supplementary Table 8). For module characterization using EASE, analysis was restricted for each module to genes with positive k_{ME} values ($P < 0.001$). Population files were comprised of

probe sets retained following mask application (n = 18,631 [HG-U133A] and n = 10,553 [HG-U95A/v2]). All available categorical systems were searched. To control for multiple comparisons, the global false discovery rate (FDR) was calculated for all systems in each module (1000 iterations). Categorical systems with a global FDR < 0.05 were deemed significantly enriched and are reported in Supplementary Table 8.

Modules were also characterized by correlating MEs with available sample information such as age, gender, and cortical area (Supplementary Table 1). For example, to determine whether any MEs in CTX_95 were significantly correlated with expression in primary visual cortex, an indicator variable was created (1 = primary visual cortex samples, 0 = all other samples). This indicator variable was then correlated (Pearson) with all MEs. A Bonferroni correction was applied based on the number of modules in the network. Finally, modules were also characterized through visual inspection using VisANT[46].

Module visualization

Visualizations of all modules from CTX, CN, and CB are presented in Supplementary Figure 4. For each module, pairwise TO values were calculated for the top 1% of all probe sets based on $|k_{ME}|$. A second filter was applied to select only those gene pairs for which both members exhibited higher $|k_{ME}|$ for the module in question than for any other module in the network. From this list, 150 pairs of genes with the greatest TO were depicted using VisANT (http://visant.bu.edu/)[46]. The "Spring Embedded Relaxing" layout algorithm was used to confer partial network structures, which were then manually adjusted for clarity. In these visualizations, modular structure is defined by the connections between genes; distances are irrelevant. Genes with expression levels that were negatively correlated are connected by black lines; all other

genes were positively correlated (except for the black module [M11], where red lines denote negative correlations). Numbers appended to gene symbols denote the $|k_{ME}|$ rank (i.e. RMM) for the corresponding probe set (some genes are represented by multiple probe sets). Genes with >= 20 depicted connections appear as large nodes, followed by genes with 10–19 connections that appear as medium nodes, followed by genes with < 10 connections that appear as small nodes.

Module eigengene network comparisons

To explore the higher-order structure of gene coexpression networks and the relationships between modules, module eigengene (ME) networks[47] were created. An ME network describes the relationships between modules based on the correlations between MEs[47]. For each dataset, Pearson correlation coefficients were calculated for all pairwise comparisons of MEs. Comparisons of ME networks between datasets were restricted to conserved modules. Correlation preservation between MEs I,J in networks k_1 and k_2 was assessed using the following formula[47]:

$$CP_{IJ}^{(k_1,k_2)} = 1 - \left(\frac{|R_{IJ}^{(k_1)} - R_{IJ}^{(k_2)}|}{2} \right) \qquad (1)$$

where $R^{(k1)}_{IJ}$ is the ME Pearson correlation matrix for all conserved modules (labeled by indices IJ) in network k_1, and similarly for network k_2. In addition, average linkage hierarchical "consensus" clustering of eigengenes in ME networks k_1 and k_2 was performed using the following dissimilarity measure[47] (I,J again label eigengenes):

$$DM_{IJ}^{(k_1,k_2)} = 1 - \left(\frac{R_{IJ}^{(k_1)} + R_{IJ}^{(k_2)}}{2} \right) \qquad (2)$$

ME networks were depicted as heat maps using the "image.plot" function in R, with red corresponding to positive correlations and green corresponding to negative correlations

(Supplementary Figure 6). To facilitate visual evaluation of ME network heat maps, MEs were ordered using average linkage hierarchical clustering with 1-correlation as the dissimilarity measure, followed by re-ordering of branches within the restrictions imposed by the dendrogram such that the correlation of adjacent MEs was maximized.

Comparisons of module membership (k_{ME}) between brain regions

Because k_{ME} is itself a correlation, comparisons of k_{ME} between networks (e.g. brain regions) is equivalent to assessing the significance of differences in correlations from samples of different sizes. To compare k_{ME} values for probe set i relative to module j in network k, we first normalized these values using the Fisher transformation:

$$z_{ijk} = 0.5 * \log\left(\frac{1 + k_{ME_{ijk}}}{1 - k_{ME_{ijk}}} \right) \qquad (3)$$

For comparison between networks $k1$ and $k2$, the difference between the resulting z scores for probe set i relative to module j was divided by the joint standard error:

$$zdiff = \frac{z_{ijk1} - z_{ijk2}}{\sqrt{1/(n_1 - 3) + 1/(n_2 - 3)}} \qquad (4)$$

where z_{ijk1} and z_{ijk2} represent the normalized correlations for probe set i relative to module j in network $k1$ and network $k2$, respectively, and n1 and n2 represent the sample sizes. This z-score was converted into a two-sided p-value based upon the normal distribution. These p-values and their corresponding z-scores are reported for all probe sets for all pairwise comparisons of conserved modules between CTX, CN, and CB in Supplementary Table 11, along with mean expression levels and differential expression (DE) p-values. To assess the significance of DE, scaled expression data from CTX, CN, and CB were pooled and normalized as described above. For batch normalization[11], samples from each study were assigned to a single batch, with tissue

(CTX, CN, or CB) designated as a covariate. DE p-values were calculated using a Bayesian t-test from the R package bayesreg[40] as described above.

Immunohistochemistry

Postmortem human brain tissue samples were obtained through the UCLA Pathology Department under the UCLA human subject guidelines. Individuals did not have evidence of neuropathological conditions and four of five patients died from non-CNS complications; the fifth patient died from a brain infarct that did not compromise the area of interest. Tissue was used from five individuals aged 51 to 81 y.o. The region of the subventricular zone at the head of the caudate was excised from formalin-fixed brain under the direction of a neuropathologist. Tissue was embedded in paraffin and sectioned at 7 μM intervals. Sections were rehydrated, boiled in citric acid buffer for antigen retrieval, and incubated in 0.3% hydrogen peroxide following standard procedures. Non-specific binding was blocked using PBS containing 5% milk, 0.2% triton-X, and 2% normal goat serum at room temperature for 1h. Tissue was incubated with primary antibody diluted in blocking solution at 4°C overnight. The following antibodies and dilutions were used: ALDH1L1 mouse monoclonal (Abcam, ab56777; 1:500), ASCL1 rabbit polyclonal (Abcam, ab38556; 1:50), CD24 mouse monoclonal (Abcam, ab19704; 1:100), connexin 43 (GJA1) rabbit polyclonal (Santa Cruz, sc-9059; 1:100), DPYSL3 rabbit polyclonal (Chemicon, AB5454; 1:1500), GFAP rabbit polyclonal (Dako, Z0334; 1:10,000), PLTP rabbit polyclonal (Abcam, ab18990; 1:100), neuronal class III beta-tubulin (TuJ1) mouse monoclonal (Covance, MMS-435P; 1:5000). Appropriate biotinylated secondary antibodies diluted in blocking solution were applied to slides for 1h at room temperature. The chromagens 3,3'-diaminobenzidine (DAB) or Vector® SG (Vector Laboratories) were used following the

manufacturer's instructions (Vector Laboratories, VECTASTAIN ABC kits). Substitution of either chromagen for each antibody gave similar results. Due to the availability of a mouse monoclonal antibody for CD24, double labeling was performed for CD24 together with ASCL1, GJA1, or PLTP. For double-labeling experiments, slides were processed with the first primary and secondary antibody and chromagen followed by the second primary and secondary antibody and contrasting chromagen. Hematoxylin staining was conducted following standard procedures after the blocking step. Most antibodies were used on two or more individuals and yielded similar expression patterns. Two different antibodies for CD24 and GJA1 gave similar results. Omission of primary antibody did not result in detectable staining.

Identification of candidate genes with expression patterns that distinguish SVZ astrocytes from mature astrocytes

To identify candidate genes with expression patterns that distinguish SVZ astrocytes from mature astrocytes, we calculated the difference in membership for M13C and M15C (MM_{diff}) for all genes in CN (n = 18,631). We limited our search to genes with strong membership for either module (MM > 0.7) and $|MM_{diff}| > 0.4$. For genes meeting these criteria with MM15C > MM13C, we also required evidence of expression in astrocytes across brain regions (MM15 > 0.5 in CTX and CB). For genes meeting these criteria with MM13C > MM15C, we required evidence of absence of expression in astrocytes across brain regions (MM15 < 0.5 in CTX, CN, and CB).

References

1. Caceres, M. et al. Elevated gene expression levels distinguish human from non-human primate brains. *Proc Natl Acad Sci U S A* **100**, 13030-5 (2003).
2. Enard, W. et al. Intra- and interspecific variation in primate gene expression patterns. *Science* **296**, 340-3 (2002).
3. Hodges, A. et al. Regional and cellular gene expression changes in human Huntington's disease brain. *Hum Mol Genet* **15**, 965-77 (2006).
4. Iwamoto, K., Bundo, M. & Kato, T. Altered expression of mitochondria-related genes in postmortem brains of patients with bipolar disorder or schizophrenia, as revealed by large-scale DNA microarray analysis. *Hum Mol Genet* **14**, 241-53 (2005).
5. Iwamoto, K., Kakiuchi, C., Bundo, M., Ikeda, K. & Kato, T. Molecular characterization of bipolar disorder by comparing gene expression profiles of postmortem brains of major mental disorders. *Mol Psychiatry* **9**, 406-16 (2004).
6. Khaitovich, P. et al. Regional patterns of gene expression in human and chimpanzee brains. *Genome Res* **14**, 1462-73 (2004).
7. Khaitovich, P. et al. A neutral model of transcriptome evolution. *PLoS Biol* **2**, E132 (2004).
8. Ryan, M.M. et al. Gene expression analysis of bipolar disorder reveals downregulation of the ubiquitin cycle and alterations in synaptic genes. *Mol Psychiatry* **11**, 965-78 (2006).
9. Lu, T. et al. Gene regulation and DNA damage in the ageing human brain. *Nature* **429**, 883-91 (2004).
10. Zhang, J., Finney, R.P., Clifford, R.J., Derr, L.K. & Buetow, K.H. Detecting false expression signals in high-density oligonucleotide arrays by an in silico approach. *Genomics* **85**, 297-308 (2005).
11. Johnson, W.E., Li, C. & Rabinovic, A. Adjusting batch effects in microarray expression data using empirical Bayes methods. *Biostatistics* **8**, 118-27 (2007).
12. Dai, M. et al. Evolving gene/transcript definitions significantly alter the interpretation of GeneChip data. *Nucleic Acids Res* **33**, e175 (2005).
13. Gentleman, R.C. et al. Bioconductor: open software development for computational biology and bioinformatics. *Genome Biol* **5**, R80 (2004).
14. Li, J.Z. et al. Systematic changes in gene expression in postmortem human brains associated with tissue pH and terminal medical conditions. *Hum Mol Genet* **13**, 609-16 (2004).
15. Li, J.Z. et al. Sample matching by inferred agonal stress in gene expression analyses of the brain. *BMC Genomics* **8**, 336 (2007).
16. Bolstad, B.M., Irizarry, R.A., Astrand, M. & Speed, T.P. A comparison of normalization methods for high density oligonucleotide array data based on variance and bias. *Bioinformatics* **19**, 185-93 (2003).
17. Eisen, M.B., Spellman, P.T., Brown, P.O. & Botstein, D. Cluster analysis and display of genome-wide expression patterns. *Proc Natl Acad Sci U S A* **95**, 14863-8 (1998).
18. Huang, Y. et al. Systematic discovery of functional modules and context-specific functional annotation of human genome. *Bioinformatics* **23**, i222-9 (2007).
19. Ihmels, J., Bergmann, S. & Barkai, N. Defining transcription modules using large-scale gene expression data. *Bioinformatics* **20**, 1993-2003 (2004).

20. Lee, H.K., Hsu, A.K., Sajdak, J., Qin, J. & Pavlidis, P. Coexpression analysis of human genes across many microarray data sets. *Genome Res* **14**, 1085-94 (2004).
21. Stuart, J.M., Segal, E., Koller, D. & Kim, S.K. A gene-coexpression network for global discovery of conserved genetic modules. *Science* **302**, 249-55 (2003).
22. Zhou, X., Kao, M.C. & Wong, W.H. Transitive functional annotation by shortest-path analysis of gene expression data. *Proc Natl Acad Sci U S A* **99**, 12783-8 (2002).
23. Steffen, M., Petti, A., Aach, J., D'Haeseleer, P. & Church, G. Automated modelling of signal transduction networks. *BMC Bioinformatics* **3**, 34 (2002).
24. Schafer, J. & Strimmer, K. An empirical Bayes approach to inferring large-scale gene association networks. *Bioinformatics* **21**, 754-64 (2005).
25. Dobra, A. et al. Sparse graphical models for exploring gene expression data. *J. Multiv. Analysis* **90**, 196-212 (2004).
26. Toh, H. & Horimoto, K. Inference of a genetic network by a combined approach of cluster analysis and graphical Gaussian modeling. *Bioinformatics* **18**, 287-97 (2002).
27. Magwene, P.M. & Kim, J. Estimating genomic coexpression networks using first-order conditional independence. *Genome Biol* **5**, R100 (2004).
28. Zhang, B. & Horvath, S. A general framework for weighted gene co-expression network analysis. *Stat Appl Genet Mol Biol* **4**, Article17 (2005).
29. Barabasi, A.L. & Oltvai, Z.N. Network biology: understanding the cell's functional organization. *Nat Rev Genet* **5**, 101-13 (2004).
30. Chung, W.Y., Albert, R., Albert, I., Nekrutenko, A. & Makova, K.D. Rapid and asymmetric divergence of duplicate genes in the human gene coexpression network. *BMC Bioinformatics* **7**, 46 (2006).
31. Oldham, M.C., Horvath, S. & Geschwind, D.H. Conservation and evolution of gene coexpression networks in human and chimpanzee brains. *Proc Natl Acad Sci U S A* **103**, 17973-8 (2006).
32. Langfelder, P., Zhang, B. & Horvath, S. Defining clusters from a hierarchical cluster tree: the Dynamic Tree Cut library for R. *Bioinformatics* (2007).
33. Kerrien, S. et al. IntAct--open source resource for molecular interaction data. *Nucleic Acids Res* **35**, D561-5 (2007).
34. Horvath, S. & Dong, J. Geometric interpretation of gene coexpression network analysis. *PLoS Comput Biol* **4**, e1000117 (2008).
35. Cahoy, J.D. et al. A transcriptome database for astrocytes, neurons, and oligodendrocytes: a new resource for understanding brain development and function. *J Neurosci* **28**, 264-78 (2008).
36. Lein, E.S. et al. Genome-wide atlas of gene expression in the adult mouse brain. *Nature* **445**, 168-76 (2007).
37. Bachoo, R.M. et al. Molecular diversity of astrocytes with implications for neurological disorders. *Proc Natl Acad Sci U S A* **101**, 8384-9 (2004).
38. Rong, Y., Wang, T. & Morgan, J.I. Identification of candidate Purkinje cell-specific markers by gene expression profiling in wild-type and pcd(3J) mice. *Brain Res Mol Brain Res* **132**, 128-45 (2004).
39. Nielsen, J.A., Maric, D., Lau, P., Barker, J.L. & Hudson, L.D. Identification of a novel oligodendrocyte cell adhesion protein using gene expression profiling. *J Neurosci* **26**, 9881-91 (2006).

40. Long, A.D. et al. Improved statistical inference from DNA microarray data using analysis of variance and a Bayesian statistical framework. Analysis of global gene expression in Escherichia coli K12. *J Biol Chem* **276**, 19937-44 (2001).
41. Sugino, K. et al. Molecular taxonomy of major neuronal classes in the adult mouse forebrain. *Nat Neurosci* **9**, 99-107 (2006).
42. Grant, S.G., Marshall, M.C., Page, K.L., Cumiskey, M.A. & Armstrong, J.D. Synapse proteomics of multiprotein complexes: en route from genes to nervous system diseases. *Hum Mol Genet* **14 Spec No. 2**, R225-34 (2005).
43. Morciano, M. et al. Immunoisolation of two synaptic vesicle pools from synaptosomes: a proteomics analysis. *J Neurochem* **95**, 1732-45 (2005).
44. Nagata, T. et al. Profiling of genes associated with transcriptional responses in mouse hippocampus after transient forebrain ischemia using high-density oligonucleotide DNA array. *Brain Res Mol Brain Res* **121**, 1-11 (2004).
45. Hosack, D.A., Dennis, G., Jr., Sherman, B.T., Lane, H.C. & Lempicki, R.A. Identifying biological themes within lists of genes with EASE. *Genome Biol* **4**, R70 (2003).
46. Hu, Z. et al. VisANT 3.0: new modules for pathway visualization, editing, prediction and construction. *Nucleic Acids Res* **35**, W625-32 (2007).
47. Langfelder, P. & Horvath, S. Eigengene networks for studying the relationships between co-expression modules. *BMC Syst Biol* **1**, 54 (2007).

Supplementary Network Analysis - Illumina

Michael C. Oldham, Steve Horvath, Genevieve Konopka, Kazuya Iwamoto, Peter Langfelder, Tadafumi Kato, and Daniel H. Geschwind

"Functional Organization of the Transcriptome in Human Brain"

Summary

To provide further validation for the reproducibility of gene coexpression relationships across individuals and microarray platforms, we applied weighted gene coexpression network analysis (WGCNA)[1] to a dataset ("CTX_ILMN") generated from human cerebral cortex samples using Illumina HumanRefseq-8 microarrays[2]. The resulting gene coexpression network was compared with the "CTX" network, which was generated from human cerebral cortex samples using Affymetrix U133A microarrays and is described in detail in the journal article. A summary of these datasets is presented in Table 1.

	CTX_ILMN	CTX
Platform	Illumina HumanRefseq-8	Affymetrix U133A
# samples / # unique individuals	159 / 159	67 / 67
Cortical areas	~ 3/4 temporal, ~1/4 frontal	All frontal
Avg. age	80	48
Mean IAC^	0.943	0.970
# probe sets used for network construction	5,269	5,549
Overlap^^	31%	37%

Table 1: Summary of CTX_ILMN and CTX datasets. ^IAC = inter-array correlation. ^^Overlap = the percentage of unique gene symbols in a given network that were present in the other network.

In addition to the expected discrepancies in gene expression measurements introduced by differences in platform design between Illumina and Affymetrix microarrays, differences in the sample characteristics and representation of genes in the CTX_ILMN and CTX datasets also presented substantial heterogeneity (Table 1). Despite this heterogeneity, a majority of gene

coexpression modules identified in CTX in the journal article revealed significant evidence of overlap in CTX_ILMN, and vice versa. We show that modules corresponding to the major cell classes of human cerebral cortex were present in CTX_ILMN, as they were in each of the four Affymetrix datasets analyzed in our study. Furthermore, we show that membership for the same modules was highly correlated between CTX and CTX_ILMN, as was the case for comparisons between CTX and CTX_95 (Fig. 3 from the journal article). These results are described below and provide additional evidence that conserved gene coexpression modules reflect consistent underlying sources of variation in microarray data generated from human cerebral cortex.

Microarray data processing

Because raw data from ref. 2 were unavailable, previously normalized expression values for 5,269 transcripts that were detected in all 193 samples of the original study (and therefore had no missing values) were used as the starting point for this analysis (National Center for Biotechnology Gene Expression Omnibus: accession code GSE8919). Beginning with these data, outlier samples in CTX_ILMN (n = 34) were identified and removed. A detailed supplement containing all of the relevant R code and corresponding figure images that were used to guide our decisions to remove outlier samples in this dataset is available on our web page (http://www.genetics.ucla.edu/labs/horvath/CoexpressionNetwork/HumanBrainTranscriptome/). Briefly, inter-array correlations (IACs) were calculated by correlating samples with one another using expression levels for all 5,269 probe sets. Samples were hierarchically clustered using average linkage and 1-IAC as a distance metric to identify outliers. IACs were also averaged for each array and compared to the resulting distribution of IACs for the dataset, and samples with low average IACs relative to the distribution were removed. This approach constitutes an

unbiased method for the identification and removal of samples with aberrant gene expression levels. Following outlier removal, quantile normalization[3] was performed in R, resulting in a mean IAC of 0.943 for CTX_ILMN. Because raw data from ref. 2 were unavailable, no batch normalization was performed.

Weighted gene coexpression network construction and module detection

WGCNA was applied to CTX_ILMN using $\beta = 6$ as described in the journal article (Methods). A single topological overlap (TO) matrix (5,269 x 5,269) was constructed for CTX_ILMN and average linkage hierarchical clustering was performed to group genes based upon the TO dissimilarity measure. Using a dynamic tree-cutting method[4], 28 gene coexpression modules were identified (Fig. 1).

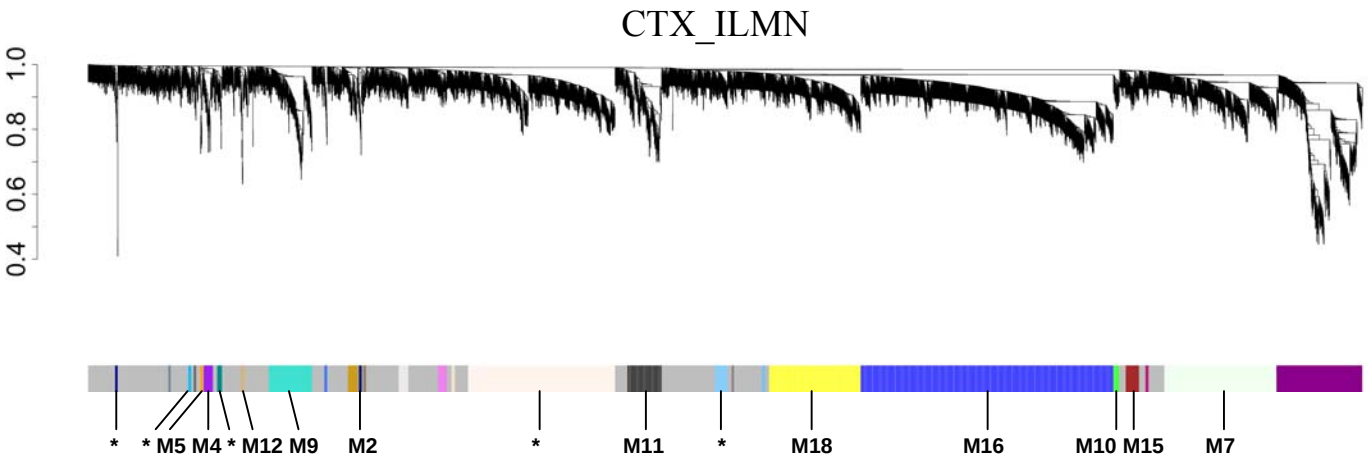

Figure 1: Illumina human cerebral cortex (CTX_ILMN) gene coexpression network. Dendrogram produced by average linkage hierarchical clustering of genes based upon topological overlap (see Methods from journal article). 28 modules of coexpressed genes in CTX_ILMN were assigned colors as indicated by the horizontal bar beneath the dendrogram. Modules with the most significant overlap between CTX_ILMN and CTX (corrected hypergeometric p-value < 0.05) were assigned the same colors and numbers as in the CTX network, with asterisks denoting modules with less significant overlap. CTX_ILMN consists of data from Illumina HumanRefseq-8 microarrays measuring expression levels in 159 human cortical samples with 5,269 probe sets.

Cross-platform validation of gene coexpression relationships

To determine whether modules from CTX and CTX_ILMN were composed of the same genes, we calculated the overlap and corresponding hypergeometric probability for each possible pair of modules in the two networks (using gene symbols as unique identifiers; see Methods from the journal article). As seen in Figure 2, a majority of gene coexpression modules identified in CTX revealed significant overlap with modules identified in CTX_ILMN, with seven of these modules showing > 50% overlap.

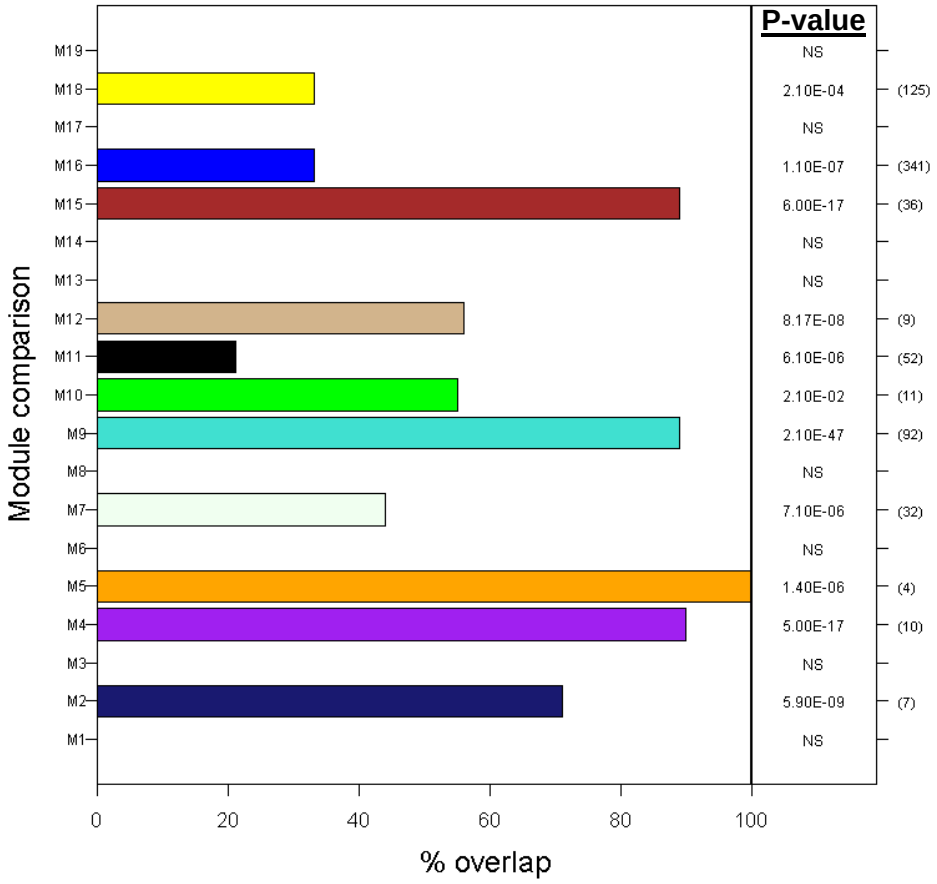

Figure 2: Gene coexpression modules in human cerebral cortex are preserved across individuals and microarray platforms. Comparison of the 19 gene coexpression modules identified in CTX with modules identified in CTX_ILMN. Modules with significant overlap (corrected hypergeometric p-value < 0.05) are depicted by horizontal colored bars. For example, M1 did not show significant overlap between CTX and CTX_ILMN, but M2 overlapped 71% with a module found in CTX_ILMN (*P* = 5.9e–09). Numbers in parentheses at right indicate the maximum possible number of shared genes per pair of modules (i.e. the denominator used to calculate percent overlap). NS = not significant.

Module membership values were calculated for all genes relative to all modules in CTX_ILMN as described in the journal article (Methods). To explore the reproducibility of module membership for individual genes between CTX and CTX_ILMN, we directly compared this quantity between the two networks for conserved modules (Fig. 3).

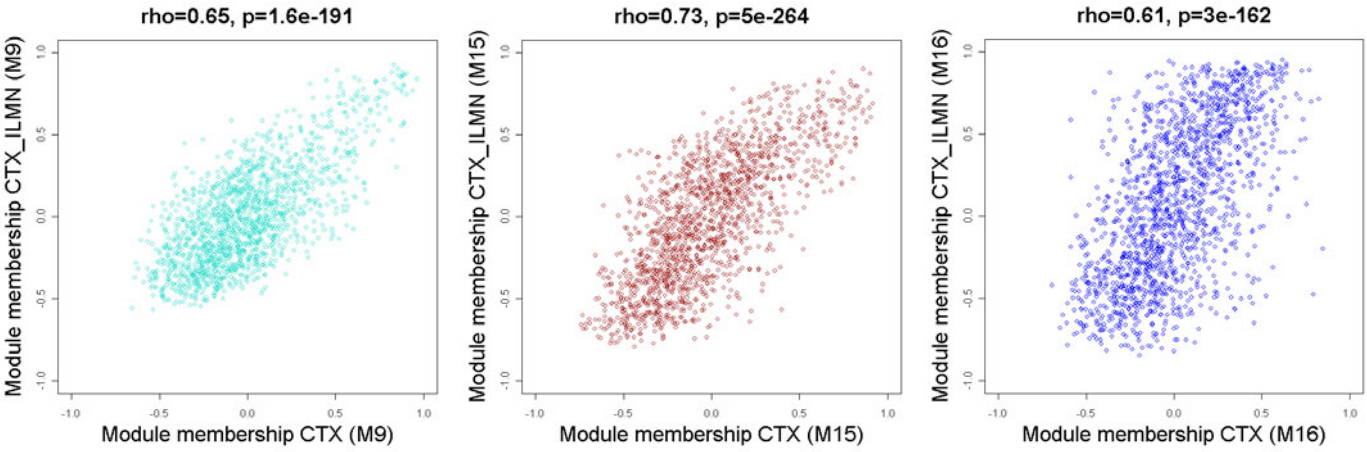

Figure 3: Module membership in human cerebral cortex is highly correlated across individuals and microarray platforms. Comparison of module membership (MM) between CTX and CTX_ILMN for M9 (left), M15 (middle), and M16 (right). For each module, the correlation (Spearman) between MM for CTX and CTX_ILMN was assessed. MM was correlated for the intersection of all genes used to construct the CTX and CTX_ILMN networks (1,598 genes).

As we observed in comparisons between Affymetrix microarray platforms (U133A [CTX] vs U95A/v2 [CTX_95]; Fig. 3 from the journal article), module membership in human cerebral cortex was remarkably consistent between Affymetrix U133A (CTX) and Illumina HumanRefseq-8 (CTX_ILMN) microarray platforms (M9: rho = 0.65, P = 1.6e–191; M15: rho = 0.73, P = 5.0e–264; M16: rho = 0.61, P = 3.0e–162; Fig. 3), despite substantial heterogeneity between these datasets (Table 1). These results validate the reproducibility of module membership values for individual genes and indicate that conserved gene coexpression modules reflect consistent underlying sources of variation in microarray data generated from human cerebral cortex.

References

1. Zhang, B. & Horvath, S. A general framework for weighted gene co-expression network analysis. *Stat Appl Genet Mol Biol* **4**, Article17 (2005).
2. Myers, A.J. et al. A survey of genetic human cortical gene expression. *Nat Genet* **39**, 1494-9 (2007).
3. Bolstad, B.M., Irizarry, R.A., Astrand, M. & Speed, T.P. A comparison of normalization methods for high density oligonucleotide array data based on variance and bias. *Bioinformatics* **19**, 185-93 (2003).
4. Langfelder, P., Zhang, B. & Horvath, S. Defining clusters from a hierarchical cluster tree: the Dynamic Tree Cut library for R. *Bioinformatics* (2007).

Supplementary Note

Michael C. Oldham, Steve Horvath, Genevieve Konopka, Kazuya Iwamoto, Peter Langfelder, Tadafumi Kato, and Daniel H. Geschwind

"Functional Organization of the Transcriptome in Human Brain"

Additional module characterization

Gene coexpression modules were characterized using five complementary approaches, as described in the journal article. To normalize comparisons across networks, module membership is reported below in terms of its rank (RMM = rank |module membership|). We focused primarily on characterizing modules with evidence of significant overlap across networks, but also characterized some modules found in only one network.

Interneurons: M6A, M23, M17

We observed that *PVALB*, a canonical marker of interneurons, exhibited strong membership for M6A (RMM = 8, P = 5.3e–15; Supplementary Table 3), M17A (RMM = 105, P = 2.0e–06; Supplementary Table 3), M17B (RMM = 4, P = 1.5e–11; Supplementary Table 4), and M23 (RMM = 17, P = 3.2e–07; Supplementary Table 4). These observations suggested that these modules might distinguish genes that are preferentially expressed in *PVALB*+ interneurons relative to other cell types in cerebral cortex. The two strongest members of M6A were *NEFH* and *VAMP1* (Supplementary Table 3 and Supplementary Fig. 4f), both of which were expressed significantly higher in a *PVALB*+ interneuron relative to pyramidal neurons in a single-cell microarray analysis of rat hippocampal CA1[1]. Using raw data from ref. 2, we identified genes with higher expression in layer 4–6 interneurons relative to other neuronal cell types isolated

from adult mouse forebrain. Both M6A (P = 7.7e–03) and M23 (P = 8.7e–04) were significantly enriched with genes from this list (Supplementary Table 7). Genes in M23 also showed increased expression in primary visual cortex relative to other cortical areas (r = 0.57, P = 1.3e–03; Supplementary Fig. 2y), as did genes in M17B (r = 0.71, P = 2.5e–06; Supplementary Fig. 2w). Collectively, these data support the conclusion that gene coexpression in these modules reflects the relative abundance of certain classes of *PVALB*+ interneurons in samples from different cortical areas.

Purkinje neurons: M6D

M6A also showed significant overlap with a module identified in cerebellum (M6D; Supplementary Table 2). The strongest members of M6D were *PVALB* and *CALB1* (Supplementary Table 6 and Supplementary Fig. 4as), both of which are highly expressed in Purkinje neurons in cerebellum[3]. These observations suggested that M6D might consist of genes that are preferentially expressed in Purkinje neurons relative to other cell types in cerebellum. Consistent with this hypothesis, Purkinje cell protein 4 (*PCP4*), considered a marker for Purkinje neurons, also exhibited strong membership for M6D (RMM = 9, P = 5.9e–09; Supplementary Table 6 and Supplementary Fig. 4as). *In situ* hybridization (ISH) data from adult mouse brain revealed elevated and often exclusive expression in Purkinje neurons for nine out of ten genes with the strongest membership for this module (Supplementary Fig. 5a–j). We also obtained a list of genes expressed in Purkinje neurons with significantly reduced expression levels in cerebella from Purkinje cell degeneration (pcd^{3J}) mice relative to wild-type littermates[4]. M6D was highly enriched with these genes (P = 6.1e–23, Supplementary Table 7). These results

indicate that M6D is comprised of genes that are preferentially expressed in Purkinje neurons relative to other cell types in cerebellum.

Microglia: M4, M5

EASE indicated that the gene ontology (GO) biological process "immune response" was significantly over-represented in M4 (*P* = 2.6e–56 [CTX]; *P* = 8.4e–09 [CTX_95]; *P* = 1.3e–24 [CN]; *P* = 1.5e–11 [CB]), along with numerous related categories such as "defense response", "response to wounding", and "response to stress" (Supplementary Table 8). Among those genes with the strongest membership for M4A were several members of the major histocompatibility class II complex, including *HLA-DRA*, *HLA-DPA1*, and *HLA-DMA*, as well as several members of the classical complement pathway, including *C1QA*, *C1QB*, and *C3* (Supplementary Table 3 and Supplementary Fig. 4d). In the brain, expression of these genes reflects the activation of microglia, the resident immune cells of the central nervous system[5]. M5 was also enriched for genes involved in the GO biological process "immune response" (*P* = 9.8e–42 [CTX]; *P* = 5.6e–11 [CTX_95]; *P* = 4.7e–04 [CN]), as well as numerous related categories (Supplementary Table 8). Expression levels of many genes with strong membership for M5A have been shown to increase significantly in microglia in response to activation with interferon-gamma[6], including *PSMB9*, *SERPING1*, *STAT1*, and *CASP1* (Supplementary Table 3). These data indicate that coexpression in M5, like M4, likely reflects activation of microglia in response to an immunogenic event. Consistent with this interpretation, coexpression in these modules was driven by a small number of individuals, some of who were represented by multiple brain regions (e.g. H46 in Supplementary Fig. 2d,al,bt), suggesting a global neuroimmunological response possibly related to cause of death.

Meningeal cells: M43

We observed that M43 was significantly enriched with genes encoding structural molecules (*P* = 9.1e–05), cell adhesion molecules (*P* = 3.7e–04), and components of the extracellular matrix (*P* = 1.5e–06) (Supplementary Table 8). In the cerebellum, meningeal cells are known to produce many components of the interstitial matrix and basement membrane[7], including fibronectin, which possessed the strongest membership of any gene for this module (Supplementary Fig. 4bh and Supplementary Table 6). Many other genes with strong membership for M43 are known to be highly expressed in meningeal cells, including *PTGDS*[8], *VIM*[9], and *BGN*[10] (Supplementary Table 6). Other genes that encode components of the extracellular matrix and exhibited strong membership for M43 included *DCN*, *MGP*, *COL6A2*, *DSP*, *FBLN1*, *FBLN5*, *COL18A1*, and *COL6A3* (Supplementary Tables 6 and 8). These data suggest that M43 consists of genes that are preferentially expressed in meningeal cells relative to other cell types in cerebellum.

Hypoxia: M12

We observed that many of the genes with the strongest membership for M12A encode transcription factors and immediate early genes, including *FOS*, *JUN*, *JUNB*, *MAFF*, and *FOSB* (Supplementary Table 3). EASE confirmed that the GO category "transcription regulator activity" was significantly over-represented in M12 for both CTX (*P* = 5.8e–07) and CB (*P* = 4.1e–03) (Supplementary Table 8). In addition, EASE identified a BBID pathway[11] related to brain ischemia as significantly over-represented in M12 for CTX (*P* = 1.3e–04) and CB (*P* = 9.7e–06) (Supplementary Table 8). Like M4 and M5, coexpression in M12 was driven by a small number of individuals (Supplementary Fig. 2l,bi). These observations suggested that

coexpression in this module might represent a CNS transcriptional response to hypoxia. To test this hypothesis, we obtained a list of genes with altered expression levels following ischemia and reperfusion in mouse hippocampus[12]. M12 was significantly enriched with genes from this list in both CTX (P = 5.6e–13) and CB (P = 2.3e–08) (Supplementary Table 7). These results provide evidence that coexpression in M12 reflects a response to hypoxia in the human brain.

Gender: M1

We observed that M1 was highly enriched with genes from chromosome Y in CTX (P = 4.8e–21), CN (P = 4.8e–16), and CB (P = 7.4e–19) (Supplementary Table 8). Among the genes with the strongest membership for M1 was *XIST*, which is expressed in females and mediates X chromosome inactivation[13]. This gene was negatively correlated with the ME for M1 in all brain regions (Supplementary Tables 3, 5, and 6). These observations suggested that M1 might distinguish genes that are differentially expressed between male and female brains. To test this hypothesis, we correlated the ME for M1 with gender status for all samples from each brain region. Gender status was highly correlated with the ME for M1 in CTX (r = 0.93, P < 2.2e–16), CN (r = 0.94, P = 2.2e–13), and CB (r = 0.98, P < 2.2e–16). These results indicate that coexpression in M1 reflects differences in gene expression between male and female brains. Interestingly, *CD24*, which exhibited extremely strong membership for M13 in CN and CTX, also possessed strong membership for M1 in cerebellum (RMM = 4, P = 2.3e–14; Supplementary Table 6). Expression of this gene in CB was significantly higher in the brains of males compared to females (Supplementary Fig. 2bh). Although most of the genes with the strongest membership for M1 are located on the sex chromosomes, some autosomal genes also revealed strong membership for this module. In CN, these included the glucocorticoid receptor

NR3C1 and the progesterone receptor subunit *PGRMC2* (Supplementary Table 5), both of which were expressed higher in males.

Synaptic function: M10, M14

We observed that M10A was highly enriched with genes encoding synaptic proteins (*P* = 5.3e–18 and *P* = 6.9e–12), neuronal markers (*P* = 9.8e–06), and genes up-regulated in glutamatergic cortical neurons (p = 1.1e–06) (Supplementary Table 7). A similar pattern was observed for M10B and M10D, including enrichment of genes encoding synaptic proteins (M10B and M10D) and genes up-regulated in glutamatergic cortical neurons (M10B) (Supplementary Table 7). Consistent with these observations, EASE identified numerous over-represented categories in M10 related to synaptic function, including "synaptic vesicle" (*P* = 2.4e–07), "synapse" (*P* = 1.9e–05), and "transmission of nerve impulse" (*P* = 1.7e–03) (Supplementary Table 8). These results support the conclusion that gene coexpression in M10 is related to glutamatergic synaptic function. Interestingly, *DICER1* exhibited very strong membership for M10A, but was negatively correlated with the ME for this module (Supplementary Table 3 and Supplementary Fig. 4j), suggesting a link between RNA interference[14] and glutamatergic synaptic function in cerebral cortex.

Analysis of M14A also revealed enrichment for genes encoding synaptic proteins (*P* = 1.6e–20 and *P* = 1.1e–13), neuronal markers (*P* = 2.2e–08), and genes up-regulated in glutamatergic cortical neurons (*P* = 1.1e–09), while M14D also exhibited significant enrichment for synaptic proteins (*P* = 1.2e–03) (Supplementary Table 7). EASE identified enrichment in M14 for numerous categories related to synaptic function, including "transmission of nerve impulse" (*P* = 4.4e–12), "synaptic transmission" (*P* = 2.0e–11), and "synaptic vesicle" (*P* = 1.9e–

05) (Supplementary Table 8). These results support the conclusion that gene coexpression in M14 is also related to glutamatergic synaptic function. Although M10 and M14 possessed similar characteristics, some functional distinctions between these modules were evident. For example, M10, but not M14, contained numerous over-represented EASE categories related to calcium channel activity, while M14 was enriched with many more EASE categories pertaining to signal transduction than M10 (Supplementary Table 8).

Organellar composition and function: M7, M2

We observed that M7 was highly enriched with genes comprising the GO cellular compartment "mitochondrion" for both CTX (P = 2.0e–16) and CB (P = 4.4e–07) (Supplementary Table 8). Other over-represented categories identified by EASE for M7 included "hydrogen ion transporter activity" (P = 2.2e–20 [CTX] and P = 2.7e–11 [CB]), "electron transport chain" (P = 5.5e–17 [CTX] and P = 7.2e–10 [CB]), "oxidative phosphorylation" (P = 9.8e–16 [CTX] and P = 2.3e–09 [CB]), and "energy metabolism" (P = 4.7e–11 [CTX] and P = 5.0e–07 [CB]) (Supplementary Table 8). Genes with strong membership for M7A included many components of the electron transport chain, including *NDUFA2*, *COX6B1*, *NDUFA13*, *COX5B*, *NDUFS8*, *ATP5H*, *NDUFB2*, *ATP5G1*, and *NDUFA7* (Supplementary Tables 3 and 8). These results provide evidence that gene coexpression in M7 is related to mitochondrial function in the human brain. Interestingly, *AQP4*, which encodes a water-specific channel important for the regulation of cell volume[15], was strongly negatively correlated with the ME for M7A (Supplementary Table 3 and Supplementary Fig. 4g), providing a previously unrecognized link between osmoregulation and energy metabolism in cerebral cortex.

EASE results indicated that another module, M2, was highly enriched with genes encoding ribosomal subunits (*P* = 2.3e–64) and elements of the KEGG pathway "translation" (*P* = 7.6e–48) (Supplementary Table 8). Although most of the genes with the strongest membership for this module encode known structural constituents of the ribosome, for some (e.g. *C6orf49* and *C10orf116*; Supplementary Table 3), association with this structure has not been previously described. The strong coexpression of these genes with so many components of the ribosome suggests that they are likely to be intimately involved with the function of this macromolecular complex and the process of translation.

Genomic clustering of coexpressed genes

EASE analysis revealed that for both CTX and CTX_95, the most significant over-represented category for M10, which was highly enriched with genes involved in glutamatergic synaptic function (see above), was chromosome 19 (*P* = 3.2e–18 [CTX] and *P* = 1.2e–14 [CTX_95]; Supplementary Table 8). Significant enrichment was also observed for M10 on chromosome 16 (*P* = 4.2e–07 [CTX] and *P* = 3.0e–03 [CTX_95]) and chromosome 22 (*P* = 1.1e–04 [CTX] and *P* = 1.2e–02 [CTX_95]) (Supplementary Table 8). Another module that was highly enriched with genes involved in glutamatergic synaptic function (M14A; see above) also showed significant enrichment for genes found on the same chromosomes (chromosome 16: *P* = 3.2e–04; chromosome 22: *P* = 3.3e–03; chromosome 19: *P* = 7.2e–03; Supplementary Table 8). These data provide evidence for genomic clustering of coexpressed genes related to glutamatergic synaptic function in human cerebral cortex.

We observed that modules related to ribosomal and mitochondrial function (M2 and M7) were also enriched with genes encoding synaptic proteins (*P* = 5.5e–12 [M2] and *P* = 2.8e–12

[M7A]; Supplementary Table 7). Like M10, these modules also showed significant enrichment for genes found on chromosome 19 (P = 4.3e–09 [M2] and P = 4.3e–12 [M7A]) and chromosome 16 (P = 8.9e–07 [M7A]) (Supplementary Table 8). These results provide evidence for the existence of coordinated transcriptional programs in human cerebral cortex underlying synaptic function, energy metabolism, and protein synthesis. Furthermore, our data indicate that this coordination may have resulted in part from genomic clustering of functionally related genes on chromosomes 16 and 19.

Generation of novel functional hypotheses regarding human disease genes on the basis of module membership

The characterization of gene coexpression modules provides an opportunity to generate novel functional hypotheses for thousands of genes expressed in the human brain, including genes involved in neurological or neuropsychiatric disease, through the principle of "guilt-by-association". For example, in CTX, *FMR1* exhibited extremely strong membership for M17A (RMM = 11, P = 1.3e–10; Supplementary Table 3), a module with characteristics of *PVALB*+ interneurons. This observation predicts that disruption of this gene, which results in fragile X mental retardation syndrome[16], should preferentially affect the function of this neuronal subtype in the adult human brain. Interestingly, a recent study identified major deficits in neocortical GABAergic inhibitory circuits in a mouse model of fragile X syndrome[17]. Specifically, this study found a 20% reduction in the density of *PVALB*+ interneurons in somatosensory cortex of mutant mice relative to wild-type mice[17]. Similarly, *SCN1B*, which encodes an auxiliary subunit of voltage-gated sodium channels and has been linked to generalized epilepsy with febrile seizures[18], exhibited extremely strong membership in CTX for M6A (RMM = 4, P < 2.2e–16;

Supplementary Table 3), another module with characteristics of *PVALB*+ interneurons. The protein encoded by this gene interacts with pore-forming subunits of voltage-gated sodium channels such as SCN1A, which has also been linked to generalized epilepsy with febrile seizures[18]. Recently, expression of *SCN1A* was localized to the axon initial segments of *PVALB*+ interneurons in mouse neocortex[19]. Like *SCN1B*, *SCN1A* also exhibited strong membership for M6A (RMM = 67, P = 9.3e–06; Supplementary Table 3). Collectively, these observations predict that the epileptic phenotype associated with disruption of *SCN1B* may be mediated by altered neurotransmission in *PVALB*+ interneurons. These examples illustrate how gene coexpression patterns within tissues can be used to generate novel functional hypotheses related to human disease genes.

Sources of sample variation in cell quantity

It is interesting to speculate on the potential sources of variation that may influence the quantities of specific cell types in different samples of brain tissue. This variation may be influenced by technical factors. For example, although samples analyzed in this study were extracted from gray matter, it is easy to imagine how different dissections might inadvertently introduce varying amounts of white matter "contamination". A sample with relatively more white matter should exhibit a spike in the expression of oligodendrocyte-related genes, perhaps similar to that seen in individual H74 in M9D (Supplementary Fig. 2ca). Because this spike applies to only a small subset of genes on the microarray, this sample was not identified as an outlier when considering all expressed genes. However, in an analysis of differential expression between two groups, asymmetric representation of such samples might erroneously suggest functional differences where none exist. Biological factors are also likely to contribute to differences in cell quantity

between samples. For example, the relative densities of certain cell types in the brain may differ between individuals[20,21]. In CTX_95 (the only dataset that included multiple samples from the same individual), expression of genes in M15B was relatively constant in cortical areas from the same individual when compared to cortical areas from different individuals (Supplementary Fig. 2ae). This observation is consistent with a role for biological factors in determining the number of astrocytes that are present in cortical samples.

References

1. Kamme, F. et al. Single-cell microarray analysis in hippocampus CA1: demonstration and validation of cellular heterogeneity. *J Neurosci* **23**, 3607-15 (2003).
2. Sugino, K. et al. Molecular taxonomy of major neuronal classes in the adult mouse forebrain. *Nat Neurosci* **9**, 99-107 (2006).
3. Bastianelli, E. Distribution of calcium-binding proteins in the cerebellum. *Cerebellum* **2**, 242-62 (2003).
4. Rong, Y., Wang, T. & Morgan, J.I. Identification of candidate Purkinje cell-specific markers by gene expression profiling in wild-type and pcd(3J) mice. *Brain Res Mol Brain Res* **132**, 128-45 (2004).
5. Walker, M.G. Z39Ig is co-expressed with activated macrophage genes. *Biochim Biophys Acta* **1574**, 387-90 (2002).
6. Moran, L.B., Duke, D.C. & Graeber, M.B. The microglial gene regulatory network activated by interferon-gamma. *J Neuroimmunol* **183**, 1-6 (2007).
7. Sievers, J., Pehlemann, F.W., Gude, S. & Berry, M. Meningeal cells organize the superficial glia limitans of the cerebellum and produce components of both the interstitial matrix and the basement membrane. *J Neurocytol* **23**, 135-49 (1994).
8. Beuckmann, C.T. et al. Cellular localization of lipocalin-type prostaglandin D synthase (beta-trace) in the central nervous system of the adult rat. *J Comp Neurol* **428**, 62-78 (2000).
9. Pasterkamp, R.J. et al. Expression of the gene encoding the chemorepellent semaphorin III is induced in the fibroblast component of neural scar tissue formed following injuries of adult but not neonatal CNS. *Mol Cell Neurosci* **13**, 143-66 (1999).
10. Junghans, U. et al. Purification of a meningeal cell-derived chondroitin sulphate proteoglycan with neurotrophic activity for brain neurons and its identification as biglycan. *Eur J Neurosci* **7**, 2341-50 (1995).
11. Becker, K.G., White, S.L., Muller, J. & Engel, J. BBID: the biological biochemical image database. *Bioinformatics* **16**, 745-6 (2000).
12. Nagata, T. et al. Profiling of genes associated with transcriptional responses in mouse hippocampus after transient forebrain ischemia using high-density oligonucleotide DNA array. *Brain Res Mol Brain Res* **121**, 1-11 (2004).
13. Penny, G.D., Kay, G.F., Sheardown, S.A., Rastan, S. & Brockdorff, N. Requirement for Xist in X chromosome inactivation. *Nature* **379**, 131-7 (1996).
14. Bernstein, E., Caudy, A.A., Hammond, S.M. & Hannon, G.J. Role for a bidentate ribonuclease in the initiation step of RNA interference. *Nature* **409**, 363-6 (2001).
15. Manley, G.T., Binder, D.K., Papadopoulos, M.C. & Verkman, A.S. New insights into water transport and edema in the central nervous system from phenotype analysis of aquaporin-4 null mice. *Neuroscience* **129**, 983-91 (2004).
16. Jin, P. & Warren, S.T. Understanding the molecular basis of fragile X syndrome. *Hum Mol Genet* **9**, 901-8 (2000).
17. Selby, L., Zhang, C. & Sun, Q.Q. Major defects in neocortical GABAergic inhibitory circuits in mice lacking the fragile X mental retardation protein. *Neurosci Lett* **412**, 227-32 (2007).
18. Yamakawa, K. Na channel gene mutations in epilepsy--the functional consequences. *Epilepsy Res* **70 Suppl 1**, S218-22 (2006).

19. Ogiwara, I. et al. Na(v)1.1 localizes to axons of parvalbumin-positive inhibitory interneurons: a circuit basis for epileptic seizures in mice carrying an Scn1a gene mutation. *J Neurosci* **27**, 5903-14 (2007).
20. Pelvig, D.P., Pakkenberg, H., Stark, A.K. & Pakkenberg, B. Neocortical glial cell numbers in human brains. *Neurobiol Aging* (2007).
21. Pakkenberg, B. et al. Aging and the human neocortex. *Exp Gerontol* **38**, 95-9 (2003).